

Unraveling hadron structure with generalized parton distributions

A.V. BELITSKY

*Department of Physics and Astronomy, Arizona State University
Tempe, AZ 85287-1504, USA*

A.V. RADYUSHKIN¹

*Physics Department, Old Dominion University
Norfolk, VA 23529, USA*

*Theory Group, Jefferson Laboratory,
Newport News, VA 23606, USA*

Abstract

The generalized parton distributions, introduced nearly a decade ago, have emerged as a universal tool to describe hadrons in terms of quark and gluonic degrees of freedom. They combine the features of form factors, parton densities and distribution amplitudes—the functions used for a long time in studies of hadronic structure. Generalized parton distributions are analogous to the phase-space Wigner quasi-probability function of non-relativistic quantum mechanics which encodes full information on a quantum-mechanical system. We give an extensive review of main achievements in the development of this formalism. We discuss physical interpretation and basic properties of generalized parton distributions, their modeling and QCD evolution in the leading and next-to-leading orders. We describe how these functions enter a wide class of exclusive reactions, such as electro- and photo-production of photons, lepton pairs, or mesons. The theory of these processes requires and implies full control over diverse corrections and thus we outline the progress in handling higher-order and higher-twist effects. We catalogue corresponding results and present diverse techniques for their derivations. Subsequently, we address observables that are sensitive to different characteristics of the nucleon structure in terms of generalized parton distributions. The ultimate goal of the GPD approach is to provide a three-dimensional spatial picture of the nucleon, direct measurement of the quark orbital angular momentum, and various inter- and multi-parton correlations.

Dedicated to Anatoly V. Efremov on occasion of his 70th anniversary

¹Also at Bogoliubov Laboratory of Theoretical Physics, JINR, Dubna, Russia.

Contents

1 Preface	6
2 Unraveling layers of matter: from atoms to partons	7
2.1 Quantum mechanical observables	9
2.1.1 Atomic form factor and momentum density	10
2.1.2 Wigner distribution	11
2.1.3 Wigner distribution of a quantum oscillator	12
2.1.4 Experimental access to Wigner distributions	13
2.2 Nucleon observables	14
2.2.1 Nucleon electromagnetic form factors	14
2.2.2 Form factors in the Breit frame and charge distributions	16
2.2.3 Nucleon structure functions	20
2.2.4 Infrared safety	21
2.2.5 Incoherence and scale separation	23
2.2.6 QCD parton distributions	25
2.2.7 Parton distributions as momentum densities in the Bjorken frame	29
2.2.8 Parton distributions in the rest frame	30
2.3 Quark phase-space distribution	31
2.4 Exclusive versus inclusive processes	32
3 Classification and properties of GPDs	33
3.1 Twist-two operators	33
3.1.1 Quark operators	34
3.1.2 Gluon operators	36
3.2 Operator matrix elements and GPDs	37
3.2.1 Time-ordering and support	38
3.2.2 Counting GPDs	40
3.2.3 Boost invariance of GPDs	41
3.2.4 Spin-zero hadrons	41
3.2.5 Spin-one-half hadrons	42
3.2.6 A comment on gluonic matrix elements	43
3.2.7 Spin-one hadrons	43
3.2.8 Implications of time reversal and hermiticity	44
3.3 Forward limit	47
3.3.1 Spin-zero hadrons	47
3.3.2 Spin-one-half hadrons	48
3.3.3 Spin-one hadrons	49
3.4 Form factors	50
3.4.1 Spin-zero hadrons	50
3.4.2 Spin-one-half hadrons	51
3.4.3 Spin-one hadrons	53
3.5 Polynomiality and skewness dependence	54
3.5.1 Spin-zero hadrons	56
3.5.2 Spin-one-half hadrons	57
3.6 GPDs and the proton spin puzzle	59

3.6.1	Axial coupling from polarized deeply inelastic scattering	60
3.6.2	Axial coupling from semileptonic decays of hyperons	61
3.6.3	Angular momentum of proton's constituents	63
3.6.4	Gravitational form factors	64
3.7	Wave functions and distribution amplitudes	67
3.7.1	Meson distribution amplitudes	68
3.7.2	Nucleon wave function with orbital momentum	69
3.7.3	Partonic content of GPDs	74
3.7.4	Overlap representation of GPDs	75
3.8	Double distributions	76
3.8.1	Gauge transformation of double distributions	78
3.8.2	Radon tomography of double distributions with GPDs	81
3.8.3	Nucleon double distributions	83
3.9	Analytic properties of DDs and GPDs	84
3.10	Impact-parameter parton distributions	85
3.10.1	Electromagnetic form factors in the Bjorken frame	85
3.10.2	Skewless GPDs as impact-parameter distributions	87
3.10.3	GPDs in impact-parameter space	90
3.11	Positivity constraints on GPDs	93
3.11.1	Inequalities relating GPDs and ordinary distributions	94
3.11.2	Inequalities in impact parameter representation	96
3.11.3	General inequalities	96
3.12	Chiral properties of GPDs	98
3.12.1	Pion GPDs	99
3.12.2	Nucleon GPDs	103
3.13	Modeling GPDs	106
3.13.1	Longitudinal dynamics	106
3.13.2	Longitudinal-transverse interplay	108
3.13.3	D-term	109
3.13.4	Nonfactorizable GPD ansätze	109
3.14	Visualizing proton via Wigner distributions	111
3.15	Limitations of GPDs as Wigner distributions	112
3.16	Transition GPDs	114
3.16.1	Baryon octet to octet transitions	114
3.16.2	Baryon octet to decuplet transitions	116
3.16.3	Implications of the large- N_c for decuplet-octet transitions	118
4	Evolution equations	122
4.1	Divergences of perturbation theory and scale dependence	123
4.2	Factorization and evolution	124
4.3	Coordinate-space evolution equations	125
4.3.1	Symmetry properties	127
4.3.2	One-loop results	128
4.4	Momentum-space evolution equations	129
4.4.1	One-loop results	131
4.4.2	From coordinate to momentum-space kernels	132

4.4.3	Reduction to inclusive kernels	133
4.4.4	Reduction to exclusive kernels	135
4.4.5	From exclusive to inclusive kernels	136
4.5	Evolution of double distributions	138
4.6	Diagonalization of the mixing matrix	139
4.6.1	Representations of the collinear conformal algebra	140
4.6.2	Conformal operators	142
4.6.3	Autonomous renormalization of conformal operators	145
4.7	Diagonalization of generalized evolution kernels	147
4.7.1	Normalization of anomalous dimensions	148
4.7.2	Inclusive to exclusive reconstruction at leading order	149
4.8	Asymptotic distribution amplitudes	151
4.9	Conformal symmetry breaking	151
4.9.1	Anomaly in the trace of energy momentum tensor	153
4.9.2	Conformal Ward identities	154
4.9.3	Commutator constraints for conformal anomalies	155
4.9.4	NLO constraint and non-diagonal anomalous dimensions	156
4.10	Solutions of renormalization group equation	157
4.10.1	Mixing of conformal operators	158
4.10.2	Restoration of conformal covariance in conformal limit	158
4.10.3	Solution with running coupling	159
4.11	Solution of evolution equations for GPDs	160
4.11.1	One-loop evolution in coordinate space	160
4.11.2	“Difficulties” with eigenfunctions	162
4.11.3	Orthogonal polynomial reconstruction	163
4.11.4	Next-to-leading order: nonsinglet sector	164
4.11.5	Next-to-leading order: singlet sector	166
4.11.6	Asymptotic GPDs in singlet sector	169
4.11.7	Two-loop evolution in momentum space	170
4.11.8	Solution of evolution equations for double distributions	170
4.11.9	Effective forward distributions	173
5	Compton scattering beyond leading order and power	178
5.1	Compton scattering in Bjorken limit	178
5.1.1	Structure of the Compton amplitude in generalized Bjorken limit	179
5.1.2	Compton amplitude in symmetric variables	183
5.1.3	One-loop factorization in symmetric variables	185
5.1.4	Hadronization corrections of the final-state photon	186
5.2	Restoration of electromagnetic gauge invariance	189
5.2.1	Tree-level twist-three Compton amplitude	190
5.2.2	Lorentz structure of the Compton amplitude	194
5.3	Twist-three GPDs	196
5.3.1	Geometric twist decomposition of operators	196
5.3.2	Twist-three GPDs for spin-zero target	198
5.3.3	Twist-three GPDs for spin-one-half target	200
5.3.4	Properties of the kinematical kernels	202

5.3.5	Discontinuities of twist-three GPDs	204
5.3.6	Factorization of the Compton amplitude at twist-three	204
5.3.7	Sum rules for twist-three GPDs	205
5.4	Compton form factors of the nucleon	206
5.4.1	Twist-three CFFs	207
5.4.2	Small- x_B behavior of Compton form factors	208
5.4.3	One-loop corrections to twist-two CFFs	210
5.5	Application of conformal operator product expansion	212
5.6	Target mass corrections	217
5.6.1	Twist decomposition and harmonic polynomials	217
5.6.2	Spin-zero target	220
5.6.3	Spin-one-half target	224
5.6.4	Twist-four mass corrections	225
6	Phenomenology of GPDs	226
6.1	Leptoproduction of a real photon	227
6.1.1	Kinematics of leptoproduction of the photon	228
6.1.2	Cross section for leptoproduction of the photon	230
6.1.3	Angular dependence	233
6.1.4	Bethe-Heitler amplitude squared	233
6.1.5	DVCS amplitude squared	235
6.1.6	Interference of Bethe-Heitler and DVCS amplitudes	236
6.1.7	Angular harmonics in terms of GPDs	237
6.1.8	Determination of Compton form factors from interference	239
6.1.9	Physical observables and access to GPDs	240
6.1.10	Asymmetries	242
6.1.11	Electron and positron beam options	244
6.1.12	Electron or positron beam option	246
6.1.13	Remarks on state-of-the-art of DVCS	247
6.2	Leptoproduction of lepton pairs	247
6.2.1	Mapping the surface of GPDs	247
6.2.2	Cross section for lepton pair electroproduction	248
6.2.3	Kinematics of the lepton pair electroproduction	250
6.2.4	Generating function for angular dependence	253
6.2.5	Angular dependence of the cross section	256
6.2.6	Squared virtual Compton amplitude	258
6.2.7	Interference of virtual Compton and Bethe-Heitler amplitudes	260
6.2.8	Squared Bethe-Heitler amplitude	263
6.2.9	Single-spin asymmetries	265
6.2.10	Charge and angular asymmetries	266
6.2.11	Advantages of lepton pair electroproduction	268
6.3	Hard exclusive production of mesons	270
6.3.1	Feynman versus hard mechanism in elastic form factors	271
6.3.2	Quark counting rules	272
6.3.3	GPDs and form factors	274
6.3.4	Exclusive meson production and QCD factorization	279

6.3.5	Electroproduction of pseudoscalar mesons	281
6.3.6	Electroproduction of vector mesons	282
6.3.7	Electroproduction of delta isobar	283
6.3.8	Cross sections for electroproduction of mesons	283
6.3.9	Perturbative corrections to meson production	285
6.3.10	Nonperturbative corrections	286
7	Outlook	288
A	Conventions	292
A.1	Representations of the Clifford algebra	293
A.2	Spin-1/2 spinors	294
A.3	Spin-1 vector field	297
A.4	Spin-3/2 Rarita-Schwinger spin-vector	298
A.5	Particle states	299
A.6	Color algebra	300
B	Light-cone vectors and tensors	300
B.1	Compton frame	301
B.2	Breit frame	302
B.3	Drell-Yan frame	303
C	Optical theorem	303
D	Light-cone quantization of QCD	305
E	Improved Belinfanté energy-momentum tensor	307
F	Basics of the Skyrme model	309
G	Computation techniques for evolution equations	311
G.1	Feynman rules	311
G.2	Momentum integrals	313
G.3	Renormalization in covariant gauges	314
G.4	Renormalization of composite operators	315
G.5	Construction of evolution equations in coordinate space	316
G.5.1	Covariant gauge formalism	317
G.5.2	Light-cone gauge formalism with ML prescription	321
G.6	Construction of evolution equations in momentum space	323
G.6.1	Renormalization in light-cone gauge with PV prescription	323
G.6.2	Evolution kernels in momentum space	325
G.7	Generalized step functions	327
H	Evolution of nonsymmetric double distributions	328
H.1	Evolution kernels for nonsymmetric double distributions	329
H.2	Solution of evolution equation for double distributions	332
H.3	Asymptotic shape of double distributions	334

I Elements of the conformal group	335
I.1 Conformal algebra	336
I.2 Induced representations	337
J Scheme transformation matrix	338
K Two-loop anomalous dimensions	340
K.1 Even-parity sector	340
K.2 Odd-parity sector	342
K.3 Maximal-helicity sector	343
K.4 Supersymmetric relations between anomalous dimensions	343
L Twist separation in light-ray operators	345

1 Preface

The concept of generalized parton distributions (GPDs) was developed as a modern tool to deliver a detailed description of the microscopic structure of hadrons in terms of their elementary constituents [1, 2, 3, 4, 5, 6]. The need for GPDs is dictated by the present-day situation in hadronic physics. The fundamental particles which form hadrons are long known to be quarks and gluons, whose interactions are described by the Lagrangian of quantum chromodynamics (QCD). However, this knowledge is not sufficient at the moment to perform reliable, fully quantitative calculations starting from first principles, since the precise mechanism of hadron formation from the underlying quark and gluonic degrees of freedom is not completely known and quantifiable to our dissatisfaction. We have to resort to hints from experimental measurements in order to understand how QCD works and ultimately resolve “the long-distance problem” of QCD. The standard way out of these complications is to use certain phenomenological functions. The well-known examples include form factors, parton densities, and distribution amplitudes. The new functions—generalized parton distributions—are hybrids of these “old” functions which, in their turn, are the limiting cases of the “new” ones. There are several existing reviews dedicated to thorough discussion of diverse aspect of GPDs [7, 8, 9, 10]. Though the subject is common, these reviews differ in the extent of the covered material, in the emphasis on particular techniques and approaches to the GPD studies, and in the degree of detail in the presentation of computations. The aim of the present endeavor is to give a review of the theory of generalized parton distributions, with discussion of calculation machinery sufficiently detailed to enable an interested reader to derive many results without heavy use of original publications as well as to provide a self-consistent compendium of analytical formulas.

The review is organized as follows. In Section 2, we discuss general quantum-mechanical aspects of investigating the structure of matter emphasizing similarities of studies on atomic, nuclear and quark/gluon levels. In particular, we address the issue of interpreting the experimentally observable quantities in terms of charge, magnetization, etc., distributions, and discuss Wigner distributions, the closest quantum-mechanical analog of the generalized parton distributions. In Section 3, we give the classification of GPDs according to the quantum numbers of the composite operators which represent them, and by the type of the hadronic matrix elements involved. The consideration in that section is limited to the leading-twist distributions. The twist-three functions are addressed later in subsection 5.3. Section 4 is devoted to the evolution of generalized parton

distributions. We discuss evolution kernels for the light-cone operators in the coordinate representation, their transformation into the momentum space, diagonalization of the mixing matrix, and interrelation between “inclusive” and “exclusive” kernels. The use of the conformal symmetry allows to understand many features of the evolution equations on a deeper level. This is also a topic of a detailed discussion in Section 4. The subject of Section 5 is the virtual Compton amplitude, the major building block of the electron-hadron Compton scattering process, potentially the cleanest source of information about GPDs. We present a thorough study of the Compton amplitude including its gauge-invariant tensor decomposition, one-loop corrections to the short-distance coefficient function and power suppressed contributions, including twist-three and target mass effects. In Section 6, we give a comprehensive discussion of a few exclusive reactions where GPDs can be measured or accessed, including deeply virtual Compton scattering, doubly deeply virtual Compton scattering and hard exclusive meson production. In the concluding Section 7, we outline a few directions, where significant improvements in the theory of GPDs can be made. A number of appendices serve as a technical supplement to the material presented in the main text.

2 Unraveling layers of matter: from atoms to partons

The wisdom goes back to the ancient Greeks who philosophized that matter consists of tiny particles—atoms. However, the subatomic structure of matter remained an unsolved puzzle till the beginning of the 20th century when radioactivity was discovered and used by Rutherford in his seminal experiments on large-angle scattering of α -particles off atoms where the outcome suggested that the atom bears a localized core—the nucleus. On the other hand, electron beams were found to pass through atoms with no or very little deflection forcing Lenard to hypothesize that atoms have “wide empty spaces inside”. The α -particles scattered more frequently than their “cousins” β -particles, which produced very low, barely observable rates due to tiny cross sections and, available at the time, luminosity of the beam. Similar experiments but rather with light sources or room-temperature neutrons are exploited nowadays to study the crystal’s lattice. If a crystal is placed in front of a source of visible light, the object will merely leave a shadow on a screen behind it and one will not be able to detect elementary building blocks which form it. Obviously, the visible light, having the wavelength $\lambda_{\text{light}} \sim 0.4 - 0.7 \mu\text{m}$, cannot do the job and resolve the internal structure of a crystal. The size of an individual atom, say, hydrogen, is of order $R_{\text{atom}} \sim (\alpha_{\text{em}} m_e)^{-1} \sim (10 \text{ KeV})^{-1}$. Therefore, to “see” individual atoms in crystals one has to use light sources with a comparable or smaller wavelength $\lambda_\gamma \leq R_{\text{atom}}$, or equivalently, of energy $E_\gamma \geq R_{\text{atom}}^{-1}$. To do this kind of “nano-photography” a beam of X-rays is needed. To go further into the structure of atoms one has to resort to even more energetic probes.

After the discovery of the nucleus’ building blocks—the nucleons (i.e., protons and neutrons)—the attention has been shifted to the extensive study of these “elementary” particles. However, their elementarity has been questioned since Stern’s experiments in 1932 [11] which measured magnitude of the proton’s magnetic moment about three times larger than that of the expected. Hofstadter’s experiments [12] with elastic electron scattering off nucleons, $eN \rightarrow e'N'$, which accessed proton’s electromagnetic form factors revealed the deviation from those of a point-like object and demonstrated for the first time that the nucleon has a spatial extent of order of one femtometer. To probe femtometer scales, we rely on scattering experiments with high-energy lepton beams, where the point-like nature of leptons does not represent an extra uncertainty in the interpretation of the data contrary to beams of composite particles. Inelastic lepton-nucleon

scattering experiments, $\ell N \rightarrow \ell' X$, conducted at Stanford Linear Accelerator Center [13] fulfilled this goal which led to the ultimate discovery of a new layer of matter by observing events with the transfer of a large momentum from the electron to the proton. If the proton would be a hard ball or a diffuse distribution of matter, such kind of scattering would be improbable. An analogy to the latter is from the early days of atomic physics when, according to the Thompson's model, the atom was thought to consist of negatively charged electrons embedded into a jelly-like medium of positive charge. Thus the results of the experiment were explained by conjecturing the existence of point-like constituents inside the proton which absorb a highly virtual γ^* -quantum emitted by the electron in the course of the scattering process.

An earlier theoretical description of deeply inelastic events resulted into the scaling hypothesis by Bjorken [14], stating that cross sections measured there must not depend on dimensionful parameters, like particle virtualities. Further development resulted into the formulation of the Feynman's parton model [15, 16]. According to the parton model, the hadron at high energy can be viewed as a composition of a number of constituents—the partons—which behave as an incoherent bunch of quanta at small space-time separations, and the interaction of the probe happens with one of them. Current algebra analysis of the deeply inelastic cross section had favored the quarks to be fermions with spin one-half [17]. It was quite tempting to identify these partons with Gell-Mann and Zweig's quarks. This experimental discovery, which triggered theoretical minds to reconsider the contemporary physical concepts, was analogous to, if not greater than, the Rutherford's experiments in atomic physics. The Feynman's partons were naturally identified with quark and gluon degrees of freedom described by a nonabelian gauge field theory of strong interactions with unbroken $SU(3)$ group—Quantum Chromodynamics (QCD).

The path which led to this fundamental finding was rather long. The analysis of divergences of charge renormalization resulted in the discovery of the asymptotic freedom [18, 19, 20] in nonabelian gauge theories. The vacuum in general is a polarizable medium of virtual particles. In abelian gauge theories the former is dielectric, i.e., the medium screens the charge, and it becomes weaker at finite distances—a lump of positive charge pulls negative charges from the medium toward itself which partially neutralizes it causing its weakening at a distance. If the charge is point-like, i.e., has zero radius, it would be screened completely at finite distances. This is a well-known zero charge problem [21, 22]. For a finite-size charge the interaction becomes stronger at smaller distances and inevitably it reaches the magnitude where the perturbation theory becomes inapplicable. Of course, this inconsistency of the resummed theory is achieved only at asymptotically high energy, so that this triviality of interaction is irrelevant as soon as one discusses processes at Earth energies. Contrary, when nonabelian fields are present the response of spin-one quanta is paramagnetic [23, 24] so that effective coupling decreases with rising energy.

The finding of the vanishing nonabelian charge at small distances has put into its spot the concept of the gauged color group. Quantum Chromodynamics, baptized by Gell-Mann and discussed earlier in the works by Fritzsch, Gell-Mann and Leutwyler [25], has emerged as the theory of strong interactions. Its Lagrangian

$$\mathcal{L}_{\text{QCD}}(z) = \frac{i}{2}\bar{\psi}(z) \left(\vec{\mathcal{D}}_\mu - \vec{\mathcal{D}}_\mu \right) \gamma^\mu \psi(z) - \frac{1}{4}F_{\mu\nu}^a(z)F_a^{\mu\nu}(z) \quad (2.1)$$

describes the minimal interaction between the quarks and the glue, introduced through the covariant derivatives

$$\vec{\mathcal{D}}_\mu = \vec{\partial}_\mu - ig t^a A_\mu^a(z), \quad \vec{\mathcal{D}}_\mu = \vec{\partial}_\mu + ig t^a A_\mu^a(z). \quad (2.2)$$

QCD predicts the desired Bjorken scaling at short distances which is, however, broken by logarithmic corrections computable from first principles [26, 27]. It took quite a while before experiments,

having a sufficiently large window in the momentum transfer, had found a confirmation for the scaling violation [28] intrinsic to renormalizable field theories.

The short-distance structure of the strong interaction dynamics was established, and another even more fundamental issue arose: long distance behavior of the theory. No free quarks have been observed. Instead, when emitted in a given process they conspire to form a color neutral object and fragment into observable hadrons. When the process involves a hard momentum transfer they form jets. This was yet another indirect evidence in favor of the quark-gluon substructure of hadrons. The studies of jets explicitly demonstrated that they carry genuine properties, computable from the first principles, of their predecessors—quarks and gluons [29]. This unusual property of the color gauge theory is the infrared slavery of hadron’s constituents, or confinement, which has been proven to be the most outstanding problem of strong interaction physics. No efficient analytical tool has been developed so far to tackle the task. We have, however, a rough physical picture according to which quarks inside a hadron are bound by a string of glue. Once the quarks are separated far enough so that the stretching force overwhelms the string tension, the latter breaks down only by means of a creation of a quark-antiquark pair from the vacuum at its ends. The quarks never show up free. With the development of lattice techniques, there is a growing compelling evidence toward this description.

The nucleon represents a relativistic multi-particle quantum system in a bound state whose dynamics is driven by strong interactions. The exhaustive exploration of its structure and confining dynamics of its constituents is a cherished goal of strong-interaction physics. This is the subject of the present review within the framework of generalized parton distributions—a set of hadron characteristics probing hadrons from a variety of different angles. This approach is phenomenological and uses experimental data as an input in theoretical considerations in order to draw solid conclusions about the internal structure of the proton and its siblings.

2.1 Quantum mechanical observables

Before we move on to a detailed analysis of tools and observables used to unravel the nucleon’s content, let us draw a few close analogies from nonrelativistic quantum mechanics. We hope that this will be extremely instructive and insightful for the main subject of our analysis.

A quantum mechanical system is determined by its wave function ψ . Acquiring the latter from theoretical considerations, like solving the Schrödinger equation, or from experimental measurements, allows one to predict any physical observable for a given system. The bulk of experimentally accessible quantities is sensitive only to the absolute value of the wave function via measurements of cross sections. The phase of the wave function is thus essentially unattainable there. To circumvent the difficulty, one has to measure correlations of wave functions or, more generally, the density matrix ρ . For a pure state,

$$\rho(\mathbf{r}_1, \mathbf{r}_2) = \psi^*(\mathbf{r}_1)\psi(\mathbf{r}_2), \quad (2.3)$$

and thus the wave function is known once the density matrix is determined. If one is able to measure the density matrix by means of the interference of a test system with a reference source, possessing a priori known characteristics, this will then serve the purpose of reconstructing the missing phase of the wave function. Succeeding in this endeavor, complete information on a quantum mechanical system can be acquired.

2.1.1 Atomic form factor and momentum density

Let us recall a few physical observables which are conventionally used to probe a quantum mechanical system and measure its wave function.

First, the spatial distribution of matter (or charge) in a system can be probed through elastic scattering of electrons, photons, or neutrons, etc. The physical quantity that one measures is the elastic form—also called structure—factor $F(\Delta)$ which depends on the three-momentum transfer to the system Δ . It is expressed (upon removing a point-like core due to scattering off the atomic nucleus) as a Fourier transform of the absolute value squared of the atomic wave function $\rho(\mathbf{r}) = |\psi(\mathbf{r})|^2$ with respect to the position three-vector $\mathbf{r} = (r^x, r^y, r^z)$:

$$\rho(\mathbf{r}) = \int d^3\Delta e^{i\Delta \cdot \mathbf{r}/\hbar} F(\Delta). \quad (2.4)$$

One can easily compute the tail of the form factor for the scattering on a bound state in a Coulomb potential, $V(\mathbf{r}) \sim 1/|\mathbf{r}|$, at large momentum transfers. In the momentum space the latter behaves as $V(\mathbf{p}) \sim 1/\mathbf{p}^2$. Then the solution to the Schrödinger equation,

$$i\frac{d}{dt}\psi(\mathbf{r}) = (H_0 + V(\mathbf{r}))\psi(\mathbf{r}), \quad (2.5)$$

where $H_0 = \mathbf{p}^2/(2m)$ and $V(\mathbf{r})$ are the free-particle Hamiltonian and the interaction potential, respectively, is given by

$$\psi(\mathbf{p}) = \frac{\int d^3\mathbf{p}' V(\mathbf{p} - \mathbf{p}') \psi(\mathbf{p}')}{E - \mathbf{p}^2/(2m)} \underset{|\mathbf{p}| \rightarrow \infty}{\approx} \text{const.} \frac{\psi(\mathbf{r} = 0)}{\mathbf{p}^4}.$$

Here all the quantities are Fourier transformed into the momentum space. In the evaluation of the second equality we took into account that the kinetic energy obviously dominates and we also neglected the dependence on \mathbf{p}' in the argument of the potential compared to the large momentum \mathbf{p} . The resulting integral is a Fourier transform of the wave function at the origin. Thus,

$$F(\Delta) = \int d^3\mathbf{p} \psi^*(\mathbf{p}) \psi(\mathbf{p} + \Delta) \underset{|\Delta| \rightarrow \infty}{\approx} \psi(\Delta) \int d^3\mathbf{p} \psi^*(\mathbf{p}) \approx \text{const.} \frac{|\psi(\mathbf{r} = 0)|^2}{\Delta^4}.$$

The second approach to study the properties of a quantum mechanical system is designed to measure the population of its constituents with a given momentum, or the momentum distribution, through knock-out scattering. The momentum density is expressed in terms of the absolute value of the momentum-space wave function $n(\mathbf{p}) = |\psi(\mathbf{p})|^2$. An example of a nonrelativistic quantum system where this quantity is measured is superfluid helium (see, e.g., Ref. [30]). In the neutron-scattering experiment, the distribution of angles and energies of a neutron beam passing through a sample of helium is recorded, while the state of the liquid helium after the scattering is not detected. At high momentum transfer, when a neutron scatters off single atoms, the impulse approximation holds and the cross section $\sigma(p^z)$ as a function of momentum p^z is expressed via the relation

$$\sigma(p^z) \sim \int dp^x dp^y n(\mathbf{p})$$

in terms of the Fourier transform of a single-particle density matrix

$$n(\mathbf{p}) = \int \frac{d^3\mathbf{r}_1}{(2\pi\hbar)^3} \frac{d^3\mathbf{r}_2}{(2\pi\hbar)^3} e^{i\mathbf{p} \cdot (\mathbf{r}_1 - \mathbf{r}_2)/\hbar} \varrho(\mathbf{r}_1, \mathbf{r}_2). \quad (2.6)$$

For a pure state, it reduces to the square of the coordinate space wave function, $\varrho(\mathbf{r}_1, \mathbf{r}_2) = \psi^*(\mathbf{r}_1)\psi(\mathbf{r}_2)$. The momentum distribution of liquid helium $n(\mathbf{p})$ at $\mathbf{p} = 0$ determines the Bose-Einstein condensate. Another well-known example of nonrelativistic momentum density is the nucleon distributions in a nucleus measured through quasielastic electron scattering.

2.1.2 Wigner distribution

As we emphasized, the observables outlined above probe only the diagonal elements of the density matrix either in the coordinate or momentum space. Thus, one is unable to get complete information on the quantum-mechanical state. The off-diagonal elements of the density matrix remain unknown and one lacks phases of the wave function. The question arises whether there exists an experimental observable which, on the one hand, is sensitive to the phase structure of the wave function and, on the other hand, has an intuitive interpretation. The answer to this question turns out to be positive.

An equivalent to the density matrix approach and a classically more comprehensive description of a quantum mechanical system is achieved by means of a partially Fourier-transformed density matrix known as the Wigner quasi-probability distribution [31, 32],

$$W(\mathbf{r}, \mathbf{p}) = \int \frac{d^3 R}{(2\pi\hbar)^3} e^{-i\mathbf{p}\cdot\mathbf{R}/\hbar} \psi^*(\mathbf{r} - \frac{1}{2}\mathbf{R}) \psi(\mathbf{r} + \frac{1}{2}\mathbf{R}) , \quad (2.7)$$

where \mathbf{r} and \mathbf{p} are *c*-numbers, not operators. Because it involves wave functions at different spatial separations, it obviously possesses complete knowledge on their imaginary phases, just like the density matrix does. It has the following important features.

- The Wigner distribution is advantageous over the density matrix since it is real:

$$W^*(\mathbf{r}, \mathbf{p}) = W(\mathbf{r}, \mathbf{p}) . \quad (2.8)$$

- It has a certain classical limit and thus can be thought of as an extension of an intuitive classical concept to quantum physics. Namely, in classical physics the state of a particle is specified by its position \mathbf{r} and momentum \mathbf{p} . In a gas of classical identical particles, the single-particle properties are described by a phase-space distribution $f(\mathbf{r}, \mathbf{p})$ representing the density of particles at a phase-space point (\mathbf{r}, \mathbf{p}) . Time dependence of the distribution is governed by the Boltzmann equation (or Liouville equation, in case the particles are not interacting). In quantum mechanics, the position and momentum operators do not commute; hence, in principle one cannot talk about the joint momentum and position distribution of particles. Indeed, a quantum-mechanical wave function depends either on spatial coordinates or on the momenta, but never both, unless they are not reciprocal variables.

The Wigner distribution can, to some extent, be thought of as a distribution of a quantum particle in the position and momentum spaces simultaneously. The nonclassical feature of the Wigner function is that it cannot be fully treated as a bona fide joint density of probability since it possesses patches of “negative probability” due to interference of quantum phases. The quantum-mechanical uncertainty principle restricts the amount of localization that a Wigner distribution can have. Therefore, the uncertainty principle leads to a “fuzzy” phase-space description of the system compared to the “sharp” determination of its momentum or coordinate observables separately. In the classical limit, $W(\mathbf{r}, \mathbf{p})$ reduces to the usual

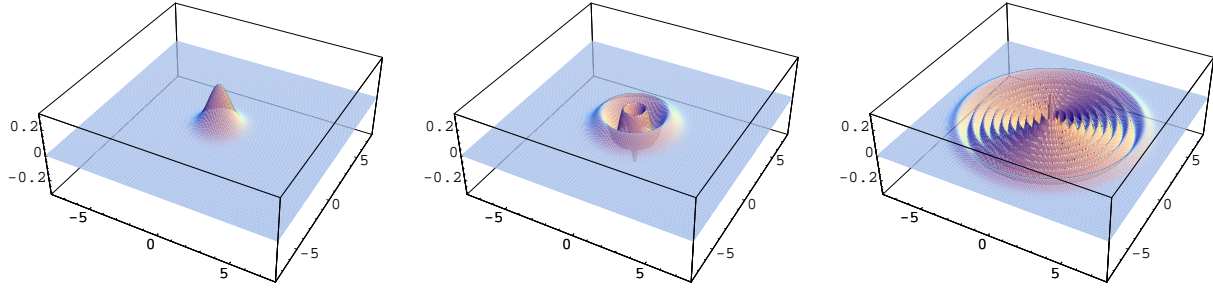


Figure 1: The Wigner function for lowest-lying quantum states of the harmonic oscillator, $n = 0$, $n = 2$ and higher level $n = 10$. The peak for $n = 0$ state is the most probable phase-space point of a particle at rest. The most probable orbit of the quantum oscillator is shown by the outermost circular orbit in phase space from the solution of classical equations of motion for the classical oscillator, see $n = 10$.

phase-space distribution and hence becomes positive definite. The Wigner quasi-probability provides an appealing opportunity to describe a quantum state using the classical concept of the phase space. The advantage of the Wigner function is that it is real and it contains complete information about the interference.

- One can calculate any dynamical quantity $\hat{\mathcal{O}}(\hat{\mathbf{r}}, \hat{\mathbf{p}})$ by performing averages of the Wigner distribution (as if it were a classical distribution) with the symbol of the operator $\mathcal{O}(\mathbf{r}, \mathbf{p})$, where the momentum and the coordinates are ordered according to the Weyl association rule [32],

$$\langle \hat{\mathcal{O}} \rangle = \int d^3\mathbf{p} d^3\mathbf{r} W(\mathbf{r}, \mathbf{p}) \mathcal{O}_{\text{Weyl}}(\mathbf{r}, \mathbf{p}). \quad (2.9)$$

- The marginal projections of the Wigner function lead to the familiar space and momentum probability densities, namely;

$$\int d^3\mathbf{p} W(\mathbf{r}, \mathbf{p}) = \rho(\mathbf{r}), \quad \int \frac{d^3\mathbf{r}}{(2\pi\hbar)^3} W(\mathbf{r}, \mathbf{p}) = n(\mathbf{p}). \quad (2.10)$$

2.1.3 Wigner distribution of a quantum oscillator

Let us illustrate the concept of the Wigner distribution using as an example the simplest system: the one-dimensional harmonic oscillator. The Wigner distribution for the n th excited state of the one-dimensional harmonic oscillator of energy $E_n = \hbar\omega (n + \frac{1}{2})$ is [33]

$$W_n(r, p) = \frac{(-1)^n}{\pi\hbar} e^{-2H/(\hbar\omega)} L_n \left(\frac{4H}{\hbar\omega} \right), \quad (2.11)$$

where H stands for the classical Hamiltonian

$$H(r, p) = \frac{p^2}{2m} + \frac{m\omega^2 r^2}{2},$$

and L_n is the n th order Laguerre polynomial. Figure 1 gives a graphical demonstration of a few lowest-order Wigner distributions.

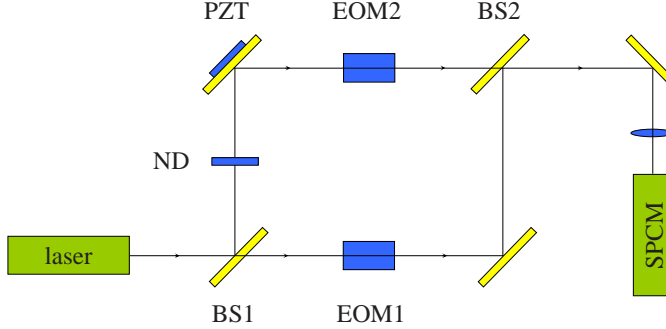


Figure 2: Mach-Zender interferometric scheme for the measurement of the quantum-mechanical Wigner distribution of a light mode. BS1 and BS2 denote the low-reflection beam splitters. The quantum state is prepared using the neutral density filter ND and a mirror mounted on a piezoelectric translator PZT. The electro-optic modulators EOM1 and EOM2 control, respectively, the amplitude and the phase of the point at which the Wigner function is measured. The signal field is focused on a single photoncounting module SPCM.

In the classical limit, the Wigner distribution is expected to become a classical phase-space distribution. For systems which are statistical ensembles, the limit $\hbar \rightarrow 0$ is often well behaved. For example, for an ensemble of harmonic oscillators at finite temperature, the Wigner distribution becomes the classical Boltzmann distribution as $\hbar \rightarrow 0$, see, e.g., [34]. For a single-particle state, discussed here, the limit is more subtle. In the quasiclassical limit—vanishing Planck constant and large quantum numbers—the Wigner distribution of the harmonic oscillator turns into a mathematical distribution which resides on classical trajectories, $E_\infty = n\hbar\omega = \text{fixed}$

$$\lim_{\hbar \rightarrow 0, n \rightarrow \infty} W_n(r, p) \sim \delta(H(r, p) - E_\infty), \quad (2.12)$$

and implies that in the quasiclassical limit most of oscillations with $H(r, p) < E_\infty$ nearly average to zero after integration with a smooth test function. This result can be easily understood from the semiclassical form of the wave function,

$$\psi(r) = C(r)e^{iS(r)/\hbar}, \quad (2.13)$$

with the classical action S . Substituting this into Eq. (2.7), reduced to the one-dimensional case, and expanding S to first order in r , one gets the quasiclassical Wigner distribution

$$W(r, p) = |C|^2 \delta \left(p - \frac{\partial S(r)}{\partial r} \right), \quad (2.14)$$

where the argument of the delta function describes a family of classical trajectories, cf. Eq. (2.12).

The Wigner function incorporates quantum mechanical effects and at the same time can be viewed as an analogue of the classical phase-space distribution, encoding the distribution of observable quantities.

2.1.4 Experimental access to Wigner distributions

The usefulness of the Wigner distribution concept from the viewpoint of phenomenological applications is driven by the possibility of its experimental measurement. To this end, one has to

be able to access the correlations of wave functions. The quantum-mechanical Wigner distribution is indeed a measurable observable. The actual measurement has been performed for a simplest physical quantum system—the quantum state of a light mode (a pulse of laser light of a given frequency)—employing ideas of Vogel and Risken [35]. It was accessed via the method of homodyne tomography [36], which is based on measuring marginal observables and subsequent reconstruction by the inverse Radon transformation (see, [37] for a review and Section 3.8.2 below). The same Wigner distribution was accessed also by a more direct measurement by means of the photon counting techniques based on a Mach-Zender interferometric scheme [38]; see Fig. 2. As we will see later in this paper, the experimental setup to measure the nucleon’s content via the concept of generalized parton distribution (GPDs) has very close resemblance of this setup.

2.2 Nucleon observables

Both marginal projections of the Wigner distribution in quantum mechanics—the charge distribution and the momentum density—have their analogues in QCD. Moreover, they share to some extent the probabilistic interpretation of their non-relativistic “cousins”, though not literally, since they are plagued by complications due to the relativistic nature of the problem and the settings where these observables are measured. In particular, exploring the internal structure of the proton or neutron two methods are conventionally used: (i) elastic reactions which measure form factors, and (ii) inelastic scattering experiments which accesses momentum distributions of nucleon’s constituents.

Both approaches are complementary, but bear similar drawbacks. The form factors do not yield direct information about the velocity of the constituents, whereas the momentum distribution does not give information on their spatial location. Quantum-mechanically, the phase structure is totally washed out as well. As we emphasized in the previous section, more complete description of the microscopic state lies in the correlation between the momentum and coordinate space distributions: information of where a particle is located and, at the same time, with what velocity it travels. However, the quantum-mechanical interpretation will be obviously affected not only by the relativistic effects we mentioned before but also by accommodation of the intrinsic interference phenomena. Nonetheless, the notion of correlated position and momentum distributions of quarks and gluons is very interesting, and it is clear that the physics of a phase-space distribution must be very rich. Let us start by reviewing in what circumstances the relativistic form factors and parton distributions survive the nonrelativistic statistical interpretation.

2.2.1 Nucleon electromagnetic form factors

In this subsection, we re-examine interpretation of electromagnetic form factors of the proton regarding intrinsic ambiguities associated with this interpretation. The electromagnetic form factors are defined by the matrix element between the nucleon states with different four-momenta of the quark electromagnetic current,

$$j^\mu(x) = \sum_{q=u,d,\dots} Q_q \bar{\psi}_q(x) \gamma^\mu \psi_q(x), \quad (2.15)$$

where the quark charges take values

$$Q_u = Q_c = \frac{2}{3}, \quad Q_d = Q_s = -\frac{1}{3}.$$

Because the nucleon is a spin one-half particle, the matrix element is parametrized by two form factors,

$$\langle p_2 | j^\mu(0) | p_1 \rangle = \bar{u}(p_2) \left\{ \gamma^\mu F_1(\Delta^2) + \frac{i\sigma^{\nu\mu}\Delta_\nu}{2M_N} F_2(\Delta^2) \right\} u(p_1), \quad (2.16)$$

known as Dirac F_1 and Pauli F_2 form factors. They depend on the momentum transfer² $\Delta = p_1 - p_2$. Our conventions for the Dirac matrices and the nucleon bispinor $u(p)$ are summarized in Appendix A.

At zero momentum transfer, the form factors are normalized to static properties of the nucleon. They can be inferred by studying the zero-recoil limit of the matrix element, $p = p_1 \rightarrow p_2$. Introducing the operators of charge and the magnetic moment at a time slice $t = 0$ (they do not change in time due to the current conservation)

$$Q \equiv \int d^3r j^0(r), \quad \boldsymbol{\mu} \equiv \int d^3r [\mathbf{r} \times \mathbf{j}(\mathbf{r})], \quad (2.17)$$

one finds the normalization

$$\frac{\langle p | Q | p \rangle}{\langle p | p \rangle} = F_1(0), \quad \frac{\langle p | \boldsymbol{\mu} | p \rangle}{\langle p | p \rangle} = \frac{\mathbf{s}}{M_N} (F_1(0) + F_2(0)), \quad (2.18)$$

where the three-vector of spin $\mathbf{s} = \frac{1}{2}w^*\boldsymbol{\sigma}w$ is expressed in terms of Weyl spinors w (see Appendix A.2). The above relation for the magnetic moment can be easily derived by introducing a Fourier transform of the matrix element of spatial current, and expanding the exponential to the linear term in the momentum transfer Δ ;

$$\int d^3r e^{-i\Delta \cdot r} \langle p_2 | \mathbf{j}(\mathbf{r}) | p_1 \rangle \approx \int d^3r (1 - i\Delta \cdot \mathbf{r}) \langle p_2 | \mathbf{j}(\mathbf{r}) | p_1 \rangle$$

Making use of the identity $(\mathbf{r} \cdot \Delta)\mathbf{j} = [[\mathbf{r} \times \mathbf{j}] \times \Delta]$ and the condition of the steady electromagnetic current $\nabla \cdot \mathbf{j} = 0$, one compares the matrix element to the expression in term of form factors to find the equality (2.18).

It was realized long ago that the physical interpretation of the nucleon form factors in terms of charge and magnetization distributions is obscured by relativistic effects [39]. Consider a system of size R and mass M . In a relativistic quantum theory, the system cannot be localized to a precision better than its Compton wavelength $1/M$ (starting from this section, we set $\hbar = 1$). As a consequence, the static size of the system cannot be defined to a precision better than $1/M$. If $R \gg 1/M$, which is the case for all nonrelativistic systems, this is not a significant constraint. One can probe the internal structure of such a system with a wavelength $\lambda \sim 1/|\Delta|$ comparable to or even much smaller than R , but still large enough compared to $1/M$ so that the probe does not induce an appreciable recoil in the test system. A familiar example is the hydrogen atom for which $R_{\text{atom}} M_{\text{atom}} \sim M_{\text{atom}}/(m_e \alpha_{\text{em}}) \sim 10^5$, and the form factor can be measured through electron scattering with momentum transfer $|\Delta| \ll M_{\text{atom}}$.

²Usually, a convention with the opposite sign is used for the momentum transfer in form factor definitions, $\Delta = p_2 - p_1$. The motivation is clear: the initial hadron gets the momentum transfer $p_2 - p_1$ from the electron. However, the most important class of physical processes involving GPDs is deeply virtual photon or meson electroproduction, in which a spacelike virtual photon converts into a real photon or a meson, requiring a positive energy transfer $E_1 - E_2$ from the initial hadron to the virtual photon. To avoid writing *positive* quantities as *minus negative* ones, we will stick to the convention $\Delta = p_1 - p_2$ throughout the paper.

When the probing wavelength is comparable to $1/M$, the form factors are no longer determined by the internal structure alone. They also contain the dynamical effects of Lorentz boosts because the initial and final nucleons have different momenta due to non-negligible recoil. In a relativistic quantum theory, the boost operators involve nontrivial dynamical effects which result in the nucleon wave function being different in different frames (in the instant form of quantization). Therefore in the region $|\Delta| \sim M$, the physical interpretation of form factors is complicated because of the entanglement of the internal and the center-of-mass motion in relativistic dynamics. In the limit $|\Delta| \gg M$, form factors depend crucially on the physical mechanism producing the overall change of the nucleon momentum. The structural effect involved is a very small part of the total nucleon wave function since it corresponds to a few lowest Fock states only.

For the nucleon, $M_N R_N \sim 4$. Although much less certain than in the case of the hydrogen atom, it still seems sensible to have a rest-frame picture for the electromagnetic form factors, as long as one keeps in mind that equally justified definitions of the nucleon sizes can differ by the effects of order $1/M_N(R_N M_N)$. The form factors at $|\Delta| \geq M_N \sim 1 \text{ GeV}$ cannot be interpreted solely as information gained about the internal structure of the nucleon.

To further clarify the uncertainty involved in the interpretation of the electromagnetic form factors, let us review an explanation offered originally by Sachs [40] and recently re-examined in Ref. [41].

2.2.2 Form factors in the Breit frame and charge distributions

To establish the notion of a (charge) distribution, one needs to create a wave packet representing a static nucleon localized at \mathbf{R} ,

$$|\mathbf{R}\rangle = \int \frac{d^3\mathbf{p}}{(2\pi)^3} e^{i\mathbf{p}\cdot\mathbf{R}} \Psi(\mathbf{p}) |\mathbf{p}\rangle, \quad (2.19)$$

where $\Psi(\mathbf{p})$ is the momentum space profile. The plane wave state $|\mathbf{p}\rangle$ is normalized in a relativistic-invariant manner, as defined in Appendix A, so that

$$\int \frac{d^3\mathbf{p}}{(2\pi)^3} (2E_{\mathbf{p}}) |\Psi(\mathbf{p})|^2 = 1$$

in order to have $\langle \mathbf{R} | \mathbf{R} \rangle = 1$. The wave packet Ψ is not an eigenstate of the free Hamiltonian. Therefore, as time progresses, the wave packet will spread. The characteristic dispersion time is proportional to

$$t_{\text{char}} \sim \int d^3\mathbf{p} (M_N/\mathbf{p}^2) |\Psi(\mathbf{p})|^2.$$

It is long for a nonrelativistic system. But for a relativistic particle, the spread could happen much faster compared to the characteristic time scale of a weakly-interacting probe. The actual form of the wave packet profile, however, does not matter since we want to capture structural information of the particle itself and not of the auxiliary wave packet.

Having localized the wave packet at $\mathbf{R} = 0$, we can use Eq. (2.19) to calculate, for example, the charge distribution in the wave packet,

$$\rho(\mathbf{r}) = \langle \mathbf{R} = 0 | j^0(\mathbf{r}) | \mathbf{R} = 0 \rangle, \quad (2.20)$$

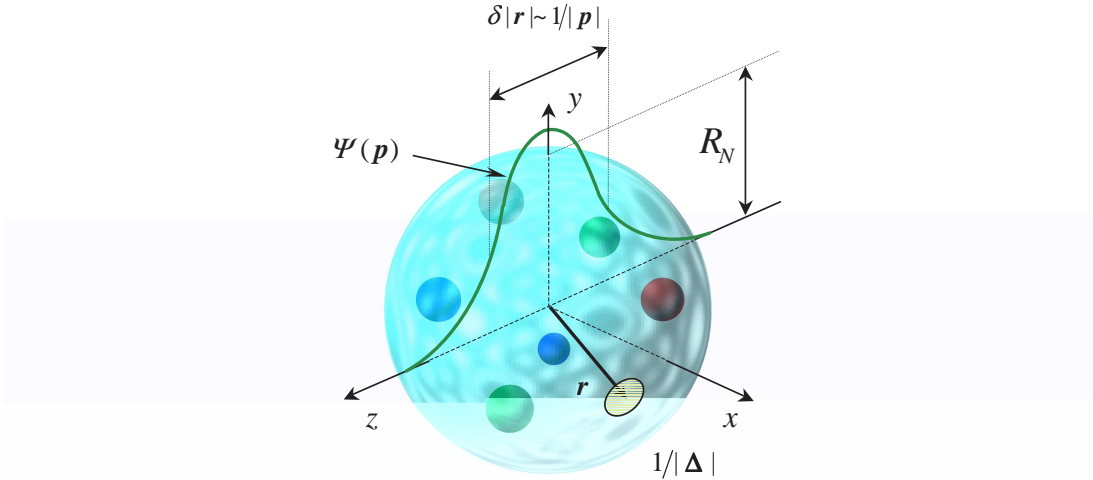


Figure 3: Localization of the nucleon with a wave packet.

where \mathbf{r} measures the relative distance to the center, $\mathbf{R} = 0$, see Fig. 3. Taking its Fourier transform, one gets

$$\begin{aligned} F(\Delta) &\equiv \int d^3\mathbf{r} e^{-i\Delta \cdot \mathbf{r}} \rho(\mathbf{r}) \\ &= \int \frac{d^3\mathbf{p}}{(2\pi)^3} \Psi^*(\mathbf{p} - \frac{1}{2}\Delta) \Psi(\mathbf{p} + \frac{1}{2}\Delta) \langle \mathbf{p} - \frac{1}{2}\Delta | j^0(0) | \mathbf{p} + \frac{1}{2}\Delta \rangle , \end{aligned} \quad (2.21)$$

where we have changed the momentum integration variables, with \mathbf{p} representing now the average momentum of the initial and final nucleons. It is important to emphasize that the resolution momentum Δ is now linked to the difference in the initial and final state momenta. In non-relativistic quantum systems, because of large masses involved, the momentum transfer causes little disturbance in velocity, and hence the initial and final states have practically the same internal wave functions. In relativistic systems, this is the origin of the difficulty in interpreting the form factor: we do not have a matrix element involving the same nucleon state before and after the interaction.

To have a situation free from ambiguities, several conditions have to be imposed on momenta to avoid dangerous regions where the interpretation can be affected by relativity, wave nature of the microscopic objects or the wave packet used for the localization. Namely (see Fig. 3):

- To remove the effects of the wave packet, the necessary condition on $\Psi(\mathbf{p})$ is that the coordinate-space size of the wave packet must be much smaller than the size of the test system, the nucleon,

$$\delta|\mathbf{r}| \ll R_N .$$

- The probing wavelength, or the resolution scale, must be large compared with the size of the wave packet, since one is not interested in details of the wave packet itself:

$$\delta|\mathbf{r}| \ll 1/|\Delta| .$$

- The size of the wave packet must be larger than the Compton wavelength of the proton so as to be insensitive to the wave nature of the proton. This results in

$$\delta|\mathbf{r}| \gg 1/M_N .$$

The corresponding restriction on momenta allowed in the wave packet is $|\mathbf{p}| \ll M_N$.

Therefore, the combined constraint on the wave packet profile is

$$1/R_N \ll |\Delta| \ll |\mathbf{p}| \ll M_N , \quad (2.22)$$

where the size of the wave packet is $\delta|\mathbf{r}| \sim 1/|\mathbf{p}|$. It is easy to see that the available window in the case of the proton is very narrow since $R_N M_N \sim 1/4$.

The first two conditions allow us to ignore the Δ dependence in Ψ so that $\Psi(\mathbf{p} \pm \frac{1}{2}\Delta) \approx \Psi(\mathbf{p})$ and, therefore,

$$F(\Delta) = \int \frac{d^3\mathbf{p}}{(2\pi)^3} |\Psi(\mathbf{p})|^2 \langle \mathbf{p} - \frac{1}{2}\Delta | j_0(0) | \mathbf{p} + \frac{1}{2}\Delta \rangle . \quad (2.23)$$

The extreme limit of the last inequality in Eq. (2.22) yields a wave packet with a zero-momentum nucleon

$$|\Psi(\mathbf{p})|^2 = \frac{(2\pi)^3}{2M_N} \delta^{(3)}(\mathbf{p}) . \quad (2.24)$$

Thus, one gets,

$$2M_N F(\Delta) = \langle -\frac{1}{2}\Delta | j_0(0) | \frac{1}{2}\Delta \rangle . \quad (2.25)$$

This is the matrix element of the charge density in the Breit frame. The latter has a unique property of the absence of the energy transfer from the incoming to the outgoing nucleons, so that the hadronic four-momenta read

$$p_1 = (E, \frac{1}{2}\Delta) , \quad p_2 = (E, -\frac{1}{2}\Delta) . \quad (2.26)$$

Thus the form factor (2.25) is related (up to a factor) to the Sachs electric form factor as

$$F(\Delta) = G_E(-\Delta^2) w_2^* w_1$$

which is a superposition of the Dirac and Pauli form factors

$$G_E(-\Delta^2) = F_1(-\Delta^2) - \frac{\Delta^2}{4M_N^2} F_2(-\Delta^2) . \quad (2.27)$$

The Weyl spinors w_2^* , w_1 are the remnants of the Dirac bispinors. Hence, we arrive at a textbook interpretation of G_E as a Fourier transform of the nucleon charge distribution normalized to the electric charge (2.18). Likewise, the magnetic form factor G_M is a Fourier transform of the magnetization distribution

$$\langle -\frac{1}{2}\Delta | \mathbf{j}(0) | \frac{1}{2}\Delta \rangle = 2i[\Delta \times \mathbf{s}] G_M(-\Delta^2) , \quad (2.28)$$

where

$$G_M(-\Delta^2) = F_1(-\Delta^2) + F_2(-\Delta^2) . \quad (2.29)$$

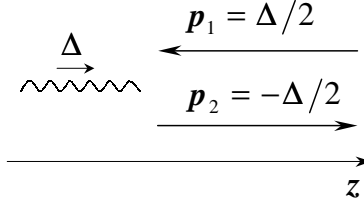


Figure 4: Breit frame for the $\gamma^* p \rightarrow p'$ process.

Several times throughout our discussion we quoted the proton radius. What was meant by this is the root-mean-square radius, defined as

$$R_N^2 = \langle \mathbf{r}^2 \rangle_E \equiv \int d^3\mathbf{r} \mathbf{r}^2 \rho(\mathbf{r}) = -6 \frac{\partial G_E(-\Delta^2)}{\partial \Delta^2}, \quad (2.30)$$

and related to the slope of the electric form factor G_E . In the literature, one can find other definitions of the proton charge radius, for instance, $\langle \mathbf{r}^2 \rangle_D$, which is related to the slope of the Dirac form factor F_1 , rather than G_E .

The helicity of the proton is well defined in the Breit frame since the incoming and outgoing particles' momenta are collinear to the same direction. In this reference frame, the helicity non-flip transition is determined by the electric form factor G_E , while the helicity-flip transition is determined by the magnetic one, G_M . Of course, these assignments are frame dependent since by a Lorentz boost one can reverse the direction of the proton motion and thus changes the sign of proton's helicity.

As we already emphasized before, the exceptional role of the Breit frame is the absence of the energy exchange, distinguishing this unique frame by the possibility of an unambiguous definition of the spatial Fourier transform of the transition matrix elements of the electromagnetic current. Of course, charge and magnetization distributions defined in such a way are not equivalent to the rest-frame densities. This is due to the presence of the Lorentz contraction effects along the direction Δ when $\Delta^2 \gg 4M_N^2$, which makes the nucleon look like a pancake. If one attempts to compute a form factor boosted to the rest frame of the nucleon, the Lorentz transformation tends to cut off its the momentum dependence at high momentum transfer [42] so that one effectively finds $F(\Delta^2) \rightarrow F(\Delta^2/\sqrt{1 - \Delta^2/4M_N^2})$. However, the procedure is not unique and thus it merely results in yet another definition of what one means by the charge distribution. Several types of prescriptions for extracting the static charge distributions from available data on form factors have been used in recent analyses (see [43]). Another physically-motivated approach is to find a relation between the Fourier transform of a static charge density and the form factor of a model obtained by boosting the wave function. For instance, one can obtain such relations in the context of the Skyrme model [44]. Different models lead to relations which differ by corrections of order $1/M_N$.

As we will establish later in Sect. 3.10.1, relativistic corrections and Lorentz contraction effects are found to disappear in the infinite momentum frame. In this frame, the nucleon has an infinitely large effective mass; hence, for physics in the transverse dimensions, we are back to the nonrelativistic case. In particular, one can localize the nucleon in the transverse coordinate space with no recoil corrections at all. The Dirac form factor F_1 is found to be related to the charge

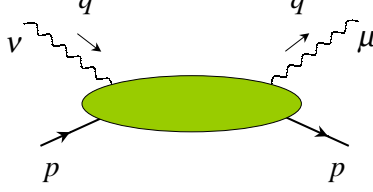


Figure 5: Hadronic tensor of deep inelastic scattering cross section determining the imaginary part of the forward Compton scattering amplitude $\gamma^*(q)N(p) \rightarrow \gamma^*(q)N(p)$.

distribution in transverse plane, with information along the longitudinal z -direction integrated out. The price one pays for eliminating the relativistic corrections is one spatial dimension.

2.2.3 Nucleon structure functions

Let us discuss now the observables probing the nucleon content through inelastic processes, namely, the lepton-hadron deeply inelastic scattering. Right before the incoming lepton hits the target, it fluctuates into a lepton and a photon, $e(k) \rightarrow e(k')\gamma^*(q)$; the latter interacts with the target $|p\rangle$ fragmenting into a number of hadrons in the final state $|n\rangle$ with the total momentum $P_n = \sum_{k=1}^N p_k$. Since the electromagnetism is very weak compared to strong interactions involved in the reaction dynamics, one can restrict the analysis to a single-photon exchange.

The amplitude of this process is described by the current-to-current coupling,

$$\mathcal{A}_n = L_\mu(k, k') \langle n | j^\mu(0) | p \rangle , \quad (2.31)$$

of the hadronic transition amplitude $\langle n | j_\mu | p \rangle$ via the local quark electromagnetic current (2.15) and the leptonic current

$$L^\mu(k, k') = \frac{i}{q^2} \bar{u}(k') \gamma^\mu u(k) .$$

The measurement is totally inclusive with respect to the final states and only the scattered lepton is detected. Neglecting the phase-space factor, the cross section reads:

$$\sigma_{\text{DIS}} = \frac{\alpha_{\text{em}}^2}{4\pi} \sum_n |\mathcal{A}_n|^2 (2\pi)^4 \delta^{(4)}(p + q - P_n) = \frac{\alpha_{\text{em}}^2}{q^4} L_\mu^\dagger L_\nu W^{\mu\nu} , \quad (2.32)$$

where, using the completeness condition (A.49) in summation over the final states, we introduce the hadronic tensor

$$W^{\mu\nu} = \frac{1}{4\pi} \int d^4 z e^{iq \cdot z} \langle p | j^\mu(z) j^\nu(0) | p \rangle , \quad (2.33)$$

represented diagrammatically in Fig. 5 with the shown assignments of indices and particle's momenta.

The decomposition of the hadronic tensor in independent Lorentz tensors introduces the structure functions. For the spin one-half target the most general form of $W^{\mu\nu}$ reads

$$\begin{aligned} W^{\mu\nu} = & - \left(g^{\mu\nu} - \frac{q^\mu q^\nu}{q^2} \right) F_1(x_B, Q^2) + \frac{1}{p \cdot q} \left(p^\mu - \frac{p \cdot q}{q^2} q^\mu \right) \left(p^\nu - \frac{p \cdot q}{q^2} q^\nu \right) F_2(x_B, Q^2) \\ & - \frac{i}{p \cdot q} \varepsilon^{\mu\nu\rho\sigma} q_\rho s_\sigma g_1(x_B, Q^2) - \frac{i}{p \cdot q} \varepsilon^{\mu\nu\rho\sigma} q_\rho \left(s_\sigma - \frac{s \cdot q}{p \cdot q} p_\sigma \right) g_2(x_B, Q^2) . \end{aligned} \quad (2.34)$$

The un- and polarized structure functions F_i and g_i , respectively, depend on two variables: space-like momentum of the probe and the Bjorken variable,

$$q^2 \equiv -Q^2, \quad x_B \equiv \frac{Q^2}{2p \cdot q}. \quad (2.35)$$

The hadronic tensor is related via the optical theorem—analogous to that discussed in the Appendix C for the case of the vacuum expectation value of two electromagnetic currents—to the imaginary part

$$W^{\mu\nu} = \frac{1}{2\pi} \Im m T^{\mu\nu}, \quad (2.36)$$

of the forward Compton scattering amplitude

$$T^{\mu\nu} = i \int d^4z e^{iq \cdot z} \langle p | T \{ j^\mu(z) j^\nu(0) \} | p \rangle, \quad (2.37)$$

determined by the chronological product of quark electromagnetic currents (2.15).

In the deeply inelastic reaction, the photon interacting with the target acts as a probe. The resolution is set by the inverse of the photon virtuality Q^2 . Thus, the nucleon is probed with the resolution $\approx (0.2 \text{ fm})/(Q \text{ in GeV})$. Since the nucleon's size is $R_N \sim 1 \text{ fm}$, one concludes that for Q^2 of order of a few GeV^2 , the photon penetrates the nucleon interior and interacts with its constituents. This is the regime which initiates a hard scattering: the electron has to pass close to one of the partons, i.e., at the distance $z^2 \sim 1/Q^2$, to exchange a photon of virtuality Q^2 . The structure functions have a very important property of scaling, i.e., Q^2 -independence, in the Bjorken limit;

$$Q^2 \rightarrow \infty, \quad x_B = \text{fixed}.$$

Analogous kinematical conditions will be imposed on other reactions discussed in the present review which warrant the light-cone distance dominance in scattering amplitudes and, hence, legitimate the application of powerful methods of perturbative QCD.

2.2.4 Infrared safety

Let us study the question whether the hadronic tensor is indeed sensitive to the structural information about the nucleon. The argument is generic and does not rely on the details of the interaction [45]; we have only to keep in mind that the QCD coupling constant is growing at large space-time scales. Thus we replace QCD perturbation theory with a quantum-mechanical one applying it to the Schrödinger equation with a scattering potential V (Eq. (2.5)). The solution of this equation will be expressed in terms of asymptotic states at the infinite past where the interaction is switched off adiabatically. The free-particle equation, $V = 0$, gives

$$\psi_0(t) = \exp(-itE_m)|\omega_m\rangle$$

with the stationary states which form a complete basis $\sum_m |\omega_m\rangle\langle\omega_m| = 1$. The solution of the full equation is expanded in free-particle states at the time t ,

$$\psi(t) = \sum_m |\omega_m\rangle S_m. \quad (2.38)$$

S_m is the evolution operator of the system from the unperturbed state $\psi(-\infty) = |\omega_0\rangle$, where $V(-\infty) = 0$, to an observed state $|\omega_m\rangle$ at the time t via a successive sequence of interactions and the free propagation through intermediate states.

$$S_m = \int_{-\infty}^{\infty} d\tau_m e^{-i(E_{m-1}-E_m)\tau_m} V_{m-1} \int_{-\infty}^{\tau_m} d\tau_{m-1} e^{-i(E_{m-2}-E_{m-1})\tau_{m-1}} V_{m-2} \dots V_1 \int_{-\infty}^{\tau_2} d\tau_1 e^{-i(E_0-E_1)\tau_2}. \quad (2.39)$$

The summation in repeated indices runs over states which are eigenfunctions of the free equations of motion, $V_m = \langle m|V|m\rangle$ is a matrix element of a perturbation—the interaction potential—between the states corresponding to free particle propagation. The combined phase of the exponentials

$$\text{phase} = \sum_{n=1}^m E_n(\tau_n - \tau_{n-1}).$$

is the free particle action: recall that $S = -\int d\tau H$. At this point, one immediately concludes:

- As long as the total phase—the free particle action—is time dependent, there is no sensitivity to long-time scales where the coupling constant grows. In this case, cancellations of long-time contributions occur due to the oscillatory nature of the integrand.
- However, if the phase is stationary, which corresponds to a stationary classical action, particles travel along their classical trajectories and the amplitude becomes sensitive to large-time dynamics.

Since α_s is large at large space-time scales, one cannot reliably evaluate the amplitude using the perturbative expansion, and the effects of quark confinement are relevant. In the opposite situation, called “the infrared safety” the quark confinement is not relevant, and the amplitude can be computed from the perturbation theory alone to the leading power accuracy in the momentum transfer q^μ . This gives an intuitive illustration of the Coleman-Norton theorem [46], which is an essential part in all the proofs of factorization theorems in QCD. Within the field-theoretical framework, the above intuitive argument can be presented in a more rigorous fashion in the form of the Landau equations for singularities of Feynman graphs.

However, there is only a very limited number of completely infrared safe quantities. They include the hadronic width of the electroweak Z -boson, jet and total inclusive cross sections in the electron-positron annihilation into hadrons $e^+e^- \rightarrow X$ [29]. In the latter case one has

$$\sigma_{\text{tot}}(q^2) = \frac{1}{2\pi} \sum_n \langle 0 | j_\mu(0) | n \rangle \langle n | j^\mu(0) | 0 \rangle (2\pi)^4 \delta^{(4)} \left(\sum_i^n p_i - q \right), \quad (2.40)$$

where the summation is performed with respect to the n -particle final states having the total momentum $\sum_i^n p_i$. The cross section (2.40) is expressed, according to the optical theorem (see Appendix C), in terms of the absorptive part of the vacuum polarization by

$$\sigma_{\text{tot}}(q^2) = \frac{1}{\pi} \Im m i \int d^4 z e^{iq \cdot z} \langle 0 | T \{ j_\mu(z) j^\mu(0) \} | 0 \rangle, \quad (2.41)$$

The argument given above suggests that this quantity will be infrared safe. Indeed, once the pair of quark and antiquark is created by the source j_μ , they travel back-to-back with the speed

of light in the opposite directions and cannot reassemble into a physical state absorbed by the $j_\mu^\dagger = j^\mu$. Since there are no classical trajectories which would allow this process, the observable is not sensitive to the infrared physics.

The discussion of the vacuum polarization in Minkowski space is complicated by its non-analytic behavior in the form of branch cuts in q^2 . They correspond to the production thresholds of hadrons. On the other hand, the QCD description involves quarks and gluons which are produced and propagate to infinite distances. Of course, there is an implicit assumption here that the latter will inevitably fragment into hadrons. A reliable theoretical evaluation can be done only for the q^2 values away from the production of physical states. To achieve this one has to use the dispersion relation which is the crucial element of the optical theorem. Making the Wick rotation and going to Euclidean space $-q^2 = Q^2$ gives

$$i \int d^4 z e^{iq \cdot z} \langle 0 | T \{ j_\mu(z) j^\mu(0) \} | 0 \rangle = \int_0^\infty dM^2 \frac{\sigma_{\text{tot}}(M^2)}{Q^2 + M^2}, \quad (2.42)$$

where the left-hand side is now an analytic function of Q^2 . In the deep Euclidean region, $Q_\mu \rightarrow \infty$, the distances probed in the current correlator are very small, $z^\mu \rightarrow 0$, due to the Heisenberg uncertainty principle, so one can safely use the QCD perturbation theory. When the virtualities are not asymptotically large, one should include power corrections using the local operator product expansion in short-distance singularities:

$$j_\mu(z) j^\mu(0) = C_0(z^2) \mathbb{1} + \sum_d C_d(z^2) \mathcal{O}_d(0), \quad (2.43)$$

where the first term is a purely perturbative contribution and the sum runs over dimension- d local operators. For example, in the massless case the lowest operator is $\mathcal{O}_4(0) = F_{\mu\nu}^a(0) F_a^{\mu\nu}(0)$. After the Fourier transformation, this series is translated into the power series expansion in $1/Q^2$. Matching both sides in Eq. (2.42) one finds that the weighted integral of the physical cross section $\sigma_{\text{tot}}(q^2)$ is related to the quantities computed using the partonic language. Therefore, the integral over the physical resonance spectrum corresponds to the integrals over the quark continuum. This is the idea of the quark-hadron duality which states that the physical cross section coincides in average with the partonic one.

The hadronic tensor, discussed in the previous section in relation to deeply inelastic scattering, has a more complicated structure than the total e^+e^- to hadrons cross section. The question is whether it can be expressed through the same chronological product of two electromagnetic currents, albeit, in different matrix elements? This is considered in the next section.

2.2.5 Incoherence and scale separation

A hard scattering cross section having at least one hadron in the initial state (like the deeply inelastic scattering cross section) cannot be infrared safe since in the preparation of the asymptotic hadron state its constituents have strongly interacted among themselves for a long time in a bound state. Obviously, the wave functions of quarks in a bound state differs from what it would be if they were free, and this difference inevitably affects the cross section.

Since the number of partons that carry the bulk of the hadron momentum is small, the photon usually will “see” only one parton per collision. The probability for coherent scattering on an n -parton configuration is suppressed by n th power of the photon virtuality,

$$\mathcal{P}_n \sim \left(\frac{|\delta \mathbf{z}_\perp|^2}{\pi R_N^2} \right)^n \sim \frac{1}{(Q^2 \pi R_N^2)^n}, \quad (2.44)$$

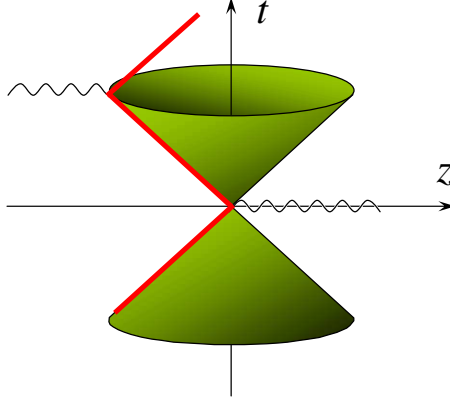


Figure 6: Pinch surface: space-time trajectory of the struck quark in the hadron.

where πR_N^2 is the transverse area of the nucleon. These power-suppressed corrections go under the name of higher twists. Thus, in leading approximation at high Q^2 one can restrict all considerations to the photon scattering on a single parton. This is known as handbag approximation. Compared to the inclusive annihilation mentioned above, the underlying physical picture for the forward Compton scattering on a quark admits a classical trajectory, see Fig. 6. A quark taken from the hadron absorbs the virtual photon at $t = 0$ and, as a result, accelerates. Then it re-emits a photon at later $t > 0$ and falls in the same momentum state. After the energy is freed into the final state the parton merges back into the parent hadron. As we already discussed above, the process is not infrared safe and depends on the quark binding inside the nucleon. The points of absorption and emission are separated by a light-like distance. The character of relevant distances in the Compton amplitude is a consequence of deep Euclidean kinematics, $Q^2 \rightarrow \infty$. Large virtualities, Q^2 , and energies, $\nu \equiv p \cdot q$, at fixed Bjorken variable x_B , probe short-distance and time structure of the process, respectively. To derive the relevant distances in deeply inelastic scattering, let us switch to a reference frame where the target proton is at rest and the virtual photon's three-momentum points in the direction opposite to the z -axis. Then

$$q^\mu = \left(\frac{Q^2}{2Mx_B}, 0, 0, -\frac{Q^2}{2Mx_B} \sqrt{1 + 4M^2x_B^2/Q^2} \right). \quad (2.45)$$

When Q^2 is large, the light-cone components of the momentum transfer (see Appendix B for conventions) can be approximated by

$$q^- \sim Q^2 / (Mx_B), \quad q^+ \sim Mx_B. \quad (2.46)$$

The integrand in Eq. (2.32) is an oscillatory function and thus gives vanishing result unless the distances involved are

$$z^- \sim 1 / (Mx_B), \quad z^+ \sim Mx_B / Q^2. \quad (2.47)$$

Therefore, provided transverse separations z_\perp are small, the deeply inelastic scattering probes strong interaction dynamics close to the light-cone $z^2 \approx 0$, and we can neglect the dependence on all coordinate components except for z^- . The latter is called the Ioffe time [47] and has the meaning of the longitudinal distance probed in the process. Its Fourier conjugate variable is the fraction x of the nucleon momentum carried by a parton interacting with the probe. In the lowest order approximation, $x = x_B$.

The hard subprocess occupies a very small space-time volume. On the other hand, the scales involved in the formation of the hadron nonperturbative wave function are much larger, of order of a typical hadronic scale, 1 GeV. Hence, it is quite likely that the two scales are uncorrelated and will not interfere. Thus, although the process depends on the hadronic state from which a given constituent has come, this is basically irrelevant for the hard interactions. Moreover, all final state interactions cancel in the deeply inelastic process. This is exhibited by the relation (2.32) following from the optical theorem. Thus, there is no sensitivity to the soft final-state interaction and all information about long-distance physics is encoded into a function which reflects the internal structure of the proton, the so-called quark (gluon) distribution. The quantum mechanical incoherence property of physics at different scales results in the factorization property of the structure functions (2.34)

$$F_i(x_B, Q^2) = \int_{x_B}^1 \frac{dx}{x} C_i(x_B/x, Q^2/\mu^2) q(x; \mu^2). \quad (2.48)$$

Here q is the quark distribution, which depends on the momentum fraction x of the parent proton, and C is a perturbatively computable short-distance quark-photon cross section. This is the basis for the predictive power of perturbative QCD.

The factorized expression for the structure functions has several fundamental properties. The parton distributions are universal objects and connect otherwise unrelated processes, like deeply inelastic scattering and Drell-Yan production of lepton pairs in proton-proton collisions $pp \rightarrow \ell^+ \ell^- X$, etc. Second, the formula implies that the momentum scale dependence of leading term in $1/Q^2$ expansion can be computed from first principles. This will be the subject of Section 4.

2.2.6 QCD parton distributions

Let us establish now the operator content of QCD parton distributions. The starting point of the analysis is the expression (2.33) for the hadronic tensor. Inserting the complete set of hadronic states, $\sum_n |n\rangle\langle n| = 1$, in the form (A.50), with a state $|n\rangle$ consisting of n particles with the total momentum $P_n = \sum_{k=1}^n p_k$ and certain quantum numbers, one gets

$$W^{\mu\nu} = \frac{1}{4\pi} \sum_n \int \prod_{k=1}^n \frac{d^3 p_k}{2E_{p_k}(2\pi)^3} (2\pi)^4 \delta^{(4)} \left(\sum_{l=1}^n p_l - p - q \right) \langle p | j^\mu(0) | p_1, \dots, p_n \rangle \langle p_1, \dots, p_n | j^\nu(0) | p \rangle, \quad (2.49)$$

where the summation over n implies the summation over the multiplicity and quantum numbers of particles populating the final state. For the photon scattering on a single parton with momentum ℓ , we separate the final state into the current fragmentation and the target fragmentation regions. The first one consists of an outgoing struck quark which forms a jet with momentum p_J and the second one is formed by target spectators with momentum $P_{\bar{n}}$, $P_n = p_J + P_{\bar{n}}$. The tree scattering amplitude corresponding to Fig. 7 (a) is given by

$$\langle p_J, \bar{n} | j^\nu(0) | p \rangle_{(0)} = \bar{u}(p_J) \gamma^\nu \langle \bar{n} | \psi(0) | p \rangle, \quad (2.50)$$

where \bar{u} is the Dirac spinor of the scattered quark. Substituting Eq. (2.50) into (2.49) we get the structure function $F_1(x_B, Q^2)$:

$$F_1(x_B, Q^2) = \frac{1}{2} \int^{Q^2} d^2 \mathbf{k}_\perp f^q(x_B, \mathbf{k}_\perp) \quad (2.51)$$

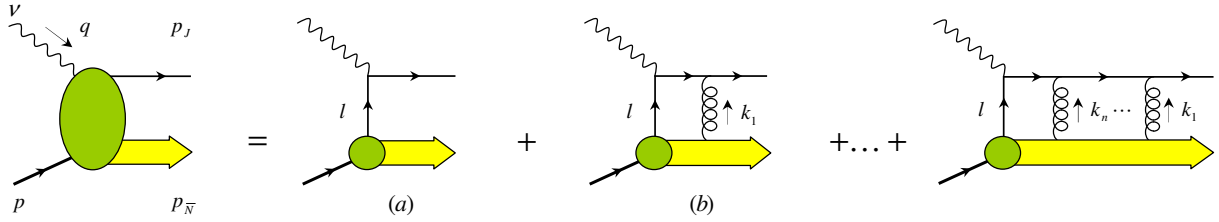


Figure 7: Multi-gluon attachments to the struck quark in deeply inelastic scattering which factorize to form the path-ordered exponential.

$$= \frac{1}{4} \int^{Q^2} d^2 \mathbf{k}_\perp \int \frac{dz^-}{2\pi} \frac{d^2 \mathbf{z}_\perp}{(2\pi)^2} e^{ix_B p^+ z^- - i \mathbf{k}_\perp \cdot \mathbf{z}_\perp} \langle p | \bar{\psi}(0, \mathbf{0}) \gamma^+ \psi(z^-, \mathbf{z}_\perp) | p \rangle .$$

Here, $f^q(x_B, \mathbf{k}_\perp)$ is the transverse momentum-dependent parton distribution in the tree-level approximation, with $xp^+ n^{*\mu}$ and k_\perp^μ being the light-cone and transverse components of the quark momentum k^μ ,

$$k^\mu \approx xp^+ n^{*\mu} + k_\perp^\mu ,$$

as explained in Appendix B. Note, that the parton distribution (2.51) is not gauge invariant as it stands, since the quark fields are not at the same space-time point.

The gauge invariance of the parton distributions is restored after one performs resummation over the multiple rescatterings of the observed final state jet with the target fragments [48, 49, 50], see Fig. 7. It is sufficient to consider the contribution from a single-gluon exchange in Fig. 7 (b). It involves all the subtleties, the all-order result being a straightforward generalization. The one-gluon amplitude is given by

$$\langle p_J, \bar{n} | j^\nu(0) | p \rangle_{(1)} = g \bar{u}(p_J) \int \frac{d^4 k_1}{(2\pi)^4} \langle \bar{n} | \mathcal{A}(k_1) S(p_J - k_1) \gamma^\nu \psi(0) | p \rangle , \quad (2.52)$$

with the free quark propagator $S(k)$. It is convenient to use now a frame similar to the Drell-Yan frame defined in Appendix B.3. By looking at the light-cone expansion of the quark propagator

$$S(p_J - k) \approx - \frac{p_J^- \gamma^+ + \mathbf{k}_\perp}{2p_J^- k^+ + \mathbf{k}_\perp^2 - i0} , \quad (2.53)$$

one immediately notices that the scaling contribution in the Bjorken limit $p_{J-} \rightarrow \infty$ arises actually from two regions rather than one. They correspond to

- the extraction of the large p_J^- component both from the numerator and the denominator (usually only this term is considered);
- scaling terms surviving the limit $k^+ \rightarrow 0$ before p_J^- is sent to infinity.

Obviously, the latter contribution is anomalous. Thus, we find for the amplitude of the one-gluon exchange [50],

$$\begin{aligned} \bar{u}(p_J) \langle \bar{n} | \mathcal{A}(k) S(p_J - k) \gamma_\nu \psi(0) | p \rangle &\approx - \frac{1}{k^+ - i0} \bar{u}(p_J) \gamma_\nu \langle \bar{n} | A^+(k_1) \psi(0) | p \rangle \\ &+ \bar{u}(p_J) \frac{\gamma_\perp^\alpha \mathbf{k}_\perp \gamma_\nu}{\mathbf{k}_\perp^2 - i0} \langle \bar{n} | \mathbf{A}_\perp^\alpha(k^+ = 0, \mathbf{k}_\perp) \psi(0) | p \rangle . \end{aligned} \quad (2.54)$$

The first term comes from the expansion of the eikonal phase acquired by a fast-propagating charge [51, 52, 53]. The second term is something else. Its Fourier transform sets the argument of the gauge field at $z^- = \infty$ [50]. To see the effect of this term we make use of the following representation of the transverse field [54]

$$\mathbf{A}_\perp^\alpha(\infty, \mathbf{z}_\perp) = -\nabla_\perp^\alpha \int_{\mathbf{z}_\perp}^\infty d\mathbf{z}'_\perp \cdot \mathbf{A}_\perp(\infty, \mathbf{z}'_\perp), \quad (2.55)$$

with $\nabla_\perp^\alpha = \partial/\partial z_\perp^\alpha$. The Fourier transform acquires a factor of transverse momentum $\nabla_\perp^\alpha \rightarrow i\mathbf{k}_\perp^\alpha$, and one sees that the transverse propagator cancels and only the contour integral of the gauge field in the transverse direction is left. Resumming to all orders, one finds the complete result for the amplitude [50]:

$$\langle p_J, \bar{n}|j^\nu(z)|p\rangle = \bar{u}(p_J)\gamma^\nu \langle \bar{n}|\Psi_\infty(z_-, \mathbf{z}_\perp)|p\rangle, \quad (2.56)$$

where we introduced a “gauge-invariant” quark field Ψ_∞ . Compared to the elementary quark field, it is augmented by the gauge links attached to it,

$$\Psi_\infty(z_-, \mathbf{z}_\perp) \equiv [\infty, \infty; \infty, \mathbf{z}_\perp][\infty, \mathbf{z}_\perp; z^-, \mathbf{z}_\perp] \psi(z_-, \mathbf{z}_\perp). \quad (2.57)$$

One gauge link runs along the light cone

$$[\infty, \mathbf{z}_\perp; z^-, \mathbf{z}_\perp] = P \exp \left(ig \int_{z^-}^\infty dz'^- A^+(z'^-, \mathbf{z}_\perp) \right), \quad (2.58)$$

and then the integration path continues in the transverse direction producing another gauge link

$$[\infty, \infty; \infty, \mathbf{z}_\perp] = P \exp \left(-ig \int_{\mathbf{z}_\perp}^\infty d\mathbf{z}'_\perp \cdot \mathbf{A}_\perp(\infty, \mathbf{z}'_\perp) \right). \quad (2.59)$$

Multiplying (2.56) by its complex conjugate, we obtain the expression for the gauge invariant transverse momentum-dependent parton distribution [50]

$$f^q(x, \mathbf{k}_\perp) = \frac{1}{2} \int \frac{dz^-}{2\pi} \frac{d^2 \mathbf{z}}{(2\pi)^2} e^{ixp^+ z^- - i\mathbf{k}_\perp \cdot \mathbf{z}_\perp} \langle p | \bar{\Psi}_\infty(0, \mathbf{0}) \gamma^+ \Psi_\infty(z^-, \mathbf{z}_\perp) | p \rangle. \quad (2.60)$$

If there is an initial rather than the final state interaction, the direction of the Wilson lines is changed: they come from the past to the interaction point. Hence, in a generic situation, the quark field entering the distribution

$$\Psi_{\infty \operatorname{sgn}(z^0)}(z^-, \mathbf{z}_\perp) \equiv [\infty \cdot \operatorname{sgn}(z^0), \infty; \infty \cdot \operatorname{sgn}(z^0), \mathbf{z}_\perp][\infty \cdot \operatorname{sgn}(z^0), \mathbf{z}_\perp; z^-, \mathbf{z}_\perp] \psi(z^-, \mathbf{z}_\perp) \quad (2.61)$$

acquires the phase in which the direction where the Wilson lines are pointing is determined by the physical process in question. It is reflected by $\operatorname{sgn}(z_0)$ in the integration limit. In deeply inelastic and Drell-Yan type processes $z_0 > 0$ and $z_0 < 0$, respectively. The sign of z_0 depends on whether interactions generating the eikonal phase occur after or before the struck quark is hit by the probe. In this formulation, the purely collinear parton distributions are the integrals of the more general distributions depending also on the transverse momentum

$$\begin{aligned} f^q(x, \mu^2) &= \int^{\mu^2} d^2 \mathbf{k}_\perp f^q(x, \mathbf{k}_\perp) \\ &= \frac{1}{2} \int \frac{dz^-}{2\pi} e^{ixp^+ z^-} \langle p | \bar{\psi}(0, \mathbf{0}) \gamma^+ [0, \mathbf{0}; z^-, \mathbf{0}] \psi(z^-, \mathbf{0}) | p \rangle. \end{aligned} \quad (2.62)$$

We schematically exhibited the appearance of the cutoff scale dependence of the transverse momentum integrals.

For positive x , the function $f^q(x, \mu^2)$ can be interpreted as the quark density $q(x, \mu^2)$, while for negative momentum fractions x it is understood as the (minus) antiquark density:

$$f^q(x, \mu^2) = q(x, \mu^2)\theta(x) - \bar{q}(-x, \mu^2)\theta(-x). \quad (2.63)$$

In the Bjorken limit, the structure functions are expressed in terms of quark distributions. For instance, the proton polarization-independent structure functions are

$$\begin{aligned} F_1(x_B, Q^2) &= \frac{1}{2x_B} F_2(x_B, Q^2) \\ &= \frac{1}{2} \sum_q Q_q^2 (q(x_B, Q^2) + \bar{q}(x_B, Q^2)), \end{aligned} \quad (2.64)$$

The proportionality of F_1 and F_2 structure functions is a consequence of the fact that the spin of quarks is one-half [17]. It is instructive to introduce a specific combination of F_1 and F_2 , the longitudinal structure function

$$F_L \equiv F_2 - 2x_B F_1. \quad (2.65)$$

For an unpolarized target, the structure functions are related to the absorption cross sections of transversely and longitudinally polarized photons

$$\begin{aligned} \sigma_T^{\gamma^*} &= \frac{2\pi^2 \alpha_{\text{em}}^2}{KM_N} \sum_{\lambda=\uparrow\downarrow} \varepsilon_\mu^{\lambda*} W^{\mu\nu} \varepsilon_\nu^\lambda \xrightarrow{Q^2 \rightarrow \infty} \frac{4\pi^2 \alpha_{\text{em}}^2}{KM_N} F_1(x_B), \\ \sigma_L^{\gamma^*} &= \frac{4\pi^2 \alpha_{\text{em}}^2}{KM_N} \varepsilon_{L\mu} W^{\mu\nu} \varepsilon_{L\nu} \xrightarrow{Q^2 \rightarrow \infty} \frac{4\pi^2 \alpha_{\text{em}}^2}{KM_N} \frac{1}{2x_B} F_L(x_B), \end{aligned}$$

respectively, with K being the photon flux factor. There are two widely used conventions for it, due to Gilman [55]

$$K = |\mathbf{q}| = \frac{p \cdot q}{M_N} \sqrt{1 + 4M_N^2 x_B^2 / Q^2}, \quad (2.66)$$

and another one due to Hand [56]

$$K = \frac{M_R^2 - M_N^2}{2M_N} = \frac{p \cdot q}{M_N} (1 - x_B), \quad (2.67)$$

where M_R is the mass of the intermediate state. In the Bjorken limit, $F_1 \gg F_L$ for spin-one-half constituents, while for scalar partons the inequality is reversed, $F_1 \ll F_L$. As is well known, the experimental verification of the first inequality established the firm foundation for identification of partons with Gell-Mann–Zweig quarks.

Analogous relations hold for the polarized structure function g_1 , the only difference is that spin-weighted rather than spin averaged quark parton species enter the leading order prediction,

$$g_1(x_B, Q^2) = \frac{1}{2} \sum_q Q_q^2 (\Delta q(x_B, Q^2) + \Delta \bar{q}(x_B, Q^2)). \quad (2.68)$$

The definition of Δq , $\Delta \bar{q}$ differs from Eq. (2.62) by the presence of the chiral matrix, i.e., $\gamma^+ \rightarrow \gamma^+ \gamma^5$. We will discuss these in more detail in subsequent sections.

2.2.7 Parton distributions as momentum densities in the Bjorken frame

Let us turn to the physical picture of the deep-inelastic event. A very intuitive interpretation of parton distributions arises in the so-called Bjorken frame, where the proton moves along the z -axis and the photon moves in the x, y plane:

$$p^\mu = \left(\mathcal{P} + \frac{M_N^2}{4\mathcal{P}}, 0, 0, \mathcal{P} - \frac{M_N^2}{4\mathcal{P}} \right), \quad q^\mu = (\omega, q^x, q^y, 0). \quad (2.69)$$

Sending the proton's momentum to infinity,

$$\mathcal{P} \rightarrow \infty, \quad (2.70)$$

defines the infinite-momentum frame in which the energy of the virtual photon vanishes

$$\omega = \frac{p \cdot q}{\mathcal{P} + M_N^2/(4\mathcal{P})} \simeq \frac{\mathcal{Q}^2}{2x_B\mathcal{P}} \rightarrow 0. \quad (2.71)$$

Thus, there is no energy exchange between the lepton and the probed quark. The photon momentum becomes purely transverse: $\mathcal{Q}^2 \rightarrow \mathbf{q}_\perp^2$. Thus, in the Bjorken frame the virtual photon is absorbed over a very short time in a very small spatial area:

- A typical interaction time of constituents is inversely proportional to the energy deficit of a given fluctuation of a particle with the energy E_0 and three-momentum \mathbf{k}_0 into two partons with energies $E_{1,2}$ and three-momenta $\mathbf{k}_{1,2}$, where $\mathbf{k}_i = (\mathbf{k}_{\perp i}, x_i p^z)$. Namely,

$$\delta t \sim \frac{1}{\delta E} = \frac{1}{E_0 - E_1 - E_2} \sim \frac{x_0 x_1 x_2 p_z}{x_1 x_2 \mathbf{k}_{\perp 0}^2 - x_0 x_2 \mathbf{k}_{\perp 1}^2 - x_0 x_1 \mathbf{k}_{\perp 2}^2} \rightarrow \infty \quad (2.72)$$

as $p_z \rightarrow \infty$. Therefore, one can treat partons as almost free in the infinite momentum frame due to the time dilation (2.72). During the time of transiting the target, the virtual photon “sees” the nucleon’s constituents in a frozen state which is thus describable by an instantaneous distribution of partons. Here it is instructive to make an analogy with the X-ray crystallography. Recall that an X-ray scattered off atoms reveals the crystal’s structure owing to the fact that the oscillations of atoms in the lattice sites can be neglected. Atoms can be considered at rest during the time when X-rays pass through the crystal.

- The highly virtual photon probes the transverse distance

$$\delta|\mathbf{z}_\perp| \sim \frac{1}{|\mathbf{q}_\perp|} = \frac{1}{\mathcal{Q}} \quad (2.73)$$

in the longitudinally Lorentz-contracted hadron.

To acquire a physically sensible picture for the parton distributions in the Bjorken frame, one should use the light-like gauge $A^+ = 0$. In this physical gauge, the gauge link in the definition of the collinear parton distribution function disappears. In the formalism of the light-cone quantization reviewed in Appendix D (see [57]), the leading-twist parton distributions are defined by the “good” components of the field operators $\bar{\psi}\gamma^+\psi = \bar{\psi}_+\gamma^+\psi_+$. Notice that the good components of quark and gluon fields behave as free only at the light-cone time $z^+ = 0$, which is where these operators enter the definition of parton distributions. This reflects the physics of the parton model: partons

are treated as free just during the short time when they are “seen” by a probe like that of a highly virtual photon in a hard process. Notice also that the parton states obtained by creation operators acting on the vacuum are defined with the reference to the time of this hard interaction, rather than with that to the far past or far future. The reason is obvious: we do not treat partons as observable particles, since they are not in light of the quark confinement. Substituting Eq. (D.8) into (2.62) gives

$$\begin{aligned} f^q(x)|_{x>0} &= \frac{1}{2x} \sum_{\lambda=\uparrow\downarrow} \int \frac{d^2\mathbf{k}_\perp}{(2\pi)^3} \frac{\langle p|b_\lambda^\dagger(xp^+, \mathbf{k}_\perp)b_\lambda(xp^+, \mathbf{k}_\perp)|p\rangle}{\langle p|p\rangle}, \\ f^q(x)|_{x<0} &= \frac{-1}{2x} \sum_{\lambda=\uparrow\downarrow} \int \frac{d^2\mathbf{k}_\perp}{(2\pi)^3} \frac{\langle p|d_\lambda^\dagger(xp_+, \mathbf{k}_\perp)d_\lambda(xp_+, \mathbf{k}_\perp)|p\rangle}{\langle p|p\rangle}, \end{aligned} \quad (2.74)$$

where b^\dagger and d^\dagger are the creation operators of a quark and an anti-quark, respectively, with longitudinal momentum $k^+ \equiv xp^+$ and transverse momentum \mathbf{k}_\perp , and $|p\rangle$ is a hadronic state with a definite light-cone energy p^+ normalized by $\langle p|p\rangle = 2p^+(2\pi)^3\delta^{(3)}(0)$. For positive momentum fractions, the parton distribution is identical to the number of quarks with a given momentum xp^+ in a fast-moving proton, while for negative x it measures the number of antiquarks. Thus, interpretation of parton distribution functions as parton number densities [16] is obvious in the infinite momentum frame. The positivity of parton distributions is also obvious, since in the light-cone quantization one can cast them in the form,

$$f^q(x) = \frac{1}{\sqrt{2}} \sum_n |\langle n|\psi_+(0)|p\rangle|^2 \delta((1-x)p^+ - P_n^+),$$

where $P_n = p_1 + p_2 + \dots + p_n$ is the momentum of intermediate particle states.

2.2.8 Parton distributions in the rest frame

The definition of the parton distribution (2.62) is boost independent. One can check that the z -boost independence translates into the reparametrization invariance of parton distributions with respect to the rescaling of light-cone vectors. Namely, the transformation

$$n^\mu \rightarrow \varrho n^\mu, \quad n^{*\mu} \rightarrow \varrho^{-1} n^{*\mu} \quad (2.75)$$

leaves the parton distributions intact. As a result, we can use parton distributions in any frame. However, a clear separation of quarks from antiquarks for positive and negative momentum fractions x , respectively, as well as the probabilistic parton picture will hold only in the infinite momentum frame, since in any other frame the partons will be strongly interacting.

By transforming all momenta to the rest frame, we see that the parton distribution is determined by a measurement on the space-time surface $z^+ = 0$, i.e., the measurement is not an instantaneous event. The variable x is intrinsic to the light-cone operator: it is a Fourier conjugate to the separation of quark fields on the light cone. It maps into the momentum fraction of quarks only in the formalism of light-cone quantization which is equivalent to the Feynman parton model in the infinite momentum frame. It is easy to see that in the rest frame of the nucleon, the Feynman variable x is just a special combination of the off-shell energy k^0 and momentum k^z ,

$$x = \frac{k^0 + k^z}{M_N}.$$

In other words, the parton distribution is the distribution of quarks projected along a special direction in the four-dimensional energy-momentum space. The quarks with different k^0 and k^z can have the same x , and furthermore, the quarks are naturally off-shell.

2.3 Quark phase-space distribution

To parallel the description of a quantum state in nonrelativistic quantum mechanics by means of the Wigner distribution, we introduce a similar concept within the field-theoretical context of QCD [58, 59, 41]. We generalize the concept of phase-space distributions to the case of relativistic quarks and gluons in the proton by promoting the wave functions of quantum-mechanical states to the field operators acting on the Hilbert space of quantum states. We introduce the (equal light-cone time) Wigner operator defining it by [59, 41]

$$\mathcal{W}^q(k^+, \mathbf{k}_\perp; \mathbf{r}) = \int \frac{dz^-}{2\pi} \frac{d^2\mathbf{z}_\perp}{(2\pi)^2} e^{-ik^+z^- + i\mathbf{k}_\perp \cdot \mathbf{z}_\perp} \bar{\Psi}_\infty(\mathbf{r} + z) \gamma^+ \Psi_\infty(\mathbf{r} - z). \quad (2.76)$$

We restricted the definition by taking the correlation at equal light-cone time since only such correlations are accessible in high-energy experiments. Here \mathbf{r} is the quark position and $k^\mu = (k^+, k^- = 0, \mathbf{k}_\perp)$ is the momentum conjugate to the space-time separation $z^\mu = (z^+ = 0, z^-, \mathbf{z}_\perp)$. Physically k^μ is the sum of incoming and outgoing partons' momenta. The parton phase-space distribution is determined by the matrix element of this operator sandwiched between the states of a localized proton (2.19), namely

$$W^q(x, \mathbf{k}_\perp; \mathbf{r}) = \langle \mathbf{R} = 0 | \mathcal{W}^q(k^+, \mathbf{k}_\perp; \mathbf{r}) | \mathbf{R} = 0 \rangle. \quad (2.77)$$

Its Fourier transform with respect to the three-dimensional coordinate \mathbf{r} determines the generalized momentum-space correlation function

$$2M_N \int \frac{d^3\mathbf{r}}{(2\pi)^3} e^{i\Delta \cdot \mathbf{r}} W^q(x, \mathbf{k}_\perp; \mathbf{r}) \equiv \mathcal{F}^q(x, \mathbf{k}_\perp; \eta, \Delta_\perp). \quad (2.78)$$

In the Breit frame³, where the incoming and outgoing momenta are given by Eq. (2.26), we have⁴

$$\mathcal{F}^q(x, \mathbf{k}_\perp; \eta, \Delta_\perp^2) = \int \frac{dz^-}{2\pi} \frac{d^2\mathbf{z}_\perp}{(2\pi)^2} e^{ixz^- p^+ - i\mathbf{k}_\perp \cdot \mathbf{z}_\perp} \langle -\frac{1}{2}\Delta | \bar{\Psi}_\infty(-z) \gamma^+ \Psi_\infty(z) | \frac{1}{2}\Delta \rangle. \quad (2.79)$$

Since there is an axial symmetry of the high-energy scattering with the z -axis directed along the momentum of the incoming proton, it is natural to separate the longitudinal and transverse kinematical variables. The longitudinal variables include the “external” parameter of skewness η and the “internal” Feynman momentum fraction x , defined as

$$\eta \equiv \frac{\Delta^+}{p^+} = \frac{\Delta^z}{2E}, \quad x \equiv \frac{k^+}{p^+} = \frac{k^0 + k^z}{2E}, \quad (2.80)$$

respectively. The rightmost expressions in each of the two definitions hold in the above “brick wall” frame. Here the incoming (outgoing) proton energy is $E = \sqrt{M_N^2 + \Delta^2/4}$. We use twice the average proton momentum p and the momentum transfer Δ ,

$$p = p_1 + p_2, \quad \Delta = p_1 - p_2. \quad (2.81)$$

³The limitation of this procedure will be discussed below in Section 3.15.

⁴An analogous \mathbf{k}_\perp unintegrated function was introduced for gluons in Ref. [60], without any reference to the Breit frame.

Obviously, Eq. (2.79) is a generating function of all known high-energy observables of the proton based on generalized parton distributions. The Wigner distributions are related to:

- the generalized parton distributions (GPDs) by a Fourier transformation and a marginal projection over the transverse parton momentum:

$$F^q(x, \eta, \Delta_\perp^2) = \int d^2\mathbf{k}_\perp \mathcal{F}^q(x, \mathbf{k}_\perp; \eta, \Delta_\perp^2). \quad (2.82)$$

- the unintegrated forward parton distributions via a simple reduction

$$f^q(x, \mathbf{k}_\perp) = 4\mathcal{F}^q(x, 2\mathbf{k}_\perp; \eta = 0, \Delta_\perp^2 = 0). \quad (2.83)$$

The factor of 2 accompanying \mathbf{k} in the argument of \mathcal{F} is a consequence of the reduction of the vector k^μ to the forward limit where it becomes twice the quark momentum.

The function $W(x; \mathbf{r})$ is not a probability density. It is a three-dimensional quasi-probability distribution of quarks with a selected Feynman variable x . We remind the reader again that the light-cone momentum is understood here in its rest-frame sense as merely a special combination of the off-shell energy and momentum along z : $x \sim k^0 + k^z$. A few special limiting cases of the parameter space endow the reduced Wigner functions with the density of probability property. They are:

- The Mellin moments with respect to the Feynman variable x of the Wigner distribution yield various form factors. The first moment gives the electromagnetic form factors discussed above, the second moment corresponds to gravitational form factors (both discussed in detail below), and higher moments generate form factors of higher-spin probes.
- The r^z -integrated skewless GPD (set to $\eta \sim p^z = 0$) yields a reduced Wigner distribution [58, 59] that coincides with the two-dimensional density $q(x; \mathbf{r}_\perp)$ which is the Soper's impact-parameter parton distribution [61]. Integrating it over \mathbf{r}_\perp gives the usual Feynman parton distribution.

The Wigner function gives a classical realization of phase-space distributions in regions where its magnitude is larger than typical quantum fluctuations. For the QCD case, the semiclassical picture arises most naturally for a large nucleus with radius much larger than its Compton wavelength, $R_A \gg \lambda_A \sim 1/M_A$.

Unfortunately, the generic Wigner function (2.79) is not accessible experimentally, however, its first marginal projection (2.82) is. The rest of our discussion will be dedicated solely to the development of the theory and phenomenology of GPDs.

2.4 Exclusive versus inclusive processes

Deeply inelastic scattering experiments discussed in the preceding paragraphs, and other inclusive reactions, have been used for over the last three decades as one of the major sources of information on the complicated long distance dynamics of hadron constituents. However, information on the nucleon's parton structure obtained in this way can only be used to access inclusive properties of hadrons, like parton distributions. It is insufficient to constrain the detailed picture of the hadron

wave function, which is the probability amplitude describing the hadron as a superposition of partonic states, e.g., for the proton,

$$|p\rangle = \psi_{uud}|uud\rangle + \psi_{uudg}|uudg\rangle + \psi_{uudgg}|uudgg\rangle + \psi_{uud\bar{q}q}|uud\bar{q}q\rangle + \dots, \quad (2.84)$$

with precise assignment of particular spin, flavor, longitudinal momentum fractions and transverse momenta to each of the hadron constituents bound inside the hadron. For instance, the quark distribution addressed above is given (schematically) by the absolute value squared of the proton wave function,

$$f^q(x) = \int dx' \int d^2\mathbf{k} d^2\mathbf{k}' |\psi_{uud}^*(x, 1-x-x', x'; \mathbf{k}, \mathbf{k}', -\mathbf{k}-\mathbf{k}')|^2, \quad (2.85)$$

(see Section 3.7 for a more precise formula) with longitudinal momentum fractions x of the struck and spectator quarks as well as their transverse momenta kept explicit. In $f^q(x)$, all the transverse momenta of the partons are integrated out. This obviously simplifies the theoretical description, but the result lacks a plethora of important features of the strong interaction physics.

There is a large class of hadronic reactions where one gets a more direct access to the wave functions. Exclusive processes are defined as scattering reactions where the kinematical parameters of all initial and final state particles are specified. From the experimental point of view, this implies that all outgoing particles are detected. The reactions include elastic lepton-hadron scattering giving information about hadronic form factors, hadron decays, hadron-hadron scattering, leptoproduction of photons and mesons off hadrons.

Exclusive rates drop much faster with momentum transfer than their inclusive counterparts. Contrary to deeply inelastic scattering, exclusive reaction rates depend on the state of the hadronic system prior as well as after the hard collision. It is a consequence of the coherent scattering of hadron constituents by an external probe such that partons can form a single outgoing hadron rather than a jet of particles. Because on the higher sensitivity to the long-distance effects these processes on the one hand can shed more light on the quark confinement but on the other hand they are more challenging for theoretical analyses.

3 Classification and properties of GPDs

The reduced phase-space distributions of partons (2.82) in the nucleon are Fourier transforms of generalized parton distributions. GPDs may be treated as a formal generalization of the matrix elements of non-local light-cone operators to the case of off-forward kinematics. They arise in a number of exclusive and diffractive processes, to the detailed analysis of which we dedicate several subsequent sections of this review.

In the present section, we give the classification of generalized parton distributions according to the quantum numbers of the operators they are represented by as well as by the hadron states these operators are sandwiched in. We consider first the leading-twist distributions. The twist-three functions will be addressed in Section 5.3.

3.1 Twist-two operators

The leading terms in the asymptotic regime for hard processes are given by operators of the lowest twist. In deeply inelastic scattering, such operators are associated with contributions exhibiting

Bjorken scaling. Formally, the geometric twist is defined as dimension in mass units minus the Lorentz spin of the operator

$$\tau = d - s. \quad (3.1)$$

A spin- s tensor transforms as an irreducible representation of the Lorentz group. The maximal spin for a given number of Lorentz indices is achieved when they are all symmetrized. The irreducibility implies that the reduction to lower-spin tensors is not possible: as a consequence, the contraction of any pair of indices with the metric tensor gives zero. Thus, the Lorentz structure has to be traceless, and its construction is straightforward. For instance, the twist-two spin- j operator built from scalar fields in a non-gauge theory is given by

$$\mathcal{R}_{\mu_1 \dots \mu_j}^{2,\phi\phi}(0) = \mathbf{S}_{\mu_1 \dots \mu_j} \phi^\dagger(0) i \vec{\partial}_{\mu_1} \dots i \vec{\partial}_{\mu_j} \phi(0), \quad (3.2)$$

where the left-right derivative is

$$\vec{\partial}_\mu \equiv \vec{\partial}_\mu - \vec{\partial}_\mu. \quad (3.3)$$

In $\mathcal{R}^{\tau,aa}$, the superscript τ stands for the twist of the operator and a specifies the particle content: QCD quarks $a = q$ and gluons $a = g$ or scalars $a = \phi$ (the latter are used for demonstration purposes only). The operation \mathbf{S} denotes the symmetrization of the corresponding Lorentz indices and trace subtraction. For example, in the case of a two-index tensor it is

$$\mathbf{S}_{\mu_1 \mu_2} t_{\mu_1 \mu_2} = \frac{1}{2!} \left(t_{\mu_1 \mu_2} + t_{\mu_2 \mu_1} - \frac{1}{2} g_{\mu_1 \mu_2} g^{\nu_1 \nu_2} t_{\nu_1 \nu_2} \right).$$

A constructive all-order definition of this operation is given below in Section 5.6.1. In case of scalar fields ϕ , the dimension of the operator with j derivatives is $d = 2d_\phi + j$. Since the dimension of ϕ is $d_\phi = 1$, we have $\tau = 2$. The towers of twist-two spin- j operators can be conveniently summed into a non-local form and one can also define the notion of twist for non-local light-ray operators in terms of Taylor expansion,

$$\mathcal{O}^{\phi\phi}(-z^-, z^-) = \phi^\dagger(-z^-) \phi(z^-) = \sum_{j=0}^{\infty} \frac{(-iz^-)^j}{j!} n^{\mu_1} \dots n^{\mu_j} \mathcal{R}_{\mu_1 \dots \mu_j}^{2,\phi\phi}(0). \quad (3.4)$$

When fermions and gauge bosons enter the game, one has to separate first the different spin projections contained in a given field operator. This can be done in a most concise manner in the light-cone formalism (see Appendix D). Below, we outline the construction separately for quark and gluon bilocal operators.

3.1.1 Quark operators

The four-component fermion field ψ , by means of the projection operators [62]

$$\psi = \psi_+ + \psi_-, \quad \psi_\pm \equiv \Pi^\pm \psi, \quad \Pi^\pm \equiv \frac{1}{2} \gamma^\mp \gamma^\pm, \quad (3.5)$$

is decomposed in two terms ψ_\pm that have the following light-cone spin:

$$\Sigma^{-+} \psi_\pm = \pm \frac{1}{2} \psi_\pm. \quad (3.6)$$

Here $\Sigma^{\mu\nu} \equiv \frac{1}{4} [\gamma^\mu, \gamma^\nu]$ is the spin tensor. Since the canonical dimension of the fermion field is $d_q = 3/2$, one finds that the ψ_+ -component has the twist $\tau_q = 1$ since its spin is $s_q = 1/2$.

Similarly, for the ψ_- -component one finds $s_q = -1/2$ and thus $\tau_q = 2$. Therefore, only the ψ_+ component enters a nonlocal operator of the minimal twist. Going from the four-component to Weyl spinors, the chiral projection of the “good” components yields two independent fields

$$\psi_{+\uparrow} = \frac{1}{2}(1 + \gamma^5)\psi_+, \quad \psi_{+\downarrow} = \frac{1}{2}(1 - \gamma^5)\psi_+. \quad (3.7)$$

The right $\psi_{+\uparrow}$ and left $\psi_{+\downarrow}$ projections of the “good” light-cone spinors possess a single nonvanishing component only, which describes a state with a definite helicity. The helicity operator is conventionally defined as (see Appendix A.2)

$$h \equiv \frac{1}{2}\bar{\mathbf{e}}_\perp^i \mathbf{e}_\perp^j \Sigma^{ij} = i\Sigma^{12}, \quad \mathbf{e}_\perp^i = (\bar{\mathbf{e}}_\perp^i)^* = (1, i), \quad (3.8)$$

with eigenvalues designating their helicity

$$h\psi_{+\uparrow} = \frac{1}{2}\psi_{+\uparrow}, \quad h\psi_{+\downarrow} = -\frac{1}{2}\psi_{+\downarrow}. \quad (3.9)$$

The counting of independent bilocal quark operators is especially transparent within this formulation, since left and right fields each contain a single non-vanishing component only. Namely, the fields

$$\psi_{+\uparrow} = \begin{pmatrix} \lambda_\uparrow \\ 0 \end{pmatrix}, \quad \psi_{+\downarrow} = \begin{pmatrix} 0 \\ \bar{\chi}_\downarrow \end{pmatrix},$$

with one-component two-dimensional Weyl spinors

$$\lambda_\uparrow \sim \begin{pmatrix} 1 \\ 0 \end{pmatrix}, \quad \bar{\chi}_\downarrow \sim \begin{pmatrix} 0 \\ 1 \end{pmatrix},$$

realize the $(0, \frac{1}{2})$ and $(\frac{1}{2}, 0)$ representations of the Lorentz group, respectively. Let us use them to build all distinct helicity combinations for the two-particle leading twist operators, i.e., $(\frac{1}{2}, 0) \otimes (\frac{1}{2}, 0) = (0, 0) \oplus (1, 0)$ and $(\frac{1}{2}, 0) \otimes (0, \frac{1}{2}) = (\frac{1}{2}, \frac{1}{2})$. We can build four distinct combinations and put them back into a covariant four-dimensional form

$$\lambda_\uparrow^* \lambda_\uparrow \pm \bar{\chi}_\downarrow^* \bar{\chi}_\downarrow = \frac{1}{\sqrt{2}}\bar{\psi} \left\{ \begin{array}{c} \gamma^+ \\ \gamma^+ \gamma^5 \end{array} \right\} \psi, \quad \lambda_\uparrow^* \bar{\chi}_\downarrow \pm \bar{\chi}_\downarrow^* \lambda_\uparrow = \frac{i}{\sqrt{2}}\bar{\psi} \left\{ \begin{array}{c} i\sigma^{+2} \\ \sigma^{+1} \end{array} \right\} \psi.$$

The latter two operators are merely two components of a two-dimensional vector. Notice that since $\sigma^{\mu\nu}$ and $\sigma^{\mu\nu}\gamma^5$ are not independent, the latter vertex will not appear as a possible Dirac structure. As an outcome of this simple analysis we can introduce the following three leading-twist bilocal quark operators:

$$\mathcal{O}^{qq}(z_1^-, z_2^-) = \bar{\psi}(z_1^-)[z_1^-, z_2^-]\gamma^+ \psi(z_2^-), \quad (3.10)$$

$$\tilde{\mathcal{O}}^{qq}(z_1^-, z_2^-) = \bar{\psi}(z_1^-)[z_1^-, z_2^-]\gamma^+ \gamma^5 \psi(z_2^-), \quad (3.11)$$

$$\mathcal{T}_\mu^{qq}(z_1^-, z_2^-) = \bar{\psi}(z_1^-)[z_1^-, z_2^-]\sigma^{+\perp}_\mu \psi(z_2^-). \quad (3.12)$$

The gauge link is added here to make the operator explicitly gauge invariant if other than the light-cone gauge $A^+ = 0$ is used. As discussed in the introduction, the path-ordered exponentials appear in physical observables as a consequence of the final (DIS) or initial (DY) state interactions.

3.1.2 Gluon operators

For a gauge field, in order to clearly identify its different spin components, one has to project the Lorentz indices of the strength tensor $F^{\mu\nu}$ onto the longitudinal light-cone directions and the transverse space with the two-dimensional metric $g_{\mu\nu}^\perp$. The light-cone spin assignments for different projections of $F^{\mu\nu}$ are as follows

$$\Sigma^{-+} F_\perp^{\pm\mu} = \pm F_\perp^{\pm\mu}, \quad \Sigma^{-+} F^{+-} = \Sigma^{-+} F_{\perp\perp}^{\mu\nu} = 0, \quad (3.13)$$

where

$$\Sigma^{\mu\nu} F^{\rho\sigma} = g^{\mu\rho} F^{\nu\sigma} - g^{\nu\rho} F^{\mu\sigma} - g^{\mu\sigma} F^{\nu\rho} + g^{\nu\sigma} F^{\mu\rho}.$$

Since the canonical dimension of the strength tensor $F^{\mu\nu}$ is $d_g = 2$, the $F_\perp^{+\mu}$ -component possesses the twist $\tau_g = 1$ since its spin is $s_g = 1$. For F^{+-} and $F_{\perp\perp}^{\mu\nu}$ -components one gets $s_g = 0$ and therefore $\tau_g = 2$, while the $F_\perp^{-\mu}$ -component $s_g = -1$ and $\tau_g = 3$. Consequently, the minimal twist is associated with the $F_\perp^{+\mu}$ -component only.

The product of two vectors, each transforming as $(\frac{1}{2}, \frac{1}{2})$, can be decomposed into irreducible representations of the Lorentz group as $(\frac{1}{2}, \frac{1}{2}) \otimes (\frac{1}{2}, \frac{1}{2}) = (0, 0) \oplus ((1, 0) \oplus (0, 1)) \oplus (1, 1)$. In terms of tensors this reads

$$g_\perp^{\mu\alpha} g_\perp^{\nu\beta} = \frac{1}{2} g_\perp^{\mu\nu} g_\perp^{\alpha\beta} + \frac{1}{2} \varepsilon_\perp^{\mu\nu} \varepsilon_\perp^{\alpha\beta} + \tau_{\perp\mu\nu; \rho\sigma}^{\mu\nu; \rho\sigma} \tau_{\perp\alpha\beta; \rho\sigma}^{\alpha\beta},$$

with the two-dimensional tensors being

$$g_\perp^{\perp\mu\nu} \equiv g_{\mu\nu} - n_\mu n_\nu^* - n_\nu n_\mu^*, \quad (3.14)$$

$$\varepsilon_\perp^{\perp\mu\nu} \equiv \varepsilon^{\alpha\beta\rho\sigma} g_{\alpha\mu}^\perp g_{\beta\nu}^\perp n_\rho^* n_\sigma, \quad (3.15)$$

$$\tau_{\perp\mu\nu; \rho\sigma}^{\perp} \equiv \frac{1}{2} g_{\mu\rho}^\perp g_{\nu\sigma}^\perp + \frac{1}{2} g_{\mu\sigma}^\perp g_{\nu\rho}^\perp - \frac{1}{2} g_{\mu\nu}^\perp g_{\rho\sigma}^\perp. \quad (3.16)$$

The totally antisymmetric tensor is normalized as $\varepsilon^{0123} = 1$. The totally symmetric and traceless in two pair of indices tensor $\tau_{\perp\mu\nu; \rho\sigma}^{\perp}$ possesses the properties

$$\tau_{\perp\mu\nu; \rho\sigma}^{\perp} \tau_{\perp\mu\nu; \rho'\sigma'}^{\perp} = \tau_{\perp\rho\sigma; \rho'\sigma'}^{\perp}, \quad \tau_{\perp\mu\nu; \rho\sigma}^{\perp} = \tau_{\perp\rho\sigma; \mu\nu}^{\perp}, \quad \tau_{\perp\mu\mu; \rho\sigma}^{\perp} = 0, \quad \tau_{\perp\mu\nu; \mu\nu}^{\perp} = 2.$$

Hence, there are three independent Lorentz structures for twist-two two-particle gluonic operators.

This can be easily understood from counting two-gluon helicity states in the formalism of the light-cone quantization. To this end, we build the holomorphic and anti-holomorphic combinations of the gauge potential in the light-cone gauge

$$A_\perp \equiv A^x + iA^y, \quad \bar{A}_\perp \equiv A^x - iA^y. \quad (3.17)$$

They describe left and right circular polarizations with helicity -1 and $+1$, respectively. Namely

$$h A_\perp = -A_\perp, \quad h \bar{A}_\perp = \bar{A}_\perp. \quad (3.18)$$

Both of them are scalars with respect to the light-cone spin operator Σ^{-+} , i.e., $\Sigma^{-+} A = \Sigma^{-+} \bar{A} = 0$. Since the light-cone derivative carries one unit of spin, so will the derivatives of the (anti-) holomorphic potentials. In the covariant form, they are related to the gluon field-strength tensors

$$\partial^+ A_\perp = F^{+x} - i\tilde{F}^{+x} = i(F^{+y} - i\tilde{F}^{+y}), \quad \partial^+ \bar{A}_\perp = F^{+x} + i\tilde{F}^{+x} = -i(F^{+y} + i\tilde{F}^{+y}).$$

For further convenience, we introduce the gluon negative- and positive-helicity covariant fields

$$F_{[-]\perp}^{+\mu} = F_{\perp}^{+\mu} - i\tilde{F}_{\perp}^{+\mu}, \quad F_{[+]\perp}^{+\mu} = F_{\perp}^{+\mu} + i\tilde{F}_{\perp}^{+\mu}, \quad (3.19)$$

respectively. Here the dual gluon field strength is defined as $\tilde{F}^{\mu\nu} \equiv \frac{1}{2}\varepsilon^{\mu\nu\rho\sigma}F_{\rho\sigma}$, so that $\tilde{F}_{\perp}^{+\mu} = \varepsilon_{\perp}^{\mu\nu}F_{\nu}^{+\perp}$ for two-dimensional transverse indices. From the positive- and negative-helicity operators we build the even- and odd-parity combinations

$$\left(F_{[-]\perp}^{+\mu} F_{[+]\perp}^{+\nu} \pm F_{[+]\perp}^{+\mu} F_{[-]\perp}^{+\nu} \right) g_{\mu\nu}^{\perp} = 4 \left\{ \begin{array}{c} g_{\mu\nu}^{\perp} \\ i\varepsilon_{\mu\nu}^{\perp} \end{array} \right\} F_{\perp}^{+\mu} F_{\perp}^{\nu+},$$

as well as the maximal-helicity operators

$$\left(F_{[+]\perp}^{+\mu} F_{[+]\perp}^{+\nu} \pm F_{[-]\perp}^{+\mu} F_{[-]\perp}^{+\nu} \right) = 4\tau_{\perp}^{\mu\nu;\rho\sigma} \left\{ \begin{array}{c} F_{\rho}^{+\perp} F_{\sigma}^{\perp+} \\ i\tilde{F}_{\rho}^{+\perp} F_{\sigma}^{\perp+} \end{array} \right\}.$$

According to this nomenclature we introduce three leading-twist gluonic operators:

$$\mathcal{O}^{gg}(z_1^-, z_2^-) = F_a^{+\mu}(z_1^-)[z_1^-, z_2^-]^{ab}g_{\mu\nu}F_b^{\nu+}(z_2^-), \quad (3.20)$$

$$\tilde{\mathcal{O}}^{gg}(z_1^-, z_2^-) = F_a^{+\mu}(z_1^-)[z_1^-, z_2^-]^{ab}i\varepsilon_{\mu\nu}^{\perp}F_b^{\nu+}(z_2^-), \quad (3.21)$$

$$\mathcal{T}_{\mu\nu}^{gg}(z_1^-, z_2^-) = F_a^{+\rho}(z_1^-)[z_1^-, z_2^-]^{ab}\tau_{\mu\nu;\rho\sigma}^{\perp}F_b^{\sigma+}(z_2^-), \quad (3.22)$$

augmented by the Wilson line in the adjoint representation

$$[z_1^-, z_2^-]^{ab} = P \exp \left(g \int_{z_2^-}^{z_1^-} dz'^- f^{abc} A_c^+(z'^-, \mathbf{0}_{\perp}) \right),$$

to respect gauge invariance. The links obey the following obvious properties

$$[z_1^-, z_2^-]^{ab} = [z_2^-, z_1^-]^{ba}, \quad [z_1^-, z_2^-]^{ab} = [z_1^-, z_3^-]^{ac}[z_3^-, z_2^-]^{cb}.$$

The construction we have just presented can be extended to higher twist multi-particle operators which have the largest number of constituent fields out of the set of all possible operators of twist- N for a given Lorentz spin. Namely, these operators are constructed from N “good” fields, ψ_+ and $F_{\perp}^{+\mu}$ living on the light cone. Let us reiterate that the twist of such nonlocal operators equals the number of elementary fields involved, and they are known in QCD as quasipartonic operators [63].

3.2 Operator matrix elements and GPDs

The leading-twist generalized parton distributions arise as coefficients in the decomposition of the off-forward hadronic matrix elements of the bilocal operators introduced in the previous section. For the scalar operator (3.4), one gets⁵

$$F^\phi(x, \eta, \Delta^2) = p^+ \int \frac{dz^-}{2\pi} e^{ixz^-p^+} \langle p_2 | \mathcal{O}^{\phi\phi}(-z^-, z^-) | p_1 \rangle. \quad (3.23)$$

⁵The presence of the factor p^+ is a consequence of the z -boost invariance of the generalized parton distributions, as will be explained in Section 3.2.3.

The variable x , just like for the usual parton distribution functions, is the Fourier conjugate to the Ioffe time. In terms of the outgoing k_1 and incoming k_2 parton's momenta one can write x as

$$x = \frac{k_1^+ + k_2^+}{p^+}.$$

GPDs also depend on the invariant t -channel momentum transfer $\Delta^2 = (p_1 - p_2)^2$ and skewness

$$\eta = \frac{\Delta^+}{p^+}.$$

We recall that we define the momentum transfer as $\Delta = p_1 - p_2$, with the sign opposite to the usual convention used for form factors. This choice⁶ guarantees that η is positive for exclusive deeply virtual lepton-hadron scattering processes. Thus, the plus components of the incoming and outgoing parton's momenta are

$$k_1^+ = \frac{x + \eta}{2} p^+ \quad \text{and} \quad k_2^+ = \frac{x - \eta}{2} p^+,$$

respectively. This parametrization corresponds to the symmetric conventions of Refs. [1] and [2]. Another parametrization used in the literature, corresponds to nonforward parton distributions [6]. In this case, the parton momenta are measured in units of the incoming hadron's momentum p_1 . Then

$$k_1^+ = X p_1^+ \quad \text{and} \quad k_2^+ = (X - \zeta) p_1^+.$$

The parameters X, ζ are related to x, η by

$$\eta = \frac{\zeta}{2 - \zeta}, \quad x = \frac{X - \zeta/2}{1 - \zeta/2}, \quad X = \frac{x + \eta}{1 + \eta}, \quad X - \zeta = \frac{x - \eta}{1 + \eta}.$$

We will not use these variables in our presentation (see Ref. [6] and Ref. [7] for more details).

3.2.1 Time-ordering and support

Let us discuss first the issue of whether the operators defining GPDs have to be chronologically or normal ordered. Generally since they enter as a part of a Feynman diagram describing the physical process, all fields are time-ordered including those present in the two-particle operators $\mathcal{O}^{\phi\phi}(-z^-, z^-)$ determining the hadronic function in question. Argumentation given below does not depend on the spin of constituent or the target, so we can use the scalar-field operator (3.4) to this end. We thus define

$$F^\phi(x, \eta, \Delta^2) = p^+ \int \frac{dz^-}{2\pi} e^{ixz^- p^+} \langle p_2 | T\{\phi^\dagger(-z^-)\phi(z^-)\} | p_1 \rangle. \quad (3.24)$$

Our goal is to demonstrate that since the elementary fields enter the operator at equal light-cone time $z^+ = 0$, the usual chronological ordering can be omitted [64, 65, 6, 66]. Notice that it is not even required that the fields have to be separated by a light-like distance: the argument holds even for the transverse-momentum dependent functions. The function $F^\phi(x, \eta, \Delta^2)$ can be treated as a projection

$$F^\phi(x, \eta, \Delta^2) = \int_{-\infty}^{\infty} dk^+ d^2 \mathbf{k}_\perp \delta \left(x - \frac{k^+}{p^+} \right) \int_{-\infty}^{\infty} dk^- \mathcal{A}(k^+, \mathbf{k}), \quad (3.25)$$

⁶Notice that in a large number of papers η is defined with an opposite sign.



Figure 8: Longitudinal momentum flow in GPDs (left). GPDs as an off-shell parton-hadron scattering amplitude (right).

of a general Green function

$$\mathcal{A}(k) = \int \frac{d^4 z}{(2\pi)^4} e^{ik \cdot z} \langle p_2 | T\{\phi^\dagger(-z)\phi(z)\} | p_1 \rangle$$

for (off-shell) parton scattering on a hadron, $\phi(-k_1) + h(p_1) \rightarrow \phi(-k_2) + h(p_2)$, with z^μ being here a four-dimensional vector with all components nonvanishing. The next step is to demonstrate that the integral over the k^- component of the Green function \mathcal{A} is identical to the integral over its discontinuity,

$$\int_{-\infty}^{\infty} dk^- \mathcal{A}(k^+, \mathbf{k}) = \int_{-\infty}^{\infty} dk^- \text{disc}_{k^-} \mathcal{A}(k^+, \mathbf{k}).$$

Thus we have to incorporate the analytical properties of \mathcal{A} as a function of Mandelstam variables $s = (p_1 - k_1)^2$ and $u = (p_2 + k_1)^2$ and parton virtualities $k_1^2 = (k - \Delta)^2/4$ and $k_2^2 = (k + \Delta)^2/4$. As usual, we will assume that the singularity structure of the non-perturbative matrix element coincides with that of the matrix element given in terms of Feynman diagrams, i.e., in perturbation theory. Then \mathcal{A} has no poles when $\Re k_i^2 < 0$ (for ‘‘negative virtualities’’) and no production thresholds in the corresponding channels for negative Mandelstam invariants, $\Re(s, u) < 0$.

To make correspondence between the $s-$, $u-$, k_1^2- and k_2^2- singularities of the Green function \mathcal{A} and singularities in the k^- plane, one should express k^- in terms of these invariants:

$$k_a^- = \frac{4k_1^2 + (\mathbf{k}_\perp + \Delta_\perp)^2}{2(k^+ + \Delta^+)} - \Delta^-, \quad k_b^- = \frac{4s + \mathbf{k}_\perp^2}{2(k^+ - p^+)} + p^-, \quad (3.26)$$

$$k_c^- = \frac{4k_2^2 + (\mathbf{k}_\perp - \Delta_\perp)^2}{2(k^+ - \Delta^+)} + \Delta^-, \quad k_d^- = \frac{4u + \mathbf{k}_\perp^2}{2(k^+ + p^+)} - p^-, \quad (3.27)$$

where $k^+ = xp^+$ and $\Delta^+ = \eta p^+$ are related to the external variables x and η . The k^- arises in the denominators of propagators with the causal Feynman prescription $k^2 + i0$ and, therefore, produce singularities of Feynman integrals in the complex plane while the prescription determines the position of the contour bypassing them,

$$\int_{-\infty}^{\infty} dk^- \mathcal{F}(k^- + i0 \cdot k_p^+),$$

with $p = a, b, c, d$ and k_p^+ being the denominators in above k_p^- . Considering different regions of the momentum space, the singularities k_p^- migrate in the complex k^- plane and so will or will not

contribute to the k^- contour integral. As we can see from the denominators of k^- , the sign change occurs at $x = -1, -\eta, \eta, 1$ and thus four regions have to be discussed (i) $|x| > 1$, (ii) $\eta < x < 1$, (iii) $-1 < x < -\eta$, and (iv) $|x| < \eta$. Let us discuss a couple of regions.

- In the region $|x| > 1$, all singularities are situated on the same side of $\Im m k^-$, since the denominators of $k_{a,b,c,d}^-$ are either all positive for $x > 1$, or all negative for $x < -1$. Therefore, we can close the integration contour in half-plane free of singularities and assuming that \mathcal{A} vanishes fast enough as $|k^-| \rightarrow \infty$ we can drop the integral over the contour at infinity and get zero for the GPD. Thus [6, 67, 66],

$$F^\phi(x, \eta, \Delta^2) = 0, \quad |x| > 1. \quad (3.28)$$

- In case $\eta < x < 1$, the s singularities are in the upper half plane, while the rest are in the lower. So we wrap the integration contour about the s -channel production threshold which results into the difference of integrals evaluated along the upper and lower sides of the branches of the cut, and result into the discontinuity

$$\int_{-\infty}^{\infty} dk^- \mathcal{A}(k^+, \mathbf{k}) = \int_{-\infty}^{\infty} dk^- \text{disc}_s \int \frac{d^4 z}{(2\pi)^4} e^{ik \cdot z} \langle p_2 | T \mathcal{O}^{\phi\phi}(-z, z) | p_1 \rangle.$$

This is just what we wanted. The derivation works for any η including the forward limit $\eta = 0$. In this sense, GPDs in this region are analogous to the usual parton densities.

The other regions are considered in a similar way [66]. In particular, in the $-1 < x < -\eta$ region, one gets the u -discontinuity in the final formula instead of the s -discontinuity, and GPDs there are analogous to the antiquark densities. The $|x| < \eta$ region is specific to the nonforward kinematics: it disappears in the forward limit. The GPDs in this region correspond to discontinuities in k_1^2 and u or k_2^2 and s . They can be interpreted as the (generalized) distribution amplitude describing the sharing of the longitudinal momentum transfer ηp^+ within the quark-antiquark pair emitted by the initial (or absorbed by the final) hadron. The support properties of GPDs can be also studied using their relation to double distributions, see Section 3.8.

3.2.2 Counting GPDs

For the operator matrix element of the transition of a spin- s_1 hadron into a spin- s_2 hadron, one can have $(2s_1 + 1) \times (2s_2 + 1)$ hadron helicity combinations. Notice that GPDs can initiate helicity-flip transitions. This is possible due to the nonvanishing momentum exchange between the initial and final states, which can produce a non-zero orbital angular momentum compensating the helicity deficit between the initial and final state polarizations. In case of parton helicity non-flip transitions we have one ($n = 1$) operator of even and one of odd parity, i.e., $\lambda_\uparrow^* \lambda_\uparrow \pm \bar{\chi}_\downarrow^* \bar{\chi}_\downarrow$, respectively. On the other hand, there are two operators ($n = 2$), $\lambda_\uparrow^* \bar{\chi}_\downarrow$ and $\bar{\chi}_\downarrow^* \lambda_\uparrow$ for the helicity-flip transitions (recall the open Lorentz index in the maximal-helicity operators). To get the total number of amplitudes, we have to multiply the number of hadron-helicity combinations by the number of quark operators which initiate the transition $n \times (2s_1 + 1) \times (2s_2 + 1)$. Not all of the amplitudes are independent, however. It turns out that the subsequent reduction works differently for generalized parton distributions compared to the ordinary parton densities. Only the application of the spatial-parity inversion results in a reduction of their number, contrary to the case of forward parton distributions, where the time reversal provides further relations

between superficially independent functions. The number of independent parton densities equals the number of independent helicity-conserving helicity amplitudes allowed by parity and time reversal invariance, see Section 3.2.8 below. The number of generalized parton distributions is obtained by counting helicity amplitudes under the constraints due to the spatial parity only. The time-reversal invariance, on the contrary, determines the overall phases and important symmetry properties of separate generalized parton distributions but does not relate them to each other.

In the following few sections, we will discuss only flavor-diagonal GPDs, i.e., the transitions not changing the internal quantum numbers of the incoming hadron in the final state. We will introduce the number of independent GPDs on a case-by-case basis. The general strategy can be found in Refs. [5, 68, 69, 70, 71]. The flavor-nondiagonal functions will be addressed later in Section 3.16.

3.2.3 Boost invariance of GPDs

As explained in Appendix B, and was mentioned in the introduction, Lorentz symmetry implies that GPDs do not change under the reparametrization of the light-cone vectors

$$n^{*\mu} \rightarrow \varrho n^{*\mu}, \quad n^\mu \rightarrow \varrho^{-1} n^\mu,$$

which implies in turn that they are also invariant under

$$k^- \rightarrow \varrho k^-, \quad k^+ \rightarrow \varrho^{-1} k^+. \quad (3.29)$$

One easily observes that indeed the definition of GPDs given above have this symmetry.

3.2.4 Spin-zero hadrons

For a spin-zero target there are two pairs of twist-two quark and gluon GPDs, which arise from the operator matrix elements of the even-parity and maximal-helicity operators introduced in Section 3.1. Namely,

$$\langle p_2 | \mathcal{O}^{qq}(-z^-, z^-) | p_1 \rangle = p^+ \int_{-1}^1 dx e^{-ixp^+z^-} H^q(x, \eta, \Delta^2), \quad (3.30)$$

$$\langle p_2 | \mathcal{T}_\mu^{qq}(-z^-, z^-) | p_1 \rangle = p^+ \int_{-1}^1 dx e^{-ixp^+z^-} H_T^q(x, \eta, \Delta^2) \frac{\Delta_\mu^\perp}{2M}, \quad (3.31)$$

$$\langle p_2 | \mathcal{O}^{gg}(-z^-, z^-) | p_1 \rangle = \frac{1}{4}(p^+)^2 \int_{-1}^1 dx e^{-ixp^+z^-} H^g(x, \eta, \Delta^2), \quad (3.32)$$

$$\langle p_2 | \mathcal{T}_{\mu\nu}^{gg}(-z^-, z^-) | p_1 \rangle = \frac{1}{4}(p^+)^2 \int_{-1}^1 dx e^{-ixp^+z^-} H_T^g(x, \eta, \Delta^2) \tau_{\mu\nu, \rho\sigma}^\perp \frac{\Delta^\rho \Delta^\sigma}{4M^2}. \quad (3.33)$$

The GPDs defined by the aligned parton-helicity operators are allowed due to nonzero orbital angular momentum between the initial and final state hadrons. They die out with vanishing momentum transfer $\Delta = 0$.

3.2.5 Spin-one-half hadrons

In case of a spin-one-half target it is convenient to express the expectation values of local operators in terms of spinor bilinears

$$\begin{aligned} b &= \bar{u}(p_2)u(p_1), & \tilde{b} &= \bar{u}(p_2)\gamma^5u(p_1), \\ h^\mu &= \bar{u}(p_2)\gamma^\mu u(p_1), & \tilde{h}^\mu &= \bar{u}(p_2)\gamma^\mu\gamma^5u(p_1), \\ t^{\mu\nu} &= \bar{u}(p_2)i\sigma^{\mu\nu}u(p_1), & \tilde{t}^{\mu\nu} &= \bar{u}(p_2)i\sigma^{\mu\nu}\gamma^5u(p_1). \end{aligned} \quad (3.34)$$

Obviously, the dual tensor bilinear $\tilde{t}^{\mu\nu}$ is obtained from $t^{\mu\nu}$ by contraction with the totally antisymmetric ϵ -tensor and can, therefore, be eliminated from the list of independent operators. Furthermore, equations of motion show that in each parity sector there are relations between the structures (3.34)

$$\begin{aligned} p^\mu b &= (M_{H_2} + M_{H_1})h^\mu - t^{\nu\mu}\Delta_\nu, & \Delta^\mu b &= -(M_{H_2} - M_{H_1})h^\mu - t^{\nu\mu}p_\nu, \\ \Delta^\mu \tilde{b} &= -(M_{H_2} + M_{H_1})\tilde{h}^\mu - \tilde{t}^{\nu\mu}p_\nu, & p^\mu \tilde{b} &= (M_{H_2} - M_{H_1})\tilde{h}^\mu - \tilde{t}^{\nu\mu}\Delta_\nu, \end{aligned} \quad (3.35)$$

where $M_{H_{1/2}}$ is the mass of the incoming/outgoing hadron. The ultimate result of this consideration suggests that matrix elements for spin-one-half target can be expressed in terms of a few Dirac bilinears chosen to be

$$h^\mu, \quad e^\mu = \frac{t^{\nu\mu}\Delta_\nu}{M_{H_2} + M_{H_1}}, \quad \tilde{h}^\mu, \quad \tilde{e}^\mu = -\frac{\Delta^\mu \tilde{b}}{M_{H_2} + M_{H_1}}. \quad (3.36)$$

For further use, we give the light-cone projection of two of Eqs. (3.35), namely,

$$b = (M_{H_2} + M_{H_1})\frac{h^+ - e^+}{p^+}, \quad \tilde{b} = -(M_{H_2} + M_{H_1})\frac{\tilde{e}^+}{\Delta^+}. \quad (3.37)$$

Thus, for the vector and axial-vector operators there are two independent Dirac structures [2], while for the maximal-helicity quark operator there are four structures [69]. The decomposition of the matrix elements for particular operators yields

$$\langle p_2 | \mathcal{O}^{qq}(-z^-, z^-) | p_1 \rangle = \int_{-1}^1 dx e^{-ixp^+z^-} \left\{ h^+ H^q(x, \eta, \Delta^2) + e^+ E^q(x, \eta, \Delta^2) \right\}, \quad (3.38)$$

$$\langle p_2 | \tilde{\mathcal{O}}^{qq}(-z^-, z^-) | p_1 \rangle = \int_{-1}^1 dx e^{-ixp^+z^-} \left\{ \tilde{h}^+ \tilde{H}^q(x, \eta, \Delta^2) + \tilde{e}^+ \tilde{E}^q(x, \eta, \Delta^2) \right\}, \quad (3.39)$$

$$\begin{aligned} \langle p_2 | \mathcal{T}_\mu^{qq}(-z^-, z^-) | p_1 \rangle &= \int_{-1}^1 dx e^{-ixp^+z^-} \left\{ t_{-\mu}^\perp H_T^q(x, \eta, \Delta^2) + \frac{p^+ e_\mu^\perp}{M_N} \tilde{H}_T^q(x, \eta, \Delta^2) \right. \\ &\quad \left. - \frac{1}{2M_N} (\Delta_\mu^\perp h^+ - \Delta^+ h_\mu^\perp) E_T^q(x, \eta, \Delta^2) - \frac{p^+ h_\mu^\perp}{2M_N} \tilde{E}_T^q(x, \eta, \Delta^2) \right\}. \end{aligned} \quad (3.40)$$

The Dirac bilinears used here are those introduced in Eq. (3.34). Note, that compared to Ref. [69], we have dropped the terms proportional to transverse components of p^μ since we have in mind a DIS-type frame where $p_\perp^\mu = 0$, see Appendix B.

For the gluonic GPDs, we have a basically identical parametrization

$$\langle p_2 | \mathcal{O}^{gg}(-z^-, z^-) | p_1 \rangle = \frac{1}{4} p^+ \int_{-1}^1 dx e^{-ixp^+z^-} \left\{ h^+ H^g(x, \eta, \Delta^2) + e^+ E^g(x, \eta, \Delta^2) \right\}, \quad (3.41)$$

$$\langle p_2 | \tilde{\mathcal{O}}^{gg}(-z^-, z^-) | p_1 \rangle = \frac{1}{4} p^+ \int_{-1}^1 dx e^{-ixp^+z^-} \left\{ \tilde{h}^+ \tilde{H}^g(x, \eta, \Delta^2) + \tilde{e}^+ \tilde{E}^g(x, \eta, \Delta^2) \right\}, \quad (3.42)$$

$$\begin{aligned} \langle p_2 | \mathcal{T}_{\mu\nu}^{gg}(-z^-, z^-) | p_1 \rangle &= \frac{1}{4} p^+ \int_{-1}^1 dx e^{-ixp^+z^-} \left\{ t^{+\perp}_\sigma H_T^g(x, \eta, \Delta^2) + \frac{p^+ e_\sigma^\perp}{M_N} \tilde{H}_T^g(x, \eta, \Delta^2) \right. \\ &\quad \left. - \frac{1}{2M_N} (\Delta_\sigma^\perp h^+ - \Delta^+ h_\sigma^\perp) E_T^g(x, \eta, \Delta^2) - \frac{p^+ h_\sigma^\perp}{2M_N} \tilde{E}_T^g(x, \eta, \Delta^2) \right\} \tau_{\mu\nu; \sigma\rho}^\perp \frac{-\Delta_\rho}{2M_N}. \end{aligned} \quad (3.43)$$

The decomposition for even and odd parity operators given here has been introduced in Ref. [5], while the maximal-helicity gluon sector was addressed in full in [69] (see also [73, 74] for an earlier discussion).

For further reference, we introduce a target-independent, boost-invariant form of GPDs. They formally have the same form as the parametrizations for the scalar target (3.30), for instance for the parity-even sector,

$$\langle p_2 | \mathcal{O}^{qq}(-z^-, z^-) | p_1 \rangle = p^+ \int_{-1}^1 dx e^{-ixp^+z^-} F^q(x, \eta, \Delta^2), \quad (3.44)$$

$$\langle p_2 | \mathcal{O}^{gg}(-z^-, z^-) | p_1 \rangle = \frac{(p^+)^2}{4} \int_{-1}^1 dx e^{-ixp^+z^-} F^g(x, \eta, \Delta^2), \quad (3.45)$$

however, the involved functions F^a ($a = q, g$) admit subsequent expansion in Dirac bilinears,

$$F^a(x, \eta, \Delta^2) = \frac{h^+}{p^+} H^a(x, \eta, \Delta^2) + \frac{e^+}{p^+} E^a(x, \eta, \Delta^2).$$

The odd parity and the maximal-helicity functions are deduced from the above by simple substitutions of operators and corresponding GPD functions.

3.2.6 A comment on gluonic matrix elements

Calculating Feynman diagrams, corresponding to a given process, one needs to work with gauge potentials rather than with the gauge covariant field strength tensors. The conversion formula is given by [4, 6]

$$\begin{aligned} \int \frac{dz^-}{2\pi} e^{ixz^-p^+} \langle p_2 | A_a^\mu(-z^-) A_b^\nu(z^-) | p_1 \rangle &= \frac{\delta_{ab}}{N_c^2 - 1} \frac{1}{(\eta - x - i0)(x + \eta - i0)} \\ &\times \left\{ \frac{1}{2} g_\perp^{\mu\nu} F^g(x, \eta, \Delta^2) - \frac{i}{2} \varepsilon_\perp^{\mu\nu} \tilde{F}^g(x, \eta, \Delta^2) + \tau_\perp^{\mu\nu; \rho\sigma} F_{T\rho\sigma}^g(x, \eta, \Delta^2) \right\}, \end{aligned} \quad (3.46)$$

in terms of the target-independent boost invariant gluonic GPDs, introduced in the preceding section.

3.2.7 Spin-one hadrons

Finally, let us address GPDs for spin-one hadrons, deuteron being the most obvious suspect. We take the polarization vectors for the incoming and outgoing deuteron as $\varepsilon_1^\mu \equiv \varepsilon^\mu(p_1)$ and $\varepsilon_2^\mu \equiv \varepsilon^\mu(p_2)$, respectively. We need to parametrize the non-local vector and axial-vector operators. Representing the tensor structures as $\varepsilon_{2\mu}^*(V^{\mu\nu}, A^{\mu\nu})\varepsilon_{1\nu}$ in these two cases, one should keep only the tensors which do not vanish when contracted with $\varepsilon_{1\mu}, \varepsilon_{2\nu}$, given the orthogonality conditions

$\varepsilon_1 \cdot p_1 = \varepsilon_2 \cdot p_2 = 0$ for the polarization vectors. With the constraints from parity invariance, one finds that $V^{\mu\nu}$ contains five linear independent tensor structures [75]

$$g_{\beta\alpha}, \quad p_\beta n_\alpha, \quad n_\beta p'_\alpha, \quad p_\beta p'_\alpha, \quad n_\beta n_\alpha.$$

Similarly, the $A^{\mu\nu}$ tensors are linear combinations of the seven tensor structures

$$\begin{aligned} & \varepsilon_{\mu\nu\beta\alpha} p^\mu p'^\nu, \quad \varepsilon_{\mu\nu\beta\alpha} n^\mu p^\nu, \quad \varepsilon_{\mu\nu\beta\alpha} n^\mu p'^\nu, \quad \varepsilon_{\mu\nu\rho\beta} p^\mu p'^\nu n^\rho n_\alpha, \quad \varepsilon_{\mu\nu\rho\beta} p^\mu p'^\nu n^\rho p'_\alpha, \\ & \varepsilon_{\mu\nu\rho\alpha} p^\mu p'^\nu n^\rho n_\beta, \quad \varepsilon_{\mu\nu\rho\alpha} p^\mu p'^\nu n^\rho p_\beta. \end{aligned}$$

Using the Schouten identity, see Appendix A, one can show that only four out of these seven are linearly independent.

Thus, the generalized parton distributions for a deuteron target are defined as [75, 76]

$$\begin{aligned} \langle p_2 | \mathcal{O}^{qq}(-z^-, z^-) | p_1 \rangle &= \int_{-1}^1 dx e^{-ixp^+z^-} \left\{ -p^+(\varepsilon_2^* \cdot \varepsilon_1) H_1^q(x, \eta, \Delta^2) \right. \\ &\quad + (\varepsilon_1^+(\varepsilon_2^* \cdot p) + \varepsilon_2^{+*}(\varepsilon_1 \cdot p)) H_2^q(x, \eta, \Delta^2) - \frac{p^+}{2M_D^2} (\varepsilon_2^* \cdot p)(\varepsilon_1 \cdot p) H_3^q(x, \eta, \Delta^2) \\ &\quad \left. + (\varepsilon_1^+(\varepsilon_2^* \cdot p) - \varepsilon_2^{+*}(\varepsilon_1 \cdot p)) H_4^q(x, \eta, \Delta^2) + \frac{1}{p^+} \left(4M_D^2 \varepsilon_1^+ \varepsilon_2^{+*} + \frac{1}{3}(p^+)^2 (\varepsilon_2^* \cdot \varepsilon_1) \right) H_5^q(x, \eta, \Delta^2) \right\}, \end{aligned} \quad (3.47)$$

$$\begin{aligned} \langle p_2 | \tilde{\mathcal{O}}^{qq}(-z^-, z^-) | p_1 \rangle &= \int_{-1}^1 dx e^{-ixp^+z^-} \left\{ M_D^2 \varepsilon_{2\mu}^* \varepsilon_{1\nu} \tilde{H}_1^q(x, \eta, \Delta^2) \right. \\ &\quad - \Delta_\mu (\varepsilon_{1\nu}(\varepsilon_2^* \cdot p) + \varepsilon_{2\nu}^*(\varepsilon_1 \cdot p)) \tilde{H}_2^q(x, \eta, \Delta^2) \\ &\quad \left. - \Delta_\mu (\varepsilon_{1\nu}(\varepsilon_2^* \cdot p) - \varepsilon_{2\nu}^*(\varepsilon_1 \cdot p)) \tilde{H}_3^q(x, \eta, \Delta^2) - \Delta_\mu (\varepsilon_{1\nu} \varepsilon_2^{+*} + \varepsilon_{2\nu}^* \varepsilon_1^+) \tilde{H}_4^q(x, \eta, \Delta^2) \right\} \frac{i}{M_D^2} \varepsilon^{+\rho\mu\nu} p_\rho. \end{aligned} \quad (3.48)$$

Finally, the gluon distributions in the deuteron are parametrized analogously to quark GPDs. They can be deduced from the above definitions by replacing the bilocal quark operators by the gluon ones, i.e., $\mathcal{O}^{qq} \rightarrow \mathcal{O}^{gg}$, changing the GPDs on the right-hand side, H^q to $\frac{1}{4}p^+H^g$, as was done in Eq. (3.41). The extra factor of p^+ is needed to have a boost-independent definition of GPDs. Note that H_i^g 's are even and \tilde{H}_i^g 's are odd in momentum fraction x . Other symmetry properties will be established below.

3.2.8 Implications of time reversal and hermiticity

Now we are in a position to discuss the implications of the time-reversal invariance on the symmetry properties of GPDs. The time-reversal operation involves the complex conjugation of states. This can be easily observed in a simple example of the non-relativistic Schrödinger equation where the time derivative is accompanied by the imaginary unity. Thus the time-reversal operator \mathcal{T} , defined on the Hilbert space of particle states, induces a complex conjugation on any c -function standing to its right, $\mathcal{T}f = f^*\mathcal{T}$. As a consequence, it is an antiunitary operation [77]

$$\langle \Omega_2 | \mathcal{T}^\dagger \mathcal{T} | \Omega_1 \rangle = \langle \Omega_2 | \Omega_1 \rangle^* = \langle \Omega_1 | \Omega_2 \rangle. \quad (3.49)$$

This equality can be easily verified by expanding the state $|\Omega_2\rangle$ in a complete basis of states. This is to be contrasted with the action of a unitary operator \mathcal{U} which obeys $\langle \Omega_1 | \mathcal{U}^\dagger \mathcal{U} | \Omega_2 \rangle = \langle \Omega_1 | \Omega_2 \rangle$, for instance the operator of spatial parity $\mathcal{U} = \mathcal{P}$.

Consider the matrix element of the \mathbf{z}_\perp -dependent bilocal operator

$$\mathcal{O}(-z^-, -\mathbf{z}_\perp; z^-, \mathbf{z}_\perp) = \Phi_\infty^\dagger(-z^-, -\mathbf{z}_\perp) \Gamma \Phi_\infty(z^-, \mathbf{z}_\perp)$$

built by sandwiching the Dirac/Lorentz structure Γ between the elementary fields Φ with the Wilson lines attached to them, in order to make the operator gauge invariant. Assuming covariant gauges in which the gauge potential is local and vanishes at infinity, we can write

$$\Phi_\infty(z^-, \mathbf{z}_\perp) = [\infty, \mathbf{z}_\perp; z^-, \mathbf{z}_\perp] \Phi(z^-, \mathbf{z}_\perp),$$

similarly to the notation introduced in Eq. (2.57). For the operator matrix element, the complex-conjugated version of Eq. (3.49) implies

$$\begin{aligned} \langle \Omega_2 | \mathcal{O}(-z^-, -\mathbf{z}_\perp; z^-, \mathbf{z}_\perp) | \Omega_1 \rangle &= \langle \Omega_2 | \mathcal{T}^\dagger \mathcal{T} \mathcal{O}(-z^-, -\mathbf{z}_\perp; z^-, \mathbf{z}_\perp) | \Omega_1 \rangle^* \\ &= \langle \Omega_2 | \mathcal{T}^\dagger \mathcal{T} \Phi_\infty^\dagger(-z^-, -\mathbf{z}_\perp) \mathcal{T}^\dagger \Gamma^* \mathcal{T} \Phi_\infty(z^-, \mathbf{z}_\perp) \mathcal{T}^\dagger \mathcal{T} | \Omega_1 \rangle^*. \end{aligned} \quad (3.50)$$

In the second line, we “commuted” \mathcal{T} through Γ and inserted two more antiunitary operations. They induce two extra complex conjugations compensating each other in the total result. Note, that the light-ray operator lives on the light-cone. Since the light-cone coordinate is a combination of the usual time and coordinate, and the latter will not be transformed under the time-reversal, thus (inconveniently) changing the minus coordinate into the plus one, it is instructive to augment the above equation (3.50) by inserting (three times) the unitary operation of spatial parity inversion $\mathcal{P}^\dagger \mathcal{P} = 1$. Thus, it is convenient to discuss the transformation of the light-cone correlation functions with respect to the combined time and spatial parity reversal. These discrete operations act in the following way on the quark

$$\begin{aligned} \mathcal{T} \psi(z^0, \mathbf{z}) \mathcal{T}^\dagger &= \eta_T T \psi(-z^0, \mathbf{z}), & \mathcal{P} \psi(z^0, \mathbf{z}) \mathcal{P}^\dagger &= \eta_P \gamma^0 \psi(z^0, -\mathbf{z}), \\ \mathcal{T} \bar{\psi}(z^0, \mathbf{z}) \mathcal{T}^\dagger &= \eta_T^* \bar{\psi}(-z^0, \mathbf{z}) T, & \mathcal{P} \bar{\psi}(z^0, \mathbf{z}) \mathcal{P}^\dagger &= \eta_P^* \bar{\psi}(z^0, -\mathbf{z}) \gamma^0, \end{aligned}$$

and gluon fields

$$\mathcal{T} A_a^\mu(z^0, \mathbf{z}) \mathcal{T}^\dagger = A_a^a(-z^0, \mathbf{z}), \quad \mathcal{P} A_a^\mu(z^0, \mathbf{z}) \mathcal{P}^\dagger = A_a^a(z^0, -\mathbf{z}).$$

Here $T = -i\gamma^5 C$ where C is the charge-conjugation matrix from Appendix A and $|\eta_i|^2 = 1$. Finally, the combined reversal of the time and spatial parity of a single-particle state with the four-momentum p^μ and spin four-vector s^μ is

$$\mathcal{T} \mathcal{P} |p^\mu, s^\mu\rangle = e^{i\chi(s)} |p^\mu, -s^\mu\rangle, \quad (3.51)$$

where the phase factor $\chi(s) = \chi_0 + \pi(s - s^z)$ depends on the intrinsic parity χ_0 of the state, its spin s and spin projection s^z on the quantization axis. Hermiticity, on the other hand, leads to

$$\langle \Omega_2 | \Phi_\infty^\dagger(-z^-, -\mathbf{z}_\perp) \Gamma \Phi_\infty(z^-, \mathbf{z}_\perp) | \Omega_1 \rangle^* = \langle \Omega_1 | \Phi_{-\infty}^\dagger(z^-, \mathbf{z}_\perp) \Gamma^\dagger \Phi_{-\infty}(-z^-, \mathbf{z}_\perp) | \Omega_2 \rangle. \quad (3.52)$$

As a simple demonstration of the implications of the above transformations for corresponding GPDs, let us see what is the result of their action on the bilocal light-cone quark vector operator (in the light-cone gauge), with $\Phi = \psi$ and $\Gamma = \gamma^0 \gamma^+$, sandwiched between the hadronic states. The space-time reversal gives

$$\begin{aligned} \langle p_2, s_2 | \bar{\psi}(-z^-) \gamma^+ \psi(z^-) | s_1, p_1 \rangle &= e^{i[\chi(s_2) - \chi(s_1)]} \langle p_2, -s_2 | \bar{\psi}(-z^-) T^\dagger \gamma^0 (\gamma^+)^* T \gamma^0 \psi(z^-) | -s_1, p_1 \rangle^* \\ &= e^{i[\chi(s_2) - \chi(s_1)]} \langle p_1, -s_1 | \bar{\psi}(-z^-) C (\gamma^+)^T C \psi(z^-) | -s_2, p_2 \rangle \\ &= e^{i[\chi(s_2) - \chi(s_1)]} \langle p_1, -s_2 | \bar{\psi}(-z^-) \gamma^+ \psi(z^-) | -s_2, p_2 \rangle. \end{aligned} \quad (3.53)$$

On the other hand, the hermiticity immediately implies that

$$\langle p_2, s_2 | \bar{\psi}(-z^-) \gamma^+ \psi(z^-) | s_1, p_1 \rangle^* = \langle p_1, s_1 | \bar{\psi}(z^-) \gamma^+ \psi(-z^-) | s_2, p_2 \rangle. \quad (3.54)$$

These transformations lead to the following conditions on GPDs [7, 69].

- Spin-zero target: The time-reversal and hermiticity result in

$$H^q(x, \eta, \Delta^2) = H^q(x, -\eta, \Delta^2), \quad (H^q)^*(x, \eta, \Delta^2) = H^q(x, -\eta, \Delta^2), \quad (3.55)$$

respectively. The time reversal changes the sign of η because the initial and final state are interchanged. Thus, the GPDs are real functions and they are even under the sign change of the skewness parameter. The last property has profound implications on the functional dependence of GPDs on the skewness, which we will discuss below in Section 3.5.

- Spin-one-half target:

$$F^q(x, \eta, \Delta^2) = F^q(x, -\eta, \Delta^2) \quad (3.56)$$

for $F = H, \tilde{H}, E, \tilde{E}, H_T, \tilde{H}_T, E_T$, and

$$\tilde{E}_T^q(x, \eta, \Delta^2) = -\tilde{E}_T^q(x, -\eta, \Delta^2). \quad (3.57)$$

Notice that the spin-dependent phases $\chi(s_i)$ in Eq. (3.53) cancel with analogous factors arising from the transformation of hadronic wave functions in the parametrization of the matrix elements when one converts the Dirac bispinors of negative spin u_{-s} to the one with positive spin u_s . Taking the complex conjugates of Eqs. (3.38) – (3.40) gives, on the other hand,

$$(F^q)^*(x, \eta, \Delta^2) = F^q(x, -\eta, \Delta^2), \quad (3.58)$$

for all distributions except \tilde{E}_T^q . For the latter, one gets

$$(\tilde{E}_T^q)^*(x, \eta, \Delta^2) = -\tilde{E}_T^q(x, -\eta, \Delta^2). \quad (3.59)$$

Taking these constraints together we see that all eight distributions are required to be real-valued as a consequence of the time-reversal invariance. In other words, this symmetry fixes the phases of the distributions, but does not require any linear combination of them to be zero.

The result that E_T^q and \tilde{E}_T^q have opposite behavior under time reversal, (see Eqs. (3.56) and (3.57)), could have been anticipated from the inspection of the tensors that multiply these GPDs in their definition (3.40). Namely, Δ changes sign under $p_1 \leftrightarrow p_2$ but p does not. As we have seen, this does not constrain either of these distributions to be zero. It is interesting to note that this situation changes if instead of the bilocal quark-antiquark operator in Eq. (3.40) one considers the local one,

$$\langle p_2 | \bar{\psi}(0) i\sigma^{\mu\nu} \psi(0) | p_1 \rangle. \quad (3.60)$$

The time-reversal invariance does imply now that the form factor multiplying the fourth bilinear, $\bar{u}(p_2)(\gamma^\mu p^\nu - p^\mu \gamma^\nu)u(p_1)$, must vanish. Since the result must not depend on η , one finds

$$\int_{-1}^1 dx \tilde{E}_T^q(x, \eta, \Delta^2) = 0. \quad (3.61)$$

Thus, one finds that, by time reversal invariance, there are only three independent form factors for the local matrix element (3.60) but four independent generalized quark distributions to describe the bilocal matrix element (3.40). In other words, the first moment of \tilde{E}_T^q is zero by the time reversal symmetry, but its higher moments, $\int dx x^n \tilde{E}_T^q(x, \eta, \Delta^2)$ with $n > 0$ are nonzero. In fact, the higher moments correspond to local matrix elements as in (3.60) but contain additional derivatives. The corresponding Lorentz tensors have rank larger than two, and allow more than three independent form factors.

- Spin-one target: combining hermiticity and time-reversal conditions one finds that all nine GPDs are real. However, their behavior under time reversal is not uniform and one gets [75]:

$$\begin{aligned} H_i^q(x, \eta, \Delta^2) &= H_i^q(x, -\eta, \Delta^2), & i &= 1, 2, 3, 5, \\ H_4^q(x, \eta, \Delta^2) &= -H_4^q(x, -\eta, \Delta^2), \\ \tilde{H}_i^q(x, \eta, \Delta^2) &= \tilde{H}_i^q(x, -\eta, \Delta^2), & i &= 1, 2, 4, \\ \tilde{H}_3^q(x, \eta, \Delta^2) &= -\tilde{H}_3^q(x, -\eta, \Delta^2). \end{aligned} \quad (3.62)$$

As a consequence of the antisymmetry of GPDs H_4^q and \tilde{H}_3^q under the reversal of the skewness parameter, one finds the sum rules [75]

$$\int_{-1}^1 dx H_4^q(x, \eta, \Delta^2) = \int_{-1}^1 dx \tilde{H}_3^q(x, \eta, \Delta^2) = 0. \quad (3.63)$$

The behavior of gluon GPDs under the time reversal is the same as in (3.62) for the corresponding quark distributions.

Let us reiterate the findings of this section. For non-forward kinematics the time-reversal invariance fixes the overall phases of generalized parton distributions and determines their symmetry properties with respect to the skewness sign change, but it does not reduce the number of GPDs deduced from the generic counting of allowed structures in the matrix elements based on the number of non-vanishing parton-hadron helicity amplitudes.

3.3 Forward limit

Generalized parton distributions satisfy a number of remarkable constraints which make them partially ‘‘known’’ in certain kinematical regions. Indeed, we observe a close analogy of the operator definition of GPDs with that for the conventional parton densities discussed in the introduction. Obviously, the former will reduce to the latter when we set the t -channel momentum transfer to be zero, i.e., take $\Delta = 0$. Let us analyze this reduction for targets of different spins.

3.3.1 Spin-zero hadrons

The parton distributions in spin-zero targets are defined by a single function for each operator matrix element. The leading twist densities are

$$\langle p | \mathcal{O}^{qq}(0, z^-) | p \rangle = 2p^+ \int_0^1 dx \left\{ q(x) e^{-ixp^+ z^-} - \bar{q}(x) e^{ixp^+ z^-} \right\}, \quad (3.64)$$

$$\langle p | \mathcal{O}^{gg}(0, z^-) | p \rangle = (p^+)^2 \int_0^1 dx \left\{ e^{-ixp^+ z^+} + e^{ixp^+ z^-} \right\} x g(x). \quad (3.65)$$

Notice that for practical purposes the quark $q(x)$ and antiquark $\bar{q}(x)$ distributions, both defined for positive momentum fractions $x > 0$, can be combined together into a single functions $f_q(x)$ which “lives” in the interval $-1 \leq x \leq 1$ as demonstrated in Eq. (2.63). The quark distributions are measurable in high-energy experiments like deeply inelastic scattering and Drell-Yan lepton pair production. In case of the pion target, the fits of parton distributions to available experimental data can be found in Refs. [78, 79]. Other (pseudo)scalar targets arise if nuclei are taken into consideration as possible targets. The spin-zero GPDs (3.30) – (3.33) yield, via the forward limiting procedure $\Delta \rightarrow 0$ such that $p_1 = p_2 \equiv p$, the conventional parton distributions,

$$H^q(x, 0, 0) = f^q(x) = q(x)\theta(x) - \bar{q}(-x)\theta(-x).$$

Analogous relations hold for gluons with obvious substitutions of $q(x)$ by $xg(x)$ and $\bar{q}(-x)$ by $xg(-x)$.

3.3.2 Spin-one-half hadrons

For non-zero spin targets—spin-one-half being the first nontrivial example—one is allowed for polarized quark Δq and antiquark $\Delta\bar{q}$ densities in addition to unpolarized distributions $q(x)$ and $\bar{q}(x)$ due to the existence of the spin pseudovector s^μ . More than this, the set of parton distributions for spin-one-half targets takes the advantage of the entire variety of the available twist-two operators introduced in Section 3.1 and leads to the introduction of the chiral-odd quark densities $\delta q(x)$, which do not show up though in conventional deeply inelastic lepton-hadron experiments. The complete set of the operator matrix elements is parametrized as follows,

$$\langle p | \mathcal{O}^{qq}(0, z^-) | p \rangle = 2p^+ \int_0^1 dx \left\{ q(x)e^{-ixp^+z^-} - \bar{q}(x)e^{ixp^+z^-} \right\}, \quad (3.66)$$

$$\langle p | \tilde{\mathcal{O}}^{qq}(0, z^-) | p \rangle = 2s^+ \int_0^1 dx \left\{ \Delta q(x)e^{-ixp^+z^-} + \Delta\bar{q}(x)e^{ixp^+z^-} \right\}, \quad (3.67)$$

$$\langle p | \mathcal{T}_\mu^{qq}(0, z^-) | p \rangle = 2\tilde{s}_\mu^\perp \int_0^1 dx \left\{ \delta q(x)e^{-ixp^+z^-} - \delta\bar{q}(x)e^{ixp^+z^-} \right\}, \quad (3.68)$$

making use of the nucleon polarization vector s^μ . Here we defined also the “dual” spin vector $\tilde{s}_\mu^\perp = i\varepsilon_{\mu\nu}^\perp s_\perp^\nu$ since the conventional definition of the transversity distribution involves the Dirac matrix $\sigma^{+\perp}\gamma^5$ rather than $\sigma^{+\perp}$ used in our Eq. (3.68). Thus, the forward limit provides a restriction on the GPDs H and \tilde{H} :

$$H(x, 0, 0) = f^q(x) = q(x)\theta(x) - \bar{q}(-x)\theta(-x), \quad (3.69)$$

$$\tilde{H}(x, 0, 0) = \Delta f^q(x) = \Delta q(x)\theta(x) + \Delta\bar{q}(-x)\theta(-x), \quad (3.70)$$

where we introduced again the functions $(f_q, \Delta f_q)$ having support for positive and negative momentum fractions. As it is clear from these conventions, the antiquark distributions are determined by the obvious relations $f^q(-x) = -\bar{q}(x)$ and $\Delta f^q(-x) = \Delta\bar{q}(x)$ for the chiral-even parity-even and odd cases, respectively. They have to be complemented by the equation

$$\delta\bar{q}(x) = -\delta f^q(-x)$$

for the chiral odd density. No constraints arise on GPDs E and \tilde{E} , since their Dirac structure vanishes as $\Delta \rightarrow 0$.

Recalling the definitions of the gluonic distributions,

$$\langle p | \mathcal{O}^{gg}(0, z^-) | p \rangle = (p^+)^2 \int_0^1 dx \left\{ e^{-ixp^+z^+} + e^{ixp^+z^-} \right\} xg(x), \quad (3.71)$$

$$\langle p | \tilde{\mathcal{O}}^{gg}(0, z^-) | p \rangle = s^+ p^+ \int_0^1 dx \left\{ e^{-ixp^+z^-} - e^{ixp^+z^-} \right\} x\Delta g(x), \quad (3.72)$$

we get for gluon GPDs

$$H^g(x, 0, 0) = xg(x)\theta(x) - xg(-x)\theta(-x), \quad (3.73)$$

$$\tilde{H}^g(x, 0, 0) = x\Delta g(x)\theta(x) + x\Delta g(-x)\theta(-x), \quad (3.74)$$

and no reduction formula for the maximal-helicity gluon sector since the forward operator matrix elements of the operator $\mathcal{T}_{\mu\nu}^g$ between the spin-one-half hadronic states vanishes identically by means to quark-hadron helicity conservation. In the off-forward case it is lifted due to the injection of a non-zero orbital momentum of parton via the nonvanishing momentum transfer Δ .

The unpolarized quark distribution is customarily separated into valence and sea contributions. Namely, for unpolarized functions one writes

$$f^q(x) = f^{q,\text{val}}(x) + f^{q,\text{sea}}(x), \quad (3.75)$$

with

$$f^{q,\text{val}}(x) = q^{\text{val}}(x)\theta(x) \equiv \{q(x) - \bar{q}(x)\}\theta(x), \quad f^{q,\text{sea}}(x) = \bar{q}(x)\theta(x) - \bar{q}(-x)\theta(-x).$$

Analogously, one defines valence and sea quark distributions in the polarized case

$$\Delta f^q(x) = \Delta f^{q,\text{val}}(x) + \Delta f^{q,\text{sea}}(x), \quad (3.76)$$

with

$$\Delta f^{q,\text{val}}(x) = \Delta q^{\text{val}}(x)\theta(x) \equiv \{\Delta q(x) - \Delta \bar{q}(x)\}\theta(x), \quad \Delta f^{q,\text{sea}}(x) = \bar{\Delta}q(x)\theta(x) + \Delta \bar{q}(-x)\theta(-x).$$

Except for transversity distribution $\delta q(x)$, the nucleon parton distributions are well constrained by experimental data in a wide range of momentum fractions x . The fits to world data can be found in Refs. [80, 81, 82] and [83, 84, 85, 86, 87] for the unpolarized and polarized parton densities, respectively.

3.3.3 Spin-one hadrons

Finally, let us comment on the forward limit of the spin-one GPDs. Recall, that in the parton model there are three independent structure functions in deep inelastic scattering off a deuteron, i.e., F_1 , b_1 , g_1 , whose probabilistic interpretation in terms of quark densities reads [88]

$$\begin{aligned} F_1(x) &= \frac{1}{6} \sum_q Q_q^2 [q^1(x) + q^{-1}(x) + q^0(x) + \bar{q}^1(x) + \bar{q}^{-1}(x) + \bar{q}^0(x)], \\ b_1(x) &= \frac{1}{4} \sum_q Q_q^2 [2q^0(x) - q^1(x) - q^{-1}(x) + 2\bar{q}^0(x) - \bar{q}^1(x) - \bar{q}^{-1}(x)], \\ g_1(x) &= \frac{1}{2} \sum_q Q_q^2 [q_\uparrow^1(x) - q_\uparrow^{-1}(x) + \bar{q}_\uparrow^1(x) - \bar{q}_\uparrow^{-1}(x)]. \end{aligned} \quad (3.77)$$

Here $q_{\uparrow(\downarrow)}^\lambda(x)$ represents the probability to find a quark with momentum fraction x and positive (negative) helicity in a deuteron target of helicity λ . The unpolarized quark densities q^λ are defined as $q^\lambda(x) = q_\uparrow^\lambda(x) + q_\downarrow^\lambda(x)$. From parity considerations, one has $q_\uparrow^\lambda = q_\downarrow^{-\lambda}$. The densities for antiquarks are defined in a similar way. Note, that the probabilistic interpretation for F_1 and g_1 is similar to that in the spin-one-half case. However, the function b_1 does not appear for spin-one-half targets. In the forward limit, the only structures in Eq. (3.47) that survive are those proportional to H_1 , H_5 and \tilde{H}_1 , because in that limit we have $\Delta = 0$ and $\varepsilon_1 \cdot p = \varepsilon_2 \cdot p = 0$. This yields

$$\begin{aligned} H_1^q(x, 0, 0) &= \frac{1}{3} [q^1(x) + q^{-1}(x) + q^0(x)] \theta(x) - \frac{1}{3} [\bar{q}^1(-x) + \bar{q}^{-1}(-x) + \bar{q}^0(-x)] \theta(-x), \\ H_5^q(x, 0, 0) &= \frac{1}{2} [2q^0(x) - q^1(x) - q^{-1}(x)] \theta(x) - \frac{1}{2} [2\bar{q}^0(-x) - \bar{q}^1(-x) - \bar{q}^{-1}(-x)] \theta(-x), \quad (3.78) \\ \tilde{H}_1^q(x, 0, 0) &= [q_\uparrow^1(x) - q_\uparrow^{-1}(x)] \theta(x) \\ &\quad + [\bar{q}_\uparrow^1(-x) - \bar{q}_\uparrow^{-1}(-x)] \theta(-x). \end{aligned}$$

Note that the sum rule [75]

$$0 = \int_{-1}^1 dx H_5^q(x, 0, 0) = \frac{1}{2} \int_0^1 dx [2q^0(x) - q^1(x) - q^{-1}(x) - 2\bar{q}^0(x) + \bar{q}^1(x) + \bar{q}^{-1}(x)], \quad (3.79)$$

corresponding to the parton model result $\int_0^1 b_1(x) = 0$ of Refs. [89, 90, 91], obtained under the assumption that the quark sea $q - \bar{q}$ does not contribute to this integral, and the vanishing of the integral

$$\int_{-1}^1 dx \tilde{H}_4^q(x, 0, 0) = 0, \quad (3.80)$$

follow from the fact that the local limit of the matrix element of the light-cone operator cannot involve the “auxiliary” light-like vector n^ν in its parametrization.

3.4 Form factors

Another interesting limit of GPDs reduces them to the hadronic form factors. We already discussed form factors in the introductory section. Here we elaborate on this issue in greater detail, starting from spin-zero hadrons and finishing with the spin-one deuteron. Form factors arise as coefficients in the expansion of matrix elements of local currents in Dirac/Lorentz structures. It is useful to define form factors for each particular quark flavor. The lowest Lorentz-spin local operators are the electromagnetic current

$$j_q^\mu(z) = \bar{\psi}_q(z) \gamma^\mu \psi_q(z), \quad (3.81)$$

and the axial-vector current available through weak interaction of leptons with hadrons

$$j_q^{5\mu}(z) = \bar{\psi}_q(z) \gamma^\mu \gamma^5 \psi_q(z). \quad (3.82)$$

The tensor chiral-odd current is not directly measurable with any known probe.

3.4.1 Spin-zero hadrons

A spin-zero hadron has only one form factor

$$\langle p_2 | j_q^\mu(0) | p_1 \rangle = p^\mu F^q(\Delta^2). \quad (3.83)$$

The reduction formula, obviously, is given by

$$\int_{-1}^1 dx H^q(x, \eta, \Delta^2) = F^q(\Delta^2). \quad (3.84)$$

The disappearance of the skewness dependence on the right-hand side of this sum rule, as well as for other targets discussed below, will be explained in Section 3.5. The well-known example of a spin-zero “target” is the charged pion, in which case

$$F_{\pi^+} = Q_u F^u - Q_d F^d. \quad (3.85)$$

3.4.2 Spin-one-half hadrons

Starting with spin-one-half hadrons, the matrix elements of the axial-vector current are also non-zero. Analogously to the proton matrix elements of the electromagnetic current (2.15), we define form factors for each species of quarks separately

$$\langle p_2 | j_q^\mu(0) | p_1 \rangle = h^\mu F_1^q(\Delta^2) + e^\mu F_2^q(\Delta^2), \quad (3.86)$$

and analogously for the axial-vector current

$$\langle p_2 | j_q^{5\mu}(0) | p_1 \rangle = \tilde{h}^\mu G_A^q(\Delta^2) + \tilde{e}^\mu G_P^q(\Delta^2), \quad (3.87)$$

with axial G_A and pseudoscalar G_P form factors multiplied by the Dirac bilinears, introduced in Section 3.2.5. Note, that in the case of axial current one can also write a term $\Delta_\nu \bar{u}(p_2) \sigma^{\nu\mu} \gamma^5 u(p_1)$ which is similar to the electric dipole moment of the nucleon. However, it is forbidden by the time-reversal invariance.

Thus, the first moments of the twist-two GPDs are equal to the corresponding quark form factors in the nucleon

$$\begin{aligned} \int_{-1}^1 dx H^q(x, \eta, \Delta^2) &= F_1^q(\Delta^2), & \int_{-1}^1 dx E^q(x, \eta, \Delta^2) &= F_2^q(\Delta^2), \\ \int_{-1}^1 dx \tilde{H}^q(x, \eta, \Delta^2) &= G_A^q(\Delta^2), & \int_{-1}^1 dx \tilde{E}^q(x, \eta, \Delta^2) &= G_P^q(\Delta^2), \end{aligned} \quad (3.88)$$

i.e., Dirac, Pauli, axial, and pseudoscalar form factors, respectively. The conventional proton F_i^p and neutron F_i^n electromagnetic form factors are given in terms of quark ones

$$F_i^p = Q_u F_i^u + Q_d F_i^d, \quad F_i^n = Q_d F_i^u + Q_u F_i^d, \quad (3.89)$$

where in the second relation we used the isospin symmetry to express quark operator matrix elements in the neutron in terms of the ones in the proton, $\langle n | \bar{d}d | n \rangle = \langle p | \bar{u}u | p \rangle$ and $\langle n | \bar{u}u | n \rangle = \langle p | \bar{d}d | p \rangle$. Analogously we define decompositions for other form factors. The normalization of the proton and neutron form factors at zero recoil are given in Table 1.

Thus, the valence u - and d -quark form factors⁷ can be extracted from the proton and neutron form factors via the formulas

$$F_i^{u,\text{val}}(\Delta^2) = 2F_i^p(\Delta^2) + F_i^n(\Delta^2), \quad F_i^{d,\text{val}}(\Delta^2) = F_i^p(\Delta^2) + 2F_i^n(\Delta^2). \quad (3.90)$$

⁷The name reflects the relation of these particular combination of hadronic form factors at zero recoil to the valence-quark sum rules for forward parton densities.

i	$F_1^i(0)$	$F_2^i(0)$	$G_A^{(3)i}(0)$	$G_P^{(3)i}(0)$
(p)roton	1	$\kappa^p = 1.79$	$g_A^{(3)p} = 1.267$	$4g_A^{(3)p}(0)M_N^2/m_\pi^2$
(n)eutron	0	$\kappa^n = -1.93$	$g_A^{(3)n} = -1.267$	$4g_A^{(3)n}(0)M_N^2/m_\pi^2$

Table 1: Normalization of nucleon electromagnetic and isovector axial and pseudoscalar form factors. An exact isospin symmetry ($M_N = M_p = M_n$) is implied for the axial form factors such that the isovector axial constants coincide up to an overall sign, $g_A^{(3)} = g_A^{(3)p} = -g_A^{(3)n}$.

The latter are known from experimental measurements accessing the Sachs electric and magnetic form factors, introduced earlier in Section 2.2.2. The latter are related to the above Dirac and Pauli form factors by a set of covariant equations

$$G_E^i(\Delta^2) = F_1^i(\Delta^2) + \frac{\Delta^2}{4M^2} F_2^i(\Delta^2), \quad G_M^i(\Delta^2) = F_1^i(\Delta^2) + F_2^i(\Delta^2). \quad (3.91)$$

and can be parametrized by dipole formulas in the small- Δ^2 region

$$\begin{aligned} G_E^p(\Delta^2) &= \frac{1}{1 + \kappa_p} G_M^p(\Delta^2) = \frac{1}{\kappa_n} G_M^n(\Delta^2) \equiv G_D(\Delta^2) = \left(1 - \frac{\Delta^2}{0.71 \text{ GeV}^2}\right)^{-2}, \\ G_E^n(\Delta^2) &= 0. \end{aligned} \quad (3.92)$$

Here we introduced the nucleon dipole form factor G_D , which is used as a first order approximation for the Δ^2 dependence. Available experimental data are rather well fitted by this simple form with certain deviations at higher momentum transfers $|\Delta^2| > 2 \text{ GeV}^2$. Note that we have set the neutron electric form factor equal to zero since at small $|\Delta^2|$ it vanishes as a first power of Δ^2 with $-1/6$ times the neutron charge radius r_n^2 as a coefficient, which is quite small, $r_n^2 \approx -0.113 \text{ fm}^2$. A modern summary of experimental results can be found in Ref. [92].

The parametrizations for the sea-quark form factors, dubbed for their connection to the first moment of the sea quark parton distributions, are guided by the counting rules, discussed later in Section 6.3.2. A plausible model ansatz then reads in terms of Sachs form factors

$$G_E^{\text{sea}}(\Delta^2) = \frac{1}{1 + \kappa_{\text{sea}}} G_M^{\text{sea}}(\Delta^2) = \left(1 - \frac{\Delta^2}{m_{\text{sea}}^2}\right)^{-3}, \quad (3.93)$$

with yet another mass cutoff m_{sea} . The slope of F_1^{sea} is given by $B_{\text{sea}} = \partial F_1^{\text{sea}} / \partial \Delta^2|_{\Delta^2=0} = 3/m_{\text{sea}}^2 - \kappa_{\text{sea}}/4M^2$.

The axial form factors are given analogously by

$$G_A^{i,\text{val}}(\Delta^2) = \left(1 - \frac{\Delta^2}{1.1 \text{ GeV}^2}\right)^{-2}, \quad G_A^{\text{sea}}(\Delta^2) = \left(1 - \frac{B_A}{3} \Delta^2\right)^{-3}, \quad (3.94)$$

where i runs over u - and d -quark species. The first of these relations is driven by experimental data, while the latter is merely a rough model. The slope B_A is considered as a free parameter, which should be fixed from experimental data. Last but not least, the isovector pseudoscalar

form factor, having the flavor structure for the proton $G_P^{(3)} = \langle p | \bar{u}u - \bar{d}d | p \rangle$, is dominated by the pion-pole contribution,

$$G_P^{(3)}(\Delta^2) \approx \frac{4g_A^{(3)} M_N^2}{m_\pi^2 - \Delta^2}, \quad (3.95)$$

valid at $|\Delta| \sim m_\pi \approx 0.14$ GeV and the residue of the pole being proportional to the triplet axial constant $g_A^{(3)}$.

3.4.3 Spin-one hadrons

The conventional form factor decomposition of the vector and axial currents for spin-1 hadrons [93, 94] is given by

$$\begin{aligned} \langle p_2 | j_q^\mu(0) | p_1 \rangle &= -G_1^q(\Delta^2)(\varepsilon_2^* \cdot \varepsilon_1)p^\mu \\ &\quad + G_2^q(\Delta^2)\left(\varepsilon_1^\mu(\varepsilon_2^* \cdot p) + \varepsilon_2^{*\mu}(\varepsilon_1 \cdot p)\right) - G_3^q(\Delta^2)(\varepsilon_1 \cdot p)(\varepsilon_2^* \cdot p)\frac{p^\mu}{2M_D^2}, \end{aligned} \quad (3.96)$$

$$\langle p_2 | j_q^{5\mu}(0) | p_1 \rangle = i\tilde{G}_1^q(\Delta^2)\varepsilon^{\mu\nu\rho\sigma}\varepsilon_{2\nu}^*\varepsilon_{1\rho}p_\sigma + i\tilde{G}_2^q(\Delta^2)\varepsilon^{\mu\nu\rho\sigma}\Delta_\nu p_\rho\frac{\varepsilon_{1\sigma}^*(\varepsilon_2^* \cdot p) + \varepsilon_{2\sigma}^*(\varepsilon_1 \cdot p)}{M_D^2}, \quad (3.97)$$

The matrix elements are defined here flavor by flavor; to get form factors for a particular hadron, one must weight the flavor components with appropriate electromagnetic or weak charges and sum over flavors.

Integrating the matrix elements defining the twist-two GPDs in the deuteron target we obtain the sum rules

$$\begin{aligned} \int_{-1}^1 dx H_i^q(x, \eta, \Delta^2) &= G_i^q(\Delta^2), \quad i = 1, 2, 3, \\ \int_{-1}^1 dx \tilde{H}_i^q(x, \eta, \Delta^2) &= \tilde{G}_i^q(\Delta^2), \quad i = 1, 2, \\ \int_{-1}^1 dx H_4^q(x, \eta, \Delta^2) &= \int_{-1}^1 dx \tilde{H}_3^q(x, \eta, \Delta^2) = 0, \\ \int_{-1}^1 dx H_5^q(x, \eta, \Delta^2) &= \int_{-1}^1 dx \tilde{H}_4^q(x, \eta, \Delta^2) = 0. \end{aligned} \quad (3.98)$$

For H_4 , \tilde{H}_3 and H_5 , \tilde{H}_4 , the integrals do not correspond to form factors of the local vector or axial currents and therefore vanish. In the case of H_4 and \tilde{H}_3 this is due to the time reversal constraints, whereas the definitions of H_5 and \tilde{H}_4 involve the tensor $n^\mu n^\nu / (p^+)^2$, whose analogue cannot appear in the decomposition of local currents due to Lorentz invariance. Some of them we already established in Section 3.3.3.

The set of form factors G_1 , G_2 , and G_3 may be expressed in terms of the charge monopole, magnetic dipole, and charge quadrupole form factors:

$$\begin{aligned} G_C(\Delta^2) &= \left(1 + \frac{2\tau}{3}\right)G_1(\Delta^2) - \frac{2\tau}{3}[G_2(\Delta^2) - (1 + \tau)G_3(\Delta^2)], \\ G_M(\Delta^2) &= G_2(\Delta^2), \quad G_Q(\Delta^2) = G_1(\Delta^2) - G_2(\Delta^2) + (1 + \tau)G_3(\Delta^2), \end{aligned}$$

with $\tau \equiv -\Delta^2/(4M^2)$. The normalization of these form factors is given by

$$G_C(0) = 1, \quad G_M(0) = \mu_d = 1.714, \quad G_Q(0) = Q_d = 25.83. \quad (3.99)$$

A parameterization for the deuteron form factors inspired by the quark counting rules for large $|\Delta^2|$ can be found in Ref. [95]:

$$\begin{aligned} G_C(\Delta^2) &= \frac{G_D^2(\frac{1}{4}\Delta^2)}{1+2\tau} \left[\left(1 - \frac{2}{3}\tau\right) g_{00}^+ + \frac{8}{3}\sqrt{2\tau}g_{+0}^+ - \frac{2}{3}(1-2\tau)g_{+-}^+ \right], \\ G_M(\Delta^2) &= \frac{G_D^2(\frac{1}{4}\Delta^2)}{1+2\tau} \left[2g_{00}^+ - \frac{2(1-2\tau)}{\sqrt{2\tau}}g_{+0}^+ - 2g_{+-}^+ \right], \\ G_Q(\Delta^2) &= \frac{G_D^2(\frac{1}{4}\Delta^2)}{1+2\tau} \left[-g_{00}^+ + \sqrt{\frac{2}{\tau}}g_{+0}^+ - \frac{1+\tau}{\tau}g_{+-}^+ \right]. \end{aligned} \quad (3.100)$$

The function $G_D(\Delta^2)$ here is the standard dipole parameterization for the nucleon form factor (3.92). The helicity amplitudes in the infinite momentum frame are given by [96]

$$g_{00}^+ = \sum_{i=1}^4 \frac{a_i}{\alpha_i^2 - \Delta^2}, \quad g_{+0}^+ = \sqrt{-\Delta^2} \sum_{i=1}^4 \frac{b_i}{\beta_i^2 - \Delta^2}, \quad g_{+-}^+ = -\Delta^2 \sum_{i=1}^4 \frac{c_i}{\gamma_i^2 - \Delta^2}. \quad (3.101)$$

The counting rules for large $|\Delta^2|$ predict the following behavior

$$g_{00}^+ \sim (-\Delta)^{-2}, \quad g_{+0}^+ \sim (-\Delta)^{-3}, \quad g_{+-}^+ \sim (-\Delta)^{-4}, \quad (3.102)$$

which gives together with the static properties (3.99) six constraints for twenty four fitting parameters:

$$\sum_{i=1}^4 \frac{a_i}{\alpha_i^2} = 1, \quad \sum_{i=1}^4 \frac{b_i}{\beta_i^2} = \frac{2 - \mu_d}{2\sqrt{2}M_d}, \quad \sum_{i=1}^4 \frac{c_i}{\gamma_i^2} = \frac{1 - \mu_d - Q_d}{4M_d^2}, \quad \sum_{i=1}^4 b_i = \sum_{i=1}^4 c_i = \sum_{i=1}^4 c_i \gamma_i^2 = 0. \quad (3.103)$$

To reduce this set to twelve parameters, one may introduce for each group α_i , β_i , and γ_i the algebraic relations:

$$\alpha_i^2 = \alpha_1^2 + (\alpha_4^2 - \alpha_1^2) \frac{i-1}{3} \quad \text{for } i = 1, \dots, 4. \quad (3.104)$$

We quote here the fitting parameters from Ref. [97]. They are given in Table 2.

3.5 Polynomiality and skewness dependence

Having discussed the simplest limiting cases of GPDs, we are going to address now their generic properties, like the polynomiality in the skewness parameter η . To properly address the issue, the formalism of Wilson operators is especially handy. The Taylor expansion of non-local light-cone operators results in a tower of local operators of increasing Lorentz spin. Namely, for the even-parity quark and gluon operators we have an infinite series decomposition

$$\mathcal{O}^{qq}(-z^-, z^-) = \sum_{j=0}^{\infty} \frac{1}{j!} (-iz^-)^j n^{\mu_1} n^{\mu_2} \dots n^{\mu_{j+1}} \mathcal{R}_{\mu_1 \mu_2 \dots \mu_{j+1}}^{2,qq}, \quad (3.105)$$

$$\mathcal{O}^{gg}(-z^-, z^-) = \sum_{j=0}^{\infty} \frac{1}{j!} (-iz^-)^j n^{\mu_1} n^{\mu_2} \dots n^{\mu_{j+2}} \mathcal{R}_{\mu_1 \mu_2 \dots \mu_{j+2}}^{2,gg}, \quad (3.106)$$

i	1	2	3	4
a_i [fm $^{-2}$]	1.57057	12.23792	-42.04576	Eq. (3.103)
b_i [fm $^{-1}$]	0.07043	0.14443	Eq. (3.103)	Eq. (3.103)
c_i	-0.16577	Eq. (3.103)	Eq. (3.103)	Eq. (3.103)
α_i^2 [fm $^{-2}$]	1.52501	Eq. (3.104)	Eq. (3.104)	23.20415
β_i^2 [fm $^{-2}$]	43.67795	Eq. (3.104)	Eq. (3.104)	2.80716
γ_i^2 [fm $^{-2}$]	1.87055	Eq. (3.104)	Eq. (3.104)	41.1294

Table 2: Sets of fitting parameters for the deuteron electromagnetic form factors.

in terms of the twist-two local operators

$$\mathcal{R}_{\mu_1\mu_2\dots\mu_j}^{2,qq} = \underset{\mu_1\mu_2\dots\mu_j}{\mathbf{S}} \bar{\psi} \gamma_{\mu_1} i \overset{\leftrightarrow}{\mathcal{D}}_{\mu_2} i \overset{\leftrightarrow}{\mathcal{D}}_{\mu_3} \dots i \overset{\leftrightarrow}{\mathcal{D}}_{\mu_j} \psi, \quad (3.107)$$

$$\mathcal{R}_{\mu_1\mu_2\dots\mu_j}^{2,gg} = \underset{\mu_1\mu_2\dots\mu_j}{\mathbf{S}} F_{\mu_1\nu} i \overset{\leftrightarrow}{\mathcal{D}}_{\mu_2} i \overset{\leftrightarrow}{\mathcal{D}}_{\mu_3} \dots i \overset{\leftrightarrow}{\mathcal{D}}_{\mu_{j-1}} F^\nu_{\mu_j}, \quad (3.108)$$

constructed from the elementary fields and the covariant left-right derivative acting on them,

$$\overset{\leftrightarrow}{\mathcal{D}}_\mu \equiv \overset{\rightarrow}{\mathcal{D}}_\mu - \overset{\leftarrow}{\mathcal{D}}_\mu. \quad (3.109)$$

As before, \mathbf{S} is the operation of symmetrization and trace subtraction. Analogous Taylor expansion hold for other twist-two quark and gluon operators. The matrix elements of the local operators listed above are related to the Mellin moments of generalized parton distributions introduced in the preceding section. For $j = 2$, the operators coincide with the quark and gluon parts of the classical, symmetric energy-momentum tensor (see Appendix E), namely

$$\Theta_{\mu_1\mu_2}^q = \frac{1}{2} \mathcal{R}_{\mu_1\mu_2}^{2,qq} \equiv \frac{i}{4} \bar{\psi} \left\{ \gamma_{\mu_1} \overset{\rightarrow}{\mathcal{D}}_{\mu_2} + \gamma_{\mu_2} \overset{\rightarrow}{\mathcal{D}}_{\mu_1} - \frac{1}{2} g_{\mu_1\mu_2} \not{p} \right\} \psi, \quad (3.110)$$

$$\Theta_{\mu_1\mu_2}^g = \mathcal{R}_{\mu_1\mu_2}^{2,gg} \equiv \frac{1}{2} \left\{ F_{\mu_1\nu}^a F_{a\mu_2}^\nu + F_{\mu_2\nu}^a F_{a\mu_1}^\nu - \frac{1}{2} g_{\mu_1\mu_2} F_{\mu\nu}^a F_a^\nu \right\}. \quad (3.111)$$

When the index of the Dirac matrix in the quark bilocal operator (3.10) is not contracted with the lightlike vector n^μ , the operator ceases to have a definite geometric twist-two. In the subsequent discussion, we will need a non-local form of the twist-two quark operator which results from the extraction of the leading component of the bilocal quark operator with a free Lorentz index of the Dirac matrix. This form can be found with the help of an identity [230], which can be verified by Taylor expanding the light-ray operator,

$$\begin{aligned} \mathcal{R}_\mu^{2,qq}(-z^-, z^-) &= \int_{-1}^1 du \frac{\partial}{\partial z^\mu} \bar{\psi}(-uz) \not{\epsilon}[-uz, uz] \psi(uz) \\ &= \sum_{j=0}^{\infty} \frac{1}{j!} (-iz^-)^j n^{\mu_1} \dots n^{\mu_j} \mathcal{R}_{\mu\mu_1\dots\mu_j}^{2,qq}, \end{aligned} \quad (3.112)$$

with $z^\mu = z^- n^\mu$ on the right-hand side of the equality. Obviously,

$$\mathcal{O}^{qq}(-z^-, z^-) = n^\mu \mathcal{R}_\mu^{2,qq}(-z^-, z^-).$$

The generalization to gluonic operators is straightforward. Having introduced the local Wilson operators, we are in a position to discuss the polynomiality property of Mellin momentns of GPDs, which are related to the hadronic matrix elements of these operators.

3.5.1 Spin-zero hadrons

As usual, it is instructive to start with a spin-zero target. The parametrization for the matrix elements of the completely symmetrized and traceless local Wilson operators, introduced in the preceding section, sandwiched between the corresponding states reads

$$\langle p_2 | \mathcal{R}_{\mu_1 \dots \mu_j}^{2,qq} | p_1 \rangle = \sum_{\mu_1 \dots \mu_j} \{ p_{\mu_1} \dots p_{\mu_j} H_{j,0}^q + \Delta_{\mu_1} p_{\mu_2} \dots p_{\mu_j} H_{j,1}^q + \dots + \Delta_{\mu_1} \dots \Delta_{\mu_j} H_{j,j}^q \}, \quad (3.113)$$

$$\langle p_2 | \tilde{\mathcal{R}}_{\mu_1 \dots \mu_j}^{2,qq} | p_1 \rangle = 0, \quad (3.114)$$

in terms of the form factors $H_{j,k}(\Delta^2)$, whose dependence on the squared momentum transfer Q^2 was not displayed for brevity. The vanishing of the matrix element of the odd parity operator is a simple consequence of the fact that one cannot form a “twist-two” axial-vector, i.e., involving only collinear momenta, for a spin-zero hadron. Thus, only the vector operators develop non-zero expectation values. For the Lorentz spin $j \geq 1$, there are exactly $j+1$ form factors $H_{j,k}$ as had been established in Refs. [7, 68]. Further, it is convenient to introduce a generating function of the coefficients H_{jk} . One can see that, after contraction of the open Lorentz indices in Eq. (3.113) with the light-cone vectors n_μ and summation over resulting Wilson operators as in Eqs. (3.105) and (3.106), one immediately establishes a relation to the Mellin moments of GPDs

$$H_{j,k}^q(\Delta^2) = \frac{1}{k!} \left. \frac{d^k}{d\eta^k} \right|_{\eta=0} \int_{-1}^1 dx x^{j-1} H^q(x, \eta, \Delta^2), \quad (3.115)$$

where $0 \leq k \leq j$, $1 \leq j$. This equation demonstrates that any given x^{j-1} moment of the GPD $H^q(x, \eta, \Delta^2)$ is a polynomial in skewness η of order j . Since this GPD is an even function of skewness, as a consequence of the time-reversal invariance, only the Lorentz structures even in Δ survive in Eq. (3.113).

Later on in Section 5 of this review, we will analyze the operator product expansion for the off-forward Compton amplitude, which gives access to GPDs. This will require the consideration of hadronic matrix elements of non-local twist-two operators with an open Lorentz index, like Eq. (3.112), and their parametrization in terms of twist-two GPDs. Having the decomposition (3.113) and the relation (3.115) at hand, the problem of designing the corresponding operator matrix elements can be easily solved. To this end, we have to project both sides of Eq. (3.113) with the product of the light-cone vectors $n_{\mu_2} \dots n_{\mu_j}$, leaving the index μ_1 intact. The obvious relation

$$n_{\mu_1} \dots n_{\mu_j} \sum_{\mu \mu_1 \dots \mu_j} \Delta^\mu \dots \Delta^{\mu_k} p^{\mu_{k+1}} \dots p^{\mu_j} = \frac{(p^+)^j}{j+1} \{ (j+1-k)p^\mu \eta^k + k \Delta^\mu \eta^{k-1} \}, \quad (3.116)$$

is then translates into an equation for the off-forward matrix element of Wilson operators,

$$n^{\mu_1} \dots n^{\mu_j} \langle p_2 | \mathcal{R}_{\mu \mu_1 \dots \mu_j}^{2,qq} | p_1 \rangle = p_\mu (p^+)^j \left(1 - \frac{\eta}{j+1} \frac{d}{d\eta} \right) H_{j+1}^q(\eta) + \Delta_\mu (p^+)^j \frac{1}{j+1} \frac{d}{d\eta} H_{j+1}^q(\eta). \quad (3.117)$$

Here the coefficients in front of the two terms on the right-hand side of Eq. (3.116) become differential operators in skewness acting on $H_{j+1}(\eta)$. The latter is related to the Mellin moments of GPDs,

$$H_j^q(\eta) = \int_{-1}^1 dx x^{j-1} H^q(x, \eta) = \sum_{k=0}^j \eta^k H_{j,k}^q, \quad (3.118)$$

The moments $H_{j+1}^q(\eta)$ can be found directly from the + component of the operator $\mathcal{R}_+^{2,qq}$. Obviously,

$$n^\mu n^{\mu_1} \dots n^{\mu_j} \langle p_2 | \mathcal{R}_{\mu\mu_1\dots\mu_j}^{2,qq} | p_1 \rangle = (p^+)^{j+1} H_{j+1}^q(\eta).$$

As a consequence of symmetrization, Eq. (3.117) contains a Wandzura-Wilczek term proportional to $\Delta_\mu^\perp = \Delta_\mu - \eta p_\mu$, which effectively enters as a twist-three contribution to the scattering amplitude, as we will demonstrate later in Section 5.3. Finally, the matrix element of the twist-two light-ray operator (3.112) can be obtained in a straightforward manner by resummation:

$$\langle p_2 | \mathcal{R}_\mu^{2,qq}(-z^-, z^-) | p_1 \rangle = \int_{-1}^1 dx e^{-iz^- p^+ x} \left(p_\mu H^q(x, \eta) + \Delta_\mu^\perp \int_{-1}^1 dy W_2(x, y) \frac{d}{d\eta} H^q(x, \eta) \right), \quad (3.119)$$

where the kernel $W_2(x, y)$ is given by

$$W_2(x, y) = \frac{1}{y} \theta(x) \theta(y - x) - \frac{1}{x} \theta(-x) \theta(x - y). \quad (3.120)$$

3.5.2 Spin-one-half hadrons

In parallel to the discussion in the previous section, the nucleon matrix element of twist-two quark operators are parametrized via a set of “form factors” as follows⁸

$$\begin{aligned} \langle p_2 | \mathcal{R}_{\mu_1\dots\mu_j}^{2,qq} | p_1 \rangle &= \sum_{\rho\mu_1\dots\mu_j} h_{\mu_1} \{ p_{\mu_2} \dots p_{\mu_j} A_{j,0}^q + \dots + \Delta_{\mu_2} \dots \Delta_{\mu_j} A_{j,j-1}^q \} \\ &+ \sum_{\mu_1\dots\mu_j} \frac{b}{2M_N} \{ p_{\mu_1} \dots p_{\mu_j} B_{j,0}^q + \Delta_{\mu_1} p_{\mu_2} \dots p_{\mu_j} B_{j,1}^q + \dots + \Delta_{\mu_1} \dots \Delta_{\mu_j} B_{j,j}^q \}, \end{aligned} \quad (3.121)$$

where the structure in the second line is identical to Eq. (3.113). Analogous relations hold for the parity odd and chiral odd operator matrix elements, though the form factor counting comes out different [68, 69, 70, 71]. We used the Gordon identities (3.35) in the above equation to reduce the tensor structure involving $t^{\mu\nu}$ to the other two Dirac bilinears. This is useful since one can use many results derived for the scalar target. As we discussed above, there is an important constraint on the matrix elements (3.121) imposed by the time-reversal invariance. Namely, the coefficients accompanying Lorentz structures with odd powers of the momentum transfer Δ should vanish [7], so that

$$A_{j,2n+1}^q = B_{j,2n+1}^q = 0.$$

The nonvanishing form factors $A_{j,k}$ and $B_{j,k}$ are related to the moments of GPDs

$$A_j^q(\eta) = \int_{-1}^1 dx x^{j-1} A^q(x, \eta) = \sum_{k=0}^{j-1} \eta^k A_{j,k}^q, \quad B_j^q(\eta) = \int_{-1}^1 dx x^{j-1} B^q(x, \eta) = \sum_{k=0}^j \eta^k B_{j,k}^q. \quad (3.122)$$

Another equivalent representation for the matrix elements of twist-two operators widely used in the literature is achieved by reduction of the scalar Dirac bilinear b accompanied by at least one vector p_μ using the Gordon identity back to the vector n^μ and tensor $t^{\mu\nu}$ Dirac bilinears. This

⁸Do not confuse these $A_{j,k}$ and $B_{j,k}$ form factors with the ones introduced in Ref. [2].

gives

$$\begin{aligned} \langle p_2 | \mathcal{R}_{\mu_1 \dots \mu_j}^{2,qq} | p_1 \rangle &= \sum_{\mu_1 \dots \mu_j} h_{\mu_1} \{ p_{\mu_2} \dots p_{\mu_j} H_{j,0}^q(\Delta^2) + \dots + \Delta_{\mu_2} \dots \Delta_{\mu_j} H_{j,j-1}^q(\Delta^2) \} \\ &\quad + \sum_{\mu_1 \dots \mu_j} e_{\mu_1} \{ p_{\mu_2} \dots p_{\mu_j} E_{j,0}^q(\Delta^2) + \dots + \Delta_{\mu_2} \dots \Delta_{\mu_j} E_{j,j-1}^q(\Delta^2) \} \\ &\quad + \sum_{\mu_1 \dots \mu_j} \frac{b}{2M_N} \Delta_{\mu_1} \dots \Delta_{\mu_j} D_j^q(\Delta^2), \end{aligned} \quad (3.123)$$

where

$$H_{j,k}^q = A_{j,k}^q + B_{j,k}^q, \quad E_{j,k}^q = -B_{j,k}^q, \quad D_j^q = B_{j,j}^q. \quad (3.124)$$

The reduced matrix elements H^q , E^q and D^q are related to the moments of parity-even quark generalized parton distributions [1, 2, 6] via

$$\begin{aligned} \int_{-1}^1 dx x^{j-1} H^q(x, \eta, \Delta^2) &= \sum_{k=0}^{j-1} \eta^k H_{j,k}^q(\Delta^2) + \eta^j D_j^q(\Delta^2), \\ \int_{-1}^1 dx x^{j-1} E^q(x, \eta, \Delta^2) &= \sum_{k=0}^{j-1} \eta^k E_{j,k}^q(\Delta^2) - \eta^j D_j^q(\Delta^2). \end{aligned} \quad (3.125)$$

For gluon GPDs, the modification of the above formulas is very straightforward. The parametrization of the parity-even gluon matrix elements in terms of form factors H^g , E^g and D^g reads in complete analogy to (3.123)

$$\begin{aligned} \langle p_2 | \mathcal{R}_{\mu_1 \dots \mu_j}^{2,gg} | p_1 \rangle &= \frac{1}{2} \sum_{\mu_1 \dots \mu_j} h_{\mu_1} \{ p_{\mu_2} \dots p_{\mu_{j-1}} H_{j,0}^g(\Delta^2) + \dots + \Delta_{\mu_2} \dots \Delta_{\mu_{j-1}} H_{j,j-2}^g(\Delta^2) \} p_{\mu_j} \\ &\quad + \frac{1}{2} \sum_{\mu_1 \dots \mu_j} e_{\mu_1} \{ p_{\mu_2} \dots p_{\mu_{j-1}} E_{j,0}^g(\Delta^2) + \dots + \Delta_{\mu_2} \dots \Delta_{\mu_{j-1}} E_{j,j-2}^g(\Delta^2) \} p_{\mu_j} \\ &\quad + \frac{1}{2} \sum_{\mu_1 \dots \mu_j} \frac{b}{2M_N} \Delta_{\mu_1} \dots \Delta_{\mu_j} D_j^g(\Delta^2), \end{aligned} \quad (3.126)$$

with form factors related to moments of gluon GPDs (3.41) via

$$\begin{aligned} \frac{1}{2} \int_{-1}^1 dx x^{j-2} H^g(x, \eta, \Delta^2) &= \sum_{k=0}^{j-2} \eta^k H_{j,k}^g(\Delta^2) + \eta^j D_j^g(\Delta^2), \\ \frac{1}{2} \int_{-1}^1 dx x^{j-2} E^g(x, \eta, \Delta^2) &= \sum_{k=0}^{j-2} \eta^k E_{j,k}^g(\Delta^2) - \eta^j D_j^g(\Delta^2). \end{aligned} \quad (3.127)$$

The reduction of the value of the Lorentz spin in the exponential of the Mellin integrand on the left-hand side of these equations by one unit $j \rightarrow j-1$ is an obvious consequence of the increased spin of gluon operators compared to the quark ones. Notice that while quark GPDs do not possess definite symmetry properties under the exchange $x \rightarrow -x$, the gluon GPDs do. Namely, due to the fact that gluon and antiguons are the same particles, one finds

$$\begin{aligned} H^g(-x, \eta, \Delta^2) &= H^g(x, \eta, \Delta^2), & E^g(-x, \eta, \Delta^2) &= E^g(x, \eta, \Delta^2), \\ \tilde{H}^g(-x, \eta, \Delta^2) &= -\tilde{H}^g(x, \eta, \Delta^2), & \tilde{E}^g(-x, \eta, \Delta^2) &= -\tilde{E}^g(x, \eta, \Delta^2), \end{aligned} \quad (3.128)$$

for parity-even and parity-odd GPDs, respectively. This charge conjugation property allows one to reduce the integral in Eq. (3.127) to the domain $0 \leq x \leq 1$.

In establishing the relation between the nucleon matrix elements of the twist-two operator with the open Lorentz index (3.112) and the nucleon form factors, the only difference from the case of spin-zero target arises in the implementation of the symmetrization procedure, namely,

$$n_{\mu_1} \dots n_{\mu_j} S_{\mu\mu_1 \dots \mu_j} h^\mu \Delta^{\mu_1} \dots \Delta^{\mu_k} p^{\mu_{k+1}} \dots p^{\mu_j} = \frac{(p^+)^{j-1}}{j+1} \{ h^\mu \eta^k p^+ + (j-k)p^\mu h^+ \eta^k + k \Delta^\mu h^+ \eta^{k-1} \},$$

and provides a new structure

$$\begin{aligned} n^{\mu_1} \dots n^{\mu_j} \langle p_2 | \mathcal{R}_{\mu\mu_1 \dots \mu_j}^{2,qq} | p_1 \rangle &= \frac{(p^+)^{j-1}}{j+1} \left((j+1)p_\mu h^+ + h_\mu - p_\mu h^+ + \Delta_\mu^\perp h^+ \frac{d}{d\eta} \right) A_{j+1}(\eta) \quad (3.129) \\ &+ \frac{b}{2M_N} \left\{ p_\mu (p^+)^j \left(1 - \frac{\eta}{j+1} \frac{d}{d\eta} \right) + \Delta_\mu (p^+)^j \frac{1}{j+1} \frac{d}{d\eta} \right\} B_{j+1}^q(\eta). \end{aligned}$$

It is easy to perform the inverse Mellin transformation to establish the corresponding relations to GPDs. To this end, one should match the integrand of the momentum fraction integrals to the moment form $x^j f(x)$. The procedure yields the equation

$$\begin{aligned} \langle p_2 | \mathcal{R}_\mu^{2,qq}(-z^-, z^-) | p_1 \rangle &= \int_{-1}^1 dx e^{-ixz^- p^+} \int_0^1 dy \left\{ \left(h_\mu - \frac{h^+}{p^+} p_\mu \right) W_2(x, y) (H + E)(y, \eta) \right. \\ &\quad \left. + \left(p_\mu \delta(x-y) + \Delta_\mu^\perp W_2(x, y) \frac{d}{d\eta} \right) \left(\frac{h^+}{p^+} H + \frac{e^+}{p^+} E \right) (y, \eta) \right\}, \quad (3.130) \end{aligned}$$

where we returned to the conventional basis of Dirac structures by means of the identity (3.37) and conventional GPDs, related to the ones defined in Eq. (3.122) by

$$A^q = H^q + E^q, \quad B^q = -E^q. \quad (3.131)$$

It is also useful to note that the identity $2M_N(p^+ h^\mu - p^\mu h^+) = (p^+ t^{\nu\mu} - p^\mu t^{\nu+})\Delta_\nu$ allows to reduce the structure accompanying E in the first line of Eq. (3.130) to the expected tensor form (3.38). Contracting the expression (3.130) with the vector n_μ we obtain conventional definitions of twist-two GPDs.

Since there are no further subtleties related to spin-one targets, we will not discuss polynomiality properties of their GPDs here.

3.6 GPDs and the proton spin puzzle

One of the motivations to study GPDs is their profound relation to the distribution of angular momentum of quarks and gluons in the proton. As is by now well known, the EMC measurement of the fraction of the proton spin carried by quarks, $\frac{1}{2}\Delta\Sigma$,

$$\sum_q \langle p | j_q^{5\mu}(0) | p \rangle = \Delta\Sigma s^\mu, \quad (3.132)$$

in polarized deeply inelastic scattering demonstrated that, instead of the much anticipated result $\Delta\Sigma^{\text{QM}} = 1$, which is a prediction of the naive quark model of the nucleon, the experimental

$Q^2(\text{GeV}^2)$	Γ_1^p	Γ_1^n	$\Gamma_1^p - \Gamma_1^n$	Ref.
5	0.118 ± 0.008	-0.058 ± 0.009	0.176 ± 0.007	[106]
10	0.120 ± 0.016	-0.078 ± 0.021	0.198 ± 0.023	[107, 108]
5	0.121 ± 0.018	-0.075 ± 0.021	$0.174 + 0.024 - 0.012$	[108]

Table 3: Experimental data on Γ_1^p , Γ_1^n , and Bjorken sum rule $\Gamma_1^p - \Gamma_1^n$ in the $\overline{\text{MS}}$ scheme.

finding was only about 20% of this. This “spin crisis” triggered an enormous flood of theoretical and experimental activity. Theoretical resolution of the spin puzzle was sought via many complementary ways including the anomalous contributions due to gluons [98, 99, 100], large negative polarization of strange quarks, significant role of the orbital angular momentum of constituents [101, 2], etc. (see Refs. [102, 103, 104, 105] for reviews). The experimental verification of the EMC finding is coming from several sources, including deeply inelastic scattering and leptonic decays of hyperons.

3.6.1 Axial coupling from polarized deeply inelastic scattering

The measurement of the polarized spin-dependent structure function g_1 , see Eq. (2.34), gives access to the helicity-dependent quark distribution functions, and thus to the fraction of hadron spin carried by quarks deduced from their first Mellin moment,

$$\Gamma_1 = \int_0^1 dx g_1(x) = \frac{1}{2} \sum_q Q_q^2 \int_0^1 dx (\Delta q(x) + \Delta \bar{q}(x)) \equiv \frac{1}{2} \sum_q Q_q^2 (\Delta q + \Delta \bar{q}) . \quad (3.133)$$

We have omitted the QCD radiative corrections to this parton model formula and did not display the dependence of all quantities on the virtuality of the resolving photon. The measurement of the structure functions on the proton and neutron targets allows one to measure the following combinations of the axial constants

$$\Gamma_1^p = \frac{1}{9} \left(\frac{3}{4} g_A^{(3)} + \frac{1}{4} g_A^{(8)} + g_A^{(0)} \right) , \quad \Gamma_1^n = \frac{1}{9} \left(-\frac{3}{4} g_A^{(3)} + \frac{1}{4} g_A^{(8)} + g_A^{(0)} \right) , \quad (3.134)$$

which are superpositions of the first moments of polarized quark densities,

$$\begin{aligned} g_A^{(0)} &= (\Delta u + \Delta \bar{u}) + (\Delta d + \Delta \bar{d}) + (\Delta s + \Delta \bar{s}) \equiv \Delta \Sigma , \\ g_A^{(3)} &= (\Delta u + \Delta \bar{u}) - (\Delta u + \Delta \bar{u}) , \\ g_A^{(8)} &= (\Delta u + \Delta \bar{u}) + (\Delta d + \Delta \bar{d}) - 2(\Delta s + \Delta \bar{s}) . \end{aligned} \quad (3.135)$$

The difference between the first moments of the proton and neutron structure functions is fixed by the Bjorken sum rule to the isovector axial coupling,

$$\Gamma_1^p - \Gamma_1^n = \frac{1}{6} g_A^{(3)} . \quad (3.136)$$

This equation is a consequence of the current algebra and isospin symmetry. Recent experimental data for the integrals Γ_1^p and Γ_1^n are summarized in Table 3. The deeply inelastic scattering data

alone do not allow to extract all axial constants since the octet and singlet constants enter in the same combination into the proton and neutron sum rules. Thus one has to resort to other sources of information in order to separate different flavor contributions. Such knowledge is provided by hyperon decays complemented by the use of the $SU(3)$ flavor symmetry, as discussed next.

3.6.2 Axial coupling from semileptonic decays of hyperons

Semileptonic decays of hyperons $B \rightarrow B' e^- \bar{\nu}_e$ measure the transition matrix element of the charged weak current,

$$\langle B | \bar{\psi}_q \gamma^\mu (1 - \gamma^5) \psi_{q'} | B' \rangle, \quad \psi_q \equiv \begin{pmatrix} u \\ d \\ s \end{pmatrix} \quad (3.137)$$

The approximate $SU(3)$ flavor symmetry of strong interactions allows one to relate the above matrix elements among each other so that one deduces the flavor-diagonal transitions, required for the spin sum rule, in terms of experimentally measured flavor-changing decays. Let us give a few details on the derivation of the $SU(3)$ -flavor relations, since we will use the very same identities for flavor-changing GPDs introduced in Section 3.16.

The $SU(3)$ baryon octet is represented conventionally by a matrix labeled with a row index a and a column index b ,

$$B^a{}_b = \begin{pmatrix} \frac{1}{\sqrt{6}}A + \frac{1}{\sqrt{2}}\Sigma^0 & \Sigma^+ & p \\ \Sigma^- & \frac{1}{\sqrt{6}}A - \frac{1}{\sqrt{2}}\Sigma^0 & n \\ \Xi^- & \Xi^0 & -\frac{2}{\sqrt{6}}A \end{pmatrix}, \quad (3.138)$$

so that, e.g., the proton is the element $B^1{}_3 = p$. The Lagrangian describing the transition $B \rightarrow B'$ within the baryon octet via the octet current has two $SU(3)$ invariant couplings, since there are two distinct $\mathbf{8}$'s in the product of two, $\mathbf{8} \otimes \mathbf{8} = \mathbf{1} \oplus \mathbf{8} \oplus \mathbf{8} \oplus \mathbf{10} \oplus \overline{\mathbf{10}} \oplus \mathbf{27}$. This yields the symmetric (D) and antisymmetric (F) invariants [109]

$$\begin{aligned} \mathcal{L}_{\mathbf{8} \rightarrow \mathbf{8}} &= D \text{tr}\{\bar{B}, B\}M - F \text{tr}[\bar{B}, B]M \\ &= (D - F)\bar{B}^a{}_b M^c{}_a B^b{}_c + (D + F)\bar{B}^b{}_c M^c{}_a B^a{}_b. \end{aligned} \quad (3.139)$$

Here $\bar{B} \equiv B^\dagger$ is a hermitian conjugated matrix, e.g., $\bar{B}^3{}_1 = \bar{p}$, and the matrix $M^a{}_b$ describes the octet of local vector $\Gamma = \gamma^\mu$ and axial $\Gamma = \gamma^\mu \gamma^5$ currents,

$$M^{q'}{}_q = \bar{\psi}_q \Gamma \psi_{q'} - \frac{1}{3} \delta_{qq'} \sum_{q''} \bar{\psi}_{q''} \Gamma \psi_{q''} \quad (3.140)$$

with corresponding two inequivalent sets of D and F constants, F_V, D_V and F_A, D_A , respectively. Actually, these are not constants at all but rather form factors due to the nonzero recoil $\Delta = p_1 - p_2$ in the transition matrix element. There are as many of them as there are independent structures in the decomposition of the matrix elements (3.137) in terms of Dirac bilinears, as, e.g., in Eqs. (3.86) and (3.87), with possible extra terms. However, since the recoil momentum in these decays is negligible compared to the hyperon masses, $|\Delta| \ll M$, one can use the static approximation and take all form factors as constants at $\Delta = 0$. This also implies that the limitation of the consideration to the vector and axial charges is legitimate. Since the $SU(3)$ vector current is a generator of $SU(3)$ transformations, its matrix elements are fixed uniquely by the $SU(3)$ group

structure constants f^{abc} , such that $F_V = 1$ and $D_V = 0$. These are the matrix elements of the axial currents that are measured in these decays, $F_A = F$, $D_A = D$.

For the transitions governed by the $M^u_d = \bar{d}u$ current, the Lagrangian gives

$$\begin{aligned}\mathcal{L}_{\mathbf{8} \rightarrow \mathbf{8}} &= \sqrt{\frac{2}{3}}D\bar{\Lambda}(\bar{d}u)\Sigma^- + \sqrt{\frac{2}{3}}D\bar{\Sigma}^+(\bar{d}u)\Lambda \\ &+ (D+F)\bar{p}(\bar{d}u)n + \sqrt{2}F\bar{\Sigma}^0(\bar{d}u)\Sigma^- - \sqrt{2}F\bar{\Sigma}^+(\bar{d}u)\Sigma^0 + (D-F)\bar{\Xi}^0(\bar{d}u)\Xi^- + \dots,\end{aligned}\quad (3.141)$$

with ellipsis standing for other flavor transitions. One can immediately read off the strengths for the corresponding transitions

$$\begin{aligned}\langle \Lambda | \bar{u}d | \Sigma^- \rangle &= \langle \Sigma^+ | \bar{u}d | \Lambda \rangle = \sqrt{\frac{2}{3}}D, & \langle p | \bar{u}d | n \rangle &= D+F, \\ \langle \Sigma^0 | \bar{u}d | \Sigma^- \rangle &= -\langle \Sigma^+ | \bar{u}d | \Sigma^0 \rangle = \sqrt{2}F, & \langle \Xi^0 | \bar{u}d | \Xi^- \rangle &= D-F.\end{aligned}\quad (3.142)$$

Extracting the proton-to-proton transitions from the above Lagrangian, we get

$$\mathcal{L}_{\mathbf{8} \rightarrow \mathbf{8}} = \bar{p} \left\{ \frac{1}{6}(3F-D)(\bar{u}u + \bar{d}d - 2\bar{s}s) + \frac{1}{2}(D+F)(\bar{u}u - \bar{d}d) \right\} p + \dots, \quad (3.143)$$

and, as a result⁹,

$$\langle p | \bar{u}u - \bar{d}d | p \rangle = D+F, \quad \langle p | \bar{u}u + \bar{d}d - 2\bar{s}s | p \rangle = 3F-D. \quad (3.144)$$

Solving these equations for the F and D couplings in terms of matrix elements, we obtain as a result the $SU(3)$ relations for the octet-to-octet transitions, for instance,

$$\langle p | \bar{u}u - \bar{d}d | p \rangle = \langle n | \bar{d}u | p \rangle. \quad (3.145)$$

Thus, certain combinations of D and F decay constants are related to the triplet and octet axial constants (3.135) via

$$g_A^{(3)} = F + D, \quad g_A^{(8)} = 3F - D. \quad (3.146)$$

The experimental data for a few decay modes are given in Table 4, wherefrom we conclude that $D = 0.79 \pm 0.07$ and $F = 0.47 \pm 0.10$. Thus, the triplet axial constant parametrizing the strength of the neutron decay [110]

$$g_A^{(3)} = 1.2670 \pm 0.0035$$

is in a wonderful agreement with the Bjorken sum rule, see Eq. (3.136) and Table 3. The octet coupling is extracted from other hyperon decays, summarized in Table 4, resulting in

$$g_A^{(8)} = 0.58 \pm 0.03.$$

⁹Since the numerical factors appearing in the above Lagrangian can be confusing, let us give a schematic derivation of these relations. The hadronic state is created from the vacuum by a creation operator $|H\rangle = b_H^\dagger|0\rangle$, and in the quark/hadron field ψ only the annihilation operator is needed $\psi = b$ (we did not display the quark/hadron wave function). Thus, we compute the matrix element of the (H)eisenberg operator in perturbation theory defined, of course, in the (D)irac representation with the Lagrangian (3.143):

$$\begin{aligned}\langle p | \bar{u}u - \bar{d}d | p \rangle_H &= \langle p | :(\bar{u}u - \bar{d}d) : \mathcal{L}_{\mathbf{8} \rightarrow \mathbf{8}} | p \rangle_D = \langle p | :(\bar{u}u - \bar{d}d) : \frac{1}{2}(D+F) : \bar{p}(\bar{u}u - \bar{d}d) p : | p \rangle_D \\ &= \frac{1}{2}(D+F)\langle 0 | b_p b_p^\dagger : (\bar{u}u - \bar{d}d) :: (\bar{u}u - \bar{d}d) : b_p b_p^\dagger | 0 \rangle_D = \frac{1}{2}(D+F)\langle 0 | : \bar{u}u :: \bar{u}u : + : \bar{d}d :: \bar{d}d : | 0 \rangle_D \\ &= D+F,\end{aligned}$$

where the operator inside :: is subject to normal ordering. In the last but one term, we have kept only pairing of quarks of the same flavor. We use normalization $\langle 0 | : \bar{u}u :: \bar{u}u : | 0 \rangle_D = \langle 0 | : \bar{d}d :: \bar{d}d : | 0 \rangle_D = 1$.

Axial transition	Matrix element	Strength	Experimental value
$n \rightarrow p$	$\langle p \bar{u}d n \rangle$	$D + F$	1.2670 ± 0.0035
$\Xi^- \rightarrow \Lambda^0$	$\langle \Lambda^0 \bar{u}s \Xi^- \rangle$	$\frac{1}{\sqrt{6}}(3F - D)$	0.25 ± 0.05
$\Sigma^- \rightarrow n$	$\langle n \bar{u}s \Sigma^- \rangle$	$D - F$	0.340 ± 0.017
$\Lambda \rightarrow p$	$\langle p \bar{u}s \Lambda^0 \rangle$	$-\frac{1}{\sqrt{6}}(3F + D)$	-0.718 ± 0.015

Table 4: Experimental data on hyperon decays [110] which measure the strength of axial transitions.

Taking into account the QCD radiative corrections, which affect the coefficients with which the axial constants enter the sum rule (3.133) by multiplicative factors [111] on the right-hand side, one extracts the singlet axial constant and thus the fraction of the nucleon spin carried by the quarks to be [85]

$$\Delta\Sigma = 0.29 \pm 0.10$$

at $Q^2 = 4 \text{ GeV}^2$ in the $\overline{\text{MS}}$ scheme. At the same time the values extracted by experimental collaborations vary from $\Delta\Sigma = 0.23 \pm 0.04 \pm 0.06$ at $Q^2 = 5 \text{ GeV}^2$ for SLAC E155 [106] to $\Delta\Sigma = 0.19 \pm 0.05 \pm 0.04$ at $Q^2 = 1 \text{ GeV}^2$ for SMC [107, 108]. As we emphasized before, this value is in sharp contradiction with the expectations of the naive quark model of hadrons.

3.6.3 Angular momentum of proton's constituents

Thus, the spin carried by quarks cannot account for the whole spin of the proton. The question arises as to where the other sources of the hadron spin are resided. To resolve successfully the issue, recall that the tensor of the angular momentum is expressed solely in terms of the improved energy-momentum tensor (see Appendix E)

$$M^{\mu\nu;\rho} = x^\mu \Theta^{\rho\nu} - x^\nu \Theta^{\rho\mu}.$$

The charge

$$\mathbb{M}^{\mu\nu} = \int d^3z M^{\mu\nu;0}(z)$$

generates Lorentz transformations and obeys the standard $SO(3, 1)$ algebra (see Eq. (I.9) in Appendix I). The three-vector of angular momentum determined from this charge as coordinate moment of the three-vector of the momentum flow $\boldsymbol{\Theta} = (\Theta^{01}, \Theta^{02}, \Theta^{03})$,

$$J^i = \frac{1}{2} \varepsilon^{ijk} \mathbb{M}^{jk} = \int d^3z [\mathbf{z} \times \boldsymbol{\Theta}(\mathbf{z})]^i \quad (3.147)$$

can be rewritten in the form [101, 2]

$$\mathbf{J} = \int d^3z \left\{ \frac{1}{2} \psi^\dagger(\mathbf{z}) \boldsymbol{\Sigma} \psi(\mathbf{z}) - \psi^\dagger(\mathbf{z}) [\mathbf{z} \times i\mathcal{D}] \psi(\mathbf{z}) + [\mathbf{E}(\mathbf{z}) \times \mathbf{B}(\mathbf{z})] \right\}, \quad (3.148)$$

which appears to have the meaning of the quark spin and orbital angular momentum with covariant momentum $i\mathcal{D}$ for the first two terms, respectively, and the gluon angular momentum for the last

one, expressed in terms of the Poynting vector $[\mathbf{E} \times \mathbf{B}]$ of chromoelectric \mathbf{E} and chromomagnetic \mathbf{B} fields. Let us note, that, for a gauge particle, a further decomposition of its angular momentum into its spin and orbital components is not possible. A hand waving argument goes as follows [112]: In quantum mechanics, the wave function of a spin- s particle is a symmetric rank- $2s$ spinor having $(2s+1)$ components, which transform into each other under the rotation of the coordinate system. The orbital wave function is related to the coordinate dependence of wave functions and is given by the spherical harmonics of order L for the angular momentum L of the system. Therefore, in order to distinguish clearly between the spin and orbital momentum, the spin and coordinate properties must be independent. As it is obvious, this condition is not fulfilled for gauge particles whose description in terms of field operators inevitably involves a gauge condition. For instance, in the Coulomb gauge, the gluon wave function is given by the three-potential $\mathbf{A}^a(x)$ equivalent to the second rank spinor which, however, is a subject to the gauge-fixing condition $\nabla \cdot \mathbf{A}^a(x) = 0$. As a result, the coordinate dependence of the vector cannot be independently defined for each of its components and leads to the inability to separate in a gauge-invariant manner the spin and orbital degrees of freedom. For suggestions of a break-up of the gluon angular momentum into its spin and orbital parts within the context of the QCD parton model picture, we refer the reader to Refs. [113, 114]. Within this framework, the gluon spin can be identified with the first moment of the polarized gluon density $\Delta g(x)$ (see Eq. (3.72)) in the light-cone gauge and then promoted to a gauge-invariant operator matrix element making use of relations such as Eq. (D.13). Analogous consideration can applied to the gluon orbital part, however, the matrix element of the corresponding operator does not show up in any physical processes and thus presumably lack any phenomenological significance [114].

For a proton at rest, with its spin vector \mathbf{s} pointing in the positive z -direction or for a proton moving along z and in the helicity-up state, the matrix element of the third component of the angular-momentum operator determines the total proton spin in terms of separate contributions from spin and orbital angular momentum of its constituents [2, 115]

$$\langle p, s^z | J^z | p, s^z \rangle = \frac{1}{2} \Delta \Sigma(\mu^2) + \sum_q L^q(\mu^2) + J^g(\mu^2) \equiv \sum_q J^q(\mu^2) + J^g(\mu^2) = \frac{1}{2}, \quad (3.149)$$

where the meaning of different terms is self-explanatory. We introduced an explicit renormalization scale dependence for separate terms which are not conserved in distinction to the total sum which has zero anomalous dimension and, hence, is scale-invariant.

3.6.4 Gravitational form factors

There are no known processes where the forward matrix element of the angular momentum operator (3.149) can be measured. The angular momentum three-vector is a coordinate moment of the momentum three-vector. A similar situation occurred previously in case of electromagnetic form factors where the nucleon magnetic moment, which corresponds to the coordinate moment of the electric current, was given by zero-recoil limit of the non-forward matrix element of the electromagnetic current. Similarly, the form factors in the off-forward matrix element of the energy-momentum tensor will allow to access the coordinate moment of the three-momentum operator. Since graviton couples to the symmetric energy-momentum tensor (see Appendix E) these gravitational form factors would be “measurable” in elastic graviton-nucleon scattering. Obviously, such an experiment is not feasible. As we will discuss later in this paper, one can access them in light-cone dominated Compton scattering. This was the seminal observation in Ref. [2].

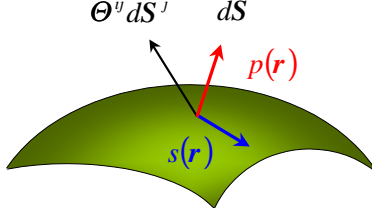


Figure 9: Pressure and shear on the nucleon's surface, considered as a continuous medium.

The quark (3.110) and gluon (3.111) components of the QCD energy-momentum tensor have the following form factor decomposition [116, 2]

$$\langle p_2 | \Theta^{a,\mu\nu} | p_1 \rangle = \frac{1}{2} \left(H^a(\Delta^2) p^{\{\mu} h^{\nu\}} + E^a(\Delta^2) p^{\{\mu} e^{\nu\}} + D^a(\Delta^2) \frac{\Delta^\mu \Delta^\nu - g^{\mu\nu} \Delta^2}{2M_N} b \right) \pm \tilde{D}(\Delta^2) M_N g^{\mu\nu} b, \quad (3.150)$$

where $a = q, g$ and the symmetrization of indices is defined as $\{\mu\nu\} = \frac{1}{2}(\mu\nu + \nu\mu)$. The form factors introduced here are related to the ones arising in the decomposition of the twist-two vector operators (3.123) via

$$H^a = H_{2,0}^a, \quad E^a = E_{2,0}^a, \quad D^a = D_2^a. \quad (3.151)$$

Note that contrary to the electromagnetic form factors, the form factors of the quark and gluon parts of the energy-momentum tensor separately depend on the resolution μ (not displayed explicitly) of the hard probe they are measured with. This is a consequence of their non-conservation, which is reflected in the presence of an extra form factor \tilde{D} . It disappears in the form factor decomposition of the total energy-momentum tensor $\Theta^{\mu\nu} = \Theta^{q,\mu\nu} + \Theta^{g,\mu\nu}$. In the following, we discuss only matrix elements of the total energy-momentum tensor and thus eliminate the superscript $a = q, g$ from the form factors. Due to the conservation of the total energy-momentum tensor, all of its form factors are scale independent. Finally, let us add for completeness the tensor decomposition of the matrix element of a spin-zero target,

$$\langle p_2 | \Theta^{\mu\nu} | p_1 \rangle = \frac{1}{2} (p^\mu p^\nu \theta_2(\Delta^2) + (g^{\mu\nu} \Delta^2 - \Delta^\mu \Delta^\nu) \theta_1(\Delta^2)). \quad (3.152)$$

In order to uncover the physical interpretation of the form factors in the parametrization (3.150), one performs the same analysis with wave packets as was done for the matrix element of the quark electromagnetic current in Section 2.2.2. As a result the Breit-frame gravitational form factors naturally appear to be the Fourier transforms of spatial characteristics of the nucleon [117, 118, 119, 120].

- The time component Θ^{00} is the energy density and thus its matrix element between the proton states localized at $\mathbf{R} = \mathbf{0}$ measures the mass distribution inside the nucleon. Its is related to the gravito-electric form factor [117, 118, 119, 120],

$$\int d^3 r e^{-i\Delta \cdot r} \langle \mathbf{0} | \Theta^{00}(\mathbf{r}) | \mathbf{0} \rangle = M_N \sqrt{1 + \frac{\Delta^2}{4M_N^2}} w_2^* w_1 \left(H - \frac{\Delta^2}{4M_N^2} (E - D) \right) (-\Delta^2). \quad (3.153)$$

Note that the mass distribution of constituents is different from their charge distribution due to the presence of electromagnetically neutral gluons inside hadrons which do not contribute to the electromagnetic form factors. At zero recoil, $\Delta = 0$, the matrix element of the energy-momentum tensor gives the nucleon's momentum fractions carried by its constituents¹⁰ which is obviously

$$H(0) = \sum_{a=q,g} H^a(0) = \sum_{a=q,g} \int_{-1}^1 dx x f^a(x) = 1. \quad (3.154)$$

The separate components of this sum

$$P^a = \int_{-1}^1 dx x f^a(x), \quad (3.155)$$

define the fraction of hadron's momentum carried by the a -parton and are measurable in deeply inelastic scattering.

- The time-spatial component of the energy-momentum tensor $\Theta \equiv (\Theta^{01}, \Theta^{02}, \Theta^{03})$ defines the three-dimensional distribution of the orbital angular momentum and is related to the nucleon gravito-magnetic form factor

$$\int d^3r e^{-i\Delta \cdot r} \langle \mathbf{0} | \Theta^{0k}(r) | \mathbf{0} \rangle = \frac{i}{4} \sqrt{1 + \frac{\Delta^2}{4M_N^2}} w_2^* [\Delta \times \boldsymbol{\sigma}]^k w_1 (H + E) (-\Delta^2). \quad (3.156)$$

To clearly see the physical content, we expand both sides of this equation up to terms linear in the momentum transfer Δ and finds

$$\langle \mathbf{0} | \mathbf{J} | \mathbf{0} \rangle = \int d^3r \langle \mathbf{0} | [r \times \boldsymbol{\Theta}(r)] | \mathbf{0} \rangle = \frac{s}{2} (H(0) + E(0)), \quad (3.157)$$

cf. (3.147). Thus, the gravito-magnetic form factor is normalized at zero recoil to the fractions of total nucleon spin carried by the angular momentum of quarks and gluons [2],

$$J^a = \frac{1}{2} (H^a(0) + E^a(0)), \quad (3.158)$$

with total angular momentum being, of course, the nucleon spin

$$\sum_q J^q + J^g = \frac{1}{2}.$$

This result, together with Eq. (3.154) immediately implies that the total gravitomagnetic moment is zero [121, 122, 123] (cf. [124])

$$\sum_q E^q(0) + E^g(0) = 0. \quad (3.159)$$

¹⁰Note however that the contributing time components of the energy momentum tensor in Eq. (3.153) do contain interaction dependent terms in the light-cone gauge $A^+ = 0$ and thus differ in interpretation from the momentum sum rule (3.155) which involves the matrix element of the interaction-independent light-cone projection of energy-momentum tensor $\langle p | \Theta^{++} | p \rangle$. See Ref. [114] for a thorough discussion on this issue.

- Finally, the spatial components of the energy-momentum tensor in the Breit frame allow one to separate the remaining form factor $D(\Delta^2)$,

$$\int d^3\mathbf{r} e^{-i\Delta \cdot \mathbf{r}} \langle \mathbf{0} | \Theta^{jk}(\mathbf{r}) | \mathbf{0} \rangle = \frac{\Delta^j \Delta^k - \Delta^2 \delta^{jk}}{4M_N} \sqrt{1 + \frac{\Delta^2}{4M_N^2}} w_2^* w_1 D(-\Delta^2). \quad (3.160)$$

Considering the nucleon as a continuous medium of partons, the stress tensor $\Theta^{ij}(\mathbf{r})$ is a density of flow of the i -th component of the momentum in the direction of the j -th axis through the unit area in a unit time interval. In other words, it characterizes the force $\Theta^{ij} dS^j$ experienced by quarks in an infinitesimal surface element dS^j at a distance \mathbf{r} from the center of the nucleon. We can introduce the following parametrization of the total static stress tensor

$$\langle \mathbf{0} | \Theta^{jk}(\mathbf{r}) | \mathbf{0} \rangle = s(\mathbf{r}) \left(\frac{r^i r^j}{\mathbf{r}^2} - \frac{1}{3} \delta^{ij} \right) + p(\mathbf{r}) \delta^{ij}, \quad (3.161)$$

in terms of the scalar functions which describe shear the $s(\mathbf{r})$ and pressure $p(\mathbf{r})$, see Fig. 9. They are related to each other by conservation of the total energy-momentum tensor. The function $p(\mathbf{r})$ can be interpreted as the radial distribution of the “pressure” inside the nucleon. Thus a detailed distribution of forces can be extracted from the Δ^2 -dependence of $D(\Delta^2)$. Namely, substituting Eq. (3.161) into Eq. (3.160) one finds that this form factor is related to the Fourier transform of the shear

$$\sqrt{1 + \frac{\Delta^2}{4M_N^2}} \Delta^2 D(-\Delta^2) w_2^* w_1 = 6M_N \int d^3\mathbf{r} e^{-i\Delta \cdot \mathbf{r}} s(\mathbf{r}) \left(\frac{r^i r^j}{\mathbf{r}^2} - \frac{1}{3} \delta^{ij} \right) \frac{\Delta^j \Delta^k}{\Delta^2}. \quad (3.162)$$

By taking the light-cone projection of the energy-momentum tensor and comparing it to the polynomial form of the moments of generalized parton distributions (3.125), one finds the following relations

$$\begin{aligned} \int_{-1}^1 dx x H^q(x, \eta, \Delta^2) &= H^q(\Delta^2) + \eta^2 D^q(\Delta^2), & \int_{-1}^1 dx x E^q(x, \eta, \Delta^2) &= E^q(\Delta^2) - \eta^2 D^q(\Delta^2), \\ \int_0^1 dx H^g(x, \eta, \Delta^2) &= H^g(\Delta^2) + \eta^2 D^g(\Delta^2), & \int_0^1 dx E^g(x, \eta, \Delta^2) &= E^g(\Delta^2) - \eta^2 D^g(\Delta^2). \end{aligned} \quad (3.163)$$

As it is clear from our presentation, the Δ^2 -dependence of the GPDs provides us with a very detailed spatial images of the nucleon. So far, we have addressed just their lowest two moments. As we found, the first moment corresponds to electromagnetic and weak form factors, while the second is expressed through the gravitational form factors. These two moments give charge, magnetization, mass and angular momentum distributions inside the proton. Higher moments of GPDs correspond to coupling of the higher-spin probes to the proton and shed light on its more complicated characteristics.

3.7 Wave functions and distribution amplitudes

As should be anticipated from our previous discussion and graphical representation of GPDs in Fig. 8, in case when the incoming or outgoing momentum is set to zero, a GPD reduces to a

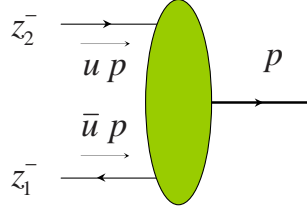


Figure 10: Two-particle distribution amplitude.

function of a single variable. This function formally resembles the meson distribution amplitude. A meson distribution amplitude (DA) actually parametrizes a vacuum-to-hadron or hadron-to-vacuum matrix element of a non-local light-cone operator¹¹

$$\langle p | \bar{\psi}(z_1^-) \gamma^+ \psi(z_2^-) | 0 \rangle = -ip^+ f_M \int_0^1 du e^{ip^+(uz_1^- + \bar{u}z_2^-)} \phi_M(u). \quad (3.164)$$

Expressing DA in the light-cone formalism in terms of creation and annihilation operators, as shown in Fig. 10,

$$if_M \phi_M(u) = \frac{1}{\sqrt{u\bar{u}}} \sum_{\lambda=\uparrow\downarrow} \int \frac{d^2 \mathbf{k}_\perp}{(2\pi)^3} \frac{\langle p | b_\lambda^\dagger(u p^+, \mathbf{k}_\perp) d_{-\lambda}^\dagger(\bar{u} p^+, -\mathbf{k}_\perp) | 0 \rangle}{\langle p | p \rangle}, \quad (3.165)$$

one can see that the function is obviously not a density.

The discussion of distribution amplitudes and their \mathbf{k}_\perp -unintegrated generalization (wave functions) has double purpose. First, distribution amplitudes enter as building blocks into numerous exclusive processes via factorization theorems together with GPDs (see Section 6.3.4). Thus they should be treated as another unknown factors in the description of these processes, and they should be understood in order to use those particular reactions for extraction of GPDs. Second, the light-cone wave functions are genuinely fundamental objects encoding information about hadronic structure on the amplitude level. They can be used to represent a number of hadronic observable in their terms. Formally, this reduces the problem of describing hadronic processes to the computation of the wave functions from first principles. In the following few sections, we provide first a short classification of meson distribution amplitudes, to be used later on in the process of description of hard exclusive meson production. Next, we outline the theory of baryon wave functions with non-zero orbital angular momentum, and use them in the study of the overlap representation of GPDs.

3.7.1 Meson distribution amplitudes

Leading twist meson distribution amplitudes (3.164), which will appear in our discussion of phenomenology of hard exclusive meson production, are classified below in few important cases by the spin and parity of hadrons involved. Let us provide a compendium of results.

- Pseudoscalar distribution amplitudes:

$$\langle \pi^+(p) | \bar{u}(z_1^-) \gamma^+ \gamma^5 d(z_2^-) | 0 \rangle = -ip^+ f_\pi^+ \int_0^1 du e^{ip^+(uz_1^- + \bar{u}z_2^-)} \phi_\pi(u), \quad (3.166)$$

¹¹Here we do not display the gauge links. Their presence is tacitly implied.

param. \ M	π^+	K^-	ρ^+	ρ^0	ω
f_M , MeV	132	159 ± 1.3	195 ± 7	216 ± 5	195
a_1^M	0	0.10 ± 0.12	0	0	0
a_2^M	0.19	-	0.18 ± 0.10	-0.1 ± 0.2	-
a_4^M	-0.13	-	-	-	-

Table 5: Decay constants [110] and magnitude of the first nontrivial harmonics in the partial wave expansion of mesonic distribution amplitudes at the scale $\mu^2 \approx 1 \text{ GeV}^2$ for π^+ [126] (also $a_{2j} \sim 10^{-3}$ for $i = 3, 4, 5$ was given there), K^- [127, 128] (however, cf. [129]), ρ^+ [125], ρ^0 [130].

$$\langle K^+(p) | \bar{u}(z_1^-) \gamma^+ \gamma^5 s(z_2^-) | 0 \rangle = -ip^+ f_K^+ \int_0^1 du e^{ip^+(uz_1^- + \bar{u}z_2^-)} \phi_K(u). \quad (3.167)$$

Notice that as a consequence of the $SU(2)$ and charge symmetry we have the relations between matrix elements involving kaons

$$\begin{aligned} \langle K^+(p) | \bar{u}(z_1^-) \gamma^+ \gamma^5 s(z_2^-) | 0 \rangle &= \langle K^-(p) | \bar{s}(z_1^-) \gamma^+ \gamma^5 u(z_2^-) | 0 \rangle \\ &= \langle K^0(p) | \bar{d}(z_1^-) \gamma^+ \gamma^5 s(z_2^-) | 0 \rangle = \langle \bar{K}^0(p) | \bar{s}(z_1^-) \gamma^+ \gamma^5 d(z_2^-) | 0 \rangle. \end{aligned} \quad (3.168)$$

- Distribution amplitudes of longitudinally polarized vector mesons:

$$\begin{aligned} \langle \rho_L^+(p) | \bar{u}(z_1^-) \gamma^+ d(z_2^-) | 0 \rangle &= p^+ f_\rho^+ \int_0^1 du e^{ip^+(uz_1^- + \bar{u}z_2^-)} \phi_\rho(u), \quad (3.169) \\ \langle \rho_L^0(p) | \frac{1}{\sqrt{2}} (\bar{u}(z_1^-) \gamma^+ u(z_2^-) - \bar{d}(z_1^-) \gamma^+ d(z_2^-)) | 0 \rangle &= p^+ f_\rho^0 \int_0^1 du e^{ip^+(uz_1^- + \bar{u}z_2^-)} \phi_\rho(u), \\ \langle \omega_L^0(p) | \frac{1}{\sqrt{2}} (\bar{u}(z_1^-) \gamma^+ u(z_2^-) + \bar{d}(z_1^-) \gamma^+ d(z_2^-)) | 0 \rangle &= p^+ f_\omega^0 \int_0^1 du e^{ip^+(uz_1^- + \bar{u}z_2^-)} \phi_\omega(u). \end{aligned}$$

A convenient partial-wave expansion of distribution amplitudes is accomplished in terms of Gegenbauer polynomials, the eigenfunctions of QCD evolution equations (this will be explained in the next chapter),

$$\phi_M(u) = 6u\bar{u} \sum_{n=0}^{\infty} a_n^M C_n^{3/2}(2u-1), \quad a_0^M = 1. \quad (3.170)$$

The decay constants and hadronic parameters a_n^M for different mesons are summarized in Table 5.

3.7.2 Nucleon wave function with orbital momentum

The Fock decomposition of a hadronic state is made in components with increasing number of constituents populating the hadron. It starts with the minimally possible configuration, which is a quark-antiquark pair for a meson or three quarks for a baryon. Below, we limit our discussion to the lowest three-quark component of the nucleon wave functions and classify them with respect to quark orbital angular momentum [131]. These wave functions are used both to unravel information contained in matrix elements and to provide a nonperturbative description of nucleon observables where the orbital momentum plays a significant role, like for instance the Pauli form factor [134],

135, 123, 132], or the hadron helicity-flip GPD E^q [123, 131] encoding the magnitude of angular momentum carried by the quarks, etc. We consider below the proton state with helicity-up and introduce the parametrization of the vacuum-to-proton matrix elements at equal light-cone time $z^+ = 0$ in terms of coordinate-space wave function with quark orbital angular momentum L^z . The following three-quark spin and orbital momentum configurations are possible in order to build up the nucleon state with the projection $s_p^z = 1/2$ of its spin:

$$\begin{aligned} s_p^z = 1/2 : \quad & \uparrow\downarrow\uparrow = \sum_q s_q^z = 1/2, & L^z = 0, \\ & \downarrow\downarrow\uparrow = \sum_q s_q^z = -1/2, & L^z = 1, \\ & \uparrow\uparrow\uparrow = \sum_q s_q^z = 3/2, & L^z = -1, \\ & \downarrow\downarrow\downarrow = \sum_q s_q^z = -3/2, & L^z = 2. \end{aligned} \quad (3.171)$$

They correspond to the following set of coordinate-space wave functions parametrizing three-quark operators with the quantum numbers of the proton [131].

• $L^z = 0$:

$$\begin{aligned} \langle 0 | \frac{\varepsilon^{abc}}{\sqrt{6}} (u_{+\uparrow}^a(z_1) C \gamma^+ u_{+\downarrow}^b(z_2)) d_{+\uparrow}^c(z_3) | p_\uparrow \rangle &= \psi_1(z_1, z_2, z_3) p^+ u_{+\uparrow}(p), \\ \langle 0 | \frac{\varepsilon^{abc}}{\sqrt{6}} (u_{+\uparrow}^a(z_1) C i \sigma^{+i} u_{+\downarrow}^b(z_2)) d_{+\uparrow}^c(z_3) | p_\uparrow \rangle &= (\psi_1(z_1, z_3, z_2) + \psi_1(z_2, z_3, z_1)) p^+ \gamma^i u_{+\uparrow}(p). \end{aligned} \quad (3.172)$$

• $L^z = 1$:

$$\begin{aligned} \langle 0 | \frac{\varepsilon^{abc}}{\sqrt{6}} (u_{+\uparrow}^a(z_1) C \gamma^+ u_{+\downarrow}^b(z_2)) d_{+\downarrow}^c(z_3) | p_\uparrow \rangle &= -i (\nabla_{1\perp} \psi_3(z_1, z_2, z_3) + \nabla_{2\perp} \psi_4(z_1, z_2, z_3)) p^+ u_{+\uparrow}(p), \\ \langle 0 | \frac{\varepsilon^{abc}}{\sqrt{6}} (u_{+\downarrow}^a(z_1) C i \sigma^{+i} u_{+\uparrow}^b(z_2)) d_{+\uparrow}^c(z_3) | p_\uparrow \rangle &= i (\nabla_{+1}^i (\psi_4(z_3, z_1, z_2) - \psi_3(z_3, z_1, z_2) - \psi_3(z_3, z_2, z_1)) \\ &\quad + \nabla_{+2}^i (\psi_4(z_3, z_2, z_1) - \psi_3(z_3, z_2, z_1) - \psi_3(z_3, z_1, z_2))) p^+ u_{+\uparrow}(p). \end{aligned} \quad (3.173)$$

• $L^z = -1$:

$$\begin{aligned} \langle 0 | \frac{\varepsilon^{abc}}{\sqrt{6}} (u_{+\uparrow}^a(z_1) C i \sigma^{+i} u_{+\uparrow}^b(z_2)) d_{+\uparrow}^c(z_3) | p_\uparrow \rangle &= i (\nabla_{-1}^i (\psi_5(z_1, z_3, z_2) - \psi_5(z_1, z_2, z_3)) + \nabla_{-2}^i (\psi_5(z_2, z_3, z_1) - \psi_5(z_2, z_1, z_3))) p^+ u_{+\uparrow}(p), \end{aligned} \quad (3.174)$$

• $L^z = 2$:

$$\begin{aligned} \langle 0 | \frac{\varepsilon^{abc}}{\sqrt{6}} (u_{+\downarrow}^a(z_1) C i \sigma^{+i} u_{+\downarrow}^b(z_2)) d_{+\downarrow}^c(z_3) | p_\uparrow \rangle &= 2i^2 \mathbf{S}_{ij} \left(\nabla_{+1}^i \nabla_{\perp 2}^j (\psi_6(z_1, z_2, z_3) + \psi_6(z_2, z_1, z_3) - \psi_6(z_1, z_3, z_2) - \psi_6(z_2, z_3, z_1)) \right. \\ &\quad \left. + \nabla_{+1}^i \nabla_{\perp 1}^j \psi_6(z_1, z_3, z_2) + \nabla_{+2}^i \nabla_{\perp 1}^j \psi_6(z_2, z_1, z_3) \right) p^+ u_{+\uparrow}(p), \end{aligned} \quad (3.175)$$

where in the last equality we introduced the symmetrization and trace subtraction operation for two-dimensional indices \mathbf{S}_{ij} $t_{ij} \equiv \frac{1}{2}(t_{ij} + t_{ji} - \delta_{ij} t_{kk})$. The charge conjugation matrix C used above

is defined in Eq. (A.8) and $\nabla_\perp \equiv \partial/\partial z_\perp$ is the transverse derivative. We also introduced the holomorphic and antiholomorphic derivatives

$$\nabla_-^i \equiv \nabla^i - i\varepsilon^{ij}\nabla^j = e_\perp^i \frac{\partial}{\partial z_\perp}, \quad \nabla_+^i \equiv \nabla^i + i\varepsilon^{ij}\nabla^j = \bar{e}_\perp^i \frac{\partial}{\partial \bar{z}_\perp} \quad (3.176)$$

with respect to holomorphic $z_\perp \equiv z^x + iz^y$ and antiholomorphic $\bar{z}_\perp \equiv z^x - iz^y$ coordinates. The two-dimensional vectors involved here were previously introduced in Eq. (3.8).

The Fourier transform of the coordinate-space wave functions leads to the conventional light-cone wave functions,

$$\psi(z_1, z_2, z_3) = \int [dx][d^2\mathbf{k}_\perp] \psi(\kappa_1, \kappa_2, \kappa_3) \exp \left(-ip^+ \sum_{i=1}^3 x_i z_i^- + i \sum_{i=1}^3 \mathbf{k}_{i\perp} \cdot \mathbf{z}_{i\perp} \right), \quad (3.177)$$

where we used a short-hand notation for the argument of the momentum-space wave function

$$\kappa_i \equiv (x_i, \mathbf{k}_{i\perp}) = (x_i, k_i^x, k_i^y). \quad (3.178)$$

We have taken into account that the wave functions depend on the momentum variables via the light-cone momentum fractions $x_i = k_i^+/p^+$ and transverse momenta $\mathbf{k}_{i\perp}$ with respect to the momentum of the parent hadron. This is an immediate consequence of the Lorentz invariance on the light cone. The integration measures are¹²

$$[dx] \equiv \delta(x_1 + x_2 + x_3 - 1) \prod_{i=1}^3 dx_i, \quad [d^2\mathbf{k}_\perp] \equiv (2\pi)^3 \delta^{(2)}(\mathbf{k}_{1\perp} + \mathbf{k}_{2\perp} + \mathbf{k}_{3\perp}) \prod_{i=1}^3 \frac{d^2\mathbf{k}_{i\perp}}{(2\pi)^3}. \quad (3.179)$$

Using the definitions of the coordinate-space wave functions, one can easily find the nucleon state in terms of components possessing different angular momentum,

$$|p_\uparrow\rangle = |p_\uparrow\rangle_{L=0} + |p_\uparrow\rangle_{L=1} + |p_\uparrow\rangle_{L=-1} + |p_\uparrow\rangle_{L=2}, \quad (3.180)$$

by evaluating the matrix elements with the nucleon state (3.172) – (3.175) at zero light-cone time, see Appendix D. A simple calculation yields the nucleon states expressed via the momentum space wave functions defined in Eq. (3.177),

$$\begin{aligned} |p_\uparrow\rangle_{L=0} &= \frac{1}{2} \int \frac{[dx][d^2\mathbf{k}_\perp]}{\sqrt{x_1 x_2 x_3}} \psi_1(\kappa_1, \kappa_2, \kappa_3) \\ &\times \frac{\varepsilon^{abc}}{\sqrt{6}} b_u^{a\dagger}(\kappa_1, \uparrow) \left\{ b_u^{b\dagger}(\kappa_2, \downarrow) b_d^{c\dagger}(\kappa_3, \uparrow) - b_d^{b\dagger}(\kappa_2, \downarrow) b_u^{c\dagger}(\kappa_3, \uparrow) \right\} |0\rangle, \end{aligned} \quad (3.181)$$

$$\begin{aligned} |p_\uparrow\rangle_{L=1} &= \frac{1}{2} \int \frac{[dx][d^2\mathbf{k}_\perp]}{\sqrt{x_1 x_2 x_3}} \left\{ k_{1\perp} \psi_3(\kappa_1, \kappa_2, \kappa_3) + k_{2\perp} \psi_4(\kappa_1, \kappa_2, \kappa_3) \right\} \\ &\times \frac{\varepsilon^{abc}}{\sqrt{6}} \left\{ b_u^{a\dagger}(\kappa_1, \uparrow) b_u^{b\dagger}(\kappa_2, \downarrow) b_d^{c\dagger}(\kappa_3, \downarrow) - b_d^{a\dagger}(\kappa_1, \uparrow) b_u^{b\dagger}(\kappa_2, \downarrow) b_u^{c\dagger}(\kappa_3, \downarrow) \right\} |0\rangle, \end{aligned} \quad (3.182)$$

$$|p_\uparrow\rangle_{L=-1} = \frac{1}{2} \int \frac{[dx][d^2\mathbf{k}_\perp]}{\sqrt{x_1 x_2 x_3}} \bar{k}_{1\perp} \psi_5(\kappa_1, \kappa_2, \kappa_3)$$

¹²Our conventions for the integration measures as well as the relation between the coordinate and momentum space wave functions differ from the ones accepted in Ref. [10] where the standard Brodsky-Lepage normalization [240] was assumed.

$$\times \frac{\varepsilon^{abc}}{\sqrt{6}} b_u^{a\dagger}(\kappa_1, \uparrow) \left\{ b_d^{b\dagger}(\kappa_2, \uparrow) b_u^{c\dagger}(\kappa_3, \uparrow) - b_u^{b\dagger}(\kappa_2, \uparrow) b_d^{c\dagger}(\kappa_3, \uparrow) \right\} |0\rangle , \quad (3.183)$$

$$|p_\uparrow\rangle_{L=2} = \frac{1}{2} \int \frac{[dx][d^2\mathbf{k}_\perp]}{\sqrt{x_1x_2x_3}} k_{1\perp} k_{3\perp} \psi_6(\kappa_1, \kappa_2, \kappa_3) \\ \times \frac{\varepsilon^{abc}}{\sqrt{6}} b_u^{a\dagger}(\kappa_1, \downarrow) \left\{ b_d^{b\dagger}(\kappa_2, \downarrow) b_u^{c\dagger}(\kappa_3, \downarrow) - b_u^{b\dagger}(\kappa_2, \downarrow) b_d^{c\dagger}(\kappa_3, \downarrow) \right\} |0\rangle . \quad (3.184)$$

Here we introduced the holomorphic and antiholomorphic momenta

$$k_{i\perp} \equiv k_i^x + i k_i^y, \quad \bar{k}_{i\perp} \equiv k_i^x - i k_i^y \quad (3.185)$$

respectively. The state with zero orbital angular momentum is normalized as follows

$${}_{L=0}\langle p_{2\uparrow}|p_{1\uparrow}\rangle_{L=0} = 4p_1^+(2\pi)^3 \delta(p_1^+ - p_2^+) \delta^{(2)}(\mathbf{p}_{1\perp} - \mathbf{p}_{2\perp}) \int [dx][d^2\mathbf{k}_\perp] |\psi_1(\kappa_1, \kappa_2, \kappa_3)|^2 . \quad (3.186)$$

The proton state with helicity-down can be obtained from the above Eqs. (3.181) – (3.184) making use of the Jacob-Wick transformation \mathcal{Y} ,

$$\mathcal{Y}|p_{s^z}\rangle \equiv e^{-i\pi J^y} \mathcal{P}|p_{s^z}\rangle = (-1)^{s-s^z} |p_{-s^z}\rangle \quad (3.187)$$

which consists of a sequence of the spatial reflection \mathcal{P} (see Section 3.2.8) and the spatial rotation J^y (3.147) by 180° around the y -axis [133].

A few comments are in order concerning the properties of wave functions. As we know from Section 3.2.8, under the reversal of spatial parity, the three-components of the proton momentum change their sign, so that (p^0, \mathbf{p}) becomes $(p^0, -\mathbf{p})$. Under the time reversal, the momentum changes in the same way. Therefore, under combined time-reversal and parity transformations, the momentum of the proton is left intact (see Eq. (3.51)). The same is true for the quark momenta. On the other hand, the helicity changes sign under the combined parity and time reversal, and hence the proton state $|p_\uparrow\rangle$ is transformed into $|p_\downarrow\rangle$. Similar changes occur for the quark states. As we mentioned before, the time reversal acting on c -numbers replaces them with their complex conjugates. Thus, under the combined reflection of space and time, a positive-helicity proton state becomes a negative-helicity state $|p_\downarrow\rangle$, with complex-conjugated wave function; flipped quark helicities, and $k^x \pm ik^y$ becoming $k^x \mp ik^y$. The transformed state is also accompanied by the phase factors $(-1)^{s-s^z}$ (see Eq. (3.51)). Comparing the resulting expression with the ones calculated by means of the Jacob-Wick transformation (3.187), which does not involve the complex conjugation, we find that all of the wave function amplitudes must be real,

$$\psi_i^* = \psi_i . \quad (3.188)$$

This result, however, holds provided the gauge condition imposed on the gluon field is also invariant under the discrete symmetries. In the light-cone gauge, the condition $A^+ = 0$ does not fix the gauge completely, one must specify additional boundary conditions for the gauge field (see Appendix D). This additional gauge fixing might not be invariant under the combined parity and time reversal. For example, the advanced and retarded boundary conditions transform into each other under the time reversal transformation; however, the principal value prescription is self-conjugate. In the former two cases, the wave function no longer obey the reality condition.

Finally, it is instructive to establish relations between the wave functions with non-zero orbital angular momentum and higher-twist distribution amplitudes, which involve the “bad” component

of the quark field. This can be done for the twist-four distribution amplitudes where a complete classification is available [136]. The bridge is built by integrating the momentum-space wave functions over the transverse momentum with appropriate weight factors. The definitions of the twist-four distribution amplitudes may be found in Ref. [136]. For reference purposes, we present here the expression for the leading twist-three proton's distribution amplitude

$$\begin{aligned} \langle 0 | \frac{\varepsilon^{abc}}{\sqrt{6}} (u_{+\uparrow}^a(z_1^-) C \gamma^+ u_{+\downarrow}^b(z_2^-)) d_{+\uparrow}^c(z_3^-) | p_\uparrow \rangle \\ = p^+ u_{+\uparrow}(p) \int [dx] \exp \left(-ip^+ \sum_{i=1}^3 x_i z_i^- \right) \Phi_3(x_1, x_2, x_3). \end{aligned} \quad (3.189)$$

and the complete set of twist-four distribution amplitudes¹³

$$\begin{aligned} \langle 0 | \frac{\varepsilon^{abc}}{\sqrt{6}} (u_{+\uparrow}^a(z_1^-) C \gamma^+ u_{+\downarrow}^b(z_2^-)) \gamma^- d_{-\uparrow}^c(z_3^-) | p_\uparrow \rangle \\ = M_N u_{+\downarrow}(p) \int [dx] \exp \left(-ip^+ \sum_{i=1}^3 x_i z_i^- \right) \Phi_4(x_1, x_2, x_3), \end{aligned} \quad (3.190)$$

$$\begin{aligned} \langle 0 | \frac{\varepsilon^{abc}}{\sqrt{6}} (u_{+\uparrow}^a(z_1^-) C \gamma_\perp^i u_{-\downarrow}^b(z_2^-)) \gamma_\perp^i d_{+\downarrow}^c(z_3^-) | p_\uparrow \rangle \\ = -M_N u_{+\uparrow}(p) \int [dx] \exp \left(-ip^+ \sum_{i=1}^3 x_i z_i^- \right) \Psi_4(x_1, x_2, x_3), \end{aligned} \quad (3.191)$$

$$\begin{aligned} \langle 0 | \frac{\varepsilon^{abc}}{\sqrt{6}} (u_{-\uparrow}^a(z_1^-) C u_{+\uparrow}^b(z_2^-)) d_{+\uparrow}^c(z_3^-) | p_\uparrow \rangle \\ = -\frac{M_N}{2} u_{+\uparrow}(p) \int [dx] \exp \left(-ip^+ \sum_{i=1}^3 x_i z_i^- \right) \Xi_4(x_1, x_2, x_3). \end{aligned} \quad (3.192)$$

Neglecting the dynamical quark-gluon correlations, the desired connection between Eqs. (3.172) – (3.175) and Eqs. (3.190) – (3.192) is found by solving the free Dirac equation $\not{\partial}\psi = 0$ for the “bad” components,

$$\psi_-(z^-, \mathbf{z}_\perp) = \frac{i}{2} \int \frac{dz'^-}{2\pi} \int \frac{dx}{x} e^{ix(z^- - z'^-)} \gamma^+ \boldsymbol{\gamma}_\perp \cdot \boldsymbol{\nabla}_\perp \psi_+(z'^-, \mathbf{z}_\perp), \quad (3.193)$$

where the prescription on the pole in x has to be chosen according to the boundary condition on the gauge field (see Appendix D). Using the expressions for nucleon state (3.180), we finally get the representation for the distribution amplitudes in terms of the wave functions [132]

$$\Phi_3(x_1, x_2, x_3) = \int [d^2 \mathbf{k}_\perp] \psi_1(\kappa_1, \kappa_2, \kappa_3), \quad (3.194)$$

$$\Phi_4(x_2, x_1, x_3) = \frac{1}{M_N x_3} \int [d^2 \mathbf{k}_\perp] \mathbf{k}_{3\perp} \cdot (\mathbf{k}_{1\perp} \psi_3(\kappa_1, \kappa_2, \kappa_3) + \mathbf{k}_{2\perp} \psi_4(\kappa_1, \kappa_2, \kappa_3)), \quad (3.195)$$

$$\Psi_4(x_1, x_2, x_3) = \frac{1}{M_N x_2} \int [d^2 \mathbf{k}_\perp] \mathbf{k}_{2\perp} \cdot (\mathbf{k}_{1\perp} \psi_3(\kappa_1, \kappa_2, \kappa_3) + \mathbf{k}_{2\perp} \psi_4(\kappa_1, \kappa_2, \kappa_3)), \quad (3.196)$$

¹³Note that we have changed the overall normalization of these distribution amplitude as compared to the original definition in Ref. [136], namely our Φ is $\Phi = \frac{-1}{2\sqrt{6}} \Phi_{[136]}$.

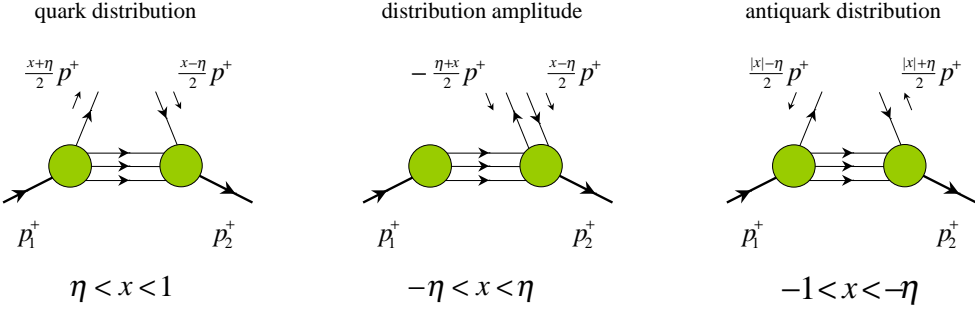


Figure 11: Partonic content of generalized parton distributions in different regions of the momentum-fraction space.

$$\Xi_4(x_1, x_2, x_3) = \frac{1}{M_N x_1} \int [d^2 \mathbf{k}_\perp] \mathbf{k}_{1\perp} \cdot \left(\mathbf{k}_{1\perp} \left(\psi_5(\kappa_1, \kappa_3, \kappa_2) - \psi_5(\kappa_1, \kappa_2, \kappa_3) \right) + \mathbf{k}_{2\perp} \left(\psi_5(\kappa_2, \kappa_3, \kappa_1) - \psi_5(\kappa_2, \kappa_1, \kappa_3) \right) \right). \quad (3.197)$$

Note the interchange of the first and second arguments in Φ_4 !

3.7.3 Partonic content of GPDs

To get a clear physical understanding of the structure of GPDs with respect to the interplay of the Feynman momentum fraction and the skewness dependence, it is instructive to use the light-cone approaches, like we did for the parton distributions in Eq. (2.74) and distribution amplitudes in Eq. (3.165). In the light-cone quantization formalism, the even-parity generalized parton distribution of a quark can be written in terms of creation and annihilation operators. In the region $x > \eta$, it has the representation [7, 137, 138]

$$F^q(x, \eta, \Delta^2)|_{x>\eta} = \frac{1}{\sqrt{x^2 - \eta^2}} \sum_{\lambda=\uparrow\downarrow} \int \frac{d^2 \mathbf{k}_\perp}{(2\pi)^3} \times \frac{\langle p_2 | b_\lambda^\dagger \left(\frac{1}{2}(x - \eta)p^+, \mathbf{k}_\perp - \frac{1}{2}\Delta_\perp \right) b_\lambda \left(\frac{1}{2}(x + \eta)p^+, \mathbf{k}_\perp + \frac{1}{2}\Delta_\perp \right) | p_1 \rangle}{\langle p | p \rangle}, \quad (3.198)$$

where the normalization condition $\langle p | p \rangle = 2p^+(2\pi)^3 \delta^{(3)}(0)$ is implied. This representation has the form resembling the expression for the quark distribution, cf. (2.74), and coincides with it when $p_1 = p_2$. In the region $x < -\eta$, the GPD has the form analogous to the antiquark distribution,

$$F^q(x, \eta, \Delta^2)|_{x<-\eta} = -\frac{1}{\sqrt{x^2 - \eta^2}} \sum_{\lambda=\uparrow\downarrow} \int \frac{d^2 \mathbf{k}_\perp}{(2\pi)^3} \times \frac{\langle p_2 | d_\lambda^\dagger \left(\frac{1}{2}(|x| - \eta)p^+, \mathbf{k}_\perp - \frac{1}{2}\Delta_\perp \right) d_\lambda \left(\frac{1}{2}(|x| + \eta)p^+, \mathbf{k}_\perp + \frac{1}{2}\Delta_\perp \right) | p_1 \rangle}{\langle p | p \rangle}. \quad (3.199)$$

Finally, in the central region $|x| < \eta$

$$F^q(x, \eta, \Delta^2)|_{|x|<\eta} = -\frac{1}{\sqrt{\eta^2 - x^2}} \sum_{\lambda=\uparrow\downarrow} \int \frac{d^2 \mathbf{k}_\perp}{(2\pi)^3} \times \frac{\langle p_2 | b_\lambda^\dagger \left(\frac{1}{2}(x - \eta)p^+, \mathbf{k}_\perp - \frac{1}{2}\Delta_\perp \right) d_{-\lambda}^\dagger \left(-\frac{1}{2}(x + \eta)p^+, -\mathbf{k}_\perp - \frac{1}{2}\Delta_\perp \right) | p_1 \rangle}{\langle p | p \rangle}, \quad (3.200)$$

we recover the form analogous to that encountered in the distribution amplitude (3.165). These representations are graphically illustrated in Fig. 11. Thus, in different regions of the momentum-fraction space, GPDs share common properties with conventional inclusive parton densities for $|x| > \eta$, and exclusive distribution amplitudes for $|x| < \eta$, which illustrates their hybrid nature with respect to the longitudinal momentum.

3.7.4 Overlap representation of GPDs

In order to exhibit further their partonic content, the generalized parton distribution can be represented in terms of the light-cone wave functions. Restricting ourselves only to the lowest Fock component of the nucleon wave function—i.e., that containing the minimal number of constituents—one can express a GPD in terms of wave functions only in the “inclusive” domain $|x| > \eta$. The “exclusive” central region obviously requires the interference of hadron wave functions which differ by two constituents, as can be seen from the middle graph in Fig. 11, and thus involve three- and five-particle light-cone wave functions. In the absence of a complete classification scheme for the latter, we will not discuss this sector at all. For a generic representation in all regions of the momentum fraction space, we refer to Refs. [139, 138].

Let us give a sample formula for the d -quark¹⁴ helicity nonflip combination of GPDs via the wave functions introduced in Section 3.7.2 for $\Delta_\perp = 0$. Using the Dirac bilinears in the light-cone frame given in Eq. (A.34), we get the expression in terms of the wave function with zero orbital angular momentum $L^z = 0$, thus neglecting contributions with $|L^z| > 0$,

$$H^d(x, \eta, \Delta_{\min}^2) - \frac{\eta^2}{1-\eta^2} E^d(x, \eta, \Delta_{\min}^2) = \int [dx] [d^2 \mathbf{k}_\perp] \quad (3.201)$$

$$\times \left\{ \delta(x_3 - x) \psi_1^* \left(\frac{x_1}{1-\eta}, \frac{x_2}{1-\eta}, \frac{x_3 - \eta}{1-\eta}, \mathbf{k}_{1\perp}, \mathbf{k}_{2\perp}, \mathbf{k}_{3\perp} \right) \psi_1 \left(\frac{x_1}{1+\eta}, \frac{x_2}{1+\eta}, \frac{x_3 + \eta}{1+\eta}, \mathbf{k}_{1\perp}, \mathbf{k}_{2\perp}, \mathbf{k}_{3\perp} \right) \right.$$

$$\left. + \delta(x_2 - x) \psi_1^* \left(\frac{x_1}{1-\eta}, \frac{x_2 - \eta}{1-\eta}, \frac{x_3}{1-\eta}, \mathbf{k}_{1\perp}, \mathbf{k}_{3\perp}, \mathbf{k}_{3\perp} \right) \psi_1 \left(\frac{x_1}{1+\eta}, \frac{x_2 + \eta}{1+\eta}, \frac{x_3}{1+\eta}, \mathbf{k}_{1\perp}, \mathbf{k}_{2\perp}, \mathbf{k}_{3\perp} \right) \right\}.$$

The additional terms with the overlap of $\psi_{3,4}$ with ψ_5 are quite analogous to the displayed ones, however, they enter suppressed by a typical factor $\langle \mathbf{k}_\perp^2 \rangle / M_N^2$, where $\langle \mathbf{k}_\perp^2 \rangle^{-1/2} \approx 300$ MeV is the average transverse momentum of quarks in the hadron wave function. Notice that for $\Delta_\perp = 0$, the invariant momentum transfer squared Δ^2 does not vanish but rather takes some minimal value

$$\Delta_{\min}^2 = -\frac{4\eta^2 M_N^2}{1-\eta^2}. \quad (3.202)$$

When $\eta = 0$, one gets the conventional overlap representation of Feynman’s parton distributions. In case $\Delta_\perp \neq 0$, the formula has to be modified as follows. Consider a reference frame where the incoming hadron has no transverse momentum $\mathbf{p}_{\perp 1} = 0$, while the outgoing proton carries a non-vanishing transverse momentum equal to the total momentum transferred $\mathbf{p}_{\perp 2} = -\Delta_\perp$. Then, the arguments of the final-state wave functions change to

$$\mathbf{k}_i \rightarrow \mathbf{k}_i - \frac{1-x_i}{1-\eta} \Delta_\perp \quad (3.203)$$

¹⁴The only reason to chose the d -quark is that the expression is more concise in this case, since there is only one d -quark in the lowest Fock component of the proton wave function.

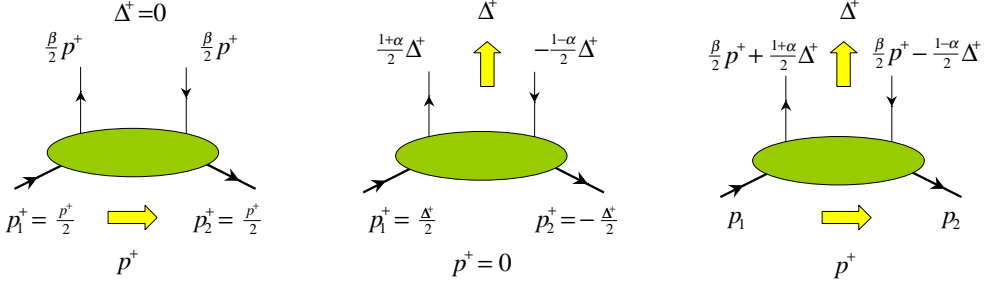


Figure 12: Momentum flow in a double distribution.

for the active parton, i.e., those with $i = 3$ and $i = 2$ for the first and second term of Eq. (3.201), respectively, and

$$\mathbf{k}_i \rightarrow \mathbf{k}_i + \frac{x_i}{1-\eta} \Delta_{\perp}, \quad (3.204)$$

for the remaining passive partons. This shift is well-known from the Drell-Yan formula for elastic form factors [206]. The representation in the region $x < -\eta$ is obtained by reversing the overall sign and replacing $x \rightarrow -x$ in the argument of the δ -function.

The hadron helicity flip amplitude expressed in terms of the GPD E can be represented in terms of the interference of the spherically symmetric wave function ψ_1 and those with non-zero orbital angular momentum, i.e., $E \sim c_1 \psi_1^* \psi_3 + c_2 \psi_1^* \psi_4 + c_3 \psi_5^* \psi_6 + \text{h.c.}$ [131].

3.8 Double distributions

Another complimentary and instructive way to look at GPDs is to treat them as kinematic ‘‘hybrids’’ of the usual parton densities $q(\beta)$ and distribution amplitudes $\phi(\alpha)$. Indeed, $q(\beta)$ corresponds to the forward limit $\Delta = 0$ of the generalized parton distributions, when the momentum p flows only in the s -channel and the outgoing parton carries the momentum $\beta p^+ / 2$ of its parent hadron with momentum $p^+ / 2$ (see Fig. 12). On the other hand, if we take $p = 0$, the momentum Δ flows in the t -channel only and is shared in fractions $(1+\alpha)\Delta^+ / 2$ and $(1-\alpha)\Delta^+ / 2$ between the partons (both momenta treated as outgoing). In general case, we deal with superposition of two momentum fluxes; then the plus components k_i^+ of the parton momenta k_i can be represented as

$$k_1^+ = \beta \frac{p^+}{2} + \frac{1+\alpha}{2} \Delta^+, \quad k_2^+ = \beta \frac{p^+}{2} - \frac{1-\alpha}{2} \Delta^+. \quad (3.205)$$

This decomposition corresponds to the following parametrization for the matrix element of the composite operator (3.4) constructed out of scalar field operators ϕ , [1, 3, 4, 6, 140].

$$\begin{aligned} \langle p_2 | \mathcal{O}^{\phi\phi}(-z^-, z^-) | p_1 \rangle &= \int_{\Omega} d\beta d\alpha e^{-i\beta z^- p^+ - i\alpha z^- \Delta^+} f^{\phi}(\beta, \alpha, \Delta^2) \\ &= \int_{-1}^1 dx e^{-ix z^- p^+} F^{\phi}(x, \eta, \Delta^2). \end{aligned} \quad (3.206)$$

In the second line we have given for comparison the parametrization in terms of a GPD, see Eq. (3.23).

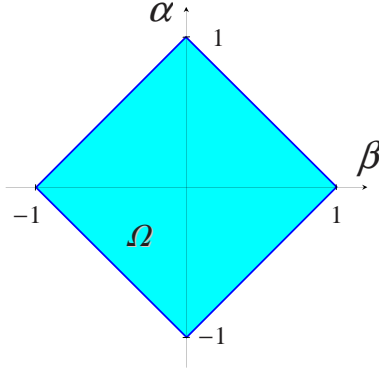


Figure 13: Support region of double distributions.

The support area for $f^\phi(\beta, \alpha, \Delta^2)$ is shown in Fig. 13. For any Feynman diagram, the spectral constraint $|\beta| + |\alpha| \leq 1$ can be proved in the α -representation [1, 6] using the approach of Ref. [141]. Hence,

$$\int_{\Omega} d\beta d\alpha = \int_{-1}^1 d\beta \int_{-1+|\beta|}^{1-|\beta|} d\alpha. \quad (3.207)$$

Comparing Eq. (2.62) with the $\Delta = 0$ limit of the DD definition (3.206) one can find the “reduction formulas” relating the double distribution $f(\beta, \alpha, \Delta^2 = 0)$ to the scalar parton distribution

$$\int_{-1+\beta}^{1-\beta} d\alpha f^\phi(\beta, \alpha, \Delta^2 = 0) = f^\phi(\beta). \quad (3.208)$$

Hence, the positive- β and negative- β components of the double distribution $f^\phi(\beta, \alpha, \Delta^2 = 0)$ can be treated as nonforward generalizations of quark and antiquark densities, respectively. The usual “forward” densities $q(\beta)$ and $\bar{q}(\beta)$ are thus given by integrating $f^\phi(\beta, \alpha, \Delta^2 = 0)$ over vertical lines $\beta = \text{const}$ for $\beta > 0$ and $\beta < 0$, respectively.

Due to hermiticity and time-reversal invariance properties of nonforward matrix elements, established in Section 3.2.8, the DDs are even functions [142] of the variable α , which is conjugate to the skewness η

$$f^\phi(\beta, \alpha, \Delta^2) = f^\phi(\beta, -\alpha, \Delta^2). \quad (3.209)$$

Equation (3.206) allows one to establish a relation between the GPD $F^\phi(x, \eta, \Delta^2)$ and the DD $f^\phi(\beta, \alpha, \Delta^2)$. The former is given as an integral of the latter, namely,

$$F^\phi(x, \eta, \Delta^2) = \int_{-1}^1 d\beta \int_{-1+|\beta|}^{1-|\beta|} d\alpha \delta(\beta + \eta\alpha - x) f^\phi(\beta, \alpha, \Delta^2). \quad (3.210)$$

The α -integration in the DD can be done by means of the delta-function with the result

$$F^\phi(x, \eta) = \int_{-1}^1 \frac{d\beta}{\eta} \Xi(\beta|x, \eta) f^\phi\left(\beta, \frac{x-\beta}{\eta}\right), \quad (3.211)$$

where the step function defining the integration limits reads

$$\begin{aligned} \Xi(\beta|x, \eta) = & \theta(x > \eta)\theta\left(\frac{x+\eta}{1+\eta} > \beta > \frac{x-\eta}{1-\eta}\right) + \theta(-\eta > x)\theta\left(\frac{x+\eta}{1-\eta} > \beta > \frac{x-\eta}{1+\eta}\right) \\ & + \theta(\eta > x > -\eta)\theta\left(\frac{x+\eta}{1+\eta} > \beta > \frac{x-\eta}{1+\eta}\right). \end{aligned} \quad (3.212)$$

In this derivation, DDs are the starting point, while GPDs are obtained from them by an integration. However, even if one starts directly with GPDs, the latter possess the *polynomiality property* which can be naturally incorporated only within the formalism of double distributions. Namely, the x^j moment of $F^\phi(x, \eta, \Delta^2)$ must be a j th order polynomial of η . This restriction on the interplay between x and η dependence of $F^\phi(x, \eta, \Delta^2)$ follows [7] from the simple fact that the Lorentz indices $\mu_1 \dots \mu_j$ of the nonforward matrix element of a local twist-two operator $\mathcal{R}_{\mu_1 \dots \mu_j}^{2,\phi\phi}$ can be carried either by p_μ or by Δ_μ , as we clarified in Section 3.5. As a result,

$$\begin{aligned} n^{\mu_1} \dots n^{\mu_j} \langle p_2 | \mathcal{R}_{\mu_1 \dots \mu_j}^{2,\phi\phi} | p_1 \rangle &= n^{\mu_1} \dots n^{\mu_j} \left\{ p_{\mu_1} \dots p_{\mu_j} F_{j,0}^\phi + \Delta_{\mu_1} \dots p_{\mu_j} F_{j,1}^\phi + \dots + \Delta_{\mu_1} \dots \Delta_{\mu_j} F_{j,j}^\phi \right\} \\ &= \sum_{k=0}^j (p^+)^{j-k} (\Delta^+)^k F_{j,k}^\phi = (p^+)^j \sum_{k=0}^j \eta^k F_{j,k}^\phi. \end{aligned} \quad (3.213)$$

The derivation of GPDs from DDs automatically satisfies the polynomiality condition (3.213), since

$$\int_{-1}^1 dx x^j F^\phi(x, \eta) = \int_{\Omega} d\beta d\alpha (\beta + \eta\alpha)^j f^\phi(\beta, \alpha) = \sum_{k=0}^j \eta^k \binom{j}{k} \int_{\Omega} d\beta d\alpha \beta^{j-k} \alpha^k f^\phi(\beta, \alpha) \quad (3.214)$$

Thus, the coefficients $F_{j,k}^\phi$ are given by

$$F_{j,k}^\phi = \binom{j}{k} \int_{\Omega} d\beta d\alpha \beta^{j-k} \alpha^k f^\phi(\beta, \alpha) \equiv \binom{j}{k} f_{j,k}^\phi, \quad (3.215)$$

i.e., they are proportional to the combined $\beta^{j-k} \alpha^k$ moments of the DD $f^\phi(\beta, \alpha)$. The symmetry and support properties of DDs dictate a nontrivial interplay between j and k dependence of $F_{j,k}^\phi$'s which should be respected in the process of modeling GPDs. After this observation, the use of DDs is a natural step in building consistent parametrizations of GPDs.

3.8.1 Gauge transformation of double distributions

So far we have dealt with the matrix elements of a scalar operator of a spinless field (3.206). However, in the case of a vector twist-two operator \mathcal{R}_μ^2 built either from spin-zero ($\phi^\dagger \partial^\mu \phi$) or spin-one-half ($\bar{\psi} \gamma^\mu \psi$) fields, there is an open vector index μ . As a result, there appear extra Lorentz structures in the decomposition of the matrix element which one should keep to avoid violation of the polynomiality condition for GPDs. This complication was studied in Ref. [143], where it was proposed to add an extra term, the so-called D-term [143] concentrated in the central region $|x| \leq \eta$ only. Such contributions may arise from the t -channel exchange of mesonic-like states.

To illustrate the problem, let us consider the parametrization of the vector quark operator $\mathcal{R}_\mu^{2,qq}(-z, z)$ in terms of double distributions. Its matrix element has two components

$$\langle p_2 | \mathcal{R}_\mu^{2,qq}(-z^-, z^-) | p_1 \rangle = f^q(z^-) p_\mu + g^q(z^-) \Delta_\mu. \quad (3.216)$$

Multiplying $\mathcal{R}_\mu^{2,qq}$ with n^μ one immediately finds

$$\langle p_2 | \mathcal{O}^{qq}(-z^-, z^-) | p_1 \rangle = \int_{\Omega} d\beta d\alpha e^{-iz^- (\beta p^+ + \alpha \Delta^+)} \{ p^+ f^q(\beta, \alpha) + \Delta^+ g^q(\beta, \alpha) \}, \quad (3.217)$$

where we introduced two double distributions corresponding to two structures in Eq. (3.216). The function $f^q(\beta, \alpha)$ is even in α , just as DD for the scalar operator, while $g^q(\beta, \alpha)$ is odd in α because Δ changes sign under the reversal of time. The corresponding GPD can be written as

$$H^q(x, \eta) = \int_{\Omega} d\beta d\alpha \delta(\beta + \eta\alpha - x) \{f^q(\beta, \alpha) + \eta g^q(\beta, \alpha)\}. \quad (3.218)$$

Note, that the α -symmetry properties of $f^q(\beta, \alpha)$ and $g^q(\beta, \alpha)$ guarantee that $H^q(x, \eta)$ is even in η . The x^j moments of $H^q(x, \eta)$ are now given by

$$\begin{aligned} \int_{-1}^1 dx x^j H^q(x, \eta) &\equiv \sum_{k=0}^{j+1} \eta^k H_{j+1,k}^q \\ &= f_{j,0}^q + \sum_{k=1}^j \eta^k \frac{j!}{k!(j-k+1)!} [(j-k+1)f_{j,k}^q + kg_{j,k-1}^q] + \eta^{j+1} g_{j,j}^q, \end{aligned} \quad (3.219)$$

where $f_{j,k}^q$ and $g_{j,k}^q$, similarly to (3.215), are defined as $\beta^{j-k}\alpha^k$ moments of the relevant DD. The $j+1$ subscript in element $H_{j+1,k}^q$ indicates the total number of vector indices of the corresponding local operator and also the highest possible power η^{j+1} of η in the expansion of the x^j moment of $H^q(x, \eta)$. The η^{j+1} term can be obtained only from the DD $g^q(\beta, \alpha)$. Alternatively, the zeroth power of η can be obtained only from the DD $f^q(\beta, \alpha)$. The η^k powers with $1 \leq k \leq j$ come both from the $f^q(\beta, \alpha)$ and $g^q(\beta, \alpha)$ DDs in the combination $(j-k+1)f_{j,k}^q + kg_{j,k-1}^q$. As a result, the coefficients $H_{j+1,k}^q$ do not change under the transformation

$$f_{j,k}^q \rightarrow f_{j,k}^q + k\lambda_{j,k}^q, \quad g_{j,k-1}^q \rightarrow g_{j,k-1}^q + (j-k+1)\lambda_{j,k}^q. \quad (3.220)$$

This means that separation of $H_{j+1,k}^q$ coefficients into f^q and g^q parts is not unambiguous [143, 144]. However, in the double distribution representation (3.217), f^q and g^q contributions look like quite distinct terms since they enter with different factors: p^+ and Δ^+ , respectively. One can get rid of the latter integrating (3.217) by parts. Assuming that DDs vanish at the boundaries of the support region Ω , we obtain

$$z^- \langle p_2 | \mathcal{O}^{qq}(-z^-, z^-) | p_1 \rangle = -i \int_{\Omega} d\beta d\alpha e^{-iz^-(\beta p^+ + \alpha \Delta^+)} \left\{ \frac{\partial}{\partial \beta} f^q(\beta, \alpha) + \frac{\partial}{\partial \alpha} g^q(\beta, \alpha) \right\}. \quad (3.221)$$

Thus, the functions f^q and g^q are defined modulo a “gauge transformation” [144]

$$f^q(\beta, \alpha) \rightarrow f^q(\beta, \alpha) + \frac{\partial}{\partial \alpha} \lambda^q(\beta, \alpha), \quad g^q(\beta, \alpha) \rightarrow g^q(\beta, \alpha) - \frac{\partial}{\partial \beta} \lambda^q(\beta, \alpha), \quad (3.222)$$

with $\lambda^q(\beta, \alpha)$ being an odd function of α , vanishing at the boundaries of the DD support region¹⁵. Since the $f_{j,0}^q$ term in (3.220) is unambiguously coming from an f^q -type DD, while the $g_{j,j}^q$ term only comes from a g^q -type one, in general, the λ^q -transformation cannot completely eliminate either one of the two DDs. But there are two possibilities of “almost complete” elimination.

- First, one can associate all the coefficients $H_{j+1,k}^q$ except the $k = j+1$ one with an f^q -type DD treating them as $\binom{j}{k} f_{j,k}^q$, and consider only the last coefficient $H_{j+1,j+1}^q = g_{j,j}^q$ as coming from a g^q -type contribution. This decomposition corresponds to [143]

$$H^q(x, \eta) = \int_{\Omega} d\beta d\alpha \delta(\beta + \eta\alpha - x) f_D^q(\beta, \alpha) + \text{sgn}(\eta) D^q(x/\eta), \quad (3.223)$$

¹⁵This restriction can be omitted, see Ref. [145] for the analysis of the situation when DD does not vanish on the boundaries of the support region.

where $f_D^q(\beta, \alpha)$ satisfies

$$\frac{\partial f_D^q(\beta, \alpha)}{\partial \beta} = \frac{\partial f^q(\beta, \alpha)}{\partial \beta} + \frac{\partial}{\partial \alpha} \left[g^q(\beta, \alpha) - \delta(\beta) D^q(\alpha) \right], \quad (3.224)$$

and the D -term [143] is given by

$$\int_{-1}^1 d\alpha \alpha^j D^q(\alpha) = g_{j,j}^q \quad \text{or} \quad D^q(\alpha) = \int_{-1+|\alpha|}^{1-|\alpha|} d\beta g^q(\beta, \alpha). \quad (3.225)$$

Since $D^q(\alpha)$ has the $|\alpha| \leq 1$ support, the D -term in GPD is entirely concentrated in the central region $|x| \leq |\eta|$. Obviously, $D^q(\alpha)$ is an antisymmetric function $D^q(\alpha) = -D^q(-\alpha)$ since $g^q(\beta, \alpha)$ is odd in α .

- Alternatively, we can decide that only the lowest coefficient $H_{j,0}^q$ is related to an f^q -type contribution (given by $f_{j,0}^q$) and treat all other $H_{j,k}^q$ coefficients as $\binom{j}{k-1} g_{j,k-1}^q$, thus associating them with a g^q -type DD. In this case [145]

$$H^q(x, \eta) = f^q(x) + \eta \int_{\Omega} d\beta d\alpha \delta(\beta + \eta\alpha - x) g_F^q(\beta, \alpha), \quad (3.226)$$

where now $g_F^q(\beta, \alpha)$ is a solution of

$$\frac{\partial g_F^q(\beta, \alpha)}{\partial \alpha} = \frac{\partial g_F^q(\beta, \alpha)}{\partial \alpha} - \frac{\partial}{\partial \beta} \left[f^q(\beta, \alpha) - \delta(\alpha) f^q(\beta) \right], \quad (3.227)$$

and $f^q(\beta)$ is the forward parton distribution

$$f^q(\beta) = \int_{-1+|\beta|}^{1-|\beta|} d\alpha f^q(\beta, \alpha). \quad (3.228)$$

- Another possibility [146] is the so-called one-component DD. To understand the idea behind it, notice that, in case of scalar quarks, the local operators $\phi^\dagger \partial^\mu \partial^{\mu_1} \dots \partial^{\mu_j} \phi$ that appear in the expansion of the vector bilocal operator $\phi^\dagger(0) \partial^\mu \phi(z^-)$ are the same as in the expansion of the scalar bilocal operator $\phi^\dagger(0) \phi(z^-)$. The only difference is that the index μ is treated as external in the vector case. Thus, the matrix element of the local operator with j derivatives in the expansion of the scalar operator coincides with the matrix element of the vector-type local operator which has $j-1$ “expansion” derivatives. Evidently, both operators can be parametrized by the same DD $f^\phi(\beta, \alpha)$ of the scalar operator. One should just realize that in the vector case one should take the x^{j-1} moment of $F^\phi(x, \eta)$ (or x^j moment of $F^\phi(x, \eta)/x$) to get matrix element of the local operator with total j derivatives. This gives

$$F^\phi(x, \eta) = x \int_{\Omega} d\beta d\alpha \delta(\beta + \eta\alpha - x) f^\phi(\beta, \alpha). \quad (3.229)$$

Due to the delta function, we have $x = \beta + \eta\alpha$.

Obviously, one can use this definition also for a vector bilocal operator built from spin-one-half fields. The parametrization of the scalar matrix elements yields

$$\langle p_2 | \mathcal{R}_\mu^{2,qq}(-z^-, z^-) | p_1 \rangle = \int_{\Omega} d\beta d\alpha (\beta p_\mu + \alpha \Delta_\mu) h^q(\beta, \alpha) e^{-i\beta z^- p^+ - i\alpha z^- \Delta^+}, \quad (3.230)$$

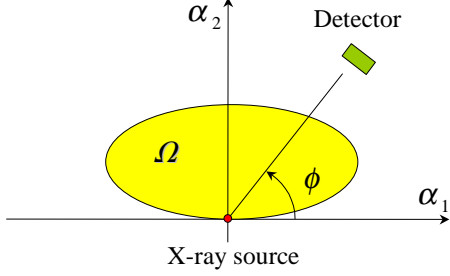


Figure 14: The Radon transformation and the analogue of the setup of the X-ray computed tomography. The X-ray source is at the center of coordinates and the detector measures the intensity I of the beam after its passes through the object confined within the area Ω .

where the DD $h^q(\beta, \alpha)$ can be defined through the coefficients $H_{j,k}^q$ of the η^k expansion (3.220) of the vector operator

$$H_{j,k}^q \equiv \binom{j}{k} \int_{\Omega} d\beta d\alpha \beta^{j-k} \alpha^k h^q(\beta, \alpha). \quad (3.231)$$

The parametrization (3.231) corresponds to the choice in (3.218)

$$f_h^q(\beta, \alpha) = \beta h^q(\beta, \alpha), \quad g_h^q(\beta, \alpha) = \alpha h^q(\beta, \alpha).$$

The λ^q -transformation producing this result is a solution to the equation

$$\left(\beta \frac{\partial}{\partial \beta} + \alpha \frac{\partial}{\partial \alpha} \right) \lambda^q(\beta, \alpha) = -\alpha f^q(\beta, \alpha) + \beta g^q(\beta, \alpha), \quad (3.232)$$

which is

$$\lambda^q(\beta, \alpha) = \int_1^\infty dt \left[\alpha f^q(t\beta, t\alpha) - \beta g^q(t\beta, t\alpha) \right]. \quad (3.233)$$

The D -term and the forward parton density are related to $h^q(\beta, \alpha)$ by

$$D^q(\alpha) = \alpha \int_{-1+|\alpha|}^{1-|\alpha|} d\beta h^q(\beta, \alpha), \quad f^q(\beta) = \beta \int_{-1+|\beta|}^{1-|\beta|} d\alpha h^q(\beta, \alpha). \quad (3.234)$$

- Finally, in Ref. [147] a DD was introduced, which embeds a prefactor $(1-x)^{2s}$ from a GPD of spin- s parton in front of the DD integral. The relation of this DD to those we discussed above is not straightforward.

3.8.2 Radon tomography of double distributions with GPDs

The relation (3.210) is known as the Radon transformation, since it is a one-dimensional slice of a two-dimensional function [37],

$$\mathcal{R}(I, \mathbf{n}) = \int_{\Omega} d^2\boldsymbol{\alpha} \delta(I - \mathbf{n} \cdot \boldsymbol{\alpha}) \tau(\boldsymbol{\alpha}), \quad (3.235)$$

along the direction specified by a two-dimensional unit vector \mathbf{n} (see Fig. 14)

$$\mathbf{n} = (\cos \phi, \sin \phi).$$

For a function $\tau(\boldsymbol{\alpha})$ with the same support Ω as for the double distribution and the angle ϕ fixed by the skewness η ,

$$\phi = \arctan \eta.$$

we arrive at the above relation (3.210) between the GPD

$$F(x, \eta) = \cos \phi \mathcal{R}(x \cos \phi, \mathbf{n}),$$

and the double distribution

$$\tau(\boldsymbol{\alpha} = (\beta, \alpha)) = f(\beta, \alpha).$$

An explicit formula for the inverse Radon transform of the DD $h^q(\beta, \alpha)$ in terms of $H^q(x, \eta)$ can be obtained by incorporating the single-DD representation for the twist-two operator $\mathcal{R}_\mu^{2,qq}$ (3.230) [146] and is achieved in a few easy steps. The first step consists in equating the right-hand sides of Eqs. (3.119) and (3.230) and projecting the Lorentz index μ onto the transverse plane such that it does not interfere with longitudinal integrations performed at subsequent stages. Next, one Fourier transforms both sides of the resulting equality with respect to the skewness $\eta = \Delta^+/p^+$. Integrating out the arising delta-function accompanying the DD, one gets a factor of $|z^- p^+|^{-1}$. Since the last step will consist in the Fourier transformation with respect to z^- , it is instructive to use the following Fourier representation for $|z^- p^+|$:

$$|a| = -\frac{1}{\pi} \text{PV} \int_{-\infty}^{\infty} \frac{d\tau}{\tau^2} e^{i\tau a}, \quad (3.236)$$

where the principal value prescription is understood as [149]

$$\begin{aligned} \text{PV} \int_{-\infty}^{\infty} \frac{d\tau}{\tau^2} \mathcal{F}(\tau) &\equiv \frac{1}{2} \int_{-\infty}^{\infty} d\tau \mathcal{F}(\tau) \left\{ \frac{1}{(\tau + i0)^2} + \frac{1}{(\tau - i0)^2} \right\} \\ &= \int_{-\infty}^{\infty} \frac{d\tau}{\tau^2} \{ \mathcal{F}(\tau) + \mathcal{F}(-\tau) - 2\mathcal{F}(0) \}. \end{aligned} \quad (3.237)$$

Carrying out the advertised Fourier transform with respect to the light-cone separation z^- , we find

$$\alpha h^q(\beta, \alpha) = -\frac{1}{2\pi^2} \int_{-\infty}^{\infty} dx \int_{-\infty}^{\infty} d\eta \text{PV} \frac{1}{(\beta + \eta\alpha - x)^2} \int_{-\infty}^{\infty} dx' W_2(x, x') \frac{d}{d\eta} H^q(x', \eta),$$

where W_2 kernel was introduced in Eq. (3.120). Finally, we perform the x integration and integrate by parts with respect to η . Dropping the surface term, we recover the result [146]

$$h^q(\beta, \alpha) = \frac{1}{2\pi^2} \int_{-\infty}^{\infty} d\eta \int_{-\infty}^{\infty} \frac{dx}{x} \text{PV} \left\{ \frac{1}{(\beta + \eta\alpha)^2} - \frac{1}{(\beta + \eta\alpha - x)^2} \right\} H^q(x, \eta). \quad (3.238)$$

This form of the inverse Radon transformation is similar to that given in Ref. [150]. Note that the inversion kernel in Eq.(3.238) compensates the singularity of the $1/x$ factor, so that the integral over x exists even if the function $H^q(x, \eta)/x$ has a non-integrable singularity at $x = 0$. In case when $H^q(x, \eta)/x$ is integrable, the first term in the integrand of Eq. (3.238) can be safely neglected, being proportional to $\delta(\beta)\delta(\alpha)$ (see Eq. (3.229)).

According to Eq. (3.223), the Radon transform of the $f_D^q(\beta, \alpha)$ (3.223) is given by $(H^q - D^q)$. The inverse transformation gives

$$f_D^q(\beta, \alpha) = -\frac{1}{2\pi^2} \int_{-\infty}^{\infty} d\eta \int_{-\infty}^{\infty} dx \text{PV} \frac{1}{(\beta + \eta\alpha - x)^2} \left\{ H^q(x, \eta) - \text{sgn}(\eta) D^q \left(\frac{x}{\eta} \right) \right\}. \quad (3.239)$$

Here the term $1/(\beta + \eta\alpha)^2$ was omitted as explained above. Since both $H^q(x, \eta)$ and $D^q(x/\eta)$ can be expressed through $h^q(\beta, \alpha)$, one can also write $f_D^q(\beta, \alpha)$ in terms of $h^q(\beta, \alpha)$. The explicit expression was given in Ref. [146]:

$$f_D^q(\beta, \alpha) = \beta h^q(\beta, \alpha) - \frac{d}{d\alpha} \alpha \int d\beta' W_2(\beta, \beta') \beta' h^q(\beta', \alpha). \quad (3.240)$$

In this sense, both f_D^q and D^q functions in (3.223) can be treated as different projections of the same function h^q . Also, it is easy to recognize

$$\lambda_h^q(\beta, \alpha) = -\alpha \int d\beta' W_2(\beta, \beta') \beta' h^q(\beta', \alpha) \quad (3.241)$$

as the λ^q -transformation from the one-component DD representation (3.230) to (3.223).

3.8.3 Nucleon double distributions

In the present section, for reference purposes, we give a single component representation of DDs for the spin-one-half target. We introduce the parametrization using the decomposition in terms of Dirac bilinears h^μ and b for the unpolarized sector,

$$\begin{aligned} & \langle p_2 | \mathcal{O}^{qq}(-z^-, z^-) | p_1 \rangle \\ &= \int_{\Omega} d\beta d\alpha e^{-i\beta z^- p^+ - i\alpha z^- \Delta^+} \left\{ h^+ h_A^q(\beta, \alpha, \Delta^2) + \frac{b}{2M_N} (\beta p^+ + \alpha \Delta^+) h_B^q(\beta, \alpha, \Delta^2) \right\}, \end{aligned} \quad (3.242)$$

and \tilde{h}^μ and \tilde{b} for the polarized one,

$$\begin{aligned} & \langle p_2 | \tilde{\mathcal{O}}^{qq}(-z^-, z^-) | p_1 \rangle \\ &= \int_{\Omega} d\beta d\alpha e^{-i\beta z^- p^+ - i\alpha z^- \Delta^+} \left\{ \tilde{h}^+ \tilde{h}_A^q(\beta, \alpha, \Delta^2) + \frac{\tilde{b}}{2M_N} (\beta p^+ + \alpha \Delta^+) \tilde{h}_B^q(\beta, \alpha, \Delta^2) \right\}. \end{aligned} \quad (3.243)$$

For gluons, the parametrization in terms of the same bilinears can be obtained from these by simple substitutions: $\mathcal{O}^{qq} \rightarrow \mathcal{O}^{gg}$ on the left-hand side and $h_A^q \rightarrow \frac{1}{4} p^+ h_A^g$, $h_B^q \rightarrow \frac{1}{4} (\beta p^+ + \alpha \Delta^+) h_B^g$ on the right-hand side of Eq. (3.242). Similar replacements are done for the gluon equivalent of Eq. (3.243) with symbols dressed by tildes.

The moments of DDs h_A^q and h_B^q from Eq. (3.242) are related to the form factors and GPDs introduced in Eqs. (3.121) and (3.122). Namely,

$$B_{j,k}^q = \frac{1}{k!} \frac{\partial^k}{\partial \eta^k} \Big|_{\eta=0} \int_{-1}^1 dx x^{j-1} B^q(x, \eta) = \binom{j}{k} \int_{\Omega} d\beta d\alpha \beta^{j-k} \alpha^k h_B^q(\beta, \alpha) \quad (3.244)$$

$$A_{j,k}^q = \frac{1}{k!} \frac{\partial^k}{\partial \eta^k} \Big|_{\eta=0} \int_{-1}^1 dx x^{j-1} A^q(x, \eta) = \binom{j-1}{k} \int_{\Omega} d\beta d\alpha \beta^{j-k-1} \alpha^k h_A^q(\beta, \alpha), \quad (3.245)$$

where $j \geq 1$ and the index k varies in the interval $0 \leq k \leq j$ for B^q and $0 \leq k \leq j-1$ for A^q structure. This is an immediate consequence of the polynomiality condition: the j -th moment of the functions $A^a(x, \eta)$ and $B^q(x, \eta)$ are polynomials of order $(j-1)$ and j in η , respectively. Matching the parametrization (3.242) into the one in terms of GPDs $A^q(x, \eta)$ and $B^q(x, \eta)$ introduced in Section 3.5.2 one immediately finds

$$A^q(x, \eta) = \int_{\Omega} d\beta d\alpha \delta(\beta + \eta\alpha - x) h_A^q(\beta, \alpha), \quad (3.246)$$

$$B^q(x, \eta) = x \int_{\Omega} d\beta d\alpha \delta(\beta + \eta\alpha - x) h_B^q(\beta, \alpha), \quad (3.247)$$

and analogous relations for the odd parity DDs (3.243). The relation of GPDs A^q and B^q in terms of the standard H^q and E^q can be found in Eq. (3.131). Finally, for the axial channel in the analogous parametrization with Dirac bilinears \tilde{h}^μ and \tilde{b} as in Eq. (3.121), the GPDs \tilde{A}^q and \tilde{B}^q are identical to the conventional \tilde{H}^q and \tilde{E}^q .

3.9 Analytic properties of DDs and GPDs

The formalism of DDs also allows one to easily establish some important properties of skewed distributions. Notice that due to the cusp at the upper corner of the DD support rhombus, the length of the integration line depends nonanalytically on x for $x = \pm\eta$. Hence, unless the double distribution identically vanishes in a finite region around the upper corner of the DD support rhombus, the x -dependence of the relevant GPDs *must be nonanalytic* at the border points $x = \pm\eta$. Still, the length of the integration line is a continuous function of x . As a result, if the double distribution $f(\beta, \alpha, \Delta^2)$ is not too singular for small β , the skewed distribution $H(x, \eta, \Delta^2)$ is continuous at the nonanalyticity points $x = \pm\eta$. Because of the $1/(\xi \pm x)$ factors present in hard amplitudes entering exclusive processes, as discussed later in Section 6, this property is crucial for perturbative factorization of exclusive amplitudes involving GPDs, when the external kinematics sets $\eta = \xi$. These features are manifested in model ansätze that will be discussed in Section 3.13.1.

In principle, we cannot exclude the possibility that the functions $f(\beta, \alpha, \Delta^2)$ have singular terms at $\beta = 0$ proportional to $\delta(\beta)$ or its derivative(s). Such terms have no projection onto the usual parton densities. We will denote them by $f_{\text{ex}}(\beta, \alpha; \Delta^2)$. They may be interpreted as coming from the t -channel meson-exchange type contributions. In this case, the partons just share the plus-component of the momentum transfer Δ : information about the initial hadron momentum is lost if the exchanged particle of mass m_M can be described by a pole propagator $1/(\Delta^2 - m_M^2)$. Hence, the meson-exchange contributions to a double distribution may look like

$$f_{\text{ex}}^+(\beta, \alpha, \Delta^2) \sim \delta(\beta) \frac{\varphi_M^+(\alpha)}{m_M^2 - \Delta^2}, \quad f_{\text{ex}}^-(\beta, \alpha, \Delta^2) \sim \delta'(\beta) \frac{\varphi_M^-(\alpha)}{m_M^2 - \Delta^2}, \quad (3.248)$$

etc., where $\varphi_M^\pm(\alpha)$ are the functions¹⁶ related to the distribution amplitudes of the relevant mesons. The two examples given above correspond to β -even (C -odd) and β -odd (C -even) parts of the double distribution $f(\beta, \alpha, \Delta^2)$. As an obvious consequence of the time-reversal symmetry of DDs (3.209), the functions $\varphi_M^\pm(\alpha)$ for singular contributions $f_M^\pm(\beta, \alpha, \Delta^2)$ are even functions $\varphi_M^\pm(\alpha) = \varphi_M^\pm(-\alpha)$ of α both for β -even and β -odd components. If the amplitude $\varphi_M(\alpha)$ vanishes

¹⁶These distribution amplitudes are expressed via the one introduced in Section 3.7.1 by means of the change of the argument $\varphi_M(\alpha) = \phi_M(\frac{1+\alpha}{2})$.

at the end-points $\alpha = \pm 1$, the $H_{\text{ex}}(x, \eta, \Delta^2)$ part of GPD vanishes at $x = \pm \eta$. The total function $H(x, \eta; \Delta^2)$ is then continuous at the nonanalyticity points $x = \pm \eta$. In the C -even case, one can get a continuous GPD in this case only if the derivative $\varphi'(\alpha)$ vanishes at the end points.

3.10 Impact-parameter parton distributions

In our presentation, GPDs were introduced as generalizations of the concept of the non-relativistic Wigner function to the quantum phase-space quasi-probability distribution in the nucleon. Thus, the partonic Wigner distributions are not endowed with the density of probability interpretation: they intrinsically have patches of “negative probability” due to the fact that they represent the interference of two amplitudes, one for the outgoing parton from the initial nucleon and another for the incoming parton in the final-state nucleon.

In this section, we demonstrate that in a particular case of zero value of the skewness parameter, the generalized parton distributions acquire a well-defined probability interpretation in the infinite-momentum frame similar to the conventional collinear parton distribution functions. Moreover, the resulting picture does not suffer from the presence of large relativistic corrections inevitably affecting the rest-frame description. The price for this advantage is the lack of one spatial dimension: instead one has a picture in two (transverse) spatial dimensions and one (longitudinal) momentum direction. Note, that the orthogonality of momentum and spatial degrees of freedom allows one to circumvent constraints from the quantum mechanical uncertainty principle.

The probability interpretation of the skewness-independent function $H(x, \eta = 0, \Delta_\perp^2)$ was available, though not widely known, for a long time [61], where an equivalent function was treated as a two-dimensional Fourier transform of the impact-parameter dependent parton distribution $f(x, \mathbf{r}_\perp)$. Recently, this concept was revived in a series of papers in Refs. [151, 152, 153].

3.10.1 Electromagnetic form factors in the Bjorken frame

Let us use the Bjorken frame adopted for discussion of form factors. In this case, the average momentum of initial and outgoing nucleon can be chosen to have only the time and z components, while the momentum transfer can be made purely transverse. To get an explicit form, one can take the general result from Appendix B where one sets $\eta = 0$ and use the reparametrization invariance to choose $\varrho = \sqrt{2}\mathcal{P}$, so that the incoming and outgoing momenta take the form

$$p_{1,2}^\mu = \left(\mathcal{P} + \frac{M_N^2 + \frac{1}{4}\Delta_\perp^2}{4\mathcal{P}}, \pm \frac{1}{2}\Delta_\perp, \mathcal{P} - \frac{M_N^2 + \frac{1}{4}\Delta_\perp^2}{4\mathcal{P}} \right), \quad \Delta^\mu = (0, \Delta_\perp, 0). \quad (3.249)$$

Since our aim is to give a transverse-space interpretation of form factors, we have to localize the nucleon in the coordinate space with an appropriately chosen two-dimensional wave packet, which possesses a definite z -component of the three-momentum,

$$|p^z, \mathbf{R}_\perp\rangle = \int \frac{d^2\mathbf{p}_\perp}{(2\pi)^2} \frac{e^{i\mathbf{p}_\perp \cdot \mathbf{R}_\perp}}{\sqrt{2E_p}} \Psi(\mathbf{p}_\perp) |p^z, \mathbf{p}_\perp\rangle. \quad (3.250)$$

Here the two-dimensional profile is related to the three-dimensional one, discussed in the introduction, by

$$\Psi(\mathbf{p}) = 2\pi\delta(p^z - p'^z) \frac{\Psi(\mathbf{p}_\perp)}{\sqrt{2E_p}}.$$

The mixed state (3.250) is normalized as

$$\langle p'^z, \mathbf{R}_\perp | p^z, \mathbf{R}_\perp \rangle = 2\pi\delta(p'^z - p^z), \quad \int \frac{d^2\mathbf{p}_\perp}{(2\pi)^2} |\Psi(\mathbf{p}_\perp)|^2 = 1. \quad (3.251)$$

Let us put this state in the center of two-dimensional plane and compute the Fourier transform of its transverse charge density

$$\begin{aligned} \int d^2\mathbf{r}_\perp e^{-i\Delta_\perp \cdot \mathbf{r}_\perp} \rho_\perp(\mathbf{r}_\perp) &\equiv \int d^2\mathbf{r}_\perp e^{-i\Delta_\perp \cdot \mathbf{r}_\perp} \langle p_2^z, \mathbf{R}_\perp = 0 | j^0(\mathbf{r}_\perp) | p_1^z, \mathbf{R}_\perp = 0 \rangle \\ &= \int \frac{d^2\mathbf{p}_\perp}{(2\pi)^2} \frac{\Psi^*(\mathbf{p}_\perp - \frac{1}{2}\Delta_\perp)}{\sqrt{2E_{\mathbf{p}_2}}} \frac{\Psi(\mathbf{p}_\perp + \frac{1}{2}\Delta_\perp)}{\sqrt{2E_{\mathbf{p}_1}}} \langle p_2^z, \mathbf{p}_\perp - \frac{1}{2}\Delta_\perp | j^0(0) | p_1^z, \mathbf{p}_\perp + \frac{1}{2}\Delta_\perp \rangle. \end{aligned} \quad (3.252)$$

To get rid of extraneous effects of the auxiliary wave packet and also to be insensitive to all kinds of corrections, the following conditions should be fulfilled (some of them are analogous to those discussed in the first section dedicated to three-dimensional interpretation of form factors):

- We require that the spatial size of the wave packet is not detectable, so it has to be smaller than the resolution scale set by the inverse momentum transfer from the initial to the final state. By uncertainty principle, this implies that typical momenta in the wave packet are larger than the momentum of the probe

$$|\mathbf{p}_\perp| \gg |\Delta_\perp|.$$

Then one can neglect Δ_\perp in the wave packet profiles (but not in matrix elements, which are sensitive to small changes in the momentum), $\Psi(\mathbf{p}_\perp \pm \frac{1}{2}\Delta_\perp) \approx \Psi(\mathbf{p}_\perp)$.

- In order to suppress relativistic corrections, and also to give the proton a well-defined longitudinal momentum, we need to avoid the energy exchange from the initial to the final state. To this end, we have to require

$$p_i^z \gg |\mathbf{p}_\perp|,$$

which results in a condition on the resolution scale [151]

$$p_i^z \gg |\Delta_\perp|. \quad (3.253)$$

In the infinite-momentum frame $\mathcal{P} \rightarrow \infty$, this will not be a restriction at all, and one can achieve simultaneously a very precise localization, since the “effective” Compton wave length $\sim 1/\sqrt{M_N^2 + \mathcal{P}^2}$ contains the longitudinal momentum \mathcal{P} [151]), and get rid of the relativistic corrections (since $p_{1,2}^0 \simeq p_{1,2}^z \simeq \mathcal{P}$).

For the helicity-non-flip transitions, the matrix element of the electromagnetic current can be easily evaluated in the infinite-momentum frame

$$\langle p_2^z, \mathbf{p}_\perp - \frac{1}{2}\Delta_\perp | j^0(0) | p_1^z, \mathbf{p}_\perp + \frac{1}{2}\Delta_\perp \rangle = 2\mathcal{P}F_1(-\Delta_\perp^2).$$

This demonstrates that, in contrast to the three-dimensional picture, the two-dimensional charge density in the infinite-momentum frame gives a well-defined, free from relativistic effects interpretation of the Fourier transform of the electromagnetic form factors as a two-dimensional charge density,

$$\int d^2\mathbf{r}_\perp e^{-i\Delta_\perp \cdot \mathbf{r}_\perp} \rho_\perp(\mathbf{r}_\perp) = F_1(-\Delta_\perp^2). \quad (3.254)$$

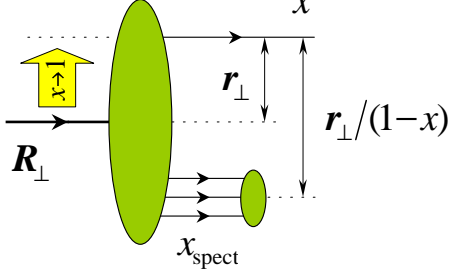


Figure 15: Distances in the impact parameter space: the transverse center-of-momentum \mathbf{R}_\perp is a reference point from where the distance to all partons is measured dressed by their momentum fractions. The distance from the active parton to the spectator system is $\mathbf{r}_\perp^s = \mathbf{r}_\perp/(1-x)$.

Note also the combinations of form factors entering the helicity-flip (non-flip) transitions in the Breit frame, discussed in Section 2.2.2, differ from those in the infinite-momentum frame as discussed at length below. This is a mere consequence of the distinction between the light-cone and conventional helicities.

The two-dimensional character of the dynamics probed by form factors in the Bjorken frame is reflected in the difference between the root-mean-square radii of the three-dimensional charge densities, determined by form factors in the Breit frame, see Eq. (2.30). Namely, in the infinite momentum frame

$$\langle \mathbf{r}_\perp^2 \rangle_D \equiv \int d^2 \mathbf{r}_\perp \mathbf{r}_\perp^2 \rho_\perp(\mathbf{r}_\perp) = -4 \frac{\partial F_1(-\Delta_\perp^2)}{\partial \Delta_\perp^2}. \quad (3.255)$$

Therefore, when one defines the charge radius in the Breit frame through the Dirac form factor, rather than the electric form factor, one gets for the ratio of the three-dimensional versus the two-dimensional radii

$$\frac{\langle \mathbf{r}^2 \rangle_D}{\langle \mathbf{r}_\perp^2 \rangle_D} = \frac{3}{2}. \quad (3.256)$$

3.10.2 Skewless GPDs as impact-parameter distributions

For the purpose of discussing high-energy observables, like conventional and generalized parton distributions, the light-cone coordinates are more appropriate than the energy-momentum variables. The former mix the transverse and longitudinal momenta unless one takes the infinite momentum limit, as we have already demonstrated in the previous subsection. For high-energy probes, these are the light-cone components of momenta which are measured. Therefore, they are more suitable for designing a viable formalism. Rewriting the relativistically-invariant momentum element in the light-cone coordinates $d^3 \mathbf{p}/(2E_p) = dp^+ d^2 \mathbf{p}_\perp / (2p^+)$ with a definite p^+ instead of a definite p^z , we change accordingly the wave-packet profile function and introduce the state

$$|p^+, \mathbf{R}_\perp\rangle = \int \frac{d^2 \mathbf{p}_\perp}{(2\pi)^2} e^{i \mathbf{p}_\perp \cdot \mathbf{R}_\perp} \Psi(\mathbf{p}_\perp) |p^+, \mathbf{p}_\perp\rangle. \quad (3.257)$$

Here we do not display the helicity of the state, it will be restored later when it will be needed for the presentation. This mixed state is normalized relativistically,

$$\langle p'^+, \mathbf{R}_\perp | p^+, \mathbf{R}_\perp \rangle = 2p^+(2\pi)\delta(p^+ - p'^+) , \quad \int \frac{d^2 \mathbf{p}_\perp}{(2\pi)^2} |\Psi(\mathbf{p}_\perp)|^2 = 1. \quad (3.258)$$

It is localized in the sense that its transverse center of momentum is at \mathbf{R}_\perp . For a state with total momentum p^+ , the transverse center of momentum is defined as [151, 152, 153].

$$\mathbf{R}_\perp \equiv \frac{1}{p^+} \int dz^- d^2 z_\perp z_\perp \Theta^{++}(z^+ = 0, z^-, z_\perp), \quad (3.259)$$

where $\Theta^{\mu\nu}$ is the energy momentum tensor. The eigenvalues of the operator \mathbf{R}_\perp on the state (3.257) have an intuitive partonic representation in the light-cone gauge. It is obtained by expressing Θ^{++} in terms of the light-cone creation and annihilation operators and noticing that, after integrating over z^- , only the terms that are diagonal in Fock space contribute, yielding

$$\mathbf{R}_\perp = \frac{\sum_i k_i^+ \mathbf{r}_{\perp,i}}{p^+} = \sum_i x_i \mathbf{r}_{\perp,i}. \quad (3.260)$$

The summation in Eq. (3.260) is over all partons in the hadron and $x_i \equiv k_i^+/p^+$ is the longitudinal momentum fraction carried by the i -th parton in the infinite momentum frame. The quantity \mathbf{R}_\perp is invariant under the transverse boost $\mathbb{M}^{+\perp}$ (see Appendix I). This result should not be surprising, since the momentum fractions x_i play here the role very similar to that of the mass fractions $m_i/\sum_i m_i$ in the expression for the center of mass in non-relativistic quantum mechanics. Working with the localized state $|p^+, \mathbf{R}_\perp\rangle$ is quite analogous to using the center-of-mass frame in nonrelativistic physics, the main difference being the change of the weight factors from the mass ratios to the longitudinal momentum fractions in the expression for the transverse center of momentum. This is related to the properties of the Galilean subgroup of transverse boosts. Note finally that \mathbf{r}_\perp measures the distance from the active quark to the hadron's center of momentum (see Fig. 15), while the distance from the active quark to the center of momentum of spectators is given by $\mathbf{r}_\perp^s = \mathbf{r}_\perp/(1-x)$.

The objects we are going to discuss in this section are the matrix elements between the state (3.257) of the partially Fourier transformed bilocal quark operators

$$\mathcal{O}^{qq}(x, \mathbf{r}_\perp) \equiv \int \frac{dz^-}{2\pi} e^{ixp^+z^-} \mathcal{O}^{qq}(-z^-, \mathbf{r}_\perp; z^-, \mathbf{r}_\perp), \quad (3.261)$$

(with the change $\mathcal{O}^{qq} \rightarrow \tilde{\mathcal{O}}^{qq}$ for the parity-odd operators). The first condition applied in the preceding section to the profile function remains unchanged. However, since now we have a fixed p^+ rather than fixed $p^z = (p^+ - p^-)/\sqrt{2}$, the latter can become negative, $p^z < 0$, if the transverse momentum is too large so that $p^+ \ll p^- = (\mathbf{p}_\perp^2 + M_N^2)/(2p^+)$. Then the desired interpretation of a proton moving with a well-defined longitudinal momentum is spoiled. This imposes a restriction on the momenta in the wave packet $|\mathbf{p}_\perp| \ll p^+$ and as a result on the attainable transverse localization, $|\Delta_\perp| \ll p^+$. This is analogous to the second condition of the preceding section, but now applied to the plus momentum. Thus, taking the proton with $p^+ \rightarrow \infty$, brings us to the situation discussed there. In the Bjorken frame, where the momenta are given by Eq. (3.249), $p^+ = \mathcal{P}/\sqrt{2}$.

To investigate the spin structure of generalized parton distributions, it is useful to represent them in a form similar to that of helicity amplitudes. Since we are dealing here with matrix elements involving two independent proton momenta, some comments are in order regarding the choice of helicity states for the protons. Note, that in the definitions of the distributions one singles out a direction that defines the light-cone coordinates (in a physical process, where these distributions appear, this direction is provided by the hard probe, such as the virtual photon in

deeply virtual Compton scattering). It is also useful to utilize this light-cone direction for defining the spin states for the protons with momenta p_1 and p_2 . This leads to the concept of light-cone helicity states [62]. Using the light-cone spinors from Appendix A.2 and results for Dirac bilinears (A.34) derived there, one can easily find for helicity-non-flip and -flip transitions [152, 154]

$$\begin{aligned} H^q(x, \eta = 0, -\Delta_\perp^2) &= \int d^2 \mathbf{r}_\perp e^{-i\Delta_\perp \cdot \mathbf{r}_\perp} \langle \frac{1}{2} p^+, \mathbf{0}_\perp, \uparrow | \mathcal{O}^{qq}(x, \mathbf{r}_\perp) | \frac{1}{2} p^+, \mathbf{0}_\perp, \uparrow \rangle, \\ -\frac{\Delta_\perp}{2M_N} E^q(x, \eta = 0, -\Delta_\perp^2) &= \int d^2 \mathbf{r}_\perp e^{-i\Delta_\perp \cdot \mathbf{r}_\perp} \langle \frac{1}{2} p^+, \mathbf{0}_\perp, \downarrow | \mathcal{O}^{qq}(x, \mathbf{r}_\perp) | \frac{1}{2} p^+, \mathbf{0}_\perp, \uparrow \rangle, \\ \tilde{H}^q(x, \eta = 0, -\Delta_\perp^2) &= \int d^2 \mathbf{r}_\perp e^{-i\Delta_\perp \cdot \mathbf{r}_\perp} \langle \frac{1}{2} p^+, \mathbf{0}_\perp, \uparrow | \tilde{\mathcal{O}}^{qq}(x, \mathbf{r}_\perp) | \frac{1}{2} p^+, \mathbf{0}_\perp, \uparrow \rangle, \end{aligned} \quad (3.262)$$

where, obviously, $p_1^+ = p_2^+ = p^+/2$ and the holomorphic transverse momentum is defined as usual, $\Delta_\perp = \Delta^x + i\Delta^y$. Note, that we have not given the expression for \tilde{E} , since it decouples in the skewless limit.

The fact that the distribution of partons in the impact parameter space is measured with respect to the transverse center of momentum (3.260) has very profound consequences on the functional form of the impact-parameter dependent distributions and, as a result, that of GPDs. When the active parton carries almost the entire momentum of the parent hadron, its momentum fraction x approaches one, while for all spectator partons $x_i \rightarrow 0$, since the sum of all momentum fractions cannot exceed unity, $\sum_{\text{spect.}} x_i = 1 - x$. Therefore, when $x = 1$, the center of momentum

$$\mathbf{R}_\perp = x\mathbf{r} + \sum_{\text{spect.}} x_i \mathbf{r}_i$$

sits right on top of the active quark, i.e., $\mathbf{R}_\perp = \mathbf{r}$ (see Fig. 15). Thus, the transverse profile narrows down and ultimately becomes concentrated at the position of the active quark $\sim \delta^{(2)}(\mathbf{r})$ [152, 155]. In other words, the transverse width of the impact-parameter dependent parton distribution

$$\langle \mathbf{r}_\perp^2(x) \rangle \equiv \left(\int d^2 \mathbf{r}_\perp \mathbf{r}_\perp^2 f^q(x, \mathbf{r}_\perp) \right) / \left(\int d^2 \mathbf{r}_\perp f^q(x, \mathbf{r}_\perp) \right), \quad (3.263)$$

should vanish as $x \rightarrow 1$. As we can see, the distance between the active parton and spectators in this asymptotic limit grows as $\mathbf{r}_\perp^s = \mathbf{r}_\perp/(1-x)$. Of course, this growth is stopped by confinement effects, so that the fast-moving active quark will not be separated from spectators by more than $|\mathbf{r}_\perp^s| \sim 1/m_h$, where m_h is some typical hadronic scale. Going away from the asymptotic limit $x \rightarrow 1$, the transverse distribution broadens out. In momentum space, such a picture implies that GPDs Fourier conjugated to the impact-parameter parton distributions must become Δ^2 -independent when the momentum fraction x approaches unity, i.e., the slope of skewless GPDs should approach zero when $x \rightarrow 1$ [152, 155, 156]. Thus, the transverse size is strongly correlated with the longitudinal momentum. This behavior was confirmed by lattice calculations of Mellin moments of GPDs. It was observed [157] that, the higher the moment, the slower is its fall-off with increasing momentum transfer, see Fig. 16.

Thus, one gets a very intuitive interpretation of skewless GPDs as Fourier transforms of impact-parameter dependent parton distributions, e.g.,

$$f_H^q(x, \mathbf{r}_\perp) = \int \frac{d^2 \Delta_\perp}{(2\pi)^2} e^{i\Delta_\perp \cdot \mathbf{r}_\perp} H^q(x, 0, -\Delta_\perp^2) = \langle p^+, \mathbf{0}_\perp, \uparrow | \mathcal{O}^{qq}(x, \mathbf{r}_\perp) | p^+, \mathbf{0}_\perp, \uparrow \rangle, \quad (3.264)$$

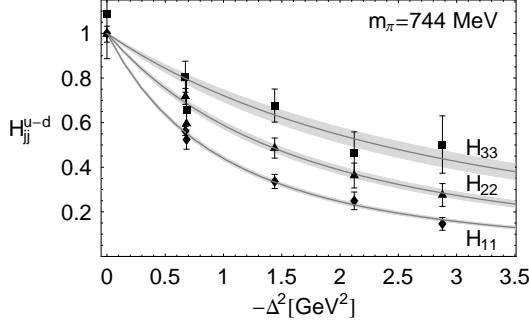


Figure 16: Lattice calculation [157] of the lowest three form factors H_{jj} with $j = 1, 2, 3$ in Mellin moments of GPDs, see Eq. (3.123).

which are simultaneous probabilities that a parton is at a certain distance \mathbf{r}_\perp from the hadron's center-of-mass and carries a fraction x of the parent hadron's momentum p [61]. These functions are positive definite, which can be seen by expressing them in terms of the creation/annihilation operators in the formalism of the light-cone quantization

$$f_H^q(x, \mathbf{r}_\perp)|_{x>0} = \frac{1}{2xp^+\delta(0^+)} \sum_{\lambda=\uparrow\downarrow} \langle \frac{1}{2}p^+, \mathbf{0}_\perp, \uparrow | b_\lambda^\dagger(\frac{x}{2}p^+, \mathbf{r}_\perp) b_\lambda(\frac{x}{2}p^+, \mathbf{r}_\perp) | \frac{1}{2}p^+, \mathbf{0}_\perp, \uparrow \rangle. \quad (3.265)$$

The partially Fourier transformed annihilation operator used here is given by

$$b_\lambda(k^+, \mathbf{r}_\perp) = \int \frac{d^2 k_\perp}{(2\pi)^3} e^{i\mathbf{k}_\perp \cdot \mathbf{r}_\perp} b_\lambda(k^+, \mathbf{k}_\perp).$$

The helicity-flip distributions can be brought to the diagonal form—to endow them with a probabilistic interpretation—by going to the transverse-spin basis

$$|\pm\perp\rangle = \frac{1}{\sqrt{2}}(|\uparrow\rangle \pm |\downarrow\rangle),$$

where

$$\langle \downarrow | \mathcal{O} | \uparrow \rangle = \langle +\perp | \mathcal{O} | +\perp \rangle - \langle -\perp | \mathcal{O} | -\perp \rangle.$$

Thus, GPDs regain a probabilistic interpretation once one sets skewness $\eta = 0$. The function $f^q(x, \mathbf{r}_\perp)$ is a three-dimensional hybrid distribution in one-dimensional momentum and two-dimensional coordinate space. After integrating over \mathbf{r}_\perp , one recovers the Feynman parton distribution. On the other hand, after integration over x one gets the impact-parameter space distribution which is the Fourier transform of the elastic form factor [158, 154, 118, 119, 159]. The pictorial comparison of parton distributions, form factors and skewless GPDs and information one accesses by studying these functions is demonstrated in Fig. 17. Notice that the right-most graph demonstrates the phenomenon of shrinking of the width of the impact-parameter distribution with increasing x and the vanishing of the height of the peak, just due to the fact that the probability to observe a single quark carrying the whole momentum of the proton is negligible.

3.10.3 GPDs in impact-parameter space

So far we have discussed GPDs for zero skewness and observed that they regain the probabilistic interpretation analogous to the Feynman parton distributions. Once one lifts the restriction of

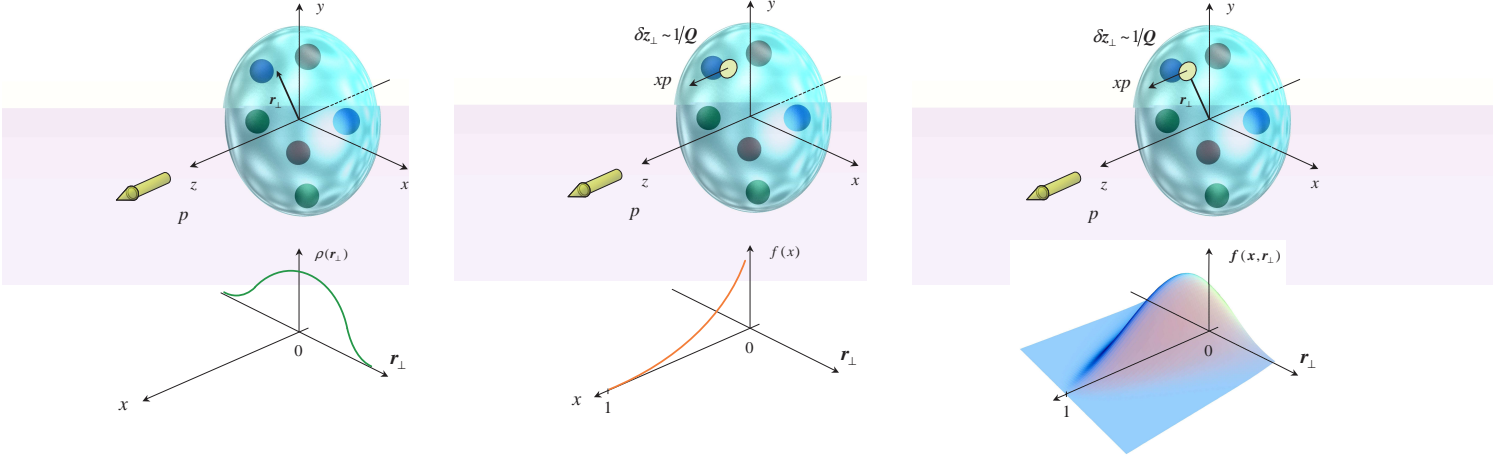


Figure 17: Probabilistic interpretation of form factors, parton densities and generalized parton distributions at $\eta = 0$ in the infinite momentum frame $p_z \rightarrow \infty$.

absence of the longitudinal momentum transfer in the t -channel, GPDs cease to be densities, rather, they become interference functions or quasiprobabilities according to their identification with Wigner distributions. There is a number of new features and interesting subtleties which appear in the impact parameter representation for $\eta \neq 0$, and now we are going to discuss them [154].

Since our goal is to evaluate the matrix element of the non-local operator (3.261) sandwiched between the mixed states (3.257), we need to know the dependence on the transverse momenta with arbitrary $\mathbf{p}_{1\perp}$ and $\mathbf{p}_{2\perp}$. As it was already indicated by the evaluation of the Dirac bilinears in Appendix A.2, these momenta cease to enter in the combination $\Delta_\perp = \mathbf{p}_{1\perp} - \mathbf{p}_{2\perp}$, unless one chooses the “transverse” Breit frame $\mathbf{p}_{1\perp} = -\mathbf{p}_{2\perp} = \frac{1}{2}\Delta_\perp$. Since $\mathbf{p}_{i\perp}$ ’s enter as integration variables in (3.257), we cannot pick this reference frame from the start, and are allowed to impose any conditions only after the integrations have been performed. The Lorentz-covariant combinations of Dirac bilinears analyzed in Appendix A.2, are found to depend on the combination¹⁷ $p_{1\perp}/p_1^+ - p_{1\perp}/p_1^+$ (see, e.g., Eq. (A.34)). This is not an accident but a direct consequence of the transverse Lorentz-boost invariance of GPDs. These transformations leave the plus-momentum invariant and change the transverse momentum in proportion to a parameter \mathbf{v}_\perp ,

$$p^+ \rightarrow p^+, \quad \mathbf{p}_\perp \rightarrow \mathbf{p}_\perp - p^+ \mathbf{v}_\perp. \quad (3.266)$$

As a consequence of this invariance, for generically defined unconstrained momenta $\mathbf{p}_{1\perp}$ and $\mathbf{p}_{2\perp}$, a given GPD is a function

$$F^q(x, \eta, \mathbf{D}_\perp) = \langle p_2 | \mathcal{O}^{qq}(x, \mathbf{0}_\perp) | p_2 \rangle \quad (3.267)$$

of the momentum fraction x , skewness η and the Lorentz invariant combination of transverse momenta¹⁸

$$\mathbf{D}_\perp \equiv \frac{2}{p^+} (\mathbf{p}_{1\perp} p_2^+ - \mathbf{p}_{2\perp} p_1^+) = (1 - \eta) \mathbf{p}_{1\perp} - (1 + \eta) \mathbf{p}_{2\perp}. \quad (3.268)$$

¹⁷Notice that for zero skewness, $p_1^+ = p_2^+$, this combination collapses to Δ_\perp/p_1^+ and thus momentum-space matrix elements do depend solely on Δ_\perp making the analysis of the previous section legitimate.

¹⁸Note that our vector \mathbf{D}_\perp differs from the one introduced originally in Ref. [154] by a global factor.

The four-dimensional momentum transfer squared is re-expressed in terms of \mathbf{D}_\perp via

$$\Delta^2 = \Delta_{\min}^2 - \frac{\mathbf{D}_\perp^2}{1 - \eta^2}, \quad (3.269)$$

where the minimum momentum transfer squared is defined in Eq. (3.202) and formally coincides with the transverse Breit-frame expression (B.15). Obviously $\mathbf{D}_\perp \stackrel{\text{Breit}}{=} \Delta_\perp$.

Sandwiching the Fourier transformed light-cone operator (3.261) between the mixed states (3.257) and changing the integration variables from $\mathbf{p}_{1\perp}$ and $\mathbf{p}_{2\perp}$ to \mathbf{D}_\perp and \mathbf{p}_\perp , one immediately finds

$$\begin{aligned} \langle p_2^+, \mathbf{r}_{2\perp} | \mathcal{O}^{qq}(x, \mathbf{0}_\perp) | p_1^+, \mathbf{r}_{1\perp} \rangle &= \int \frac{d^2 \mathbf{D}_\perp}{(2\pi)^2} e^{-i \mathbf{D}_\perp \cdot \mathbf{r}_{1\perp}/(1-\eta)} F^q(x, \eta, \mathbf{D}_\perp) \\ &\times \int \frac{d^2 \mathbf{p}_\perp}{(2\pi)^2} e^{i \mathbf{p}_\perp \cdot [(1-\eta)\mathbf{r}_{2\perp} - (1+\eta)\mathbf{r}_{1\perp}]} \Psi^* \left((1-\eta)\mathbf{p}_\perp \right) \Psi^* \left((1+\eta)\mathbf{p}_\perp + \mathbf{D}_\perp/(1-\eta) \right), \end{aligned} \quad (3.270)$$

where $p_1^+ = (1+\eta)p^+/2$ and $p_2^+ = (1-\eta)p^+/2$. Requiring that the second exponential reduces to unity, one introduces

$$\mathbf{r}_\perp = -\frac{\mathbf{r}_{1\perp}}{1-\eta} = -\frac{\mathbf{r}_{2\perp}}{1+\eta}. \quad (3.271)$$

We impose the normalization condition on the wave packet

$$\mathcal{N}_\Psi = \int \frac{d^2 \mathbf{p}_\perp}{(2\pi)^2} \Psi^* \left((1-\eta)\mathbf{p}_\perp - \frac{1}{2}\mathbf{D}_\perp/(1+\eta) \right) \Psi^* \left((1+\eta)\mathbf{p}_\perp + \frac{1}{2}\mathbf{D}_\perp/(1-\eta) \right) = 1,$$

implying that it is a slowly varying function of its argument. Notice that if one chooses a ‘nailed down’ proton state in the coordinate space, which corresponds to $\Psi = 1$, the normalization factor becomes divergent $\mathcal{N}_{\Psi=1} = \delta^{(2)}(\mathbf{r}_\perp = 0)$. Then, making use of (3.271), one immediately finds from Eq. (3.270)

$$\langle p_2^+, -\eta \mathbf{r}_\perp | \mathcal{O}^{qq}(x, \mathbf{r}_\perp) | p_1^+, \eta \mathbf{r}_\perp \rangle = \int \frac{d^2 \mathbf{D}_\perp}{(2\pi)^2} e^{i \mathbf{D}_\perp \cdot \mathbf{r}_\perp} F^q(x, \eta, \mathbf{D}_\perp), \quad (3.272)$$

where we have used $\langle \mathbf{r}_{2\perp} - \mathbf{r}_\perp | \mathcal{O}(\mathbf{0}_\perp) | \mathbf{r}_{1\perp} - \mathbf{r}_\perp \rangle = \langle \mathbf{r}_{2\perp} | \mathcal{O}(\mathbf{r}_\perp) | \mathbf{r}_{1\perp} \rangle$ resulting from translation invariance in the impact parameter space. Now, one can safely impose the transverse Breit frame condition: the functional dependence of GPDs on that condition will not change. A very important lesson one learns [154] is that the presence of a non-zero longitudinal momentum exchange in the t -channel affects the transverse separation of incoming and outgoing hadrons (see Fig. 18). As a result, the overlap between these states decreases with increasing skewness. It is interesting to notice that, for the partons, also, the transverse shift depends only on the skewness but not on the momentum fraction x . Therefore, information on the transverse localization of partons is not washed out in quantities integrated over x with an arbitrary weight depending on longitudinal momenta. It is exactly the form in which GPDs arise in a number of high energy processes discussed later in this review.

Incorporating Eq. (A.34) to evaluate the light-cone helicity matrix elements, one finds the following set of equations [154]

$$\sqrt{1-\eta^2} \left(H(x, \eta, -\Delta_\perp^2) - \frac{\eta^2}{1-\eta^2} E(x, \eta, -\Delta_\perp^2) \right) \quad (3.273)$$

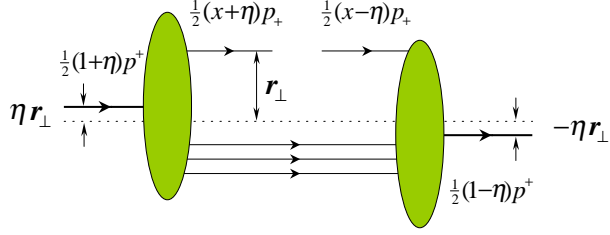


Figure 18: Interpretation of GPDs in the impact parameter space for non-zero skewness. The distributions of partons in transverse plane is measured with respect to the two-hadron center of momentum. Each of the hadrons is shifted away from it in the opposite directions linearly proportional to the longitudinal deficit η .

$$\begin{aligned}
&= \int d^2 \mathbf{r}_\perp e^{-i\Delta_\perp \cdot \mathbf{r}_\perp} \langle p_2^+, -\eta \mathbf{r}_\perp, \uparrow | \mathcal{O}^{qq}(x, \mathbf{r}_\perp) | p_1^+, \eta \mathbf{r}_\perp, \uparrow \rangle, \\
-\frac{\Delta_\perp}{2M_N \sqrt{1-\eta^2}} E(x, \eta, -\Delta_\perp^2) &= \int d^2 \mathbf{r}_\perp e^{-i\Delta_\perp \cdot \mathbf{r}_\perp} \langle p_2^+, -\eta \mathbf{r}_\perp, \downarrow | \mathcal{O}^{qq}(x, \mathbf{r}_\perp) | p_1^+, \eta \mathbf{r}_\perp, \uparrow \rangle, \\
\sqrt{1-\eta^2} \left(\tilde{H}(x, \eta, -\Delta_\perp^2) - \frac{\eta^2}{1-\eta^2} \tilde{E}(x, \eta, -\Delta_\perp^2) \right) &= \int d^2 \mathbf{r}_\perp e^{-i\Delta_\perp \cdot \mathbf{r}_\perp} \langle p_2^+, -\eta \mathbf{r}_\perp, \uparrow | \tilde{\mathcal{O}}^{qq}(x, \mathbf{r}_\perp) | p_1^+, \eta \mathbf{r}_\perp, \uparrow \rangle, \\
-\frac{\eta \Delta_\perp}{2M_N \sqrt{1-\eta^2}} \tilde{E}(x, \eta, -\Delta_\perp^2) &= \int d^2 \mathbf{r}_\perp e^{-i\Delta_\perp \cdot \mathbf{r}_\perp} \langle p_2^+, -\eta \mathbf{r}_\perp, \downarrow | \tilde{\mathcal{O}}^{qq}(x, \mathbf{r}_\perp) | p_1^+, \eta \mathbf{r}_\perp, \uparrow \rangle.
\end{aligned}$$

A more correct form for the third argument of GPDs in Eq. (3.267) is to write it as the four-dimensional momentum transfer via Eq. (3.269). We hope that our shorter notation will not lead to confusion. Note, finally, that the zero-skewness limit of Eqs. (3.262) reproduces the results of the previous section.

3.11 Positivity constraints on GPDs

To carry out realistic modeling of generalized parton distributions, the latter have to obey several first-principle constraints, like the reduction to the usual parton densities and form factors, and have to fulfill the polynomiality condition in the skewness parameter, as we established in previous sections. Another nontrivial property of GPDs is reflected by so-called positivity constraints. The terminology is introduced by analogy with inequalities satisfied by forward parton densities. As was demonstrated in Eq. (2.74), the latter are expressed as a diagonal matrix element of the number-of-particles operator, $\langle p | b^\dagger b | p \rangle$, or as a norm $|\mathcal{A}|^2 = |b|p\rangle|^2$, of the state $\mathcal{A} = b|p\rangle$ created with the action of the quark annihilation operator b on the hadronic state $|p\rangle$. As a result, the parton density is explicitly positive definite and can be treated as a probability. On the other hand, generalized parton distributions correspond to non-diagonal matrix elements, for instance, $\langle p_2 | b^\dagger b | p_1 \rangle$ in one of the inclusive regions (3.198), and therefore they describe the overlap $(\mathcal{A}_2^* \mathcal{A}_1)$ of the state $\mathcal{A}_2 = b|p_2\rangle$ with $\mathcal{A}_1 = b|p_1\rangle$, rather than the norm. The Cauchy inequality $|\mathcal{A}_2^* \mathcal{A}_1| \leq |\mathcal{A}_2| |\mathcal{A}_1|$ will be the basic tool for getting positivity constraints on GPDs.

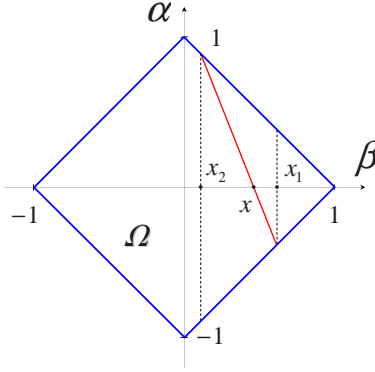


Figure 19: Integration line producing $H(x, \eta, \Delta^2)$.

When non-diagonal matrix elements are parametrized by several GPDs, e.g., by H and E for spin-one-half hadrons, the positivity constraints restrict possible values of particular combinations of $H(x, \eta, \Delta^2)$ and $E(x, \eta, \Delta^2)$, with the bounds set in terms of the forward parton densities $q(y)$ taken at particular values of its argument y depending on both x and η . Moreover, one can build the states $\mathcal{A}_{1,2}$ as arbitrary superpositions of $b|p\rangle$ type states and this implies that, in principle, there is an infinite set of positivity constraints. This presents a serious challenge for building consistent models of GPDs.

3.11.1 Inequalities relating GPDs and ordinary distributions

As a first demonstration, let us address inequalities which arise between GPDs in the inclusive domain and standard forward parton densities. In case when $x > \eta$, the integration contour over DDs producing $H^q(x, \eta, -\Delta^2)$ (see Fig. 19) is inside the region between two vertical lines generating the usual parton distributions $q(x_2)$ and $q(x_1)$ being functions of the momentum fractions

$$x_1 = \frac{x + \eta}{1 + \eta}, \quad x_2 = \frac{x - \eta}{1 - \eta},$$

cf. Eq. (3.212). Then

$$H^q(x, \eta, \Delta^2)|_{x \geq \eta} = \int_{x_2}^{x_1} \frac{d\beta}{\eta} f^q \left(\beta, \frac{\beta - x}{\eta} \right). \quad (3.274)$$

The combinations x_1, x_2 have a very simple interpretation: they measure the momentum of the initial or final parton in units of the momentum of the relevant hadron. Assuming a monotonic decrease of the double distribution $f^q(\beta, \alpha)$ in the β -direction and a universal normalized profile in the α -direction, we conclude that $H^q(x, \eta, \Delta^2 = 0)$ is larger than $q(x_1)$ but smaller than $q(x_2)$, $q(x_1) < H^q(x, \eta, \Delta^2 = 0) < q(x_2)$. Moreover, if the slope of parton densities $q(x)$ gets steeper when $x \rightarrow 0$, which is the case for any x^{-a} behavior with $a > 0$, then we may expect that $H^q(x, \eta, \Delta^2 = 0)$ is smaller than the average of $q(x_1)$ and $q(x_2)$:

$$H^q(x, \eta, \Delta^2 = 0) \leq \frac{1}{2} [q(x_1) + q(x_2)].$$

An inequality of this kind was originally proposed in Refs. [160, 7]. The basic idea used in the derivation is to treat GPDs as nondiagonal matrix elements of the form $\langle \Psi_{\text{out}} | \Psi_{\text{in}} \rangle$ and then to use

the Schwartz inequality

$$\langle \Psi_{\text{out}} | \Psi_{\text{in}} \rangle \leq \frac{1}{2} \left[\langle \Psi_{\text{in}} | \Psi_{\text{in}} \rangle + \langle \Psi_{\text{out}} | \Psi_{\text{out}} \rangle \right],$$

interpreting the diagonal matrix elements in terms of the forward parton densities. One step further into strengthening the constraint [161] was to use the form involving the geometric average

$$\langle \Psi_{\text{out}} | \Psi_{\text{in}} \rangle \leq \sqrt{|\Psi_{\text{in}}| |\Psi_{\text{out}}|}.$$

To this end, the GPDs are written as

$$H(x, \eta) = \sum_S \langle \Psi_{\text{out}}(x, \eta; S) | \Psi_{\text{in}}(x, \eta; S) \rangle, \quad (3.275)$$

where $|\Psi_{\text{in}}(x, \eta; S)\rangle$ describes the probability amplitude that the incoming nucleon with momentum $\frac{1}{2}(1+\eta)p$ converts into a parton with momentum $\frac{1}{2}(x+\eta)p$ and spectators S , while $\langle \Psi_{\text{out}}(x, \eta; S)|$ describes the recombination of the spectator system S and a parton with momentum $\frac{1}{2}(x-\eta)p$ into the outgoing hadron with momentum $\frac{1}{2}(1-\eta)p$. Then the Cauchy-Schwartz inequality states

$$\left| \sum_S \langle \Psi_{\text{out}}(x, \eta; S) | \Psi_{\text{in}}(x, \eta; S) \rangle \right|^2 \leq \sum_S \langle \Psi_{\text{in}}(x, \eta; S) | \Psi_{\text{in}}(x, \eta; S) \rangle \sum_{S'} \langle \Psi_{\text{out}}(x, \eta; S') | \Psi_{\text{out}}(x, \eta; S') \rangle. \quad (3.276)$$

The forward matrix elements give the usual parton densities. For instance, for a spinless target,

$$\sum_S \langle \Psi_{\text{in}}(x, \eta; S) | \Psi_{\text{in}}(x, \eta; S) \rangle = q(x_1) \quad , \quad \sum_S \langle \Psi_{\text{out}}(x, \eta; S) | \Psi_{\text{out}}(x, \eta; S) \rangle = q(x_2). \quad (3.277)$$

As a result, one obtains for the quark distributions [161, 140, 168]

$$H^q(x, \eta, \Delta^2) \leq \sqrt{q(x_1)q(x_2)}. \quad (3.278)$$

Similarly, for the gluon distributions, taking into account extra factors of x present in their definitions, gives the inequality

$$H^g(x, \eta, \Delta^2) \leq \sqrt{(1-\eta^2)x_1x_2g(x_1)g(x_2)}. \quad (3.279)$$

For unpolarized quarks in the nucleon, inequalities involve both H and E GPDs. In particular, (3.278) was modified in Ref. [162] into

$$\left| H - \frac{\eta^2}{1-\eta^2} E \right| \leq \sqrt{\frac{q(x_1)q(x_2)}{1-\eta^2}}. \quad (3.280)$$

The same inequality, with the change $H \rightarrow \tilde{H}$, $E \rightarrow \tilde{E}$, holds for polarized quark GPDs [163]. The inequality (3.280) was enhanced in [164] to

$$\left(H(x, \eta, \Delta^2) - \frac{\eta^2}{1-\eta^2} E(x, \eta, \Delta^2) \right)^2 + \left(\frac{|\Delta_\perp|}{2M_N(1-\eta^2)} E(x, \eta, \Delta^2) \right)^2 \leq \frac{q(x_1)q(x_2)}{1-\eta^2}. \quad (3.281)$$

This relation also gives a constraint on the helicity-flip GPD E itself [164, 162]:

$$\frac{|\Delta_\perp|}{2M_N\sqrt{1-\eta^2}} |E(x, \eta, \Delta^2)| < \sqrt{q(x_1)q(x_2)}. \quad (3.282)$$

3.11.2 Inequalities in impact parameter representation

All inequalities discussed in the previous subsection compare Δ^2 -dependent GPDs $F^q(x, \eta, \Delta^2)$ with forward parton densities $q(x)$ which have no Δ^2 -dependence. Since GPDs are expected to decrease with increasing $|\Delta^2|$, the inequalities at lowest attainable Δ^2 are the strongest. In fact, it is possible to construct inequalities in which GPDs are compared to other GPDs which are also decreasing with $|\Delta^2|$. The simplest example is obtained by taking $\eta = 0$ and switching to the impact parameter representation (3.264). Then an analogue of (3.282) is [165],

$$|\nabla_{\perp} f_E^q(x, 0, \mathbf{r}_{\perp})| < 2M_N f_H^q(x, 0, \mathbf{r}_{\perp}), \quad (3.283)$$

where the subscript $F = H, E$ indicates the origin of the impact-parameter-dependent parton distribution from the corresponding GPD (see Section 3.10.2). For discussion of other inequalities in the $\eta = 0$ case see Refs. [166, 152, 167, 151]. There exist also inequalities [154] between skewed ($\eta \neq 0$) and skewless ($\eta = 0$) \mathbf{r}_{\perp} -dependent impact parameter distributions:

$$\sqrt{1 - \eta^2} |f_H^q(x, \eta, \mathbf{r}_{\perp})| \leq \sqrt{f_H^q\left(x_1, 0, \frac{\mathbf{r}_{\perp}}{1 + \eta}\right) f_H^q\left(x_2, 0, \frac{\mathbf{r}_{\perp}}{1 - \eta}\right)}, \quad (3.284)$$

where the third argument of the impact-parameter distributions correspond to the distance between the probed quark and the transverse center-of-momentum of the hadron [154], as we demonstrated in Section 3.10.3.

3.11.3 General inequalities

The derivation of inequalities is usually based on the positivity of the norm of a Hilbert vector given by a superposition of states like $b(x_i)|h(p_i, \lambda_i)\rangle$, where $b(x_i)$ is the annihilation operator of the quark with the momentum $x_i p_i$ and $|h(p_i, \lambda_i)\rangle$ is a hadronic state with momentum p_i and helicity λ_i . Choosing independent weights c_i for each state gives [168]

$$\left| \sum_i c_i b(x_i) |h(p_i, \lambda_i)\rangle \right|^2 \geq 0. \quad (3.285)$$

In the original example (3.276) only two states Ψ_{in} and Ψ_{out} were incorporated into the superposition. Taking a general superposition, one may hope to derive the most generic inequalities [168]. To this end, one constructs a general quark-hadron superposition. It is given by a four-dimensional integral involving integration over the hadron three-momentum and the quark longitudinal momentum. Hence, the squared norm is an eight-dimensional integral. One integration is removed by the longitudinal momentum conservation. As explained in [168], by using the impact parameter representation for GPDs, the remaining seven-dimensional integral can be reduced to a two-dimensional one with respect to variables x and η :

$$\sum_{\lambda_1 \lambda_2} \int_{-1}^1 d\eta \int_{\eta}^1 \frac{dx}{(1-x)^5} p_{\lambda_2}^*(y_2) p_{\lambda_1}(y_1) f_{\lambda_2 \lambda_1}\left(x, \eta, \frac{y_1 y_2}{1-x} \mathbf{r}_{\perp}\right) \geq 0, \quad (3.286)$$

where $f_{\lambda_2 \lambda_1}$ is a generic notation for the impact parameter representation of quark GPDs in the helicity basis. The arguments of the p -functions

$$y_1 = \frac{1-x}{1+\eta}, \quad y_2 = \frac{1-x}{1-\eta}$$

correspond to the light-cone momentum of the spectator system measured in units of the initial or final hadron, respectively. Since the functions p_λ are arbitrary, this relation generates an infinite set of inequalities. In case of spin-zero hadrons, the \mathbf{r}_\perp -space functions $f_{\lambda_2\lambda_1}$ are simply $f^q = f_H^q$, while for spin-one-half case, they were obtained in Eq. (3.273) so that their matrix takes the form

$$f_{\lambda_2\lambda_1}^q(x, \eta, -\Delta_\perp) = \sqrt{1-\eta^2} \begin{pmatrix} H^q - \frac{\eta^2}{1-\eta^2} E^q & \frac{\bar{\Delta}}{2M_N(1-\eta^2)} E^q \\ -\frac{\Delta}{2M_N(1-\eta^2)} E^q & H^q - \frac{\eta^2}{1-\eta^2} E^q \end{pmatrix}_{\lambda_2\lambda_1}. \quad (3.287)$$

By choosing appropriate functions p_λ in (3.286) one can obtain various inequalities [168], including those discussed earlier. In particular, taking $p(z) = c_1\delta(z - y_1) + c_2\delta(z - y_2)$ and optimizing the resulting inequality with respect to c_1 and c_2 gives Eq. (3.284). Furthermore, taking $c_i = d_i \exp(-p_{i\perp}\Delta_\perp)$ and optimizing with respect to d_1 and d_2 one obtains Eq. (3.278). It was checked in Refs. [168, 161] that inequalities obtained in this way are not destroyed by one-loop evolution, which will be discussed in Section 4.

In Ref. [147] it was demonstrated that the general positivity constraint (3.286) is equivalent to the following representation for GPDs in the impact-parameter space

$$f^q(x, \eta, \mathbf{r}_\perp) = (1-x)^2 \sum_n Q_n(y_1, (1-\eta)\mathbf{r}_\perp) Q_n(y_2, (1+\eta)\mathbf{r}_\perp), \quad (3.288)$$

valid in the inclusive domain $|x| < \eta$. Recalling that the momentum-fraction interpretation of parameters y_1, y_2 , we can interpret the functions Q_n as the \mathbf{r}_\perp -space transforms of objects similar to the light-cone wave functions (see the explanation in Ref. [10] after Eq. (198)). In other words, Eq. (3.288) has the structure of the generalized overlap representation, cf. Section 3.7.4. The prefactor $(1-x)^2$ is specific for spin-one-half partons. For a generic spin- s parton, it is $(1-x)^{2s+1}$ [147].

The positivity constraints are, of course, satisfied by perturbative diagrammatic representation. In particular, for a toy scalar model—scalar quarks of mass m_ϕ coupled to a scalar meson having the mass m_M —the contribution of the triangle diagram corresponding to the matrix element of the bilocal operator (3.4) takes the form [169]

$$f^\phi(x, \eta, \mathbf{r}_\perp) = \frac{1-x}{4\pi} V_0(y_1, (1-\eta)\mathbf{r}_\perp) V_0(y_2, (1+\eta)\mathbf{r}_\perp), \quad (3.289)$$

where the generalized impact-parameter light cone wave functions

$$V_0(y, \mathbf{r}_\perp) = \frac{1}{4\pi y} \int_0^\infty \frac{d\sigma}{\sigma} \exp\left(-\frac{\mathbf{r}_\perp^2}{4\sigma y^2} - \sigma(m_\phi^2 - y(1-y)m_M^2)\right), \quad (3.290)$$

can be concisely expressed through the McDonald function K_0 . Feynman diagrams also satisfy the polynomiality conditions. Thus, a possible strategy for model building is to construct GPDs by superposition of expressions corresponding to perturbative diagrams [170, 147] or having similar structure [169].

The positivity constraints provide a very sensitive test for self-consistency of model expressions for GPDs. For instance, the triangle diagram for the bilocal vector operator $\phi^\dagger(-z^-)\partial^\mu\phi(z^-)$ in the scalar toy model [170] has both the p^μ term corresponding to F -type DD and the Δ^μ part contributing to G -type DD. As observed in [171], a GPD built from the F -type part alone

violates even the simplest positivity condition of Eq. (3.278) type. At the moment, it seems that the most promising way to satisfy both the polynomiality conditions and the infinite set of the positivity constraints is to combine the generic representation (3.288) with the formalism of double distributions. Only a first step [170, 147, 169] has been made in this direction so far.

3.12 Chiral properties of GPDs

Although the dependence of GPDs on the momentum fraction variables x and η cannot be handled analytically from first principles, but only through elaborate phenomenological modeling, the dependence on the transverse momentum transfer is quite a different story. The small- Δ^2 dependence can be revealed through an effective field theory description at scales of order of the chiral symmetry breaking. The conventional approach uses Goldstone bosons of the spontaneously broken chiral symmetry as independent degrees of freedom within the framework of chiral perturbation theory (χ PT). The construction of effective operators is performed by means of the standard power counting of χ PT, which relies on the fact that the Goldstone bosons do not interact at zero momentum.

In the present section, we review the application of χ PT to the pion and nucleon GPDs. We limit ourselves to the $SU(2)$ χ PT. We consider single-nucleon systems and, in order to have a consistent power counting, we use the formalism of the heavy baryon χ PT. It treats the nucleon as a non-relativistic infinitely heavy particle [172]. We present the results at one loop level of χ PT. In this way, we compute the leading non-analytic corrections of the type $|\Delta^2| \ln |\Delta^2|$ to GPDs, where $M_N^2 \gg |\Delta^2| \sim m_\pi^2$. Such corrections are universal and allow us to get an insight into the structure of GPDs at small momentum transfer. Note, that ultraviolet divergences generated by one-loop diagrams should be absorbed into the coefficients of next-to-leading order counterterms in the chiral expansion, as this domain is not described correctly by low-momentum meson Lagrangian.

The calculational procedure is rather straightforward. First, one constructs composite operators from the nucleon and pion fields which match the quantum numbers of the operators built on the quark-gluon level, e.g., local Wilson operators (3.107) – (3.108) or their light-cone generating functions (3.10) – (3.20). The operators made of nucleon and pion fields are added to the effective Lagrangian [173, 174]. Then one uses the heavy-baryon chiral perturbation theory [172] (for a review, see [175]) for computation of the tree-level and one-loop contributions. In our case, one needs the leading order pion-nucleon Lagrangian

$$\mathcal{L}_{\text{LO}} = \bar{N}_v \{ i v \cdot \mathcal{D} + 2g_A S \cdot \mathcal{A} \} N_v + \frac{f_\pi^2}{8} \text{tr} \{ \partial^\mu \Sigma \partial_\mu \Sigma^\dagger \} + \lambda \text{tr} \{ M_q (\Sigma + \Sigma^\dagger) \}. \quad (3.291)$$

Here, N_v is the heavy-nucleon field operator, depending on the four-velocity v^μ and normalized by $N_v(0)|p\rangle = u_v(p)|0\rangle$. The relation of the heavy-nucleon spinor u_v to the usual one u is given in Appendix A.2, along with other useful relations required to perform calculations. The notation $S_\mu \equiv \frac{i}{2}\sigma_{\mu\nu}\gamma_5 v^\nu$ is used for the Pauli-Lubanski spin vector. The nonlinear chiral Σ field is constructed from the triplet of the pion fields

$$\Sigma \equiv \xi^2 = \exp \left(\frac{i\sqrt{2}}{f_\pi} \pi^a \tau^a \right), \quad (3.292)$$

where $f_\pi = 132$ MeV is the pion decay constant and τ^a are the flavor Pauli matrices. The axial-vector and vector (hidden in the covariant derivative $\mathcal{D}_\mu \equiv \partial_\mu + \mathcal{V}_\mu$) pion potentials are given by

expressions

$$\mathcal{V}_\mu \equiv \frac{1}{2} (\xi^\dagger \partial_\mu \xi + \xi \partial_\mu \xi^\dagger) , \quad \mathcal{A}_\mu \equiv \frac{i}{2} (\xi^\dagger \partial_\mu \xi - \xi \partial_\mu \xi^\dagger) . \quad (3.293)$$

The field Σ and the coupling λ , that occur in the effective Lagrangian, are subject to the chiral counting rules:

$$\Sigma \sim \mathcal{O}(\delta^0), \quad \partial^\mu \Sigma \sim \mathcal{O}(\delta^1), \quad \lambda \sim \mathcal{O}(\delta^2), \quad (3.294)$$

with δ being a small parameter of the chiral expansion. In our subsequent consideration it will be the t -channel momentum transfer Δ^μ . From (3.294), one finds that the leading order effective Lagrangian is of the order of Δ^2 . For the purposes of the present discussion, we will need just the first non-trivial term in the expansion of the potentials in the pion fields, namely,

$$\mathcal{A}_\mu = -\frac{1}{\sqrt{2}f_\pi} \partial_\mu \pi^a \tau^a + \dots, \quad \text{and} \quad \mathcal{V}_\mu = \frac{i}{(\sqrt{2}f_\pi)^2} \varepsilon_{abc} \pi^a \partial_\mu \pi^b \tau^c + \dots ,$$

respectively. In the mass term, the coefficient λ , accompanying the quark mass matrix $M_q = \text{diag}(m_u, m_d)$, is related to the quark condensate via $\lambda = -\frac{1}{2}\langle\bar{\psi}\psi\rangle$.

3.12.1 Pion GPDs

We start with pion GPDs [176]. Since the isosinglet and isotriplet GPDs possess different chiral properties, it is instructive to study them separately. These functions are related to the following combinations of flavor-specific GPDs (3.30) as

$$H_\pi^{(0)} = H_\pi^u + H_\pi^d, \quad H_\pi^{(1)} = H_\pi^u - H_\pi^d. \quad (3.295)$$

The isospin symmetry relates GPDs of different pion species among each other,

$$H_{\pi^+}^{u+d} = H_{\pi^-}^{u+d} = H_{\pi^0}^{u+d}, \quad H_{\pi^+}^{u-d} = -H_{\pi^-}^{u-d}, \quad H_{\pi^0}^{u-d} = 0. \quad (3.296)$$

These combinations have definite transformation properties under the time-reversal and charge conjugation symmetries

$$H_\pi^{(I)}(x, \eta) = H_\pi^{(I)}(x, -\eta), \quad H_\pi^{(I)}(x, \eta) = (-1)^{1-I} H_\pi^{(I)}(-x, \eta). \quad (3.297)$$

Before we compute their chiral behavior in low momentum transfer as well as the pion mass, let us present a few exact results based on their Goldstone nature. Namely, from the soft-pion theorems it was established in Ref. [72] that

$$H_\pi^{(0)}(x, \eta = 1, \Delta^2 = 0) = 0, \quad H_\pi^{(1)}(x, \eta = 1, \Delta^2 = 0) = \phi_\pi \left(\frac{1+x}{2} \right). \quad (3.298)$$

for isoscalar $I = 0$ and isovector $I = 1$ sectors. On the other hand, since the x -moment of GPDs should be a polynomial in η with the highest power of η no larger than two (see Eq. (3.115)), one finds [72] that

$$\int_{-1}^1 dx x H_\pi^{(0)}(x, \eta, \Delta^2 = 0) = (1 - \eta^2) \sum_q P^q, \quad (3.299)$$

where P^q is the fraction of the pion's momentum carried by the flavor- q quark. Notice that due to the chiral nature of the pion, the second moment depends on a single rather than two

independent non-perturbative parameters as it is the case in the generic case of a spinless target. As we established in Eqs. (3.154) and (3.155), the value of P^q is related to the inclusive parton distributions through

$$P^q = \int_{-1}^1 dx x f^q(x) = \int_0^1 dx x (q(x) + \bar{q}(x)) . \quad (3.300)$$

This quantity depends on the resolution scale, which is not displayed. The sum rule for the pion GPD (3.299) imposes a constraint on the pion D -term,

$$D^q(\alpha) = -\frac{5}{4} P^q (1 - \alpha^2) \left\{ C_1^{3/2}(\alpha) + \dots \right\} ,$$

thus fixing the magnitude of the leading term exactly.

Now we are in a position to figure out the dependence on the soft momentum transfer and m_π using χ PT. First notice, that different light-cone components of the t -channel momentum transfers have different scaling in χ PT. Namely, Δ^+ is of order one since it forms the scaling variable η , while the soft expansion parameter will be the transverse momentum transfer $\delta = \Delta_\perp$. Making use of this power counting procedure, we have to construct effective hadronic operators made from the non-linear pion field Σ and its derivatives, which will substitute the partonic operator (3.10) parametrizing GPDs at low energy scales. Depending on the type of the light-cone component of the derivative acting on Σ , one finds the following scaling rules in the infinite momentum frame:

$$\partial^+ \Sigma \sim \mathcal{O}(\Delta_\perp^0), \quad \partial^- \Sigma \sim \mathcal{O}(\Delta_\perp^2), \quad \nabla_\perp \Sigma \sim \mathcal{O}(\Delta_\perp) . \quad (3.301)$$

Using the building blocks (3.301), one derives effective field theory operators in terms of the Goldstone degrees of freedom by matching the quantum numbers of the twist-two operators (3.10). The analysis, which exhibits the symmetry properties of the composite pion operators can be done in terms of local Wilson operators. To the leading order in the chiral expansion, one finds that the lowest spin-one operator in the isoscalar sector vanishes identically—as a consequence of the charge conjugation property of the nonlinear pion field $\tau^2 \Sigma^\dagger \tau^2 = \Sigma^T$ and unitarity—so that the first nontrivial isoscalar operator has spin two,

$$\mathcal{O}_\mu^{(0)\pi} = \text{tr} \left\{ \Sigma \partial_\mu \Sigma^\dagger \right\} = 0, \quad \mathcal{O}_{\mu_1 \mu_2}^{(0)\pi} = f_\pi^2 a_2^\pi \underset{\mu_1 \mu_2}{\mathbf{S}} \text{tr} \left\{ \partial_{\mu_1} \Sigma \partial_{\mu_2} \Sigma^\dagger \right\} , \quad (3.302)$$

On the other hand, even the spin-two operator in the isovector sector is zero,

$$\underset{\mu_1 \mu_2}{\mathbf{S}} \text{tr} \left\{ \tau^a \partial_{\mu_1} \Sigma \partial_{\mu_2} \Sigma^\dagger \right\} = 0 . \quad (3.303)$$

Actually, the origin of this equation is more general than the chiral limit. On the parton level is corresponds to the vanishing of the first Mellin moment of the isovector combination of GPDs $H^{u-d}(x, \eta, \Delta^2)$ (see Eq. (3.30)) which is an even function in x as a consequence of the isospin symmetry of the quark operator and its odd parity under the charge conjugation. One can further classify all high-spin local pion operators according to this scheme [117]. It is much more convenient however to deal with non-local pion operators, which effectively resum the entire series of Wilson operators. Namely, relying on general symmetry considerations one can introduce the operator [176]:

$$\begin{aligned} \mathcal{O}^\pi(z^-) = \frac{f_\pi^2}{8} \int_{-1}^1 d\beta \int_{-1+|\beta|}^{1-|\beta|} d\alpha f(\beta, \alpha) & \left\{ \Sigma((\alpha + \beta)z^-) i \vec{\partial}^+ \Sigma^\dagger((\alpha - \beta)z^-) \right. \\ & \left. + \Sigma^\dagger((\alpha + \beta)z^-) i \vec{\partial}^+ \Sigma((\alpha - \beta)z^-) \right\} , \end{aligned} \quad (3.304)$$

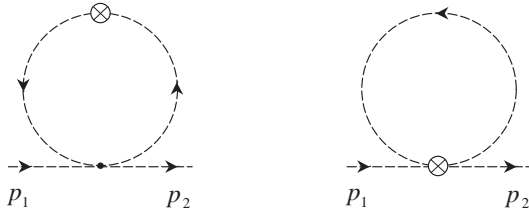


Figure 20: Chiral loops generating non-analytic behavior of pion GPDs. The four-pion vertex in the leftmost diagram originates from the expansion of effective Lagrangian \mathcal{L}_{LO} .

which is an $SU(2)$ matrix. Its trace with τ^A , $\text{tr } \tau^A \mathcal{O}^\pi$, and expansion in local operators can be shown to yield only the operators with required symmetry and structure, with (3.302) and (3.303) being the first terms in Taylor series in powers of the Ioffe time z^- . In the above definition $f(\beta, \alpha)$ is a generating function of a tower of low-energy constants. It is a double distribution, discussed in the preceding section, though to the lowest order in the chiral expansion. The low-energy constants match the partonic degrees of freedom to the pionic: their values are not determined within the effective field theory and rather considered as phenomenological parameters. There is a number of pion operators with more than two Σ fields since their insertion does not alter the twist of the composite operator, however, they do not contribute to the one-loop matrix elements we are interested in here and will be totally omitted.

The pion GPDs are defined in terms of (3.304) as a matrix element of the hadronic operator

$$\int \frac{dz^-}{2\pi} e^{-ixp^+z^-} \langle \pi^b(p_2) | \text{tr } \tau^C \mathcal{O}^\pi(z^-) | \pi^a(p_1) \rangle = \frac{1}{2} \text{tr}(\tau^C \tau^a \tau^b) H_\pi^{(I)}(x, \eta, \Delta), \quad (3.305)$$

where $\tau^A = (\mathbb{1}, \tau^a)$ and the index A runs over the values $A = 0, 1, 2, 3$. The above formula introduces both the isovector (of isospin $I[a] = 1$) and isoscalar (of isospin $I[0] = 0$) GPDs.

Notice that the first moment of the double distribution $f^{(I)}$ is matched to known nonperturbative parameters

$$\int_{\Omega} d\alpha d\beta f^{(0)}(\beta, \alpha) \beta = \sum_q P^q = a_2^\pi \quad (3.306)$$

$$\int_{\Omega} d\alpha d\beta f^{(1)}(\beta, \alpha) = 1. \quad (3.307)$$

As it is clear from the context, the low-energy constant a_2^π is related to the momentum fraction of the pion carried by quarks and gluons forming it. For an on-shell pion at low normalization point $\mu^2 \approx 0.3 \text{ GeV}^2$ one has [78] $a_2^{\pi,q} \approx 0.7$ and respectively $a_2^{\pi,g} \approx 0.3$ due to the momentum conservation. The interpretation of the generating functions $f^{(I)}(\beta, \alpha)$ as DDs implies that these functions depend on the factorization scale μ . The functional dependence on this parameter is described by evolution equations to be discussed in the following sections. For the sake of brevity, we do not write this argument explicitly.

Computation of the Feynman diagrams in Fig. 20 yields the following expressions for pion GPDs with leading non-analytic corrections included [176, 177]

$$H_\pi^{(0)}(x, \eta, \Delta^2) = \Phi^{(0)} \left(\frac{x}{\eta}, \frac{1}{\eta} \right) + \frac{\theta(\eta - |x|)}{2(4\pi f_\pi)^2} (m_\pi^2 - 2\Delta^2) \int_{-1}^1 d\sigma \ln m_\pi^2(\sigma) \Phi^{(0)} \left(\frac{x}{\eta}, \sigma \right),$$

$$H_\pi^{(1)}(x, \eta, \Delta^2) = \left(1 - 2\frac{m_\pi^2 \ln m_\pi^2}{(4\pi f_\pi)^2}\right) \Phi^{(1)}\left(\frac{x}{\eta}, \frac{1}{\eta}\right) + \frac{\theta(\eta - |x|)}{(4\pi f_\pi)^2 \eta} \int_{-1}^1 d\sigma m_\pi^2(\sigma) \ln m_\pi^2(\sigma) \frac{\partial}{\partial \sigma} \Phi^{(1)}\left(\frac{x}{\eta}, \sigma\right), \quad (3.308)$$

where

$$m_\pi^2(\sigma) \equiv m_\pi^2 - (1 - \sigma^2) \frac{\Delta^2}{4}$$

and

$$\Phi^{(I)}(u, v) = \int_{\Omega} d\alpha d\beta f^{(I)}(\beta, \alpha) \{v\delta(u - \alpha - v\beta) - (1 - I)\delta(u - \alpha - \beta)\},$$

with the integration going over the same simplex Ω as for conventional DDs. Note that the argument of the chiral logarithms can be made dimensionless by introducing a chiral cut-off Λ_χ^2 , the dependence on which cancels between these one-loop expressions and the next-to-leading order counterterms in the derivative expansion of the effective chiral Lagrangian \mathcal{L}_{NLO} [178].

Let us discuss a few limiting cases of Eq. (3.308).

- Conventional form factors are found by forming the first two moments of pion GPDs,

$$\int_{-1}^1 dx H_\pi^{(1)}(x, \eta, \Delta^2) = 2F_{\pi+}(\Delta^2), \quad (3.309)$$

$$\int_{-1}^1 dx x H_\pi^{(0)}(x, \eta, \Delta^2) = \theta_2(\Delta^2) - \eta^2 \theta_1(\Delta^2), \quad (3.310)$$

with the pion electromagnetic and gravitational form factors defined in Eqs. (3.85) and (3.152), respectively. Integrating the one-loop expression (3.308), we thus obtain the well-known results for the leading non-analytic contribution to the pion electromagnetic [178] and gravitational form factors [179]

$$F_\pi(\Delta^2) = 1 - 2\frac{m_\pi^2 \ln m_\pi^2}{(4\pi f_\pi)^2} + \frac{1}{(4\pi f_\pi)^2} \int_{-1}^1 d\sigma m_\pi^2(\sigma) \ln m_\pi^2(\sigma), \quad (3.311)$$

$$\theta_2(\Delta^2) = P^q, \quad (3.312)$$

$$\theta_1(\Delta^2) = P^q \left(1 + \frac{m_\pi^2 - 2\Delta^2}{2(4\pi f_\pi)^2} \int_{-1}^1 d\sigma (1 - \sigma^2) \ln m_\pi^2(\sigma)\right), \quad (3.313)$$

respectively.

- Parton densities are found by taking the skewless limit. Note, however, that the limit $\eta \rightarrow 0$ and the chiral limit $m_\pi \rightarrow 0$ do not commute in Eq. (3.308). To reproduce the results obtained recently in Refs. [173, 174], we have to send $\eta \rightarrow 0$ before $m_\pi \rightarrow 0$. This yields

$$q(x) = q_0(x) \left(1 - 2\frac{m_\pi^2 \ln m_\pi^2}{(4\pi f_\pi)^2}\right) + 2\delta(x) \frac{m_\pi^2 \ln m_\pi^2}{(4\pi f_\pi)^2}, \quad (3.314)$$

with $q_0(x)$ being the quark distribution in the chiral limit.

3.12.2 Nucleon GPDs

Undoubtedly, the most profound manifestation of the chiral symmetry in the dynamics of nucleon GPDs is the appearance of the pion pole in the isovector combination $\tilde{E}^{u-d} = \tilde{E}^u - \tilde{E}^d$. Analogously to the behavior of the pseudoscalar nucleon form factor introduced in Eq. (3.95), the quark-antiquark pair determining the operator content of GPD \tilde{E} can fluctuate into an off-shell pion and due to its Goldstone nature \tilde{E}^{u-d} develops this transition develops a pole in Δ^2 . The explicit chiral symmetry breaking proportional to m_q gives a small mass to the pion so that the pole is shifted from zero to the physical value $\Delta^2 = m_\pi^2$. At the pole, the single pion exchange dominates over other resonances with the same quantum numbers, such that it is possible to have a legitimate approximation for $|\Delta^2| \leq m_\pi^2$. Continuing to the physical region of space-like Δ^2 , one writes for the proton [142, 183]

$$\tilde{E}^{u-d}(x, \eta, \Delta^2 \rightarrow m_\pi^2) = \frac{\theta(\eta - |x|)}{2\eta} \phi_\pi \left(\frac{x + \eta}{2\eta} \right) \frac{4g_A^{(3)} M_N^2}{m_\pi^2 - \Delta^2}, \quad (3.315)$$

where the bound state of the quark-antiquark pair is determined by the pion leading twist distribution amplitude (3.166). By means of the Goldberger-Treiman, the pion-nucleon coupling constant $g_{\pi NN}$ was reduced to the isovector axial constant $g_A^{(3)}$, $f_\pi g_{\pi NN} = \sqrt{2} M_N g_A^{(3)}$. Using the isospin symmetry one can finally write for specific flavor components

$$\tilde{E}^u = -\tilde{E}^d = \frac{1}{2} \tilde{E}^{u-d}. \quad (3.316)$$

Now we turn to the chiral expansion of other nucleon GPDs [117]. Under the chiral $SU(2)_L \otimes SU(2)_R$ group, the quark operators determining their content transform under either isovector $(3, 1) \oplus (1, 3)$ or isoscalar $(1, 1)$ representations. These correspond to the flavor non-singlet $\mathcal{R}^{2,qq,a}$ and singlet $\mathcal{R}^{2,qq,0}$ quark operators, respectively,

$$\mathcal{R}_{\mu_1 \mu_2 \dots \mu_j}^{2,qq,A} = \mathbf{S}_{\mu_1 \mu_2 \dots \mu_j} \bar{\psi} \tau^A \gamma_{\mu_1} i \vec{\mathcal{D}}_{\mu_1} i \vec{\mathcal{D}}_{\mu_2} \dots i \vec{\mathcal{D}}_{\mu_j} \psi. \quad (3.317)$$

For the purpose of a unique translation of the Lorentz-covariant matrix elements in Eq. (3.123) into non-relativistic ones, it is convenient to use the Breit reference frame [180, 181], as we discussed at length in Section 2.2.2. Exploiting the results from the Appendix A.2, the decomposition (3.123) transforms in the Breit frame into the equation

$$\begin{aligned} \langle p_2 | \mathcal{R}_{\mu_1 \dots \mu_j}^{2,qq,A} | p_1 \rangle &= \mathbf{S}_{\mu_1 \dots \mu_j} \bar{u}_v(p_2) \tau^A u_v(p_1) v_{\mu_1} \{ (2M_N)^{j-1} G_{j,0}^E v_{\mu_2} \dots v_{\mu_j} + \dots + G_{j,j-1}^E \Delta_{\mu_2} \dots \Delta_{\mu_j} \} \\ &+ \mathbf{S}_{\mu_1 \dots \mu_j} \frac{\bar{u}_v(p_2) \tau^A [S_{\mu_1}, S \cdot \Delta] u_v(p_1)}{M_N} \{ (2M_N)^{j-1} G_{j,0}^M v_{\mu_2} \dots v_{\mu_j} + \dots + G_{j,j-1}^M \Delta_{\mu_2} \dots \Delta_{\mu_j} \} \\ &+ \mathbf{S}_{\mu_1 \dots \mu_j} \frac{\bar{u}_v(p_2) \tau^A u_v(p_1)}{2M_N} \Delta_{\mu_1} \dots \Delta_{\mu_j} D_j, \end{aligned} \quad (3.318)$$

where for brevity we did not display the dependence of the form factors G_{jk}^E , G_{jk}^M and D_j on the momentum transfer Δ^2 and dropped higher-order corrections in the ratio Δ^2/M_N^2 . Obviously due to the constraint from the time-reversal invariance (see Section 3.2.8) the form factors accompanying the odd power of the momentum transfer Δ_μ has to be set to zero. The electric- and

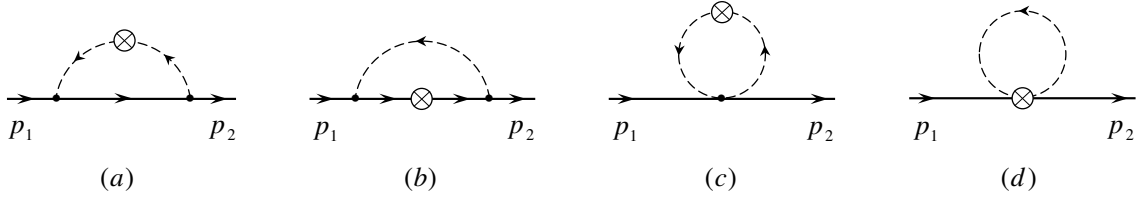


Figure 21: One loop diagrams contributing to the nucleon matrix elements of the twist-two operators. One should also add diagrams with self-energy insertions into the external lines, which are not displayed explicitly here.

magnetic-type form factors G_{jk}^E and G_{jk}^M are related to the previously introduced H_{jk} and E_{jk} in Eq. (3.123) via

$$G_{jk}^E = H_{jk} + \frac{\Delta^2}{4M_N^2} E_{jk}, \quad G_{jk}^M = H_{jk} + E_{jk}. \quad (3.319)$$

Note, that $G_{1,0}^E$ and $G_{1,0}^M$ correspond to the standard Sachs nucleon electromagnetic form factors (3.91),

$$G_{1,0}^E = G_E, \quad G_{1,0}^M = G_M. \quad (3.320)$$

They have been extensively discussed in the literature [180, 181], and therefore we will not address their chiral properties here.

To proceed with the analysis of chiral loops, let us complement the basis of pion operators, discussed in the preceding section, by adding hadronic twist-two operators bilinear in the heavy nucleon fields. The nucleon operators admit the form that mimics the tensor decomposition of the off-forward matrix elements (3.318). The leading operators contributing to isoscalar and isovector combinations of $G_{j,0}^E$ and $G_{j,0}^M$ are

$$\begin{aligned} \mathcal{O}_{\mu_1\mu_2\dots\mu_j}^{N,A} &= a_j^N (2M_N)^{j-1} \sum_{\mu_1\dots\mu_j} \mathbf{S} v_{\mu_1} \dots v_{\mu_j} \bar{N}_v \tau_{\xi+}^A N_v \\ &+ b_j^N (2M_N)^{j-1} (-i\partial^\nu) \sum_{\mu_1\dots\mu_j} \mathbf{S} v_{\mu_1} \dots v_{\mu_{j-1}} \bar{N}_v \tau_{\xi+}^A \frac{[S_{\mu_j}, S_\nu]}{M} N_v + \dots, \end{aligned} \quad (3.321)$$

where

$$\tau_{\xi+}^A \equiv \frac{1}{2} (\xi \tau^A \xi^\dagger + \xi^\dagger \tau^A \xi). \quad (3.322)$$

As in the pion case, the coefficients a^N and b^N , matching partonic and hadronic descriptions, are unknown, and have to be determined from experimental data. Subleading operators are derived from this expression by replacing the factors of the four-velocity v^μ in the Lorentz structure by derivatives. Note, that, due to the time-reversal symmetry restrictions, one should always replace an even number of velocities. In order to mimic the D -term structure, one further introduces a subleading operator,

$$\dots + c_2^N \frac{1}{2M} \sum_{\mu_1\mu_2} \mathbf{S} (-i\partial_{\mu_1})(-i\partial_{\mu_2}) \bar{N}_v \tau_{\xi+}^A N_v.$$

Having constructed the operator basis, the leading-order chiral behavior is then deduced from the Feynman graphs displayed in Fig. 21. The isoscalar form factors receive contributions only from the diagrams 21 (a) and (c), since (b) and (d) vanish identically. Their calculation is straightforward making use of the leading order chiral lagrangian (3.291) and yields [117]

$$G_{2,0}^E(\Delta^2) = a_2^N + 3a_2^\pi \frac{g_A^2 \pi}{2M_N(4\pi f_\pi)^2} \left\{ (2m_\pi^2 - \Delta^2) \int_{-1}^1 d\sigma \sqrt{m_\pi^2(\sigma)} + \frac{4}{3} m_\pi^3 \right\},$$

$$\begin{aligned} G_{2,0}^M(\Delta^2) &= b_2^N + 3 \frac{g_A^2}{(4\pi f_\pi)^2} \int_{-1}^1 d\sigma \left\{ a_2^\pi m_\pi^2(\sigma) - 2b_2^N m_\pi^2 \delta(\sigma - 1) \right\} \ln m_\pi^2(\sigma), \\ D_2(\Delta^2) &= c_2^N + 3a_2^\pi \frac{g_A^2 \pi}{4(4\pi f_\pi)^2} M_N (2m_\pi^2 - \Delta^2) \int_{-1}^1 d\sigma \frac{1 - \sigma^2}{\sqrt{m_\pi^2(\sigma)}}. \end{aligned} \quad (3.323)$$

Notice the absence of the one-loop contributions to the form factors $G_{2,0}^E$ and D_2 from the nucleon operators. This is a consequence of a cancellation of the one-loop contribution (c) by the self-energy insertions into the external lines. We completely absorb all analytic contributions present in (3.323) into counterterms. Another comment concerns $G_{2,0}^E$. The pion operators generate $1/M_N$ -suppressed contributions to this structure. Therefore, by power counting we must add $\mathcal{O}(1/M_N)$ bilinear nucleon operators constructed from one large and one small component of the nucleon field, and also analogous terms stemming from the chiral Lagrangian. Lorentz invariance unambiguously fixes their coefficients, and no new low energy constants arise. However, the effect of these contributions in form factors is Δ^2 -independent and analytic in the pion mass. Thus, we will not compute them, although they can be anticipated to generate an additional term $-5a_2^N g_A^2 m_\pi^3 / (32\pi f_\pi^2 M_N)$ to the right-hand side of $G_{2,0}^E$ in Eq. (3.323) required by the momentum sum rules. Also, there arises a Foldy-like term $(b_j^N - a_j^N)\Delta^2/(4M_N^2)$ in $G_{j,0}^E$, just like in the form factor case [181], from contributions of small nucleon field components in the heavy-mass expansion of relativistic nucleon operators.

Sum rules for the total momentum and spin of the nucleon (pion) impose the following constraints on the coefficients a_2^N and b_2^N (a_2^π),

$$a_2^{N,q} + a_2^{N,g} = 1, \quad b_2^{N,q} + b_2^{N,g} = 1, \quad a_2^{\pi,q} + a_2^{\pi,g} = 1. \quad (3.324)$$

The latter two equations imply that the total gravitomagnetic moment of the nucleon vanishes [123] (cf. Eq. (3.159)).

The leading $(j, 0)$ -structures of the higher j -moments ($j > 2$) do not receive non-analytic contributions in the momentum transfer Δ^2 at the next-to-leading order in the chiral expansion due to the absence of relevant pion operators. Thus, one gets [117]

$$G_{j,0}^E(\Delta^2) = a_j^N + \dots, \quad G_{j,0}^M(\Delta^2) = b_j^N \left(1 - 6 \frac{g_A^2 m_\pi^2}{(4\pi f_\pi)^2} \ln m_\pi^2 + \dots \right), \quad (3.325)$$

where the ellipsis stand for analytic contributions from one-loop diagrams and counterterms, which are suppressed by at least $m_\pi^2/(4\pi f_\pi)^2$.

Due to the absence of the pion cloud contributions in diagrams (a) and (b), no non-analytic dependence on the momentum transfer arises at this order of χ PT. However, the diagrams (c) and (d) develop chiral logarithms in the pion mass of the form

$$G_{2,0}^F(\Delta^2) = f_2^N \left\{ 1 - \frac{2m_\pi^2}{(4\pi f_\pi)^2} (\chi_F g_A^2 + 1) \ln m_\pi^2 \right\}, \quad (3.326)$$

where the overall coefficients $f_2^N = (a_2^N, b_2^N, c_2^N)$ depend on the form factor $G_{2,0}^F$ in question and χ_F takes the values $\chi_F = 3, 2, 3$ for $G_{2,0}^F = G_{2,0}^E, G_{2,0}^M, D_2$, respectively. It is implied that one adds counterterms to the right-hand side of these equations linear in m_π^2 whose (unknown) coefficients absorb minimally the ultraviolet divergences resulting from loop integrals and also the Foldy-like term, as discussed after Eq. (3.323). The leading structures of the higher moments $G_{j,0}^E$ and

$G_{j,0}^M$, apart from the change of an overall normalization $b_2^N \rightarrow b_j^N$ and $a_2^N \rightarrow a_j^N$, have the same dependence on the chiral logarithms as in Eq. (3.326). Finally, let us note that one also can include the delta-isobar as a dynamical degree of freedom in χ PT. Such kind of analysis was performed for the orbital angular momentum sum rule (3.158) in Ref. [174].

A pragmatic application of the results outlined in the present section can be either in evolution of experimental measurements for the angular momentum sum rule (3.158) from nonzero to zero recoil or in chiral extrapolations of lattice data normally taken at very high “ m_π ” all the way down to the physical point.

3.13 Modeling GPDs

The studies in the previous sections of generic properties of GPDs and their asymptotic behavior in different regions of the momentum-fraction space allow to develop some “semi-realistic” models for them. Of course, the final word about their validity is reserved to experimental measurements. There exists a number of estimates of the functional form of GPDs based on various models of the hadronic structure, including the chiral soliton quark model [182, 143, 183, 9, 184, 185, 186, 187, 188], bag model [189, 190], constituent quark models [191, 192, 194], instanton techniques [193], light-cone frameworks [195, 170], Bethe-Salpeter [196, 197, 198] and Schwinger-Dyson [171, 199] approaches. The first-principle lattice simulations [157, 200, 201, 202] provided estimates for several off-forward matrix elements of local operators and constrained their functional dependence on the momentum transfer Δ^2 . First transverse lattice results were reported in Ref. [203]. In this section, we will discuss how available information can be used for construction of ansätze for GPDs based on very general principles. This will be done in a few steps. Since GPDs depend on two longitudinal variables, x and η , and one transverse Δ^2 , we address first the question of modeling the longitudinal dynamics, setting $\Delta^2 = 0$. Then we consider interplay of longitudinal Feynman momentum and transverse momentum Δ_\perp dependence. Finally, we combine the two models together building a single three-variable function.

3.13.1 Longitudinal dynamics

We will rely here upon the approach that uses double distributions in order to constrain plausible functional forms of the dependence on the s - and t -channel longitudinal momenta x and η . As already announced, we consider first the limiting case $\Delta^2 = 0$. First, let us make two observations. The β -variable of a double distribution $f(\beta, \alpha)$ can be interpreted as a fraction of the momentum p carried by the parton. The reduction formula (3.208) states that the integral over α gives the usual parton density $f(\beta)$. When combined together they suggest that the profile of $f(\beta, \alpha)$ in the β -direction follows the shape of parton density $f(\beta)$. Thus, it makes sense to write

$$f(\beta, \alpha) = \pi(\beta, \alpha) f(\beta), \quad (3.327)$$

where the function $\pi(\beta, \alpha)$ is normalized by the condition

$$\int_{-1+|\beta|}^{1-|\beta|} d\alpha \pi(\beta, \alpha) = 1. \quad (3.328)$$

It characterizes the profile of $f(\beta, \alpha)$ in the t -channel α -direction. The profile function should be symmetric with respect to $\alpha \rightarrow -\alpha$ as a consequence of the time-reversal invariance (3.209),

see Section 3.2.8. For a fixed β , the function $\pi(\beta, \alpha)$ describes how the longitudinal momentum transfer Δ^+ is shared between the two partons. Hence, the shape of $\pi(\beta, \alpha)$ should look like a symmetric meson distribution amplitude $\varphi(\alpha)$. Recalling that the support region for DDs is restricted by $|\alpha| \leq 1 - |\beta|$, to get a more close analogy with DAs, we rescale α as $\alpha = (1 - |\beta|)\gamma$ introducing the variable γ with β -independent limits: $-1 \leq \gamma \leq 1$. The simplest model is to assume that the γ -profile is a universal function $g(\gamma)$ for all β 's. As we already emphasized, in general this function does not have to vanish at the boundary of its support [145]. To proceed, we disregard this complication and assume that the double distribution is zero on the boundary of its support region. More elaborated models may require lifting this condition. As possible simple choices for $g(\gamma)$ one can take $\delta(\gamma)$, with no spread in γ -direction, $(1 - \gamma^2)^b$ which is a characteristic shape for the asymptotic limit of the quark and gluon distribution amplitudes for $b = 1$ and $b = 2$, respectively, as we will explain in the next chapter. In terms of (β, α) variables, all of these models can be summarized by a single formula

$$\pi(\beta, \alpha; b) = \frac{\Gamma(b + \frac{3}{2})}{\sqrt{\pi}\Gamma(b+1)} \frac{[(1-\beta)^2 - \alpha^2]^b}{(1-\beta)^{2b+1}}, \quad (3.329)$$

with a parameter b . In the limiting case $b = \infty$, we have $\pi(\beta, \alpha; \infty) = \delta(\alpha)$.

Let us analyze the structure of GPDs obtained from these simple models. In particular, taking $f(\beta, \alpha; \infty) = \delta(\alpha)f(\beta)$ gives the simplest model

$$H(x, \eta, \Delta^2 = 0) = f(x)$$

in which the GPDs at $\Delta^2 = 0$ have no skewness dependence at all and coincide with the usual parton distributions. For some values of b , one can find analytic expressions for GPDs also, provided that the functional form of the forward density is not very involved. Taking, for instance,

$$f(\beta) = \frac{\Gamma(5-n)}{\Gamma(4)\Gamma(1-n)} \frac{(1-\beta)^3}{\beta^n} \theta(\beta), \quad \pi(\beta, \alpha; 1) = \frac{3}{4} \frac{(1-\beta)^2 - \alpha^2}{(1-\beta)^3}, \quad (3.330)$$

gives a simple analytical representation for the corresponding GPD,

$$H(x, \eta, \Delta^2 = 0) = \frac{(1 - \frac{n}{4})}{\eta^3} \left\{ \theta(x > -\eta) \left(\frac{x + \eta}{1 + \eta} \right)^{2-n} (\eta^2 - x + (2 - n)\eta(1 - x)) - (\eta \rightarrow -\eta) \right\}. \quad (3.331)$$

It is evident that no odd powers of η would appear in the x^j -th moments of this function. Furthermore, this expression is explicitly non-analytic for $x = \pm\eta$. This is true even if n is integer. Discontinuity at $x = \pm\eta$, however, appears only in the second derivative of $H(x, \eta, \Delta^2 = 0)$, while the function itself and its first derivatives are continuous so that the model curves for $H(x, \eta)$ are very smooth.

In the case of singlet quark distributions, the DDs $f_{\text{singl}}(\beta, \alpha)$ should be odd functions of β . Still, we can use the model like (3.331) for the $\beta > 0$ part, but take $f_{\text{singl}}(\beta, \alpha)|_{\beta \neq 0} = A f(|\beta|, \alpha) \text{sgn}(\beta)$. Note, that $n \geq 1$ is the usual situation for standard parametrizations of singlet quark distributions. Then the integral producing $H_{\text{singl}}(x, \eta)$ in the $|x| \leq \eta$ region diverges for $\alpha \rightarrow x/\eta$. However, due to the antisymmetry of $f_{\text{singl}}(\beta, \alpha)$ with respect to $\beta \rightarrow -\beta$ and its symmetry with respect to $\alpha \rightarrow -\alpha$, the singularity at $\alpha = x/\eta$ can be integrated using the principal value prescription.

3.13.2 Longitudinal-transverse interplay

Above, we have discussed hypothetical GPDs with no transverse dynamics, setting $\Delta^2 = 0$ from the start. Now we are going to discuss the dependence on $\Delta^2 \neq 0$ in a simplified situation when $\eta = 0$. Even in this case, a first principle, model independent way to do this is currently not available, we have to rely on some assumptions. The simplest idea is to assume a complete factorization of longitudinal and transverse dependence, like $H^q(x, \eta = 0, \Delta^2) = f^q(x)F^q(\Delta^2)$, with $f^q(x)$ being a forward parton density and $F^q(\Delta^2)$ the relevant form factor. To be specific, for H^q and E^q GPDs of the proton the factorized ansatz implies that the Δ^2 dependence is accumulated in Dirac and Pauli form factors $F_1^q(\Delta^2), F_2^q(\Delta^2)$, respectively. Since the latter are defined through the matrix element of the electromagnetic (or, in general, vector) current, only the valence parts of H^q and E^q can be modeled in terms of F_1^q and F_2^q . Thus, for the flavor- q valence quark contribution we would write

$$H^{u,\text{val}}(x, \eta = 0, \Delta^2) = \frac{1}{2}F_1^u(\Delta^2) f^{u,\text{val}}(x), \quad H^{d,\text{val}}(x, \eta = 0, \Delta^2) = F_1^d(\Delta^2) f^{d,\text{val}}(x), \quad (3.332)$$

and analogously for the valence part of the helicity-flip function E^q , with obvious replacements everywhere of the Dirac F_1^q by the Pauli F_2^q form factor. Note however that the x -dependence of E^q is not constrained by the forward parton density f^q so this is an ad hoc assumption. The presence of the factor 1/2 in the u -quark distribution in the proton is a consequence of corresponding normalization of its form factor $F_1^u(0) = 2$ and parton density $\int dx f^{u,\text{val}}(x) = 2$. The expression of the quark form factors in terms of the measured proton and nucleon electromagnetic form factors was given earlier in Section 3.4.2.

This factorized form cannot, however, be even remotely correct since as we established in the previous section, at large values of the Feynman momentum $x \rightarrow 1$, the Δ^2 -dependence must become weaker. In other words, the higher the Mellin moment of GPDs, the flatter is the dependence on the momentum transfer. Due to a limited kinematical coverage in the t -channel momentum transfer Δ^2 in experiments, theoretical estimates confronted to data are currently insensitive to this feature, however.

A hint for a nontrivial and phenomenologically viable interplay between the x and Δ^2 dependence arises from the Regge theory. Recall that the high-energy dependence of, say, elastic $p_1 + p_2 \rightarrow p'_1 + p'_2$ scattering amplitudes is governed by linear Regge trajectories $\alpha_q(\Delta^2) = \alpha_q + \alpha'_q \Delta^2$ with $\Delta = p_1 - p'_1$, so that the physical cross section goes like $\sigma \sim s^{\alpha_q(\Delta^2)}$ as a function of the center-of-mass energy $s = (p_1 + p_2)^2$. In our case the role of s is taken by the (inverse) momentum fraction x which in the physical process is equal to the generalized Bjorken variable $x = x_B \sim s^{-1}$. Therefore, at small- x one can take as a working hypothesis for the non-forward parton distribution [9, 118]

$$f^q(x, \Delta^2) \equiv H^q(x, \eta = 0, \Delta^2) \xrightarrow{x \rightarrow 0} x^{-\alpha_q(\Delta^2)} = e^{-\alpha_q(\Delta^2) \ln x}.$$

This behavior was recently refined in dedicated studies in Refs. [205, 415]. Note, that this form satisfies the general requirement that the Δ^2 -dependence should disappear in the $x \rightarrow 1$ limit. Furthermore, the relevant form factor is determined by the x -integral of $f^q(x, \Delta^2)$. The latter admits the form

$$f^q(x, \Delta^2) \sim x^{-\alpha_q - \alpha'_q(1-x)^p \Delta^2} (1-x)^N. \quad (3.333)$$

The requirement of a controlled transverse size of the hadron and, therefore, finiteness of the spectator distance \mathbf{r}_\perp^s (see Fig. 15) at large- x where

$$f^q(x \rightarrow 1, \Delta^2) \sim e^{\alpha_q(1-x) + \alpha'_q(1-x)^{p+1}} (1-x)^N$$

requires $p \geq 1$ [155]. Notice, that phenomenologically, the form with $p = 0$ and $\alpha' \sim 1\text{GeV}^{-2}$ works fine up to at least $x \sim 0.5$ [204]. The form factor asymptotics at large Δ^2 is governed by the large- x behavior of $f^q(x, \Delta)$ and is given by

$$F(\Delta^2 \rightarrow \infty) \sim |\Delta^2|^{-(N+1)/(p+1)}.$$

The Drell-Yan relation requires $p = 1$ [206] and is consistent with the above observations. Thus Eq. (3.333) with $p = 1$ provides a function with a plausible interplay between longitudinal and transverse dynamics.

3.13.3 D-term

We have discussed so far only the first component of the two-component form of GPDs which can be reconstructed from a non-singular double distribution (3.223). The second component—the *D*-term—is entirely concentrated inside the central region $|x| \leq \eta$. Originally, it was inspired by the chiral quark-soliton model analysis and was parametrized as [143]

$$D(\alpha, \Delta^2 = 0) = (1 - \alpha^2) \sum_{n=0}^{\infty} d_n C_{2n+1}^{3/2}(\alpha), \quad (3.334)$$

where the expansion goes in odd powers of Gegenbauer polynomials due to the antisymmetry of the *D*-term, $D(-\alpha) = -D(\alpha)$. The first few parameters were found within the model [182, 9] as well as recently extracted from lattice simulations [157, 200]. For the lowest term, the results deduced from them are

$$d_0^{\chi\text{QSM}} = -4.0 \frac{1}{N_f}, \quad d_0^{\text{latt}} = d_0^u \approx d_0^d \approx -0.5, \quad (3.335)$$

where N_f is the number of active flavors. Both predictions are plagued by uncontrollable uncertainties. In the lattice case, the effect of disconnected diagrams was not calculated. However they are known to produce a sizable negative contribution [207]. Once the latter are properly taken into account the lattice result might approach the model calculation. For our subsequent estimates we choose an intermediate value $d_0 = -1.0$.

To account for the Δ^2 -dependence one can assume the simplistic form

$$D(\alpha, \Delta^2) = \left(1 - \frac{\Delta^2}{m_D^2}\right)^{-3} D(\alpha, \Delta^2 = 0), \quad (3.336)$$

with the mass scale $m_D^2 = 0.6\text{ GeV}^2$.

3.13.4 Nonfactorizable GPD ansätze

Now, we are in a position to give semi-realistic models for GPDs. The q -flavor double distribution will be decomposed into the valence and sea components, $f^q = f^{q,\text{val}} + f^{q,\text{sea}}$. Both of them are related to the non-forward quark distribution $f^q(\beta, \Delta^2)$ with a profile function π , as was discussed in Section 3.13.1,

$$f^{q,\text{val}}(\beta, \alpha, \Delta^2) = f^{q,\text{val}}(\beta, \Delta^2) \theta(\beta) \pi(|\beta|, \alpha; b_{\text{val}}), \quad (3.337)$$

$$f^{q,\text{sea}}(\beta, \alpha, \Delta^2) = (\bar{f}^q(\beta, \Delta^2) \theta(\beta) - \bar{f}^q(-\beta, \Delta^2) \theta(-\beta)) \pi(|\beta|, \alpha; b_{\text{sea}}), \quad (3.338)$$

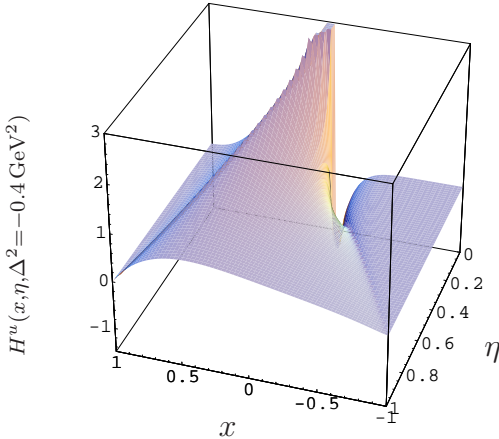


Figure 22: The u -quark GPD at $\Delta^2 = -0.4 \text{ GeV}^2$ as a function of the Feynman momentum x and skewness η . Positive (negative) values of the distribution correspond to quark (antiquarks) contributions to the GPD.

where at $\Delta^2 = 0$ the function $f^q(\beta, \Delta^2 = 0)$ reduces to the conventional parton densities.

Below we give separately the parametrization for the unpolarized and polarized non-forward parton distributions. They have to be plugged into Eq. (3.337) and then used to reconstruct GPDs by means of Eq. (3.211).

- Unpolarized GPDs. In our model we use the GRV leading order quark distributions [82] with discarded flavor asymmetry of the sea. Then the nonforward distributions read

$$\begin{aligned} f^{u,\text{val}}(\beta, \Delta^2) &= 1.239\beta^{-\alpha_v - \alpha'_v(1-\beta)^{1/2}\Delta^2} \left(1 - 1.8\sqrt{\beta} + 9.5\beta\right) (1-\beta)^{2.72}, \\ f^{d,\text{val}}(\beta, \Delta^2) &= 0.761\beta^{-\alpha_v - \alpha'_v(1-\beta)^{1/2}\Delta^2} \left(1 - 1.8\sqrt{\beta} + 9.5\beta\right) (1-\beta)^{3.62}, \\ \bar{f}^u(\beta, \Delta^2) &= \bar{f}^d(\beta, \Delta^2) = 0.76\beta^{-\alpha_s - \alpha'_s(1-\beta)^{3/2}\Delta^2} \left(1 - 3.6\sqrt{\beta} + 7.8\beta\right) (1-\beta)^{9.1}. \end{aligned} \quad (3.339)$$

They are assumed to be defined at the same renormalization scale as the forward quark distributions used for their construction, i.e., $\mu_{\text{LO}}^2 = 0.26 \text{ GeV}^2$. These models closely reproduce the quark form factors with the dipole parametrization of the proton and neutron Sachs form factors in the low $|\Delta^2| < 3 \text{ GeV}^2$ region. The Regge intercepts and slope parameters are taken to be

$$\begin{aligned} \alpha_v &= 0.52, & \alpha'_v &= 1.1 \text{ GeV}^{-2}, \\ \alpha_s &= 0.85, & \alpha'_s &= 0.3 \text{ GeV}^{-2}. \end{aligned} \quad (3.340)$$

The Regge parameters for the valence quarks are numerically close to those of the ρ -reggeons. Since the sea quarks are generated by the gluon radiation, their Regge parameters are analogous to that of the pomeron. We use $p = 1/2$ exponentials instead of $p = 1$ dictated by the Drell-Yan relation, since this value fits better the form factor at small and moderate Δ^2 . For $p = 1$, one can get a reasonable fit at moderate Δ^2 with $\alpha'_u = 1.6 \text{ GeV}^2$. For the α -profile of the DDs we use in our estimates $b_{\text{val}} = b_{\text{sea}} = 1$, though for the sea-quark distribution this value is not a consequence of asymptotic considerations, rather $b_{\text{sea}} = 2$ is

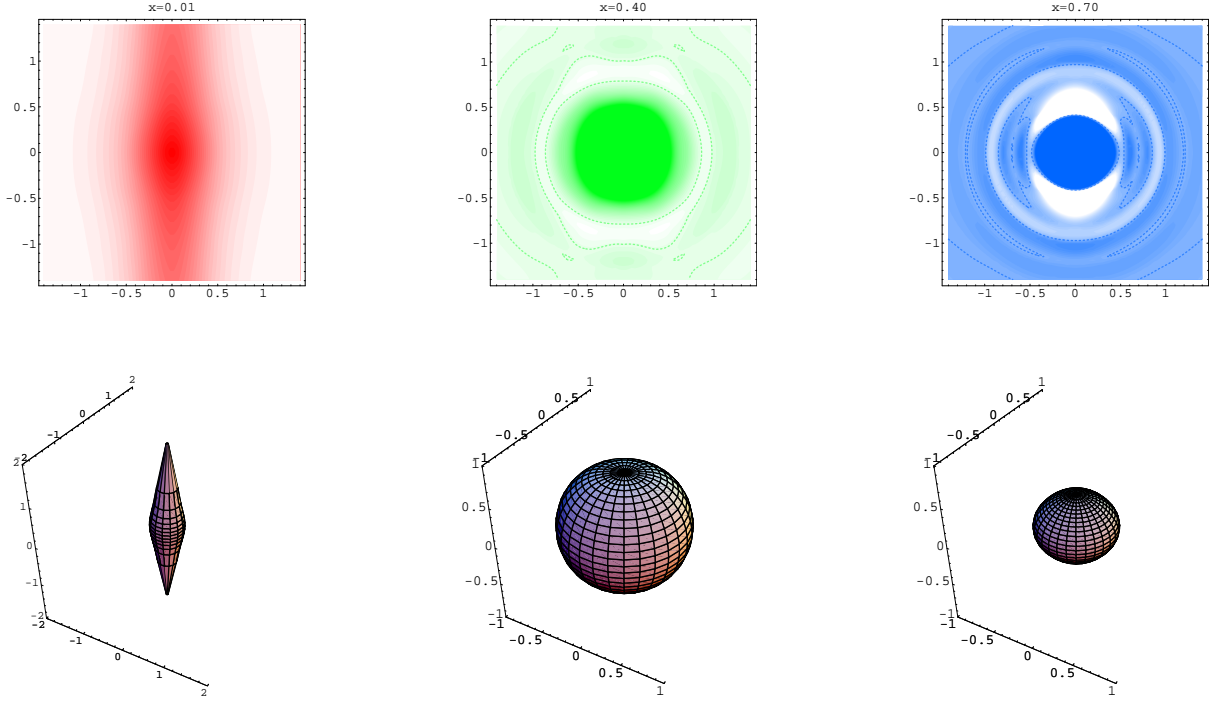


Figure 23: The u -quark Wigner distribution W^u at different values of the Feynman parameter for non-factorizable ansatz of generalized parton distributions (3.339). The vertical and horizontal axis corresponds to r^z and $|\mathbf{r}_\perp|$, respectively, measured in femtometers. The [dashed] contours separate regions of positive [darker areas] and negative [lighter areas] densities. Below each contour plot we presented the shape of three-dimensional isodensity contours [$W^u = \text{const}$].

a legitimate choice [10] (see Eqs. (136) and (255) there). The model of the u -quark GPD at $\Delta^2 = -0.4 \text{ GeV}^2$ is demonstrated in Fig. 22.

- Polarized GPDs. The model is quite analogous to the unpolarized case:

$$\Delta f^q(\beta, \Delta^2) = \eta_q A_q x^{a_q - \alpha'_q \Delta^2(1-\beta)} (1 - \beta)^{b_q} \left(1 + \gamma_q \beta + \rho_q \sqrt{\beta} \right). \quad (3.341)$$

The parameters are fixed by the GSA forward densities [83] at $\mu^2 = 4 \text{ GeV}^2$ in the $\Delta^2 = 0$ limit, and the slopes $\alpha'_u = 1.15 \text{ GeV}^{-2}$, $\alpha'_d = 1.0 \text{ GeV}^{-2}$ were chosen to fit the dipole form of the axial form factor at low $|\Delta^2| < 3 \text{ GeV}^2$ with the effective mass $m_A^2 = 0.9 \text{ GeV}^2$ for the valence GPD. For the sea-quark distribution, we take $\alpha'_s = 0.3 \text{ GeV}^{-2}$.

Let us emphasize that the models we have developed here serve solely an illustration purpose. More realistic GPDs have to be developed by means of combined fits to available data in different kinematical regions as was done in recent works [205, 415]. Presently, we address only quarks. The spatial distribution of gluons was studied in Refs. [208, 209].

3.14 Visualizing proton via Wigner distributions

Making use of the above models we can plot the phase-space quasi-probability distribution of partons inside the proton, following Ref. [41]. According to our earlier discussion, the Wigner func-

tion of a quark $W^q(x, \mathbf{r})$ is obtained from GPDs in the Breit frame through the three-dimensional Fourier transformation with respect to the three-momentum Δ (see Section 2.3):

$$W^q(x, \mathbf{r}) = \int \frac{d^3\Delta}{(2\pi)^3} e^{i\Delta \cdot \mathbf{r}} H^q \left(x, \Delta_z / \sqrt{\Delta^2 + 4M_N^2}, -\Delta^2 \right).$$

We consider the quark Wigner quasi-probabilities resulting from the parametrization for the GPDs given above. In Fig. 23 we show the up-quark Wigner distributions calculated from $H^u(x, \eta, \Delta^2)$ for a few values of the Feynman momentum $x = \{0.01, 0.4, 0.7\}$. The intensity of the plots indicates the magnitude of the positive density distribution. The lighter areas indicate negative values, which are divided by the level zero, shown by dashed contours. The plots exhibit significant dependence of the quark distribution on the longitudinal momentum fraction x . The image is rotationally symmetric in the transverse \mathbf{r}_\perp -plane. At small x , the distribution extends far beyond the nominal nucleon size along the longitudinal z direction. The physical explanation for this is that the position space uncertainty of the quarks is large when x is small, and therefore the quarks are de-localized along the longitudinal direction. This de-localization reflects the part of the nucleon wave function, and shows long-range correlations as verified in high-energy scattering. On the other hand, at larger x , the momentum along the z direction is of order of nucleon mass, and the quarks are localized to within $1/M_N$.

3.15 Limitations of GPDs as Wigner distributions

Let us analyze whether our interpretation of GPDs as Fourier transforms of Wigner distributions receives any limitations from relativity and quantum effects. To this end, consider the nucleon matrix element of the light-ray operator

$$\langle p_2 | \mathcal{O}^{qq}(-z^-, z^-) | p_1 \rangle.$$

Since we are interested in the Breit-frame interpretation of GPDs, we should impose restrictions on momenta involved, similar to the ones used in discussion of form factors, in order to avoid dangerous regions where relativistic and quantum effects will spoil the interpretation. We construct the same wave packet as in the analysis of the nucleon form factors in Section 2.2.2. This allows one to find a sequence of inequalities between the longitudinal Δ^z and transverse Δ_\perp resolution scales of the probe and typical momenta p^z , \mathbf{p}_\perp of the wave packet as in Eq. (2.22). A straightforward consideration in one-to-one correspondence with the one performed in Section 2.2.2 yields inequalities for the transverse momenta

$$1/R_N \ll |\Delta_\perp| \ll |\mathbf{p}_\perp| \ll M_N. \quad (3.342)$$

The consideration for longitudinal variables is nontrivial, since the probe is non-local in the light-like direction. Thus, the following three longitudinal distance scales are involved (see Fig. 24). The longitudinal position of partons r^z is set in the Breit frame by the skewness $r^z \sim 1/\Delta^z \sim 1/(\eta E)$ (see Eq. (2.80)). A typical longitudinal momentum in the wave packet sets its intrinsic fuzziness $\delta r^z \sim 1/p^z$. Finally, since the probe is non-local, we have an extra degree of freedom—the Ioffe time z^- . The latter is a variable Fourier conjugate to the the Feynman momentum $x = k^+/p^+$ (which has the meaning of the parton momentum relative to that of the parent hadron in the infinite momentum frame as was established in Section 2.2.7). The non-locality grows with decreasing parton momentum fraction x , $z^- \sim 1/(xE)$. This correlation length is set by the distance which

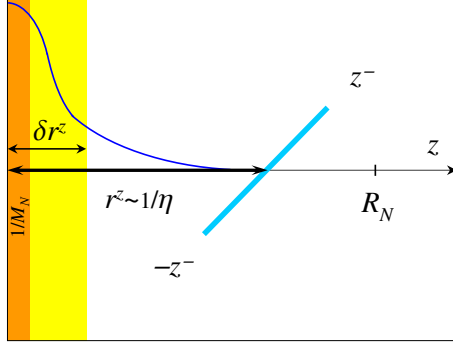


Figure 24: Distance scales for the Wigner distribution in the Breit frame. The Compton wavelength and the radius of the proton are $1/M_N$ and R_N , respectively. The partons are probed at longitudinal distances r^z in the proton localized by means of a wave packet of the size δr^z with a probe whose non-locality is z^- .

the quark-antiquark pair, originating from the decay of the probe, propagates in the Breit frame from the space-time point of its creation to recombination back into the off-shell gauge boson. So z^- can exceed the nucleon size.

First, we have to analyze consequences of the uncertainty on the longitudinal localization of the proton state. Obviously, to be insensitive to the structure of the residual wave packet itself one has to set the condition that its fuzziness δr^z be much smaller than the resolving distances r^z within the hadron, $\delta r^z \ll r^z$. This translates into the condition in the reciprocal (momentum) space

$$|\Delta^z| \ll |p^z| \ll M_N, \quad (3.343)$$

with the right-most inequality being the limitation due to the finite Compton wavelength of the nucleon. Next, the non-locality of the probe in the longitudinal direction z^- cannot be larger than the distances r^z it scans,

$$|z^-| \ll r^z. \quad (3.344)$$

When one makes the Fourier transformation of the above matrix element with respect to the Ioffe time, one has to impose this restriction on the light-cone distances. This immediately implies that the Feynman momentum x probed in the proton cannot be smaller than $1/r^z$, i.e., $x \gg 1/(Er^z) \sim \eta$. If this condition is omitted, there will be a quantum uncertainty arising from the fuzziness of the picture for very large Ioffe times. This consideration results in a limitation on the static picture of GPDs (in the Breit frame) as Fourier transforms of Wigner distributions. GPDs admit this interpretation only in a limited region of the parameter space, as we have just established.

The unpolarized nucleon GPD in the Breit frame is given by [117]

$$\frac{1}{2M_N} F^q(x, \eta, \Delta^2) = \left(H^q - \frac{\Delta^2}{4M_N^2} E^q \right) (x, \eta, \Delta^2) + \frac{i}{M_N} [\Delta \times \mathbf{s}]^z (H^q + E^q) (x, \eta, \Delta^2), \quad (3.345)$$

where, for brevity, we set $w_2^* w_1 = 1$ and \mathbf{s} is defined as in Eq. (2.18). The physical content of the functions involved is revealed by examining their spin structure. The matrix element in Eq.

(3.345) demonstrates that the first term is independent of the proton spin, and is considered as the charge density

$$\rho(x, \mathbf{r}) = \int \frac{d^3\Delta}{(2\pi)^3} e^{i\Delta \cdot \mathbf{r}} \left(H - \frac{\Delta^2}{4M_N^2} E \right) (x, \eta, \Delta^2). \quad (3.346)$$

The second term depends on the proton spin and can be regarded as the third component of the vector current

$$j^z(x, \mathbf{r}) = \frac{i}{M_N} \int \frac{d^3\Delta}{(2\pi)^3} e^{i\Delta \cdot \mathbf{r}} [\Delta \times \mathbf{s}]^z (H + E) (x, \eta, \Delta^2). \quad (3.347)$$

The E -term generates a convection current due to the orbital angular momentum of massless quarks and vanishes when all quarks are in the s -orbit. The physics in separating F^q into ρ and j^z can be seen from the Dirac matrix γ^+ selected by the high-energy probes, which is a combination of time and space components. Because the current distribution has no spherical symmetry, the quark density seen in the infinite momentum frame, $\rho + j^z$, is deformed in the impact parameter space [151]. This is the kinematic effect of Lorentz transformations.

The Wigner distributions introduced above allow one to calculate the single-quark properties using the classical concept of average in the phase space. If one integrates over the momentum fraction x in $\rho(x, \mathbf{r})$, one recovers the spherical charge distribution. On the other hand, integrating over x in $j^z(x, \mathbf{r})$ one obtains the electric current distribution. In the latter case, if the integral is weighted with x , one gets the mechanical momentum density.

3.16 Transition GPDs

So far we have discussed GPDs involving the same hadron in the initial and final state. There is, however, a number of reactions which change the flavor of partons during the hard scattering. This could be either due to weak interactions, or if the original quark goes into a flavored meson, so that a quark with a different flavor joins the outgoing baryon in the final state. In the present section, we address these quantities and also show how one can relate them to the diagonal ones making use of some approximations. Obviously, since there is a flavor exchange between the incoming and outgoing baryons, there are no gluonic GPDs associated with these transitions.

Contrary to the diagonal case, there are no positivity constraints on the transition GPDs, since they do not become densities in any limit, like the forward limit for the diagonal GPDs. The transition GPDs rather describe the correlations between the wave function of the resonance and that of the nucleon. Throughout our discussion, we will assume that resonances are stable hadrons, and thus the corresponding GPDs do not contain the final-state strong-interaction phases. An alternative description would be in terms of the hadrons actually observed in the detector. The relevant GPD

$$\langle H_1 H_2 | \mathcal{O}^{qq'} | p \rangle,$$

describes the transition from the initial state nucleon (say, the proton p) to the final state hadrons H_1, H_2 with a given invariant mass close to that of the resonance H that decays into them. In this case, the imaginary phases have to be introduced.

3.16.1 Baryon octet to octet transitions

Let us start with discussion of matrix elements describing transitions between hadrons within the baryon octet. They are very interesting phenomenologically since they involve matrix elements of

operators containing the strange quark. For instance, matrix elements of the even and odd parity light-ray operators for the transition $p \rightarrow \Sigma^+$ can be decomposed as

$$\begin{aligned}\langle \Sigma^+(p_2) | \mathcal{O}^{sd}(-z^-, z^-) | p(p_1) \rangle &= \int_{-1}^1 dx e^{-ixp^+z^-} \{ h^+ H_{p\Sigma^+}(x, \eta, \Delta^2) + e^+ E_{p\Sigma^+}(x, \eta, \Delta^2) \}, \\ \langle \Sigma^+(p_2) | \tilde{\mathcal{O}}^{sd}(-z^-, z^-) | p(p_1) \rangle &= \int_{-1}^1 dx e^{-ixp^+z^-} \{ \tilde{h}^+ \tilde{H}_{p\Sigma^+}(x, \eta, \Delta^2) + \tilde{e}^+ \tilde{E}_{p\Sigma^+}(x, \eta, \Delta^2) \},\end{aligned}\quad (3.348)$$

where the flavor structure of the operators should be understood as $\mathcal{O}^{sd} = \bar{s}\gamma^+d$, etc. The first moments of these functions are related to the vector and axial transition form factors within the baryon octet [9]

$$\int_{-1}^1 dx H_{p\Sigma^+}(x, \eta, \Delta^2) = F_1^{p\Sigma^+}(\Delta^2) - \eta F_3^{p\Sigma^+}(\Delta^2), \quad (3.349)$$

$$\int_{-1}^1 dx E_{p\Sigma^+}(x, \eta, \Delta^2) = F_2^{p\Sigma^+}(\Delta^2) + \eta F_3^{p\Sigma^+}(\Delta^2), \quad (3.350)$$

$$\int_{-1}^1 dx \tilde{H}_{p\Sigma^+}(x, \eta, \Delta^2) = G_A^{p\Sigma^+}(\Delta^2) + \frac{M_{\Sigma^+} - M_N}{M_{\Sigma^+} + M_N} G_{\text{eff}}^{p\Sigma^+}(\Delta^2), \quad (3.351)$$

$$\int_{-1}^1 dx \tilde{E}_{p\Sigma^+}(x, \eta, \Delta^2) = G_P^{p\Sigma^+}(\Delta^2) + \frac{1}{\eta} G_{\text{eff}}^{p\Sigma^+}(\Delta^2). \quad (3.352)$$

Compared to the parametrization of the matrix elements of the conserved vector (3.86) and axial currents (3.87), there are two extra form factors, the weak electricity term F_3 in the vector current case

$$\langle \Sigma^+(p_2) | \bar{s}\gamma^\mu d(0) | p(p_1) \rangle = h^\mu F_1^{p\Sigma^+}(\Delta^2) + e^\mu F_2^{p\Sigma^+}(\Delta^2) - \frac{b\Delta^\mu}{M_{\Sigma^+} + M_N} F_3^{p\Sigma^+}(\Delta^2), \quad (3.353)$$

and the effective pseudoscalar term G_{eff} in the axial one,

$$\langle \Sigma^+(p_2) | \bar{s}\gamma^\mu \gamma^5 d(0) | p(p_1) \rangle = \tilde{h}^\mu G_A^{p\Sigma^+}(\Delta^2) + \tilde{e}^\mu G_P^{p\Sigma^+}(\Delta^2) + \frac{\tilde{t}^{\nu\mu} \Delta_\nu}{M_{\Sigma^+} + M_N} G_{\text{eff}}^{p\Sigma^+}(\Delta^2). \quad (3.354)$$

The parametrization is given in terms of the same bilinears as before, however, with the outgoing wave function one corresponding to the hyperon. Both the F_3 and G_{eff} terms appear due to the violation of the exact flavor symmetry by the non-zero strange quark mass. They can be safely neglected otherwise, of course, with a very high confidence for the strangeness-free transitions.

Now we are in a position to use the $SU(3)$ symmetry in order to relate all transition GPDs within the octet to those of the diagonal generalized quark distributions in the proton. The Lagrangian of the octet baryon coupling has been given before in Eq. (3.139). The only replacement we have to make there is to treat M^a_b as an octet of non-local light-ray quark operators,

$$M^{q'}_q = \mathcal{O}^{qq'}(-z^-, z^-) - \frac{1}{3} \delta^{qq'} \sum_{q''} \mathcal{O}^{q''q''}(-z^-, z^-), \quad (3.355)$$

and similarly for the odd parity and maximal-helicity operators—the Dirac structure is irrelevant. By the same token as in Section 3.6.1, we can read off the strength of interaction in terms of

the “constants” D and F , see Eq. (3.142). Removing them from the resulting relations, we can re-express all the transition GPDs in terms of the q -flavor quark distribution in the proton [9]

$$\begin{aligned} H_{pn} &= H^u - H^d, \\ H_{p\Lambda} &= -\frac{1}{\sqrt{6}} (2H^u - H^d - H^s), & H_{n\Lambda} &= -\frac{1}{\sqrt{6}} (2H^d - H^u - H^s), \\ H_{p\Sigma^+} &= -H^d + H^s, & H_{n\Sigma^+} &= -H^u + H^s, \\ H_{p\Sigma^0} &= -\frac{1}{\sqrt{2}} (H^d - H^s), & H_{n\Sigma^0} &= -\frac{1}{\sqrt{2}} (H^u - H^s). \end{aligned} \quad (3.356)$$

The quark content of GPDs on the left-hand side of the equation are given by flavor-changing quark operators $\mathcal{O}^{q'q}$. Obviously, these are the same relations as those for the octet decay constants, addressed in Section 3.6. These relations are expected to hold to reasonable accuracy, except for the distributions \tilde{E} , where the presence of the psedoscalar-meson pole induces a strong violation of the flavor $SU(3)$ symmetry due to significant difference of the meson masses within the octet.

3.16.2 Baryon octet to decuplet transitions

The transition amplitudes between the nucleon and the Δ isobar have been under an intensive scrutiny for a long time because, among other things, they allowed to address the question of the nucleon and its first resonance “deformation”. The selection rules, for instance, for the electromagnetic decay $\Delta \rightarrow N\gamma^*$ allow, apart from the magnetic, also for the electric and the Coulomb quadrupole transitions. The latter two vanish in a naive models with spherical symmetry, hence the term. In this sense, the electric and Coulomb quadrupole form factors quantify the amount of the deformation and its dependence on the radial distance from the center-of-mass.

The “nucleon-to-delta” generalized parton distributions bring much more into quantifying the precise partonic dynamics of these transitions, describing their dependence with respect to a number of kinematical variables they depend upon. According to our analysis in Section 3.2.2, there are eight independent quark-helicity conserving transitions, hence, there will be eight independent quark GPDs. Let us define the quark matrix elements for, say, the transition $p \rightarrow \Delta^{++}$ and determine the rest by making use of the $SU(3)$ flavor symmetry, as was done in the previous section for transitions within the baryon octet. There are four GPDs for the even parity operators¹⁹

$$\langle \Delta^{++}(p_2) | \mathcal{O}^{ud}(-z^-, z^-) | p(p_1) \rangle = \int_{-1}^1 dx e^{-ixp^+z^-} \bar{u}_\nu(p_2) \left\{ \frac{\Delta^\mu n^\nu - \Delta^\nu n^\mu}{M_N} \left(\gamma_\mu G_1(x, \eta, \Delta^2) \right. \right. \\ \left. \left. + \frac{p_\mu}{M_N} G_2(x, \eta, \Delta^2) - \frac{\Delta_\mu}{M_N} G_3(x, \eta, \Delta^2) \right) + \frac{\Delta^+ \Delta^\nu}{M_N^2} G_4(x, \eta, \Delta^2) \right\} \gamma^5 u(p_1), \quad (3.357)$$

and four for the odd parity case

$$\langle \Delta^{++}(p_2) | \tilde{\mathcal{O}}^{ud}(-z^-, z^-) | p(p_1) \rangle = \int_{-1}^1 dx e^{-ixp^+z^-} \bar{u}_\nu(p_2) \left\{ \frac{\Delta^\mu n^\nu - \Delta^\nu n^\mu}{M_N} \left(\gamma_\mu \tilde{G}_1(x, \eta, \Delta^2) \right. \right. \\ \left. \left. + \frac{p_\mu}{M_N} \tilde{G}_2(x, \eta, \Delta^2) \right) + n^\nu \tilde{G}_3(x, \eta, \Delta^2) + \frac{\Delta^+ \Delta^\nu}{M_N^2} \tilde{G}_4(x, \eta, \Delta^2) \right\} u(p_1). \quad (3.358)$$

¹⁹Notice that our parametrization differs from the one in Ref. [9] in the number of independent GPDs—we have more by one in the parity-even operator matrix element to match the number of helicity amplitudes involved in the transition—as well the basis of tensor structures used in the decomposition.

Here, u^μ is the Rarita-Schwinger spinor, whose properties are summarized in Appendix A.4. The γ^5 matrix was added to match the negative parity of the Δ^{++} . In the local limit, this parametrization reduces

$$\int_{-1}^1 dx G_i(x, \eta, \Delta^2) = G_i(\Delta^2), \quad \int_{-1}^1 dx \tilde{G}_i(x, \eta, \Delta^2) = \tilde{G}_i(\Delta^2), \quad (3.359)$$

to the $p \rightarrow \Delta^{++}$ transition form factors [210, 211, 212],

$$\langle \Delta^{++}(p_2) | \bar{u} \gamma^\mu d(0) | p(p_1) \rangle = u_\nu(p_2) \left\{ \frac{\Delta^\rho g^{\mu\nu} - \Delta^\nu g^{\mu\rho}}{M_N} \left(\gamma_\rho G_1(\Delta^2) + \frac{p_\rho}{M_N} G_2(\Delta^2) \right. \right. \\ \left. \left. - \frac{\Delta_\rho}{M_N} G_3(\Delta^2) \right) + \frac{\Delta^\mu \Delta^\nu}{M_N^2} G_4(\Delta^2) \right\} \gamma^5 u(p_1), \quad (3.360)$$

$$\langle \Delta^{++}(p_2) | \bar{u} \gamma^\mu \gamma^5 d(0) | p(p_1) \rangle = u_\nu(p_2) \left\{ \frac{\Delta^\rho g^{\mu\nu} - \Delta^\nu g^{\mu\rho}}{M_N} \left(\gamma_\rho \tilde{G}_1(\Delta^2) + \frac{p_\rho}{M_N} \tilde{G}_2(\Delta^2) \right) \right. \\ \left. + g^{\mu\nu} \tilde{G}_3(\Delta^2) + \frac{\Delta^\mu \Delta^\nu}{M_N^2} \tilde{G}_4(\Delta^2) \right\} u(p_1).$$

The partial conservation of the vector and the axial currents implies that

$$G_4 \stackrel{\text{PCVC}}{\approx} 0, \quad \tilde{G}_4 \stackrel{\text{PCAC}}{\approx} \frac{M_N^2}{m_\pi^2 - \Delta^2} \tilde{G}_3. \quad (3.361)$$

However, for the transitions in which s -quark is involved, the symmetry is broken by its mass. This breaking is fully responsible for nonvanishing $G_4^{(q \rightarrow s)} \sim m_s$.

In case of the electromagnetic current, the form factors G_i are related to the standard magnetic $M1$, electric $E2$ and Coulomb $C2$ form factors by the following set of relations [212]

$$6M_N M_\Delta (M_\Delta + M_N) \begin{pmatrix} G_{M1} \\ G_{E2} \\ G_{C2} \end{pmatrix} = \begin{pmatrix} (M_\Delta + M_N)(3M_\Delta + M_N) - \Delta^2 & 2(M_\Delta^2 - M_N^2) & 2\Delta^2 \\ M_\Delta^2 - M_N^2 + \Delta^2 & 2(M_\Delta^2 - M_N^2) & 2\Delta^2 \\ 4M_\Delta^2 & 2(3M_\Delta^2 + M_N^2 - \Delta^2) & 2(M_\Delta^2 - M_N^2 + \Delta^2) \end{pmatrix} \begin{pmatrix} M_N G_1 \\ M_\Delta G_2 \\ M_\Delta G_3 \end{pmatrix}. \quad (3.362)$$

Some of these transition form factors have been accessed by experimental measurements. A very concise and convenient compendium of their parametrizations can be found in Refs. [214, 215].

Let us now derive $SU(3)$ relations between transition GPDs. To this end, we have to write down the most general $SU(3)$ invariant couplings of the non-local light-ray operators (3.355) to octet and decuplet baryons. A simple symmetry argument shows that such a Lagragian contains one term since $\mathbf{8}$ appears only once in the product $\mathbf{8} \otimes \mathbf{10} = \mathbf{8} \oplus \mathbf{10} \oplus \mathbf{27} \oplus \mathbf{35}$. It reads

$$\mathcal{L}_{\mathbf{8} \rightarrow \mathbf{10}} = E (T^{abc} \varepsilon_{cde} M^d{}_a \bar{B}^e{}_b + \text{h.c.}), \quad (3.363)$$

where the components of the totally symmetric tensor T^{abc} describing the decuplet are identified

with the particles as follows (see [216, 217])

$$T^{ijk} : \quad \begin{matrix} & & & & \Delta^{++} & \frac{1}{\sqrt{3}}\Delta^+ & \frac{1}{\sqrt{3}}\Sigma^{*+} \\ & & & & \frac{1}{\sqrt{3}}\Delta^+ & \frac{1}{\sqrt{3}}\Delta^0 & \frac{1}{\sqrt{6}}\Sigma^{*0} \\ & & & & \frac{1}{\sqrt{3}}\Sigma^{*+} & \frac{1}{\sqrt{6}}\Sigma^{*0} & \frac{1}{\sqrt{3}}\Xi^{*0} \\ & & & & \frac{1}{\sqrt{3}}\Delta^+ & \frac{1}{\sqrt{3}}\Delta^0 & \frac{1}{\sqrt{6}}\Sigma^{*0} \\ & & & & \frac{1}{\sqrt{3}}\Delta^0 & \Delta^- & \frac{1}{\sqrt{3}}\Sigma^{*-} \\ & & & & \frac{1}{\sqrt{6}}\Sigma^{*0} & \frac{1}{\sqrt{3}}\Sigma^{*-} & \frac{1}{\sqrt{3}}\Xi^{*-} \\ & & & & \frac{1}{\sqrt{3}}\Sigma^{*+} & \frac{1}{\sqrt{6}}\Sigma^{*0} & \frac{1}{\sqrt{3}}\Xi^{*0} \\ & & & & \frac{1}{\sqrt{6}}\Sigma^{*0} & \frac{1}{\sqrt{3}}\Sigma^{*-} & \Omega \end{matrix} . \quad (3.364)$$

For instance, $T^{111} = \Delta^{++}$, $T^{122} = \frac{1}{\sqrt{3}}\Delta^0$, etc. Expanding the invariant Lagrangian in the component form, one finds for transitions involving the proton

$$\mathcal{L}_{8 \rightarrow 10} = E \left(\Delta^{++}\mathcal{O}^{ud} + \frac{1}{\sqrt{3}}\Sigma^{*+}\mathcal{O}^{sd} - \frac{1}{\sqrt{3}}\Delta^0\mathcal{O}^{du} - \frac{1}{\sqrt{6}}\Sigma^{*0}\mathcal{O}^{su} - \frac{1}{\sqrt{3}}\Delta^+(\mathcal{O}^{uu} - \mathcal{O}^{dd}) \right) \bar{p} + \text{h.c.} \quad (3.365)$$

Analogously, one finds terms with the neutron. As usual, the coefficients in front of different interaction terms encode the strength of the transitions. Following the same procedure as that outlined in Section 3.6.2, we find the following $SU(3)$ relations between matrix elements

$$\begin{aligned} \langle \Delta^{++} | \mathcal{O}^{ud} | p \rangle &= -\sqrt{3} \langle \Delta^0 | \mathcal{O}^{du} | p \rangle = -\frac{\sqrt{3}}{2} \langle \Delta^+ | \mathcal{O}^{uu} - \mathcal{O}^{dd} | p \rangle \\ &= -\sqrt{6} \langle \Sigma^{*0} | \mathcal{O}^{su} | p \rangle = \sqrt{3} \langle \Sigma^{*+} | \mathcal{O}^{sd} | p \rangle, \\ &= -\langle \Delta^- | \mathcal{O}^{du} | n \rangle = \sqrt{3} \langle \Delta^+ | \mathcal{O}^{ud} | n \rangle = -\frac{\sqrt{3}}{2} \langle \Delta^0 | \mathcal{O}^{uu} - \mathcal{O}^{dd} | n \rangle \\ &= \sqrt{6} \langle \Sigma^{*0} | \mathcal{O}^{sd} | n \rangle = -\sqrt{3} \langle \Sigma^{*-} | \mathcal{O}^{su} | n \rangle. \end{aligned} \quad (3.366)$$

These relations hold irrespective to all other quantum numbers assigned to bilocal quark operators, and they provide relations between GPDs. For instance, the $p \rightarrow \Delta^{++,+,0}$ transition GPDs obey the equations

$$G_{p\Delta^{++}}^{ud} = -\frac{\sqrt{3}}{2} G_{p\Delta^+}^{uu-dd} = -\sqrt{3} G_{p\Delta^0}^{du}. \quad (3.367)$$

Here, we did not display the index $i = 1, \dots, 4$ distinguishing different species of GPDs for a given transition. Instead, we exhibited their partonic flavor content and the hadronic transition involved.

3.16.3 Implications of the large- N_c for decuplet-octet transitions

It turns out that one can further reduce the GPDs for the $p \rightarrow \Delta^+$ transitions to the diagonal $p \rightarrow p$ GPDs. This can be done by using the multicolor limit, which proved to be extremely

fruitful phenomenologically over the last few decades since it captures many of the salient features of the baryon physics. In this limit, the mesons and baryons are described by interpolating fields

$$M = \sum_{i=1}^{N_c} \bar{\psi}_i \psi^i, \quad B = \varepsilon_{i_1 i_2 \dots i_{N_c}} \psi^{i_1} \psi^{i_2} \dots \psi^{i_{N_c}}.$$

Thus, a baryon is viewed as built from N_c quarks, so its mass grows linearly in the number of colors $M \sim N_c$, while the meson mass is of order N_c^0 . The meson decay constants $M \rightarrow \bar{\psi}\psi$ scale as $N_c^{1/2}$, while the triple-meson vertices vanish as $N_c^{-1/2}$. Therefore, the meson theory becomes weakly coupled at large N_c , and ultimately becomes free as $N_c \rightarrow \infty$, so that mesons become stable in the multicolor world, and this approach cannot be used for the description of the physical meson spectrum.

For baryons, the situation is quite the opposite. The meson-baryon-baryon coupling scales like $N_c^{1/2}$, so that the baryon theory becomes strongly coupled as N_c grows. There are a few ways for realization of the large- N_c limit for baryons. It is either the large- N_c quark model (or the contracted $SU(4)$, using the modern language) or the bosonic description in which the baryon arises as a topologically stable soliton of a mesonic field theory. The simplest version of the latter is the Skyrme model (see Appendix F). The nucleon and the delta isobar represent different rotational modes of the same object—chiral soliton. In the large- N_c limit, the Δ isobar is degenerate in mass with the nucleon, i.e., $M_\Delta - M_N \sim \mathcal{O}(N_c^{-1})$. A leading order prediction in $1/N_c$ is a genuine property of QCD rather than a consequence of model considerations, because the analysis of the leading large- N_c order contributions is purely kinematical. It relies on simple group theoretical arguments only: no dynamical assumptions have to be made.

Before we explain the main steps in the derivation of the large- N_c relations, let us make it clear under what circumstances such relations may be valid. GPDs depend on three independent kinematical variables, so let us see what constraints and conditions are imposed on them by taking the multicolor limit.

- Since the (incoming and outgoing) baryon is heavy, $M \sim \mathcal{O}(N_c)$, its four-momentum p_i^μ is dominated by its time component, and is of the same order as the mass. Next observation is that the sum of all parton momenta—the active and spectators—gives that of the parent hadron, $k + \sum_{\text{spectators}} k = p$. Then, because $p \sim \mathcal{O}(N_c)$, each of its N_c partons carries the momentum $k \sim \mathcal{O}(N_c^0)$. Hence, $x \equiv k^+ / p^+ \approx \sqrt{2}k^+ / M \sim \mathcal{O}(N_c^{-1})$.
- Since the baryons are considered as non-relativistic particles in the infinite-mass limit, there should be no significant recoil transferred to the outgoing particle. This suggests that the t -channel momentum $|\Delta^2| \ll M^2$, thus at least $\Delta^2 \sim \mathcal{O}(N_c^0)$.
- In the Breit frame, which is very suitable for discussing the non-relativistic reduction of relativistic expressions, there is no energy exchange between the incoming and outgoing hadrons, and the momentum transfer is three-dimensional. Thus, as we established earlier, the skewness in the heavy-baryon limit is $\eta = \Delta^z / (2M) \sim \mathcal{O}(N_c^{-1})$, and it is parametrically of the same order as the Feynman momentum fraction x .

The analysis shows [460], that the only unsuppressed matrix elements are mediated by scalar-isoscalar $\mathcal{O} = \sum_q \bar{\psi}_q \psi_q$ and vector-iso-vector $\mathcal{O}^{ai} \sim \bar{\psi}_{q'} \gamma^i \tau_{q'q}^a \psi_q$ operators in the spin-flavor basis, with the spin of the state equal to its isospin,

$$\langle S' = I', S'_3, I'_3 | \mathcal{O} | S = I, S_3, I_3 \rangle, \quad \langle S' = I', S'_3, I'_3 | \mathcal{O}^{ai} | S = I, S_3, I_3 \rangle. \quad (3.368)$$

Here the state of a particle is parametrized in terms of its spin, which equals to isospin, and their projections. The rest, i.e., scalar-isovector and vector-isoscalar, transitions are subleading in the large N_c counting.

Let us demonstrate how to relate GPDs for the proton-to-delta to the diagonal proton-to-proton transitions. As an example, we consider matrix elements of the odd parity quark operators. First, we need to understand what kind of nucleon-to-nucleon GPDs are matched into those for the nucleon-to-delta transitions. In order to do this, we perform the non-relativistic reduction of Dirac bilinears standing in front of the nucleon-nucleon GPDs. As we advocated before, this can be consistently done by going to the Breit frame first (see Section 2.2.2) and then taking the limit of the heavy baryon mass $M_N = M_\Delta \equiv M \gg \Delta^2$. As one can see from Eqs. (A.29), the resulting structures contain the spin Pauli matrix sandwiched between two Weyl spinors. Thus, all the structures will be of leading order in the multi-color limit, provided that one takes the isovector combination of quark operators

$$\tilde{\mathcal{O}}^{(3)} = \tilde{\mathcal{O}}^{uu} - \tilde{\mathcal{O}}^{dd}. \quad (3.369)$$

We will take the spin up states for incoming and outgoing nucleons. In this case the q -flavor quark operator matrix elements yields

$$\begin{aligned} \langle p_\uparrow(p_2) | \tilde{\mathcal{O}}^{qq}(-z^-, z^-) | p_\uparrow(p_2) \rangle &= \sqrt{2}M \int_{-1}^1 dx e^{-ixp^+z^-} \\ &\times \left\{ \tilde{H}^q(x, \eta, \Delta^2) - \frac{\Delta_z^2}{4M^2} \left(\tilde{E}^q(x, \eta, \Delta^2) + \frac{1}{2}\tilde{H}^q(x, \eta, \Delta^2) \right) \right\}, \end{aligned} \quad (3.370)$$

which has to be combined into the isovector combination (3.369). For the analogous proton-to-delta transition, using the Rarita-Schwinger spin-vector (see Appendix A.4) we find

$$\begin{aligned} \langle \Delta_\uparrow^+(p_2) | \tilde{\mathcal{O}}^{(3)}(-z^-, z^-) | p_\uparrow(p_1) \rangle &= \frac{2M}{\sqrt{3}} \int_{-1}^1 dx e^{-ixp^+z^-} \left\{ \frac{\Delta_z}{M} \left(\tilde{G}_1(x, \eta, \Delta^2) + \tilde{G}_2(x, \eta, \Delta^2) \right) \right. \\ &\left. + \tilde{G}_3(x, \eta, \Delta^2) - \frac{\Delta_z^2}{M^2} \tilde{G}_4(x, \eta, \Delta^2) \right\}, \end{aligned} \quad (3.371)$$

where we do not indicate the hadronic transition involved, as was done in the preceding section, $\tilde{G}_i = \tilde{G}_{i,p\Delta^+}^{uu-dd}$. Thus, we observe that the isovector combination of proton-to-proton functions $\tilde{H}^u - \tilde{H}^d$ is matched into \tilde{G}_3 , while the combination $(\tilde{E}^u - \tilde{E}^d) + \frac{1}{2}(\tilde{H}^u - \tilde{H}^d)$ into \tilde{G}_4 . Finally, we see that in the large- N_c limit

$$\tilde{G}_1 = -\tilde{G}_2. \quad (3.372)$$

According to the large- N_c limit, the nucleon and the delta-isobar are eigenstates of the same object, the chiral soliton. In terms of the matrix elements of the quark operators, we have the relation

$$\sqrt{2}\langle p_\uparrow | \tilde{\mathcal{O}}^{(3)} | p_\uparrow \rangle = \langle \Delta_\uparrow^+ | \tilde{\mathcal{O}}^{(3)} | p_\uparrow \rangle. \quad (3.373)$$

Substituting Eqs. (3.370) and (3.371) into this relation and equating the coefficients in front of different powers of the momentum transfer Δ_z , we ultimately find

$$\tilde{G}_3 = \sqrt{3} \left(\tilde{H}^u - \tilde{H}^d \right), \quad (3.374)$$

$$\tilde{G}_4 = \frac{\sqrt{3}}{4} \left\{ \left(\tilde{E}^u - \tilde{E}^d \right) + \frac{1}{2} \left(\tilde{H}^u - \tilde{H}^d \right) \right\}. \quad (3.375)$$

Analogous considerations apply to the vector operators. For the proton-to-proton matrix element, the non-relativistic reduction results in

$$\langle p_\downarrow(p_2) | \mathcal{O}^{qq}(-z^-, z^-) | p_\uparrow(p_1) \rangle = -\frac{\Delta}{\sqrt{2}} \int_{-1}^1 dx e^{-ixp^+z^-} (H^q(x, \eta, \Delta^2) + E^q(x, \eta, \Delta^2)) , \quad (3.376)$$

while for the transition to the delta isobar we have

$$\langle \Delta_\downarrow^+(p_2) | \mathcal{O}^{(3)}(-z^-, z^-) | p_\uparrow(p_1) \rangle = -\frac{\Delta}{\sqrt{3}} \int_{-1}^1 dx e^{-ixp^+z^-} G_1(x, \eta, \Delta^2) , \quad (3.377)$$

where we kept only the leading contribution that matches into the leading contribution in the diagonal transition. Thus, one gets

$$G_1 = \sqrt{3} (H^u - H^d) + \sqrt{3} (E^u - E^d) . \quad (3.378)$$

The relations (3.374) – (3.378) relate the “unknown” $p \rightarrow \Delta^+$ to “known” $p \rightarrow p$ GPDs. Using $SU(3)$ relations of the previous section, one relates all other $\mathbf{8} \rightarrow \mathbf{10}$ matrix elements to those of the flavor-diagonal proton transitions.

The relation (3.378) correctly reproduces the known large- N_c prediction between the isovector combination of the proton and neutron magnetic moments,

$$\int_{-1}^1 dx (H^u - H^d + E^u - E^d)(x, \eta, \Delta^2 = 0) = \mu_p - \mu_n ,$$

and the $p \rightarrow \Delta^+$ transition magnetic moment $\mu_{\Delta^+ p}$. The latter is determined by the zero-recoil limit of the magnetic form factor associated with the matrix element of the electromagnetic current G_{M1}^{em} . This electromagnetic form factor is related the first moment of the isovector GPD for the same transition $p \rightarrow \Delta^+$ via the equation

$$\int_{-1}^1 dx G_1(x, \eta, \Delta^2 = 0) = 2G_1^{\text{em}}(\Delta^2 = 0) = 3G_{M1}^{\text{em}}(\Delta^2 = 0) \equiv \sqrt{6}\mu_{\Delta^+ p} ,$$

where in the first equality, we have used Eq. (F.8), while in the second, the large-mass approximation of Eq. (3.362) for the $p \rightarrow \Delta^+$ electromagnetic form factors.

One can establish more precise scaling rules for the GPDs making use of known results for large- N_c scaling of nucleon form factors [218, 219, 220], and also the parametric dependence of the kinematical variables on the number of colors, as discussed above. As a result, one arrives at the following set of scaling rules for the isosinglet [9]

$$\begin{aligned} H^u + H^d &\sim \mathcal{O}(N_c^2) , & E^u + E^d &\sim \mathcal{O}(N_c^2) , \\ \tilde{H}^u + \tilde{H}^d &\sim \mathcal{O}(N_c) , & \tilde{E}^u + \tilde{E}^d &\sim \mathcal{O}(N_c^3) , \end{aligned} \quad (3.379)$$

and isovector combinations

$$\begin{aligned} H^u - H^d &\sim \mathcal{O}(N_c^2) , & E^u - E^d &\sim \mathcal{O}(N_c^3) , \\ \tilde{H}^u - \tilde{H}^d &\sim \mathcal{O}(N_c) , & \tilde{E}^u - \tilde{E}^d &\sim \mathcal{O}(N_c^4) . \end{aligned} \quad (3.380)$$

These relation then allow to neglect the isovector combinations of \tilde{H} and H GPDs compared to those of \tilde{E} and E in Eqs. (3.374) and (3.378), respectively.

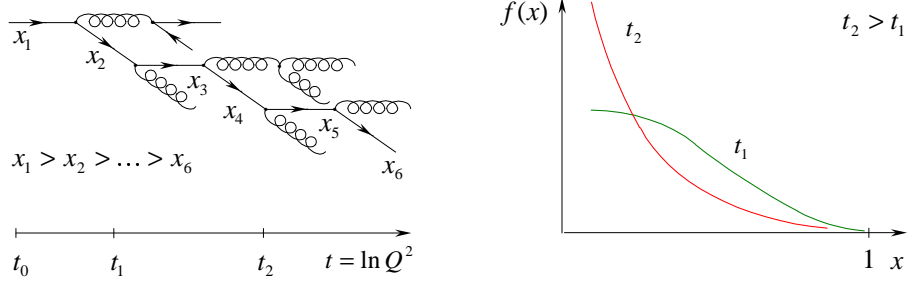


Figure 25: Multiple emission of partons (left) from the active quark diminishes its momentum via redistribution between the particles it spawns. This shower decreases its momentum when measured at later and later “times” $t = \ln Q^2$ and results in scaling violation in parton distributions.

4 Evolution equations

Having discussed nonperturbative characteristics of GPDs, we turn to the exploration of their perturbative properties. Recall, that during a deep-inelastic scattering event, the virtual photon of high virtuality Q^2 exchanged between the lepton and the proton acts as an almost local probe which, due to the uncertainty principle, selects distances inversely proportional to its virtuality $|\delta z_\perp| \sim 1/Q$. The variation in the resolution scale changes the granularity of the observed picture, or put it into the current context, the density of the parton number $q(x)$ for a given momentum fraction x . Suppose that the hard probe of a certain wavelength can resolve a parton having momentum $x p^\mu$. By refining the probe’s resolution, the same parton will be seen as a system of several partons, each carrying a smaller momentum fraction $x_i < x$ due to the momentum conservation $x = \sum_i x_i$. Thus, the parton distribution $q(x)$ depends on the virtuality of the current $q(x) \rightarrow q(x, Q^2)$ and, as a result, the Bjorken scaling is violated.

The qualitative description outlined above can be put in a rigorous theoretical framework. In QCD, like in any theory with a dimensionless coupling constant, the scaling violation is logarithmic and, due to asymptotic freedom, can be computed to arbitrary accuracy within perturbation theory, the limit being set only by the technical ability to actually perform the computation.

The general features of the QCD evolution can be understood in the following way. An active quark can emit a gluon (or several gluons) before the actual interaction with the photon has occurred, as illustrated on the left drawing in Fig. 25. When it radiates a gluon, the quark loses a portion of its original momentum. Though the loss can be small for each particular event, the quark, being a relativistically moving particle tends to emit more gluons. The bremsstrahlung of many gluons drifts the quark momentum into the low- x region. Since the gluons, in their turn, can dissociate into quark-antiquark pairs, there is a proliferation of quarks with small momentum fractions and, correspondingly, a decrease of the parton density in the large- x domain. Thus, the probability to find a quark with a small momentum fraction is higher at larger Q^2 , as shown on the right part of Fig. 25. Therefore, one sees more and more quarks (or gluons) in the cloud forming the parent “fat” quark.

The physical picture behind the evolution of generalized parton distributions is more involved. As we established in previous sections, in different regions of the longitudinal momentum of the annihilated and created partons, these functions resemble either parton densities or distribution amplitudes. The scaling violation in parton distributions considered as an example above is espe-

cially transparent and intuitive since one is dealing with probabilities. The distribution amplitudes do not have a classical interpretation, and the evolution of DAs reflects their quantum nature. We will discuss the qualitative features of the evolution of GPDs later in this chapter. Now we will concentrate on the description of several calculational frameworks which allow one to quantify the phenomenon.

4.1 Divergences of perturbation theory and scale dependence

Formally, the scaling violation arises due to the unrestricted growth of the parton's transverse momentum in perturbation theory. This can be explicitly demonstrated by computing the probability of the soft gluon emission²⁰ from a quark. The amplitude in this kinematic region takes the form (see, e.g., [112])

$$i\mathcal{A}_{q \rightarrow qg}(p) = \overrightarrow{p} \cdot \overrightarrow{p-k} / k = i \frac{\not{p} - \not{k}}{(p-k)^2} ig \not{v}(k) u(p) \simeq g \frac{p \cdot \varepsilon(k)}{p \cdot k} u(p), \quad (4.1)$$

where we used the fact that the quark momentum is light-like $p^\mu = p^- n^\mu$ with $p^- \sim Q$, so that $p \cdot k \gg k^2 \sim p^2$. The emission probability is then

$$\int \frac{d^3 \mathbf{k}}{2E_{\mathbf{k}}(2\pi)^3} |\mathcal{A}_{q \rightarrow qg}(p)|^2 = \frac{\alpha_s}{\pi^2} \bar{u}(p) u(p) \int \frac{dk^+}{k^+} \int \frac{d^2 \mathbf{k}_\perp}{\mathbf{k}_\perp^2}, \quad (4.2)$$

with $p^\mu = n^{*\mu}$. Both the longitudinal and transverse integrals here are logarithmically divergent. These divergences have different nature. The longitudinal k^+ integral can be converted into the integral over the fraction x , which cannot exceed one, so only the soft $x \rightarrow 0$ divergence remains. It does not induce the Q -dependence, hence this is not the phenomenon we are interested in now. It is rather an artifact of the soft-gluon approximation. The scaling violation is related to the structure of the transverse momentum integral. Its divergence at the lower limit, when $\mathbf{k}_\perp \rightarrow 0$, corresponds to situation when the final quark momentum ($p - k$) is collinear to the initial momentum p . The *collinear divergence* converts into the $\ln p^2$ (mass singularity) if no approximation is made [221]. The divergence on the upper limit is regulated by the kinematics of deep inelastic scattering which restricts \mathbf{k}_\perp at a value of order Q . Thus, for a one-loop diagram one obtains a $\ln Q^2/p^2$ contribution as a correction to the parton density, and the naive scaling is violated. For a diagram with n gluons, one can obtain the $(\ln Q^2/p^2)^n$ contribution. It comes from integration over the region where the successive $\mathbf{k}_{i\perp}$'s are strongly ordered. This means that the leading logarithm $(\ln Q^2/p^2)^n$ for an n -rung ladder diagram (see Fig. 26) comes from the region

$$\begin{aligned} |\mathbf{k}_{n\perp}| &\ll \dots \ll |\mathbf{k}_{2\perp}| \ll |\mathbf{k}_{1\perp}| \ll Q, \\ k_n^- &\ll \dots \ll k_2^- \ll k_1^-, \\ k_n^+ &\geq \dots \geq k_2^+ \geq k_1^+. \end{aligned} \quad (4.3)$$

The last line here reflects the decrease of the longitudinal quark momentum due to the gluon emission (cf. Fig. 25 left). The hierarchy in the second line is a consequence of the on-shellness of intermediate states $k_i^2 = 2k_i^+ k_i^- - \mathbf{k}_{i\perp}^2 = 0$ and the inequalities in the other two lines. If one is interested in contributions with non-leading powers of $\ln Q^2$ or higher-order non-logarithmic α_s

²⁰The gluon is soft when all four components of its momentum are much smaller than Q , i.e., $k^\mu \sim (\lambda, \lambda, \lambda, \lambda)$ and $\lambda \ll Q$. However, we can still apply perturbation theory if $\lambda \gg \Lambda_{\text{QCD}}$.

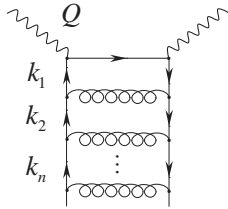


Figure 26: Ladder diagrams producing the dominant contribution in the leading logarithmic to the structure functions of deeply inelastic scattering and resulting into logarithmic scaling violation.

corrections, the strong ordering in \mathbf{k}_\perp is lifted. It is worth mentioning here that the resulting evolution equations in momentum space can be interpreted in terms of the kinetic equilibration of partons in the effective “time” $t \equiv \ln Q^2$ [222].

4.2 Factorization and evolution

An important observation is that the parameter Q in this calculation serves as an ultraviolet (UV) cut-off for the \mathbf{k}_\perp integral. This allows one to treat the Q^2 -dependence of parton densities as a particular case of the dependence on the UV regularization parameter μ^2 and to apply the renormalization group to organize the summation of the $\ln Q^2$ contributions. Once the renormalization group applicability is established, one can use the full power of this formalism and compute the evolution effects to a given order of perturbation theory.

Within the QCD factorization approach, the DIS structure functions are represented as the convolution

$$F_i(x_B, Q^2) = \int_{x_B}^1 \frac{dx}{x} C_i(x_B/x, Q^2/\mu^2) q(x; \mu^2) \quad (4.4)$$

of the coefficient function $C(x_B/x, Q^2/\mu^2)$ and the parton distributions $q(x; \mu^2)$ given by the matrix elements of composite operators. By construction, the factorization scale μ separates large virtualities from the small ones. For the coefficient function C determined by the large momentum integration, the scale μ serves as a cut-off at the lower limit of the \mathbf{k}_\perp integration, i.e., as the regularization parameter for the mass singularities. At the same time, it serves as the upper limit for the \mathbf{k}_\perp integration (i.e., as an UV cut-off) in matrix elements defining the parton distributions. The crucial property is the multiplicative renormalizability of the relevant composite operators expressed by the renormalization group equation

$$\frac{d}{d \ln \mu^2} q(x, \mu^2) = \int_x^1 \frac{dy}{y} P(x/y; \alpha_s(\mu^2)) q(y; \mu^2). \quad (4.5)$$

It is the well-known Dokshitzer-Gribov-Lipatov-Altarelli-Parisi (DGLAP) equation [222, 223, 224]. Since the structure functions $F_i(x_B, Q^2)$, being physical observables, do not depend on the arbitrary momentum separation scale μ^2

$$\frac{dF_i(x_B, Q^2)}{d \ln \mu^2} = 0, \quad (4.6)$$

the same evolution kernels $P(z; \alpha_s)$ appear in the evolution equations for the coefficient functions

$$\frac{d}{d \ln \mu^2} C_i(x; Q^2/\mu^2, \alpha_s(\mu^2)) = - \int_x^1 \frac{dy}{y} C_i(y; Q^2/\mu^2, \alpha_s(\mu^2)) P(x/y; \alpha_s(\mu^2)).$$

Since the coefficient functions are given by integration over large momenta, the evolution kernels are computable in perturbation theory. To get rid of complications due to gluons, one can consider a specific combination of the DIS cross sections where gluonic contributions drop out and which picks up a specific flavor combination of quarks, the so-called non-singlet parton distributions q_{NS} . It is given, for instance, by the difference of the scattering cross sections on the proton and neutron targets, the nonsinglet cross section $\sigma^p - \sigma^n \equiv \sigma^{\text{NS}}$. Then the evolution is governed by a single kernel $P_{\text{NS}}(x; \alpha_s(\mu^2))$. It is given by an infinite series expansion in α_s ,

$$P_{\text{NS}}(x; \alpha_s) = \sum_{n=0}^{\infty} \left(\frac{\alpha_s}{2\pi} \right)^{n+1} P_{\text{NS}}^{(n)}(x). \quad (4.7)$$

For the singlet quark distribution

$$q_s = \sum_q (q + \bar{q}), \quad (4.8)$$

the evolution is more complicated since the quarks can mix with gluons and, therefore, the evolution equation takes the form

$$\frac{d}{d \ln \mu^2} \begin{pmatrix} q_s \\ g \end{pmatrix}(x; \mu^2) = \int_x^1 \frac{dy}{y} \begin{pmatrix} P^{qq} & P^{qg} \\ P^{gq} & P^{gg} \end{pmatrix}(x/y; \alpha_s(\mu^2)) \begin{pmatrix} q_s \\ g \end{pmatrix}(y; \mu^2). \quad (4.9)$$

The splitting functions are defined as decay probabilities,

$$P^{ab}(x; \alpha_s(\mu^2)) = |A_{a \rightarrow bc}|^2, \quad (4.10)$$

having the perturbative expansion like in Eq. (4.7). The leading order amplitudes A contributing to one-loop DGLAP kernels are represented in Fig. 27 (left). The solution of the DGLAP evolution equations combined with higher order QCD radiative corrections allows to obtain a perfect description of experimental data for the unpolarized deeply inelastic cross section, shown in Fig. 27 (right).

4.3 Coordinate-space evolution equations

As we know, the generalized parton distributions are determined by off-forward matrix elements of bilocal operators living on the light cone. These are the same operators that define the forward parton distribution. As long as the separation of the field operators is neither zero $z^\mu = 0$ nor light-like $z^2 = 0$, the renormalization of the product $\Phi^*(0)\Phi(z)$ is trivially reduced to the familiar renormalization constants \mathcal{Z}_Φ of the fundamental field operators Φ . However, if $z^\mu = 0$ or $z^2 = 0$, additional divergences enter the game, since the product of (at least) two field operators located at the same space-time point (or on the light cone) produces an ill-defined quantity from the point of view of the theory of distributions, and the corresponding infinities have to be regularized and subtracted. This corresponds to the ultraviolet divergencies discussed above within the context of the momentum-space evolution equations.

Evolution equations for all “momentum-fraction” functions, i.e., parton densities, distribution amplitudes and generalized parton distributions, arise from the same set of renormalization group equations for the light-ray operators (3.10) and (3.20). The formalism was developed by several groups in early and mid eighties [226, 227, 228, 230].

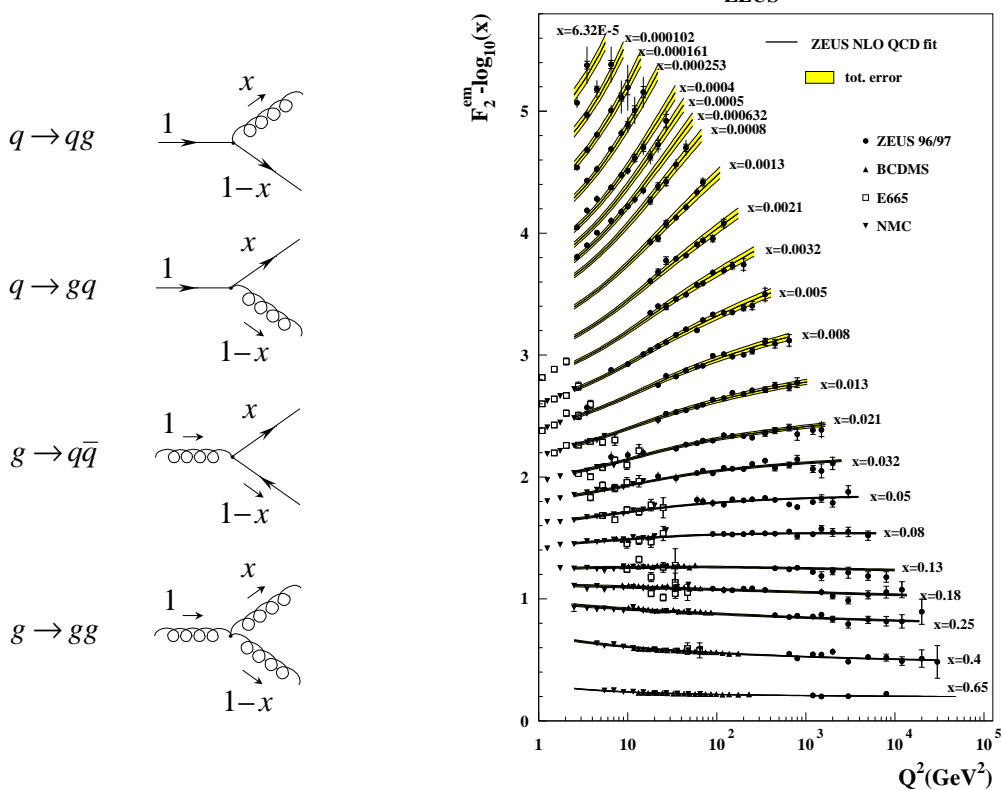


Figure 27: Elementary $a \rightarrow bc$ parton splitting amplitudes encountered at each step of the evolution (left) and a fit to experimental data [225] (right) implementing them (dressed with next-to-leading order perturbative corrections) in the evolution equation (4.9).

In the following we will discuss the flavor singlet case, where the quark and gluon operators mix with each other. For brevity we introduce the two dimensional vector

$$\mathcal{O}(z_1^-, z_2^-) \equiv \begin{pmatrix} \frac{1}{2} \sum_q (\mathcal{O}^{qq}(z_1^-, z_2^-) \mp \mathcal{O}^{qq}(z_2^-, z_1^-)) \\ \mathcal{O}^{gg}(z_1^-, z_2^-) \end{pmatrix}, \quad (4.11)$$

where the plus and minus signs stand for the axial $\tilde{\mathcal{O}}$ and vector channel \mathcal{O} , respectively. Note that due to the Bose symmetry, the gluon operator also has definite symmetry with respect to the interchange of $z_1^- \leftrightarrow z_2^-$, i.e., it is (anti)symmetric in the case of (axial)vector operator. The two-vector \mathcal{O} obeys the renormalization group equation

$$\frac{d}{d \ln \mu^2} \mathcal{O}(z_1^-, z_2^-) = \int_0^1 du \int_0^1 dv \mathcal{K}(u, v) \mathcal{O}(\bar{u}z_1^- + uz_2^-, vz_1^- + \bar{v}z_2^-), \quad (4.12)$$

(here and below $\bar{u} \equiv 1 - u$ and analogously for other variables) with the perturbative kernel having an expansion in perturbation series

$$\mathcal{K}(u, v) = \sum_{n=1}^{\infty} \left(\frac{\alpha_s}{2\pi} \right)^n \mathcal{K}_{(n)}(u, v). \quad (4.13)$$

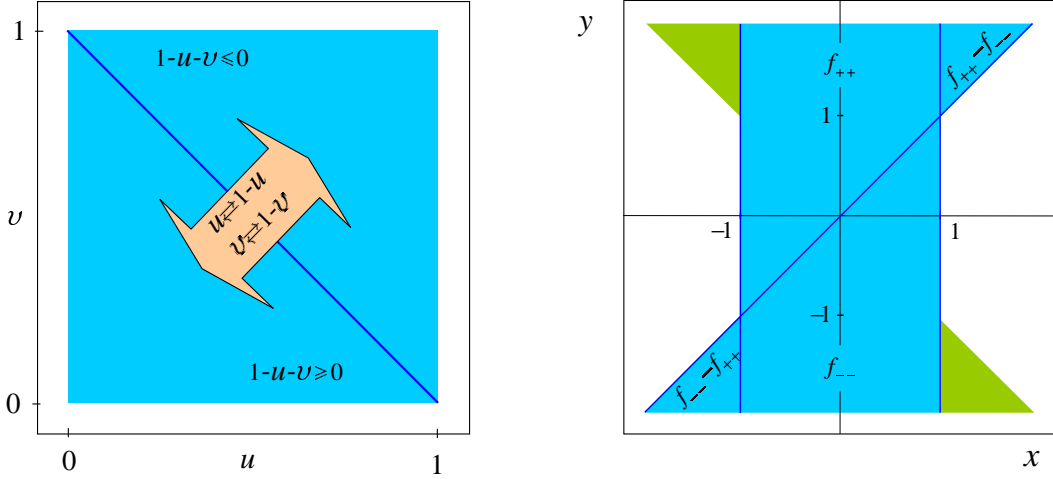


Figure 28: Support of the singlet anomalous dimensions \mathcal{K} in the light-cone position (a) and fraction (b) representation. In (b) we show the support of the momentum-space kernel which arises from $1 - u - v \geq 0$ of the light-cone position representation (blue) and from $1 - u - v \leq 0$ (left-top and right-bottom green corners). We use a short-hand notation in the graph $f_{\pm\pm} = f(\pm x, \pm y)$ with f defined by Eq. (4.40).

The evolution kernel is a two-by-two matrix

$$\mathcal{K}(u, v) = \begin{pmatrix} \mathcal{K}^{qq} & \frac{z_2^- - z_1^-}{i} \mathcal{K}^{qg} \\ \frac{i}{z_2^- - z_1^-} \mathcal{K}^{qq} & \mathcal{K}^{gg} \end{pmatrix}. \quad (4.14)$$

which explicitly depends on the light-cone position $z_2^- - z_1^-$ in the mixed channels.

Finally let us add that nonsinglet (or valence) combinations of even and odd parity operators,

$$\mathcal{O}_{\text{NS}}^{qq}(z_1^-, z_2^-) = \frac{1}{2} (\mathcal{O}^{qq}(z_1^-, z_2^-) + \mathcal{O}^{qq}(z_2^-, z_1^-)), \quad \widetilde{\mathcal{O}}_{\text{NS}}^{qq}(z_1^-, z_2^-) = \frac{1}{2} (\widetilde{\mathcal{O}}^{qq}(z_1^-, z_2^-) - \widetilde{\mathcal{O}}^{qq}(z_2^-, z_1^-)), \quad (4.15)$$

have an autonomous evolution, i.e., they do not mix with gluons.

4.3.1 Symmetry properties

The first important issue to understand is the anatomy of the evolution kernels for GPDs, which arise from the support property of the kernels \mathcal{K} . This problem can be solved by means of the α or Feynman-parameter representation of Green functions with a non-local operator insertion. It is sufficient to work in the light-cone gauge and to formally generalize the α -representation for the gluon propagator [1]. From these studies one can deduce the support of the kernels shown in Fig. 28 (a):

$$\mathcal{K}(u, v) \neq 0, \quad \text{for } 0 \leq u, v \leq 1; \quad 0, \quad \text{otherwise}. \quad (4.16)$$

Invariance under charge conjugation implies the following symmetry relation

$$\mathcal{K}(u, v) = \mathcal{K}(v, u). \quad (4.17)$$

It is also worth noting that the symmetry properties of the flavor singlet operators with respect to the interchange of their light cone arguments, i.e., $z_1^- \leftrightarrow z_2^-$, can be used to map the region $u + v \geq 1$ into $1 \geq u + v$ by the substitution $u \rightarrow 1 - v$ and $v \rightarrow 1 - u$. Here the region $1 \geq u + v$ corresponds in the forward case to quark-quark mixing which occurs already at leading order, while $u + v \geq 1$ appears due to a quark-antiquark interaction.

4.3.2 One-loop results

The calculations of the one-loop kernels are rather straightforward. A detailed exposition of the formalism on a simple example of the non-singlet quark operator $\mathcal{O}_{\text{NS}}^{qq}$ is given in Appendix G.5. The one-loop kernels have the support only in the lower triangle of the diagram 28, i.e.,

$$\mathcal{K}_{(0)}^{ab}(u, v) = \theta(1 - u - v) \kappa^{ab}(u, v). \quad (4.18)$$

To avoid displaying the step-function in all formulas, we assume below that $u + v \leq 1$, and merely list all the kernels for twist-two operators which we classified in Section 3.1.

- Even parity sector [229, 230, 3, 4, 6, 231]:

$$\mathcal{K}_{(0)}^{qq,V}(u, v) = C_F \left\{ 1 + [\bar{u}/u]_+ \delta(v) + [\bar{v}/v]_+ \delta(u) - \frac{1}{2} \delta(u) \delta(v) \right\}, \quad (4.19)$$

$$\mathcal{K}_{(0)}^{qg,V}(u, v) = 2T_F N_f \{ 1 - u - v + 4uv \}, \quad (4.20)$$

$$\mathcal{K}_{(0)}^{gg,V}(u, v) = C_F \{ \delta(v) \delta(u) + 2 \}, \quad (4.21)$$

$$\mathcal{K}_{(0)}^{gg,V}(u, v) = C_A \left\{ 4(1 - u - v + 3uv) + [\bar{u}^2/u]_+ \delta(v) + [\bar{v}^2/v]_+ \delta(u) \right\} - \frac{1}{2} (\beta_0 + 6C_A) \delta(u) \delta(v). \quad (4.22)$$

- Odd parity sector [232, 231]:

$$\mathcal{K}_{(0)}^{qg,A}(u, v) = C_F \left\{ 1 + [\bar{u}/u]_+ \delta(v) + [\bar{v}/v]_+ \delta(u) - \frac{1}{2} \delta(u) \delta(v) \right\}, \quad (4.23)$$

$$\mathcal{K}_{(0)}^{qg,A}(u, v) = 2T_F N_f \{ 1 - u - v \}, \quad (4.24)$$

$$\mathcal{K}_{(0)}^{gg,A}(u, v) = C_F \{ \delta(v) \delta(u) - 2 \}, \quad (4.25)$$

$$\mathcal{K}_{(0)}^{gg,A}(u, v) = C_A \left\{ 4(1 - u - v) + [\bar{u}^2/u]_+ \delta(v) + [\bar{v}^2/v]_+ \delta(u) \right\} - \frac{1}{2} (\beta_0 + 6C_A) \delta(u) \delta(v). \quad (4.26)$$

- Maximal-helicity sector [233, 74]:

$$\mathcal{K}_{(0)}^{qq,T}(u, v) = C_F \left\{ [\bar{v}/v]_+ \delta(u) + [\bar{u}/u]_+ \delta(v) - \frac{1}{2} \delta(u) \delta(v) \right\}, \quad (4.27)$$

$$\mathcal{K}_{(0)}^{gg,T}(u, v) = C_A \left\{ [\bar{u}^2/u]_+ \delta(v) + [\bar{v}^2/v]_+ \delta(u) \right\} - \frac{1}{2} (\beta_0 + 6C_A) \delta(u) \delta(v). \quad (4.28)$$

The plus-prescription here is defined as

$$\left[\frac{f(u)}{u} \right]_+ \equiv \frac{f(u)}{u} - \delta(u) \int_0^1 dv \frac{f(v)}{v}. \quad (4.29)$$

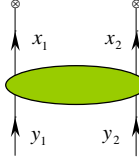


Figure 29: Momentum flow in evolution kernels.

4.4 Momentum-space evolution equations

Let us discuss the evolution equation for the target independent GPDs. In the singlet sector the quark and gluon GPDs can be organized into a two-dimensional vector in complete analogy to the light-ray operators discussed in the preceding section. Namely,

$$\mathbf{F}(x, \eta) \equiv \begin{pmatrix} \sum_q (F^q(x, \eta) \mp F^q(-x, \eta)) \\ \frac{1}{2} F^g(x, \eta) \end{pmatrix}, \quad (4.30)$$

with $-$ and $+$ signs standing for parity-even and -odd sector. Here the target-independent GPDs, entering this two-vector, are the Fourier transforms of the light-ray operators

$$\langle p_2 | \mathcal{O}^{qq}(z_1^-, z_2^-) | p_1 \rangle = p^+ \int_{-1}^1 dx e^{\frac{i}{2} p^+ ((\eta+x)z_1^- + (\eta-x)z_2^-)} F^q(x, \eta), \quad (4.31)$$

$$\langle p_2 | \mathcal{O}^{gg}(z_1^-, z_2^-) | p_1 \rangle = \frac{(p^+)^2}{4} \int_{-1}^1 dx e^{\frac{i}{2} p^+ ((\eta+x)z_1^- + (\eta-x)z_2^-)} F^g(x, \eta). \quad (4.32)$$

Identical relations hold for the maximal helicity GPDs which carry open Lorentz indices. The vector \mathbf{F} satisfies a matrix evolution equation

$$\frac{d}{d \ln \mu} \mathbf{F}(x, \eta) = - \int_{-1}^1 dy \mathbf{K} \left(\frac{\eta+x}{2}, \frac{\eta-x}{2} \middle| \frac{\eta+y}{2}, \frac{\eta-y}{2} \right) \mathbf{F}(y, \eta), \quad (4.33)$$

governed by the two-by-two matrix kernel

$$\mathbf{K}(x_1, x_2 | y_1, y_2) = \begin{pmatrix} K^{qq} & K^{qg} \\ K^{gq} & K^{gg} \end{pmatrix}, \quad (4.34)$$

having an infinite expansion in perturbative series

$$\mathbf{K}(x_1, x_2 | y_1, y_2) = \sum_{n=0}^{\infty} \left(\frac{\alpha_s}{2\pi} \right)^n \mathbf{K}_{(n)}(x_1, x_2 | y_1, y_2). \quad (4.35)$$

These kernels, via the Fourier transform incorporating Eqs. (4.31) – (4.32), are related to the light-cone position space kernels discussed in the preceding section [1, 4, 6]

$$\mathbf{K}(x_1, x_2 | y_1, y_2) = \int_0^1 du \int_0^1 dv \begin{pmatrix} -\mathcal{K}^{qq}(u, v) & \mathcal{K}^{qg}(u, v) \partial_{x_1} \\ \mathcal{K}^{gq}(u, v) \partial_{x_1}^{-1} & -\mathcal{K}^{gg}(u, v) \end{pmatrix} \delta(x_1 - y_1(1-u) - y_2v), \quad (4.36)$$

where we have used the momentum conservation condition $\sum_{i=1}^2(x_i - y_i) = 0$. The momentum fractions of incoming y_i and outgoing x_i legs can be expressed in terms of the symmetric variables as

$$x_1 = \frac{\eta + x}{2}, \quad x_2 = \frac{\eta - x}{2}, \quad y_1 = \frac{\eta + y}{2}, \quad y_2 = \frac{\eta - y}{2}.$$

We denote $\partial_{x_1} \equiv d/dx_1$ and $\partial_{x_1}^{-1} \equiv \int^{x_1} dx'_1$. The indefinite integration limits in the gq channel induces an ambiguity which, however, affects only the unphysical moments²¹ and has to be fixed “by hand”, e.g., by comparison of moments calculated in both representations. Note that this ambiguity implicitly appears also in the diagrammatic calculation of Feynman diagrams in the light-cone fraction representation and is responsible for different results available in the literature.

The representation (4.36) implies a simple scaling property of the \mathbf{K} kernel, due to which its components are in fact two-variable functions of the x/η and y/η ratios [1, 6],

$$\mathbf{K}\left(\frac{\eta + x}{2}, \frac{\eta - x}{2} \middle| \frac{\eta + y}{2}, \frac{\eta - y}{2}\right) = \frac{1}{\eta} \begin{pmatrix} k^{qq}\left(\frac{x}{\eta}, \frac{y}{\eta}\right) & \eta^{-1}k^{qg}\left(\frac{x}{\eta}, \frac{y}{\eta}\right) \\ \eta k^{gq}\left(\frac{x}{\eta}, \frac{y}{\eta}\right) & k^{gg}\left(\frac{x}{\eta}, \frac{y}{\eta}\right) \end{pmatrix}. \quad (4.37)$$

The invariance under the charge conjugation implies now the symmetry for the diagonal $k^{aa}(x, y) = k^{aa}(-x, -y)$ and off-diagonal ($a \neq b$) $k^{ab}(x, y) = -k^{ab}(-x, -y)$ elements. The connection between the parton-parton and parton-antiparton regions can be established by the substitution $y \rightarrow -y$. As we already explained for the light-cone position kernels, it is sufficient to consider the $u+v \leq 1$ part of the total support region $0 \leq u, v \leq 1$. The contribution that comes from the region $u+v \geq 1$ can be formally obtained from the first region by changing $y \rightarrow -y$. Thus, the support of the kernels extends into two additional regions in the upper-left and lower-right corners of the support diagram, see Fig. 28 (b). Then the integral representation (4.36) implies the support shown in Fig. 28 (b), or formally

$$k^{ab}(x, y) = \vartheta(x, y)f^{ab}(x, y) \pm \vartheta(-x, -y)f^{ab}(-x, -y), \quad (4.38)$$

where the $(-)$ + stands for (off-) diagonal entries. Here the step-function is

$$\vartheta(x, y) = \theta\left(\frac{y-x}{1+y}\right)\theta\left(\frac{1+x}{1+y}\right)\text{sign}(1+y) = \theta(y-x)\theta(1+x) - \theta(x-y)\theta(-1-x), \quad (4.39)$$

and f^{ab} are analytic functions related to integrals of the coordinate-space evolution kernels as

$$f^{aa}(x, y) = -\int_0^{\frac{1+x}{1+y}} dw \mathcal{K}^{aa}\left(\frac{1-x-(1-y)w}{2}, \frac{1+x-(1+y)w}{2}\right), \quad (4.40)$$

and analogously for off-diagonal elements with operators $-\partial_x$ and $-\partial_x^{-1}$ acting on the right-hand side of the equality for qg and gq kernels, respectively.

Looking at Fig. 28 one gets the impression that the whole kernel can be obtained from the region $|x|, |y| \leq 1$. Indeed, it was proved in [1] that the continuation is unique. For practical purposes, it is sufficient to replace the θ structure:

$$\theta(y-x)|_{|x|,|y|\leq 1} \rightarrow \vartheta(x, y). \quad (4.41)$$

Thus, the evolution kernels for GPDs can be considered as generalized exclusive kernels, addressed below, and their restoration from the given Efremov-Radyushkin-Brodsky-Lepage (ER-BL or exclusive) kernels is simple and unique. We will elaborate more on these issues in Section 4.4.5.

²¹ Those moments which vanish by symmetry reasons, i.e., j even (odd) in the singlet sector of the vector (axial) operators.

4.4.1 One-loop results

A very simple computation method to calculate these kernels at one-loop order is presented in Appendix G.6. It was originally suggested in Refs. [234, 63] and used there to compute all leading order off-forward evolution kernels. Recently they were recalculated by different means in a number of studies dedicated specifically to analyses of GPDs [5, 67, 235, 236]. The results for sectors with different quantum numbers are summarized below.

- Even-parity sector:

$$\begin{aligned}
K_{(0)}^{qq;V}(x_1, x_2 | y_1, y_2) &= C_F \left[\frac{x_1}{x_1 - y_1} \vartheta_{11}^0(x_1, x_1 - y_1) + \frac{x_2}{x_2 - y_2} \vartheta_{11}^0(x_2, x_2 - y_2) \right. \\
&\quad \left. + \vartheta_{111}^0(x_1, -x_2, x_1 - y_1) \right]_+, \\
K_{(0)}^{qg;V}(x_1, x_2 | y_1, y_2) &= 2T_F N_f \left[\vartheta_{112}^1(x_1, -x_2, x_1 - y_1) + 2 \frac{x_1 - y_1}{y_1 y_2} \vartheta_{111}^0(x_1, -x_2, x_1 - y_1) \right], \\
K_{(0)}^{gg;V}(x_1, x_2 | y_1, y_2) &= C_F \left[(y_1 - y_2) \vartheta_{111}^0(x_1, -x_2, x_1 - y_1) + x_1 x_2 \vartheta_{111}^1(x_1, -x_2, x_1 - y_1) \right], \\
K_{(0)}^{gg;V}(x_1, x_2 | y_1, y_2) &= C_A \left[\frac{x_1}{y_1} \left[\frac{x_1}{x_1 - y_1} \vartheta_{11}^0(x_1, x_1 - y_1) \right]_+ + \frac{x_2}{y_2} \left[\frac{x_2}{x_2 - y_2} \vartheta_{11}^0(x_2, x_2 - y_2) \right]_+ \right. \\
&\quad + 2 \frac{x_1 x_2 + y_1 y_2}{y_1 y_2} \vartheta_{111}^0(x_1, -x_2, x_1 - y_1) + 2 \frac{x_1 x_2}{y_1 y_2} \frac{x_1 y_1 + x_2 y_2}{(x_1 + x_2)^2} \vartheta_{11}^0(x_1, -x_2) \\
&\quad \left. + \left(\frac{1}{2} \frac{\beta_0}{C_A} + 2 \right) \delta(x_1 - y_1) \right].
\end{aligned} \tag{4.42}$$

- Odd-parity sector:

$$\begin{aligned}
K_{(0)}^{qq;A}(x_1, x_2 | y_1, y_2) &= K_{(0)}^{qq;V}(x_1, x_2 | y_1, y_2), \\
K_{(0)}^{qg;A}(x_1, x_2 | y_1, y_2) &= 2T_F N_f \vartheta_{112}^1(x_1, -x_2, x_1 - y_1), \\
K_{(0)}^{gg;A}(x_1, x_2 | y_1, y_2) &= C_F \left[(x_1 - x_2) \vartheta_{111}^0(x_1, -x_2, x_1 - y_1) + x_1 x_2 \vartheta_{111}^1(x_1, -x_2, x_1 - y_1) \right], \\
K_{(0)}^{gg;A}(x_1, x_2 | y_1, y_2) &= C_A \left[\frac{x_1}{y_1} \left[\frac{x_1}{x_1 - y_1} \vartheta_{11}^0(x_1, x_1 - y_1) \right]_+ + \frac{x_2}{y_2} \left[\frac{x_2}{x_2 - y_2} \vartheta_{11}^0(x_2, x_2 - y_2) \right]_+ \right. \\
&\quad + 2 \frac{x_1 y_2 + y_1 x_2}{y_1 y_2} \vartheta_{111}^0(x_1, -x_2, x_1 - y_1) + 2 \frac{x_1 x_2}{y_1 y_2} \vartheta_{11}^0(x_1, -x_2) \\
&\quad \left. + \left(\frac{1}{2} \frac{\beta_0}{C_A} + 2 \right) \delta(x_1 - y_1) \right].
\end{aligned} \tag{4.43}$$

- Maximal-spin (or transversity) sector:

$$\begin{aligned}
K_{(0)}^{qq;T}(x_1, x_2 | y_1, y_2) &= C_F \left[\left[\frac{x_1}{x_1 - y_1} \vartheta_{11}^0(x_1, x_1 - y_1) \right]_+ + \left[\frac{x_2}{x_2 - y_2} \vartheta_{11}^0(x_2, x_2 - y_2) \right]_+ \right. \\
&\quad \left. + \frac{1}{2} \delta(x_1 - y_1) \right], \\
K_{(0)}^{gg;T}(x_1, x_2 | y_1, y_2) &= C_A \left[\frac{x_1}{y_1} \left[\frac{x_1}{x_1 - y_1} \vartheta_{11}^0(x_1, x_1 - y_1) \right]_+ + \frac{x_2}{y_2} \left[\frac{x_2}{x_2 - y_2} \vartheta_{11}^0(x_2, x_2 - y_2) \right]_+ \right. \\
&\quad \left. + \left(\frac{1}{2} \frac{\beta_0}{C_A} + 2 \right) \delta(x_1 - y_1) \right].
\end{aligned} \tag{4.44}$$

The regularization of the end-point behavior $y_i \rightarrow x_i$ is achieved via the plus-prescription,

$$\left[\frac{x_1}{x_1 - y_1} \vartheta_{11}^0(x_1, x_1 - y_1) \right]_+ \equiv \frac{x_1}{x_1 - y_1} \vartheta_{11}^0(x_1, x_1 - y_1) - \delta(x_1 - y_1) \int dx'_1 \frac{x'_1}{x'_1 - y_1} \vartheta_{11}^0(x'_1, x'_1 - y_1). \quad (4.45)$$

Note that the ϑ -functions other than ϑ_0^{11} can be reduced to the latter making use of Eqs. (G.106) – (G.113). Moreover, the step-function $\vartheta(x, y)$ from the previous section is related to ϑ_0^{11} via

$$\vartheta(x, y) = (1 + y) \vartheta_0^{11}(1 + x, x - y), \quad (4.46)$$

as can be seen by matching their definitions.

The even parity kernels (4.42) possess the off-diagonal pieces in the non-physical sector as defined in the footnote 21. To cure this problem in appropriate way, so that the forward limit would not be affected, we should add certain terms to the kernels computed from Feynman diagrams

$$K^{ab} \rightarrow K^{ab} + \delta K^{ab}, \quad (4.47)$$

where [235]

$$\delta K_{(0)}^{gg;V}(x_1, x_2 | y_1, y_2) = 4T_F N_f \frac{x_1 x_2}{y_1 y_2} (y_2 - y_1) \vartheta_{11}^0(x_1, -x_2), \quad (4.48)$$

$$\delta K_{(0)}^{gg;V}(x_1, x_2 | y_1, y_2) = 2C_F x_1 x_2 (x_2 - x_1) \vartheta_{11}^0(x_1, -x_2), \quad (4.49)$$

In the forward limit $\vartheta_{11}^0(x, -x) = 0$, so that these extra terms die out.

4.4.2 From coordinate to momentum-space kernels

As we emphasized earlier, Eq. (4.40) connects the coordinate and momentum space kernels. However, since the relation was given for the momentum kernels (4.38) rather than those in Section 4.4.1, which depend on different variables, it is instructive to rewrite it. For the diagonal kernels K written in terms of x_i and y_i variables, Eq. (4.40) gives

$$K^{aa}(x_1, x_2 | y_1, y_2) = -\frac{y_1}{x_1 + x_2} \vartheta_{11}^0(x_1 - y_1, x_1) \int_0^{x_1/y_1} dw \mathcal{K}^{aa}\left(\frac{x_2 - y_2 w}{x_1 + x_2}, \frac{x_1 - y_1 w}{x_1 + x_2}\right) - \frac{y_2}{x_1 + x_2} \vartheta_{11}^0(x_2 - y_2, x_2) \int_0^{x_2/y_2} dw \mathcal{K}^{aa}\left(\frac{x_2 - y_2 w}{x_1 + x_2}, \frac{x_1 - y_1 w}{x_1 + x_2}\right), \quad (4.50)$$

where we assumed the momentum conservation $x_1 + x_2 = y_1 + y_2$. For the off-diagonal elements, as it is evident from Eq. (4.36), one should also apply the operators $-\partial_x$ and $-\partial_x^{-1}$ on the right-hand side. Having these results, one can verify that the momentum space evolution kernels (4.42) – (4.44) arise from the coordinate space ones (4.19) – (4.28).

In the one-loop case, one can do the transformation in a more explicit way by making use of Eq. (4.36). The first step of the resuction consists in rescaling of the Feynman integration variables

$$\int_0^1 du \int_0^1 dv \theta(1 - u - v) f(u, v) = \int_0^1 du \int_0^1 dv \bar{u} f(u, \bar{u}v). \quad (4.51)$$

The delta-function is eliminated then by using the general formula

$$\int_0^1 dv f(v) \delta(x - vy) = f\left(\frac{x}{y}\right) \vartheta_{11}^0(x, x - y), \quad (4.52)$$

which brings in the ϑ_{11}^0 -function of the momentum space formulation. Notice that Eq. (4.37) is now an obvious consequence of the rescaling property of the argument of the delta-function, so that

$$\vartheta_{11}^0(x, x - y) = \frac{1}{\eta} \vartheta_{11}^0\left(\frac{x}{\eta}, \frac{x - y}{\eta}\right).$$

The second integration is accomplished making use of the result

$$\begin{aligned} \int_0^1 du \bar{u}^n \vartheta_{11}^0(x_1 - y_1 \bar{u}, x_1 - \eta \bar{u}) &= \frac{1}{n} \left\{ \left[1 - \left(\frac{x_1}{\eta} \right)^n \right] \vartheta_{11}^0(x_1 - y_1, -x_2) \right. \\ &\quad \left. - \frac{y_1}{y_2} \left[\left(\frac{x_1}{\eta} \right)^n - \left(\frac{x_1}{y_1} \right)^n \right] \vartheta_{11}^0(x_1 - y_1, x_1) \right\}, \end{aligned} \quad (4.53)$$

where $\eta = x_1 + x_2 = y_1 + y_2$. As a simple demonstration of these formulas, one finds

$$\mathcal{K}_{\text{test}}^{qq}(u, v) = 1 \quad \Leftrightarrow \quad K_{\text{test}}^{qq}(x_1, x_2 | y_1, y_2) = \vartheta_{111}^0(x_1, -x_2, x_1 - y_1),$$

according to Eq. (4.36).

4.4.3 Reduction to inclusive kernels

The off-forward evolution kernels yield the usual DGLAP splitting functions when the skewness parameter is set to zero, $\eta = 0$,

$$K(x, -x | 1, -1) \equiv -P(x), \quad (4.54)$$

where $0 \leq x \leq 1$ so that $\vartheta_{11}^0(x - 1, x) = 1$. Then the leading order kernels have the form, which coincide with the well-known results, which present below for completeness.

- Even-parity sector:

$$P_{(0)}^{qq;V}(x) = C_F \left[\frac{1 + x^2}{1 - x} \right]_+, \quad (4.55)$$

$$P_{(0)}^{gg;V}(x) = 2T_F N_f \{x^2 + (1 - x)^2\}, \quad (4.56)$$

$$P_{(0)}^{gg;V}(x) = C_F \frac{1}{x} \{1 + (1 - x)^2\}, \quad (4.57)$$

$$P_{(0)}^{gg;V}(x) = 2C_A \left\{ \frac{1}{x} + \left[\frac{1}{1 - x} \right]_+ - 2 + x(1 - x) \right\} - \frac{\beta_0}{2} \delta(1 - x). \quad (4.58)$$

- Odd-parity sector:

$$P_{(0)}^{qq;A}(x) = C_F \left[\frac{1 + x^2}{1 - x} \right]_+, \quad (4.59)$$

$$P_{(0)}^{gg;A}(x) = 2T_F N_f \{x^2 - (1 - x)^2\}, \quad (4.60)$$

$$P_{(0)}^{gg;A}(x) = C_F \frac{1}{x} \{1 - (1 - x)^2\}, \quad (4.61)$$

$$P_{(0)}^{gg;A}(x) = 2C_A \left\{ 1 - 2x + \left[\frac{1}{1 - x} \right]_+ \right\} - \frac{\beta_0}{2} \delta(1 - x). \quad (4.62)$$

- Maximal-helicity sector:

$$P_{(0)}^{qq;T}(x) = C_F \left\{ 2x \left[\frac{1}{1-x} \right]_+ + \frac{3}{2} \delta(1-x) \right\}, \quad (4.63)$$

$$P_{(0)}^{gg;T}(x) = 2C_A x^2 \left[\frac{1}{1-x} \right]_+ - \frac{\beta_0}{2} \delta(1-x). \quad (4.64)$$

(4.65)

We have used the standard form of the plus-regularization of the end-point singularity,

$$\left[\frac{1}{1-x} \right]_+ \equiv \frac{1}{1-x} - \delta(1-x) \int_0^1 \frac{dx'}{1-x'}. \quad (4.66)$$

The Mellin moments of the evolution kernels define the anomalous dimensions of the basic Wilson operators (i.e., those without total derivatives)

$$\int_0^1 dx x^j P(x; \alpha_s) = -\frac{1}{2} \gamma_j^{\text{fw}}(\alpha_s). \quad (4.67)$$

As usual, the splitting functions are given by the expansion in coupling constant

$$\gamma_j^{\text{fw}}(\alpha_s) = \sum_{n=0}^{\infty} \left(\frac{\alpha_s}{2\pi} \right)^{n+1} \gamma_{(n)j}^{\text{fw}}. \quad (4.68)$$

In the lowest order, the Mellin moments of the nonsinglet parton distributions

$$q_j(\mu^2) = \int_0^1 dx x^j q(x; \mu^2) \quad (4.69)$$

have a simple evolution

$$q_j(\mu^2) = \left(\frac{\alpha_s(\mu_0^2)}{\alpha_s(\mu^2)} \right)^{\gamma_{(0)}^{qq;\text{fw}} j / \beta_0} q_j(\mu_0^2), \quad (4.70)$$

governed by the one-loop qq anomalous dimension $\gamma_{(0)j}^{qq;\text{fw}}$ and the one-loop QCD beta-functions β_0 defined in Eq. (G.29). To get the evolved parton distribution $q(x; \mu^2)$, one can use the formal reconstruction of a function from its Mellin moments

$$q(x; \mu^2) = \sum_{n=0}^{\infty} \frac{(-1)^j}{j!} \delta^{(j)}(x) q_j(\mu^2), \quad (4.71)$$

which gives

$$q(x; \mu^2) = \sum_{j=0}^{\infty} \frac{(-1)^j}{j!} \delta^{(j)}(x) \left(\frac{\alpha_s(\mu_0^2)}{\alpha_s(\mu^2)} \right)^{\gamma_{(0)j}^{qq;\text{fw}} / \beta_0} \int_0^1 dy y^j q(y; \mu_0^2). \quad (4.72)$$

Using the fact that all $\gamma_j^{qq;\text{fw}} > 0$ for $j > 0$, while the lowest $j = 0$ moment of the parton distribution corresponds to a local conserved axial/vector current with vanishing anomalous dimension, one finds

$$q(x; \mu^2 \rightarrow \infty) = \delta(x) \int_0^1 dy q(y; \mu_0^2), \quad (4.73)$$

Thus, we observe the qualitative feature of the inclusive evolution pointed out at the beginning of this chapter. Namely, when the proton is probed with infinitely fine resolution, one finds an infinite number of partons with tiny (actually zero) momentum with respect to the momentum of the parent hadron.

The expression (4.71), of course, has an obvious practical difficulty: all the derivatives of the delta function are concentrated at a single point $x = 0$, and the restoration of the correct support of the function $q(x)$ is a result of the infinite summation of a slow convergent series. In other words, Eq. (4.71) should only be understood in the sense of (mathematical) distributions, as a statement about its integration with smooth functions. A similar problem will be encountered later in this chapter when we will attempt to solve the evolution equation for GPDs using the eigenfunctions of the corresponding evolution equation.

4.4.4 Reduction to exclusive kernels

The meson and baryon distribution amplitudes discussed in Section 3.7 also evolve with the change of the resolution scale μ^2 . The meson distribution amplitudes $\phi_M(x; \mu^2)$ obey the ER-BL evolution equation [237, 238, 239, 240]

$$\frac{d}{d \ln \mu^2} \phi_M(x; \mu^2) = \int_0^1 dy V(x, y) \phi_M(y; \mu^2). \quad (4.74)$$

The functions $V(x, y)$ correspond to the $\eta = 1$ limit of the general off-forward evolution kernels:

$$K(x, 1-x|y, 1-y) \equiv -V(x, y), \quad (4.75)$$

which holds for diagonal and off-diagonal elements of the mixing matrix. Since $0 \leq x, y \leq 1$, we have $\vartheta_{11}^0(x-y, x) = \frac{1}{y}\theta(y-x)$, and it is easy to derive that the leading order ER-BL kernels have the following form²²

$$V_{(0)}^{ab}(x, y) = \theta(y-x) F^{ab}(x, y) \pm \theta(x-y) \bar{F}^{ab}(x, y); \pm \text{ for } \begin{cases} a = b \\ a \neq b \end{cases}, \quad (4.76)$$

where $\bar{F}^{ab}(x, y) \equiv F^{ab}(\bar{x}, \bar{y})$ with $\bar{x} = 1-x$ and $\bar{y} = 1-y$. The $-$ and $+$ signs in Eq. (4.76) correspond off-diagonal $a \neq b$ and diagonal $a = b$ elements, respectively, of the $V_{(0)}^{ab}$ matrix. The use of Eqs. (4.75) reproduces the kernels obtained earlier in many papers. The results are summarized below.

- Even-parity sector [237, 240, 241]:

$$F^{qg;V}(x, y) = C_F \frac{x}{y} \left\{ \frac{1}{[y-x]_+} + 1 + \frac{3}{2} \delta(x-y) \right\}, \quad (4.77)$$

$$F^{qg;V}(x, y) = 2N_f T_F \frac{x}{y^2 \bar{y}} (2x - y - 1), \quad (4.78)$$

$$F^{gq;V}(x, y) = C_F \frac{x}{y} (2y - x), \quad (4.79)$$

$$F^{gg;V}(x, y) = C_A \frac{x^2}{y^2} \left\{ \frac{1}{[y-x]_+} + 2\bar{x} + 2y(1+2\bar{x}) - \frac{1}{2} \frac{\beta_0}{C_A} \delta(x-y) \right\}. \quad (4.80)$$

²²Note that the terms with δ -function accompanied by step-functions are understood in the following way $\delta(x-y)[\theta(y-x) + \theta(x-y)] = \delta(x-y)$.

- Odd-parity sector [242, 243]:

$$F^{qq;A}(x, y) = C_F \frac{x}{y} \left\{ \frac{1}{[y-x]_+} + 1 + \frac{3}{2} \delta(x-y) \right\}, \quad (4.81)$$

$$F^{qg;A}(x, y) = -2N_f T_F \frac{x}{y^2}, \quad (4.82)$$

$$F^{gq;A}(x, y) = C_F \frac{x^2}{y}, \quad (4.83)$$

$$F^{gg;A}(x, y) = C_A \frac{x^2}{y^2} \left\{ \frac{1}{[y-x]_+} + 2 - \frac{1}{2} \frac{\beta_0}{C_A} \delta(x-y) \right\}. \quad (4.84)$$

- Maximal-helicity sector [233, 73]:

$$F^{qq;T}(x, y) = C_F \frac{x}{y} \left\{ \frac{1}{[y-x]_+} + \frac{3}{2} \delta(x-y) \right\}, \quad (4.85)$$

$$F^{gg;T}(x, y) = C_A \frac{x^2}{y^2} \left\{ \frac{1}{[y-x]_+} - \frac{1}{2} \frac{\beta_0}{C_A} \delta(x-y) \right\}. \quad (4.86)$$

All of the singularities are regularized as follows

$$\begin{aligned} \frac{\theta(y-x)}{[y-x]_+} &\equiv \frac{\theta(y-x)}{y-x} - \delta(y-x) \int_0^1 dx' \frac{\theta(y-x')}{y-x'}, \\ \frac{\theta(x-y)}{[x-y]_+} &\equiv \frac{\theta(x-y)}{x-y} - \delta(y-x) \int_0^1 dx' \frac{\theta(x'-y)}{x'-y}. \end{aligned}$$

4.4.5 From exclusive to inclusive kernels

Both inclusive DGLAP splitting functions and exclusive ER-BL kernels for mesons are particular projections (reductions) of the same general off-forward evolution kernels. In fact, there exist formulas providing a direct reduction of the ER-BL kernels to the DGLAP ones. They can be most conveniently derived if the ER-BL evolution is written in the matrix form, as an equation for the moments of the distribution amplitude

$$a_j(\mu^2) = \int_0^1 dx x^j \phi_M(x; \mu^2). \quad (4.87)$$

The coefficients a_j are proportional to the matrix elements of local operators

$$\langle p | \bar{\psi}(0) (-i \bar{\partial}^+)^j \gamma^+ \psi(0) | 0 \rangle = -i(p^+)^{j+1} f_M \int_0^1 dx x^j \phi_M(x). \quad (4.88)$$

Under evolution, these operators \mathcal{O}_j mix with the operators $(\partial^+)^{j-k} \mathcal{O}_k$ having the same total number j of vector indices but containing $j-k$ total derivatives acting on the operator \mathcal{O}_k as a whole. Since a total derivative ∂^μ just produces the overall factor p^μ in the matrix element (see footnote 24), the evolution equation for a_j 's has the form

$$\frac{d}{d \ln \mu^2} a_j(\mu^2) = -\frac{1}{2} \sum_{k=0}^j \gamma_{jk}(g) a_k(\mu^2). \quad (4.89)$$

The matrix elements γ_{jk} are related to the kernel $V(x, y)$ by

$$\int_0^1 dx x^j V(x, y) = -\frac{1}{2} \sum_{k=0}^j \gamma_{jk}(y) y^k. \quad (4.90)$$

The appearance of a polynomial in y on the right-hand side, rather than a single power y^j , is a simple consequence of fact that the evolution kernel V encodes the mixing of operators with total derivatives. The local operator

$$x^j \leftrightarrow \bar{\psi}(0)(-i \overleftarrow{\partial}^+)^j \gamma^+ \psi(0)$$

is allowed to evolve with the “probability” γ_{jk} into the operators with less “left derivatives” $\overleftarrow{\partial}^+$ and more “total derivatives” ∂^+

$$y^k \leftrightarrow (i \partial^+)^k \bar{\psi}(0)(-i \overleftarrow{\partial}^+)^{j-k} \gamma^+ \psi(0).$$

In the forward case, the operators with total derivatives have zero matrix elements, so only the diagonal term γ_{jj} survives. The latter is given by the j th moment of the DGLAP splitting function $P(z)$, and this establishes its relationship to the ER-BL kernel. In the singlet case, the relations are complicated by the quark-gluon mixing. So, we have

$$\int_0^1 dx \begin{pmatrix} x^j \\ x^{j-1} \end{pmatrix} \begin{pmatrix} V^{qq} & V^{qg} \\ V^{gq} & V^{gg} \end{pmatrix} (x, y) = -\frac{1}{2} \sum_{k=(0,1)}^j \begin{pmatrix} \gamma_{jk}^{qq} & \gamma_{jk}^{qg} \\ \gamma_{jk}^{gq} & \gamma_{jk}^{gg} \end{pmatrix} \begin{pmatrix} y^k \\ y^{k-1} \end{pmatrix}, \quad (4.91)$$

for the ER-BL kernels, and

$$\int_0^1 dx x^j \begin{pmatrix} P^{qq} & P^{qg} \\ P^{gq} & P^{gg} \end{pmatrix} (x) = -\frac{1}{2} \begin{pmatrix} \gamma_j^{qq;\text{fw}} & \gamma_j^{qg;\text{fw}} \\ \gamma_j^{gq;\text{fw}} & \gamma_j^{gg;\text{fw}} \end{pmatrix}, \quad (4.92)$$

for the splitting functions, such that $\gamma_{jj}^{ab} = \gamma_j^{ab;\text{fw}}$. To extract the diagonal elements from Eq. (4.91), we substitute y by $1/\eta$ and multiply each entry on both sides with a sufficient power of η , found by inspection. As suggested by Fig. 28, the ER-BL kernels, having the support $0 \leq x, y \leq 1$, can be extended to the entire (x, y) -plane according to the rules which we spell out later. Rescaling the integration variable and taking the limit $\eta \rightarrow 0$, we find

$$\lim_{\eta \rightarrow 0} \int_0^1 \frac{dx}{\eta} x^j \begin{pmatrix} k^{qq} & \frac{1}{\eta} k^{qg} \\ \frac{\eta}{x} k^{gq} & \frac{1}{x} k^{gg} \end{pmatrix} \left(2 \frac{x}{\eta} - 1, \frac{2}{\eta} - 1 \right) = \frac{1}{2} \begin{pmatrix} \gamma_{jj}^{qq} & \gamma_{jj}^{qg} \\ \gamma_{jj}^{gq} & \gamma_{jj}^{gg} \end{pmatrix}, \quad (4.93)$$

where we used the extended kernels in the whole region. This is done by a simple replacement of the θ functions in the ER-BL kernels by

$$\theta(y - x) \rightarrow \vartheta(2x - 1, 2y - 1) = \theta\left(1 - \frac{x}{y}\right) \theta\left(\frac{x}{y}\right) \text{sgn}(y), \quad (4.94)$$

$$\theta(x - y) \rightarrow \vartheta(1 - 2x, 1 - 2y) = \theta\left(1 - \frac{\bar{x}}{\bar{y}}\right) \theta\left(\frac{\bar{x}}{\bar{y}}\right) \text{sgn}(\bar{y}), \quad (4.95)$$

$$\theta(y - \bar{x}) \rightarrow \vartheta(1 - 2x, 2y - 1) = \theta\left(1 - \frac{\bar{x}}{y}\right) \theta\left(\frac{\bar{x}}{y}\right) \text{sgn}(y), \quad (4.96)$$

$$\theta(\bar{y} - x) \rightarrow \vartheta(2x - 1, 1 - 2y) = \theta\left(1 - \frac{x}{\bar{y}}\right) \theta\left(\frac{x}{\bar{y}}\right) \text{sgn}(\bar{y}), \quad (4.97)$$

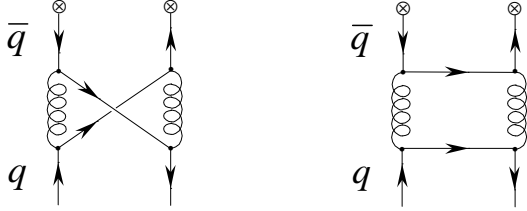


Figure 30: The typical contribution inducing the parton-antiparton mixing in evolution kernels.

where $0 \leq x, y \leq 1$ on the left-hand side of the substitution rules, while on right-hand side they are unrestricted. The last two relations are not required at leading order, since the corresponding momentum flow structures start from two loops only. The latter originate from the region $u+v \geq 1$ of the coordinate space kernels and stem from the parton-antiparton mixing. Two typical contributions inducing the quark-antiquark mixing are demonstrated in Fig. 30. Comparison with Eq. (4.92) provides us with the desired formula:

$$P(x) = \text{LIM } V(x, y) \equiv -\lim_{\eta \rightarrow 0} \frac{1}{\eta} \begin{pmatrix} k^{qq} & \frac{1}{\eta} k^{qg} \\ \frac{\eta}{x} k^{gq} & \frac{1}{x} k^{gg} \end{pmatrix} \left(2\frac{x}{\eta} - 1, 2\frac{1}{\eta} - 1 \right). \quad (4.98)$$

In particular, the step-function structures are reduced as follows

$$\theta(y-x) \rightarrow \lim_{\eta \rightarrow 0^+} \vartheta \left(2\frac{x}{\eta} - 1, 2\frac{1}{\eta} - 1 \right) = \theta(1-x)\theta(x), \quad (4.99)$$

$$\theta(x-y) \rightarrow \lim_{\eta \rightarrow 0^+} \vartheta \left(1 - 2\frac{x}{\eta}, 1 - 2\frac{1}{\eta} \right) = -\theta(1-x)\theta(x), \quad (4.100)$$

$$\theta(y-\bar{x}) \rightarrow \lim_{\eta \rightarrow 0^+} \vartheta \left(1 - 2\frac{x}{\eta}, 2\frac{1}{\eta} - 1 \right) = \theta(1+x)\theta(-x), \quad (4.101)$$

$$\theta(\bar{y}-x) \rightarrow \lim_{\eta \rightarrow 0^+} \vartheta \left(2\frac{x}{\eta} - 1, 1 - 2\frac{1}{\eta} \right) = -\theta(1+x)\theta(-x). \quad (4.102)$$

For instance, the one-loop kernels $V_{(0)}^{ab}(x, y)$ contain only the two usual θ -structures, i.e., $\theta(y-x)$ and $\theta(x-y)$. Then the LIM operation yields

$$\text{LIM } \mathbf{V}_{(0)}(x, y) = \theta(1-x)\theta(x) \lim_{\eta \rightarrow 0} \frac{1}{\eta} \begin{pmatrix} (F^{qq} - \bar{F}^{qq}) & \frac{1}{\eta} (F^{qg} + \bar{F}^{qg}) \\ \frac{\eta}{x} (F^{gq} + \bar{F}^{gq}) & \frac{1}{x} (F^{gg} - \bar{F}^{gg}) \end{pmatrix} \left(\frac{x}{\eta}, \frac{1}{\eta} \right).$$

The plus-prescription involved in the diagonal kernels is reduced as follows

$$\text{LIM } [f(x, y)]_+ = \text{LIM } f(x, y) - \delta(1-x) \int_0^1 dx \text{LIM } f(x, y) = [\text{LIM } f(x, y)]_+. \quad (4.103)$$

4.5 Evolution of double distributions

Up to now we have addressed the scale dependence of GPDs and their “off-springs”—parton densities and distribution amplitudes. Before we turn to developing analytical tools for solving

them, let us briefly consider the evolution equations for double distributions [1, 3, 4, 6]. Let us discuss the non-singlet evolution of DDs h_A^q , introduced in section 3.8.3, as an example.

The generic form of the evolution equation for the double distribution h_A^q reads

$$\frac{d}{d \ln \mu^2} h_A^q(\beta_1, \alpha_1) = \int_{\Omega} d\beta_1 d\alpha_2 R^{qq}(\beta_1, \alpha_1; \beta_2, \alpha_2) h_A^q(\beta_2, \alpha_2), , \quad (4.104)$$

where the evolution kernel R^{qq} , having the standard perturbative expansion

$$R^{qq}(\beta_1, \alpha_1; \beta_2, \alpha_2) = \sum_{n=0}^{\infty} \left(\frac{\alpha_s}{2\pi} \right)^n R_{(n)}^{qq}(\beta_1, \alpha_1; \beta_2, \alpha_2), \quad (4.105)$$

can be found in terms of the light-cone evolution kernel for non-local operators. To achieve this, we form the matrix element of both sides of Eq. (4.12) and make use of the parametrization of the resulting operator matrix elements in terms of DDs (3.242). Then by performing the inverse Fourier transform in p^+ and Δ^+ , one immediately finds

$$R^{qq}(\beta_1, \alpha_1; \beta_2, \alpha_2) = \int_0^1 du dv \mathcal{K}^{qq}(u, v) \delta(\beta_1 - \beta_2(1-u-v)) \delta(\alpha_1 - \alpha_2(1-u-v) - v + u). \quad (4.106)$$

Since the leading order coordinate kernel $\mathcal{K}_{(0)}^{qq}$ exists only in the triangle $1-u-v > 0$ there arises a spectral constraint in the integrand. The calculation can be done by means of Eqs. (4.51) – (4.52) and it yields

$$\begin{aligned} R_{(0)}^{qq}(\beta_1, \alpha_1; \beta_2, \alpha_2) &= \frac{1}{2|\beta_2|} \mathcal{K}_{(0)}^{qq} \left(\frac{1}{2}(1-\alpha_1) - \frac{\beta_1}{2\beta_2}(1-\alpha_2), \frac{\beta_1}{2\beta_2}(1+\alpha_1) - \frac{1}{2}(1+\alpha_2) \right) \\ &\times \vartheta \left(\frac{\beta_1}{\beta_2}(1-\alpha_2) - (1-\alpha_1), 0 \right) \vartheta \left((1+\alpha_1) - \frac{\beta_1}{\beta_2}(1+\alpha_2), \frac{\beta_1}{\beta_2}(1-\alpha_2) - (1-\alpha_1) \right). \end{aligned} \quad (4.107)$$

Here the spectral constraints are expressed in terms of the generalized step functions (4.39) via Eq. (4.46). Other sectors are considered analogously. We refer the reader to Appendix H for a compendium of explicit results for one-loop evolution kernel, albeit, for nonsymmetric DDs.

4.6 Diagonalization of the mixing matrix

Now we are in a position to construct a framework for the analytical solution of the evolution equations for generalized parton distributions. To start with, let us recall that the diagonalization of the leading order evolution equation (4.74) for the meson distribution amplitude (3.166)—the first nontrivial encounter of the mixing pattern involving towers of operators containing total derivatives—was found in Refs. [237, 239, 240]. It was demonstrated there that the local operators

$$\tilde{\mathbb{O}}_{jj}^{qq} \equiv i^j \bar{\psi} \gamma^+ \gamma^5 \left(\vec{\partial}^+ + \bar{\partial}^+ \right)^j C_j^{3/2} \left(\frac{\vec{\partial}^+ - \bar{\partial}^+}{\vec{\partial}^+ + \bar{\partial}^+} \right) \psi,$$

expressed through the conventional Gegenbauer polynomials $C_j^{3/2}$, do not mix with other operators under renormalization for different j . In other words, operators $\tilde{\mathbb{O}}_{jj}^{qq}$ are multiplicatively renormalizable for each values of j or, equivalently, the matrix γ_{jk} is diagonal in the basis of Gegenbauer

polynomials: $\gamma_{jk} = \delta_{jk}\gamma_j$, where γ_j is the usual anomalous dimension of the forward matrix elements of the quark operators with j (left-right) derivatives. It was immediately recognized [237] that the operators $\tilde{\mathbb{O}}_{jj}^{qq}$ coincide with conformal tensors of the free field theory [244]. In fact, it was already anticipated in [245] that the conformal operators renormalize multiplicatively at one-loop order. The relationship between conformal invariance and renormalization properties of composite operators was further studied in Refs. [246, 247, 248, 249] and completely disentangled in higher orders of the perturbation theory in the culminating studies of Refs. [250, 251, 233, 252, 235, 253].

These findings suggested that the anomalous dimensions of conformal operators are enumerated by a single conserved quantum number j identified with the conformal spin of the composite operator. Therefore, one expects that this property is reflected in QCD Lagrangian and it must be manifested as its space-time symmetry. As is well-known the largest symmetry group of a massless classical four-dimensional gauge theory is the fifteen-parameter group of conformal transformations $SO(4, 2)$, which contains dilatations \mathbb{D} and special conformal transformations \mathbb{K}^μ in addition to the generators of the conventional Poincaré group with Lorentz transformations $\mathbb{M}^{\mu\nu}$ and translations \mathbb{P}^μ . The algebra as well as its representations are reviewed in Appendix I. Below we will elaborate on this issues in greater detail since these consideration allow one to understand the structure of higher order corrections in a very efficient way.

4.6.1 Representations of the collinear conformal algebra

The discussion of twist two operators, to which we restrict our consideration, allows to consider a subgroup of all conformal transformations since the former are built solely from “good” field components and “live” on the light cone. This so-called collinear conformal subgroup contains the following generators

$$\mathbb{L}^- \equiv \frac{i}{2}\mathbb{K}^- , \quad \mathbb{L}^+ \equiv i\mathbb{P}^+ , \quad \mathbb{L}^0 \equiv \frac{i}{2}(\mathbb{D} + \mathbb{M}^{-+}) , \quad (4.108)$$

projected on the light-cone with two tangent vectors n^μ and $n^{*\mu}$, as specified in Appendix B. There is yet another combination of the dilatation and the light-cone projection of the Lorentz generator

$$\mathbb{E} = i(\mathbb{D} - \mathbb{M}^{-+}) , \quad (4.109)$$

which commutes with all operators of the collinear conformal subgroup. It counts the twist

$$\tau = d - s , \quad (4.110)$$

defined in terms of the dimension d and the spin s , of the operator it acts on. The generators introduced above form a closed algebra and act non-trivially on the “good” components of the quark and gluon operators living on the light-cone, i.e., the elementary fields which enter the leading twist operators introduced in Section 3.1. They obey the $su(1, 1)$ commutation relations

$$[\mathbb{L}^+, \mathbb{L}^-] = -2\mathbb{L}^0 , \quad [\mathbb{L}^0, \mathbb{L}^\pm] = \pm\mathbb{L}^\pm \quad (4.111)$$

From this commutator algebra one concludes that \mathbb{L}^+ is a step-up operator and \mathbb{L}^- is a step-down operator. The quadratic Casimir operators is defined as

$$\mathbf{L}^2 = \mathbb{L}^0(\mathbb{L}^0 - 1) - \mathbb{L}^+\mathbb{L}^- . \quad (4.112)$$

The conformal spin is determined as an eigenvalue of the \mathbb{L}^0

$$[\mathbb{L}^0, \Phi(0)] = j\Phi(0) , \quad j \equiv \frac{1}{2}(d + s) . \quad (4.113)$$

It is composed from the dimension d and the spin s of the corresponding field $\Phi(0)$. The values that the latter takes on elementary field operators were given earlier in Eqs. (3.6) and (3.13).

Since the canonical dimension of the fermion field is $d_q = 3/2$, one finds that the “good” ψ_+ -component has the conformal spin $j_q = 1$. Similarly, for the “bad” ψ_- -component one finds $j_q = 1/2$. The canonical dimension of the field strength tensor is $d_g = 2$, the $F_{\perp}^{+\mu}$ -component has the conformal spin $j_g = 3/2$. For F^{+-} and $F_{\perp\perp}^{\mu\nu}$ -components one gets $j_g = 1$, while for the $F_{\perp}^{-\mu}$ -component one has $j_g = 1/2$. Thus, the conformal spin of “good” QCD fields is

$$j_q = 1, \quad j_g = \frac{3}{2}. \quad (4.114)$$

Now we are in a position to discuss the representation of the quantum operators $\mathbb{L}^{\pm,0}$ in the basis of quark and gluon fields.

- The representation of quantum generators acting on the quantum-field operators in terms of differential operators is derived in Appendix I using the method of induced representations. The action of quantum generators \mathbb{G} on a function Φ living on the light-cone z^- and possessing the conformal spin j

$$[\mathbb{G}, \Phi(z^-)] \equiv \hat{G}\Phi(z^-), \quad (4.115)$$

results into the following differential representation for them

$$\hat{L}^- \equiv 2jz^- + (z^-)^2 \frac{\partial}{\partial z^-}, \quad \hat{L}^+ \equiv \frac{\partial}{\partial z^-}, \quad \hat{L}^0 \equiv j + z^- \frac{\partial}{\partial z^-}. \quad (4.116)$$

The quadratic Casimir operator in this representation is defined as

$$\hat{\mathbf{L}}^2 = \hat{L}^0(\hat{L}^0 - 1) - \hat{L}^+ \hat{L}^-. \quad (4.117)$$

Note that the commutation relations for the generators in this representation differ from the generators acting on the Hilbert space by a minus sign,

$$[\hat{L}^+, \hat{L}^-] = 2\hat{L}^0, \quad [\hat{L}^0, \hat{L}^\pm] = \mp \hat{L}^\pm. \quad (4.118)$$

For a multiparticle operator, one defines the generators as

$$\hat{L}_{1\dots N}^{\pm,0} = \sum_{\ell=1}^N \hat{L}_\ell^{\pm,0}. \quad (4.119)$$

- One can choose a different representation for quantum generators, which is very handy in constructing the conformal operators [254, 255]. Namely, one can realize the generators in the basis spanned by the elements [242]

$$Z^k \equiv \frac{\partial^{+k} \Phi(0)}{\Gamma(k+2j)}, \quad (4.120)$$

with the field possessing the conformal spin j . We construct a representation by defining

$$[\mathbb{G}, f(Z)] \equiv Gf(Z), \quad (4.121)$$

for any polynomial $f(Z)$ in the variable Z . The generators G admit the following differential representation²³

$$L^- = \frac{\partial}{\partial Z}, \quad L^+ = 2jZ + Z^2 \frac{\partial}{\partial Z}, \quad L^0 = j + Z \frac{\partial}{\partial Z}. \quad (4.122)$$

These generators satisfy the same commutation relations as the original quantum generators

$$[L^+, L^-] = -2L^0, \quad [L^0, L^\pm] = \pm L^\pm. \quad (4.123)$$

It is interesting to note that this representation differs from (4.116) by a mere interchange of the functional form of the raising and lowering operators. For multi-variable functions $\chi(Z_1, Z_2, \dots, Z_N)$ the generators are obviously generalized by taking the sum of single-variable generators,

$$L_{1\dots N}^{\pm,0} = \sum_{\ell=1}^N L_\ell^{\pm,0}. \quad (4.124)$$

The quadratic Casimir operator has the same form as before

$$\mathbf{L}^2 = L^0(L^0 - 1) - L^+L^-.$$

And its action on a two-argument function is determined by the following differential operator

$$\mathbf{L}_{12}^2 = -(Z_1 - Z_2)^2 \frac{\partial}{\partial Z_1} \frac{\partial}{\partial Z_2} + 2(Z_1 - Z_2) \left(j_2 \frac{\partial}{\partial Z_1} - j_1 \frac{\partial}{\partial Z_2} \right) + (j_1 + j_2)(j_1 + j_2 - 1). \quad (4.125)$$

4.6.2 Conformal operators

In general, the Wilson operators (3.2) do not transform covariantly under the action of the $SO(4, 2)$ conformal group and, as a consequence, they do not have an autonomous renormalization. To identify operators which are eigenfunctions of the renormalization group operator, one uses the fact that at leading order of perturbation theory the latter commutes with the generators of the conformal group. Thus they possess the same eigenfunctions. Making use of the collinear $SL(2)$ subgroup of the conformal group one can organize operators containing total derivatives into conformally-covariant towers, the so-called conformal operators. They are built as a linear superposition of bilinears

$$(\partial^{+k}\Phi_1(0)) (\partial^{+n-k}\Phi_2(0)).$$

²³The derivation of generators in this representation is very straightforward making use the available representation (4.116):

$$[\mathbb{G}, Z^k] = \frac{\partial^{+k}[\mathbb{G}, \Phi]}{\Gamma(2j+k)} = \frac{\partial^{+k}\widehat{G}\Phi}{\Gamma(2j+k)} \equiv GZ^k.$$

For instance, for $\mathbb{G} = \mathbb{L}^+$ one has according to these sequence of transformations

$$[\mathbb{L}^+, Z^k] = (2j+k)Z^{k+1} = \left(2jZ + Z^2 \frac{\partial}{\partial Z} \right) Z^k,$$

which gives L^+ in Eq. (4.122).

Similarly to the construction of the ground state of the rotational symmetry in quantum mechanics, we construct the ground—also called the primary—state of the $SL(2)$ symmetry by annihilating a superposition of the aforementioned bilinear states with the step-down operator \mathbb{L}^- . The definite value of the conformal spin is assigned to them by the eigenvalues of the quadratic Casimir operator (4.125). Since we construct the state from derivatives acting on a field, to perform actual calculations it is useful to use the representation (4.122) of the conformal generators. Thus, we build the operator as a linear superposition²⁴

$$\mathbb{O}(0) = \sum_{k=0}^n c_{nk} Z_1^k Z_2^{n-k}, \quad (4.126)$$

and impose two conditions.

- The lowest-weight vector condition

$$[\mathbb{L}^-, \mathbb{O}(0)] = L_{12}^- \mathbb{O}(0) = 0, \quad (4.127)$$

with multivariable generators (4.124) for $N = 2$.

- Assignment of the eigenvalue J of the conformal spin to the conformal primary

$$[\mathbb{L}^2, \mathbb{O}(0)] = \mathbf{L}_{12}^2 \mathbb{O}(0) = J(J-1) \mathbb{O}(0), \quad (4.128)$$

where the two-particle Casimir operators is given in Eq. (4.125).

The solution to the first equation is any translation-invariant function $\mathbb{O} \sim f(Z_2 - Z_1)$ or, since we are interested in local operators, a polynomial of an arbitrary order $\mathbb{O} \sim (Z_2 - Z_1)^n$, so that the coefficients c_{jk} are given by binomial coefficients. The second condition immediately relates the order of the polynomial to the conformal spin

$$J = n + j_1 + j_2, \quad (4.129)$$

with j_a for $a = 1, 2$ being the conformal spin of the elementary field Φ_a . Thus, we come to the definition of conformal operators

$$\mathbb{O}_j(0) = i^{j-j_1-j_2+2} \frac{\Gamma(j+j_1-j_2+2)\Gamma(j+j_2-j_1+2)}{\Gamma(j-j_1-j_2+3)} (Z_2 - Z_1)^{j-j_1-j_2+2}, \quad (4.130)$$

where we introduced $j = J-2$. Here, the overall factor is chosen such that in the basis spanned by elementary fields with derivatives, the operator will be given in terms of the Jacobi polynomials,

$$P_j^{(\alpha, \beta)}(x) = \frac{1}{2^j} \sum_{k=0}^j \binom{j+\alpha}{k} \binom{j+\beta}{j-k} (x-1)^{j-k} (x+1)^k. \quad (4.131)$$

As usual,

$$\binom{j}{k} = \frac{\Gamma(j+1)}{\Gamma(k+1)\Gamma(j-k+1)}$$

²⁴Notice that since the operators are sandwiched between states with different momenta, one cannot “integrate by parts” by moving derivatives from one field to another, like one does in the forward matrix elements, and reduce the whole tower of operators for $0 \leq k \leq n$ to a single one. In other words operators with total derivatives do matter since $\langle p_2 | i\partial^+ \mathbb{O} | p_1 \rangle = \langle p_2 | [\mathbb{O}, \mathbb{P}^+] | p_1 \rangle = \Delta^+ \langle p_2 | \mathbb{O} | p_1 \rangle = \eta p^+ \langle p_2 | \mathbb{O} | p_1 \rangle \neq 0$.

is the binomial coefficient. In the explicit form, the conformal operator reads

$$\mathbb{O}_j(0) = \Phi_1(0)(i\partial^+)^{j-j_1-j_2+2} P_{j-j_1-j_2+2}^{(2j_1-1, 2j_2-1)} \left(\vec{\mathcal{D}}^+/\partial^+ \right) \Phi_2(0), \quad (4.132)$$

where we have used the notations

$$\partial_\mu \equiv \vec{\partial}_\mu + \bar{\partial}_\mu, \quad \vec{\mathcal{D}}_\mu \equiv \vec{\mathcal{D}}_\mu - \bar{\mathcal{D}}_\mu,$$

for the total and left-right derivatives, respectively. Then, the non-local product $\Phi_1(0)\Phi_2(z^-)$ can be expanded over the conformal operators:

$$\begin{aligned} \Phi_1(0)\Phi_2(z^-) &= \sum_{n=0}^{\infty} \frac{(2n+2j_1+2j_2-1)\Gamma(n+2j_1+2j_2-1)}{\Gamma(n+2j_1)\Gamma(n+2j_2)} \\ &\quad \times (-iz^-)^n \int_0^1 du u^{n+2j_1-1} \bar{u}^{n+2j_2-1} \mathbb{O}_{j=n+j_1+j_2-2}(uz^-). \end{aligned} \quad (4.133)$$

We implied the $A^+ = 0$ gauge here to be able to neglect the path-ordered exponentials.

The conformal spin- $(j+2)$ representation space is spanned by the conformal operator $\mathbb{O}_j(0)$ and its descendants generated by applying the step-up operator \mathbb{L}^+

$$\mathbb{O}_{jl}(0) = i^{l-j+j_1+j_2-2} \underbrace{[\mathbb{L}^+, \dots, [\mathbb{L}^+, [\mathbb{L}^+, \mathbb{O}_j(0)]] \dots]}_{l-j+j_1+j_2-2} = (i\partial_+)^{l-j+j_1+j_2-2} \mathbb{O}_j(0), \quad (4.134)$$

to the vacuum state $\mathbb{O}_{jj}(0) \equiv \mathbb{O}_j(0)$. As it is clear from the commutation relations, the momentum generator \mathbb{P}^+ is a raising operator, while the special conformal generator \mathbb{K}^- is a lowering operator, see Fig. 31. The dilatation \mathbb{D} and the Lorentz \mathbb{M}^{-+} generators are diagonal operators. Then the infinitesimal variations of the conformal operators under the light-cone algebra are

$$\begin{aligned} \delta^P \mathbb{O}_{jl} &= i[\mathbb{O}_{jl}, \mathbb{P}^+] = i\mathbb{O}_{jl+1}, \\ \delta^M \mathbb{O}_{jl} &= i[\mathbb{O}_{jl}, \mathbb{M}^{-+}] = -(l+s_1+s_2)\mathbb{O}_{jl}, \\ \delta^D \mathbb{O}_{jl} &= i[\mathbb{O}_{jl}, \mathbb{D}] = -(l+d_1+d_2)\mathbb{O}_{jl}, \\ \delta^K \mathbb{O}_{jl} &= i[\mathbb{O}_{jl}, \mathbb{K}^-] = i a(j, l) \mathbb{O}_{jl-1}, \end{aligned} \quad (4.135)$$

with

$$a(j, l) = 2(j-l)(j+l+2j_1+2j_2-1). \quad (4.136)$$

Since the conformal spins of the elementary fields coincide $j_1 = j_2$ for all phenomenologically interesting bilocal composite operators, the Jacobi polynomials can be reduced to the Gegenbauer polynomials C_k^ν :

$$P_k^{(\nu-1/2, \nu-1/2)}(x) = \frac{(\nu+1/2)_k}{(2\nu)_k} C_k^\nu(x), \quad (4.137)$$

where $(a)_n \equiv \Gamma(a+n)/\Gamma(a)$ is the Pochhammer symbol. The operators built from the same elementary fields and containing Gegenbauer polynomials in light-cone derivatives will be referred to as conformal operators, just like the operators given by Eq. (4.132). This will not lead to a confusion since we are not going to discuss the mixed-field operators in this review. Thus, we introduce the quark and gluon conformal operators,

$$\mathbb{O}_{jl}^{qq} = \bar{\psi}(i\partial^+)^l \gamma^+ C_j^{3/2} \left(\vec{\mathcal{D}}^+/\partial^+ \right) \psi, \quad \mathbb{O}_{jl}^{gg} = F^+_\mu(i\partial^+)^{l-1} C_{j-1}^{5/2} \left(\vec{\mathcal{D}}^+/\partial^+ \right) F^{\mu+}, \quad (4.138)$$

and analogously for other Dirac and Lorentz structures.

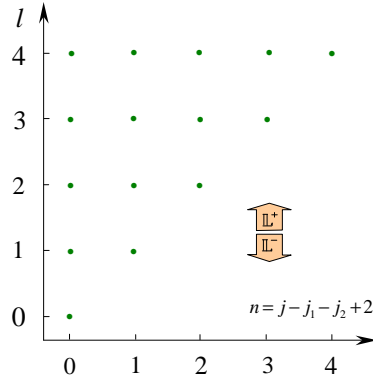


Figure 31: The tower of conformal operators is generated by the step-up operator \mathbb{L}^+ from the lowest weights \mathbb{O}_{jj} for different eigenvalues of the conformal spin j . The generator of the conformal boost \mathbb{L}^- serves as a step-down operator and decreases the Lorentz spin l of operators within a tower with the same conformal spin j .

4.6.3 Autonomous renormalization of conformal operators

An operator which generates finite Green functions with products of elementary field operators at different space-time positions is called the subtracted operator and it is defined as

$$\mathbb{O}_{jl}^R = \sum_{k=0}^j \mathcal{Z}_{jk} \mathbb{O}_{kl}. \quad (4.139)$$

From this definition, one immediately finds that it obeys the renormalization group equation

$$\frac{d}{d \ln \mu} \mathbb{O}_{jl}^R = - \sum_{k=0}^j \gamma_{jk}(g) \mathbb{O}_{kl}^R. \quad (4.140)$$

The matrix of anomalous dimensions²⁵ $\gamma_{jk}(g)$ possesses a triangular form as a consequence of the Lorentz invariance, i.e., only operators with the same number of derivatives can mix, so that $\gamma_{jk} \neq 0$ for $j \geq k$, or explicitly

$$\gamma_{jk} = \begin{pmatrix} \gamma_{jj} & \cdots & \gamma_{j0} \\ & \ddots & \vdots \\ 0 & & \gamma_{00} \end{pmatrix} \equiv \gamma_j \delta_{jk} + \gamma_{jk}^{ND} \theta_{jk}, \quad (4.141)$$

with the diagonal elements $\gamma_j \equiv \gamma_{jj}$ and non-diagonal elements separated from them by means of the discrete step function $\theta_{jk} = \{1, j > k; 0, j \leq k\}$. The anomalous dimension matrix $\gamma_{jk}(g)$ receives an infinite series expansion in perturbation theory;

$$\gamma_{jk}(g) = \sum_{n=0}^{\infty} \left(\frac{\alpha_s}{2\pi} \right)^{n+1} \gamma_{(n)jk}. \quad (4.142)$$

These anomalous dimensions induce a shift in the scaling transformation of conformal operators (4.135), i.e.,

$$\delta^D \mathbb{O}_{jl} = - \sum_{k=0}^j \{(l + d_1 + d_2) \delta_{jk} + \gamma_{jk}\} \mathbb{O}_{kl}. \quad (4.143)$$

²⁵Notice that this matrix of anomalous dimensions is different from the one introduced in Eq. (4.90). They belong to different bases of states and only their diagonal elements $j = k$ are related to each other via Eq. (K.1).

At leading order of perturbation theory, there are no counterterms for the renormalization of the coupling constant, so there are no sources of special conformal symmetry breaking in one-loop anomalous dimensions. Therefore, in this approximation the tree form of the conformal boost is preserved. The commutation relation between the dilatation and special conformal transformations then immediately leads to the following condition

$$0 = [\delta^D, \delta^K] \mathbb{O}_{jl} - \delta^K \mathbb{O}_{jl} = -i \sum_{k=1}^j \{a(j, l) - a(k, l)\} \gamma_{(0)jk} \mathbb{O}_{jl-1} = -i \sum_{k=1}^j a(j, k) \gamma_{(0)jk} \mathbb{O}_{jl-1}.$$

This imposes a constraint on the one-loop anomalous dimension matrix

$$a(j, k) \gamma_{(0)jk} = 0. \quad (4.144)$$

Since $a(j, k) \neq 0$ for $j \neq k$, the matrix γ_{jk} does not possess non-diagonal elements, but because $a(j, j) = 0$ vanishes, it can have the diagonal ones: $\gamma_{(0)jk} = \gamma_{(0)j} \delta_{jk}$. This means that conformal operators with different conformal spins do not mix with each other at leading order of perturbation theory supporting the observation made earlier. The constraint (4.144) implies that the anomalous dimensions depend only on the conformal spin, but it gives no restrictions on the form of the diagonal elements. As we already anticipate, the diagonal elements can be identified with the anomalous dimensions of Wilson operators (without total derivatives) which appear in the QCD description of the cross section of deeply inelastic scattering, which we addressed in Section 4.4.3. A slight difference in their normalization will be addressed in the subsequent section. This result also implies that the perturbative expansion of non-diagonal anomalous dimensions starts at two-loop order only

$$\gamma_{jk}^{\text{ND}} = \left(\frac{\alpha_s}{2\pi}\right)^2 \gamma_{(1)jk}^{\text{ND}} + \mathcal{O}(\alpha_s^3). \quad (4.145)$$

So far we gave a generic discussion of the mixing pattern of conformal operators \mathbb{O} in perturbation theory. As we know in the singlet sector it is the two-vector

$$\mathbf{O}_{jl} \equiv \begin{pmatrix} \mathbb{O}_{jl}^{qq} \\ \mathbb{O}_{jl}^{gg} \end{pmatrix}, \quad (4.146)$$

of the quark and gluon operators (4.138), which participates in the renormalization group evolution. It obeys the matrix equation

$$\frac{d}{d \ln \mu} \mathbf{O}_{jl} = - \sum_k \boldsymbol{\gamma}_{jk}(g) \mathbf{O}_{kl}, \quad (4.147)$$

with the two-by-two matrix of anomalous dimensions

$$\boldsymbol{\gamma}_{jk} = \begin{pmatrix} \gamma_{jk}^{qq} & \gamma_{jk}^{qg} \\ \gamma_{jk}^{gq} & \gamma_{jk}^{gg} \end{pmatrix}. \quad (4.148)$$

Each of its γ_{jk}^{ab} four elements $ab = qq, qg, gq, gg$ is of the triangular form (4.141).

4.7 Diagonalization of generalized evolution kernels

Our preceding discussion indicates that the generalized evolution kernels are diagonalizable in the basis of Gegenbauer polynomials, i.e., the two-by-two matrix of kernels can be cast in the form

$$K_{(0)}^{ab}(x_1, x_2 | y_1, y_2) = \frac{1}{2} \sum_{j=(0,1)}^{\infty} \tilde{P}_j^a(x_1, x_2) \gamma_{(0)j}^{ab} P_j^b(y_1, y_2), \quad (4.149)$$

where the two-vectors P^a ($a = q, g$) of Gegenbauer polynomials and their conjugate are

$$P_j^a(x_1, x_2) = \begin{pmatrix} C_j^{3/2} \left(\frac{x_1 - x_2}{x_1 + x_2} \right) \\ C_{j-1}^{5/2} \left(\frac{x_1 - x_2}{x_1 + x_2} \right) \end{pmatrix}, \quad \tilde{P}_j^a(x_1, x_2) = \begin{pmatrix} \frac{x_1 x_2}{n_j(\frac{3}{2})} C_j^{3/2} \left(\frac{x_1 - x_2}{x_1 + x_2} \right) \\ \frac{x_1^2 x_2^2}{n_{j-1}(\frac{5}{2})} C_{j-1}^{5/2} \left(\frac{x_1 - x_2}{x_1 + x_2} \right) \end{pmatrix}, \quad (4.150)$$

with the normalization factor being

$$n_j(\nu) = 2^{1-4\nu} \frac{\Gamma^2(1/2)\Gamma(2\nu+j)}{\Gamma^2(\nu)\Gamma(j+1)(\nu+j)}. \quad (4.151)$$

The low $j = 0$ limit in the series (4.149) stands for the quark-quark sector and $j = 1$ for the rest. The one-loop anomalous dimensions, deduced from the generalized evolution kernels from Section 4.4.1, are

- Even-parity sector [241, 242, 235, 253]:

$$\gamma_{(0)j}^{qg;V} = -C_F \left(-4\psi(j+2) + 4\psi(1) + \frac{2}{(j+1)(j+2)} + 3 \right), \quad (4.152)$$

$$\gamma_{(0)j}^{gg;V} = -24N_f T_F \frac{j^2 + 3j + 4}{j(j+1)(j+2)(j+3)}, \quad (4.153)$$

$$\gamma_{(0)j}^{gq;V} = -C_F \frac{j^2 + 3j + 4}{3(j+1)(j+2)}, \quad (4.154)$$

$$\gamma_{(0)j}^{gg;A} = -C_A \left(-4\psi(j+2) + 4\psi(1) + 8 \frac{j^2 + 3j + 3}{j(j+1)(j+2)(j+3)} - \frac{\beta_0}{C_A} \right). \quad (4.155)$$

- Odd-parity sector [256, 235, 253]:

$$\gamma_{(0)j}^{qg;A} = -C_F \left(-4\psi(j+2) + 4\psi(1) + \frac{2}{(j+1)(j+2)} + 3 \right), \quad (4.156)$$

$$\gamma_{(0)j}^{gg;A} = -24N_f T_F \frac{1}{(j+1)(j+2)}, \quad (4.157)$$

$$\gamma_{(0)j}^{gq;A} = -C_F \frac{j(j+3)}{3(j+1)(j+2)}, \quad (4.158)$$

$$\gamma_{(0)j}^{gg;A} = -C_A \left(-4\psi(j+2) + 4\psi(1) + \frac{8}{(j+1)(j+2)} - \frac{\beta_0}{C_A} \right). \quad (4.159)$$

- Maximal-helicity sector [233, 73]:

$$\gamma_{(0)j}^{qq;T} = -C_F (-4\psi(j+2) + 4\psi(1) + 3) , \quad (4.160)$$

$$\gamma_{(0)j}^{gg;T} = -C_A (-4\psi(j+2) + 4\psi(1)) + \beta_0 . \quad (4.161)$$

The anomalous dimensions depend on the Euler ψ -function which is expressed in terms of the harmonic numbers

$$\psi(n) = \frac{d}{dn} \ln \Gamma(n) = \psi(1) + \sum_{k=1}^{n-1} \frac{1}{k} , \quad (4.162)$$

with the Euler constant $\gamma_E = -\psi(1) \approx 0.577216$.

4.7.1 Normalization of anomalous dimensions

The difference of the off-diagonal entries $a \neq b$, displayed in Eqs. (4.152) – (4.161), from the forward anomalous dimensions (4.67) can be understood as follows. When one sandwiches the conformal operators \mathbb{O}_{jj} in forward matrix elements, only the term which has no total derivatives ∂^+ is relevant. Thus, one needs the leading term of Gegenbauer polynomials at large arguments, namely,

$$C_j^\nu(x) = c_j^\nu x^j + \mathcal{O}(x^{j-1}) , \quad (4.163)$$

where the coefficient is

$$c_j^\nu = \frac{2^{1-2\nu-j} \sqrt{\pi} \Gamma(2\nu+2j)}{\Gamma(j+1) \Gamma(\nu) \Gamma(\frac{1}{2}+\nu+j)} . \quad (4.164)$$

The ratio of these coefficients for quark and gluon sectors is therefore

$$\frac{c_j^{3/2}}{c_{j-1}^{5/2}} = \frac{3}{j} . \quad (4.165)$$

Keeping only the contributions surviving in the forward limit, we thus get for the quark and gluon (vector) conformal operators,

$$\mathbb{O}_{jj}^{qq} = 2^j c_j^{3/2} \bar{\psi} \gamma^+ (i\mathcal{D}^+)^j \psi + \dots , \quad \mathbb{O}_{jj}^{gg} = 2^{j-1} c_{j-1}^{5/2} F^{+\mu} (i\mathcal{D}^+)^{j-1} F_\mu^+ + \dots . \quad (4.166)$$

Here the covariant derivative \mathcal{D}^μ acts on the right and the ellipses denote terms containing total derivatives. Therefore, substituting (4.166) into Eq. (4.147), keeping the leading term only and matching it into the renormalization group equation for forward Wilson operators, we find that the forward anomalous dimensions introduced in Eq. (4.67) are related to the diagonal eigenvalues via

$$\gamma_j^{gg;\text{fw}} = \frac{j}{6} \gamma_j^{qq} , \quad \gamma_j^{gq;\text{fw}} = \frac{6}{j} \gamma_j^{qq} . \quad (4.167)$$

This explains the difference in their normalization.

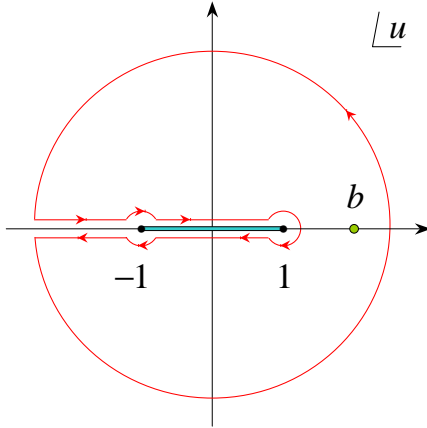


Figure 32: The integration contour for the evaluation of the integral (4.173). There is a n -th order pole in the point $u = b$ and the cut on the real axis from -1 to 1 .

4.7.2 Inclusive to exclusive reconstruction at leading order

In Section 4.4.4, we have already obtained the one-loop ER-BL evolution kernels analytically by taking the appropriate limit of generalized evolution kernels. As the formula (4.149) suggests the diagonal part (in the basis of the Gegenbauer polynomials) of the exclusive kernels can be reconstructed directly from the corresponding DGLAP analogues. The result of this reconstruction can be found analytically, at least at leading order.

The formal expression for the diagonal part of the leading order exclusive kernel admits the form identical to (4.149),

$$V_{(0)}(x, y) = -\frac{1}{2} \sum_{j=0}^{\infty} \frac{w(x|\nu)}{n_j(\nu)} C_j^\nu(2x-1) \gamma_{(0)j} C_j^\nu(2y-1), \quad (4.168)$$

where $\gamma_{(0)j}$'s are the leading order anomalous dimensions of the conformal operators, $w(x|\nu)$ is the weight factor

$$w(x|\nu) = (x\bar{x})^{\nu-1/2},$$

and $n_j(\nu)$ is the normalization factor (4.151).

Therefore, the main problem is to perform the infinite summation and construct a generating function for the exclusive evolution kernels. This goal can be achieved in two straightforward steps.

- Use the Gegenbauer's summation theorem [257],

$$\begin{aligned} & \frac{1}{n_j(\nu)} C_j^\nu(2x-1) C_j^\nu(2y-1) \\ &= 2^{2\nu} (\nu + j) \int_0^\pi \frac{d\phi}{\pi} (\sin \phi)^{2\nu-1} C_j^\nu((2x-1)(2y-1) + 4\sqrt{x\bar{x}y\bar{y}} \cos \phi). \end{aligned} \quad (4.169)$$

- Multiply both sides of Eq. (4.169) by $w(x|\nu)z^j$ and sum over j . On the right-hand side of the summation theorem, use the formula for the generating function of the Gegenbauer polynomials

$$\sum_{j=0}^{\infty} z^j C_j^\nu(a) = (1 - 2az + z^2)^{-\nu}. \quad (4.170)$$

To perform the summation, represent the “contaminating factor” $(\nu + j)$ by the differential operator $(\nu + z\partial_z)$.

Finally, changing the integration variable to $\cos\phi \equiv u$, we get the generating function for reconstruction of the exclusive kernels from the inclusive ones,

$$\begin{aligned}\mathcal{G}(z, \nu | x, y) &\equiv \sum_{j=0}^{\infty} \frac{w(x|\nu)}{n_j(\nu)} C_j^\nu(2x-1) z^j C_j^\nu(2y-1) \\ &= 2^{2\nu} \frac{\nu}{\pi} (x\bar{x})^{\nu-\frac{1}{2}} \int_{-1}^1 du (1-u^2)^{\nu-1} \frac{(1-z^2)}{[1-2a(u)z+z^2]^{\nu+1}},\end{aligned}\quad (4.171)$$

where

$$a(u) \equiv (2x-1)(2y-1) + 4u\sqrt{x\bar{x}y\bar{y}}. \quad (4.172)$$

In order to find an ER-BL evolution kernel, we have to convolute the equality (4.171) with the corresponding DGLAP splitting function and evaluate the integral on the right-hand side of this equation. Performing the external integration first leads to the integrand which is an elementary function of u . The remaining integral over u can be evaluated by considering its analytical continuation to the whole complex plane and choosing the integration contour as displayed in Fig. 32. The calculation reduces to the evaluation of the residues of the n -th order pole at the point $u = b \equiv (1 - (2x-1)(2y-1))/4\sqrt{x\bar{x}y\bar{y}}$ and at the point $u = \infty$. The final result is

$$J_n \equiv \int_{-1}^1 du \frac{\sqrt{1-u^2}}{(u-b)^n} = \pi \{ \text{res}_{u=b} + \text{res}_{u=\infty} \} \frac{\sqrt{u^2-1}}{(u-b)^n}. \quad (4.173)$$

The first residue provides a contribution proportional to difference of θ -functions, while the second one to their sum. Namely, for the $n = 1, 2$ which appear in the transformation of the one-loop splitting functions we get

$$\text{res}_{u=b} \frac{\sqrt{u^2-1}}{(u-b)^n} = \begin{cases} \frac{1}{2} \frac{y-x}{\sqrt{x\bar{x}y\bar{y}}} [\theta(y-x) - \theta(x-y)], & \text{for } n = 1 \\ \frac{1}{2} \frac{1-(2x-1)(2y-1)}{y-x} [\theta(y-x) - \theta(x-y)], & \text{for } n = 2 \end{cases}, \quad (4.174)$$

and

$$\text{res}_{u=\infty} \frac{\sqrt{u^2-1}}{(u-b)^n} = \begin{cases} -\frac{1}{4} \frac{1-(2x-1)(2y-1)}{\sqrt{x\bar{x}y\bar{y}}} [\theta(y-x) + \theta(x-y)], & \text{for } n = 1 \\ -[\theta(y-x) + \theta(x-y)], & \text{for } n = 2 \end{cases}. \quad (4.175)$$

For instance, for the qq -kernel $P_{(0)}^{qq;V}(z) = (1+z^2)/(1-z)$ with $z > 0$, we have

$$\pi \int_0^1 dz P_{(0)}^{qq;V}(z) \mathcal{G}(z, \frac{3}{2} | x, y) = \frac{1}{2y\bar{y}} J_2 - \sqrt{\frac{x\bar{x}}{y\bar{y}}} J_1, \quad (4.176)$$

where

$$J_1 = -\frac{\pi}{\sqrt{x\bar{x}y\bar{y}}} \{x\bar{y}\theta(y-x) + y\bar{x}\theta(x-y)\}, \quad (4.177)$$

$$J_2 = 2\pi \left\{ \frac{x\bar{y}}{y-x} \theta(y-x) + \frac{y\bar{x}}{x-y} \theta(x-y) \right\}, \quad (4.178)$$

which indeed coincides with the well-known result (4.77). Analogous calculations can be done for other channels. No additional subtleties arise there.

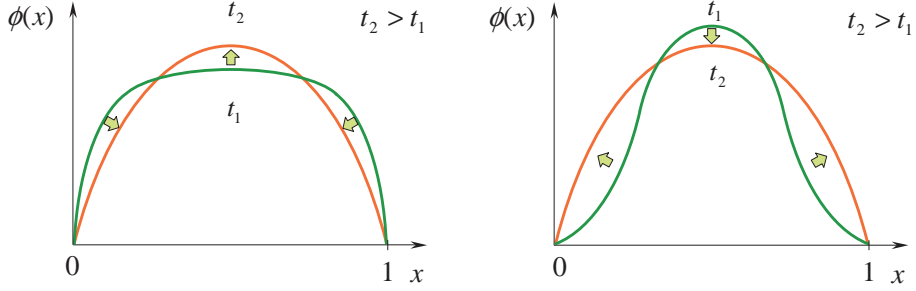


Figure 33: At very large renormalization scales a distribution amplitude is driven to its asymptotic form $(x\bar{x})^{2j-1}$.

4.8 Asymptotic distribution amplitudes

The solution to the evolution equation of a two-particle distribution amplitude can be written in the form of the conformal partial wave expansion

$$\phi(x; \mu^2) = \sum_{j=(0,1)}^{\infty} \frac{w(x|\nu)}{n_j(\nu)} C_j^\nu(2x-1) \left(\frac{\alpha(\mu_0^2)}{\alpha(\mu^2)} \right)^{\gamma_{(0)} j / \beta_0} \int_0^1 dy C_j^\nu(2y-1) \phi(y; \mu_0^2).$$

The index of the Gegenbauer polynomial is related to the conformal spin of the constituent fields $\nu_a = 2j_a - 1$, it is either $\nu_q = 3/2$ for quarks or $\nu_g = 5/2$ for gluons. The first term in the series is $j = 0(1)$ for quarks (gluons). Since the anomalous dimensions are positive, $\gamma_j > 0$ for $j > 0$, and growing with increasing j , only the lowest term of the infinite series can be kept in the asymptotic limit $\mu^2 \rightarrow \infty$

$$\phi(x; \mu^2 \rightarrow \infty) = a_0(\mu^2) (x(1-x))^{\nu-1/2}.$$

Actually, due to the conservation of the non-singlet quark current, $\gamma_0^{qq} = 0$ and this equality is exact since the lowest term does not depend on the renormalization point, $a_0 = \text{const}$. Thus, the functional form of the distribution amplitude is unambiguously fixed by applying the consequences of the conformal symmetry. The only unknown parameter left is the nonperturbative coefficient c_0 . The general trend of the evolution of an input distribution amplitude with increasing “time” $t = \ln \mu^2$ is demonstrated in Fig. 33. Analogous considerations can be used for multiparticle distribution amplitudes, with the result

$$\phi(x_1, x_2, \dots, x_N; \mu^2 \rightarrow \infty) = c(\mu^2) \prod_{k=1}^N x_k^{2j_k-1},$$

where j_k is the conformal spin of the k th constituent. However, in the present circumstances there are no symmetry reasons prohibiting the lowest operator from developing a nonzero anomalous dimension. Therefore, the coefficient c continues to evolve even in the asymptotic limit. The accuracy of representing the large- μ^2 behavior of distribution amplitudes by the lowest-order term only is determined by the ratio of the lowest and the next-to-lowest anomalous dimensions.

4.9 Conformal symmetry breaking

The conformal symmetry is not a quantum symmetry of QCD. Out of the fifteen-parameter group only its Poincaré subgroup survives when quantum corrections are taken into account. The

currents associated with dilatation and four conformal boosts are no longer conserved. This is a direct consequence of the dimensional transmutation in QCD according to which the quantum theory generates an intrinsic scale related to ultraviolet divergences. These divergences cause the QCD coupling constant to depend on this scale and change when the ultraviolet cutoff is varied. Therefore, since the conformal symmetry ensured the multiplicative renormalizability of conformal operators at leading order, in full quantum theory they will start to mix with each other. Thus, the mixing arises beyond leading order of perturbation theory as we pointed out in Eq. (4.145).

Moreover, there is yet another very subtle (scheme-dependent) source of the conformal symmetry breaking due to the very necessity of a regularization which makes the very calculation possible. The only regularization scheme implemented in QCD perturbation theory²⁶ which preserves the non-abelian gauge invariance to all orders in coupling constant is dimensional regularization and its off-springs like dimensional reduction. In these approaches, the coupling constant becomes *dimensionful* when one goes away from four-dimensional space-time $d \neq 4$, and one can expect the conformal symmetry breaking effects in renormalization of operators. It should be emphasized that the conformal invariance of the theory is destroyed even when the four-dimensional beta-function vanishes identically, since the d -dimensional function has a two-component form

$$\beta_\varepsilon(g) = -\varepsilon g + \beta(g) .$$

The first source is nonvanishing for $d \neq 4$ even if $\beta(g) = 0$. This breaking will be encoded below into the so-called special conformal anomaly matrix γ^c .

A very efficient formalism for computing higher order anomalous dimensions of conformal operators consists of a few straightforward steps relying on the following observations, some of which were established and spelled out earlier:

- The triangularity of the anomalous dimension matrix γ_{jk} implies that its eigenvalues are given by the diagonal elements and coincide with the well-known forward anomalous dimensions.
- Tree-level special conformal invariance implies that the leading order mixing matrix is diagonal. One-loop violation of the symmetry induces non-diagonal elements. Thus, the one-loop special conformal anomaly will generate two-loop anomalous dimensions.
- Scale Ward identity for the Green function with conformal operator insertion is known to be with the Callan-Symanzik equation for the latter, and thus the dilatation anomaly is the anomalous dimension of the composite operator

$$\mathbb{O}_j^R \int d^d z \Theta^\mu{}_\mu(z) \sim \sum_{k=0}^j \gamma_{jk} \mathbb{O}_k^R . \quad (4.179)$$

- The four-dimensional conformal algebra provides a relation between the anomalies of dilatation and special conformal transformations via the commutator $[\mathbb{D}, \mathbb{K}^-] = i\mathbb{K}^-$. Using the latter, one can deduce the form of the two-loop non-diagonal elements γ_{jk}^{ND} [253].

²⁶We exclude lattice regularization because it is not very convenient to use in continuous perturbative computations.

4.9.1 Anomaly in the trace of energy momentum tensor

In order to write down conformal Ward identities, one has to know the infinitesimal variation of the action in the regularized theory under the conformal symmetry. Since the dilation and the special conformal symmetry do not survive the regularization, the change of the action under these transformations will be nonvanishing. To simplify the derivation it is instructive to use the following generic variations of the Lagrangian under the \mathbb{D} and \mathbb{K}^μ transformations

$$\delta^D \mathcal{L}[\Phi] = -\partial^\mu (z_\mu \mathcal{L}[\Phi]) + d \mathcal{L}[\Phi] - d_\Phi \frac{\partial \mathcal{L}[\Phi]}{\partial \Phi} \Phi - (d_\Phi + 1) \frac{\partial \mathcal{L}[\Phi]}{\partial (\partial_\mu \Phi)} \partial_\mu \Phi, \quad (4.180)$$

$$\begin{aligned} \delta^K \mathcal{L}[\Phi] &= -\partial^\mu ((2z_\mu z_\nu - z^2 g_{\mu\nu}) \mathcal{L}[\Phi]) + 2x_\nu \left(d \mathcal{L}[\Phi] - d_\Phi \frac{\partial \mathcal{L}[\Phi]}{\partial \Phi} \Phi - (d_\Phi + 1) \frac{\partial \mathcal{L}[\Phi]}{\partial (\partial_\mu \Phi)} \partial_\mu \Phi \right) \\ &\quad - 2d_\Phi \frac{\partial \mathcal{L}[\Phi]}{\partial (\partial_\nu \Phi)} \Phi + 2i \frac{\partial \mathcal{L}[\Phi]}{\partial (\partial_\mu \Phi)} \Sigma_{\nu\mu} \Phi. \end{aligned} \quad (4.181)$$

Applying them to the dimensionally regularized $d = 4 - 2\varepsilon$ QCD Lagrangian in the covariant gauge (G.23), with the following assignment of scaling dimensions $d_g = 1$, $d_q = 3/2$, $d_{\bar{\omega}} = d - 2$ and $d_\omega = 0$ to the gluon, quark and ghost fields, respectively, one finds that the conformal variation of the action can be expressed by well classified operators: gauge invariant operators \mathcal{O}_A , BRST exact operators \mathcal{O}_B , and equation of motion (EOM) operators Ω . A further advantage of the chosen set of scale dimensions is that it allows one to use the Jackiw's conformal covariant transformation law for gauge fields [258]. The final result of the calculation can be written as

$$\delta^D S_{\text{QCD}} = \int d^d z \Delta(z), \quad \delta^K S_{\text{QCD}} = \int d^d z 2z_\mu \Delta(z), \quad (4.182)$$

where the integrand $\Delta(x)$ is expressed in terms of the regularized but unrenormalized trace anomaly of the energy-momentum tensor $\Theta_{\mu\nu}$ (E.6):

$$\begin{aligned} \Delta(z) &= -\Theta^\mu_\mu(z) - d_g \Omega_g(z) - d_q \Omega_{\bar{q}q}(z) - d_{\bar{\omega}} \Omega_{\bar{\omega}}(z) \\ &= \varepsilon \{ \mathcal{O}_A(z) + \mathcal{O}_B(z) + \Omega_{\bar{\omega}}(z) - \Omega_{\bar{q}q}(z) \} + (d - 2) \partial^\mu \mathcal{O}_{B\mu}(z). \end{aligned} \quad (4.183)$$

Here we introduced the following set of gauge invariant and BRST-exact operators

$$\mathcal{O}_A = \frac{\mathcal{Z}_3}{2} F_{\mu\nu}^a F^{a\mu\nu}, \quad \mathcal{O}_B = \frac{\delta^{\text{BRST}}}{\delta \lambda} \bar{\omega}^a \partial^\mu A_\mu^a, \quad \mathcal{O}_{B\mu} = \frac{\delta^{\text{BRST}}}{\delta \lambda} \bar{\omega}^a A_\mu^a, \quad (4.184)$$

as well as EOM operators

$$\Omega_g = A_\mu^a \frac{\delta S}{\delta A_\mu^a}, \quad \Omega_{\bar{q}q} = \frac{\delta S}{\delta \psi} \psi + \bar{\psi} \frac{\delta S}{\delta \bar{\psi}}, \quad \Omega_{\bar{\omega}} = \bar{\omega}^a \frac{\delta S}{\delta \bar{\omega}^a}. \quad (4.185)$$

It is desirable to express the variations of the action (4.182) in terms of renormalized (via the modified minimal subtraction scheme) operators as this allows one to neglect contributions proportional to the dimensional-regularization parameter ε . For this reason, one should solve the renormalization problem of the above mentioned operators [259]. A straightforward analysis yields [253]

$$\mathcal{O}_A^R(z) = \left(1 + g \frac{\partial \ln \mathcal{Z}_c}{\partial g} \right) \mathcal{O}_A(z) + \left(g \frac{\partial \ln \mathcal{X}}{\partial g} - 2\xi \frac{\partial \ln \mathcal{X}}{\partial \xi} \right) \{ \mathcal{O}_B(z) + \Omega_{\bar{\omega}}(z) + \Omega_g(z) \}$$

$$+ \left(g \frac{\partial \ln \tilde{\mathcal{Z}}_3}{\partial g} - 2\xi \frac{\partial \ln \tilde{\mathcal{Z}}_3}{\partial \xi} \right) \Omega_{\bar{\omega}}(z) + \frac{1}{2} \left(g \frac{\partial \ln \tilde{\mathcal{Z}}_2}{\partial g} - 2\xi \frac{\partial \ln \tilde{\mathcal{Z}}_2}{\partial \xi} \right) \Omega_{\bar{q}q}(z), \quad (4.186)$$

$$\begin{aligned} \mathcal{O}_B^R(z) = & \left(1 + 2\xi \frac{\partial \ln \mathcal{X}}{\partial \xi} \right) \mathcal{O}_B(z) + 2\xi \frac{\partial \ln \mathcal{X}}{\partial \xi} \left\{ \Omega_g(z) + \Omega_{\bar{\omega}}(z) \right\} + \xi \frac{\partial \ln \tilde{\mathcal{Z}}_2}{\partial \xi} \Omega_{\bar{q}q}(z) \\ & + 2\xi \frac{\partial \ln \tilde{\mathcal{Z}}_3}{\partial \xi} \Omega_{\bar{\omega}}(z), \end{aligned} \quad (4.187)$$

where the charge renormalization constant is $\mathcal{Z}_c = \mathcal{X} \mathcal{Z}_3^{-1/2}$ (see Eq. (G.24)). Thus, inserting these findings into Eq. (4.183) we obtain the renormalized anomaly in the trace of the energy-momentum tensor in $d = 4 - 2\varepsilon$ dimensions

$$\begin{aligned} \Theta^\mu{}_\mu(z) = & \frac{\beta_\varepsilon}{g} \mathcal{O}_A^R(z) + \left(\frac{\beta_\varepsilon}{g} - \gamma_g \right) \left\{ \mathcal{O}_B^R(z) + \Omega_{\bar{\omega}}(z) \right\} - \left(d_g + \gamma_g - \frac{\beta}{g} \right) \Omega_g(z) \\ & - (d_q + \gamma_q - \varepsilon) \Omega_{\bar{q}q}(z) - (d_{\bar{\omega}} + 2\gamma_{\bar{\omega}}) \Omega_{\bar{\omega}}(z) - (d-2) \partial^\mu \mathcal{O}_{B\mu}^R(z). \end{aligned} \quad (4.188)$$

We cannot set $\varepsilon = 0$ yet since $\Theta^\mu{}_\mu$ will enter in a product with the conformal operator into dilatation and special conformal Ward identities and this product contains short distance singularities which once regularized by means of dimensional regularization produce poles in $1/\varepsilon$. The latter will compensate $\mathcal{O}(\varepsilon)$ terms in $\Theta^\mu{}_\mu$ and result into finite contributions. After subtraction of the poles, the finite part generates the dilatation (see Eq. (4.179) and Eq. (4.190) below) and special conformal anomalies (see Eq. (4.191) below).

4.9.2 Conformal Ward identities

Having found the form of the variations δS_{QCD} , we can now derive the dilatation and special conformal Ward identities. It is well known that the Ward identity for the dilatation operator is the Callan-Symanzik equation,

$$\begin{aligned} \sum_k^L (d_k^{\text{can}} + z_k \cdot \partial_k) \langle \mathbb{O}_{jl}^R \Phi(z_1) \dots \Phi(z_L) \rangle & \equiv - \langle \mathbb{O}_{jl}^R \delta^D (\Phi(z_1) \dots \Phi(z_L)) \rangle \\ & = \langle (\delta^D \mathbb{O}_{jl}^R) \Phi(z_1) \dots \Phi(z_L) \rangle + \langle \mathbb{O}_{jl}^R (i \delta^D S_{\text{QCD}}) \Phi(z_1) \dots \Phi(z_L) \rangle. \end{aligned} \quad (4.189)$$

Here in the first line, we used the definition of the infinitesimal form (I.10) of the scale transformation (I.25) and, in the second line, we integrated by parts in the functional integral such that the variation is moved from the field monomial $\Phi(z_1) \dots \Phi(z_L)$ on the conformal operator and the weight of the functional measure $\exp(iS_{\text{QCD}})$. In quantum theory the Ward identity thus develops an extra term in its right-hand side due to nonvanishing variation of the regularized QCD action $\delta^D S_{\text{QCD}}$. This generates an anomaly which arises from the renormalization of the product of two composite operators: the conformal operator and the trace anomaly in the energy-momentum tensor (4.182) – (4.183),

$$\mathbb{O}_{jl}^R (\delta^D S_{\text{QCD}}) = i \sum_{k=0}^j \gamma_{jk} \mathbb{O}_{kl}^R + \dots. \quad (4.190)$$

One can see that the canonical dimension $d_j^{\text{can}} = j + 2d_\Phi$ of the conformal operator \mathbb{O}_j gets modified by the anomalous dimension,

$$d_j^{\text{can}} \rightarrow d_j^{\text{can}} + \gamma_{jj},$$

however, it also induces the mixing of conformal operators starting at two-loop order. On the other hand, in the Ward identity for the special conformal transformation, there is an anomaly that appears from the renormalization of an analogous product,

$$\mathbb{O}_{k,l}^R(\delta_-^K S_{\text{QCD}}) = \sum_{k=0}^j \gamma_{jk}^c(l) \mathbb{O}_{k,l-1}^R + \dots \quad (4.191)$$

Here $\gamma_{jk}^c(l)$ is the special conformal anomaly. It satisfies the following condition

$$\gamma_{jj}^c(j) = 0, \quad (4.192)$$

(no summation over j) which is an obvious consequence of the absence of the counterterm in Eq. (4.191) for $l = j$. Note, that $\gamma^c \neq \gamma$, so that the dilatation and special conformal symmetries are broken differently. However, their anomalies satisfy a constraint which we are going to discuss next.

4.9.3 Commutator constraints for conformal anomalies

In order to establish relations between anomalous dimensions and special conformal anomalies, one has to resort to the commutators between corresponding generators from the conformal algebra. The symbolic form of the action of the dilatation and conformal boost²⁷, derived from the conformal Ward identities, is given by²⁸ [253]

$$[\mathbb{O}_{jl}^R(0), \mathbb{D}] = i[(l+2d)\delta_{jk} + \gamma_{jk}] \mathbb{O}_{kl}^R(0) - \left[\mathbb{O}_{jl}(0) \int d^4z \Theta^\mu{}_\mu(z) \right]^R + \dots, \quad (4.193)$$

$$[\mathbb{O}_{jl}^R(0), \mathbb{K}^-] = [a(j,l)\delta_{jk} + \gamma_{jk}^c(l)] \mathbb{O}_{kl-1}^R - \left[\mathbb{O}_{jl}(0) \int d^4z 2z^- \Theta^\mu{}_\mu(z) \right]^R + \dots, \quad (4.194)$$

where the ellipses stand for the “unphysical” sector. Both of these transformations laws are valid to all orders in perturbation theory and can be used for finding relations between γ and γ^c [235, 253].

- The first of these constraints stems from the commutator $[\mathbb{D}, \mathbb{K}^\mu] = i\mathbb{K}^\mu$. It readily yields a matrix equation which reads at the conformal point $\beta(g^*) = 0$

$$[a(l) + \gamma^c(l), \gamma] = 0. \quad (4.195)$$

It is an extension of Eq. (4.144) to all orders of perturbation theory. Here the constant matrix $a_{jk}(l) = \delta_{jk}a(j,l)$ is a remnant of the leading order conformal boost of the conformal operators (4.135). This relation can be easily derived using Eqs. (4.193) and (4.194). From this constraints, one can draw very important conclusions. One immediately realizes that even at this conformal point, the modified minimal subtraction scheme, used for subtraction of UV divergences, breaks explicitly the conformal covariance, i.e., it leads to mixing of conformal operators with different conformal spins, so that $\gamma_{jk}|_{j \neq k} \neq 0$.

In QCD, the coupling is running and this commutator constraint is promoted to [251, 253]

$$\left[a(l) + \gamma^c(l) + 2\frac{\beta}{g} b(l), \gamma \right] = 0, \quad (4.196)$$

²⁷They are understood as insertions into a Green function with field monomials, i.e., $\langle [\dots] \Phi(z_1) \dots \Phi(z_L) \rangle$.

²⁸Here and below we assume the summation over repeated indices.

with the four-dimensional β -function accompanied by a new matrix

$$b_{jk}(l) = \theta_{jk} \{ 2(l+k+3)\delta_{jk} - [1 + (-1)^{j-k}](2k+3) \}. \quad (4.197)$$

- Another equation between anomalies arises from the translation invariance in the form of the commutator $[\mathbb{K}^\mu, \mathbb{P}^\nu] = -2i(g^{\mu\nu}\mathbb{D} + \mathbb{M}^{\mu\nu})$ and implies a linear relation between the same anomalies [252, 253]

$$\gamma_{jk}^c(l+1) - \gamma_{jk}^c(l) = -2\gamma_{jk}. \quad (4.198)$$

It provides an identity between the diagonal elements of the special conformal anomaly matrix and diagonal elements $\gamma_{jj} = \gamma_j$ of the anomalous dimension matrix, namely,

$$\gamma_{jj}^c(l) = -2(l-j)\gamma_j. \quad (4.199)$$

Extension of Eq. (4.198) to the case of the running strong coupling is straightforward [252, 253]

$$\gamma_{jk}^c(l+1) - \gamma_{jk}^c(l) = -2 \left(\gamma_{jk} - 2\frac{\beta}{g}\delta_{jk} \right). \quad (4.200)$$

4.9.4 NLO constraint and non-diagonal anomalous dimensions

Equation (4.196) does not impose any constraints on the diagonal elements of the anomalous dimension matrix γ_{jj} since they merely cancel in the commutator, however, it does immediately imply a relation between the non-diagonal part of the elements of the two-loop anomalous dimension matrix $\gamma_{(1)jk}^{\text{ND}}$ in terms of the one-loop special conformal anomaly, β -function and one-loop anomalous dimensions [253],

$$a(j, k)\gamma_{(1)jk}^{\text{ND}} = (\gamma_{(0)j} - \gamma_{(0)k})(\gamma_{(0)jk}^c + \beta_0 b_{jk}). \quad (4.201)$$

Here the one-loop special conformal anomaly was deduced to one-loop order from Eqs. (4.191) to be of the form

$$\gamma_{(0)jk}^c = -b_{jk}\gamma_{(0)k} + w_{jk} = a(j, k)(-d_{jk}\gamma_{(0)k} + g_{jk}), \quad (4.202)$$

where the explicit form of the matrix g_{jk} will be given below.

The generic expression (4.201) can be used to find the NLO non-diagonal anomalous dimensions for the singlet sector [253] and represented as

$$\begin{aligned} \gamma_{(1)jk}^{qq,\text{ND}} &= \left(\gamma_{(0)j}^{qq} - \gamma_{(0)k}^{qq} \right) \left\{ d_{jk} \left(\beta_0 - \gamma_{(0)k}^{qq} \right) + g_{jk}^{qq} \right\} - \left(\gamma_{(0)j}^{qq} - \gamma_{(0)k}^{qq} \right) d_{jk} \gamma_{(0)k}^{qq} + \gamma_{(0)j}^{qq} g_{jk}^{qq}, \\ \gamma_{(1)jk}^{gg,\text{ND}} &= \left(\gamma_{(0)j}^{gg} - \gamma_{(0)k}^{gg} \right) d_{jk} \left(\beta_0 - \gamma_{(0)k}^{gg} \right) - \left(\gamma_{(0)j}^{gg} - \gamma_{(0)k}^{gg} \right) d_{jk} \gamma_{(0)k}^{gg} + \gamma_{(0)j}^{gg} g_{jk}^{gg} - g_{jk}^{gg} \gamma_{(0)k}^{gg}, \\ \gamma_{(1)jk}^{gq,\text{ND}} &= \left(\gamma_{(0)j}^{gq} - \gamma_{(0)k}^{gq} \right) d_{jk} \left(\beta_0 - \gamma_{(0)k}^{gq} \right) - \left(\gamma_{(0)j}^{gq} - \gamma_{(0)k}^{gq} \right) d_{jk} \gamma_{(0)k}^{gq} + \gamma_{(0)j}^{gq} g_{jk}^{gq} - g_{jk}^{gq} \gamma_{(0)k}^{gq} \\ &\quad + \left(\gamma_{(0)j}^{gq} - \gamma_{(0)k}^{gq} \right) g_{jk}^{gq}, \\ \gamma_{(1)jk}^{gq,\text{ND}} &= \left(\gamma_{(0)j}^{gq} - \gamma_{(0)k}^{gq} \right) \left\{ d_{jk} \left(\beta_0 - \gamma_{(0)k}^{gq} \right) + g_{jk}^{gq} \right\} - \left(\gamma_{(0)j}^{gq} - \gamma_{(0)k}^{gq} \right) d_{jk} \gamma_{(0)k}^{gq} - g_{jk}^{gq} \gamma_{(0)k}^{gq}. \end{aligned} \quad (4.203)$$

The leading order diagonal anomalous dimensions has been given in Section 4.7; the d -elements are

$$d_{jk} = -\frac{1}{2}[1 + (-1)^{j-k}] \frac{(2k+3)}{(j-k)(j+k+3)}. \quad (4.204)$$

This matrix can be generated as a derivative of the Gegenbauer polynomial with respect to its index,

$$\frac{d}{d\nu} \Big|_{\nu=3/2} C_j^\nu(x) = -2 \sum_{k=0}^j d_{jk} C_k^{3/2}(x), \quad \frac{d}{d\nu} \Big|_{\nu=5/2} C_{j-1}^\nu(x) = -2 \sum_{k=1}^j d_{jk} C_{k-1}^{3/2}(x). \quad (4.205)$$

Finally, the renormalized special conformal anomalies g are:

- Even and odd parity sectors:

$$g_{jk}^{qq,V} = g_{jk}^{qq,A} = -C_F [1 + (-1)^{j-k}] \theta_{j-2,k} \frac{(3+2k)}{(j-k)(j+k+3)} \quad (4.206)$$

$$\times \left\{ 2A_{jk} + (A_{jk} - \psi(j+2) + \psi(1)) \frac{(j-k)(j+k+3)}{(k+1)(k+2)} \right\}, \quad (4.207)$$

$$g_{jk}^{gg,V} = g_{jk}^{gg,A} = -C_F [1 + (-1)^{j-k}] \theta_{j-2,k} \frac{1}{6} \frac{(3+2k)}{(k+1)(k+2)}, \quad (4.208)$$

$$g_{jk}^{gg,V} = g_{jk}^{gg,A} = -C_A [1 + (-1)^{j-k}] \theta_{j-2,k} \frac{(3+2k)}{(j-k)(j+k+3)} \quad (4.209)$$

$$\times \left\{ 2A_{jk} + (A_{jk} - \psi(j+2) + \psi(1)) \left[\frac{\Gamma(j+4)\Gamma(k)}{\Gamma(j)\Gamma(k+4)} - 1 \right] \right. \\ \left. + 2(j-k)(j+k+3) \frac{\Gamma(k)}{\Gamma(k+4)} \right\}.$$

- Maximal-helicity sector:

$$g_{jk}^{qq,T} = g_{jk}^{qq,V}, \quad (4.210)$$

$$g_{jk}^{gg,T} = -2C_A \sigma_{j-k} \theta_{j-2,k} \frac{(3+2k)}{(j-k)(j+k+3)} \quad (4.211)$$

$$\times \left\{ 2A_{jk} + (A_{jk} - \psi(j+2) + \psi(1)) \left[\frac{\Gamma(j+4)\Gamma(k)}{\Gamma(j)\Gamma(k+4)} - 1 \right] \right\}.$$

In all expressions we have introduced the matrix A whose elements are defined by

$$A_{jk} = \psi \left(\frac{j+k+4}{2} \right) - \psi \left(\frac{j-k}{2} \right) + 2\psi(j-k) - \psi(j+2) - \psi(1). \quad (4.212)$$

4.10 Solutions of renormalization group equation

We have now all the elements of the anomalous dimension matrix of conformal operators at NLO. In order to solve the renormalization group equation, it remains find its eigenvectors (the eigenvalues are given by the diagonal elements and coincide with known forward anomalous dimensions). This section is devoted to the solution of this problem. It will be shown that the eigefunctions are determined by the special conformal anomaly matrix, determined above.

4.10.1 Mixing of conformal operators

Beyond leading order, one has to perform an additional shuffling of operators in order to get the eigenstates of the renormalization group equation. Let us perform a transformation to the “conformal” renormalization scheme

$$\mathbb{O}_{jl}^{\text{R}} = \mathcal{B}_{jk} \widehat{\mathbb{O}}_{kl}^{\text{R}}, \quad (4.213)$$

where the \mathcal{B} -matrix encodes the rotation to the diagonal basis, in which the operators do not mix. This new set of operators satisfies the renormalization group equation

$$\frac{d}{d \ln \mu} \widehat{\mathbb{O}}_{jl}^{\text{R}} = -\gamma_j \widehat{\mathbb{O}}_{jl}^{\text{R}}, \quad (4.214)$$

with diagonal anomalous dimension matrix $\gamma_{jj} \equiv \gamma_j$. By definition, they do not mix. The renormalization group equation is identical to the dilatation operator, which is diagonal in this basis

$$[\widehat{\mathbb{O}}_{jl}^{\text{R}}, \mathbb{D}] = i \left(d^{\text{can}} - \mu \frac{d}{d\mu} \right) \widehat{\mathbb{O}}_{jl}^{\text{R}} = i(l + 2d + \gamma_j) \widehat{\mathbb{O}}_{jl}^{\text{R}}. \quad (4.215)$$

The solution to this equation is

$$\widehat{\mathbb{O}}_{jl}^{\text{R}}(\mu^2) = \mathcal{T} \exp \left\{ -\frac{1}{2} \int_{\mu_0^2}^{\mu^2} \frac{d\tau}{\tau} \gamma_j(\alpha_s(\tau)) \right\} \widehat{\mathbb{O}}_{jl}^{\text{R}}(\mu_0^2). \quad (4.216)$$

Since γ_j , which are two-by-two matrices in the singlet sector, do not commute in general with each other for different scales of the coupling constant, we have introduced the \mathcal{T} -ordered exponential along the “proper time” τ .

From the renormalization group equations (4.140) and (4.214), we find that the \mathcal{B} -matrix satisfies the following differential equation:

$$\beta(g) \frac{\partial}{\partial g} \mathcal{B}_{jk}(g) + (\gamma_j - \gamma_k) \mathcal{B}_{jk}(g) + \gamma_{jl}^{\text{ND}} \mathcal{B}_{lk}(g) = 0. \quad (4.217)$$

As will be shown in the following two sections, the formalism described above allows to find the corrections to the eigenfunctions analytically, since the \mathcal{B} -matrix is defined in terms of the conformal anomaly γ^c and the β -function. Below, we consider first the hypothetical conformal limit and then address the realistic case with the running coupling constant.

4.10.2 Restoration of conformal covariance in conformal limit

Our goal is to find the explicit form of the rotation matrix \mathcal{B} . It is obvious that this matrix simultaneously diagonalizes both the dilatation and conformal boosts given in Eqs. (4.193) and (4.194), respectively. Let us discuss the nonsinglet case only, since the consideration of the singlet sector does not bring any complications of principle. At the conformal point $\beta = 0$, the rotation matrix B satisfies a simplified version of Eq. (4.217), namely

$$\mathcal{B}_{jk}^{-1} \gamma_{k'k''} \mathcal{B}_{k''k} = \gamma_j \delta_{jk}, \quad (4.218)$$

(no summation on the right-hand side is implied). The last equation can be easily solved recursively using the expansion

$$\mathcal{B}_{jk} = \sum_{N=0}^{\infty} \mathcal{B}_{jk}^{(N)}, \quad \mathcal{B}_{jk}^{(0)} = \delta_{jk}. \quad (4.219)$$

Note, that the terms $\mathcal{B}_{jk}^{(N)}$ with $N \geq 1$ are purely off-diagonal matrices, i.e., their diagonal elements are identically zero. They are given in terms of the n th power of a matrix $\mathbf{b}(k)$

$$\mathcal{B}_{jk}^{(N)} = \{\mathbf{b}^N(k)\}_{jk}, \quad (4.220)$$

which possesses the elements

$$b_{k'k''}(k) = -\frac{\gamma_{k'k''}^{\text{ND}}}{\gamma_{k'} - \gamma_k}. \quad (4.221)$$

Let us demonstrate that the conformal boost is diagonal in this basis. The transformation (4.213) gives

$$[\widehat{\mathbb{O}}_{jl}^{\text{R}}, \mathbb{K}^-] = \mathcal{B}_{jk'}^{-1} \{a(k', l) \delta_{k'k''} + \gamma_{k'k''}^c(l)\} \mathcal{B}_{k''k} \widehat{\mathbb{O}}_{kl-1}^{\text{R}}. \quad (4.222)$$

First we transform the right-hand side to the form

$$\mathcal{B}_{jk'}^{-1} \{a(k', l) \delta_{k'k''} + \gamma_{k'k''}^c(l)\} \mathcal{B}_{k''k} = a(j, l) \delta_{jk} + \mathcal{B}_{jk'}^{-1} \gamma_{k'k''}^c(l) \mathcal{B}_{k''k} + \mathcal{B}_{jk'}^{-1} a(k', k) \mathcal{B}_{k',k}, \quad (4.223)$$

where we commuted $\mathcal{B}_{k''k}$ through the matrix $a_{k'k''}(l)$, first, and then used the identity

$$a(k', k) \mathcal{B}_{k',k} = -\gamma_{k'k''}^c(k) \mathcal{B}_{k''k}, \quad (4.224)$$

proved in Appendix J. This yields

$$\begin{aligned} \mathcal{B}_{jk'}^{-1} \{a(k', l) \delta_{k'k''} + \gamma_{k'k''}^c(l)\} \mathcal{B}_{k''k} &= a(j, l) \delta_{jk} + \mathcal{B}_{jk'}^{-1} (\gamma_{k'k''}^c(l) - \gamma_{k'k''}^c(k)) \mathcal{B}_{k''k} \\ &= a(j, l) \delta_{jk} + 2(k-l) \mathcal{B}_{jk'}^{-1} \gamma_{k'k''}^c \mathcal{B}_{k''k} \\ &\equiv 2(j-l)(j+l+2\nu+\gamma_j) \delta_{jk}, \end{aligned} \quad (4.225)$$

where in the second step we used Eq. (4.198) in the form $\gamma_{kk'}^c(l) - \gamma_{kk'}^c(k) = 2(k-l)\gamma_{kk'}$. Therefore, for operators transformed according to Eq. (4.213) one can restore the exact conformal covariance broken in the minimal subtraction scheme,

$$[\widehat{\mathbb{O}}_{jl}^{\text{R}}, \mathbb{K}^-] = 2(j-l)(j+l+2\nu+\gamma_j) \widehat{\mathbb{O}}_{jl-1}^{\text{R}}, \quad (4.226)$$

One observes that in the conformally covariant scheme the loop corrections to the dilatation and conformal boost are determined solely by the anomalous dimensions of conformal operators.

4.10.3 Solution with running coupling

In case of the running coupling constant, the solution of the differential equation (4.217) is more involved. First, we have to specify the boundary condition for $\mathcal{B}(g)$. Note, that in the previous case of the fixed coupling we are naturally led to a scheme with constant \mathcal{B} . In the current case, the ‘‘minimization’’ of radiative corrections corresponds to the choice $\mathcal{B}(g_0) = 1$ with $g_0 = g(\mu_0^2)$ which implies the absence of loop corrections at some initial scale μ_0 . The most important advantage of this requirement is that, contrary to our previous discussion, the initial condition for the solution of the renormalization group equation (4.216) can be easily determined by ordinary Gegenbauer operators

$$\mathbb{O}_{jl}^{\text{R}}(\mu_0) = \widehat{\mathbb{O}}_{jl}^{\text{R}}(\mu_0). \quad (4.227)$$

To two-loop accuracy, we can write equation for the first nontrivial iteration of $\mathcal{B}_{jk}(g) = \mathbb{1}_{jk} + \mathcal{B}_{jk}^{(1)}(g)$,

$$\beta(g) \frac{\partial}{\partial g} \mathcal{B}_{jk}^{(1)}(g) + (\gamma_j - \gamma_k) \mathcal{B}_{jk}^{(1)}(g) + \gamma_{jk}^{\text{ND}} = 0, \quad (4.228)$$

the solution to which can be written in the form

$$\mathcal{B}_{jk}^{(1)}(g) = - \int_{g_0}^g \frac{dg'}{\beta(g')} \exp \left(- \int_{g'}^g \frac{dg''}{\beta(g'')} \gamma_j(g'') \right) \gamma_{jk}^{\text{ND}}(g') \exp \left(- \int_g^{g'} \frac{dg''}{\beta(g'')} \gamma_k(g'') \right). \quad (4.229)$$

Having constructed compact analytical solution to renormalization group equations for conformal operators, we are ready to apply them to the evolution of GPDs.

4.11 Solution of evolution equations for GPDs

In the present section, we present an outline of methods used to solve evolution equations for generalized parton distributions. We mostly focus on the formalism of the orthogonal polynomial reconstruction which allows for a fully analytical treatment of the problem. Analogous analytical methods for coordinate-space functions, i.e., directly for non-local light-ray operators, were designed in Refs. [230, 260] for one-loop renormalization group equations. This formalism we will briefly discuss next. We continue with a short discussion of the solution of evolution equations for double distributions and the formalism of “effective” forward distributions. Then we turn to the machinery of orthogonal polynomial reconstruction. Finally, we conclude this section with a few remarks on the deficiency the truncation procedure of the expansion in polynomials and advantages of a direct numerical integration of evolution equations for GPDs.

4.11.1 One-loop evolution in coordinate space

The basis of local conformal operators, introduced and elaborated in great detail in previous sections, is not the only choice. It turns out that one can completely circumvent going through the local Taylor series expansion and construction of conformal towers in order to solve analytically the evolution equation for light-ray operators. In fact, such a procedure was developed a long time ago and is based on the expansion in terms of non-local conformal operators [230]. It was recently applied to the study of the evolution of the coordinate-space GPDs [260], which are the partial Fourier transform of GPDs with respect to the Feynman momentum x ,

$$\mathcal{F}^a(z^-, \eta, \Delta^2) \equiv \int dx e^{-ixz^- p^+} F^a(x, \eta, \Delta^2).$$

These functions are analogous to the Ioffe-time forward parton distributions [47, 261].

In order to demonstrate the basic features of the formalism we discuss the quark operator only and refer the interested reader to the original papers [230, 260, 262, 263] for an exhaustive treatment of other aspects of the formalism and discussion of the singlet sector as well. A non-local conformal operator is defined as a convolution of the light-ray operator with a coefficient function [230]

$$\mathbb{S}_j^{qq}(k) = \int_{-\infty}^{\infty} dr^- \int_0^{\infty} dz^- \Psi_j(k; r^-, z^-) \mathcal{O}^{qq} \left(\frac{r^- + z^-}{2}, \frac{r^- - z^-}{2} \right). \quad (4.230)$$

The function $\Psi_j(k; r^-, z^-)$ is found from the condition that this coherent state is an eigenfunction of the conformal Casimir operator [262]

$$[\mathbb{L}^+, \mathbb{S}_j^{qq}(k)] = -ik \mathbb{S}_j^{qq}(k), \quad [\mathbf{L}^2, \mathbb{S}_j^{qq}(k)] = (j+2)(j+1) \mathbb{S}_j^{qq}(k), \quad (4.231)$$

where we adopted the second condition from Eq. (4.128) setting there the conformal spin to $J = j+2$ (see Eq. (4.129)) with the numerical value of the quark conformal spin $j_q = 1$. Taking into

account that the operator \mathbb{L}^+ acts as a total derivative on a non-local operator, i.e., differentiation with respect to r^- , we can integrate by parts in Eq. (4.230) and get a simple equation for the wave function

$$\frac{\partial}{\partial r^-} \Psi_j(k; r^-, z^-) = ik \Psi_j(k; r^-, z^-), \quad (4.232)$$

which admits a plane-wave solution in r^-

$$\Psi_j(k; r^-, z^-) = e^{ikr^-} \psi_j(kz^-). \quad (4.233)$$

Since r^- is the center of mass of the light-ray operator \mathcal{O}^{qq} , the solution describes the propagation of the wave packet $\psi_j(kz^-)$ with momentum k , while the z^- -dependent profile $\psi_j(kz^-)$ responsible for the internal relative motion of quarks attached to the ends of the Wilson string. From the second condition in Eq. (4.231), one finds that the wave function $\psi_j(kz^-)$ satisfies the Bessel equation,

$$\left(\varrho^2 \frac{\partial^2}{\partial \varrho^2} + \varrho^2 - (j+2)(j+1) \right) \psi_j(\varrho) = 0, \quad (4.234)$$

and admits the solution

$$\psi_j(\varrho) = \left(\frac{\varrho}{k} \right)^{1/2} J_{j+3/2}(\varrho), \quad (4.235)$$

where the overall factor of $k^{-1/2}$ was chosen for normalization purposes.

By construction, the non-local conformal operator

$$\mathbb{S}_j^{qq}(k) = \int_{-\infty}^{\infty} dr^- e^{ikr^-} \int_0^{\infty} dz^- (z^-)^{1/2} J_{j+3/2}(kz^-) \mathcal{O}^{qq} \left(\frac{r^- + z^-}{2}, \frac{r^- - z^-}{2} \right) \quad (4.236)$$

possesses an autonomous scale dependence at one-loop order,

$$\mathbb{S}_j^{qq}(k; \mu^2) = \mathbb{S}_j^{qq}(k; \mu_0^2) \left(\frac{\alpha_s(\mu_0^2)}{\alpha_s(\mu^2)} \right)^{\gamma_{(0)j}^{qq}/\beta_0}. \quad (4.237)$$

This is equivalent to the multiplicative renormalization of local conformal operators discussed in the preceding sections. Now, using the Neumann series representation of the delta-function in the variable z^- [260]

$$\delta(z_1^- - z_2^-) = (z_2^-)^{1/2} (z_1^-)^{-3/2} \sum_{j=0}^{\infty} (3+2j) J_{j+3/2}(kz_1^-) J_{j+3/2}(kz_2^-), \quad (4.238)$$

and conventional Fourier representation for the delta-function in r^- we can expand the non-local light-ray operator into the infinite series in coherent states

$$\begin{aligned} \mathcal{O}^{qq} \left(\frac{r^- + z^-}{2}, \frac{r^- - z^-}{2} \right) &= \int dr'^- dz'^- \delta(r^- - r'^-) \delta(z^- - z'^-) \mathcal{O}^{qq} \left(\frac{r'^- + z'^-}{2}, \frac{r'^- - z'^-}{2} \right) \\ &= (z^-)^{-3/2} \sum_{j=0}^{\infty} (3+2j) \int \frac{dk}{2\pi} e^{ikr^-} J_{j+3/2}(kz^-) \mathbb{S}_j^{qq}(k). \end{aligned} \quad (4.239)$$

Let us point out that the conformal operators constructed in Eq. (4.236) are defined for positive integer values of the conformal spin j only [260], such that non-local operators are expanded in

infinite series (4.239). On the other hand, the decomposition found in the original work [230] uses the Kantorovich-Lebedev transformation [264] and is based on an integral representation which requires analytical continuation of the conformal spin j into the complex plane, which thus uses a continuous series representation of the collinear conformal group, rather than the discrete series adopted in the local operator expansion. The equivalence of the two solutions was demonstrated in Ref. [260], which illustrates a relation between the Kantorovich-Lebedev transformation and the Neumann series expansion.

4.11.2 “Difficulties” with eigenfunctions

Now we turn to a thorough discussion of constructing solutions to the evolution equations for GPDs in the basis of local conformal operators. As we established in Section 4.7, the one-loop evolution equation for GPDs is diagonalized in the basis of Gegenbauer polynomials. Namely, taking the nonsinglet quark sector as an example, one has the leading order equation²⁹

$$\frac{d}{d \ln \mu} F^q(x, \eta; \mu^2) = -\frac{\alpha_s(\mu^2)}{2\pi} \int_{-1}^1 \frac{dy}{\eta} k_{(0)}^{qq} \left(\frac{x}{\eta}, \frac{y}{\eta} \right) F^q(y, \eta; \mu^2) + \mathcal{O}(\alpha_s^2), \quad (4.240)$$

with the Gegenbauer polynomials $C_j^{3/2}(x)$ —defined on the interval $-1 \leq x \leq 1$ —being its eigenfunctions,

$$\int_{-1}^1 \frac{dx}{\eta} C_j^{3/2} \left(\frac{x}{\eta} \right) k_{(0)}^{qq} \left(\frac{x}{\eta}, \frac{y}{\eta} \right) = \gamma_{(0)j}^{qq} C_j^{3/2} \left(\frac{y}{\eta} \right). \quad (4.241)$$

One may try to write the solution to Eq. (4.240) as an expansion in terms of its eigenfunctions

$$F^q(x, \eta; \mu^2) = \frac{1}{\eta} \sum_{j=0}^{\infty} \frac{w(\frac{x}{\eta} | \frac{3}{2})}{\eta^j N_j(\frac{3}{2})} C_j^{3/2} \left(\frac{x}{\eta} \right) \mathbb{F}_j^q(\eta; \mu^2), \quad (4.242)$$

where the weight and normalization factors are

$$w(x|\nu) = (1-x^2)^{\nu-1/2}, \quad N_j(\nu) = 2^{1-2\nu} \frac{\Gamma^2(1/2)\Gamma(2\nu+j)}{\Gamma^2(\nu)\Gamma(j+1)(\nu+j)},$$

and the Gegenbauer moments of GPDs related to the conformal operators (4.138) via

$$\mathbb{F}_j^q(\eta; \mu^2) = \eta^j \int_{-1}^1 dx C_j^{3/2} \left(\frac{x}{\eta} \right) F^q(x, \eta; \mu^2) = (p^+)^{-j-1} \langle p_2 | \mathbb{O}_{jj}^{qq}(0) | p_1 \rangle. \quad (4.243)$$

However, one immediately faces a difficulty identical to the one we already encountered before, when we studied the eigenfunctions of the inclusive DGLAP equations. Namely, the Gegenbauer polynomials $C_j^\nu(x)$ are mutually orthogonal on the interval $-1 \leq x \leq 1$, which is their support region. Therefore, each term on the right-hand side of Eq. (4.242), vanishes outside the interval $-\eta \leq x \leq \eta$, while the left-hand side has the support in the entire region $-1 \leq x \leq 1$. Of course, the correct support on the right-hand side is restored due to the infinite summation of the slowly converging series in Gegenbauer polynomials, in the very same fashion as in Eq. (4.72). Thus, this form of the solution is not useful in practical studies of the logarithmic scaling violation of GPDs.

²⁹For brevity, we do not display the superscript NS on quantities involved.

Still, there is a feature which becomes extremely transparent in the representation (4.242). Due to fact that the Gegenbauer moments evolve autonomously

$$\mathbb{F}_j^q(\eta; \mu^2) = \mathbb{F}_j^q(\eta; \mu_0^2) \left(\frac{\alpha_s(\mu_0^2)}{\alpha_s(\mu^2)} \right)^{\gamma_{(0)j}^{qq}/\beta_0} \quad (4.244)$$

with vanishing anomalous dimension for the lowest moment of GPDs in the vector and axial-vector channels $\gamma_{(0)j=0}^{qq,A,V} = 0$, at asymptotically large scales only the lowest term in the expansion survives. As a result, the GPD is driven at asymptotically large scales to the shape

$$F^q(x, \eta; \mu^2 \rightarrow \infty) \equiv F_{\text{asy}}^q(x, \eta) = \frac{3}{4} \frac{1}{\eta} \left(1 - \frac{x^2}{\eta^2} \right) \theta(\eta - |x|) \mathbb{F}_0^q, \quad (4.245)$$

where the lowest conformal moment \mathbb{F}_0^q is related to the quark electromagnetic form factors, i.e., it is the Dirac $\mathbb{F}_0^q = F_1^q(\Delta^2)$ and Pauli $\mathbb{F}_0^q = F_2^q(\Delta^2)$ form factors for parton helicity non-flip $F^q = H^q$ and flip $F^q = E^q$ GPDs. Note that the GPD washes out completely from the “inclusive” region, i.e.,

$$F_{\text{asy}}^q(x, \eta) = 0, \quad \text{for } |x| > \eta. \quad (4.246)$$

The explicit asymptotic solutions for the singlet sector can be found below in Eqs. (4.289) and (4.291).

Of course, the formal expansion (4.242) should be understood in a sense of the mathematical distribution in the same fashion as the expansion in δ -functions of the parton distribution (4.71). To make the analogy with the inclusive case more explicit, it is easy to see that the Gegenbauer polynomials can be represented in the form involving derivative of the δ -function making use of the Rodrigues’ formula

$$(1-x^2)^{\nu-1/2} C_j^\nu(x) = 2^{1-2\nu-j} \frac{\Gamma(\frac{1}{2})\Gamma(j+2\nu)}{\Gamma(\nu)\Gamma(j+\nu+\frac{1}{2})\Gamma(j+1)} \int_{-1}^1 dv (1-v^2)^{j+\nu-\frac{1}{2}} \delta^{(j)}(v-x), \quad (4.247)$$

where $\delta^{(j)}(v-x) = \partial_v^j \delta(v-x)$. Hence, to get a meaningful result, one should convolute both sides with a smooth function first. This idea lies in the heart of the method which we will start discussing in the next section using the same nonsinglet quark example.

4.11.3 Orthogonal polynomial reconstruction

The restoration of the support properties of GPDs can be easily achieved via their expansion in a series with respect to a complete set of orthogonal, say, Gegenbauer, polynomials [267, 142], having the same support as GPDs,

$$F^q(x, \eta; \mu^2) = \sum_{j=0}^{\infty} \frac{w(x|\frac{3}{2})}{N_j(\frac{3}{2})} C_j^{3/2}(x) F_j^q(\eta; \mu^2). \quad (4.248)$$

It is straightforward to calculate the expansion coefficients F_j^q in terms of the conformal moments which evolve autonomously at leading order (4.244),

$$F_j^q(\eta; \mu^2) = \sum_{k=0}^j E_{jk}(\eta|\frac{3}{2}) \mathbb{F}_k^q(\eta; \mu^2). \quad (4.249)$$

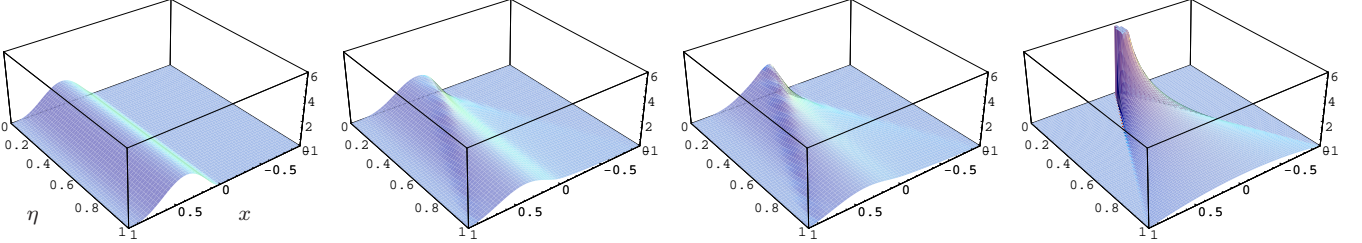


Figure 34: Evolution of a model distribution with the change of the renormalization scale. Figures from left to right show the skewless input distribution $H(x, \eta) = 60x^2(1-x)^3\theta(x)$ and its evolved shape at $\mu^2 = 2 \text{ GeV}^2$, $\mu^2 = 200 \text{ GeV}^2$ and $\mu^2 = \infty$, respectively. The qualitative features of generalized evolution are clearly seen: Partons from the inclusive region $|x| > \eta$ migrate into the exclusive domain $|x| < \eta$ and once they get there, they never come back. They are redistributed in the exclusive region $|x| < \eta$ according to the usual ERBL evolution pattern as exemplified in Fig. 33.

Using Eq. (4.247) and employing the definition of hypergeometric functions, we can write the expansion coefficients $E_{jk}(\eta|\nu)$ in a very compact form

$$\begin{aligned} E_{jk}(\eta|\nu) &= \int_{-1}^1 dx \frac{w(x|\nu)}{\eta^k N_k(\nu)} C_k^\nu(x) C_j^\nu(\eta x) \\ &= \frac{1}{2} \theta_{jk} [1 + (-1)^{j-k}] \frac{(-1)^{\frac{j-k}{2}} \Gamma(\nu + \frac{j+k}{2})}{\Gamma(\nu + k) \Gamma(1 + \frac{j-k}{2})} {}_2F_1 \left(\frac{\frac{k-j}{2}, \nu + \frac{j+k}{2}}{\nu + k + 1} \middle| \eta^2 \right). \end{aligned} \quad (4.250)$$

Since ${}_2F_1(-n, a+n; a+1; 1) = \delta_{n0}$, we immediately obtain for $\eta = 1$ that $F_j^q(1; \mu^2) = \mathbb{F}_j^q(1; \mu^2)$, which matches to the solution to ER-BL equation for the quark component of meson distribution amplitudes. The qualitative features of the evolution are demonstrated in Fig. 34 for a simple GPD.

4.11.4 Next-to-leading order: nonsinglet sector

Let us now discuss the effects of mixing of conformal moments at next-to-leading order, and how this modifies the solution to the evolution equations [269]. Again, we perform at first the expansion of GPDs in terms of a set of orthogonal polynomials

$$F^q(x, \eta; \mu^2) = \sum_{j=0}^{\infty} \frac{(1-x)^\alpha (1+x)^\beta}{n_j(\alpha, \beta)} P_j^{(\alpha, \beta)}(x) F_j^q(\eta; \mu^2). \quad (4.251)$$

Here we use the opportunity and illustrate the use of the Jacobi polynomials, “living” on the interval $-1 \leq x \leq 1$. The normalization coefficients are

$$n_j(\alpha, \beta) = \frac{\Gamma(j+\alpha+1)\Gamma(j+\beta+1)}{(2j+\alpha+\beta+1)\Gamma(j+1)\Gamma(j+\alpha+\beta+1)},$$

with parameters α, β which can be chosen from the condition of the fastest convergence of the series, which is difficult to implement in practice. The coefficients in the re-expansion in terms of

conformal moments of GPDs $\mathbb{F}_j^q(\eta; \mu^2)$

$$F_j^q(\eta; \mu^2) = \sum_{k=0}^j E_{jk}(\eta|\alpha, \beta) \mathbb{F}_k^q(\eta; \mu^2), \quad (4.252)$$

are now determined by the overlap integral

$$E_{jk}(\eta|\alpha, \beta) = \int_{-1}^1 dx \frac{w(x|\frac{3}{2})}{\eta^k N_k(\frac{3}{2})} C_k^{3/2}(x) P_j^{(\alpha, \beta)}(\eta x). \quad (4.253)$$

The results for all other classic orthogonal polynomials immediately follow from this expression. For special values of the parameters α and β , the Jacobi polynomials coincide [268] either with Gegenbauer,

$$P_j^{(\lambda-1/2, \lambda-1/2)}(x) = \frac{\Gamma(2\lambda)\Gamma(j+\lambda+\frac{1}{2})}{\Gamma(j+2\lambda)\Gamma(\lambda+\frac{1}{2})} C_j^\lambda(x),$$

or Legendre,

$$P_j^{(0,0)}(x) = P_j(x),$$

or Chebyshev polynomials of the first,

$$P_j^{(-1/2, -1/2)}(x) = \frac{\Gamma(j+\frac{1}{2})}{\sqrt{\pi} j!} T_j(x),$$

and the second kind,

$$P_j^{(1/2, 1/2)}(x) = \frac{2\Gamma(j+\frac{3}{2})}{\sqrt{\pi}(j+1)!} U_j(x). \quad (4.254)$$

Starting from two-loop order, the conformal operators start to mix and so do the Gegenbauer moments of GPDs. The latter have to be re-expanded in terms of multiplicatively renormalizable moments $\widehat{\mathbb{F}}_j^q(\eta; \mu^2)$ as

$$\mathbb{F}_j^q(\eta; \mu^2) = \sum_{k=0}^j \eta^{j-k} \mathcal{B}_{jk}(\mu^2, \mu_0^2) \mathcal{E}_k(\mu^2, \mu_0^2) \widehat{\mathbb{F}}_k^q(\eta; \mu_0^2). \quad (4.255)$$

We have chosen the normalization condition for the two evolution operators

$$\mathcal{E}_j(\mu_0^2, \mu_0^2) = 1, \quad \mathcal{B}_{jk}(\mu_0^2, \mu_0^2) = \delta_{jk}, \quad (4.256)$$

which implies

$$\widehat{\mathbb{F}}_j^q(\eta; \mu_0^2) = \mathbb{F}_j^q(\eta; \mu_0^2), \quad (4.257)$$

so that at certain normalization point μ_0 the multiplicatively renormalizable operators coincide with conformal operators, as discussed in Section 4.10.3. The two evolution operators satisfy the following evolution equations with next-to-leading order solutions.

- The diagonal evolution operator \mathcal{E} obeys the equation

$$\frac{d}{d \ln \mu} \mathcal{E}_j(\mu^2, \mu_0^2) + \gamma_j^{qq} \mathcal{E}_j(\mu^2, \mu_0^2) = 0, \quad (4.258)$$

with the two-loop solution

$$\begin{aligned}\mathcal{E}_j(\mu^2, \mu_0^2) &= \left(\frac{\alpha_s(\mu_0^2)}{\alpha_s(\mu^2)} \right)^{\gamma_{(0)j}^{qq}/\beta_0} \left(\frac{\beta_0 + \beta_1 \frac{\alpha_s(\mu^2)}{4\pi}}{\beta_0 + \beta_1 \frac{\alpha_s(\mu_0^2)}{4\pi}} \right)^{(\gamma_{(0)j}^{qq}/\beta_0 - 2\gamma_{(1)j}^{qq}/\beta_1)} \\ &\simeq \left(\frac{\alpha_s(\mu_0^2)}{\alpha_s(\mu^2)} \right)^{\gamma_{(0)j}^{qq}/\beta_0} \left\{ 1 + \left(\frac{\beta_1 \gamma_{(0)j}^{qq}}{2\beta_0^2} - \frac{\gamma_{(1)j}^{qq}}{\beta_0} \right) \frac{\alpha_s(\mu^2) - \alpha_s(\mu_0^2)}{2\pi} \right\},\end{aligned}\quad (4.259)$$

where β_0 and β_1 are the first two coefficients of the perturbative expansion of the QCD β -function, given in Appendix G.3.

- The non-diagonal evolution operator \mathcal{B} fulfills the equation

$$\frac{d}{d \ln \mu} \mathcal{B}_{jk}(\mu^2, \mu_0^2) + (\gamma_j^{qq} - \gamma_k^{qq}) \mathcal{B}_{jk}(\mu^2, \mu_0^2) + \gamma_{jl}^{qq, \text{ND}} \mathcal{B}_{lk}(\mu^2, \mu_0^2) = 0. \quad (4.260)$$

The solution to it in the two-loop approximation was given before in Eq. (4.229). Keeping the first nontrivial terms in the perturbative expansion for all functions involved, it reads

$$\mathcal{B}_{jk}(\mu^2, \mu_0^2) = \delta_{jk} - \frac{\alpha_s(\mu^2)}{2\pi} \frac{\gamma_{(1)jk}^{qq, \text{ND}}}{\gamma_{(0)j}^{qq} - \gamma_{(0)k}^{qq} + \beta_0} \left(1 - \left(\frac{\alpha_s(\mu_0^2)}{\alpha_s(\mu^2)} \right)^{(\gamma_{(0)j}^{qq} - \gamma_{(0)k}^{qq} + \beta_0)/\beta_0} \right). \quad (4.261)$$

We remind that, compared to all other renormalization-group functions, $\gamma_{jk}^{qq, \text{ND}}$ starts at two-loop order according to Eq. (4.145).

Finally, the coupling constant at two-loop order is given by the following inverse-log expansion

$$\alpha_s(\mu^2) = -\frac{4\pi}{\beta_0 \ln(\mu^2/\Lambda_{\overline{\text{MS}}}^2)} \left(1 + \frac{\beta_1}{\beta_0^2} \frac{\ln \ln(\mu^2/\Lambda_{\overline{\text{MS}}}^2)}{\ln(\mu^2/\Lambda_{\overline{\text{MS}}}^2)} \right). \quad (4.262)$$

If the input scale μ_0 at which the initial conditions for renormalization group evolution are defined is chosen very low, it is more reliable and accurate to obtain α_s in two-loop approximation by solving the exact transcendental equation

$$-\beta_0 \ln \frac{\mu^2}{\Lambda_{\overline{\text{MS}}}^2} = \frac{4\pi}{\alpha_s(\mu^2)} - \frac{\beta_1}{\beta_0} \ln \left(-\frac{4\pi}{\beta_0 \alpha_s(\mu^2)} - \frac{\beta_1}{\beta_0^2} \right). \quad (4.263)$$

The two formulas, Eqs. (4.262) and (4.263), differ by $\sim 15\%$ for $\mu^2 = 0.6 \text{ GeV}^2$, and the deviation decreases to 3% for $\mu^2 = 4 \text{ GeV}^2$. However, this source of theoretical uncertainty is conceptually irrelevant for our study.

4.11.5 Next-to-leading order: singlet sector

Finally, let us turn to the singlet sector [270]. The “two-component vector” of quark and gluon GPDs (4.30) is expanded into a series

$$\mathbf{F}(x, \eta; \mu^2) = \sum_{j=0}^{\infty} \tilde{\mathcal{P}}_j(x) \mathbf{F}_j(\eta; \mu^2), \quad (4.264)$$

involving a matrix of orthogonal polynomials

$$\tilde{\mathcal{P}}_j(x) = \begin{pmatrix} \frac{w(x|\alpha_p)}{n_j(\alpha_p)} \mathcal{P}_j^{(\alpha_p)}(x) & 0 \\ 0 & \frac{w(x|\alpha'_p)}{n_j(\alpha'_p)} \mathcal{P}_j^{(\alpha'_p)}(x) \end{pmatrix}, \quad (4.265)$$

with $w(x|\alpha_p)$ and $n_j(\alpha_p)$ being the weight and normalization factors, respectively. Re-expanding the moments $\mathbf{F}_j(\eta; \mu^2)$ in terms of the conformal moments $\mathbf{F}_k(\eta; \mu^2)$, one finds analogously to the nonsinglet sector

$$\mathbf{F}_j(\eta; \mu^2) = \sum_{k=0}^{\infty} \mathbf{E}_{jk}(\eta) \mathbf{F}_k(\eta; \mu^2). \quad (4.266)$$

The matrix of coefficients

$$\mathbf{E}_{jk}(\eta) = \begin{pmatrix} E_{jk}(\eta| \frac{3}{2}; \alpha_p) & 0 \\ 0 & E_{jk-1}(\eta| \frac{5}{2}; \alpha'_p) \end{pmatrix}, \quad (4.267)$$

consists of elements

$$E_{jk}(\eta| \nu; \alpha_p) = \int_{-1}^1 dx \frac{w(x| \nu)}{\eta^k N_k(\nu)} C_k^\nu(x) \mathcal{P}_j^{(\alpha_p)}(\eta x), \quad (4.268)$$

while the matrix of conformal moments $\mathbf{F}_k(\eta; \mu^2)$ is defined by

$$\mathbf{F}_j(\eta; \mu^2) = \int_{-1}^1 dx \begin{pmatrix} \eta^j C_j^{3/2}(x/\eta) & 0 \\ 0 & \eta^{j-1} C_{j-1}^{5/2}(x/\eta) \end{pmatrix} \mathbf{F}(x, \eta; \mu^2), \quad (4.269)$$

where the two vector of the singlet quark and gluon GPDs is given in Eq. (4.30). These conformal moments are expressed in terms of the non-forward matrix element of the two-vector of the conformal operators (4.146) as follows

$$\mathbf{F}_j(\eta; \mu^2) = 2(p^+)^{-j-1} \langle p_2 | \mathbf{O}_{jj}(0) | p_1 \rangle \quad (4.270)$$

The latter evolve according to the formula

$$\mathbf{F}_k(\eta; \mu^2) = \sum_{k=0}^j \eta^{j-k} \mathcal{B}_{jk}(\mu^2, \mu_0^2) \mathcal{E}_k(\mu^2, \mu_0^2) \hat{\mathbf{F}}_k(\eta; \mu_0^2). \quad (4.271)$$

involving two evolution operators as in the non-singlet case.

In NLO, the singlet diagonal evolution operator \mathcal{E}_j satisfies the equation

$$\frac{d}{d \ln \alpha_s(\mu^2)} \mathcal{E}_j(\mu^2, \mu_0^2) = -\frac{1}{\beta_0} \left\{ \gamma_{(0)j} + \frac{\alpha_s(\mu^2)}{2\pi} \mathbf{R}_j \right\} \mathcal{E}_j(\mu^2, \mu_0^2), \quad (4.272)$$

with the boundary condition

$$\mathcal{E}_j(\mu_0^2, \mu_0^2) = \mathbb{1} = \begin{pmatrix} 1 & 0 \\ 0 & 1 \end{pmatrix}.$$

Here

$$\mathbf{R}_j = \gamma_{(1)j} - \frac{\beta_1}{2\beta_0} \gamma_{(0)j} \quad (4.273)$$

is expressed in terms of the diagonal elements $\gamma_{jj} = \gamma_j$ of the one- and two-loop expressions of the two-by-two matrix of anomalous dimensions (4.148). The solution to Eq. (4.272) can be written as [271, 272]

$$\begin{aligned} \mathcal{E}_j(\mu^2, \mu_0^2) &= \left(\mathbf{P}_j^+ - \frac{\alpha_s(\mu^2) - \alpha_s(\mu_0^2)}{2\pi} \frac{1}{\beta_0} \mathbf{P}_j^+ \mathbf{R}_j \mathbf{P}_j^+ \right) \left(\frac{\alpha_s(\mu_0^2)}{\alpha_s(\mu^2)} \right)^{\gamma_j^+/\beta_0} \\ &\quad - \frac{\alpha_s(\mu^2)}{2\pi} \frac{\mathbf{P}_j^- \mathbf{R}_j \mathbf{P}_j^+}{\gamma_j^- - \gamma_j^+ + \beta_0} \left(1 - \left(\frac{\alpha_s(\mu_0^2)}{\alpha_s(\mu^2)} \right)^{(\gamma_j^- - \gamma_j^+ + \beta_0)/\beta_0} \right) \left(\frac{\alpha_s(\mu_0^2)}{\alpha_s(\mu^2)} \right)^{\gamma_j^+/\beta_0} \\ &\quad + (\gamma_j^+ \leftrightarrow \gamma_j^-, \mathbf{P}_j^+ \leftrightarrow \mathbf{P}_j^-), \end{aligned} \quad (4.274)$$

in terms of the projection operators

$$\mathbf{P}_j^\pm = \frac{\pm 1}{\gamma_j^+ - \gamma_j^-} (\gamma_{(0)j} - \gamma_j^\mp \mathbb{1}), \quad (4.275)$$

built from the eigenvalues of the LO anomalous dimension matrix $\gamma_{(0)j}$,

$$\gamma_j^\pm = \frac{1}{2} \left(\gamma_{(0)j}^{qq} + \gamma_{(0)j}^{gg} \pm \sqrt{\left(\gamma_{(0)j}^{qq} - \gamma_{(0)j}^{gg} \right)^2 + 4\gamma_{(0)j}^{qq}\gamma_{(0)j}^{gg}} \right). \quad (4.276)$$

The projectors obey the properties

$$(\mathbf{P}_j^\pm)^2 = \mathbf{P}_j^\pm, \quad \mathbf{P}_j^+ \mathbf{P}_j^- = 0, \quad \mathbf{P}_j^+ + \mathbf{P}_j^- = \mathbb{1}, \quad (4.277)$$

such that the expansion of the LO anomalous dimension matrix in its eigenfunctions and eigenvalues reads

$$\gamma_{(0)j} = \gamma_j^+ \mathbf{P}_j^+ + \gamma_j^- \mathbf{P}_j^-. \quad (4.278)$$

The other evolution operator \mathcal{B} , which fixes the corrections to the eigenfunctions of the NLO kernels, can be represented to the required order by

$$\mathcal{B} = \mathbb{1} + \mathcal{B}^{(1)}, \quad (4.279)$$

where only the first iteration $\mathcal{B}^{(1)}$ was kept. The latter is determined by the first order differential equation

$$\frac{d}{d \ln \alpha_s(\mu^2)} \mathcal{B}_{jk}^{(1)}(\mu^2, \mu_0^2) = -\frac{1}{\beta_0} \left\{ \gamma_{(0)j} \mathcal{B}_{jk}^{(1)}(\mu^2, \mu_0^2) - \mathcal{B}_{jk}^{(1)}(\mu^2, \mu_0^2) \gamma_{(0)k} + \frac{\alpha_s(\mu^2)}{2\pi} \gamma_{(1)jk}^{\text{ND}} \right\}, \quad (4.280)$$

and reads [270]

$$\begin{aligned} \mathcal{B}_{jk}^{(1)} &= -\frac{\alpha_s(\mu^2)}{2\pi} \left(\frac{\mathbf{P}_j^+ \gamma_{(1)jk}^{\text{ND}} \mathbf{P}_k^+}{\gamma_j^+ - \gamma_k^+ + \beta_0} \left(1 - \left(\frac{\alpha_s(Q_0^2)}{\alpha_s(\mu^2)} \right)^{(\gamma_j^+ - \gamma_k^+ + \beta_0)/\beta_0} \right) \right. \\ &\quad \left. + \frac{\mathbf{P}_j^+ \gamma_{(1)jk}^{\text{ND}} \mathbf{P}_k^-}{\gamma_j^+ - \gamma_k^- + \beta_0} \left(1 - \left(\frac{\alpha_s(\mu_0^2)}{\alpha_s(\mu^2)} \right)^{(\gamma_j^+ - \gamma_k^- + \beta_0)/\beta_0} \right) \right) \\ &\quad + (\gamma_j^+ \leftrightarrow \gamma_j^-, \mathbf{P}_j^+ \leftrightarrow \mathbf{P}_j^-), \end{aligned} \quad (4.281)$$

where $j > k$.

4.11.6 Asymptotic GPDs in singlet sector

An immediate consequence of these considerations is the functional form of the singlet GPDs at asymptotically large scales. The evolution operator \mathcal{E}_j (4.274), truncated to one-loop order in coupling, possesses two eigenfunctions, which are found with the help of the projection operators \mathbf{P}_j^\pm acting on the two-vector of Gegenbauer moments of GPDs (4.269),

$$\mathbf{P}_j^\pm \mathbf{F}_j = \frac{\pm 2}{\gamma_j^+ - \gamma_j^-} \begin{pmatrix} \gamma_{(0)j}^{qq} - \gamma_j^\mp \\ \gamma_{(0)j}^{gq} \end{pmatrix} F_j^\pm. \quad (4.282)$$

These multiplicatively combinations of conformal moments,

$$F_j^\pm = \sum_q \mathbb{F}_j^q + \frac{1}{4} \frac{\gamma_{(0)j}^{gg}}{\gamma_{(0)j}^{qq} - \gamma_j^\mp} \mathbb{F}_j^g, \quad (4.283)$$

evolve with the anomalous dimensions γ_j^\pm , respectively. The F_j^\pm are built as linear superpositions of the conformal moments of the quark GPDs, defined earlier in Eq. (4.243), and the gluon GPDs,

$$\mathbb{F}_j^g(\eta; \mu_0^2) \equiv \eta^{j-1} \int_{-1}^1 dx C_{j-1}^{5/2} \left(\frac{x}{\eta} \right) F^g(x, \eta; \mu_0^2) = 4(p^+)^{-j-1} \langle p_2 | \mathbb{O}_{jj}^{gg}(0) | p_1 \rangle. \quad (4.284)$$

In particular, one finds for $j = 1$ that F_1^- has a vanishing anomalous dimension, while F_1^+ has a positive nonzero anomalous dimension,

$$\begin{aligned} \gamma_1^- &= 0, & F_1^- &= \sum_q \mathbb{F}_1^q + \frac{3}{2} \mathbb{F}_1^g, \\ \gamma_1^+ &= \frac{8}{3} C_F + \frac{2}{3} N_f, & F_1^+ &= \sum_q \mathbb{F}_1^q - \frac{3N_f}{8C_F} \mathbb{F}_1^g. \end{aligned} \quad (4.285)$$

The former result is expected since F_1^- corresponds to the matrix element of the conserved total energy-momentum tensor, see Eqs. (3.110) and (3.111). Namely,

$$\sum_q \mathbb{F}_1^q + \frac{3}{2} \mathbb{F}_1^g = 2c_1^{3/2} (p^+)^{-2} \langle p_2 | \Theta^{q,++} + \Theta^{g,++} | p_1 \rangle. \quad (4.286)$$

The presence of the factor 3/2 in front of \mathbb{F}_1^g is an artifact of the normalization of the Gegenbauer polynomials. It can be seen to be gone when transforming to Wilson operators via Eq. (4.166). Thus at asymptotically large scales $\mu^2 \rightarrow \infty$, F_1^+ vanishes while F_1^- remains constant. Introducing $\mathbb{F}_{1,\text{asy}}^a = \mathbb{F}_1^a(\mu^2 \rightarrow \infty)$ and, temporarily, a unit normalization for asymptotic F_1^- , one can solve the two asymptotic equations

$$\sum_q \mathbb{F}_{1,\text{asy}}^q + \frac{3}{2} \mathbb{F}_{1,\text{asy}}^g = 1, \quad \sum_q \mathbb{F}_{1,\text{asy}}^q - \frac{3N_f}{8C_F} \mathbb{F}_{1,\text{asy}}^g = 0 \quad (4.287)$$

in order to find separate singlet quark and gluon components

$$\sum_q \mathbb{F}_{1,\text{asy}}^q = \frac{N_f}{4C_F + N_f}, \quad \frac{3}{2} \mathbb{F}_{1,\text{asy}}^g = \frac{4C_F}{4C_F + N_f} \quad (4.288)$$

This translates into the following asymptotic form $F_{\text{asy}}^a = F^a(\mu^2 \rightarrow \infty)$ of the singlet quark [9, 10]

$$\sum_q H_{\text{asy}}^q(x, \eta) = \frac{15}{4} \frac{N_f}{4C_F + N_f} \frac{x}{\eta^3} \left(1 - \frac{x^2}{\eta^2}\right) \theta(\eta - |x|) \sum_q \left\{ H_{2,0}^q + \eta^2 D_2^q \right\}, \quad (4.289)$$

$$\sum_q E_{\text{asy}}^q(x, \eta) = \frac{15}{4} \frac{N_f}{4C_F + N_f} \frac{x}{\eta^3} \left(1 - \frac{x^2}{\eta^2}\right) \theta(\eta - |x|) \sum_q \left\{ E_{2,0}^q - \eta^2 D_2^q \right\}, \quad (4.290)$$

and gluon GPDs

$$H_{\text{asy}}^g(x, \eta) = \frac{15}{8} \frac{4C_F}{4C_F + N_f} \frac{1}{\eta} \left(1 - \frac{x^2}{\eta^2}\right)^2 \theta(\eta - |x|) \left\{ H_{2,0}^g + \eta^2 D_2^g \right\}, \quad (4.291)$$

$$E_{\text{asy}}^g(x, \eta) = \frac{15}{8} \frac{4C_F}{4C_F + N_f} \frac{1}{\eta} \left(1 - \frac{x^2}{\eta^2}\right)^2 \theta(\eta - |x|) \left\{ E_{2,0}^g - \eta^2 D_2^g \right\}. \quad (4.292)$$

Here we restored the polynomials in form factors (3.124) (cf. Eq. (3.125)). Note that the boundary values all $F^a(\pm\eta, \eta)$ vanish in the $\mu^2 \rightarrow \infty$ limit.

4.11.7 Two-loop evolution in momentum space

Though the method of orthogonal polynomial reconstruction discussed above is rather elegant as it allows for an explicit analytic solution, its practical implementation for GPDs faces difficulties due to poor convergence of the truncated series³⁰ in certain regions of the momentum fractions space, namely, around $x = \eta$ and low x and η domain [267, 269, 270]. A robust method, free from these complications, was developed by means of a direct numerical solution [67, 274] of the integro-differential evolution equation for GPDs (4.33). Since the formalism allows straightforward generalizations to high-loop orders, the two-loop generalized evolution kernels were reconstructed in Ref. [275] bypassing direct evaluations of Feynman graphs, from the available two-loop anomalous dimensions of conformal operators presented in Section 4.9.4, inclusive splitting functions, known two-loop non-singlet evolution kernels in exclusive kinematics [276, 277, 278] and relying on supersymmetric relations, discussed in Appendix K.4, and well-understood limiting procedure outlined in Section 4.4.5. A thorough numerical analysis demonstrated a high efficiency of the formalism and revealed that the two-loop effects are strongly enhanced around $x = \eta$, while they do not exceed 25% within a very large range in other kinematical regions [279, 280].

4.11.8 Solution of evolution equations for double distributions

The multiplicative renormalization of conformal operators can be used for an efficient solution of evolution equations for double distributions. From the autonomous leading order evolution of conformal operators one can establish the eigenfunctions of the renormalization group equations in the basis of double distributions and draw interesting consequences for the functional form of the latter. For simplicity, we consider the the nucleon GPD $A(x, \eta)$ and corresponding symmetric DDs $h_A(\beta, \alpha)$ introduced in Sections 3.5.2 and 3.8.3, respectively.

Let us discuss the nonsinglet case first. Switching from the quark GPD A^q in their multiplicatively renormalizable conformal moments to the DDs h_A^q , we can write making use of Eq.

³⁰This is not the case in applications of the Jacobi polynomial reconstruction of forward parton distributions [273].

(3.246)

$$\mathbb{A}_n^q(\eta) = \eta^n \int_{-1}^1 dx C_n^{3/2} \left(\frac{x}{\eta} \right) A^q(x, \eta) = \eta^n \int_{\Omega} d\beta d\alpha C_n^{3/2} \left(\frac{\beta}{\eta} + \alpha \right) h_A^q(\beta, \alpha). \quad (4.293)$$

Using the identity

$$C_n^{3/2} \left(\frac{\beta}{\eta} + \alpha \right) = \sum_{l=0}^n \frac{\Gamma(n-l+3/2)}{\Gamma(3/2)(n-l)!} \left(\frac{2\beta}{\eta} \right)^{n-l} C_l^{3/2+n-l}(\alpha), \quad (4.294)$$

one finds

$$\mathbb{A}_n^q(\eta) = \sum_{k=0}^{[n/2]} 2^{n-2k} \frac{\Gamma(n-2k+3/2)}{\Gamma(3/2)(n-2k)!} \eta^{2k} \int_{\Omega} d\beta d\alpha \beta^{n-2k} C_{2k}^{3/2+n-2k}(\alpha) h_A^q(\beta, \alpha). \quad (4.295)$$

Hence, each $\beta^m C_l^{3/2+m}(\alpha)$ moment of the DD $h_A^q(\beta, \alpha)$ is multiplicatively renormalizable and its evolution is governed by the anomalous dimension $\gamma_{(0)m+l}^{qg;V}$ [6, 140],

$$\int_{\Omega} d\beta d\alpha \beta^m C_l^{3/2+m}(\alpha) h_A^q(\beta, \alpha; \mu^2) = \left(\frac{\alpha_s(\mu_0^2)}{\alpha_s(\mu^2)} \right)^{\gamma_{(0)m+l}^{qg;V}/\beta_0} \int_{\Omega} d\beta d\alpha \beta^m C_l^{3/2+m}(\alpha) h_A^q(\beta, \alpha; \mu_0^2). \quad (4.296)$$

In Eq. (4.295), we took into account that the DDs $h_A^q(\beta, \alpha)$ are always even in α , which gives an expansion of the Gegenbauer moments in powers of η^2 . In the nonsinglet case, the Gegenbauer moments $\mathbb{A}_n^q(\eta)$ are nonzero for even n only.

Another simple case is the evolution of the gluon distributions in pure gluodynamics. Then the multiplicatively renormalizable Gegenbauer moments of the GPD $A^g(x, \eta)$

$$\mathbb{A}_n^g(\eta) = \eta^{n-1} \int_{-1}^1 dx C_{n-1}^{5/2} \left(\frac{x}{\eta} \right) A^g(x, \eta), \quad (4.297)$$

which are vanishing only for odd n , can be rewritten in terms of the DD h_A^g :

$$\mathbb{A}_n^g(\eta) = \sum_{k=0}^{[(n-1)/2]} 2^{n-2k-1} \frac{\Gamma(n-2k+3/2)}{\Gamma(5/2)(n-2k-1)!} \eta^{2k} \int_{\Omega} d\beta d\alpha \beta^{n-2k} C_{2k}^{3/2+n-2k}(\alpha) h_A^g(\beta, \alpha). \quad (4.298)$$

Note, that the two shifts, $n \rightarrow n-1$, and $3/2 \rightarrow 5/2$ have compensated each other. Again, every combined $\beta^m C_l^{3/2+m}(\alpha)$ moment of $h_A^g(\beta, \alpha)$ is multiplicatively renormalizable and its evolution is governed by the anomalous dimension $\gamma_{(0)m+l}^{gg;V}$ [6, 140].

Since the Gegenbauer polynomials $C_l^{3/2+m}(\alpha)$ are orthogonal with the weight $(1-\alpha^2)^{m+1}$, the evolution of the β^m -moments of DDs in both cases is given by the formula [140]

$$\begin{aligned} h_{A,m}^q(\alpha; \mu^2) &\equiv \int_{-1}^1 d\beta \beta^m h_A^q(\beta, \alpha; \mu^2) \\ &= (1-\alpha^2)^{m+1} \sum_{k=0}^{\infty} h_{A,ml}^q(\mu_0^2) C_l^{m+3/2}(\alpha) \left(\frac{\alpha_s(\mu_0^2)}{\alpha_s(\mu^2)} \right)^{\gamma_{(0)m+l}^{qg;V}/\beta_0}, \end{aligned} \quad (4.299)$$

where the expansion coefficients $h_{A,m}^q$ are proportional to $\beta^m C_l^{3/2+m}(\alpha)$ moments of DDs h_A^q . The anomalous dimensions $\gamma_{(0)j}^{qq}$ increase with $j = m + l$, and, hence, the m -th β -moment of $h_A^q(\beta, \alpha; \mu^2)$ is asymptotically, i.e., $\mu^2 \rightarrow \infty$, dominated by the α -profile $(1 - \alpha^2)^{m+1}$. Such a correlation between β - and α -dependence of $h_A^q(\beta, \alpha; \mu)$ is not something exotic. Take a DD which is constant in its support region. Then its β^m -moment behaves like $(1 - |\alpha|)^{m+1}$, i.e., the width of the α profile decreases with increasing j . This result is easy to understand: due to the spectral condition $|\alpha| \leq 1 - |\beta|$, the β^m moments with larger m are dominated by regions which are narrower in the α -direction.

These observations suggests to try a model in which the moments $h_{A,m}(\alpha; \mu^2)$ have the asymptotic $(1 - \alpha^2)^{m+1}$ profile even at non-asymptotic μ^2 . This is equivalent to assuming that all the combined moments $\beta^m C_l^{3/2+m}(\alpha)$ with $l > 0$ vanish. Note that this assumption is stable with respect to evolution. Since integrating $h_{A,m}^q(\alpha; \mu^2)$ over α one should get the moments $f_m^q(\mu^2)$ of the forward density $f^q(\beta; \mu^2)$, the DD moments $h_{A,m}^q(\alpha; \mu^2)$ in this model are given by

$$h_{A,m}^q(\alpha; \mu^2) = \rho_{m+1}(\alpha) f_m^q(\mu^2), \quad (4.300)$$

where $\rho_{m+1}(\alpha)$ is the normalized profile function

$$\rho_m(\alpha) \equiv \frac{\Gamma(m + 3/2)}{\Gamma(1/2)\Gamma(m + 1)} (1 - \alpha^2)^m. \quad (4.301)$$

In the explicit form:

$$\int_{-1}^1 d\beta \beta^m h_A^q(\beta, \alpha; \mu^2) = \frac{\Gamma(m + 5/2)}{\Gamma(1/2)(m + 1)!} (1 - \alpha^2)^{m+1} \int_{-1}^1 dx x^m f^q(x; \mu^2). \quad (4.302)$$

In this relation, all the dependence on α can be trivially shifted to the left-hand side of this equation, and we immediately see that $h_A^q(\beta, \alpha; \mu^2)$ in this model is a function of $\beta/(1 - \alpha^2)$,

$$h_A^q(\beta, \alpha; \mu^2) = F^q \left(\frac{\beta}{1 - \alpha^2}; \mu^2 \right) \theta \left(0 < \frac{\beta}{1 - \alpha^2} < 1 \right). \quad (4.303)$$

A direct relation between $f^q(x; \mu^2)$ and $F^q(u; \mu^2)$ can be easily obtained using the basic fact that integrating $h_A^q(\beta, \alpha; \mu^2)$ over α one should get the forward density $f^q(x, \mu^2)$; e.g., for positive x we have

$$f^q(x) = x \int_x^1 du \frac{F^q(u)}{u^{3/2} \sqrt{u - x}}. \quad (4.304)$$

This relation has the structure of the Abel equation. Solving it for $F(u)$ we get

$$F^q(u) = -\frac{u^{3/2}}{\pi} \int_u^1 dx \frac{[f^q(x)/x]'}{\sqrt{x - u}}. \quad (4.305)$$

Thus, in this model, knowing the forward density $f^q(x)$ one can calculate the double distribution function $h_A^q(\beta, \alpha) = F^q(\beta/(1 - \alpha^2))$.

Note, however, that the model derived above violates the DD support condition $|\beta| + |\alpha| \leq 1$: the restriction $|\beta| \leq 1 - \alpha^2$ defines a larger area. Hence, the model is only applicable in a situation when the difference between two spectral conditions can be neglected. A practically important case is the shape of $A^q(x, \eta)$ for small skewness η . Indeed, calculating $A^q(x, \eta)$ for small η one

integrates the relevant DDs $h_A^q(\beta, \alpha)$ over practically vertical lines. If x is also small, both the correct $|\alpha| \leq 1 - |x|$ and model $\alpha^2 \leq 1 - |x|$ conditions can be substituted by $|\alpha| \leq 1$. Now, if $x \gg \eta$, a slight deviation of the integration line from the vertical direction can be neglected and $A^q(x, \eta)$ can be approximated by the forward limit $f^q(x)$.

Specifying the ansatz for $f^q(x)$, one can get an explicit expression for the model DD by calculating $F^q(u)$ from Eq. (4.305). However, in the simplest case when $f^q(x) = Ax^{-a}$ for small x , the result is evident without any calculation: the DD $h_A^q(\beta, \alpha)$ which is a function of the ratio $\beta/(1-\alpha^2)$ and reduces to $A\beta^{-a}$ after an integration over α must be given by $h_A^q(\beta, \alpha) = \rho_a(\alpha) f^q(\beta)$ where $\rho_a(\alpha)$ is the normalized profile function of Eq. (4.301), i.e.,

$$h_A^q(\beta, \alpha) = A \frac{\Gamma(a + 5/2)}{\Gamma(1/2) \Gamma(a + 2)} (1 - \alpha^2)^a \beta^{-a}. \quad (4.306)$$

This DD is a particular case of the general factorized ansatz $h_A^q(\beta, \alpha) = \rho_m(\alpha) f^q(\beta)$ considered in Section 3.13.1. The most nontrivial feature of this model is the correlation $m = a$ between the profile function parameter n and the power a characterizing the small- β behavior of the forward parton distribution.

Knowing the DDs $h_A^q(\beta, \alpha)$, the relevant GPDs $A^q(x, \eta)$ can be obtained in a standard way. In particular, the GPD enhancement factor $\mathcal{R}(\eta)$ for small η in this model is given by

$$\mathcal{R}^q \equiv \frac{A^q(\eta, \eta)}{f^q(\eta)} = \frac{\Gamma(2a + 2)}{\Gamma(a + 2)\Gamma(a + 1)}. \quad (4.307)$$

The use of the asymptotic profiles for DD moments $h_{A,n}^q(\alpha)$ is the basic assumption of the model described above. However, if one is interested in GPDs for small η , the impact of deviations of $h_{A,n}^q(\alpha)$ from the asymptotic profile is suppressed. Even if the higher harmonics are present in $h_{A,n}^q(\alpha)$, i.e., if the $\beta^{n-2k} C_{2k}^{3/2+n-2k}(\alpha)$ moments of $h_A^q(\beta, \alpha)$ are nonzero for $k \geq 1$ values, their contribution into the Gegenbauer moments $\mathbb{A}_n^q(\eta; \mu^2)$ is strongly suppressed by η^{2k} factors (see Eq. (4.295)). Hence, for small η , the shape of $A^q(\eta, \eta)$ for a wide variety of model α -profiles is very close to that based on the asymptotic profile model.

Absence of higher harmonics in $h_{A,n}^q(\alpha)$ is equivalent to absence of the η -dependence in the Gegenbauer moments $\mathbb{A}_n^q(\eta; \mu^2)$. The assumption that the moments $\mathbb{A}_n^q(\eta; \mu^2)$ do not depend on η is the starting point for the model of GPDs $A^q(x, \eta)$ constructed in Ref. [326]. Though the formalism of DDs is not used there, both approaches lead to identical results: the final result of Ref. [326] has the form of a DD representation for $A^q(x, \eta)$. The approach of Ref. [326] is based on the concept of effective forward distributions, which we discuss in the next subsection.

4.11.9 Effective forward distributions

Since the Gegenbauer moments $\mathbb{A}_n^a(\eta; \mu^2)$ evolve like x^n Mellin moments of the usual forward parton densities $f^q(x; \mu^2)$, it was proposed [265] to introduce effective forward distributions (EFDs) $q_\eta(x; \mu^2)$ and $g_\eta(x; \mu^2)$ as functions whose x^n Mellin moments are proportional to the Gegenbauer moments of GPDs, and which coincide with the usual parton densities in the $\eta = 0$ limit. Since

$$\mathbb{A}_n^q(\eta = 0; \mu^2) = \frac{2^n \Gamma(n + 3/2)}{\Gamma(3/2) n!} \int_{-1}^1 dx x^n f^q(x; \mu^2), \quad (4.308)$$

$$\mathbb{A}_n^g(\eta = 0, \mu^2) = \frac{2^n \Gamma(n + 3/2)}{3 \Gamma(3/2) (n - 1)!} \int_{-1}^1 dx x^n f^g(x; \mu^2), \quad (4.309)$$

EFDs are defined [326] by

$$\int_{-1}^1 dz z^n q_\eta(z; \mu^2) = \frac{\Gamma(3/2) n!}{2^n \Gamma(n+3/2)} \mathbb{A}_n^q(\eta; \mu^2), \quad (4.310)$$

$$\int_{-1}^1 dz z^n g_\eta(z; \mu) = \frac{3 \Gamma(3/2) (n-1)!}{2^n \Gamma(n+3/2)} \mathbb{A}_n^g(\eta, \mu^2). \quad (4.311)$$

To proceed further, one can use the expansion (4.133) of bilocal light-cone operators $\mathcal{O}^{aa}(-z^-, z^-)$ over the multiplicatively renormalizable local operators \mathbb{O}_n^{aa} . For quarks, it reads

$$\mathcal{O}^{qq}(0, z^-) = \sum_{n=0}^{\infty} \frac{2n+3}{2^{2n+2}(n+1)!} (-iz^-)^n \int_{-1}^1 d\alpha (1-\alpha^2)^{n+1} \mathbb{O}_n^{qq}\left(\frac{1-\alpha}{2} z^-\right). \quad (4.312)$$

Inserting it into the nonforward matrix element gives

$$A^q(x, \eta) = \sum_{n=0}^{\infty} \frac{2n+3}{2^{2n+2}(n+1)!} \int_{-1}^1 d\alpha (1-\alpha^2)^{n+1} \delta^{(n)}(x - \eta\alpha) \mathbb{A}_n^q(\eta), \quad (4.313)$$

where $\delta^{(n)}(x - \eta\alpha) = \partial_x^n \delta(x - \eta\alpha)$. This formula has a typical structure of a formal inversion of Mellin moments,

$$f(x) = \sum_{n=0}^{\infty} \frac{(-1)^n}{n!} \delta^{(n)}(x) \int_{-1}^1 dx' (x')^n f(x'). \quad (4.314)$$

In Ref. [265], it was proposed to use a form more convenient for summation over n

$$f(x) = -\frac{1}{\pi} \text{disc}_x \sum_{n=0}^{\infty} \frac{1}{x^{n+1}} \int_{-1}^1 dx' (x')^n f(x'), \quad (4.315)$$

based on treating $\delta^{(n)}(x)$ as discontinuities

$$\text{disc}_x \Phi(x) \equiv \frac{1}{2i} \left[\Phi(x + i\varepsilon) - \Phi(x - i\varepsilon) \right]. \quad (4.316)$$

of $1/x^{n+1}$. Using Eq. (4.310), it gives

$$A^q(x, \eta) = -\frac{1}{\pi} \text{disc}_x \int_{-1}^1 d\alpha \sum_{n=0}^{\infty} \frac{\Gamma(n+5/2)}{\Gamma(3/2)(n+1)!} \left(\frac{1-\alpha^2}{x-\eta\alpha}\right)^{n+1} \int_{-1}^1 dz z^n q_\eta(z). \quad (4.317)$$

Now one can perform summation over n and take discontinuity. The formal result, however, would contain a rather singular integrand $[z(1-\alpha^2)/(x-\eta\alpha)-1]^{-3/2}$ producing an end-point divergence. To get a correct result, one needs to soften the singularity by using the relation

$$\int_0^1 dz z^n q_\eta(z) = -\frac{1}{n+2} \int_0^1 dz z^{n+2} \frac{d}{dz} \left(\frac{q_\eta(z)}{z} \right), \quad (4.318)$$

obtained through integration by parts assuming that the surface terms vanish. This gives

$$A^q(x, \eta) = -\frac{1}{\pi} \int_{-1}^1 d\alpha \int_{-1}^1 dz \frac{x-\eta\alpha}{1-\alpha^2} [z(1-\alpha^2)/(x-\eta\alpha)-1]^{-1/2} \frac{d}{dz} \left(\frac{q_\eta(z)}{z} \right). \quad (4.319)$$

If one takes a model in which the effective forward distribution does not depend on η , $q_\eta(z) = q(z)$, then this expression corresponds to a double distribution representation for GPD, with the DD h_A^q given by

$$h_A^q(\beta, \alpha) = -\frac{\beta}{\pi(1-\alpha^2)} \int_{-1}^1 dz \frac{\theta(z/\beta \geq 1/(1-\alpha^2))}{\sqrt{z(1-\alpha^2)/\beta - 1}} \frac{d}{dz} \left(\frac{q(z)}{z} \right). \quad (4.320)$$

Note, that the model with η -independent ansatz for EFDs corresponds to DDs which have a nontrivial α -profile. As we already discussed, the β^n moment of such a DD has the asymptotic shape $(1-\alpha^2)^{n+1}$ for all scales μ^2 . The resulting model GPD has a nontrivial η -dependence, the fact also evident from Eq. (4.319). In other words, this model, though based solely on input from forward distributions, is not a model in which GPD $H(x, \eta)$ coincides with its forward limit $q(x)$ for all η . Such a purely forward model would require $h_A^q(\beta, \alpha) = \delta(\alpha) f^q(\beta)$.

Equation (4.320) coincides with Eq. (4.305), and, as pointed out at the end of the previous subsection, the model for $H^q(x, \eta; \mu)$ based on η -independent EFD was originally developed in Ref. [326]. The spectral condition $\beta/z \leq 1 - \alpha^2$ relating the “original” fraction z of EFD and the “produced” fraction β of DD resembles the momentum ordering $x/z \leq 1$ in the DGLAP equation: the produced fraction³¹ cannot be larger than the original one. In the present case, if the parton also takes some nonzero fraction α of the momentum transfer, the allowed values of β cannot exceed $z(1 - \alpha^2)$. However, as we already remarked, the model based on η -independent Gegenbauer moments gives DD with incorrect support $|\beta| \leq 1 - \alpha^2$. This means that EFDs must have a nontrivial η -dependence needed to secure the correct support $|\beta| \leq 1 - |\alpha|$.

For gluons, one can combine the expansion for the bilocal operator

$$\mathcal{O}^{gg}(0, z^-) = \sum_{n=0}^{\infty} \frac{3(2n+5)}{2^{2n+3}(n+2)!} (-iz^-)^n \int_{-1}^1 d\alpha (1-\alpha^2)^{n+2} \mathbb{O}_{n+1}^{gg} \left(\frac{1-\alpha}{2} z^- \right) \quad (4.321)$$

and the EFD definition (4.311). The resulting expression for $A^g(x, \eta)$ has the form close to Eq. (4.313) derived in the quark case:

$$A^g(x, \eta) = -\frac{1}{\pi} \int_{-1}^1 d\alpha \int_{-1}^1 dz \frac{(x - \eta \alpha)^2}{1 - \alpha^2} [z(1 - \alpha^2)/(x - \eta \alpha) - 1]^{-1/2} \frac{d}{dz} \left(\frac{g_\eta(z)}{z} \right). \quad (4.322)$$

The extra factor $(x - \eta \alpha)$ reflects the convention that $A^g(x, \eta)$ reduces to $xf^g(x)$ in the forward limit.

To get the inverse transformation, i.e., to express EFD $q_\eta(z; \mu^2)$ in terms of GPD $A^q(x, \eta; \mu^2)$, one can start again with EFD definition (4.310). Using expression for the Gegenbauer moments and the beta-function representation for the proportionality coefficients, one obtains³²

$$q_\eta(z) = -\frac{1}{\pi} \text{disc}_z \int_0^1 ds \frac{1}{2z\sqrt{1-s}} \sum_{n=0}^{\infty} \left(\frac{s\eta}{2z} \right)^n \int_{-1}^1 dx C_n^{3/2} \left(\frac{x}{\eta} \right) A^q(x, \eta), \quad (4.323)$$

and

$$g_\eta(z) = -\frac{1}{\pi} \text{disc}_z \int_0^1 ds \frac{3\sqrt{1-s}}{2z^2} \sum_{n=0}^{\infty} \left(\frac{s\eta}{2z} \right)^n \int_{-1}^1 dx C_n^{5/2} \left(\frac{x}{\eta} \right) A^g(x, \eta). \quad (4.324)$$

³¹For positive fractions.

³²In this construction, we follow the line of reasoning presented in Ref. [266], modifying without notice some formulas and statements of that paper where we deem it necessary.

Incorporating the generating function representation for the Gegenbauer polynomials (4.170), these equations yield

$$q_\eta(z) = -\frac{1}{\pi} \operatorname{disc}_z \int_0^1 \frac{ds}{2z\sqrt{1-s}} \int_{-1}^1 dx \frac{A^q(x, \eta)}{[1 - sx/z + s^2\eta^2/(4z^2)]^{3/2}} \quad (4.325)$$

and

$$g_\eta(z) = -\frac{1}{\pi} \operatorname{disc}_z \int_0^1 ds \frac{3\sqrt{1-s}}{2z^2} \int_{-1}^1 dx \frac{A^g(x, \eta)}{[1 - sx/z + s^2\eta^2/(4z^2)]^{5/2}}. \quad (4.326)$$

There are evident discontinuities in the integrands of these representations in the region

$$1 - \frac{s x}{z} + \frac{s^2\eta^2}{4z^2} \leq 0, \quad (4.327)$$

where the arguments of the z -dependent square roots are negative. In this region

$$|x| \geq \frac{|z|}{s} + \frac{s\eta^2}{4|z|}. \quad (4.328)$$

The function on the right hand side has minimum at $s = 2|z|/\eta$ and is equal there η . If $|z| \leq \eta/2$, the value of s at the minimum is within the range allowed for s , and integration over x goes over the $\eta \leq |x| \leq 1$ limits. Note, that the restriction $\eta \leq |x|$ means that taking these discontinuities we would include only the $\eta \leq |x|$ part of the Gegenbauer moments $\mathbb{A}_n^q(\eta)$. The $|x| \leq \eta$ part of these moments, call them $\mathbb{A}_n^{q,<}(\eta)$, can be added using Eq. (4.314), i.e., in the form of a sum of terms proportional to $\mathbb{A}_n^{q,<}(\eta) \delta^{(n)}(z)$. Whether this part can also be written in a more closed form, is an open question. An alternative way to write EFDs in analytic form is based on using DDs and is discussed at the end of this section.

Integrating by parts over x to reduce the singularity of the $3/2$ and $5/2$ roots to the integrable power $1/2$, and then taking the discontinuity of the inverse square root, one obtains

$$q_\eta(z) = -\frac{1}{\pi} \int_0^1 \frac{ds}{s\sqrt{1-s}} \int_{-1}^1 dx \frac{\theta(\text{root})}{\sqrt{-1 + sx/z - s^2\eta^2/(4z^2)}} \frac{\partial}{\partial x} A^q(x, \eta) + \delta q_\eta(z), \quad (4.329)$$

where

$$\delta q_\eta(z) \equiv \sum_{n=0}^{\infty} \frac{(-1)^n \Gamma(3/2)}{2^n \Gamma(n+3/2)} \delta^{(n)}(z) \eta^n \int_{-\eta}^{\eta} dx C_n^{3/2} \left(\frac{x}{\eta} \right) A^q(x, \eta), \quad (4.330)$$

and

$$\begin{aligned} g_\eta(z) = & \frac{2}{\pi} \int_0^1 \frac{\sqrt{1-s}}{s^2} ds \int_{-1}^1 dx \frac{\theta(\text{root})}{\sqrt{-1 + sx/z - s^2\eta^2/(4z^2)}} \frac{\partial^2}{\partial x^2} A^g(x, \eta) \\ & + \sum_{n=0}^{\infty} \frac{3(-1)^n \Gamma(3/2)}{2^n n \Gamma(n+3/2)} \mathbb{A}_{n+1}^{g,<}(\eta) \delta^{(n)}(z). \end{aligned} \quad (4.331)$$

We intentionally wrote the $|x| \leq |\eta|$ parts in two forms: in explicit form for quarks (it will be used below) and in a shorter form for gluons. The notation $\theta(\text{root})$ implies that integration over s, x is in the region specified by Eq. (4.327), where the argument of the square root is positive.

If $|z| \geq |\eta|/2$, the minimum value for $|x|$ in this region is achieved at the boundary $s = 1$, and is given by a z -dependent expression $|x|_{\min} = |z| + \eta^2/4|z|$. The support region for the first term of EFDs is

$$0 \leq |z| \leq \frac{1}{2} \left(1 + \sqrt{1 - \eta^2}\right), \quad 0 \leq |\eta| \leq 1. \quad (4.332)$$

It is smaller than the square $0 \leq |z|, \eta \leq 1$. Concerning the term coming from the $|x| \leq \eta$ integration, one may be worried that, in principle, an infinite sum of $\delta^{(n)}(z)$ terms can produce a function with any support. However, using the relation

$$\int_{-1}^1 dz \left(\frac{z}{\eta}\right)^n \delta q_\eta(z) = \frac{\Gamma(3/2) n!}{2^n \Gamma(n+3/2)} \int_{-\eta}^\eta dx C_n^{3/2} \left(\frac{x}{\eta}\right) A^q(x, \eta), \quad (4.333)$$

and taking into account that $C_n^{3/2}(x/\eta)$ are polynomials in x/η , one can see that the support region of $\delta q_\eta(z)$ is $|z| \leq \eta$. The same is true for the $|x| \leq \eta$ gluonic term.

All these complications, related to different nature of GPDs $A(x, \eta)$ in $|x| \geq \eta$ and $|x| \leq \eta$ regions, can be avoided if one writes EFDs in terms of DDs. The main point is that “DDs do not know about η ”. In quark case, using (4.295), one has

$$\int_{-1}^1 dz z^n q_\eta(z) = \sum_{k=0}^{[n/2]} \left(\frac{\eta}{2}\right)^{2k} \frac{\Gamma(n-2k+3/2)n!}{\Gamma(n+3/2)(n-2k)!} \int_{\Omega} d\beta d\alpha \beta^{n-2k} C_{2k}^{3/2+n-2k}(\alpha) h_A^q(\beta, \alpha). \quad (4.334)$$

The first terms of the η^2 expansion can be easily written:

$$\begin{aligned} \int_{-1}^1 dz z^n q_\eta(z) &= \int_{\Omega} d\beta d\alpha \left\{ \beta^n h_A^q(\beta, \alpha) \right. \\ &\quad \left. + \frac{\eta^2}{2} \theta(n-2) n(n-1) \left[\alpha^2 - \frac{1}{2n+1} \right] \beta^{n-2} h_A^q(\beta, \alpha) \right\} + \mathcal{O}(\eta^4). \end{aligned} \quad (4.335)$$

Inverting the Mellin transform, we obtain for positive³³ z

$$q_\eta(z)|_{z \geq 0} = f^q(z) + \frac{\eta^2}{2} \left\{ \frac{d^2}{dz^2} \left[h_{A,2}^q(z) - \frac{z^{3/2}}{2} \int_z^1 d\beta \frac{f^q(\beta)}{\beta^{5/2}} \right] \right\}_{+\{0,1\}} + \mathcal{O}(\eta^4), \quad (4.336)$$

where $f^q(z)$ is the forward distribution, i.e., the zeroth α -moment of the DD $h_A^q(\beta, \alpha)$, and $h_{A,2}^q(\beta)$ is the second α -moment of the DD:

$$h_{A,2}^q(\beta)|_{\beta \geq 0} = \int_{-1+\beta}^{1-\beta} d\alpha \alpha^2 h_A^q(\beta, \alpha). \quad (4.337)$$

The $\{\dots\}_{+\{0,1\}}$ prescription generalizes the standard “plus” distribution: it means that the function in the brackets should be accompanied by a subtraction procedure which guarantees that its z^0 and z^1 moments vanish (even if taken in the $z \geq 0$ region only), to comply with the structure of the generating equation (4.335). For gluons, using Eq. (4.298), one obtains

$$\begin{aligned} \int_{-1}^1 dz z^n g_\eta(z) &= \int_{\Omega} d\beta d\alpha \left\{ \beta^n h_A^g(\beta, \alpha) \right. \\ &\quad \left. + \frac{\eta^2}{2} \theta(n-3) (n-1)(n-2) \left[\alpha^2 - \frac{1}{2n+1} \right] \beta^{n-2} h_A^g(\beta, \alpha) \right\} + \mathcal{O}(\eta^4), \end{aligned} \quad (4.338)$$

³³To reconstruct the function $q_\eta(z)$ for negative z , one should use its z -symmetry.

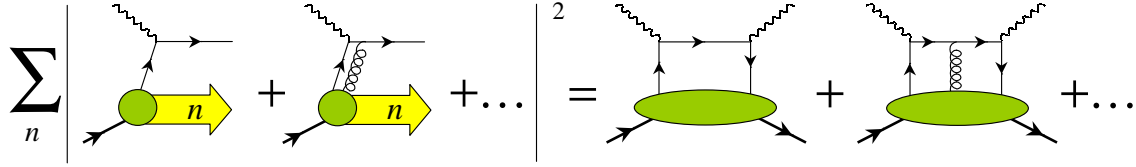


Figure 35: Hadronic structure functions of deeply inelastic scattering as a series in a number of partons participating in a hard scattering, truncated here to the lowest two terms in the Fock expansion. The first term on the right-hand side of the equality stands for the leading twist-two contribution. As was demonstrated in Section 2.2.6, it is an absolute value squared of a single-parton scattering amplitude. The second term is an interference of single- and two-particle amplitudes and corresponds to twist-three effects. The latter are power suppressed in the hard scale compared to the leading term.

and

$$g_\eta(z)|_{z \geq 0} = f^g(z) + \frac{\eta^2}{2} \left\{ z \frac{d^2}{dz^2} \left[\frac{h_{A,2}^g(z)}{z} - \frac{z^{1/2}}{2} \int_z^1 d\beta \frac{f^g(\beta)}{\beta^{5/2}} \right] \right\}_{+ \{0,1,2\}} + \mathcal{O}(\eta^4), \quad (4.339)$$

with $\{\dots\}_{+ \{0,1,2\}}$ now meaning that z^0, z^1 and z^2 moments of the function in the brackets should vanish. It is straightforward to include higher terms of the η^2 expansion.

At present, the only practical way to construct GPDs consistent with the polynomiality condition is to use factorized models “forward density (β) \otimes profile function(β, α)” for DDs. In these models, EFDs $q_\eta(z), g_\eta(z)$ can be expressed in terms of forward distributions through an expansion in η^2 , and one can study evolution of GPDs by existing codes for numerical evolution of parton densities.

5 Compton scattering beyond leading order and power

So far we have discussed the properties of the leading-twist GPDs irrespective of specific high-energy processes where they emerge and can be ultimately measured. The present section is a first step toward phenomenology of GPDs in various scattering experiments. The subject of our analysis here is the virtual Compton amplitude, a building block of the electron-nucleon Compton scattering process. We present a thorough study of the Compton amplitude including its gauge-invariant tensor decomposition, one-loop corrections to the short-distance coefficient function and power suppressed contributions including the consideration of twist-three and target mass effects.

5.1 Compton scattering in Bjorken limit

As argued in the introduction, the scattering of a virtual photon on a single parton scales at asymptotically large virtualities of the probe. The simultaneous scattering on two partons is suppressed by a power of the hard scale (see Eq. (2.44)). Since experimentally accessed processes are probed at finite values of the momentum transfer, one has to know *a priori* the magnitude of power-suppressed contributions, which also go under the name of power corrections or higher twist effects. A typical lepton-hadron cross section at high momentum transfer Q is given by a

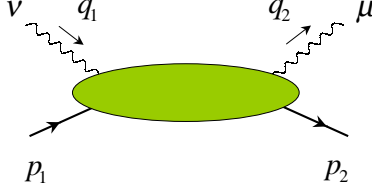


Figure 36: Virtual Compton amplitude.

series in $1/\mathcal{Q}$

$$\sigma(x_B, \mathcal{Q}^2) = \sum_{\tau=2}^{\infty} \left(\frac{\Lambda}{\mathcal{Q}} \right)^{\tau-2} \int \{dx_\tau\} C(x_B, \{x_\tau\}; \alpha_s) f(\{x_\tau\}; \mathcal{Q}^2), \quad (5.1)$$

where τ stands for the twist of contributing operators, which parametrize physics at soft scales. The first term in the expansion (5.1) corresponds to the Feynman parton model picture. Subsequent terms, standing for multi-parton correlations in hadron, reveal QCD dynamics not encoded in conventional parton densities. They manifest genuine quantum mechanical effects, since they involve interference of hadron wave functions with different numbers of constituents, see Fig. 35. Twist-three correlations are unique among all other higher-twist effects because they appear as a leading effect in certain hadronic spin asymmetries. The most familiar example is the transverse spin structure function g_2 (see Eq. (2.34)) measured in deeply inelastic scattering. Though this function is formally defined as a Fourier transform of a two-quark bilocal operator—similarly to the twist-two parton distributions, extensively discussed above—the presence of the transverse Dirac matrix γ_\perp in its vertex results in the “good-bad” field structure, in terminology of the formalism of light-cone quantization, as we explain in Appendix D. The elimination of the “bad” fields in favor of the “good” ones (D.7) yields contributions with an additional parton in the QCD light-cone operator compared to its original two-particle counterpart. This is exactly the manifestation of the interference nature of the transverse spin structure function, which makes it very attractive for studies of genuine QCD interaction effects beyond the naive parton model. Since deeply inelastic scattering is expressed in terms of the forward Compton amplitude, the effects we have just outlined will arise in a more prominent and enhanced way in the off-forward Compton amplitude, which we will address presently. As a consequence of QCD factorization theorems, proved currently to leading twist accuracy, the latter will be expressed in terms of GPDs.

5.1.1 Structure of the Compton amplitude in generalized Bjorken limit

Several versions of the leading twist factorization theorems were discussed in the literature [6, 282, 283, 284] for the amplitude of the virtual Compton scattering on a hadron, which is defined through the off-forward matrix element of the time-ordered product of two quark electromagnetic currents (2.15),

$$T_{\mu\nu} = i \int d^4z e^{iq\cdot z} \langle p_2 | T \{ j_\mu(z/2) j_\nu(-z/2) \} | p_1 \rangle. \quad (5.2)$$

To determine regions responsible for contributions with a powerlike \mathcal{Q}^{-N} behavior, it is sufficient to analyze the singularity structure due to denominators of particle propagators. The numerators, present in the QCD case, only change particular powers N , which are not important for our

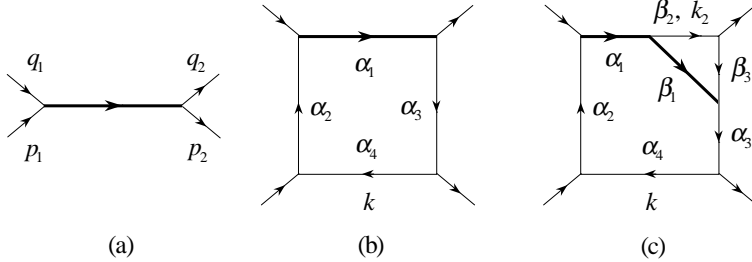


Figure 37: Lowest order perturbative diagrams exhibiting possible short-distance regimes contributing to the asymptotics of Compton scattering amplitude. Thick lines correspond to the highly virtual propagators.

analysis at this stage. Furthermore, complications due to gauge invariance in the realistic case of QCD can be treated in a rather straightforward manner. Hence, to understand basic points of the factorization approach of Ref. [6], it is instructive to address the VCS amplitude using the example of a cubic scalar model³⁴. We will concentrate on the contribution due to the s -channel diagrams, since the analysis of u -channel diagrams does not bring any new insights into the factorization property of the hadronic tensor.

The tree-level Compton amplitude, see Fig. 37 (a), is given by

$$T_{(0)} = \frac{1}{(p_1 + q_1)^2 + i0} = \frac{1}{p_1^2 + q_1^2 + 2(p_1 \cdot q_1) + i0}. \quad (5.3)$$

The scaling property is exhibited by considering, say, the kinematics when both $\mathcal{Q}^2 \equiv -q_1^2$ and $(p_1 \cdot q_1)$ are large and $q_2^2 = 0$, while keeping the Bjorken variable x_B (2.35) fixed. Neglecting the target mass p_1^2 , one obtains

$$T_{(0)} = \frac{1}{2(p_1 \cdot q_1)} \frac{1}{1 - x_B + i0} + \mathcal{O}\left(\frac{p_1^2}{p_1 \cdot q_1}\right). \quad (5.4)$$

The analysis of loop amplitudes is conveniently performed making use of the α -representation of particle's propagators (G.42). The one-loop expression for the Compton amplitude displayed in Fig. 37 (b) can then be rewritten performing the momentum integration with the help of Eq. (G.16) as

$$T_{(1)} = ig^2 \int \frac{d^4k}{(2\pi)^4} \frac{1}{k^2(k+p_1)^2(k+p_2)^2(k+p_1+q_1)^2} = \frac{g^2}{(4\pi)^2} \int_0^\infty \prod_{j=1}^4 \frac{d\alpha_j}{\varrho^2} e^{iE_1+i0_\varrho}, \quad (5.5)$$

$(0_\varrho = 0 \cdot \varrho)$ with the integrand depending on the exponent

$$E_1 = q_1^2 \frac{\alpha_1 \alpha_2}{\varrho} + q_2^2 \frac{\alpha_1 \alpha_3}{\varrho} + s \frac{\alpha_1 \alpha_4}{\varrho} + t \frac{\alpha_2 \alpha_3}{\varrho} + p_1^2 \frac{\alpha_2 \alpha_4}{\varrho} + p_2^2 \frac{\alpha_3 \alpha_4}{\varrho}. \quad (5.6)$$

and $\varrho \equiv \sum_{j=1}^4 \alpha_j$. In general, a two-to-two scattering amplitude depends on seven kinematical invariants: the usual Mandelstam variables

$$s = (p_1 + q_1)^2, \quad t = (p_1 - p_2)^2, \quad u = (p_2 - q_1)^2$$

³⁴The absence of a stable vacuum state in this model is irrelevant for the demonstration of generic perturbative properties of scattering amplitudes.

and external virtualities q_1^2 , q_2^2 , p_1^2 , p_2^2 obeying the constraint $s + t + u = q_1^2 + q_2^2 + p_1^2 + p_2^2$. It also depends on the masses m_σ of the internal lines σ (which, for brevity, were omitted in Eqs. (5.5) and (5.6) above). There exists a simple rule to derive the coefficients accompanying the momentum invariants in the exponential of the α -representation. In particular, cutting the lines 1 and 2 in Fig. 37 (b) corresponding to α -parameters α_1 and α_2 , one divides the diagram into two components with q_1^2 being the total momentum squared entering into each of them. Cutting the lines 1 and 3 gives the components corresponding to q_2^2 , for lines 1 and 4 one gets s , and so on. In general, any diagram contributing to the Compton amplitude can be written as

$$T(p_1, p_2, q_1, q_2) = \int_0^\infty \prod_{\sigma=1}^L d\alpha_\sigma \frac{G(\alpha, \{p_i\}, m_\sigma)}{D^2(\alpha)} \times \exp \left\{ iq_1^2 \frac{A_1(\alpha)}{D(\alpha)} + iq_2^2 \frac{A_2(\alpha)}{D(\alpha)} + is \frac{A_s(\alpha)}{D(\alpha)} + iu \frac{A_u(\alpha)}{D(\alpha)} + it \frac{A_t(\alpha)}{D(\alpha)} - i \sum_\sigma \alpha_\sigma (m_\sigma^2 - i\epsilon) \right\}, \quad (5.7)$$

where L is the number of its internal lines. The pre-exponential factor $G(\alpha, \{p_i\}, m_\sigma)$ results from the numerator structure of the QCD diagram, and D , A_s , A_u , A_t , A_1 , A_2 are functions of the α -parameters $\{\alpha_\sigma\}$ uniquely determined for each diagram. The D function (the “determinant” of a diagram) is given by a sum of products of the α -parameters of each set of lines the elimination of which from the diagram converts the diagram into a tree diagram (i.e., containing no loops). The A functions are given by sums of products of the α -parameters corresponding to all possible cuts of the diagram into two components each having a tree structure. A particular product of the α -parameters is multiplied by the kinematical invariant corresponding to a specified cut.

Our objective is to consider the Compton amplitude in the asymptotic limit when some of the invariants are large and some are small, and to identify the powerlike scaling contributions. The hadron masses $p_1^2 = p_2^2 = M^2$ will always be treated as small variables. The main point to realize is that if, say, s is a large invariant, the result of integration over a region where $A_s/D > \rho$ will be exponentially $\sim \exp[-s\rho]$ suppressed at large s . Only provided that A_s/D vanishes somewhere in the integration region, one can get a power-behaved contribution. This may happen either when A_s vanishes, or when D goes to infinity. In its turn, A_s can vanish only when some α -parameters vanish, and D can tend to infinity only when some α -parameters tend to infinity. In particular, for the one-loop diagram in Fig. 37 (b), there are two evident possibilities $\alpha_1 = 0$ and $\alpha_4 = 0$ that make the coefficient in front of s equal to zero in Eq. (5.6). These two choices do not exclude each other, so one can take $\alpha_1 = 0$ and/or $\alpha_4 = 0$. Less evident possibilities are $\alpha_2 \rightarrow \infty$ and/or $\alpha_3 \rightarrow \infty$. Note, that $\alpha_1 \rightarrow \infty$ or $\alpha_4 \rightarrow \infty$ do not automatically make the s -coefficient $\alpha_1\alpha_4/\rho$ vanish, since these parameters are present in the denominator factor ρ . In other words, there is a complication that when $D \rightarrow \infty$, it is quite possible that then also $A_s \rightarrow \infty$. Moreover, in the opposite situation, when $A_s \rightarrow 0$, it is also possible that $D \rightarrow 0$, and to get zero for the ratio A_s/D , the numerator A_s should vanish faster than the denominator D . The solution of the problem of finding such sets of α -parameters for which the ratio A_s/D vanishes, is facilitated by the fact that $\alpha_\sigma \rightarrow 0$ is analogous to contraction of the corresponding line σ into a point, while $\alpha_\sigma \rightarrow \infty$ corresponds to removal of the line σ from the diagram. Hence, we should find such sets of lines, whose contraction into a point (“short-distance or SD regime”) or their removal from the diagram (“infrared or IR regime”) makes the diagram independent of s , or, in general, of all large variables. The combined SD-IR regimes are also possible. In this case, the dependence on large variables is killed by contracting some lines into points and eliminating some other lines.

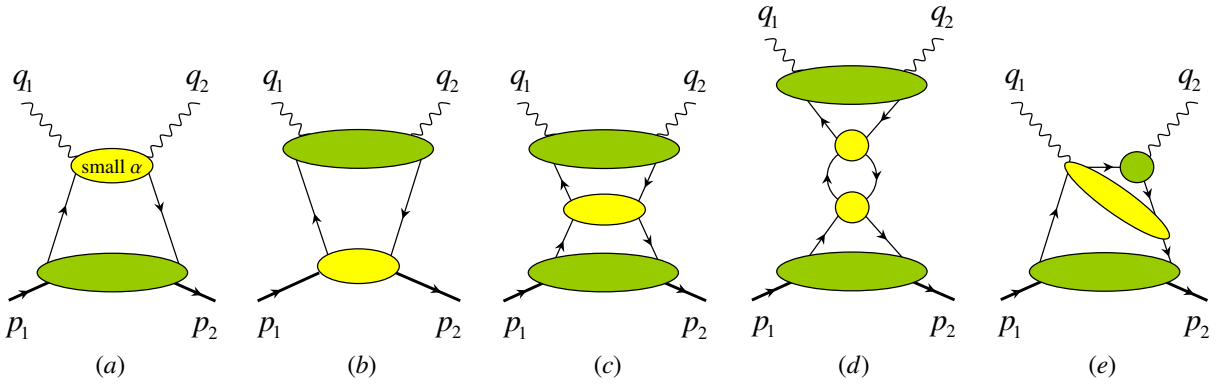


Figure 38: Short-distance regimes in the generalized Compton amplitude: the contractions (i), (ii), (iii) and (iv), discussed in the text, are represented in (a), (b), (c) and (e), respectively. A multiperipheral chain is shown in (d).

The α -representation has the advantage that the dependence of the amplitudes on the momentum invariants is displayed in the most direct way. This makes it very convenient for a general analysis of the asymptotic behavior of Feynman diagrams. Proceeding by analogy with the one-loop example, one can easily find three evident possibilities to eliminate the dependence of a four-point function on the large invariant s : (i) to contract into a point a subgraph containing the external lines with momenta q_1 and q_2 , see Fig. 38 (a), (the $\alpha_1 = 0$ regime in the one-loop case); (ii) to contract into a point a subgraph containing the external lines with momenta p_1 and p_2 , see Fig. 38 (b), (the $\alpha_4 = 0$ regime); and (iii) to contract into point a central subgraph so as to separate the sets q_1, q_2 and p_1, p_2 from each other, see Fig. 38 (c). Since small α_σ 's correspond to large virtualities, the possibility (i) corresponds to large virtualities between the q_1 and q_2 vertices, while the possibility (ii) implies that there is a large virtuality momentum flowing between the p_1 and p_2 vertices. The latter are imitating hadrons, and since the hadronic wave functions are expected to rapidly vanish at large virtualities, the contraction (ii) should be excluded from possible contributing regions. Note, that the contraction corresponding to the possibility (i) gives a “reduced” diagram that depends only on t and p_1^2, p_2^2 , but does not depend on q_1^2 and q_2^2 . If t is small, all dependence on large variables is eliminated. On the other hand, after the contraction of type (iii), the upper part still depends on q_1^2 and q_2^2 , and when one of them or both are large, one would still need to apply the type (i) contraction. When both q_1^2 and q_2^2 are small, we are not required to contract a subgraph containing the q_1, q_2 vertices, and the large- s (or u) behavior may be governed by central contractions (there may be several of them, forming a “multiperipheral” chain, see Fig. 38 (d)), with the upper nonperturbative object similar to a photon-to-photon GPD. In general, type (i) contraction eliminates the dependence on q_1^2, q_2^2, s and u . If both of q_1^2, q_2^2 are large, the type (i) contraction is the only possibility, since other contractions would involve the hadronic vertices. If t is small, the lines outside the contracted subgraph do not need to have large virtualities. One can parametrize the function describing the small-virtuality part by a nonperturbative parton distribution, and calculate the large virtuality part using perturbative QCD and asymptotic freedom. If only one of the photon virtualities, say q_1^2 is large, there is also a possibility (iv), see Fig. 38 (e). The reduced diagram in this case has an extra small-virtuality part corresponding to the distribution amplitude of the q_2 -photon. At this stage, the analysis

should be supplemented by power counting. In QCD, the possibility (iv) is suppressed by $1/q_1^2$ compared to possibility (i) [3, 5], thus if q_1^2 is large, the type (i) contraction is the only possibility to get the leading power contribution.

The kinematics when at least one of the invariants q_1^2 , q_2^2 is large and s is also large, but the ratios q_1^2/s , q_2^2/s are fixed, can be called the generalized Bjorken limit.

5.1.2 Compton amplitude in symmetric variables

In many cases, it is convenient to use symmetric combinations of particle momenta

$$q = \frac{1}{2}(q_1 + q_2), \quad p = p_1 + p_2, \quad \Delta = p_1 - p_2 = q_2 - q_1. \quad (5.8)$$

The three Mandelstam kinematical invariants can be traded for the symmetric ones, which consist of the averaged photon virtuality and two scaling variables,

$$q^2 = -Q^2, \quad \xi = \frac{Q^2}{p \cdot q}, \quad \eta = \frac{\Delta \cdot q}{p \cdot q}. \quad (5.9)$$

The latter two are called the generalized Bjorken and skewness variables, respectively. They can be re-expressed in terms of the “experimental” ones, i.e., masses of incoming and outgoing photons, and the conventional Bjorken variable

$$\mathcal{Q}^2 = -q_1^2, \quad M_{\ell\bar{\ell}}^2 = q_2^2, \quad x_B = \frac{\mathcal{Q}^2}{2p_1 \cdot q_1}, \quad (5.10)$$

respectively, via the equations:

$$Q^2 = \frac{1}{2} \left(\mathcal{Q}^2 - M_{\ell\bar{\ell}}^2 + \frac{\Delta^2}{2} \right), \quad (5.11)$$

for the averaged photon virtuality, and

$$\xi = \frac{\mathcal{Q}^2 - M_{\ell\bar{\ell}}^2 + \Delta^2/2}{2\mathcal{Q}^2/x_B - \mathcal{Q}^2 - M_{\ell\bar{\ell}}^2 + \Delta^2}, \quad \eta = \frac{\mathcal{Q}^2 + M_{\ell\bar{\ell}}^2}{2\mathcal{Q}^2/x_B - \mathcal{Q}^2 - M_{\ell\bar{\ell}}^2 + \Delta^2}, \quad (5.12)$$

for the scaling variables. Note that Q^2 and ξ can take both positive ($\mathcal{Q}^2 > M_{\ell\bar{\ell}}^2$) and negative ($\mathcal{Q}^2 < M_{\ell\bar{\ell}}^2$) values depending on the relative magnitude of spacelike and timelike photon virtualities, while $\eta > 0$ and $\eta \pm \xi > 0$. To complete the set of formulas, we give also the inverse transformations

$$M_{\ell\bar{\ell}}^2 = - \left(1 - \frac{\eta}{\xi} \right) Q^2 + \frac{\Delta^2}{4}, \quad \mathcal{Q}^2 = \left(1 + \frac{\eta}{\xi} \right) Q^2 - \frac{\Delta^2}{4}, \quad (5.13)$$

and

$$x_B = \frac{(\xi + \eta)Q^2 - \xi\Delta^2/4}{(1 + \eta)Q^2 - \xi\Delta^2/2}. \quad (5.14)$$

The generalized Bjorken limit, where the perturbative QCD approach to the general Compton amplitude makes sense and proves to be very fruitful, is characterized by sending the Mandelstam variable s and one or both photon virtualities to infinity, while keeping ξ and η finite. The most important limiting cases follow.

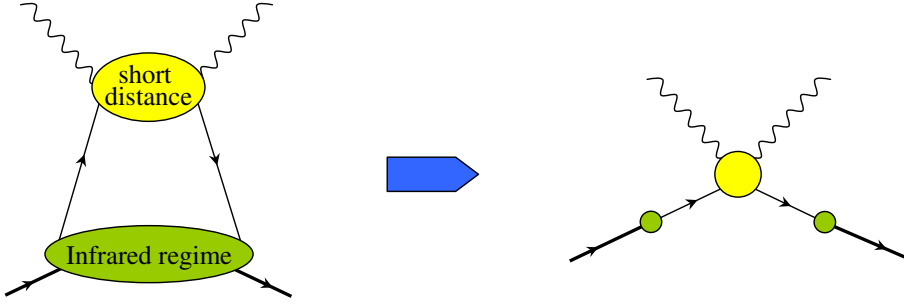


Figure 39: The diagram for the wide-angle Compton scattering and its reduced graph.

- Deeply inelastic scattering:

$$\Delta = 0, \quad \eta = 0, \quad \xi = x_B,$$

with Bjorken kinematics

$$s \sim -q_1^2 = -q_2^2 \rightarrow \infty.$$

- Deeply virtual Compton scattering:

$$q_2^2 = 0, \quad \eta \simeq \xi,$$

and

$$s \sim -q_1^2 \rightarrow \infty, \quad -\Delta^2 \ll s.$$

- Timelike Compton scattering:

$$q_1^2 = 0, \quad \eta \simeq -\xi,$$

such that

$$s \sim q_2^2 \rightarrow \infty, \quad -\Delta^2 \ll s.$$

- Doubly virtual Compton scattering:

$$q_1^2 < 0, \quad q_2^2 > 0, \quad \eta > \xi.$$

with scaling limit

$$s \sim -q_1^2 \sim q_2^2 \rightarrow \infty, \quad -\Delta^2 \ll s.$$

The region $\eta < \xi$ is accessible only when both of the photon virtualities are space-like (like in DIS). However, the Compton amplitude in such a kinematics does not correspond to a leading contribution of any known high-energy process. It arises, however, as a part of the two-photon contribution in exclusive electron-proton scattering, which measures electromagnetic form factors [281].

Another process that attracted recently a lot of attention [416, 204] is the wide-angle Compton scattering, when both photons are real and $s \sim -t \sim -u$ is large. The contraction of a subgraph containing the real-photon vertices (α_1 in the one-loop example) eliminates dependence on s and u , but the resulting object still has dependence on large variable t . For the one-loop diagram, this dependence can be eliminated by the infrared regime $\alpha_4 \rightarrow \infty$. In general case, the analog is

the situation when the α -parameters of a “soft” subgraph, connecting the incoming and outgoing nucleon vertices, tend to infinity. This corresponds to Feynman mechanism, i.e., these lines can be treated as “wee” particles carrying decreasing fractions $x < \lambda/\sqrt{-t}$ of the hadron momentum. As a result, large virtualities are not induced in the lower object, and one might talk about separation of hard and soft contributions. The factorization properties of this process need further study. In particular, they are also complicated by the possibility of combining a central type (iii) contraction with Feynman mechanism for the upper and lower components of the reduced diagram.

5.1.3 One-loop factorization in symmetric variables

Let us continue the discussion of the cubic scalar model and illustrate the mechanism of factorization of the Compton amplitude into GPDs. We will use symmetric variables which allow simultaneous treatment of different kinematical situations. The tree-level Compton amplitude, see Fig. 37 (a), is given now by

$$T_{(0)} = \frac{1}{(p_1 + q_1)^2 + i0} = \frac{1}{(p \cdot q)} \frac{1}{1 - \xi + \frac{1}{2}\epsilon + i0}, \quad (5.15)$$

where the small correction to the scaling contribution goes in powers of

$$\epsilon \equiv \frac{4M_N^2 - \Delta^2}{2(p \cdot q)}.$$

Thus, the virtuality of the propagator of the tree diagram is proportional to $(p \cdot q) = Q^2/\xi$ rather than to $Q^2 = -q^2$ as one might expect from the definition of the Compton amplitude (5.2). In this connection, we would like to note that the variable Q^2 related to the symmetric combination $q_1 + q_2$ need not be mandatorily large in the generalized Bjorken limit. Actually, this scale becomes small when the virtualities of incoming and outgoing photons cancel each other: $q_1^2 + q_2^2 = 0$. As we discussed above, to assure that the small- α regime (or short “distances” between the photon vertices) is the only possibility to get a power-law contribution for large s , one or both external photon virtualities q_1^2, q_2^2 need to be large. The momentum $q_1 + q_2$ cannot be arranged as a total momentum entering into one of the components of a Compton diagram cut into two parts, so its value is not directly relevant to the analysis of asymptotic behavior. In the generalized Bjorken limit, it is convenient to treat $(p \cdot q)$ as the basic large variable, expressing photon virtualities, Q^2 , etc. as $(p \cdot q)$ multiplied by an appropriate dimensionless coefficient. Since the variable Q^2 contains $Q^2 - M_{\ell\bar{\ell}}^2$ it is a large variable, except for a region where $Q^2 \approx M_{\ell\bar{\ell}}^2$. However, as far as Q^2 and $M_{\ell\bar{\ell}}^2$ are large, this accidental cancellation has no significance.

When $p \cdot q \rightarrow \infty$ and ξ is fixed, one recovers the scaling coefficient function $1/(x - \xi + i0)$ convoluted with the “perturbative” GPD which, to this order, is simply

$$F_{(0)}^\phi(x, \eta, \Delta^2) = \delta(1 - x). \quad (5.16)$$

At one-loop order, the exponential factor of the α -representation in Eq. (5.6) written in symmetric variables is

$$\begin{aligned} E_1 = \alpha_1 & \left\{ (1 - \xi + \frac{1}{2}\epsilon) \left(1 - \frac{\alpha_1}{\varrho} \right) - (1 + \eta + \epsilon) \frac{\alpha_2}{\varrho} - (1 - \eta + \epsilon) \frac{\alpha_3}{\varrho} \right\} (p \cdot q) + \frac{\alpha_2 \alpha_3}{\varrho} \Delta^2 \\ & + (\alpha_2 + \alpha_3) \left(1 - \frac{\alpha_2 + \alpha_3}{\varrho} \right) M_N^2. \end{aligned} \quad (5.17)$$

As we already discussed, integration in the vicinity of $\alpha_1 \rightarrow 0$ corresponds to large virtuality of the corresponding line in the Feynman diagram, the propagator between the photon vertices. To leading order in $1/(p \cdot q)$, such an integration gives

$$T_{(1)}^{\text{SD1}} = \frac{1}{(p \cdot q)} \int_{-1}^1 dx \frac{F_{(1)}^\phi(x, \eta, \Delta^2)}{x - \xi + i0}, \quad (5.18)$$

where we introduced the one-loop GPD, which absorbs all contributions which diverge when M_N goes to zero, i.e., the so-called mass singularities,

$$F_{(1)}^\phi(x, \eta, \Delta^2) = \frac{ig^2}{(4\pi)^2} \int_0^\infty \prod_{j=2}^4 d\alpha_j \delta \left(x - 1 + (1+\eta)\frac{\alpha_2}{\tilde{\varrho}} + (1-\eta)\frac{\alpha_3}{\tilde{\varrho}} \right) \frac{e^{i(\tilde{E}_1+i0_{\tilde{\varrho}})}}{\tilde{\varrho}^2}. \quad (5.19)$$

Here, $\tilde{\varrho} = \alpha_2 + \alpha_3 + \alpha_4$. Note, that $\tilde{E}_1 = E_1[\alpha_1 = 0]$ does not depend on large scales. Summing the tree and one-loop contributions, one gets a factorized expression of the form (5.18) with $F_{(1)}^\phi$ being replaced by $F^\phi = F_{(0)}^\phi + F_{(1)}^\phi + \dots$. One can easily convince oneself that the perturbative expansion of the GPD $F^\phi(x, \eta, \Delta^2)$ arises from the matrix element of the light-cone operator $\mathcal{O}^{\phi\phi}$ from Eq. (3.4):

$$F^\phi(x, \eta, \Delta^2) = p^+ \int \frac{dz^-}{2\pi} e^{ixz^- p^+} \langle p_2 | \mathcal{O}^{\phi\phi}(-z^-, z^-) | p_1 \rangle. \quad (5.20)$$

Other short-distance and infrared regimes lead to contributions which are power-suppressed compared to the leading one (5.18), see Ref. [6]. When a larger number of lines is connecting the hadronic part with hard propagators, this usually leads to the suppression of amplitudes by powers of $1/(p \cdot q)$, merely because the number of hard propagators increases. An important exception is provided by the longitudinally polarized $\varepsilon^\mu \sim p^\mu$ vector particles in gauge field theories. Namely, in QCD the quark propagator $\sim q/(p \cdot q)$ combines with the adjacent gluon vertex factor $\not{q} \sim \not{p}$ to produce an unsuppressed $\mathcal{O}(1)$ factor. Hence, one should take this contributions into account and sum over all possible insertions of gluon lines into the hard quark propagator. The summation is identical to that performed in Section 2.2.6 for conventional parton densities and yields a path-ordered exponential stretched between the elementary fields in the bilocal operator defining the GPD. The analysis of the most general handbag diagram, i.e., with a single propagator between the photon vertices and any possible configuration of lines forming the lower part, does not bring in new complications compared to the already discussed one-loop example, and can be treated in an analogous manner. In QCD case, the numerator $\sim q$ of the hard propagator combines with the Dirac spinors of the incoming and outgoing quark lines $u\bar{u} \sim \not{p}$ and cancels the power of $p \cdot q$ coming from the denominator, so that $T^{\text{SD1}} \sim \mathcal{O}((p \cdot q)^0)$.

5.1.4 Hadronization corrections of the final-state photon

When the final-state photon is timelike, the quark-antiquark pair can form an on-shell intermediate hadronic state before annihilating into the heavy photon. This corresponds to the hard momentum being re-routed around the photon vertex as shown in the diagram (c) of Fig. 37. This configuration can potentially generate an asymptotically leading contribution when the photon virtuality is low. Let us demonstrate that it is actually suppressed. The two-loop diagram in Fig. 37 (c) has the form

$$T_{(3)} = -g^4 \int \frac{d^4 k_1}{(2\pi)^4} \frac{1}{k_1^2 (k_1 + p_1)^2 (k_1 + p_2)^2 (k_1 + p_1 + p_2)^2} \quad (5.21)$$

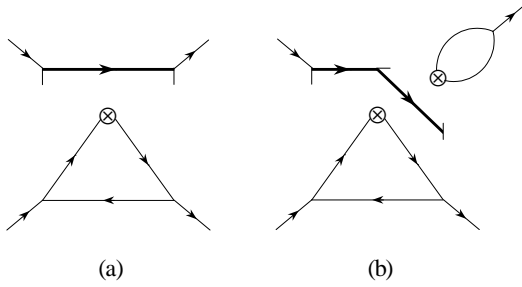


Figure 40: Short-distance regimes corresponding to loop diagrams in Fig. 37.

$$\times \int \frac{d^4 k_2}{(2\pi)^4} \frac{1}{k_2^2 (k_2 - q_2)^2 (k_2 - k_1 - q_1 - p_1)^2} = i \frac{g^4}{(4\pi)^4} \int_0^\infty \prod_{i=1}^4 d\alpha_i \prod_{j=1}^3 d\beta_j \frac{e^{i(E_2 + i0_{\alpha+\beta})}}{[\alpha\beta + \beta_1(\beta - \beta_1)]^2}$$

with $\alpha \equiv \sum_{i=1}^4 \alpha_i$ and $\beta \equiv \sum_{i=1}^3 \beta_i$. The exponential here is given by

$$E_2 = \alpha \frac{\alpha_1 + \beta_1 \left(1 - \frac{\beta_1 + \beta_3}{\beta}\right)}{\alpha + \beta_1 \left(1 - \frac{\beta_1}{\beta}\right)} \times \left\{ (1 - \xi + \frac{1}{2}\epsilon) \left(1 - \frac{\alpha_1}{\alpha} + \frac{\beta_1 \beta_3}{\alpha \beta}\right) - (1 + \eta + \epsilon) \frac{\alpha_2}{\alpha} - (1 - \eta + \epsilon) \left(\frac{\alpha_3}{\alpha} + \frac{\beta_1 \beta_3}{\alpha \beta}\right) \right\} (p \cdot q) + \frac{\alpha_2 \left(\alpha_3 + \frac{\beta_1 \beta_3}{\beta}\right)}{\alpha + \beta_1 \left(1 - \frac{\beta_1}{\beta}\right)} \Delta^2 + \left(\alpha_2 + \alpha_3 + \frac{\beta_1 \beta_3}{\beta}\right) \left(1 - \frac{\alpha_2 + \alpha_3 + \frac{\beta_1 \beta_3}{\beta}}{\alpha + \beta_1 \left(1 - \frac{\beta_1}{\beta}\right)}\right) M_N^2 + \beta_3 \left(1 - \frac{\beta_1 + \beta_3}{\beta}\right) M_{\ell\bar{\ell}}^2. \quad (5.22)$$

In the short-distance regime, i.e., $\alpha_1 \rightarrow 0$, $\beta_1 \rightarrow 0$, defining $\tilde{\alpha} = \alpha_2 + \alpha_3 + \alpha_4$ and $\tilde{\beta} = \beta_2 + \beta_3$, we get, see Fig. 40 (b),

$$T_{(3)}^{\text{SD}_2} = -\frac{g^2}{(p \cdot q)^2} \int_{-1}^1 dx \int_0^1 du \frac{F_{(1)}^\phi(x, \eta, \Delta^2) \Pi_{(1)}(u, M_{\ell\bar{\ell}}^2)}{(1-u)(x-\xi+i0)^2}, \quad (5.23)$$

where $F_{(1)}^\phi$ was given above, since $\tilde{E}_1 = E_2[\alpha_1 = \beta_i = 0]$, while

$$\Pi_{(1)}(u, M_{\ell\bar{\ell}}^2) = \frac{1}{(4\pi)^2} \int_0^\infty \prod_{j=2}^3 d\beta_j \delta\left(u - \frac{\beta_3}{\tilde{\beta}}\right) \exp\left\{i\beta_3 \left(1 - \frac{\beta_3}{\tilde{\beta}}\right) M_{\ell\bar{\ell}}^2\right\} \quad (5.24)$$

is the first term in the perturbative expansion of the correlation function

$$\Pi(u, M_{\ell\bar{\ell}}^2) = iq_2^- \int d^4 z e^{iq_2 \cdot z} \int \frac{dy^+}{2\pi} e^{-iuy^+ q_2^-} \langle 0 | T \{ \mathcal{O}^{\phi\phi}(0, y^+), j(z) \} | 0 \rangle, \quad (5.25)$$

where the ‘‘electromagnetic’’ current is $j(z) = \frac{1}{2}\phi^2(z)$. Therefore, we observe that this short-distance regime is suppressed compared to the leading one, Eq. (5.18).

In the QCD case, the suppression of contributions due to the hadronic component of the photon is milder than in the scalar example—it is only $(p \cdot q)^{-1/2}$ compared to the handbag diagram—but still persists. The structure of the reduced amplitude is the same as in Eq. (5.23), but with only one power of the hard-scattering coefficient $1/(x - \xi + i0)$ involved, and the vacuum correlator taking the following form

$$\begin{aligned} \Pi^\mu(u, q_2) &\equiv (q_2^\mu q_2^\nu - M_{\ell\bar{\ell}}^2 g^{\mu\nu}) n_\nu^* \Pi(u, M_{\ell\bar{\ell}}^2) \\ &= i \int d^4 z e^{iz \cdot q_2} \int \frac{dy^+}{2\pi} e^{-iy^+ q_2^-} \langle 0 | T \{ \bar{\psi}(0^-, 0^+, \mathbf{0}_\perp) \gamma^- \psi(0^-, y^+, \mathbf{0}_\perp), j^\mu(z) \} | 0 \rangle. \end{aligned} \quad (5.26)$$

This correlation function can be saturated, using the jargon of QCD sum rules, by the ρ -meson [286] and reads

$$\Pi(u, M_{\ell\bar{\ell}}^2) = -\frac{m_\rho^2}{g_\rho^2} \frac{\varphi_\rho(u)}{M_{\ell\bar{\ell}}^2 - m_\rho^2 + im_\rho \Gamma_\rho} + \frac{3}{4\pi^2} u(1-u) \int_{s_0}^\infty \frac{ds}{s - M_{\ell\bar{\ell}}^2 - i0}, \quad (5.27)$$

where $\phi_\rho(u)$ is the ρ -meson distribution amplitude (3.170), while $g_\rho^2/(4\pi) = 2.36 \pm 0.18$, $m_\rho = 770$ MeV and $\Gamma_\rho = 150$ MeV are the ρ -meson decay constant, mass and width, respectively. The second term on the right-hand side comes from the perturbative contribution to the correlator, known to two-loop order [286]. A part of it is dual to the ρ -meson in the interval $s \in [0, s_0]$ and is absorbed in the ρ -pole contribution given by the first term. The parameter $s_0 \approx 1.5$ GeV² is the effective continuum threshold³⁵. Due to divergence in the correlation function, one has to use a renormalized expression stemming from the subtracted dispersion relation, $\Pi_R(u, M_{\ell\bar{\ell}}^2) = \Pi(u, M_{\ell\bar{\ell}}^2) - \Pi(u, 0)$ in the Compton amplitude (5.23).

From this result, it is apparent that, besides the usual s -channel discontinuity, the VCS amplitude has an extra imaginary part associated with the conversion of the quark-antiquark pair into an on-shell intermediate hadronic state. Due to the current conservation, which implies $\bar{u}(\ell_-) \not\! q_2 u(-\ell_+) = 0$, only one Lorentz structure contributes to the leptoproduction amplitude, and the result is

$$\Pi_\mu(u, q_2) \frac{g_{\mu\nu}}{M_{\ell\bar{\ell}}^2} \bar{u}(\ell_-) \gamma_\nu u(-\ell_+) = -\Pi(u, M_{\ell\bar{\ell}}^2) \bar{u}(\ell_-) \gamma_- u(-\ell_+). \quad (5.28)$$

It should be noted, that since the skewness and the generalized Bjorken variable are not equal in general, $\eta \neq \pm\xi$, possible complications due to the singular structure of the hard coefficient function do not arise because its poles $1/(x \pm \xi)$ are away from the “turning” points $x = \pm\eta$ of GPDs corresponding to the situation when one of the partons has zero momentum fraction. Moreover, as we demonstrated in Section 3.13.1, GPDs are continuous at this point, i.e., have no jumps, so that this region does not present a problem even in the case $\eta = \pm\xi$ [6, 148, 283].

Summarizing, the leading region for the Compton amplitude in QCD has the structure depicted in Fig. 41 (a). In addition to the simplest handbag of the scalar theory, one is allowed to attach to the hard part an infinite number of zero-twist longitudinally polarized gluons A^+ . As we discussed above, their insertion does not result in power suppressed contributions, and the net effect can be factorized into the Wilson line along the trajectory of motion of the struck quark in the hard subprocess, as was explained in Section 2.2.6. It restores the color gauge invariance of the light-ray operator involved in the correlation function defining GPDs. Due to the unitary cancellation of the eikonal lines going beyond the photon absorption and emission points, the path-ordered exponential extends only between the quark fields, see Fig. 41 (b).

³⁵The approximation of the continuum contribution by a step-function threshold in the spectral density causes a divergence in the real part at $M_{\ell\bar{\ell}}^2 = s_0$, which is spurious.

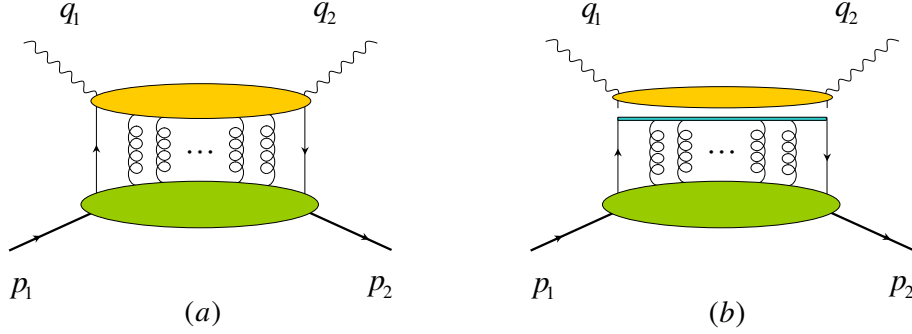


Figure 41: The leading asymptotic region in the Compton scattering amplitude (a) and the factorization of longitudinal gluons into the path-ordered exponential (b).

5.2 Restoration of electromagnetic gauge invariance

Let us illustrate the peculiarities of the off-forward kinematics on a simple example of a free Dirac fermion theory. As we will see, even and odd parity structures start to “talk” to each other in this case. The reason is that, in the off-forward kinematics, the operator product expansion should be used in its full form, including operators with total derivatives because their matrix elements are nonzero. Moreover, it is important to keep such operators in order to restore the electromagnetic gauge invariance of the two-photon amplitude defined by the chronological product $T\{j_\mu(z_1)j_\nu(z_2)\}$ of two currents $j_\mu(z) = \bar{\psi}(z)\gamma_\mu\psi(z)$. The leading light-cone singularity $(z_1 - z_2)^2 \rightarrow 0$ arises from the handbag diagram, as we established in the preceding section, and reads

$$T\{j^\mu(z_1)j^\nu(z_2)\} = i\bar{\psi}(z_1)\gamma^\mu S(z_1 - z_2)\gamma^\nu\psi(z_2) + i\bar{\psi}(z_2)\gamma^\nu S(z_2 - z_1)\gamma^\mu\psi(z_1), \quad (5.29)$$

where $S(z)$ is the coordinate-space free quark propagator

$$S(z) = \frac{\Gamma(d/2)}{2\pi^{d/2}} \frac{\not{z}}{[-z^2]^{d/2}}.$$

Taking into account the free equations of motion

$$\not{\partial}\psi = 0, \quad \not{\partial}S(z) = -i\delta^{(4)}(z),$$

it is straightforward to show that the handbag diagram respects current conservation. After performing the decomposition of the Dirac structure in Eq. (5.29) with the help of Eq. (A.13) we obtain

$$\begin{aligned} T\{j^\mu(z_1)j^\nu(z_2)\} &= S^{\mu\nu;\rho\sigma}iS_\rho(z_1 - z_2)\{\bar{\psi}(z_1)\gamma_\sigma\psi(z_2) - \bar{\psi}(z_2)\gamma_\sigma\psi(z_1)\} \\ &\quad - i\varepsilon^{\mu\nu\rho\sigma}iS_\rho(z_1 - z_2)\{\bar{\psi}(z_1)\gamma_\sigma\gamma^5\psi(z_2) + \bar{\psi}(z_2)\gamma_\sigma\gamma^5\psi(z_1)\}, \end{aligned} \quad (5.30)$$

where

$$S^{\mu\nu;\rho\sigma} \equiv g^{\mu\rho}g^{\nu\sigma} + g^{\mu\sigma}g^{\nu\rho} - g^{\mu\nu}g^{\rho\sigma}. \quad (5.31)$$

One easily finds that the current conservation does not hold separately in the parity even and odd terms. Rather, it is fulfilled due to the cancellation between terms with different parity on the right-hand side of Eq. (5.30). In other words, if one takes only the vector bilocal operator from

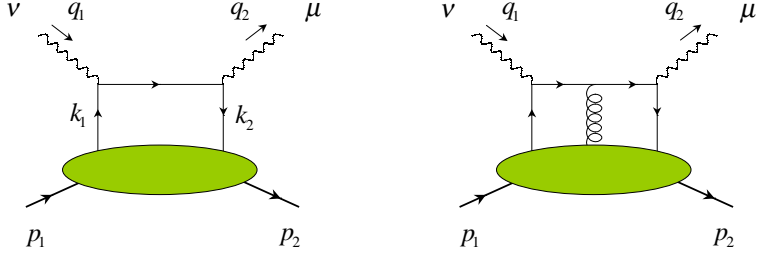


Figure 42: Two- and three-leg coefficient functions for the virtual Compton process which build up a gauge invariant amplitude to the twist-three accuracy. Addition of the u -channel diagrams is implied.

the right-hand side of Eq. (5.30) and parametrizes it through GPDs H, E , the result will not be gauge-invariant. Apparently, the gauge invariance should be restored if the contribution of the axial vector bilocal operator is added. However, the latter is parametrized at the leading twist by another set of GPDs, \tilde{H}, \tilde{E} , which, in general, are dynamically independent of H, E . From this point of view, the possibility of cancellations looks miraculous. The resolution of the puzzle lies in the fact that in the twist decomposition of $\bar{\psi}(z_1)\gamma_\mu(1, \gamma_5)\psi(z_2)$, one should take into account operators with total derivatives which formally have twist-three, but are “kinematically” related to twist-two operators. After such terms are included, one obtains gauge invariant expressions for contributions associated both with H, E and \tilde{H}, \tilde{E} GPDs [287, 288, 289, 290, 291, 292, 293, 294, 295, 296, 297, 298]. At twist-three, one should also include the interaction-dependent three-particle contributions (see Fig. 42), but this does not represent any difficulty of principle, as will be demonstrated in the next section.

5.2.1 Tree-level twist-three Compton amplitude

Let us use the ideas, we have just spelled out, and perform the calculation of the Compton amplitudes in the Bjorken region in the light-cone gauge, in which only the physical degrees of freedom propagate. Evaluating the handbag diagram in the Bjorken limit, in addition to the leading contributions, we will keep also non-leading terms linear in partons’ transverse momenta. For the s -channel diagram, we perform the reduction of the Dirac structure as follows

$$\begin{aligned} \gamma^\mu S(k_1 + q_1) \gamma^\nu \simeq & \frac{1}{(p \cdot q)(x - \xi + i0)} \left\{ S^{\mu\nu;\rho\sigma} \left(\frac{1}{2}(p \cdot q)n_\sigma + k_\sigma^\perp + \frac{1}{2}(x - \xi)p_\sigma \right) \gamma_\rho \right. \\ & \left. + i\varepsilon^{\mu\nu\rho\sigma} \left(\frac{1}{2}xp_\sigma + q_\sigma + k_\sigma^\perp \right) \gamma_\rho \gamma^5 \right\}. \end{aligned}$$

Adding the u -channel diagram gives the amplitude in the twist-three approximation

$$\begin{aligned} T_{(2)}^{\mu\nu} = & \frac{1}{2p \cdot q} \int dx \sum_q C_{(0)}^{q[-]}(x, \xi) \left\{ (p \cdot q) S^{\mu\nu;\rho\sigma} n_\sigma F_\rho^q(x, \eta) + i\varepsilon^{\mu\nu\rho\sigma} p_\sigma \left(x \tilde{F}_\rho^q(x, \eta) - \tilde{K}_\rho^q(x, \eta) \right) \right\} \\ & + \frac{1}{2p \cdot q} \int dx \sum_q C_{(0)}^{q[+]}(x, \xi) \left\{ 2i\varepsilon^{\mu\nu\rho\sigma} q_\sigma \tilde{F}_\rho^q(x, \eta) + S^{\mu\nu;\rho-} p_\sigma K_\rho^q(x, \eta) \right\}, \end{aligned} \quad (5.32)$$

where the subscript (2) on the amplitude means that it comes from the two-particle contributions in the t -channel. The tree-level coefficient functions are

$$C_{(0)}^{q[\pm]}(x, \xi) = \frac{Q_q^2}{\xi - x - i0} \pm \frac{Q_q^2}{\xi + x - i0}. \quad (5.33)$$

In Eq. (5.32) above we used the following boost-invariant parity-even

$$F_\rho^q(x, \eta) = p^+ \int \frac{dz^-}{2\pi} e^{ixz^- p^+} \langle p_2 | \mathcal{O}_\rho^{qq}(-z^-, z^-) | p_1 \rangle, \quad (5.34)$$

$$K_\rho^q(x, \eta) = \int \frac{dz^-}{2\pi} e^{ixz^- p^+} \langle p_2 | \mathcal{K}_\rho^{qq}(-z^-, z^-) | p_1 \rangle, \quad (5.35)$$

and parity-odd

$$\tilde{F}_\rho^q(x, \eta) = p^+ \int \frac{dz^-}{2\pi} e^{ixz^- p^+} \langle p_2 | \tilde{\mathcal{O}}_\rho^{qq}(-z^-, z^-) | p_1 \rangle, \quad (5.36)$$

$$\tilde{K}_\rho^q(x, \eta) = \int \frac{dz^-}{2\pi} e^{ixz^- p^+} \langle p_2 | \tilde{\mathcal{K}}_\rho^{qq}(-z^-, z^-) | p_1 \rangle \quad (5.37)$$

functions with an open Lorentz index of the Dirac matrix. They are Fourier transforms of the two-quark operators

$$\begin{aligned} \mathcal{O}_\mu^{qq}(-z^-, z^-) &= \bar{\psi}_q(-z^-) \gamma_\mu \psi_q(z^-), & \mathcal{K}_\mu^{qq}(-z^-, z^-) &= \bar{\psi}_q(-z^-) i \overleftrightarrow{\partial}_\mu^\perp \gamma^+ \psi_q(z^-), \\ \tilde{\mathcal{O}}_\mu^{qq}(-z^-, z^-) &= \bar{\psi}_q(-z^-) \gamma_\mu \gamma^5 \psi_q(z^-), & \tilde{\mathcal{K}}_\mu^{qq}(-z^-, z^-) &= \bar{\psi}_q(-z^-) i \overleftrightarrow{\partial}_\mu^\perp \gamma^+ \gamma^5 \psi_q(z^-). \end{aligned} \quad (5.38)$$

In this notation, we do not intend to perform the form factor decomposition for generalized parton distributions, so that the expression for the amplitude is valid for a target of an arbitrary spin.

The first operator in Eq. (5.38) has an open Lorentz index and contains both the twist-two and twist-three contributions. The twist-two part can be projected out by contracting the operators with the light-like vector n^μ . The operators \mathcal{K} and $\tilde{\mathcal{K}}$ reflect the transverse momentum of partons in a hadron moving along the light-cone. Neglecting them, one gets the conventional leading twist approximation to the VCS amplitude [1, 2, 3, 299, 300].

The functions introduced above are not independent, in fact, they are related to each other by means of the quark Heisenberg equation of motion, $\mathcal{D}\psi = 0$. Obviously, in the interacting theory they are related to three-particle quark-gluon-quark operators. Namely, a simple decomposition of Lorentz products and indices in terms of the light-cone Sudakov components gives the following relations

$$\begin{aligned} &\frac{\partial}{\partial z^-} \mathcal{O}_{\mu\nu}^{qq,\perp}(-z^-, z^-) - i\varepsilon_{\mu\nu}^\perp \partial^+ \tilde{\mathcal{O}}_{\perp}^{qq,\nu}(-z^-, z^-) + i\mathcal{K}_\mu^{qq}(-z^-, z^-) + i\varepsilon_{\mu\nu}^\perp \partial_\perp^\nu \tilde{\mathcal{O}}^{qq}(-z^-, z^-) \\ &+ \int dz'^- \left\{ w(z'^- - z^-) \mathcal{S}_{[-]\mu}^{ggq}(-z^-, z'^-, z^-) + w(z'^- + z^-) \mathcal{S}_{[+]\mu}^{ggq}(-z^-, z'^-, z^-) \right\} = 0, \\ &\partial^+ \mathcal{O}_{\mu\nu}^{qq,\perp}(-z^-, z^-) - i\varepsilon_{\mu\nu}^\perp \frac{\partial}{\partial z^-} \tilde{\mathcal{O}}_{\perp}^{qq,\nu}(-z^-, z^-) + \varepsilon_{\mu\nu}^\perp \tilde{\mathcal{K}}_{\nu}^{qq}(-z^-, z^-) - \partial_\mu^\perp \mathcal{O}^{qq}(-z^-, z^-) \\ &+ \int dz'^- \left\{ w(z'^- - z^-) \mathcal{S}_{[-]\mu}^{ggq}(-z^-, z'^-, z^-) - w(z'^- + z^-) \mathcal{S}_{[+]\mu}^{ggq}(-z^-, z'^-, z^-) \right\} = 0, \end{aligned}$$

where the weight $w(z^-)$ depends on the boundary conditions assumed for the gauge field, see Eq. (D.14) in Appendix D. Obviously, the total contribution will not depend on this prescription. Notice that ∂^+ is a total light-cone derivative, i.e.,

$$\partial_\mu \mathcal{O}^{\phi\phi}(-z, z) \equiv \left. \frac{\partial}{\partial a^\mu} \right|_{a=0} \mathcal{O}^{\phi\phi}(-z + a, z + a). \quad (5.39)$$

The three-particle antiquark-gluon-quark operators \mathcal{S}^{qgq} are given by

$$\begin{aligned}\mathcal{S}_{[\pm]\mu}^{qgq}(z_1^-, z_2^-, z_3^-) &= ig\bar{\psi}_q(z_1^-) \left\{ \gamma^+ F_{\mu}^{+\perp}(z_2^-) \pm i\gamma^+ \gamma^5 \tilde{F}_{\mu}^{+\perp}(z_2^-) \right\} \psi_q(z_1^-), \\ \tilde{\mathcal{S}}_{[\pm]\mu}^{qgq}(z_1^-, z_2^-, z_3^-) &= ig\bar{\psi}_q(z_1^-) \left\{ \gamma^+ \gamma^5 F_{\mu}^{+\perp}(z_2^-) \pm i\gamma^+ \tilde{F}_{\mu}^{+\perp}(z_2^-) \right\} \psi_q(z_1^-).\end{aligned}\quad (5.40)$$

Here we adopted a notation for the $N_c \times N_c$ matrix of the gauge field strength, $F_{\mu\nu} \equiv t^a F_{\mu\nu}^a$. This notation and a similar notation for the gauge potential, $A_\mu \equiv t^a A_\mu^a$, will be implied from now on whenever an adjoint $SU(3)$ index is not shown explicitly. The two functions in Eq. (5.40) are related to each other by a “duality” equation

$$i\varepsilon_{\mu\nu}^\perp \tilde{\mathcal{S}}_{[\pm]}^{qgq,\nu} = \pm \mathcal{S}_{[\pm]\mu}^{qgq}. \quad (5.41)$$

In terms of the functions introduced in Eqs. (5.35) – (5.38), these relations result in

$$\begin{aligned}x F_{\mu}^{q,\perp}(x, \eta) - \eta i\varepsilon_{\mu\nu}^\perp \tilde{F}_{\perp}^{q,\nu}(x, \eta) + i\varepsilon_{\mu\nu}^\perp \Delta_{\perp}^\nu \tilde{F}^q(x, \eta) - K_\mu^q(x, \eta) \\ - \int \frac{d\tau}{\tau} \left\{ S_{[-]\mu}^{qgq}(x - \tau, x) + S_{[+]\mu}^{qgq}(x + \tau, x) \right\} = 0,\end{aligned}\quad (5.42)$$

$$\begin{aligned}x i\varepsilon_{\mu\nu}^\perp \tilde{F}_{\perp}^{q,\nu}(x, \eta) - \eta F_{\mu}^{q,\perp}(x, \eta) + \Delta_\mu^\perp F^q(x, \eta) - i\varepsilon_{\mu\nu}^\perp \tilde{K}^{q,\nu}(x, \eta) \\ + \int \frac{d\tau}{\tau} \left\{ S_{[-]\mu}^{qgq}(x - \tau, x) - S_{[+]\mu}^{qgq}(x + \tau, x) \right\} = 0,\end{aligned}\quad (5.43)$$

where the apparent singularity in τ is regularized in accordance with the residual gauge fixing procedure, see Eqs. (D.15) and (D.16). The boost-invariant twist-two functions are determined by

$$F^q \equiv (p^+)^{-1} n^\mu F_\mu^q, \quad \tilde{F}^q \equiv (p^+)^{-1} n^\mu \tilde{F}_\mu^q. \quad (5.44)$$

The three-particle correlations $S_{[\pm]\rho}^{qgq}(x_1, x_2)$ are the functions of two independent momentum fractions

$$S_{[\pm]\rho}^{qgq}(x_1, x_2) = \int \frac{dz_1^-}{2\pi} \frac{dz_2^-}{2\pi} e^{ix_1 z_1^- p^+ + ix_2 z_2^- p^+} \langle p_2 | \mathcal{S}_{[\pm]\rho}^{qgq}(-z_1^-, z_2^-, z_1^-) | p_1 \rangle. \quad (5.45)$$

Since the two-particle contribution is related to the three-particle ones by QCD equations of motion, to get the complete result we have to evaluate the contribution from the Compton scattering on a quark-gluon-quark system. This situation is analogous to the treatment of the transverse spin structure function g_2 in deeply inelastic scattering [234]. This observation was first made in Ref. [287] and applied there to off-forward Compton scattering on a scalar target. The contribution corresponding to the diagram in Fig. 42 (b) is

$$\begin{aligned}T_{(3)}^{\mu\nu} &= \frac{1}{2p \cdot q} \int dx \int \frac{d\tau}{\tau} \sum_q C_{(0)}^{q[+]}(x, \xi) S^{\mu\nu;\rho\sigma} p_\sigma \left\{ S_{[-]\rho}^{qgq}(x - \tau, x) + S_{[+]\rho}^{qgq}(x + \tau, x) \right\} \\ &+ \frac{1}{2p \cdot q} \int dx \int \frac{d\tau}{\tau} \sum_q C_{(0)}^{q[-]}(x, \xi) S^{\mu\sigma;\nu\rho} p_\sigma \left\{ S_{[-]\rho}^{qgq}(x - \tau, x) - S_{[+]\rho}^{qgq}(x + \tau, x) \right\}.\end{aligned}\quad (5.46)$$

Summing the two-particle (5.32) and three-particle (5.46) Compton amplitudes and using Eq. (5.42) and (5.43) to remove the GPDs K_ρ^q and \tilde{K}_ρ^q , we find that the quark-gluon-quark correlation

cancels, and the result is simply

$$T^{\mu\nu} = T_{(2)}^{\mu\nu} + T_{(3)}^{\mu\nu} = \int_{-1}^1 dx \sum_q C_{(0)}^{q[-]}(x, \xi) \left\{ T_{(1)}^{\mu\nu} F^q(x, \eta) + T_{(2)}^{\mu\nu;\rho} F_{\rho}^{q,\perp}(x, \eta) \right\} \\ + \int_{-1}^1 dx \sum_q C_{(0)}^{q[+]}(x, \xi) \left\{ \tilde{T}_{(1)}^{\mu\nu} \tilde{F}^q(x, \eta) + \tilde{T}_{(2)}^{\mu\nu;\rho} \tilde{F}_{\rho}^{q,\perp}(x, \eta) \right\}. \quad (5.47)$$

The range of integration over the momentum fraction variable x is dictated by the support properties of GPDs, established in Section 3.2.1. The Lorentz tensors accompanying GPDs are

$$\begin{aligned} T_{(1)}^{\mu\nu} &= -g^{\mu\nu} + \frac{1}{p \cdot q} p^\mu (2q^\nu + \xi p^\nu + \Delta_\perp^\nu) + \frac{1}{p \cdot q} p^\nu (2q^\mu + \xi p^\mu - \Delta_\perp^\mu), \\ \tilde{T}_{(1)}^{\mu\nu} &= \frac{i}{p \cdot q} (\varepsilon^{\mu\nu\rho\sigma} p_\rho q_\sigma + \frac{1}{2} \varepsilon_{\rho\sigma}^\perp \Delta_\sigma^\perp (p^\mu g_\perp^{\rho\nu} + p^\nu g_\perp^{\rho\mu})) , \\ T_{(2)}^{\mu\nu;\rho} &= \frac{1}{p \cdot q} (q^\nu + (\xi + \frac{1}{2}\eta) p^\nu) g_\perp^{\mu\rho} + \frac{1}{p \cdot q} (q^\mu + (\xi - \frac{1}{2}\eta) p^\mu) g_\perp^{\nu\rho}, \\ \tilde{T}_{(2)}^{\mu\nu;\rho} &= \frac{i}{p \cdot q} (\varepsilon_{\mu\nu\rho\sigma} q_\sigma + \frac{1}{2} \eta \varepsilon_{\rho\sigma}^\perp (p^\mu g_\perp^{\sigma\nu} + p^\nu g_\perp^{\sigma\mu})) . \end{aligned} \quad (5.48)$$

These expressions are obviously target independent. They were found here by means of a rigorous field theoretical analysis [287, 288, 289, 291], which confirms an earlier “rule of the thumb” restoration procedure [301] suggested for the leading twist Lorentz tensor $T_{(1)}^{\mu\nu}$. Furthermore, it is easy to check that, after the twist-three corrections have been taken into account, the result is gauge invariant up to $\mathcal{O}(\Delta_\perp^2)$, i.e., up to twist-four effects:

$$q_{1\nu} T_{(i)}^{\mu\nu} = \mathcal{O}(\Delta_\perp^2) \quad \text{and} \quad q_{2\mu} T_{(i)}^{\mu\nu} = \mathcal{O}(\Delta_\perp^2).$$

To prove this, we used the Sudakov decomposition of the photon momenta given in Appendix B.1. It is interesting to note that the twist-three structures $T_{\mu\nu;\rho}^{(i)}$ give exact zero when they are simultaneously contracted both with incoming and outgoing photon momenta:

$$q_{1\nu} q_{2\mu} T_{\mu\nu;\rho}^{(i)} = 0.$$

The approximately gauge-invariant Lorentz structures introduced above can be restored to exact ones. To this end, we define two projectors

$$\mathcal{P}^{\mu\nu} \equiv g^{\mu\nu} - \frac{q_1^\mu q_2^\nu}{q_1 \cdot q_2}, \quad \mathcal{E}^{\mu\nu\rho\sigma} \equiv \varepsilon^{\alpha\beta\rho\sigma} \left(g^\mu_\alpha - \frac{p^\mu q_{2\alpha}}{p \cdot q_2} \right) \left(g^\nu_\beta - \frac{p^\nu q_{1\beta}}{p \cdot q_1} \right). \quad (5.49)$$

They satisfy the gauge invariance conditions exactly

$$\mathcal{P}^{\mu\nu} q_{2\mu} = \mathcal{P}^{\mu\nu} q_{1\nu} = \mathcal{E}^{\mu\nu\rho\sigma} q_{2\mu} = \mathcal{E}^{\mu\nu\rho\sigma} q_{1\nu} = 0.$$

One can easily see that the tensors given in Eq. (5.48) are the first terms in the Δ_\perp expansion of the following Lorentz structures

$$\begin{aligned} T_{(1)}^{\mu\nu} &= -\mathcal{P}^{\mu\rho} g_{\rho\sigma} \mathcal{P}^{\sigma\nu} + \frac{\xi}{p \cdot q} \mathcal{P}^{\mu\rho} p_\rho p_\sigma \mathcal{P}^{\sigma\nu}, & \tilde{T}_{(1)}^{\mu\nu} &= \frac{i}{p \cdot q} \mathcal{E}^{\mu\nu\rho\sigma} p_\rho q_\sigma, \\ T_{(2)}^{\mu\nu;\rho} &= \frac{\xi}{p \cdot q} (\mathcal{P}^{\mu\rho} p_\sigma \mathcal{P}^{\sigma\nu} + \mathcal{P}^{\mu\sigma} p_\sigma \mathcal{P}^{\rho\nu}), & \tilde{T}_{(2)}^{\mu\nu;\rho} &= \frac{i}{p \cdot q} \mathcal{E}^{\mu\nu\rho\sigma} q_\sigma, \end{aligned} \quad (5.50)$$

which exactly satisfy the requirements of the gauge invariance.

5.2.2 Lorentz structure of the Compton amplitude

The analysis of twist-three contributions given above allows one to find the (electromagnetically) gauge-invariant tensor decomposition of the off-forward Compton amplitude:

$$\begin{aligned} T^{\mu\nu} = & -\mathcal{P}^{\mu\rho}g_{\rho\sigma}\mathcal{P}^{\sigma\nu}\mathcal{F}_1(\xi, \eta, \Delta^2; Q^2) + \frac{1}{p \cdot q}\mathcal{P}^{\mu\rho}p_\rho p_\sigma\mathcal{P}^{\sigma\nu}\mathcal{F}_2(\xi, \eta, \Delta^2; Q^2) \\ & + \frac{i}{p \cdot q}\mathcal{E}^{\mu\nu\rho\sigma}p_\rho q_\sigma\tilde{\mathcal{F}}_1(\xi, \eta, \Delta^2, Q^2) + \mathcal{P}^{\mu\rho}\mathcal{P}^{\sigma\nu}\mathcal{T}_{\rho\sigma}(\xi, \eta, \Delta^2; Q^2) \\ & + \frac{\xi}{p \cdot q}(\mathcal{P}^{\mu\rho}p_\sigma\mathcal{P}^{\sigma\nu} + \mathcal{P}^{\mu\sigma}p_\sigma\mathcal{P}^{\rho\nu})\mathcal{F}_{3\rho}^\perp(\xi, \eta, \Delta^2; Q^2) + \frac{i}{p \cdot q}\mathcal{E}^{\mu\nu\rho\sigma}q_\sigma\tilde{\mathcal{F}}_{3\rho}^\perp(\xi, \eta, \Delta^2; Q^2). \end{aligned} \quad (5.51)$$

By analogy with terminology used in studies of deeply inelastic scattering, the functions that appear in the decomposition (5.51) will be called the Compton form factors (CFFs). Four of these functions, \mathcal{F}_1 , \mathcal{F}_2 , $\tilde{\mathcal{F}}_1$, \mathcal{T} , receive twist-two contributions as their leading term, while the other two, $\mathcal{F}_{3\rho}^\perp$ and $\tilde{\mathcal{F}}_{3\rho}^\perp$, start at twist three. Similarly to the case of the forward Compton amplitude, one can introduce the longitudinal-longitudinal helicity³⁶ amplitude

$$\mathcal{F}_L \equiv \frac{1}{\xi}\mathcal{F}_2 - \mathcal{F}_1. \quad (5.52)$$

In the preasymptotic Bjorken limit, the CFFs can be written as a power expansion in the hard scale, with each term, in its turn, being a power series in the strong coupling constant. In particular, the functions whose leading term is of twist two will be written as

$$\mathcal{F}_i(\xi, \eta, \Delta^2; Q^2) = \sum_{a=q,g} \int_{-1}^1 dx C_i^{a[-]}(x, \xi, \eta; Q^2/\mu^2) F^a(x, \eta, \Delta^2; \mu^2) + \mathcal{O}(Q^{-2}), \quad (5.53)$$

$$\tilde{\mathcal{F}}_1(\xi, \eta, \Delta^2; Q^2) = \sum_{a=q,g} \int_{-1}^1 dx C_1^{a[+]}(x, \xi, \eta; Q^2/\mu^2) \tilde{F}^a(x, \eta, \Delta^2; \mu^2) + \mathcal{O}(Q^{-2}), \quad (5.54)$$

where the index i runs over $i = 1, L$. We have explicitly introduced the factorization scale μ^2 which separates short and long distance physics. The perturbative expansion of coefficient functions in the strong coupling constant reads to the lowest two orders

$$C_i^{a[\pm]}(x, \xi, \eta; Q^2/\mu^2) = C_{i(0)}^{a[\pm]}(x, \xi) + \frac{\alpha_s}{2\pi} C_{i(1)}^{a[\pm]}(x, \xi, \eta; Q^2/\mu^2) + \mathcal{O}(\alpha_s^2). \quad (5.55)$$

The leading order quark coefficient functions for CFFs \mathcal{F}_1 and $\tilde{\mathcal{F}}_1$ are given in Eq. (5.33), i.e., $C_{1(0)}^{q[\pm]} = C_{(0)}^{q[\pm]}$. The function \mathcal{F}_L vanishes at leading order of perturbation theory,

$$\mathcal{F}_2 \stackrel{\text{LO}}{=} \xi \mathcal{F}_1. \quad (5.56)$$

This a generalization of the Callan-Gross relation (2.64), just like in the forward Compton amplitude case, it is a consequence of the spin-one-half nature of quarks. Thus, we have

$$C_{L(0)}^{q[\pm]} = 0.$$

³⁶Referring to incoming-outgoing virtual photons.

The photons can interact with gluons only through quarks, hence the contribution of gluons starts from one-loop order,

$$C_{i(0)}^{g[\pm]}(x, \xi) = 0.$$

The one-loop coefficient functions for all twist-two functions will be presented later in Section 5.4.3.

The appearance of the function \mathcal{T} in the decomposition (5.51) is a consequence of the gluon helicity-flip by two units. It arises due to nonzero orbital angular momentum in the off-forward scattering. The twist-two photon helicity-flip amplitude is absent in the handbag diagram because of the conservation of the angular momentum along the photon-parton collision axis. Since photons are vector particles, to flip its helicity one needs to compensate two units of the angular momentum. For the collinear twist-two partonic amplitude, this is only possible by a simultaneous flip of gluon helicities. Since quarks have spin one-half, their helicity flip can provide at most one unit of the angular momentum. As a consequence, twist-two photon helicity-flip amplitude is sensitive to the helicity-flip gluon distribution in a nucleon. However, a similar angular momentum conservation argument shows that such distribution is forbidden in the forward limit, i.e., in DIS on a spin-one-half target. In the off-forward case, the transverse component of the momentum transfer Δ_\perp can provide one unit of the angular momentum, so the off-forward virtual Compton scattering offers a unique opportunity to investigate the helicity-flip gluon distribution in the nucleon. The factorized form of the corresponding CFF is

$$\mathcal{T}_{\mu\nu}(\xi, \eta, \Delta^2; Q^2) = \int_{-1}^1 dx C_T^g(x, \xi, \eta; Q^2/\mu^2) F_{T\mu\nu}^g(x, \eta, \Delta^2; \mu^2) + \mathcal{O}(Q^{-2}), \quad (5.57)$$

where the boost-invariant maximal-helicity GPD $F_{T\mu\nu}^g$ is defined as

$$\langle p_2 | \mathcal{T}_{\mu\nu}^{gg}(-z^-, z^-) | p_1 \rangle = \frac{1}{4} (p^+)^2 \int_{-1}^1 dx e^{-ixp^+z^-} F_{T\mu\nu}^g(x, \eta, \Delta^2), \quad (5.58)$$

with the operator $\mathcal{T}_{\mu\nu}^{gg}$ determined in Eq. (3.22). By the same token as before, the CCF (5.57) has vanishing leading order coefficient function $C_{T(0)}^g(x, \xi) = 0$.

Finally, the functions which start from twist three are displayed in the last line of Eq. (5.51). Of course, the collinear expansion of the corresponding Lorentz structures (not taking into account the gluon helicity-flip contributions) reproduces Eq. (5.47) of the preceding section up to terms linear in the transverse momentum transfer Δ_\perp . The twist-three functions at leading order in strong coupling yield

$$\mathcal{F}_{3\mu}^\perp(\xi, \eta, \Delta^2; Q^2) = \sum_q \int_{-1}^1 dx C_{(0)}^{q[-]}(x, \xi) F_\mu^{q\perp}(x, \eta, \Delta^2; Q^2), \quad (5.59)$$

$$\tilde{\mathcal{F}}_{3\mu}^\perp(\xi, \eta, \Delta^2; Q^2) = \sum_q \int_{-1}^1 dx C_{(0)}^{q[+]}(x, \xi) \tilde{F}_\mu^{q\perp}(x, \eta, \Delta^2; Q^2). \quad (5.60)$$

At one-loop order, different components of the twist-three functions receive different radiative corrections, so that we have to decompose them first into different irreducible components. As was demonstrated in Ref. [316], the coefficient functions related to separate components for the leading twist even-parity Lorentz structure $\mathcal{T}_{(1)}^{\mu\nu}$ are no longer equal starting from one-loop order. This is due to a nonvanishing contribution of the longitudinally polarized photon scattering. The

coefficient functions of twist-three Compton form factors are also different for different components [302].

In the forward limit the discontinuity of CFFs is related to the structure functions of deeply inelastic scattering (2.34) via

$$\frac{1}{2\pi} \Im m \mathcal{F}_1(x_B, 0, 0, Q^2) = F_1(x_B, Q^2), \quad \frac{1}{2\pi} \Im m \tilde{\mathcal{F}}_1(x_B, 0, 0, Q^2) = g_1(x_B, Q^2). \quad (5.61)$$

5.3 Twist-three GPDs

Having introduced twist-three GPDs, we are in a position to explore their properties. In this section, we define twist-three skewed parton distributions and their relation to the twist-two ones.

5.3.1 Geometric twist decomposition of operators

Now we are going to present a decomposition of the two-quark operators into separate twist components to the twist-three accuracy [230, 303, 289, 290, 291, 292]. An essential ingredient of our presentation is the treatment of operators with total derivatives. Since the group-theoretical notion of twist as dimension minus spin of an operator is well defined for local operators, we will adhere to the following strategy: first, we do the Taylor expansion of a light cone operator into an infinite series of local operators; second, we extract of definite twist components; and as a final step, we resum the result back into a nonlocal form. An alternative approach—directly in terms of the light-ray operators—is described in Appendix L. In the following we will not take care of the trace terms proportional to n^ρ , since they only contribute at the twist-four level. They will be considered in Section 5.6.

We start with the Taylor expansion of Eq. (5.38) in terms of local operators

$$\mathcal{O}_\rho^{qq}(-z^-, z^-) = \sum_{j=0}^{\infty} \frac{(-iz^-)^j}{j!} n^{\mu_1} \dots n^{\mu_j} \mathcal{O}_{\rho\mu_1\dots\mu_j}^{qq}, \quad (5.62)$$

with

$$\mathcal{O}_{\rho\mu_1\dots\mu_j}^{qq} = \mathbf{S}_{\mu_1\dots\mu_j} \bar{\psi}_q \gamma_\rho i \overleftrightarrow{\mathcal{D}}_{\mu_1} \dots i \overleftrightarrow{\mathcal{D}}_{\mu_j} \psi_q. \quad (5.63)$$

To have a well-defined decomposition into twist-two and twist-three contributions, we separate the tensors $\mathcal{R}_{\rho\mu_1\dots\mu_j}^{\tau,qq}$ with $(j+1)$ indices into components transforming irreducibly with respect to the Lorentz group. Since the indices $\mu_1 \dots \mu_j$ already form an irreducible Lorentz tensor $(\frac{j}{2}, \frac{j}{2})$ of spin j , we have to decompose its product with the free Lorentz index ρ in the representation $(\frac{1}{2}, \frac{1}{2})$, which yields

$$(\frac{j}{2}, \frac{j}{2}) \otimes (\frac{1}{2}, \frac{1}{2}) = (\frac{j+1}{2}, \frac{j+1}{2}) \oplus (\frac{j}{2}, \frac{j}{2}),$$

or, using Young tableaux

$$\begin{array}{|c|c|c|c|c|} \hline \mu_1 & \mu_2 & \mu_3 & \dots & \mu_j \\ \hline \end{array} \otimes \begin{array}{|c|} \hline \rho \\ \hline \end{array} = \begin{array}{|c|c|c|c|c|} \hline \rho & \mu_1 & \mu_2 & \dots & \mu_j \\ \hline \end{array} \oplus \begin{array}{|c|c|c|c|c|} \hline \mu_1 & \mu_2 & \dots & \mu_j \\ \hline \rho \\ \hline \end{array} .$$

In terms of operators, we perform the decomposition of the non-local operator \mathcal{O}_ρ^{qq} into twist-two and twist-three components. This can easily be done by merely symmetrizing and antisymmetrizing the index ρ with the remaining indices,

$$\begin{aligned} \mathcal{O}_\rho^{qq}(-z^-, z^-) &= \mathcal{R}_\rho^{2,qq}(-z^-, z^-) + \mathcal{R}_\rho^{3,qq}(-z^-, z^-) \\ &= \sum_{j=0}^{\infty} \frac{(-iz^-)^j}{j!} n^{\mu_1} \dots n^{\mu_j} \left\{ \mathcal{R}_{\rho\mu_1\dots\mu_j}^{2,qq} + \frac{2j}{j+1} \mathcal{R}_{\rho\mu_1\dots\mu_j}^{3,qq} \right\}, \end{aligned} \quad (5.64)$$

where the operator with geometric twist $\tau = 2$ was discussed before (see Eqs. (3.107) and (3.108)), while the $\tau = 3$ operator is given by

$$\mathcal{R}_{\rho\mu_1\dots\mu_j}^{3,qq} = \sum_{\mu_1\dots\mu_j} \mathbf{A}_{\rho\mu_1\dots\mu_j} \bar{\psi}_q \gamma_\rho i \overleftrightarrow{\mathcal{D}}_{\mu_1} \dots i \overleftrightarrow{\mathcal{D}}_{\mu_j} \psi_q. \quad (5.65)$$

The antisymmetrization is defined as

$$\mathbf{A}_{\mu_1\mu_2} t_{\mu_1\mu_2} = \frac{1}{2} (t_{\mu_1\mu_2} - t_{\mu_2\mu_1}).$$

The twist-two light-cone operator was found in Eq. (3.112), while the twist-three light-ray operator contains two distinct contributions, evaluated in Appendix L. The first contribution is due to the twist-two operators with total derivatives [289, 290, 293, 304, 305, 306, 307], the second one comes from genuine three-particle twist-three operators [289]. Combining them together, one gets

$$\begin{aligned} \mathcal{R}_\rho^{3,qq}(-z^-, z^-) = & \frac{z^-}{2} \int_0^1 du \left\{ -u i \varepsilon_\rho^{+\mu\nu} \partial_\mu \left[\tilde{\mathcal{R}}_\nu^{2,qq} ((\bar{u} - u)z^-, z^-) + \tilde{\mathcal{R}}_\nu^{2,qq} (-z^-, (u - \bar{u})z^-) \right] \right. \\ & - u (\partial_\rho n_\sigma - g_{\rho\sigma} \partial_+) \left[\mathcal{R}_\sigma^{2,qq} ((\bar{u} - u)z^-, z^-) - \mathcal{R}_\sigma^{2,qq} (-z^-, (u - \bar{u})z^-) \right] \\ & + z^- \int_{-u}^u d\tau \left[(u - \tau) \mathcal{S}_{[+]_\rho}^{ggq} ((\bar{u} - u)z^-, (\tau + \bar{u})z^-, z^-) \right. \\ & \left. \left. - (u + \tau) \mathcal{S}_{[-]_\rho}^{ggq} (-z^-, (\tau - \bar{u})z^-, (u - \bar{u})z^-) \right] \right\}. \end{aligned} \quad (5.66)$$

An analogous equation holds for the parity-odd case, with obvious replacements $\mathcal{R} \leftrightarrow \tilde{\mathcal{R}}$ and $\mathcal{S} \leftrightarrow \tilde{\mathcal{S}}$. Compared to the forward scattering case, the expression for $\mathcal{R}^{3,qq}$ contains the opposite parity terms $\tilde{\mathcal{R}}^{2,qq}$. Notice also that the “center-of-mass” of two- and three-particle operators gets shifted by a total translation $\exp(\pm i\bar{u}z^- \partial^+)$. This equation gives a relation between generalized parton distributions of different “twists” when sandwiched between hadronic states.

In terms of local operators, the Eq. (5.66) reads

$$\begin{aligned} \mathcal{R}_{\rho;j}^{3,qq} = & \frac{1}{2j} \sum_{l=0}^{j-1} (j-l) (i\partial^+)^l \left\{ -\sigma_{l+1} i \varepsilon_\rho^{+\mu\nu} i \partial_\mu \tilde{\mathcal{R}}_{\nu;j-l-1}^{2,qq} - \sigma_l (i \partial_\rho n^\sigma - g_\rho^\sigma i \partial^+) \mathcal{R}_{\sigma;j-l-1}^{2,qq} \right\} \\ & - \frac{1}{j} \sum_{l=0}^{j-2} \sum_{k=1}^{j-l-1} (i\partial^+)^l \left\{ (j-k-l) \mathcal{S}_{[+]_\rho;j-l,k}^{ggq} - (-1)^l k \mathcal{S}_{[-]_\rho;j-l,k}^{ggq} \right\}, \end{aligned} \quad (5.67)$$

with

$$\sigma_l = \frac{1}{2} [1 - (-1)^l].$$

Similar equation holds for odd parity. It is obtained by replacing $\gamma^+ \rightarrow \gamma^+ \gamma^5$ and removing or dressing functions with a tilde. In Eq. (5.67) we used the convention

$$\mathcal{O}_{\rho;j} = n^{\mu_1} \dots n^{\mu_j} \mathcal{O}_{\rho\mu_1\dots\mu_j},$$

and also introduced three-particle local operators

$$\mathcal{S}_{[\pm]_\rho;j,k}^{ggq} = ig \bar{\psi}_q (i \overleftrightarrow{\partial}^+)^{k-1} \left\{ \gamma^+ F_{\rho}^{+\perp} \pm i \gamma^+ \gamma^5 \tilde{F}_{\rho}^{+\perp} \right\} (i \overleftrightarrow{\partial}^+)^{j-k-1} \psi_q. \quad (5.68)$$

5.3.2 Twist-three GPDs for spin-zero target

Turning to the analysis of twist-three GPDs, it is instructive to consider first the case of a spinless target [287, 289, 290, 293, 146, 296, 190, 308]. First, we construct the decomposition of GPDs with an open Lorentz index up to the twist-three contributions [287]

$$F_\mu^q = p_\mu H^q + \Delta_\mu^\perp H_3^q, \quad \tilde{F}_\mu^q = \tilde{\Delta}_\mu^\perp \tilde{H}_3^q, \quad (5.69)$$

where

$$\tilde{\Delta}_\perp^\rho \equiv i\varepsilon_\perp^{\rho\sigma} \Delta_\sigma^\perp. \quad (5.70)$$

The time-reversal invariance implies that

$$H_3^q(x, -\eta, \Delta^2) = -H_3^q(x, \eta, \Delta^2), \quad \tilde{H}_3^q(x, -\eta, \Delta^2) = \tilde{H}_3^q(x, \eta, \Delta^2). \quad (5.71)$$

The matrix elements of the twist-two local operators have been defined in Section 3.5 in Eqs. (3.113). Next we define the reduced matrix elements of the antiquark-gluon-quark operators. Since these operators are partially antisymmetrized, we have obviously two vectors: Δ_ρ^\perp and its “dual” $\tilde{\Delta}_\rho^\perp$ as possible tensor structures. Thus, the general decomposition of the reduced matrix elements is

$$\langle p_2 | \mathcal{S}_{[\pm]\rho;j,k}^{qgq} | p_1 \rangle = \Delta_\rho^\perp S_{[\pm]j,k}^{qgq}(p^+)^j, \quad \langle p_2 | \tilde{\mathcal{S}}_{[\pm]\rho;j,k}^{qgq} | p_1 \rangle = \tilde{\Delta}_\rho^\perp \tilde{S}_{[\pm]j,k}^{qgq}(p^+)^j. \quad (5.72)$$

The duality relation (5.41) gives $\tilde{S}_{[\pm]j,k}^{qgq} = S_{[\pm]j,k}^{qgq}$ and reduces the number of independent contributions to two instead of four. It proves convenient to introduce a mixed representation for corresponding GPDs, such that the transformed functions that depend on the position of the gluon field and a Fourier conjugate variable with respect to the distance between the two quark fields:

$$\langle p_2 | \begin{cases} \mathcal{S}_{[\pm]\rho}^{qgq}(-z^-, uz^-, z^-) \\ \tilde{\mathcal{S}}_{[\pm]\rho}^{qgq}(-z^-, uz^-, z^-) \end{cases} \Big| p_1 \rangle = (p^+)^2 \begin{Bmatrix} \Delta_\rho^\perp \\ \tilde{\Delta}_\rho^\perp \end{Bmatrix} \int dx e^{-ixp^+z^-} S_{[\pm]}^{qgq}(x, u, \eta). \quad (5.73)$$

Taking the moments with respect to the momentum fraction x yields the polynomials of order $j-2$ in the variable u :

$$S_{[\pm]j}^{qgq}(u, \eta) \equiv \int_{-1}^1 dx x^{j-2} S_{[\pm]}^{qgq}(x, u, \eta) = \sum_{k=1}^{j-1} \binom{j-2}{k-1} \left(\frac{1+u}{2}\right)^{k-1} \left(\frac{1-u}{2}\right)^{j-k-1} S_{[\pm]j,k}^{qgq}(\eta). \quad (5.74)$$

The functions $S_{[\pm]j,k}^{qgq}(\eta)$ are defined in Eq. (5.72). They are polynomials in η of order j . Finally, to obtain the matrix element of the operator $\mathcal{O}_{\rho;j}^{qq}$, we insert our findings (3.117) into the solution (5.67):

$$\begin{aligned} (p^+)^{-j} \langle p_2 | \mathcal{O}_{\rho;j}^{qq} | p_1 \rangle &= \left(p_\rho + \frac{\Delta_\rho^\perp}{\eta} \right) H_{j+1}^q(\eta) + \Delta_\rho^\perp \left\{ \sum_{k=0}^j \frac{\sigma_{j+1-k}}{j+1} \eta^{j-k} \left(\frac{d}{d\eta} - \frac{k+1}{\eta} \right) H_{k+1}^q(\eta) \right\} \\ &\quad - \Delta_\rho^\perp \sum_{k=2}^j \frac{k! \eta^{j-k}}{(j+1)(k-2)!} \int_{-1}^1 du \left\{ \frac{1-u}{2} S_{[+]k}^{qgq}(u, \eta) - (-1)^{j-k} \frac{1+u}{2} S_{[-]k}^{qgq}(u, \eta) \right\}, \end{aligned} \quad (5.75)$$

where we have used the relations

$$\begin{aligned}\int_{-1}^1 du \frac{1+u}{2} S_{[\pm]j}^{qgg}(u, \eta) &= 2 \sum_{k=1}^{j-1} \frac{k}{j(j-1)} S_{[\pm]j,k}^{qgg}(\eta), \\ \int_{-1}^1 du \frac{1-u}{2} S_{[\pm]j}^{qgg}(u, \eta) &= 2 \sum_{k=1}^{j-1} \frac{j-k}{j(j-1)} S_{[\pm]j,k}^{qgg}(\eta).\end{aligned}$$

The final step is a summation of local operators, see Eq. (5.64), that yields an expression in terms of the usual twist-two GPDs $H^q(x, \eta)$ and the mixed representation three-particle functions $S_{[\pm]}^{qgg}(y, u, \eta)$,

$$\begin{aligned}F_\mu^q(x, \eta) &= \left(p_\mu + \frac{\Delta_\mu^\perp}{\eta} \right) H^q(x, \eta) + \frac{\Delta_\mu^\perp}{\eta} \int_{-1}^1 \frac{dy}{\eta} W_+ \left(\frac{x}{\eta}, \frac{y}{\eta} \right) \left(\eta \frac{\partial}{\partial \eta} + y \frac{\partial}{\partial y} \right) H^q(y, \eta) \\ &\quad - \Delta_\rho^\perp \int_{-1}^1 \frac{dy}{\eta} \int_{-1}^1 du \left\{ \frac{1-u}{2} W'' \left(\frac{x}{\eta}, \frac{y}{\eta} \right) S_{[+]}^{qgg}(y, u, \eta) + \frac{1+u}{2} W'' \left(-\frac{x}{\eta}, -\frac{y}{\eta} \right) S_{[-]}^{qgg}(y, u, \eta) \right\}.\end{aligned}\quad (5.76)$$

Here we have introduced the kernel

$$\begin{aligned}W(x, y) &\equiv \vartheta_{11}^0(1-x, y-x) \\ &= \frac{\theta(1-x)\theta(x-y) - \theta(x-1)\theta(y-x)}{1-y},\end{aligned}\quad (5.77)$$

which enters in symmetric and antisymmetric combinations

$$W_\pm(x, y) = \frac{1}{2} \{W(x, y) \pm W(-x, -y)\}. \quad (5.78)$$

Notice that we encounter the same generalized step function as in the section devoted to the evolution of GPDs (see Appendix G.7 for a summary of formulas involving these functions). We also used the notation

$$W'' \left(\pm \frac{x}{\eta}, \pm \frac{y}{\eta} \right) \equiv \frac{d^2}{dy^2} W \left(\pm \frac{x}{\eta}, \pm \frac{y}{\eta} \right)$$

and incorporated the following result for the Mellin moments of the W -kernels

$$\int_{-1}^1 \frac{dx}{\eta} x^j W \left(\frac{x}{\eta}, \frac{y}{\eta} \right) = \sum_{k=0}^j \frac{\eta^{j-k} y^k}{j+1} \quad (5.79)$$

performing the restoration of the non-local form.

The only difference in the axial-vector case is that the corresponding operator matrix element does not possess the twist-two part for a spinless target. However, a non-vanishing twist-two contribution of the vector operator induces a kinematical term due to the Levi-Civita tensor in Eq. (5.67). Thus, the twist-three functions contain two parts, namely, the kinematical piece, expressed in terms of the twist-two function, and the term given as a correlation function of antiquark-gluon-quark operators [289]:

$$\begin{aligned}H_3^q(x, \eta) &= \frac{1}{\eta} \int_{-1}^1 \frac{dy}{\eta} W_+ \left(\frac{x}{\eta}, \frac{y}{\eta} \right) \left(\eta \frac{\partial}{\partial \eta} + y \frac{\partial}{\partial y} \right) H^q(y, \eta) + \frac{1}{\eta} H^q(x, \eta) - S_{[+]}^{qgg}(x, \eta), \\ \tilde{H}_3^q(x, \eta) &= \frac{1}{\eta} \int_{-1}^1 \frac{dy}{\eta} W_- \left(\frac{x}{\eta}, \frac{y}{\eta} \right) \left(\eta \frac{\partial}{\partial \eta} + y \frac{\partial}{\partial y} \right) H^q(y, \eta) - S_{[-]}^{qgg}(x, \eta).\end{aligned}\quad (5.80)$$

Note that the first moment of these functions with respect to x vanishes. The new dynamical information is contained in the antiquark-gluon-quark GPDs [289]

$$S_{\pm}^{qgq}(x, \eta) = \int_{-1}^1 \frac{dy}{\eta} \int_{-1}^1 du \left\{ \frac{1-u}{2} W'' \left(\frac{x}{\eta}, \frac{y}{\eta} \right) S_{[+]}^{qgq}(y, u, \eta) \pm \frac{1+u}{2} W'' \left(-\frac{x}{\eta}, -\frac{y}{\eta} \right) S_{[-]}^{qgq}(y, u, \eta) \right\}. \quad (5.81)$$

5.3.3 Twist-three GPDs for spin-one-half target

Let us address the case of realistic spin-one-half target. For the vector channel, the analysis repeating the one we outlined in the previous section yields

$$\begin{aligned} F_{\mu}^q(x, \eta) &= \left(p_{\mu} + \frac{\Delta_{\mu}^{\perp}}{\eta} \right) \left(\frac{h^+}{p^+} H^q(x, \eta) + \frac{e^+}{p^+} E^q(x, \eta) \right) \\ &+ \int_{-1}^1 \frac{dy}{\eta} \left\{ W_+ \left(\frac{x}{\eta}, \frac{y}{\eta} \right) G_{\mu}^q(y, \eta) + W_- \left(\frac{x}{\eta}, \frac{y}{\eta} \right) i\varepsilon_{\mu\nu}^{\perp} \tilde{G}^{q,\nu}(y, \eta) \right\} \\ &- \int_{-1}^1 \frac{dy}{\eta} \int_{-1}^1 du \left\{ \frac{1-u}{2} W'' \left(\frac{x}{\eta}, \frac{y}{\eta} \right) S_{[+]^{\mu}}^{qgq}(y, u, \eta) + \frac{1+u}{2} W'' \left(-\frac{x}{\eta}, -\frac{y}{\eta} \right) S_{[-]^{\mu}}^{qgq}(y, u, \eta) \right\}, \end{aligned} \quad (5.82)$$

and similarly for the axial sector,

$$\begin{aligned} \tilde{F}_{\mu}^q(x, \eta) &= \left(p_{\mu} + \frac{\Delta_{\mu}^{\perp}}{\eta} \right) \left(\frac{\tilde{h}^+}{p^+} \tilde{H}^q(x, \eta) + \frac{\tilde{e}^+}{p^+} \tilde{E}^q(x, \eta) \right) \\ &+ \int_{-1}^1 \frac{dy}{\eta} \left\{ W_+ \left(\frac{x}{\eta}, \frac{y}{\eta} \right) \tilde{G}_{\mu}^q(y, \eta) + W_- \left(\frac{x}{\eta}, \frac{y}{\eta} \right) i\varepsilon_{\mu\nu}^{\perp} G^{q,\nu}(y, \eta) \right\} \\ &- \int_{-1}^1 \frac{dy}{\eta} \int_{-1}^1 du \left\{ \frac{1-u}{2} W'' \left(\frac{x}{\eta}, \frac{y}{\eta} \right) \tilde{S}_{[+]^{\mu}}^{qgq}(y, u, \eta) + \frac{1+u}{2} W'' \left(-\frac{x}{\eta}, -\frac{y}{\eta} \right) \tilde{S}_{[-]^{\mu}}^{qgq}(y, u, \eta) \right\}. \end{aligned} \quad (5.83)$$

Here we have introduced a shorthand notation for the combinations

$$\begin{aligned} G^{q,\mu}(x, \eta) &= \left(h^{\mu} - p^{\mu} \frac{h^+}{p^+} \right) (H^q(x, \eta) + E^q(x, \eta)) \\ &+ \frac{\Delta_{\mu}^{\perp}}{\eta} \left\{ \frac{h^+}{p^+} \left(\eta \frac{\partial}{\partial \eta} + x \frac{\partial}{\partial x} \right) (H^q(x, \eta) + E^q(x, \eta)) - \frac{b}{2M_N} \left(\eta \frac{\partial}{\partial \eta} + x \frac{\partial}{\partial x} \right) E^q(x, \eta) \right\}, \end{aligned} \quad (5.84)$$

$$\begin{aligned} \tilde{G}^{q,\mu}(x, \eta) &= \left(\tilde{h}^{\mu} - p^{\mu} \frac{\tilde{h}^+}{p^+} \right) \tilde{H}(x, \eta) \\ &+ \frac{\Delta_{\mu}^{\perp}}{\eta} \left\{ \frac{\tilde{h}^+}{p^+} \left(\eta \frac{\partial}{\partial \eta} + x \frac{\partial}{\partial x} \right) \tilde{H}(x, \eta) - \frac{\tilde{b}}{2M_N} \left(\eta \frac{\partial}{\partial \eta} + x \frac{\partial}{\partial x} \right) \eta \tilde{E}(x, \eta) \right\}. \end{aligned} \quad (5.85)$$

Next, for the time being we introduce three-particle GPDs without their explicit decomposition in spinor bilinears,

$$\langle p_2 | \left\{ \begin{array}{l} \mathcal{S}_{[\pm]\mu}^{qgq}(-z^-, uz^-, z^-) \\ \tilde{\mathcal{S}}_{[\pm]\mu}^{qgq}(-z^-, uz^-, z^-) \end{array} \right\} | p_1 \rangle = (p^+)^2 \int dx e^{-ixp^+z^-} \left\{ \begin{array}{l} S_{[\pm]\mu}^{qgq}(x, u, \eta) \\ \tilde{S}_{[\pm]\mu}^{qgq}(x, u, \eta) \end{array} \right\}. \quad (5.86)$$

A general decomposition of the vector and axial-vector GPDs, in a complete basis of structures to twist-three accuracy, reads

$$F_\mu^q = p_\mu \frac{h^+}{p^+} H^q + p_\mu \frac{e^+}{p^+} E^q + \Delta_\mu^\perp \frac{h^+}{p^+} H_{3+}^q + \Delta_\mu^\perp \frac{e^+}{p^+} E_{3+}^q + \tilde{\Delta}_\mu^\perp \frac{\tilde{h}^+}{p^+} \tilde{H}_{3-}^q + \tilde{\Delta}_\mu^\perp \frac{\tilde{e}^+}{p^+} \tilde{E}_{3-}^q, \quad (5.87)$$

$$\tilde{F}_\mu^q = p_\mu \frac{\tilde{h}^+}{p^+} \tilde{H}^q + p_\mu \frac{\tilde{e}^+}{p^+} \tilde{E}^q + \Delta_\mu^\perp \frac{\tilde{h}^+}{p^+} \tilde{H}_{3+}^q + \Delta_\mu^\perp \frac{\tilde{e}^+}{p^+} \tilde{E}_{3+}^q + \tilde{\Delta}_\mu^\perp \frac{h^+}{p^+} \tilde{H}_{3-}^q + \tilde{\Delta}_\mu^\perp \frac{e^+}{p^+} \tilde{E}_{3-}^q. \quad (5.88)$$

The parametrization of the correlation functions S and \tilde{S} then can be cast in an analogous form,

$$\begin{aligned} S_{[\pm]\mu}^{qgq}(x, u, \eta) &= \Delta_\mu^\perp \frac{b}{2M} S_1^\pm + \Delta_\mu^\perp \frac{h^+}{p^+} S_2^\pm + \tilde{\Delta}_\mu^\perp \frac{\tilde{b}}{2M} S_3^\pm + \tilde{\Delta}_\mu^\perp \frac{\tilde{h}^+}{p^+} S_4^\pm, \\ \tilde{S}_{[\pm]\mu}^{qgq}(x, u, \eta) &= \Delta_\mu^\perp \frac{\tilde{b}}{2M} \tilde{S}_1^\pm + \Delta_\mu^\perp \frac{\tilde{h}^+}{p^+} \tilde{S}_2^\pm + \tilde{\Delta}_\mu^\perp \frac{b}{2M} \tilde{S}_3^\pm + \tilde{\Delta}_\mu^\perp \frac{h^+}{p^+} \tilde{S}_4^\pm, \end{aligned} \quad (5.89)$$

where duality (5.41) requires $S_i^\pm = \tilde{S}_i^\pm$.

In order to reduce the above GPDs to the form of Eqs. (5.87) and (5.88), we decompose the (axial-) vector Dirac bilinears h_μ (\tilde{h}_μ) in its twist-two and -three components making use of the Dirac equation

$$\begin{aligned} h^\mu &= p^\mu \frac{h^+}{p^+} - \eta \frac{\Delta_\perp^\mu}{\Delta_\perp^2} \left\{ \Delta^2 \frac{h^+}{p^+} - 4M_N^2 \frac{e^+}{p^+} \right\} - \frac{\tilde{\Delta}_\perp^\mu}{\Delta_\perp^2} \left\{ \Delta^2 \frac{\tilde{h}^+}{p^+} - 4M_N^2 \frac{\tilde{e}^+}{p^+} \right\}, \\ \tilde{h}^\mu &= p^\mu \frac{\tilde{h}^+}{p^+} - \eta \frac{\Delta_\perp^\mu}{\Delta_\perp^2} \left\{ (\Delta^2 - 4M_N^2) \frac{\tilde{h}^+}{p^+} - 4M_N^2 \frac{1}{\eta^2} \frac{\tilde{e}^+}{p^+} \right\} - \frac{\tilde{\Delta}_\perp^\mu}{\Delta_\perp^2} \left\{ \Delta^2 \frac{h^+}{p^+} - 4M_N^2 \frac{e^+}{p^+} \right\}. \end{aligned}$$

Here twist-four terms, proportional to n_μ^* , have been neglected. The transverse momentum squared is re-expressed in terms of the momentum difference,

$$\Delta_\perp^2 \simeq (1 - \eta^2) (\Delta^2 - \Delta_{\min}^2), \quad \Delta_{\min}^2 \simeq -4M_N^2 \frac{\eta^2}{1 - \eta^2}.$$

Note, that later on when computing physical amplitudes contributing to various exclusive processes, one can safely replace the light-like vector n^μ by q^μ , such that to twist-four accuracy

$$\frac{v^+}{p^+} \rightarrow \frac{(v \cdot q)}{(p \cdot q)}.$$

According to our discussion, all twist-three GPDs are decomposed into the so-called Wandzura-Wilczek (WW) term F_{\pm}^{WW} and a function F_{\pm}^{qgq} that contains dynamical information arising from antiquark-gluon-quark correlations:

$$F_{3\pm}^q = F_{\text{WW}\pm}^q + F_{\pm}^{qgq}, \quad (5.90)$$

where F is a unified notation for GPDs of different species

$$F = \{H, E, \tilde{H}, \eta \tilde{E}\}.$$

Notice that the pion-pole function \tilde{E} is accompanied by the skewness η . As we just discussed, the WW parts are expressed solely in terms of the twist-two functions and have the following form

$$\begin{aligned} F_{\text{WW}+}(x, \eta) &= \frac{1}{\eta} \int_{-1}^1 \frac{dy}{\eta} W_+ \left(\frac{x}{\eta}, \frac{y}{\eta} \right) \left(y \frac{\partial}{\partial y} + \eta \frac{\partial}{\partial \eta} \right) F(y, \eta) + \frac{1}{\eta} F(x, \eta) - \frac{4M_N^2}{\Delta_\perp^2} F_+^\perp(x, \eta), \\ F_{\text{WW}-}(x, \eta) &= \frac{1}{\eta} \int_{-1}^1 \frac{dy}{\eta} W_- \left(\frac{x}{\eta}, \frac{y}{\eta} \right) \left(y \frac{\partial}{\partial y} + \eta \frac{\partial}{\partial \eta} \right) F(y, \eta) - \frac{4M_N^2}{\Delta_\perp^2} F_-^\perp(x, \eta), \end{aligned} \quad (5.91)$$

for the ‘+’ and ‘-’ component of the twist-three GPDs in the WW-approximation, respectively. The functions F_\pm^\perp specifically appear for the spin-one-half targets and read

$$\begin{aligned} H_\pm^\perp(x, \eta) &= \frac{\Delta^2}{4M_N^2} \int_{-1}^1 \frac{dy}{\eta} \left\{ \eta W_\pm \left(\frac{x}{\eta}, \frac{y}{\eta} \right) (H + E)(y, \eta) + W_\mp \left(\frac{x}{\eta}, \frac{y}{\eta} \right) \tilde{H}(y, \eta) \right\}, \\ E_\pm^\perp(x, \eta) &= - \int_{-1}^1 \frac{dy}{\eta} \left\{ \eta W_\pm \left(\frac{x}{\eta}, \frac{y}{\eta} \right) (H + E)(y, \eta) + W_\mp \left(\frac{x}{\eta}, \frac{y}{\eta} \right) \tilde{H}(y, \eta) \right\}, \\ \tilde{H}_\pm^\perp(x, \eta) &= \int_{-1}^1 \frac{dy}{\eta} \left\{ \eta \left(\frac{\Delta^2}{4M_N^2} - 1 \right) W_\pm \left(\frac{x}{\eta}, \frac{y}{\eta} \right) \tilde{H}(y, \eta) + \frac{\Delta^2}{4M_N^2} W_\mp \left(\frac{x}{\eta}, \frac{y}{\eta} \right) (H + E)(y, \eta) \right\}, \\ \eta \tilde{E}_\pm^\perp(x, \eta) &= - \int_{-1}^1 \frac{dy}{\eta} \left\{ W_\pm \left(\frac{x}{\eta}, \frac{y}{\eta} \right) \tilde{H}(y, \eta) + \eta W_\mp \left(\frac{x}{\eta}, \frac{y}{\eta} \right) (H + E)(y, \eta) \right\}. \end{aligned} \quad (5.92)$$

The antiquark-gluon-quark contributions can be read off from the parametrization of the corresponding operators in Eq. (5.89).

It is important to realize that the scale dependence of the twist-three GPDs F_μ^q and \tilde{F}_μ^q is not homogeneous, namely, their different components have their own autonomous evolution in hard momentum transfer Q^2 . While in the WW-approximation the functions are expressed in terms of standard twist-two GPDs, obeying the renormalization group equations discussed at length in the previous chapter, the three-particle correlation function satisfy an independent equation. The thorough analysis of the latter reveals hidden symmetries of the problem which leads to its complete integrability [309, 310, 311, 312]. However, this is a subject of separate reviews [262, 313].

5.3.4 Properties of the kinematical kernels

In Section 5.3.2 we introduced the notion of the WW-kernels (5.78). Here, we consider their general properties [292]. To make formulas appear concise, let us adopt the following notations for the action of the WW-kernels on a test function $\tau(x, \eta)$

$$[W_\pm \otimes \tau](x, \eta) \equiv \int_{-1}^1 \frac{dy}{\eta} W_\pm \left(\frac{x}{\eta}, \frac{y}{\eta} \right) \tau(y, \eta), \quad (5.93)$$

The functions $[W_\pm \otimes \tau]$ resulting from the WW-transformation will be referred to as the WW-transform.

It is instructive to analyze two limiting cases of the WW-transformation, namely, the forward limit $\eta \rightarrow 0$ and the exclusive limit $\eta \rightarrow 1$, as well as address the issue of polynomiality and singularity structure of the WW kernels.

- In the forward limit, we easily obtain

$$\begin{aligned} \lim_{\eta \rightarrow 0} [W_+ \otimes \tau](x, \eta) &= \theta(x) \int_x^1 \frac{dy}{y} \tau(y, \eta = 0) - \theta(-x) \int_{-1}^x \frac{dy}{y} \tau(y, \eta = 0), \\ \lim_{\eta \rightarrow 0} [W_- \otimes \tau](x, \eta) &= 0. \end{aligned} \quad (5.94)$$

We can see that the action of the W_+ in the forward limit reproduces the Wandzura–Wilczek relation for the spin structure function $g_T = g_1 + g_2$ [314]. The term with $\theta(x)$ corresponds to quark distributions

$$\lim_{\Delta \rightarrow 0} \tilde{F}_\mu^{q\perp}(x, \eta, \Delta^2)|_{x>0} = h_\mu^\perp \left\{ \Delta q(x) + \int_x^1 \frac{dy}{y} \Delta q(y) \right\},$$

while the term with $\theta(-x)$ to antiquark ones. The W_- kernel disappears in the forward limit, so that this kernel is specific to off-forward kinematics.

- In the $\eta \rightarrow 1$ limit, the generalized parton distributions have the properties of meson distribution amplitudes as we demonstrated in Section 3.7.3. In this limit, the WW-transforms have the form

$$\lim_{\eta \rightarrow 1} [W_\pm \otimes \tau](x, \eta) = \frac{1}{2} \left\{ \int_{-1}^x \frac{dy}{1-y} \varphi(y) \pm \int_x^1 \frac{dy}{1+y} \varphi(y) \right\},$$

where we used the notation $\tau(x, \eta = 1) = \varphi(x)$. This equation corresponds to the WW-relations for meson distribution amplitudes derived in Refs. [125, 303]. So, we can say that the WW-transform of GPDs interpolates between the WW-relations for parton distributions and those for meson distribution amplitudes. Furthermore, the general form of the WW-kernels (5.78) allows one to derive WW relations for distribution amplitudes of mesons with arbitrary spin.

- One can easily compute the Mellin moments of the WW-transform. This was already used above in Eq. (5.79). The result for WW-transform with the W_\pm kernels is

$$\int_{-1}^1 dx x^j [W_\pm \otimes \tau](x, \eta) = \frac{1}{j+1} \int_{-1}^1 dy \left\{ \frac{y^{j+1} - \eta^{j+1}}{y - \eta} \pm \frac{y^{j+1} - (-\eta)^{j+1}}{y + \eta} \right\} \tau(u, \eta). \quad (5.95)$$

Wherfrom we can see an important property of the WW-transformation, namely, if the function $\tau(x, \eta)$ satisfies the polynomiality condition

$$\int_{-1}^1 dx x^j \tau(x, \eta) = \sum_{k=0}^{j+1} \eta^k \tau_k, \quad (5.96)$$

i.e., it is a polynomial of order $j+1$, so does its WW-transform.

Let us consider now two special cases of these Mellin moments, $j = 0, 1$. These particular moments of twist-three GPDs do not receive contribution from the “genuine twist-three” quark-gluon operators, therefore, for these particular cases the WW-approximation gives exact results. In the forward limit this observation leads to Burkhard-Cottingham ($j = 0$) [317] and Efremov-Teryaev-Leader ($j = 1$) [318] sum rules for polarized structure function g_T . Generalizations of these sum rules for generalized parton distributions have been discussed in Refs. [288, 290].

- In Ref. [290] it was demonstrated that the twist-three GPDs in the WW-approximation exhibit discontinuities at the points $x = \pm\eta$. This feature stems from the analogous properties of the WW-kernels. Namely, the discontinuities of a WW-transform at the points $x = \pm\eta$ yields

$$\begin{aligned} \lim_{\varepsilon \rightarrow 0} \left[[W_\pm \otimes \tau](\eta + \varepsilon, \eta) - [W_\pm \otimes \tau](\eta - \varepsilon, \eta) \right] &= \frac{1}{2} \text{PV} \int_{-1}^1 \frac{dy}{y - \eta} \tau(y, \eta), \\ \lim_{\varepsilon \rightarrow 0} \left[[W_\pm \otimes \tau](-\eta + \varepsilon, \eta) - [W_\pm \otimes \tau](-\eta - \varepsilon, \eta) \right] &= \pm \frac{1}{2} \text{PV} \int_{-1}^1 \frac{dy}{y + \eta} \tau(y, \eta). \end{aligned} \quad (5.97)$$

We see that for a very wide class of functions $\tau(u, \eta)$ the discontinuity of the corresponding WW-transforms is nonzero. This nonanalytic behavior of the WW-transformation may result in violation of perturbative factorization for the twist-three DVCS amplitude, since the singularity of the hard coefficient function $x = \pm\xi$ overlaps the jump of the twist-three GPDs $x = \pm\eta = \pm\xi$.

5.3.5 Discontinuities of twist-three GPDs

Using the discontinuity structure of the WW-kernels one can find the behavior of twist-three GPDs for spinless targets in the vicinity of the “turning” point $|x| = \eta$ [292, 291, 293],

$$\begin{aligned} H_3^q(\eta + 0, \eta) - H_3^q(\eta - 0, \eta) \\ = \frac{1}{2} \text{PV} \int_{-1}^1 \frac{dy}{\eta} \frac{1}{y - \eta} \left\{ \left(\eta \frac{\partial}{\partial \eta} + y \frac{\partial}{\partial y} \right) H(y, \eta) - 2 \frac{\partial^2}{\partial y^2} \int_{-1}^1 du (1+u) S_{[-]}^{qqq}(y, u, \eta) \right\}. \end{aligned} \quad (5.98)$$

Here we have tacitly assumed that GPDs vanish at the boundary $x = \pm 1$ (see Eq. 3.28)). Obviously, these discontinuities are not an artifact of the WW-approximation. Rather, they are intrinsic to the procedure of separation of twist-two and -three contributions.

Notice however, that the combination

$$F_\mu^q(x, \eta, \Delta^2) - i\varepsilon_{\mu\nu}^\perp \tilde{F}^{q\nu}(x, \eta, \Delta^2), \quad (5.99)$$

is free from discontinuities at $x = \eta$, while

$$F_\mu^q(x, \eta, \Delta^2) + i\varepsilon_{\mu\nu}^\perp \tilde{F}^{q\nu}(x, \eta, \Delta^2), \quad (5.100)$$

is continuous at $x = -\eta$. Fortunately only these combinations contribute to the VCS amplitude to twist-four accuracy as we will discuss below.

5.3.6 Factorization of the Compton amplitude at twist-three

An important observation is that the observed divergences of the twist-three DVCS amplitudes cancel in certain combinations of helicity amplitudes [292, 291, 293]. This is possible because, in the Wandzura-Wilczek approximation, the discontinuities of contributing twist-three GPDs are related to each other. Since the divergences occur only at the points $x = \pm \xi$, it is sufficient that the jumps cancel at these specific values to save factorizability. As we will see, though divergent terms are formally present in $T^{\mu\nu}$, they do not contribute to the physical Compton amplitude with a real, transverse photon in the final state.

In particular, there is no singularity problem for the amplitudes with longitudinal polarization of the virtual photon. Let us demonstrate this. We can choose a frame in which the four momentum q_1^μ of the incoming photon has no transverse components, i.e., $q_{1\perp}^\mu = 0$, and the final-state photon carries the total transverse momentum transfer $q_{2\perp}^\mu = \Delta_\perp^\mu$. Then we construct the explicit form of the longitudinal polarization vector of the incoming virtual photon. In this frame the tensor structures (5.48) of the Compton amplitude in terms of the light-cone vectors loose their symmetric form, for instance, $\tilde{T}_{(1)}^{\mu\nu} = i(\varepsilon^{\mu\nu\rho\sigma} p_\rho q_\sigma + n^{*\mu} \varepsilon_\perp^{\nu\rho} \Delta_\rho^\perp)/(p \cdot q)$. Imposing the usual normalization and orthogonality conditions, we find for the incoming polarization vector

$$\varepsilon_L^\mu(q_1) = \frac{1}{Q} \left(1 + \frac{\eta}{\xi} + \delta^2 (2\xi + \eta)^2 \right)^{-1/2} (q^\mu + \tfrac{1}{2}(2\xi + \eta)p^\mu), \quad (5.101)$$

with δ^2 determined in Eq. (B.9). The projection of the Compton scattering amplitude (5.51), with imposed on-shell $q_2^2 = 0$ condition for the outgoing photon, gives

$$T_{\mu\nu} \varepsilon_L^\nu(q_1) \simeq \frac{Q}{\xi^2 \sqrt{1+\xi}} n_\mu (\mathcal{F}_2 - \xi \mathcal{F}_1) + \frac{2\xi}{Q \sqrt{1+\xi}} \left(\mathcal{F}_{3\mu}^\perp - i\varepsilon_{\mu\nu}^\perp \tilde{\mathcal{F}}_{3\perp}^\nu \right). \quad (5.102)$$

The first term does not represent any danger. Moreover, it vanishes at leading order of perturbation theory due to the generalized Callan-Gross relation (5.56). It is the second term which is the structure of interest. A closer inspection for a scalar target immediately suggests that, it reduces to a combination of functions H_3 and \tilde{H}_3 ,

$$\mathcal{H}^3 - \tilde{\mathcal{H}}^3 = \sum_q \int_{-1}^1 \frac{dx}{x} C_{(0)}^{q[-]}(x, \xi) \left(x H_3^q(x, \xi) + \xi \tilde{H}_3^q(x, \xi) \right), \quad (5.103)$$

which is singularity-free according to Eq. (5.98) and similar equation for \tilde{H}_3 .

Analogous cancellations occur for the spin-one-half target. On the other hand, a further analysis demonstrates that the DVCS amplitude on the nucleon with transversely polarized virtual photon contains a different combination of twist-three GPDs, namely,

$$\mathcal{F}_{3\mu}^\perp + i\varepsilon_{\mu\nu}^\perp \tilde{\mathcal{F}}_{3\perp}^\nu,$$

and it does possess uncancelled discontinuities. However, in cross sections for physical observables, the contribution of this “problematic” part of the twist-three DVCS amplitude is accompanied by a contracted polarization vector of the emitted real photon. Thus it turns out to be suppressed by two powers of the hard scale, relative to the leading order result. Thus, it does not contribute to observables at the level of $\mathcal{O}(1/Q)$ power corrections and is beyond the limits of approximations involved. In other words, the DVCS differential cross section to the twist-three accuracy gets contributions only from the longitudinal part of twist-three amplitudes which is free from divergences, which could threaten the validity of the factorization.

5.3.7 Sum rules for twist-three GPDs

As we demonstrated in our previous discussion, the leading-twist GPDs are related to hadronic form factor via integral relations—sum rules. Let us analyze in the same fashion a few lowest Mellin moments of twist-three GPDs. We established in the preceding section that the twist-three GPDs are expressible in terms of “known” twist-two ones and multiparticle correlation functions. Since the moments of GPDs are related to matrix elements of local Wilson operators, thus a Mellin moment of a twist-three GPD will be a sum of two- and three-particle operators. In order to compensate for the deficit in the mass dimension of a local two-particle compared to a quark-gluon-quark operator, which has an extra gluon field, the former will be inevitably dressed with derivatives. A simple dimensional analysis suggests then that the lowest moment of a twist-three GPD, expressed in terms of a local $\bar{\psi}(0)\Gamma\psi(0)$ operator, will not have contributions from three-particle correlation, since otherwise it should possesses inverse derivatives, which would lead to a non-locality and violation of the local operator product expansion. Higher moments will contain multiparticle correlations, unless it is prohibited by symmetry reasons. Let us discuss a few cases starting with the spin-zero target and then addressing the nucleon.

- For spin-zero target, one immediately finds [290] the analogue of the Burkhardt-Cottingham sum rule

$$\int_{-1}^1 dx H_3^q(x, \eta) = -\frac{1}{2} \frac{\partial}{\partial \eta} \int_{-1}^1 dx H^q(x, \eta) = 0. \quad (5.104)$$

There is also an analogue of the Efremov-Leader-Teryaev sum rule [318] for the same distribution, which takes the form

$$\int_{-1}^1 dx x H_3^q(x, \eta) = -\frac{1}{4} \frac{\partial}{\partial \eta} \int_{-1}^1 dx x H^q(x, \eta) = \frac{\eta}{2} P^q. \quad (5.105)$$

Here, as before, P^q is the momentum fraction of the flavor- q parton in a spinless hadron, see Eq. (3.299). As just pointed out, in both cases the quark-gluon-quark operators do not contribute.

- For spin-one-half target, the first moment of the functions F_μ^q and \tilde{F}_μ^q , introduced in Eqs. (5.82) and (5.83), respectively, yields the usual electromagnetic and weak quark form factors

$$\int_{-1}^1 dx F_\mu^q(x, \eta, \Delta^2) = \langle p_2 | j_\mu^q(0) | p_1 \rangle, \quad \int_{-1}^1 dx \tilde{F}_\mu^q(x, \eta, \Delta^2) = \langle p_2 | j_\mu^{5q}(0) | p_1 \rangle.$$

This means that the twist-three functions $F_{3\pm}^q$ in Eqs. (5.87) and (5.88) have vanishing first moments,

$$\int_{-1}^1 dx F_{3\pm}^q(x, \eta, \Delta^2) = 0. \quad (5.106)$$

The most interesting information from the viewpoint of the proton spin crisis comes from the first moment of the transverse part of the parity-even function,

$$\begin{aligned} \int_{-1}^1 dx x F_\mu^{q\perp}(x, \eta, \Delta^2) &= \frac{1}{2} h_\mu^\perp \left\{ G_A^q(\Delta^2) + \int_{-1}^1 dx x (H^q(x, \eta, \Delta^2) + E^q(x, \eta, \Delta^2)) \right\} \\ &\quad - \Delta_\mu^\perp \frac{b}{4M_N} \frac{\partial}{\partial \eta} \int_{-1}^1 dx x E^q(x, \eta, \Delta^2). \end{aligned} \quad (5.107)$$

It provides complimentary knowledge on the magnitude of the angular orbital motion of quarks in building up the spin of the proton, since

$$\lim_{\Delta^2 \rightarrow 0} \left\{ G_A^q(\Delta^2) + \int_{-1}^1 dx x (H^q(x, \eta, \Delta^2) + E^q(x, \eta, \Delta^2)) \right\} = \Delta q + 2J^q. \quad (5.108)$$

The term in Eq. (5.107) proportional to $\Delta_\perp^\mu b$ measures the distribution of shear in the nucleon (see Eqs. (3.162) and (3.163)). Starting from the third moment, the sum rules receive contributions from the quark-gluon-quark operators [298].

5.4 Compton form factors of the nucleon

Since factorization theorems have not been proven for the $1/\mathcal{Q}$ suppressed contributions, in contrast to the leading twist situation [6, 282, 283], it may happen that, at this level of accuracy, the results are plagued by singularities, and that the higher twist distributions are not universal. Though, the first next-to-leading order analysis in the Wandzura-Wilczek approximation [302] demonstrated the absence of these divergences and thus favors factorization beyond leading power in hard momentum. For survival of factorization in exclusive processes it is often vital that non-perturbative functions do have specific analytic properties. For instance, in case of the pion transition form factor measured in the process $\gamma^* \gamma^* \rightarrow \pi^0$, the meson distribution amplitude should vanish at the end-points, and there are some arguments [240] that this is really the case. For DVCS an analogous requirement amounts to continuity of generalized parton distributions at $|x| = \eta$. The tree level analysis has been given in the previous section, and as we have seen, for the transverse polarization of the initial photon, one actually encounters a situation with divergent expressions, however, they do not show up when the Compton amplitude is projected on the real photon final state satisfying $\varepsilon^* \cdot q_2 = 0$ [291].

We emphasize again that, in the absence of three-particle contributions, the twist-three functions are completely known in terms of the twist-two ones, just like in the naive parton model. It is an interesting non-perturbative problem to estimate the size of the antiquark-gluon-quark matrix elements in comparison with the Wandzura-Wilczek term. For forward kinematics, recent experimental data [319] and lattice results [320] suggest that the dynamical twist-three effects encoded in three-particle operators are small. Extrapolating these findings to off-forward scattering, one can hope to use the Wandzura-Wilczek part of the relation (5.82) as a reliable model for the “transverse” twist-three GPDs F_μ^q and \tilde{F}_μ^q .

5.4.1 Twist-three CFFs

The Compton form factors introduced in (5.59) and (5.60) are given as convolutions of perturbatively calculable coefficient functions $C^{[\pm]}$ with a set of twist-two and twist-three GPDs (5.87,5.88) via

$$\begin{aligned} \left\{ \mathcal{H}^q, \mathcal{E}^q, \mathcal{H}_{3+}^q, \mathcal{E}_{3+}^q, \tilde{\mathcal{H}}_{3-}^q, \tilde{\mathcal{E}}_{3-}^q \right\} (\xi, \eta) &= \int_{-1}^1 dx C_{(0)}^{q[-]}(\xi, x) \left\{ H^q, E^q, H_{3+}^q, E_{3+}^q, \tilde{H}_{3-}^q, \tilde{E}_{3-}^q \right\} (x, \eta), \\ \left\{ \tilde{\mathcal{H}}^q, \tilde{\mathcal{E}}^q, \tilde{\mathcal{H}}_{3+}^q, \tilde{\mathcal{E}}_{3+}^q, \mathcal{H}_{3-}^q, \mathcal{E}_{3-}^q \right\} (\xi, \eta) &= \int_{-1}^1 dx C_{(0)}^{q[+]}(\xi, x) \left\{ \tilde{H}^q, \tilde{E}^q, \tilde{H}_{3+}^q, \tilde{E}_{3+}^q, H_{3-}^q, E_{3-}^q \right\} (x, \eta). \end{aligned} \quad (5.109)$$

As we already established in previous sections, only the singularity-free combination of CFFs $\mathcal{F}_{3+} - \mathcal{F}_{3-}$ can show up in physical amplitudes [290, 293, 146, 321]. The absence of divergences can be immediately seen by computing the difference of Compton form factors for a generic situation $\eta \neq \xi$, evaluating the convolutions with the coefficient functions (5.33) and making use of the identity

$$\int_{-1}^1 \frac{dx}{\eta} \frac{1}{\xi - x} W \left(\frac{x}{\eta}, \frac{y}{\eta} \right) = \frac{1}{y - \eta} \ln \left(\frac{\xi - \eta}{\xi - y} \right).$$

For instance, for unpolarized CFFs we find in the WW-approximation

$$\begin{aligned} \mathcal{H}_{\text{WW+}}^q(\xi, \eta) - \mathcal{H}_{\text{WW-}}^q(\xi, \eta) &= \frac{1}{\eta} \mathcal{H}^q(\xi, \eta) + \int_{-1}^1 \frac{dy}{\eta} C_{3(0)}^{q[-]}(\xi, \eta, x) \left(x \frac{\partial}{\partial x} + \eta \frac{\partial}{\partial \eta} \right) H^q(x, \eta) \\ &\quad - \frac{\Delta^2}{\Delta_\perp^2} \int_{-1}^1 dx \left\{ \eta C_{3(0)}^{q[-]}(\xi, \eta, x) (H^q + E^q)(x, \eta) - C_{3(0)}^{q[+]}(\xi, \eta, x) \tilde{H}^q(x, \eta) \right\}, \end{aligned} \quad (5.110)$$

where the coefficient function

$$C_{3(0)}^{q[\pm]}(\xi, \eta, x) = \frac{Q_q^2}{\xi + x} \ln \frac{\xi + \eta}{\xi - x} \pm \frac{Q_q^2}{\xi - x} \ln \frac{\xi + \eta}{\xi + x}, \quad (5.111)$$

is finite for $\eta = \xi$. Analogous relations hold for other CFFs.

In the real-photon limit $\eta = \xi$, relevant for the deeply virtual Compton scattering, a specific “effective” combination of Compton form factors contributes to all amplitudes, namely,

$$\mathcal{F}_{\text{eff}}^q \equiv -\frac{2\xi}{1 + \xi} \mathcal{F}^q + 2\xi (\mathcal{F}_{3+}^q - \mathcal{F}_{3-}^q), \quad (5.112)$$

where $\mathcal{F}_{3\pm}^q$ are defined in Eqs. (5.109). Here, the CFF \mathcal{F} in Eq. (5.112) stands for \mathcal{H} , \mathcal{E} , $\tilde{\mathcal{H}}$, and $\tilde{\mathcal{E}}$ functions. Therefore, only four new GPDs (corresponding to GPDs $F = H, E, \tilde{H}$, and \tilde{E}) remain at twist-three level. The explicit form for the effective twist-three functions yields

$$\begin{aligned}\mathcal{F}_{\text{eff}}^q(\xi) = & \frac{2}{1+\xi}\mathcal{F}^q(\xi) + 2\xi\frac{\partial}{\partial\xi}\int_{-1}^1 dx C_{3(0)}^{q[\mp]}(\xi, \xi, x)F^q(x, \xi) + \frac{8M^2\xi}{\Delta_\perp^2}\mathcal{F}_\perp^q(\xi) \\ & -2\xi\int_{-1}^1 du \int_{-1}^1 dx C_{(0)}^{qqq}(\xi, x, u) \left(S_{[+]F}^{qqq}(-x, -u, -\xi) - S_{[-]F}^{qqq}(x, u, -\xi) \right) \Big\},\end{aligned}\quad (5.113)$$

for $\mathcal{F} = \mathcal{H}, \mathcal{E}, \tilde{\mathcal{H}}$ with $C_{3(0)}^{q[-]}$ coefficient function for the first two and $C_{3(0)}^{q[+]}$ for the latter. In case of the function $\tilde{\mathcal{E}}$, the formula takes a slightly different form due to the accompanying factor of skewness η in the helicity-flip functions \tilde{E}^q , namely,

$$\begin{aligned}\tilde{\mathcal{E}}_{\text{eff}}^q(\xi) = & \frac{2}{1+\xi}\tilde{\mathcal{E}}^q(\xi) + 2\frac{\partial}{\partial\xi}\xi\int_{-1}^1 dx C_{3(0)}^{q[+]}(\xi, \xi, x)\tilde{E}^q(x, \xi) + \frac{8M^2\xi}{\Delta_\perp^2}\tilde{\mathcal{E}}_\perp^q(\xi) \\ & -2\xi\int_{-1}^1 du \int_{-1}^1 dx C_{(0)}^{qqq}(\xi, x, u) \left(S_{[+]E}^{qqq}(-x, -u, -\xi) - S_{[-]E}^{qqq}(x, u, -\xi) \right) \Big\}.\end{aligned}\quad (5.114)$$

Here we have used a new notation for the three-particle coefficient functions

$$C_{(0)}^{qqq}(\xi, x, u) = Q_q^2 \frac{\partial^2}{\partial x^2} \frac{1+u}{\xi+x} \ln\left(\frac{2\xi}{\xi-x}\right). \quad (5.115)$$

Finally, the functions \mathcal{F}_\perp^q contributing to the effective CFFs are given by

$$\begin{aligned}\mathcal{H}_\perp^q(\xi) = & -\frac{\Delta^2}{4M^2}\int_{-1}^1 dx \left\{ \xi C_{3(0)}^{q[-]}(x, \xi) (H^q + E^q)(x, \xi) - C_{3(0)}^{q[+]}(x, \xi) \tilde{H}^q(x, \xi) \right\}, \\ \mathcal{E}_\perp^q(\xi) = & \int_{-1}^1 dx \left\{ \xi C_{3(0)}^{q[-]}(x, \xi) (H^q + E^q)(x, \xi) - C_{3(0)}^{q[+]}(x, \xi) \tilde{H}^q(x, \xi) \right\}, \\ \tilde{\mathcal{H}}_\perp^q(\xi) = & \int_{-1}^1 dx \left\{ \xi \left(1 - \frac{\Delta^2}{4M^2} \right) C_{3(0)}^{q[+]}(x, \xi) \tilde{H}^q(x, \xi) + \frac{\Delta^2}{4M^2} C_{3(0)}^{q[-]}(x, \xi) (H^q + E^q)(x, \xi) \right\}, \\ \tilde{\mathcal{E}}_\perp^q(\xi) = & \frac{1}{\xi} \int_{-1}^1 dx \left\{ C_{3(0)}^{q[+]}(x, \xi) \tilde{H}^q(x, \xi) - \xi C_{3(0)}^{q[-]}(x, \xi) (H^q + E^q)(x, \xi) \right\}.\end{aligned}\quad (5.116)$$

We should note that the kinematical factor Δ_\perp^{-2} in Eqs. (5.113) and (5.114) cancels out in final results for angular harmonics of the cross section (6.23), calculated later in Sections 6.1.5 and 6.1.6, and therefore, it does not lead to spurious kinematical poles.

5.4.2 Small- x_B behavior of Compton form factors

Let us now study the properties of the DVCS CFFs for small x_B in the leading order approximation. At intermediate momentum transfer Δ^2 , this kinematics was discussed within the BFKL approach in Refs. [322, 323] and in Ref. [324] within the dipole model. The small- ξ behavior of the CFFs is governed by the small momentum fraction asymptotics of parton densities. If the latter behave like $x^{-\alpha_q}$ with $\alpha_q > 0$, then the real and imaginary parts of \mathcal{H}^q go like $\xi^{-\alpha_q}$, and the ratio of the real to imaginary part is given by $\tan((\alpha_q - 1)\pi/2) = -\cot(\alpha_q\pi/2)$. For polarized parton

densities, the small- x behavior of the Regge type $x^{-\tilde{\alpha}_q}$ induces an equivalent growth of $\tilde{\mathcal{H}}^q$ in ξ . However, the ratio of the real to imaginary part is now $\tan(\tilde{\alpha}_q \pi/2)$ instead.

This behavior can be understood in a model-independent way. The essential assumption is that double distributions can be represented in the following form

$$f^q(\beta, \alpha) = \beta^{-\alpha_q} \{d_q(0, \alpha) + \dots\}, \quad (5.117)$$

in the vicinity of the point $\beta = 0$, where the parameter α_q may depend on Δ^2 and Q^2 [9, 325], as we already addressed in Section 3.13.2. Double distributions can also have δ -like singularities at $\beta = 0$. Such contributions generate GPDs entirely concentrated in the exclusive region $|x| < \eta$ and can be interpreted as isolated mesonic-like states and treated separately. Moreover, we assume that $f(\beta, \alpha)$ and, consequently, also $d(0, \alpha)$ vanishes fast enough when it approaches the support boundary $|\beta| + |\alpha| = 1$. By “fast enough” we mean that, when $\alpha \rightarrow \pm 1$, we have $|d(0, \alpha)| < |1 \mp \alpha|^{\text{Max}(0, \alpha_q - 1) + \varepsilon}$ with $\varepsilon > 0$. Due to the symmetry properties of corresponding DDs with respect to β , it is sufficient to discuss the region $\beta > 0$ only. We also assume that $\alpha_q < 2$ in the vector and $\tilde{\alpha}_q < 1$ in the axial-vector sector to ensure the existence of certain integrals. The latter inequalities are fulfilled phenomenologically.

The usual parton densities $q(\beta)$ result from DDs after integration over α (see Eq. (3.228)). Thus, at small momentum fractions β , the parton densities are given by $\beta^{-\alpha_q} \int_{-1}^1 d\alpha d_q(0, \alpha)$. Then a straightforward calculation shows that the imaginary and real parts of the twist-two CFFs at leading order behave like [326, 327, 146, 328]

$$\begin{aligned} \Im \mathcal{H}^q(\xi, \Delta^2; Q^2) &= Q_q^2 \pi \xi^{-\alpha_q} \int_{-1}^1 d\alpha (1 - \alpha)^{-\alpha_q} d_q(0, \alpha, \Delta^2; Q^2), \\ \Re \mathcal{H}^q(\xi, \Delta^2; Q^2) &= \tan\left((\alpha_q - 1)\frac{\pi}{2}\right) \Im \mathcal{H}^q(\xi, \Delta^2; Q^2). \end{aligned} \quad (5.118)$$

An analogous formula holds for the spin-flip CFF \mathcal{E} . Note, that the D-term is not important in this limit. However, the small- ξ behavior of CFFs can, in principle, be altered by other terms concentrated at $\beta = 0$, i.e., $\frac{d^n}{d\beta^n} \delta(\beta)$. Such dependence is not excluded so far by sum rules. These $\delta^{(n)}(\beta)$ -like singularities, convoluted with the hard scattering part yield contributions proportional to ξ^{-n-1} . Due to a definite cross symmetry of the hard scattering coefficient function, the exponent n of this dependence takes odd (even) values for \mathcal{E} ($\tilde{\mathcal{E}}$), respectively. Implementing these considerations, the complete set of asymptotic formulas for small- ξ reads

$$\begin{aligned} \begin{Bmatrix} \Re \\ \Im \end{Bmatrix} \mathcal{H}^q(\xi, \Delta^2) &= \begin{Bmatrix} -\cot(\alpha_q \pi/2) \\ 1 \end{Bmatrix} N_{\mathcal{H}}^q(\Delta^2) \xi^{-\alpha_q(\Delta^2)}, \\ \begin{Bmatrix} \Re \\ \Im \end{Bmatrix} \mathcal{E}^q(\xi, \Delta^2) &= \begin{Bmatrix} -\cot(\beta_q \pi/2) \\ 1 \end{Bmatrix} N_{\mathcal{E}}^q(\Delta^2) \xi^{-\beta_q(\Delta^2)} + \begin{Bmatrix} 1 \\ 0 \end{Bmatrix} M_{\mathcal{E}}^q(\Delta^2) \xi^{-2p}, \\ \begin{Bmatrix} \Re \\ \Im \end{Bmatrix} \tilde{\mathcal{H}}^q(\xi, \Delta^2) &= \begin{Bmatrix} \tan(\tilde{\alpha}_q \pi/2) \\ 1 \end{Bmatrix} N_{\tilde{\mathcal{H}}}^q(\Delta^2) \xi^{-\tilde{\alpha}_q(\Delta^2)}, \\ \begin{Bmatrix} \Re \\ \Im \end{Bmatrix} \tilde{\mathcal{E}}^q(\xi, \Delta^2) &= \begin{Bmatrix} \tan(\tilde{\beta}_q \pi/2) \\ 1 \end{Bmatrix} N_{\tilde{\mathcal{E}}}^q(\Delta^2) \xi^{-\tilde{\beta}_q(\Delta^2)} + \begin{Bmatrix} 1 \\ 0 \end{Bmatrix} \frac{F_{\pi}^q(\Delta^2)}{2\xi} + \begin{Bmatrix} 1 \\ 0 \end{Bmatrix} M_{\tilde{\mathcal{E}}}^q(\Delta^2) \xi^{-2\tilde{p}-1}, \end{aligned} \quad (5.119)$$

where at zero recoil $\alpha_q(\Delta^2 = 0) = \alpha_q$ and $\tilde{\alpha}_q(\Delta^2 = 0) = \tilde{\alpha}_q = a_q$ coincide with the “Regge intercepts” of the forward parton distributions (3.339) and (3.341), respectively. The constants

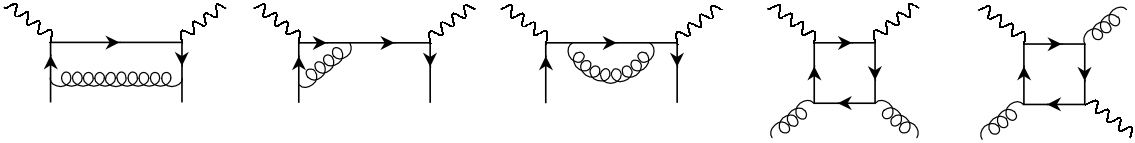


Figure 43: One-loop coefficient functions for quark and gluon GPDs in the Compton amplitude.

$p, \tilde{p} \geq 1$ are positive integers that reflect the appearance of isolated meson-like states. They provide the dominant contributions to the spin-flip CFFs and could overwhelm the small- x_B behavior of the spin non-flip CFFs. Note also, that because of the well-constrained dependence at small and large ξ , and a simple shape of the (partonic) CFFs, one can extend the parametrization (5.119) in the whole kinematical region of the generalized Bjorken variable by allowing for a weak ξ -dependence of the normalization N -factors and phases, keeping however the M -factors ξ -independent. Equations (5.119) for unpolarized \mathcal{H}, \mathcal{E} and polarized $\tilde{\mathcal{H}}, \tilde{\mathcal{E}}$ GPDs are in agreement with relations stemming from derivative analyticity for corresponding scattering amplitudes A and \tilde{A} ,

$$\Re e \frac{A}{s} = \tan \left(\frac{\pi}{2} \frac{d}{d \ln s} \right) \Im m \frac{A}{s}, \quad \Re e \tilde{A} = \tan \left(\frac{\pi}{2} \frac{d}{d \ln s} \right) \Im m \tilde{A},$$

—even and odd, respectively, under crossing symmetry $s \leftrightarrow u$ [329, 330]. These are obtained from dispersion relations by approximating the amplitude with a simple Regge-pole form, $A \sim s^{\alpha_M}$, and resumming the Taylor expansion in logarithms of the energy s , see, e.g., [10].

5.4.3 One-loop corrections to twist-two CFFs

So far the analysis of the Compton amplitudes was carried out in Born approximation. For reliable phenomenological analyses of experimental observables, one has to know the magnitude of higher order effects in coupling constant. To match the two-loop evolution of GPDs, analyzed in full in Section 4, one has to complement it with one-loop corrections to hard coefficient functions.

The next-to-leading coefficient functions $C_{i(1)}^{a[\pm]}$ (5.55) have been found in a number of studies by computing the one-loop Feynman diagrams shown in Fig. 43. To simplify the presentation, let us extract the color factors and quark charges from them and split the coefficient functions into two terms, one of which entirely absorbs the renormalization group logarithm of the hard scale Q^2 ,

$$C_{i(1)}^{q[\pm]}(x, \xi, \eta; Q^2/\mu^2) \equiv C_F Q_q^2 \left[c_{i(1)}^{q[\pm]}(x, \xi, \eta) + \kappa_{i(1)}^{q[\pm]}(x, \xi, \eta) \ln(Q^2/\mu^2) \right], \quad (5.120)$$

$$C_{i(1)}^{g[\pm]}(x, \xi, \eta; Q^2/\mu^2) \equiv 2T_F \sum_q Q_q^2 \left[c_{i(1)}^{g[\pm]}(x, \xi, \eta) + \kappa_{i(1)}^{g[\pm]}(x, \xi, \eta) \ln(Q^2/\mu^2) \right]. \quad (5.121)$$

The index i runs here over two values in the even-parity sector $i = 1, L$ and it is $i = 1$ in the odd-parity one. One more value is obviously possible: $i = T$ corresponding to the gluon transversity, i.e., the maximal-helicity sector. The parameter $\mu^2 = \mu_{\overline{\text{MS}}}^2$ is the renormalization scale in the $\overline{\text{MS}}$ scheme. Varying it—normally within the range $Q^2/2 \leq \mu^2 \leq 2Q^2$ —one can achieve minimization of the one-loop corrections by choosing the optimal value. The reduced coefficient functions are summarized below for different sectors.

- Parity-even sector [315, 233, 316, 282]

$$\begin{aligned}
c_{1(1)}^{q[-]}(x, \eta, \xi) &= -\frac{9}{2} \frac{1}{\xi - x} - \frac{3(2x\xi - x^2 - \eta^2)}{2(\xi - x)(x^2 - \eta^2)} \ln \left(1 - \frac{x}{\xi}\right) + \frac{\xi^2 + x^2 - 2\eta^2}{2(\xi - x)(x^2 - \eta^2)} \ln^2 \left(1 - \frac{x}{\xi}\right) \\
&\quad + \frac{3x(\xi^2 - \eta^2)}{(\xi^2 - x^2)(x^2 - \eta^2)} \ln \left(1 - \frac{\eta}{\xi}\right) + \frac{x(\xi - \eta)(x^2 - 2\eta\xi - 2\eta^2 - \xi^2)}{2(\xi^2 - x^2)\eta(x^2 - \eta^2)} \ln^2 \left(1 - \frac{\eta}{\xi}\right) \\
&\quad + (\xi \leftrightarrow -\xi), \\
c_{1(1)}^{g[-]}(x, \eta, \xi) &= \frac{4\xi^2 - 4x\xi + x^2 - \eta^2}{2(x^2 - \eta^2)^2} \ln \left(1 - \frac{x}{\xi}\right) - \frac{2\xi^2 - 2x\xi + x^2 - \eta^2}{4(x^2 - \eta^2)^2} \ln^2 \left(1 - \frac{x}{\xi}\right) \\
&\quad + \frac{(\xi - \eta)(x^2 - 4\eta\xi - \eta^2)}{2\eta(x^2 - \eta^2)^2} \ln \left(1 - \frac{\eta}{\xi}\right) - \frac{(\xi - \eta)(x^2 - 2\eta\xi - \eta^2)}{4\eta(x^2 - \eta^2)^2} \ln^2 \left(1 - \frac{\eta}{\xi}\right) \\
&\quad + (\xi \leftrightarrow -\xi).
\end{aligned}$$

- Parity-odd sector [233, 316, 282]

$$\begin{aligned}
c_{1(1)}^{q[+]}(x, \eta, \xi) &= -\frac{9}{2} \frac{1}{\xi - x} + \frac{x^2 + 3\eta^2 - 2x\xi - 2\xi^2}{(\xi - x)(x^2 - \eta^2)} \ln \left(1 - \frac{x}{\xi}\right) + \frac{\xi^2 + x^2 - 2\eta^2}{2(\xi - x)(x^2 - \eta^2)} \ln^2 \left(1 - \frac{x}{\xi}\right) \\
&\quad + \frac{(\xi - \eta)(\xi^2 + 2x^2 + 3\eta\xi)}{(\xi^2 - x^2)(x^2 - \eta^2)} \ln \left(1 - \frac{\eta}{\xi}\right) - \frac{(\xi - \eta)(\xi^2 + x^2 + 2\eta\xi)}{2(\xi^2 - x^2)(x^2 - \eta^2)} \ln^2 \left(1 - \frac{\eta}{\xi}\right) \\
&\quad - (\xi \leftrightarrow -\xi), \\
c_{1(1)}^{[+]g}(x, \eta, \xi) &= -\frac{3x^2 + \eta^2 - 4x\xi}{2(x^2 - \eta^2)^2} \ln \left(1 - \frac{x}{\xi}\right) - \frac{2x\xi - x^2 - \eta^2}{4(x^2 - \eta^2)^2} \ln^2 \left(1 - \frac{x}{\xi}\right) \\
&\quad - \frac{2x(\xi - \eta)}{(x^2 - \eta^2)^2} \ln \left(1 - \frac{\eta}{\xi}\right) + \frac{x(\xi - \eta)}{2(x^2 - \eta^2)^2} \ln^2 \left(1 - \frac{\eta}{\xi}\right) - (\xi \leftrightarrow -\xi). \tag{5.122}
\end{aligned}$$

- Longitudinal sector [316]

$$\begin{aligned}
c_{L(1)}^{q[-]}(x, \eta, \xi) &= -\frac{2\xi}{(x^2 - \eta^2)} \ln \left(1 - \frac{x}{\xi}\right) + \frac{2x\xi}{\eta(x^2 - \eta^2)} \ln \left(1 - \frac{\eta}{\xi}\right) + (\xi \leftrightarrow -\xi), \\
c_{L(1)}^{g[-]}(x, \eta, \xi) &= \frac{2\xi(\xi - x)}{(x^2 - \eta^2)^2} \ln \left(1 - \frac{x}{\xi}\right) + \frac{\xi(x^2 - 2\eta\xi + \eta^2)}{\eta(x^2 - \eta^2)^2} \ln \left(1 - \frac{\eta}{\xi}\right) + (\xi \leftrightarrow -\xi).
\end{aligned}$$

- Maximal-helicity sector [73, 74]

$$c_{T(1)}^g(x, \eta, \xi) = -\frac{1}{x^2 - \eta^2} \left\{ 1 + \frac{\xi^2 - \eta^2}{\omega^2(x^2 - \eta^2)} \ln \frac{\xi^2 - x^2}{\xi^2 - \eta^2} \right\}. \tag{5.123}$$

The functions accompanying the logarithm of the ratio of the hard-to-renormalization scale are given by the convolution³⁷ of the leading order quark coefficient functions (5.33) with corresponding one-loop evolution kernels (4.37) from Section 4.4.1,

$$\kappa_{1(1)}^{a[\mp]}(x, \xi, \eta) \sim Q_q^{-2} \int_{-1}^1 dz C_{(0)}^{q[\mp]}(z, \xi) k^{qa, V/A} \left(\frac{z}{\eta}, \frac{x}{\eta} \right), \quad \text{with } a = q, g, \tag{5.124}$$

³⁷See the following Section 5.5 for details.

if the mixing is allowed, and have the following explicit form

$$\begin{aligned}\kappa_{1(1)}^{q[\pm]}(x, \xi, \eta) &= \frac{3}{2} \frac{1}{\xi - x} + \frac{\xi^2 + x^2 - 2\eta^2}{(\xi - x)(x^2 - \eta^2)} \ln \left(1 - \frac{x}{\xi} \right) \\ &\quad + \frac{x(\xi - \eta)(x^2 - 2\eta\xi - 2\eta^2 - \xi^2)}{(\xi^2 - x^2)\eta(x^2 - \eta^2)} \ln \left(1 - \frac{\eta}{\xi} \right) \pm (\xi \leftrightarrow -\xi),\end{aligned}\tag{5.125}$$

$$\begin{aligned}\kappa_{1(1)}^{g[-]}(x, \xi, \eta) &= -\frac{2\xi^2 - 2x\xi + x^2 - \eta^2}{2(x^2 - \eta^2)^2} \ln \left(1 - \frac{x}{\xi} \right) \\ &\quad - \frac{(\xi - \eta)(x^2 - 2\eta\xi - \eta^2)}{2\eta(x^2 - \eta^2)^2} \ln \left(1 - \frac{\eta}{\xi} \right) + (\xi \leftrightarrow -\xi),\end{aligned}\tag{5.126}$$

$$\kappa_{1(1)}^{g[+]}(x, \xi, \eta) = -\frac{2x\xi - x^2 - \eta^2}{2(x^2 - \eta^2)^2} \ln \left(1 - \frac{x}{\xi} \right) + \frac{x(\xi - \eta)}{(x^2 - \eta^2)^2} \ln \left(1 - \frac{\eta}{\xi} \right) - (\xi \leftrightarrow -\xi).\tag{5.127}$$

Other functions are zero

$$\kappa_{L(1)}^{q[-]}(x, \xi, \eta) = \kappa_{L(1)}^{g[-]}(x, \xi, \eta) = \kappa_{T(1)}^g(x, \xi, \eta) = 0.\tag{5.128}$$

Notice that in the real-photon limit $q_2^2 = 0$, relevant for DVCS, all singular logarithmic contributions vanish at least linearly in $(\xi - \eta)$, supporting the factorizability of the DVCS amplitude. Therefore, the DVCS coefficient functions are easily obtainable from the above expressions by setting $\eta = \xi$ there. Let us point out that recently one-loop coefficient functions due to heavy flavors propagating in loops were reported in Ref. [331].

In the following section, we will demonstrate a formalism to reconstruct the one-loop coefficient functions by means of conformal operator product expansion. It avoids explicit loop calculations and is based on known next-to-leading forward coefficient functions. The presentation will be rather technical and a practitioner who is interested in final results rather than the use of the QCD machinery to deduce them, can skip entirely the following Section 5.5.

5.5 Application of conformal operator product expansion

The next-to-leading order coefficient functions for off-forward Compton amplitudes were deduced in the previous section by an explicit calculation of perturbative one-loop diagrams. However, instead one could have used implications of the conformal symmetry and avoid any computations of loop integrals completely. To this end, let us note that in Section 4, we found that the off-forward evolution kernels at leading order of perturbation theory are defined entirely by the forward splitting functions. Or in other words, the off-forward kernels are diagonalized by conformal partial waves—conformal operators—and their eigenvalues are determined solely by the forward anomalous dimensions of operators without total derivatives. Thus, as we demonstrated in Section 4.7.2 one can unambiguously restore the off-forward evolution kernels from the forward ones. By the same token, as we will demonstrate in this section, one can reconstruct the off-forward coefficient functions.

As we explained before, the redefinition of conformal representations by shifting the scale dimensions of fields, given originally in terms of their canonical mass dimensions, by the anomalous ones, makes the theory respect conformal covariance. However, the effect of the running of the gauge coupling inevitably breaks the conformal symmetry. Therefore, supposing the existence of a nontrivial zero g^* of the β -function ($\beta(g^*) = 0$) a conformally covariant OPE can be proven to

exist even for interacting theory. Below we will shortly outline some of the points which are of relevance for our further discussion.

Instead of constructing the operator product expansion in terms of local Wilson operators, we can automatically take care of operators with total derivatives by expanding over the basis of conformal operators. Keeping the Lorentz indices open, the latter read for quarks

$$\mathbb{O}_{\mu_0 \mu_1 \dots \mu_k}^{qq} = \sum_{\ell=0}^k e_{k\ell}(j_q) \underset{\mu_0 \dots \mu_k}{\mathbf{S}} \bar{\psi} \gamma_{\mu_0} i \vec{\partial}_{\mu_1} \dots i \vec{\partial}_{\mu_\ell} i \overleftarrow{\partial}_{\mu_{\ell+1}} \dots i \overleftarrow{\partial}_{\mu_{k-\ell}} \psi, \quad (5.129)$$

where the expansion coefficient for a generic conformal spin j field is

$$e_{k\ell}(j) \equiv \frac{(-1)^{k-\ell}(4j+k-2)!(2j-1)!(2j+k-1)!}{(4j-2)!\ell!(k-\ell)!(k-\ell+2j-1)!(\ell+2j-1)!} \quad (5.130)$$

The descendants are obtained by acting with the step-up operators on the above operator

$$\mathbb{O}_{k;\mu_0 \mu_1 \dots \mu_l}^{qq} \equiv [\dots [[\mathbb{O}_{\mu_0 \mu_1 \dots \mu_k}^{qq}, \mathbb{P}_{\mu_{k+1}}], \mathbb{P}_{\mu_{k+2}}], \dots \mathbb{P}_{\mu_\ell}], \quad (5.131)$$

with l Lorentz indices, $(l-k)$ of which are attached to total derivatives. Contracting the open Lorentz indices with the light-like vectors n^μ we get the conventional definition of the quark conformal operator

$$\mathbb{O}_{kl}^{qq} \equiv n^{\mu_0} n^{\mu_1} \dots n^{\mu_k} \mathbb{O}_{k;\mu_0 \mu_1 \dots \mu_l}^{qq}. \quad (5.132)$$

We will apply the expansion in terms of the conformal operators to the product of two electromagnetic currents. As can be seen from our results in Section 5.2.1, for the leading twist contribution only the transverse components of the Lorentz indices do contribute. The other tensor structures are suppressed by at least one inverse power of the hard scale. Thus the expansion of a product of two electromagnetic currents takes the form

$$j_\perp(z) j_\perp(0) = \sum_{k=0}^{\infty} \left(\frac{1}{z^2} \right)^{d_j - t_k / 2} \sum_{l=k}^{\infty} c_{kl} (z^-)^{l+2s_q} \mathbb{O}_{kl}^{qq}(0), \quad (5.133)$$

where $d_j = 3$ is the mass dimensional of the electromagnetic current, $t_k = d_k - k - 2s_q = 2$ is the twist of the composite operator \mathbb{O}_{kk}^{qq} and $s_q = 1/2$ is the spin of the quark. Actually, one can resum the infinite series with respect to l . To this end one has to deduce a recursion relation for the expansion coefficients c_{kl} . Acting on the left-hand side of Eq. (5.133) with the step-down conformal boost operator, we get

$$\begin{aligned} [j_\perp(z) j_\perp(0), \mathbb{K}^-] &= i (2d_j z^- - z^2 \partial^- + 2z^- z^\mu \partial_\mu) j_\perp(z) j_\perp(0) \\ &\simeq 2i \sum_{k=0}^{\infty} \left(\frac{1}{z^2} \right)^{d_j - t_k / 2} \sum_{l=k}^{\infty} (j_k + l - k) c_{kl} (z^-)^{l+2s_q+1} \mathbb{O}_{kl}^{qq}. \end{aligned} \quad (5.134)$$

While applying \mathbb{K}^- on the right-hand side of the equality (5.133), we find

$$[j_\perp(z) j_\perp(0), \mathbb{K}^-] \simeq -2 \sum_{k=0}^{\infty} \left(\frac{1}{z^2} \right)^{d_j - t_k / 2} \sum_{l=k}^{\infty} (l - k + 1) (2j_k + l - k) c_{kl+1} (z^-)^{l+2s_q+1} \mathbb{O}_{kl}^{qq}, \quad (5.135)$$

where we have used the covariant transformation law for conformal operators established in Eq. (4.135). Here $j_k = 2j_q + k$ is the conformal spin of the conformal operator \mathbb{O}_{kl}^{qq} . By comparing both sides of the equation, we can get the following recursion relation

$$c_{k,l+1} = -i \frac{(j_k + l - k)}{(l - k + 1)(2j_k + l - k)} c_{kl},$$

the solution to which is given by

$$c_{kl} = (-i)^{l-k} \frac{\Gamma(j_k + l - k) \Gamma(2j_k)}{(l - k)! \Gamma(2j_k + l - k) \Gamma(j_k)} c_{kk}. \quad (5.136)$$

Substituting these coefficients into (5.133) one can resum contributions of total derivatives, $\mathbb{O}_{kl}^{qq} = (i\partial^+)^{l-k} \mathbb{O}_{kk}^{qq}$, with the result

$$j_\perp(z) j_\perp(0) = \sum_{k=0}^{\infty} c_{kk} \frac{\Gamma(2j_k)}{\Gamma^2(j_k)} \left(\frac{1}{z^2}\right)^{d_j - t_k/2} (z^-)^{k+2s_q} \int_0^1 du (u\bar{u})^{j_k-1} \mathbb{O}_{kk}^{qq}(uz^-), \quad (5.137)$$

which constitutes the conformal operator product expansion [332]. Note that the right-hand side can be expressed in terms of the confluent hypergeometric function ${}_1F_1$. Now sandwiching this expression between off-forward hadronic states and transforming it into the momentum space, we find the Compton amplitudes

$$\begin{aligned} T_{\perp\perp} &= i \int d^4 z e^{iq\cdot z + i\Delta\cdot z/2} \langle p_2 | T \{ j_\perp(z) j_\perp(0) \} | p_1 \rangle \\ &= \sum_{k=0}^{\infty} c'_k \left(\frac{\mu^2}{Q^2}\right)^{2-d_j+t_k/2} \int_0^1 du (u\bar{u})^{j_k-1} \left(1 - \frac{\eta}{\xi}(1-2u)\right)^{d_j - k - t_k/2 - 3} \xi^{-k-1} \mathbb{F}_k^q(\eta), \end{aligned} \quad (5.138)$$

as an expansion in terms of the Gegenbauer moments of the quark GPDs (4.243). Here μ^2 is the normalization scale. So far the analysis was performed in noninteracting theory, i.e., in tree approximation. By switching on strong interactions, the conformal spin and the canonical dimensions get shifted by anomalous dimensions, since the canonical dimension of conformal operators \mathbb{O}_{kk}^{qq} changes accordingly (cf. Sections 4.9.2 and 4.10.2)

$$d_k^{\text{can}} \rightarrow d_k = k + 2d_q + \gamma_k^{qq}(\alpha_s).$$

The expansion coefficients c'_k are promoted to functions of the coupling constant α_s which are related to the Wilson coefficients of deeply inelastic scattering. Apart from already present at tree level quark operator matrix elements, the amplitude also acquires gluon operators starting from one-loop order. From the above result for the Compton amplitude we can read off the expression for the Compton form factors. For instance, for the quark contribution to the Compton form factor $\mathcal{F}_1(\xi, \eta)$ one immediately finds

$$\begin{aligned} \mathcal{F}_1(\xi, \eta) &= \sum_k \sigma_k c_k^{\text{DIS}}(\alpha_s) \frac{2^{k+2} B(k+1, k+2)}{B(k+2 + \gamma_k^{qq}/2, k+2 + \gamma_k^{qq}/2)} \left(\frac{\mu^2}{Q^2}\right)^{\gamma_k/2} \\ &\times \int_0^1 du (u\bar{u})^{k+1+\gamma_k^{qq}/2} \left(1 - \frac{\eta}{\xi}(1-2u)\right)^{-k-1-\gamma_k^{qq}/2} \xi^{-k-1} \widehat{\mathbb{F}}_k^q(\eta), \end{aligned} \quad (5.139)$$

where $\sigma_k \equiv \frac{1}{2}[1+(-1)^{k+1}]$, $B(a, b) = \Gamma(a)\Gamma(b)/\Gamma(a+b)$ is the Euler beta function and $\widehat{\mathbb{F}}_k^q$ define the conformally covariant moments (4.213), which renormalize autonomously at the conformal point $\beta(g^*) = 0$. Due to the normalization condition (4.227), these conformally covariant operators coincide with ordinary conformal operators at low normalization point μ_0 , i.e., $\widehat{\mathbb{F}}_k^q(\mu_0) = \mathbb{F}_k^q(\mu_0)$. Therefore, below we will display all equations at μ_0 so that to avoid the hat-symbol on top of moments. Analogously in the parity-odd Compton form factor $\widetilde{\mathcal{F}}_1$, one replaces σ_k by σ_{k+1} and \mathbb{F} by $\widetilde{\mathbb{F}}$. Also one trades the DIS unpolarized Wilson coefficient c_k^{DIS} by the one of polarized scattering. Obviously, at leading order, $\gamma_k^{qq} = 0$ and $c_k = 1$. This reproduces the normalization accepted before. Obviously, in the forward case it reduces to the conventional expansion of the structure function in the unphysical region $x_B > 1$,

$$\mathcal{F}_1(\xi = x_B, \eta = 0) = F_1(x_B) = \sum_k \frac{\sigma_k}{x_B^{k+1}} \langle p | \bar{\psi} \gamma^+(i\partial^+)^k \psi(0) | p \rangle. \quad (5.140)$$

where we limited the perturbative expansion to leading order only.

Let us demonstrate how to use the conformal operator product expansion in order to find one-loop off-forward coefficient functions [252, 233], which were computed above making use of the standard Feynman rule formalism. For demonstration purposes, let us use the odd-parity gluon sector. By expanding the prediction of the conformal operator product expansion (5.139) to first order in the strong coupling constant

$$\widetilde{\mathcal{F}}_1(\xi, \eta) = \widetilde{\mathcal{F}}_1^{(0)}(\xi, \eta) + \frac{\alpha_s}{2\pi} \widetilde{\mathcal{F}}_1^{(1)}(\xi, \eta) + \mathcal{O}(\alpha_s^2), \quad (5.141)$$

we obtain for the next-to-leading correction in this sector

$$\begin{aligned} \widetilde{\mathcal{F}}_1^{(1)}(\xi, \eta) &= \sum_q Q_q^2 \sum_k \frac{\sigma_{k+1}}{N_f} \left\{ \widetilde{c}_{(1)k}^{qg} - \frac{1}{2} \gamma_{(0)k}^{qg;A} \ln \left(\frac{Q^2}{\mu^2} \right) + \frac{1}{2} \gamma_{(0)k}^{qg;A} \frac{d}{d\varrho} \right\} \Big|_{\varrho=0} \\ &\times \frac{2^k B(k+1, k+2)}{B(k+2+\varrho, k+2+\varrho)} \int_0^1 du (u\bar{u})^{k+1+\varrho} \left(1 - \frac{\eta}{\xi} (1-2u) \right)^{-k-1-\varrho} \xi^{-k-1} \widetilde{\mathbb{F}}_k^g(\eta), \end{aligned} \quad (5.142)$$

with conformally covariant moments of the gluon GPD coinciding with conventional conformal moments at low normalization point were defined in Eq. (4.284). Note that the factor 4 in $\widetilde{\mathbb{F}}_k^g$ (4.284) explains the relative normalization of Eqs. (5.139) and (5.142). The forward Wilson coefficient function in Eq. (5.142) is [98, 333]

$$\widetilde{c}_{(1)k}^{qg} = \frac{6}{k} \int_0^1 dx x^j 2T_F N_f \left[(2x-1) \ln \frac{1-x}{x} + 3 - 4x \right] = \frac{1}{2} \gamma_{(0)k}^{qg;A} [\psi(k+1) - \psi(1) + 1]. \quad (5.143)$$

Here we have multiplied the forward coefficient function with the factor $6/k$ taking into account the difference in the normalization of Wilson and conformal operators (see Eq. (4.166)). The above prediction from the operator product expansion consists of two terms,

$$\widetilde{\mathcal{F}}_1^{(1)}(\xi, \eta) = \widetilde{\mathcal{F}}_1^{(1),\text{ev}}(\xi, \eta) + \widetilde{\mathcal{F}}_1^{(1),\text{cf}}(\xi, \eta), \quad (5.144)$$

—the correction due to renormalization group evolution of conformal operators $\widetilde{\mathcal{F}}_1^{(1),\text{ev}}$ and the next-to-leading order correction to the coefficient function $\widetilde{\mathcal{F}}_1^{(1),\text{cf}}$. While the second one is the

quantity in question, the former was already found in our earlier discussion of the evolution of GPDs. It reads

$$\tilde{\mathcal{F}}_1^{(1),\text{ev}}(\xi, \eta) = \sum_q C_{(0)}^{q[+]}(x, \xi) \otimes \frac{1}{8N_f} \left\{ \Phi_{(1)}^{qg;A}(x, y, \eta) - K_{(0)}^{qg;A}(x, y, \eta) \ln \left(\frac{Q^2}{\mu^2} \right) \right\} \otimes \tilde{F}^g(y, \eta). \quad (5.145)$$

Here to simplify formulas, we used the convention for the convolution

$$\tau_1(x, y) \otimes \tau_2(y, z) \equiv \int dy \tau_1(x, y) \tau_2(y, z).$$

The correction to the eigenfunction of the next-to-leading evolution equation reads

$$\Phi_{(1)}^{qg;A}(x, y, \eta) = (1 - \text{diag})S(x, z) \otimes K_{(0)}^{qg;A}(z, y, \eta). \quad (5.146)$$

It reproduces the result for conformal operators when one form Gegenbauer moments with it (see Eqs. (4.196) and (4.224)). The shift operator is defined as

$$S(x, y) \otimes w(y|\nu)C_k^\nu(x) \equiv \frac{d}{d\varrho} \Big|_{\varrho=0} w(y|\nu + \varrho)C_k^{\nu+\varrho}(x),$$

while the subtraction of the diagonal contribution in the basis of conformal operators yields for a test function $\tau(x, u)$

$$C_k^\nu(x) \otimes (1 - \text{diag})\tau(x, y) = \sum_{l=0}^k (\tau_{kl} - \tau_{kk}\delta_{kl}) C_k^\nu(y).$$

Expanding Eq. (5.145) in conformal partial waves, we find

$$\begin{aligned} \tilde{\mathcal{F}}_1^{(1),\text{ev}}(\xi, \eta) &= \sum_q Q_q^2 \sum_k \frac{\sigma_{k+1}}{2N_f} \gamma_{(0)k}^{qg;A} \left\{ \frac{d}{d\varrho} - \ln \left(\frac{Q^2}{\mu^2} \right) \right\} \Big|_{\varrho=0} \\ &\times \frac{2^k B(k+1, k+2)}{B(k+2+\varrho, k+2+\varrho)} \int_0^1 du (u\bar{u})^{k+1+\varrho} \left(1 - \frac{\eta}{\xi} (1-2u) \right)^{-k-1} \xi^{-k-1} \tilde{\mathbb{F}}_k^g(\eta). \end{aligned} \quad (5.147)$$

Using Eq. (5.144) to solve for $\mathcal{F}_1^{(1),\text{cf}}$ one finds from the difference of the conformal operator product expansion (5.142) and next-to-leading evolution corrections $\tilde{\mathcal{F}}_1^{(1),\text{ev}}$ the one-loop correction to the coefficient function

$$\begin{aligned} \tilde{\mathcal{F}}_1^{(1),\text{cf}}(\xi, \eta) &= C_{1(1)}^{g[+]}(x, \xi, \eta; 1) \otimes \tilde{F}^g(x, \eta) = \sum_q Q_q^2 \sum_k \frac{\sigma_{k+1}}{N_f} \left\{ \tilde{c}_{(1)k}^{qg} + \frac{1}{2} \gamma_{(0)k}^{qg;A} \frac{d}{d\varrho} \right\} \Big|_{\varrho=0} \\ &\times \frac{2^k B(k+1, k+2)}{B(k+2, k+2)} \int_0^1 du (u\bar{u})^{k+1} \left(1 - \frac{\eta}{\xi} (1-2u) \right)^{-k-1-\varrho} \xi^{-k-1} \tilde{\mathbb{F}}_k^g. \end{aligned} \quad (5.148)$$

The resummation of this series is straightforward and gives the next-to-leading coefficient function in the form of a convolution³⁸,

$$C_{1(1)}^{g[+]}(y, \xi, \eta; 1) = \sum_q Q_q^2 \left\{ \frac{1 - \ln \left(1 - \frac{x}{\xi} \right)}{\xi - x - i0} + \frac{1 - \ln \left(1 + \frac{x}{\xi} \right)}{\xi + x - i0} \right\} \otimes \frac{1}{8N_f} K_{(0)}^{qg;A}(x, y, \eta). \quad (5.149)$$

Evaluating the integrals we indeed reproduce the result for the off-forward coefficient function (5.122), computed before by means of Feynman diagrams. Presently we deduced it without any loop-integrals calculation but merely relying on the conformal symmetry.

³⁸The presence of the logarithm in the coefficient function can be easily understood since $\frac{\ln x}{x} = -\frac{d}{d\varrho}|_{\varrho=0} x^{-1-\varrho}$.

5.6 Target mass corrections

The leading-twist approximation to hard processes in QCD is affected both by radiative corrections in the strong coupling constant and higher twist power suppressed contributions. The former were addressed in preceding sections. In case when the energy scale of the reaction turns out to be rather low, $Q^2 \sim 2 - 4 \text{ GeV}^2$, one has to take care of power suppressed effects since they modify significantly the scaling behavior of corresponding cross sections. Power corrections can be divided into two classes according to their origin: dynamical and kinematical. The dynamical corrections reflect multiparton correlations inside hadrons [334], i.e., new information not contained in the leading-twist distributions. The kinematical corrections include the power-suppressed contributions which can be expressed in terms of the twist-two functions. We already discussed the Wandzura-Wilczek type contributions [314] arising from separation of composite operators into components with definite symmetry properties with respect to the Lorentz group. Another prominent class accommodates target mass corrections [335]. They stem from the subtraction of traces in Wilson operators possessing a well defined geometrical twist.

In this section, we describe a formalism for resummation of the target mass corrections for the virtual Compton scattering amplitude. Since the present day studies of DVCS involve momentum transfers of the order of a few GeV, the ratio of the nucleon mass to the momentum transfer can produce corrections as large as 30% to the leading twist massless results. Despite being suppressed by an extra power of the hard momentum scale, the target mass corrections can still compete at available energies with twist-three effects. There exists a standard formalism [335] for resumming target mass corrections in deeply inelastic scattering (see also [336] for an earlier first discussion of the topic). However, it is not readily applicable to off-forward processes since new towers of Lorentz structures develop in matrix elements of local operators and they cannot be handled in a fashion proposed in [335]. A discussion of mass effects in exclusive processes with simpler kinematics of distribution amplitudes can be found in Ref. [337].

To resum infinite series of mass corrections, it is again more efficient to use double distributions $h^q(\beta, \alpha, \Delta^2)$ from Section 3.8.3 rather than GPDs $F^q(x, \eta, \Delta^2)$ [339]. This allows one to represent all-order results in a compact fashion. Once this is accomplished, one can use the inverse Radon transformation (3.238) to express DDs in terms of GPDs. Regretfully, this step can hardly be used for successful phenomenological applications. However, each term in the expansion of the resummed expressions in powers of $(M^2/Q^2)^j$ can be straightforwardly cast in the conventional language of GPDs. The formalism is described in the following two sections, and as a demonstration, we resum target mass effects resulting from trace terms of twist-two operators. The restriction to leading twist approximation in the Compton amplitude leads to the violation of electromagnetic gauge invariance as we described at length in Section 5.2. The problem of resumming mass effects stemming from higher twist operator matrix elements was not addressed in the literature so far. Therefore, it might be premature to use presently derived results for numerical evaluation of the magnitude of hadronic mass effects in physical cross sections.

5.6.1 Twist decomposition and harmonic polynomials

The goal of the present section is to construct the operator product expansion for the off-forward Compton amplitude (5.2) taking the entire tower of target mass corrections into account. Since the latter originate from the trace subtraction in the definition of the local Wilson operators (3.107), the effects will be thus entirely kinematical in nature. Hence, we can neglect dynamical higher twists stemming from multiparticle operators and restrict our attention to two-particle

contributions only. In this approximation, the Fourier transformed two-photon amplitude is given by

$$T^{\mu\nu} = \frac{1}{\pi^2} \sum_q Q_q^2 \int d^4 z \frac{z_\sigma}{[-z^2 + i0]^2} \langle p_2 | \cos(z \cdot q) S^{\mu\nu;\rho\sigma} \mathcal{O}_\rho^{qq}(-z/2, z/2) + \sin(z \cdot q) \varepsilon^{\mu\nu\rho\sigma} \tilde{\mathcal{O}}_\rho^{qq}(-z/2, z/2) | p_1 \rangle, \quad (5.150)$$

where \mathcal{O}_ρ^{qq} and $\tilde{\mathcal{O}}_\rho^{qq}$ are defined in Eqs. (3.10) and (3.11), respectively. Presently, we will keep the separation z^μ between the quark fields non-light-like.

To solve the problem, we have to extract the increasing-twist traceless components from the contributing operators. Such a procedure was designed in Section 5.3.1 for light-like interquark separations $z^2 = 0$. Since the latter condition is lifted now, the twist separation has to be modified. The general strategy is the following. Since a transparent formalism can be devised in terms of local Wilson operators, we expand first the non-local operators \mathcal{O}_ρ^{qq} and $\tilde{\mathcal{O}}_\rho^{qq}$ in Taylor series, e.g., for the even parity sector,

$$\mathcal{O}_\rho^{qq}(-z, z) = \sum_{j=0}^{\infty} \frac{(-i)^j}{j!} z^{\mu_1} \dots z^{\mu_j} \mathcal{O}_{\rho\mu_1\dots\mu_j}^{qq}(0) \equiv \sum_{j=0}^{\infty} \frac{(-i)^j}{j!} \mathcal{O}_{\rho;j}^{qq}(0), \quad (5.151)$$

with

$$\mathcal{O}_{\rho\mu_1\dots\mu_j}^{qq}(0) = \bar{\psi}_q \gamma_\rho i \vec{\mathcal{D}}_{\mu_1} \dots i \vec{\mathcal{D}}_{\mu_j} \psi_q. \quad (5.152)$$

In terms of local operators, it is straightforward to symmetrize and antisymmetrize the open Lorentz index ρ with the rest, as we already demonstrated in Section 5.3.1. Therefore, we can decompose the original operator $\mathcal{O}_\rho^{qq}(-z, z)$ into its symmetric and antisymmetric components,

$$\mathcal{O}_\rho^{qq}(-z, z) = \mathcal{O}_\rho^{qq,\text{sym}}(-z, z) + \mathcal{O}_\rho^{qq,\text{asym}}(-z, z). \quad (5.153)$$

When expanded in Taylor series of the type (5.151), they generate a tower of Wilson operators (cf. (3.107) and (5.65))

$$\mathcal{O}_{\rho;j}^{qq,\text{sym}} = z^{\mu_1} \dots z^{\mu_j} \bar{\psi}_q \gamma_{\{\rho} i \vec{\mathcal{D}}_{\mu_1} \dots i \vec{\mathcal{D}}_{\mu_j\}} \psi_q, \quad (5.154)$$

$$\mathcal{O}_{\rho;j}^{qq,\text{asym}} = \frac{2j}{j+1} z^{\mu_1} \dots z^{\mu_j} \bar{\psi}_q \gamma_{[\rho} i \vec{\mathcal{D}}_{\{\mu_1} \dots i \vec{\mathcal{D}}_{\mu_j\}} \psi_q. \quad (5.155)$$

The curly $\{\dots\}$ and square $[\dots]$ brackets denote the symmetrization and antisymmetrization of the corresponding Lorentz indices (including the combinatoric factors), respectively. Notice that the symmetrization is performed without the trace subtraction. Obviously, if one neglects dynamical twist-four and higher effects, one has $z^\rho \mathcal{O}_\rho^{qq}(-z, z) = z^\rho \mathcal{O}_\rho^{qq,\text{sym}}(-z, z)$ and the same holds true for local operators. The symmetric Wilson operators can be concisely represented as

$$\mathcal{O}_{\rho;j}^{qq,\text{sym}} = \frac{1}{j+1} \frac{\partial}{\partial z^\rho} z^\sigma \mathcal{O}_{\sigma;j}^{qq}, \quad \mathcal{O}_{\rho;j}^{qq} \equiv z^{\mu_1} \dots z^{\mu_j} \mathcal{O}_{\rho\mu_1\dots\mu_j}^{qq}. \quad (5.156)$$

The same formulas are valid in the axial sector $\tilde{\mathcal{O}}_\rho^{qq}$.

As a next step, we subtract traces from $\mathcal{O}_\rho^{qq,\text{sym}}$ and $\mathcal{O}_\rho^{qq,\text{asym}}$, thus rewriting the decomposition (5.153) in the form

$$\mathcal{O}_\rho^{qq}(-z, z) = \mathcal{R}_\rho^{2,qq}(-z, z) + \mathcal{R}_\rho^{3,qq}(-z, z) + \mathcal{R}_\rho^{r,qq}(-z, z), \quad (5.157)$$

which then gives definite twist-two $\mathcal{R}_\rho^{2,qq}$ and twist-three $\mathcal{R}_\rho^{3,qq}$ operators. Even higher twist operators are encoded in $\mathcal{R}_\rho^{r,qq}$. A systematic construction of traceless operators can be effectively achieved making use of the concept of the so-called harmonic polynomials [340]. The construction of harmonic polynomials goes as follows. A rank- j (not necessarily symmetric and definitely not traceless) tensor $T_{\mu_1 \dots \mu_j}$ is contracted first with j four-vectors z^μ ,

$$T_j(z) \equiv z^{\mu_1} \dots z^{\mu_j} T_{\mu_1 \dots \mu_j}. \quad (5.158)$$

The traceless tensor $\bar{T}_{\mu_1 \dots \mu_j}$

$$\bar{T}_j(z) = z^{\mu_1} \dots z^{\mu_j} \bar{T}_{\mu_1 \dots \mu_j} = z^{\mu_1} \dots z^{\mu_j} \sum_{\mu_1 \dots \mu_j} \mathbf{S} T_{\mu_1 \dots \mu_j}, \quad (5.159)$$

is built from (5.158) by means of the operation \mathbf{S} introduced in Section 3.1. However, so far we did not have its algebraic definition. This is accomplished by noticing that $\bar{T}_j(z)$ satisfies the condition [340]

$$\square \bar{T}_j(z) = 0, \quad \square \equiv \frac{\partial}{\partial z^\mu} \frac{\partial}{\partial z_\mu}. \quad (5.160)$$

Then, the traceless and symmetric tensor $\bar{T}_{\mu_1 \dots \mu_j}$ can be represented as a polynomial H_j of the j -th order in the variable $z^2 \square$ acting on $T_j(z)$

$$\bar{T}_j(z) = H^j(z^2, \square) T_j(z). \quad (5.161)$$

Substituting (5.161) into (5.159) one finds the explicit expression for the polynomials [340, 230, 338]

$$H^j(z^2, \square) = \sum_{k=0}^{[j/2]} \frac{\Gamma(j-k+1)}{k! \Gamma(j+1)} \left(-\frac{z^2 \square}{4} \right)^k, \quad (5.162)$$

which are dubbed harmonic polynomials.

For the case at hand, the tensor $T_{\mu_1 \dots \mu_j}$ is given by the local Wilson operator (5.152). It is important to realize that the derivatives $\partial/\partial z^\mu$ in Eq. (5.161) act on the coordinates z^μ which are contracted with the tensor indices of the operator in question and not on the quark fields³⁹. Compared to the example (5.158), the operators $\mathcal{O}_{\rho \mu_1 \dots \mu_j}^{qq}$ possess an open Lorentz index ρ . Therefore, the equation defining the harmonic polynomials has to be complemented by yet another one. The tracelessness condition now reads

$$\square \mathcal{R}_{\rho;j}^{\tau,qq} = 0, \quad \frac{\partial}{\partial z_\rho} \mathcal{R}_{\rho;j}^{\tau,qq} = 0, \quad (5.163)$$

for each twist $\tau = 2, 3$. Straightforward algebra yields the decomposition (cf. (5.64))

$$\mathcal{O}_{\rho;j}^{qq} = \mathcal{R}_{\rho;j}^{2,qq} + \frac{2j}{j+1} \mathcal{R}_{\rho;j}^{3,qq} + \mathcal{R}_{\rho;j}^{r,qq}, \quad (5.164)$$

with the traceless twist-two and -three operators [338, 339]

$$\mathcal{R}_{\rho;j}^{2,qq} = \frac{1}{j+1} \frac{\partial}{\partial z^\rho} H^{j+1}(z^2, \square) z^\sigma \mathcal{O}_{\sigma;j}^{qq}, \quad j \geq 0, \quad (5.165)$$

$$\mathcal{R}_{\rho;j}^{3,qq} = \frac{1}{2j} \left[g_{\rho\sigma} z^\mu \frac{\partial}{\partial z^\mu} - z_\sigma \frac{\partial}{\partial z^\rho} \right] \left[g^{\sigma\tau} - \frac{1}{j+1} z^\sigma \frac{\partial}{\partial z_\tau} \right] H^j(z^2, \square) \mathcal{O}_{\tau;j}^{qq}, \quad j \geq 1, \quad (5.166)$$

³⁹This is, by the way, the reason that we write the derivatives as $\partial/\partial z^\mu$ rather than ∂_μ .

and the remainder being

$$\begin{aligned}\mathcal{R}_{\rho;j}^{r,qq} = & \frac{1}{j+1} \left\{ \frac{\partial}{\partial z^\rho} [1 - H^{j+1}(z^2, \square)] z^\sigma + \left[g_\rho^\sigma z^\mu \frac{\partial}{\partial z^\mu} - z^\sigma \frac{\partial}{\partial z^\rho} \right] [1 - H^j(z^2, \square)] \right. \\ & \left. + \frac{1}{j+1} \left[z_\rho z^\mu \frac{\partial}{\partial z^\mu} - z^2 \frac{\partial}{\partial z^\rho} \right] \frac{\partial}{\partial z_\sigma} H^j(z^2, \square) \right\} \mathcal{O}_{\sigma;j}^{qq}.\end{aligned}$$

It is an easy task to check that the operators $\mathcal{R}_{\rho;j}^{\tau,qq}$ ($\tau = 2, 3$) are indeed traceless. To this end, one uses

$$\square H^j(z^2, \square) \mathcal{O}_{\mu;j}^{qq} = 0$$

and the Euler theorem

$$z^\nu \frac{\partial}{\partial z^\nu} \frac{\partial}{\partial z_\mu} H^j(z^2, \square) \mathcal{O}_{\mu;j}^{qq} = (j-1) \frac{\partial}{\partial z_\mu} H^j(z^2, \square) \mathcal{O}_{\mu;j}^{qq}.$$

When we set $z^2 = 0$ in these equations, we reproduce the earlier results given in Eqs. (3.107) and (5.65). The operator $\mathcal{R}_{\rho;j}^{r,qq}$ generates effects proportional to the total derivative squared ∂^2 as well as multiparticle operators

$$\mathcal{R}_{\rho;j}^{r,qq} \sim -\partial^2 \mathcal{R}_{\rho;j}^{2,qq} + \text{multiparticle operators}.$$

The latter are not included into our consideration as we pointed out at the beginning of this section. When $\mathcal{R}_{\rho;j}^{r,qq}$ is sandwiched between states with different momenta, the total derivative term produces contributions proportional to the momentum transfer squared Δ^2 . Limiting our present analysis to the situation $M^2 \gg |\Delta^2|$, with M^2 being the hadron mass, we will also neglect the latter in what follows (see, however, Appendix L).

5.6.2 Spin-zero target

After these preliminary remarks, let us turn to the discussion of the general framework for the resummation of kinematical mass corrections. Up to now, the problem was addressed at leading twist only [289]. Unfortunately, as we described in detail in Section 5.2.1, this approximation violates the electromagnetic gauge invariance. Since the target mass corrections stemming from higher twist terms are not available, we restrict our present consideration to the leading twist sectors only. The major steps in performing the resummation are: parametrization of off-forward matrix elements of symmetric local operators in terms of moments of DDs, subtraction of traces using the harmonic projectors H^j , subsequent Fourier transformation to the momentum space and, finally, resummation of infinite series.

To illustrate the main features of the formalism, we consider a spinless target. As before, to leading twist accuracy only matrix elements of the parity even operators are relevant in this case. To evaluate them, we perform as a first step the form factor decomposition of the symmetric quark operator as follows

$$\langle p_2 | \mathcal{O}_{\rho\mu_1 \dots \mu_j}^{qq,\text{sym}} | p_1 \rangle = p_{\{\rho} p_{\mu_1} \dots p_{\mu_j\}} H_{j+1,0}^q + \dots + \Delta_{\{\rho} \Delta_{\mu_1} \dots \Delta_{\mu_j\}} H_{j+1,j+1}^q + \dots , \quad (5.167)$$

where $\{\dots\}$ denotes as usual the symmetrization. The ellipsis stands for terms containing the metric tensor, which disappear when we subsequently apply the harmonic polynomial H^j to this

expression. After the projection via Eq. (5.165), one gets

$$\begin{aligned}\langle p_2 | \mathcal{R}_{\rho;j}^{2,qq} | p_1 \rangle &= \frac{1}{j+1} \partial_\rho H^{j+1}(z^2, \square) \sum_{k=0}^{j+1} (z \cdot p)^{j+1-k} (z \cdot \Delta)^k H_{j+1,k}^q \\ &= z_{\mu_1} \dots z_{\mu_j} \underset{\rho\mu_1 \dots \mu_j}{\mathbf{S}} \left\{ p_\rho p_{\mu_1} \dots p_{\mu_j} H_{j+1,0}^q + \dots + \Delta_\rho \Delta_{\mu_1} \dots \Delta_{\mu_j} H_{j+1,j+1}^q \right\}.\end{aligned}\quad (5.168)$$

The first line gives a compact expression for the subtracted operator, which is extremely convenient for further derivations, and is the basis of the formalism.

On the other hand, we can project out the twist-two operator from Eq. (5.167) by contracting all Lorentz indices with the light-like vector n_μ . After such a projection, the trace terms disappear. This observation suggests that the coefficients $H_{j+1,k}^q$ in front of the Lorentz tensors are related to the reduced matrix elements of the light-cone operators and can be represented in terms of the moments of conventional leading twist GPDs or DDs via (cf. Eq. (3.231))

$$H_{j,k}^q = \frac{1}{k!} \frac{\partial^k}{\partial \eta^k} \Big|_{\eta=0} \int_{-1}^1 dx \ x^{j-1} H^q(x, \eta) = \binom{j}{k} \int_{\Omega} d\beta d\alpha \ \beta^{j-k} \alpha^k h^q(\beta, \alpha) \quad (5.169)$$

where $0 \leq k \leq j$, $1 \leq j$. Consequently, the parametrizations⁴⁰ of the matrix element of the non-local symmetric operator $\mathcal{O}_\rho^{qq,\text{sym}}$ and the light-ray operator $\mathcal{R}_\rho^{2,qq}$ coincides up to terms proportional to z_ρ , Δ_ρ^\perp or z^2 :

$$\langle p_2 | \mathcal{O}_\rho^{qq,\text{sym}}(-z, z) | p_1 \rangle = \int_{\Omega} d\beta d\alpha \ h^q(\beta, \alpha) \mathcal{P}_\rho e^{-iz \cdot \mathcal{P}} + \dots, \quad (5.170)$$

where $\mathcal{P}_\mu \equiv \beta p_\mu + \alpha \Delta_\mu$.

Now, it is easy to perform the resummation of matrix elements of traceless local operators. Substitution of Eq. (5.169) into Eq. (5.168) yields

$$\langle p_2 | \mathcal{R}_{\rho;j}^{2,qq} | p_1 \rangle = \int_{\Omega} d\beta d\alpha \ h^q(\beta, \alpha) \frac{1}{j+1} \partial_\rho H^{j+1}(z^2, \square) (z \cdot \mathcal{P})^{j+1}. \quad (5.171)$$

The action of the harmonic polynomials on the scalar product standing to its right generates conventional Chebyshev polynomials (4.254), which form an irreducible representation of the orthogonal group $SO(4)$ [340], i.e., the Euclidean Lorentz group,

$$H^j(z^2, \square) (z \cdot \mathcal{P})^j = \left(\frac{z^2 \mathcal{P}^2}{4} \right)^{j/2} U_j \left(\frac{z \cdot \mathcal{P}}{\sqrt{z^2 \mathcal{P}^2}} \right). \quad (5.172)$$

Since a typical contribution of twist-two Wilson operators to the Compton amplitude (5.150) has the form

$$\int d^4 z e^{iz \cdot q} \frac{z_\sigma}{[-z^2]^k} \langle p_2 | \mathcal{R}_{\rho;j}^{2,qq} | p_1 \rangle = \langle p_2 | \mathcal{R}_{\rho\mu_1 \dots \mu_j}^{2,qq} | p_1 \rangle \int d^4 z e^{iz \cdot q} \frac{z_\sigma z_{\mu_1} \dots z_{\mu_j}}{[-z^2]^k},$$

the Fourier transformation can be done using the following formula

$$\int d^4 z e^{iz \cdot q} \frac{z_{\mu_1} \dots z_{\mu_j}}{[-z^2]^k} = (-i)^{j+1} 2^{4-2k+j} \pi^2 \frac{\Gamma(2-k+j)}{\Gamma(k)} \frac{q_{\mu_1} \dots q_{\mu_j}}{[-q^2]^{2-k+j}},$$

⁴⁰As discussed in Section 3.8.1, this is an example of the DD parametrization by a single function [146].

which is a generalization of Eq. (G.21). Here on the right-hand side of the equality, we dropped all terms involving the metric tensor $g_{\mu_i \mu_k}$, since they vanish when contracted with the traceless tensor $\mathcal{R}_{\rho \mu_1 \dots \mu_j}^{2,qq}$. This yields

$$\begin{aligned} & \int d^4 z e^{iz \cdot q} \frac{z_\sigma}{[-z^2]^2} \frac{z_{\mu_1}}{2} \dots \frac{z_{\mu_j}}{2} \langle p_2 | \mathcal{R}_{\rho \mu_1 \dots \mu_j}^{2,qq} | p_1 \rangle \\ &= i^{j+2} \pi^2 \Gamma(j+1) \frac{1}{q^2} \Pi_{\sigma \mu_1} \frac{q_{\mu_2}}{q^2} \dots \frac{q_{\mu_j}}{q^2} \langle p_2 | \mathcal{R}_{\rho \mu_1 \dots \mu_j}^{2,qq} | p_1 \rangle, \end{aligned} \quad (5.173)$$

where we introduced a tensor

$$\Pi_{\mu\nu} \equiv g_{\mu\nu} - \frac{2}{q^2} q_\mu q_\nu, \quad \Pi_{\mu\rho} \Pi_{\rho\nu} = g_{\mu\nu}. \quad (5.174)$$

Assembling all results together, we find the contribution of the twist-two operators to the Compton amplitude (5.150)

$$\begin{aligned} & \int d^4 x e^{iz \cdot q} \frac{z_\sigma}{[-z^2]^2} \langle p_2 | \mathcal{R}_\rho^{2,qq} \left(-\frac{z}{2}, \frac{z}{2} \right) | p_1 \rangle \\ &= 2\pi^2 \left\{ \frac{q_\sigma}{q^2} \sum_{j=0}^{\infty} \langle p_2 | \mathcal{R}_{\rho[j]}^{2,qq} | p_1 \rangle - \frac{1}{2} \Pi_{\sigma\tau} \frac{\partial}{\partial q_\tau} \sum_{j=1}^{\infty} \frac{1}{j} \langle p_2 | \mathcal{R}_{\rho[j]}^{2,qq} | p_1 \rangle \right\}. \end{aligned} \quad (5.175)$$

Here we have used a new convention

$$\mathcal{R}_{\rho[j]}^{2,qq} = \frac{q_{\mu_1}}{q^2} \dots \frac{q_{\mu_j}}{q^2} \mathcal{R}_{\rho \mu_1 \dots \mu_j}^{2,qq}, \quad (5.176)$$

for contraction of the twist-two local operators $\mathcal{R}^{2,qq}$ with the four-vectors q^μ/q^2 and also exploited the identity

$$\frac{\partial}{\partial \frac{q_\sigma}{q^2}} = q^2 \Pi_{\sigma\tau} \frac{\partial}{\partial q_\tau}.$$

To evaluate the sums in (5.175), we substitute (5.172) in (5.171) and replace z_μ by q_μ/q^2 . This gives the local traceless matrix elements $\langle p_2 | \mathcal{R}_{\rho[j]}^{2,qq} | p_1 \rangle$ in terms of the Chebyshev polynomials. The summation in Eq. (5.175) can now be done with the help of the generating function for the Chebyshev polynomials (4.254)

$$G_U(a, b) \equiv \sum_{j=0}^{\infty} a^j U_j(b) = (1 - 2ab + a^2)^{-1}. \quad (5.177)$$

The required j -dependent coefficient in the series is obtained by integrating both sides of the equation with appropriate weights. In this way one obtains the sums needed for calculation of (5.175),

$$\begin{aligned} & \sum_{j=0}^{\infty} \frac{a^{j+1}}{(j+1)} U_{j+1}(b) = \int_0^a \frac{da'}{a'} (G_U(a', b) - 1), \\ & \sum_{j=1}^{\infty} \frac{a^{j+1}}{j(j+1)} U_{j+1}(b) = \int_0^a da' \int_0^{a'} \frac{da''}{(a'')^2} (G_U(a'', b) - 1 - 2a''b). \end{aligned} \quad (5.178)$$

Here $a = \frac{1}{2}\sqrt{\mathcal{P}^2/q^2}$ and $b = q \cdot \mathcal{P}/\sqrt{q^2\mathcal{P}^2}$. This immediately leads to

$$\sum_{j=0}^{\infty} \langle p_2 | \mathcal{R}_{\rho[j]}^{2,qq} | p_1 \rangle = q^2 \Pi_{\rho\tau} \frac{\partial}{\partial q_\tau} \int_{\Omega} d\beta d\alpha h^q(\beta, \alpha) \quad (5.179)$$

$$\begin{aligned} & \times \left\{ \frac{1 - \sqrt{1 + \mathcal{M}^2}}{2\sqrt{1 + \mathcal{M}^2}} \ln \left(1 + \frac{1 - \sqrt{1 + \mathcal{M}^2}}{2\Xi} \right) - \frac{1 + \sqrt{1 + \mathcal{M}^2}}{2\sqrt{1 + \mathcal{M}^2}} \ln \left(1 + \frac{1 + \sqrt{1 + \mathcal{M}^2}}{2\Xi} \right) \right\}, \\ & \sum_{j=1}^{\infty} \frac{1}{j} \langle p_2 | \mathcal{R}_{\rho[j]}^{2,qq} | p_1 \rangle = -q^2 \Pi_{\rho\tau} \frac{\partial}{\partial q_\tau} \int_{\Omega} d\beta d\alpha h^q(\beta, \alpha) \\ & \times \left\{ \frac{1}{\Xi} + \frac{1 - \sqrt{1 + \mathcal{M}^2}}{2\sqrt{1 + \mathcal{M}^2}} \left(1 + \frac{1 - \sqrt{1 + \mathcal{M}^2}}{2\Xi} \right) \ln \left(1 + \frac{1 - \sqrt{1 + \mathcal{M}^2}}{2\Xi} \right) \right. \\ & \left. - \frac{1 + \sqrt{1 + \mathcal{M}^2}}{2\sqrt{1 + \mathcal{M}^2}} \left(1 + \frac{1 + \sqrt{1 + \mathcal{M}^2}}{2\Xi} \right) \ln \left(1 + \frac{1 + \sqrt{1 + \mathcal{M}^2}}{2\Xi} \right) \right\}, \end{aligned} \quad (5.180)$$

where we introduced the variables

$$\Xi \equiv \frac{Q^2}{q \cdot \mathcal{P}} = \frac{\xi}{\beta + \eta\alpha}, \quad \mathcal{M}^2 \equiv \frac{Q^2 \mathcal{P}^2}{(q \cdot \mathcal{P})^2} = \Xi^2 \frac{4M^2 \beta^2}{Q^2} \left\{ 1 - \frac{\Delta^2}{4M^2} \left(1 - \frac{\alpha^2}{\beta^2} \right) \right\}. \quad (5.181)$$

After inserting (5.179) and (5.180) into Eq. (5.175) one should perform differentiation with respect to q_μ , which is done by means of the formula for a test function τ

$$q^2 \Pi_{\mu\nu} \frac{\partial}{\partial q_\nu} \tau(\mathcal{M}^2, \Xi) = \left\{ 2\mathcal{M}^2 (q_\mu + \Xi \mathcal{P}_\mu) \frac{\partial}{\partial \mathcal{M}^2} - \mathcal{P}_\mu \frac{\partial}{\partial \Xi^{-1}} \right\} \tau(\mathcal{M}^2, \Xi). \quad (5.182)$$

Finally, one needs to contract the resulting equation with the tensor $S^{\mu\nu;\rho\sigma}$ to get the hadronic tensor

$$T_{\mu\nu}^2 = \sum_q Q_q^2 \int_{\Omega} d\beta d\alpha h^q(\beta, \alpha) \left\{ - \left(g_{\mu\nu} - \frac{q_\mu q_\nu}{q^2} \right) \mathcal{C}_1 + \frac{1}{q \cdot \mathcal{P}} \left(\mathcal{P}_\mu + \frac{q_\mu}{\Xi} \right) \left(\mathcal{P}_\nu + \frac{q_\nu}{\Xi} \right) \mathcal{C}_2 \right\}, \quad (5.183)$$

with mass-dependent coefficient functions

$$\begin{aligned} \mathcal{C}_1 &= \frac{4\Xi - \mathcal{M}^2(1 - \Xi)}{\Xi [4\Xi(1 + \Xi) - \mathcal{M}^2]} + \frac{\mathcal{M}^2(2\Xi - \mathcal{M}^2)}{4\Xi (1 + \mathcal{M}^2)^{3/2}} \ln \left(\frac{1 - \sqrt{1 + \mathcal{M}^2} + 2\Xi}{1 + \sqrt{1 + \mathcal{M}^2} + 2\Xi} \right) + (\Xi \rightarrow -\Xi), \\ \mathcal{C}_2 &= \frac{4\Xi - \mathcal{M}^2(1 - \Xi)}{(1 + \mathcal{M}^2) [4\Xi(1 + \Xi) - \mathcal{M}^2]} + \frac{3\mathcal{M}^2(2\Xi - \mathcal{M}^2)}{4(1 + \mathcal{M}^2)^{5/2}} \ln \left(\frac{1 - \sqrt{1 + \mathcal{M}^2} + 2\Xi}{1 + \sqrt{1 + \mathcal{M}^2} + 2\Xi} \right) \\ &\quad - (\Xi \rightarrow -\Xi). \end{aligned} \quad (5.184)$$

To pick up the correct sheet of the Riemann surface for the logarithm, it is necessary to restore the suppressed Feynman prescription $Q^2 \rightarrow Q^2 - i0$ in (5.173). In the forward limit, Eq. (5.183) coincides with the well-known result [335]. As expected the current conservation is fulfilled in the forward case but violated for off-forward kinematics. The leading order massless (generalized) Callan–Gross relation [345] $\mathcal{C}_2 = \Xi \mathcal{C}_1$ is also broken by target mass corrections.

5.6.3 Spin-one-half target

In case of a spin-one-half target, the matrix elements $\langle p_2 | \mathcal{R}_{\rho;j}^{2,qq} | p_1 \rangle$ are represented in terms of the vectors p , Δ and a set of (independent) Dirac bilinears, characterizing the spin content of the target. It is convenient to use the same Dirac structures h_ρ, b and $\tilde{h}_\rho, \tilde{b}$ as previously in Section 3.5.2 in order to exploit the scalar sector analyzed above. Thus, the matrix element of, e.g., vector operator is parametrized according to

$$\begin{aligned} \langle p_2 | \mathcal{O}_{\rho\mu_1\dots\mu_j}^{qq,\text{sym}} | p_1 \rangle &= h_{\{\rho} p_{\mu_1} \cdots p_{\mu_j\}} A_{j+1,0}^q + \cdots + h_{\{\rho} \Delta_{\mu_1} \cdots \Delta_{\mu_j\}} A_{j+1,j}^q \\ &\quad + \frac{b}{2M_N} \{ p_{\{\rho} p_{\mu_1} \cdots p_{\mu_j\}} B_{j+1,0}^q + \cdots + \Delta_{\{\rho} \Delta_{\mu_1} \cdots \Delta_{\mu_j\}} B_{j+1,j+1}^q \} + \dots, \end{aligned} \quad (5.185)$$

where again the ellipses denote terms proportional to the metric tensor, which do not contribute to harmonic projections. The non-local twist-two vector operator is given by

$$\begin{aligned} \langle p_2 | \mathcal{R}_\rho^{2,qq}(-z, z) | p_1 \rangle &= \int_{\Omega} d\beta d\alpha \left\{ h_A^q(\beta, \alpha) h \cdot \partial^\mathcal{P} + h_B^q(\beta, \alpha) \frac{b}{2M_N} \mathcal{P} \cdot \partial^\mathcal{P} \right\} \\ &\quad \times \partial_\rho \sum_{j=0}^{\infty} \frac{(-i)^j}{j!(j+1)^2} \left(\frac{z^2 \mathcal{P}^2}{4} \right)^{(j+1)/2} U_{j+1} \left(\frac{z \cdot \mathcal{P}}{\sqrt{z^2 \mathcal{P}^2}} \right), \end{aligned} \quad (5.186)$$

in terms of DDs introduced in Section 3.8.3. Here we have generated the factor of z in $h \cdot z$ by the differentiation with respect to \mathcal{P} . The same trick was done with the b form factor for the purpose of a uniform representation. The same equation holds for the axial operator.

The Fourier transform and the resummation are done in the same vein as for a spinless target, and the result is

$$\begin{aligned} T_{\mu\nu}^2 &= \sum_q Q_q^2 \int_{\Omega} d\beta d\alpha \left\{ \left(\tilde{h}_A^q(\beta, \alpha) \tilde{h} \cdot \partial^\mathcal{P} + \tilde{h}_B^q(\beta, \alpha) \frac{\tilde{b}}{2M_N} \mathcal{P} \cdot \partial^\mathcal{P} \right) \frac{i}{q \cdot \mathcal{P}} \varepsilon_{\mu\nu\rho\sigma} q_\rho \mathcal{P}_\sigma \tilde{\mathcal{C}}_1 \right. \\ &\quad + \left(h_A^q(\beta, \alpha) h \cdot \partial^\mathcal{P} + h_B^q(\beta, \alpha) \frac{b}{2M_N} \mathcal{P} \cdot \partial^\mathcal{P} \right) \\ &\quad \left. \times \left(- \left(g_{\mu\nu} - \frac{q_\mu q_\nu}{q^2} \right) \mathcal{C}_1 + \frac{1}{q \cdot \mathcal{P}} \left(\mathcal{P}_\mu + \frac{q_\mu}{\Xi} \right) \left(\mathcal{P}_\nu + \frac{q_\nu}{\Xi} \right) \mathcal{C}_2 \right) \right\}, \end{aligned} \quad (5.187)$$

with massive coefficient functions

$$\begin{aligned} \mathcal{C}_1 &= \frac{[2\Xi(1+2\mathcal{M}^2) - \mathcal{M}^4]L_-}{4\Xi(1+\mathcal{M}^2)^{3/2}} - \frac{L_+}{2(1+\mathcal{M}^2)} - \frac{\mathcal{M}^2 L}{2(1+\mathcal{M}^2)^{3/2}} + (\Xi \rightarrow -\Xi), \\ \mathcal{C}_2 &= \frac{[2\Xi(1+4\mathcal{M}^2) - 3\mathcal{M}^4]L_-}{4(1+\mathcal{M}^2)^{5/2}} - \frac{\Xi(1-2\mathcal{M}^2)L_+}{2(1+\mathcal{M}^2)^2} - \frac{3\Xi\mathcal{M}^2 L}{2(1+\mathcal{M}^2)^{5/2}} - (\Xi \rightarrow -\Xi), \\ \tilde{\mathcal{C}}_1 &= \frac{L_-}{2(1+\mathcal{M}^2)^{1/2}} - \frac{L_+}{2(1+\mathcal{M}^2)} - \frac{\mathcal{M}^2 L}{2(1+\mathcal{M}^2)^{3/2}} + (\Xi \rightarrow -\Xi), \end{aligned} \quad (5.188)$$

expressed via

$$\begin{aligned} L_{\pm} &\equiv \ln \frac{1 - \sqrt{1 + \mathcal{M}^2} + 2\Xi}{2\Xi} \pm \ln \frac{1 + \sqrt{1 + \mathcal{M}^2} + 2\Xi}{2\Xi}, \\ L &\equiv \text{Li}_2 \left(-\frac{1 - \sqrt{1 + \mathcal{M}^2}}{2\Xi} \right) - \text{Li}_2 \left(-\frac{1 + \sqrt{1 + \mathcal{M}^2}}{2\Xi} \right) \end{aligned}$$

logarithms and Euler dilogarithms $\text{Li}_2(x) = - \int_0^x \frac{dy}{y} \ln(1-y)$.

5.6.4 Twist-four mass corrections

As we mentioned earlier, the resummed mass corrections can be expressed in terms of GPDs by means of the inverse Radon transform (3.238), which however involves them in unphysical regions of the momentum space. Hence, this step does not prove useful in phenomenological applications. However, every term in the mass expansion, M^2/Q^2 , can be easily converted into the conventional representation with GPDs involved only in the region of their support. Let us demonstrate this for the expanded Compton form factor \mathcal{F}_1 for a (pseudo) scalar target (5.184). To the first non-trivial order, i.e., to $\mathcal{O}(M^4/Q^4)$ accuracy, the latter reads in the DD form

$$\begin{aligned} \mathcal{F}_1 \approx \sum_q Q_q^2 \int_{\Omega} d\beta d\alpha h^q(\beta, \alpha) & \left\{ \left(C_1^{(0)}(\Xi^{-1} - i0) + C_1^{(0)}(-\Xi^{-1} - i0) \right) \right. \\ & \left. + \frac{M^2}{Q^2} \beta^2 \Xi^2 \left(C_1^{(1)}(\Xi^{-1} - i0) + C_1^{(1)}(-\Xi^{-1} - i0) \right) \right\}. \end{aligned}$$

Here in the approximation $M^2 \gg \Delta^2$, we set

$$\mathcal{M}^2 \approx 4 \frac{M^2}{Q^2} \beta^2 \Xi^2$$

and introduced the mass-independent coefficient functions

$$C_1^{(0)}(\Xi^{-1}) = -(1 + \Xi)^{-1}, \quad C_1^{(1)}(\Xi^{-1}) = (1 + \Xi)^{-2} + 2 \ln \left(\frac{\Xi}{1 + \Xi} \right).$$

To switch from the DD to the usual GPD representation, we need the following general result

$$\begin{aligned} \int_{\Omega} d\beta d\alpha \left\{ \frac{\alpha^n}{\beta^n} \right\} \mathcal{C}(\Xi^{-1}) h^q(y, z) & \quad (5.189) \\ & = \int dx \mathcal{C}\left(\frac{x}{\xi}\right) \int dy V_1^{(n)}(x, y) \left\{ \prod_{k=0}^{n-1} \left(-y \frac{\partial}{\partial y} - \eta \frac{\partial}{\partial \eta} - k \right) \right\} H^q(y, \eta), \end{aligned}$$

where the kernels are expressed in terms of generalized step-functions (G.105),

$$V_1^{(n)}(x, y) = \frac{(y - x)^{n-1}}{(n-1)!} \vartheta_{11}^0(x, x-y). \quad (5.190)$$

Substituting these expressions back into Eq. (5.189) yields

$$\begin{aligned} \mathcal{F}_1 \approx \sum_q Q_q^2 \int_{-1}^1 dx \int_{-1}^1 dy & \left\{ \left(C_1^{(0)}\left(\frac{x}{\xi} - i0\right) + C_1^{(0)}\left(-\frac{x}{\xi} - i0\right) \right) \delta(x - y) \right. \\ & \left. - \frac{M^2}{Q^2} \left(C_1^{(1)}\left(\frac{x}{\xi} - i0\right) + C_1^{(1)}\left(-\frac{x}{\xi} - i0\right) \right) V_1^{(2)}(x, y) \left(y \frac{\partial}{\partial y} + \eta \frac{\partial}{\partial \eta} + 1 \right) \right\} H^q(y, \eta), \end{aligned} \quad (5.191)$$

which has now the desired form. Completely analogous manipulations produce the GPD representation for all other form factors.

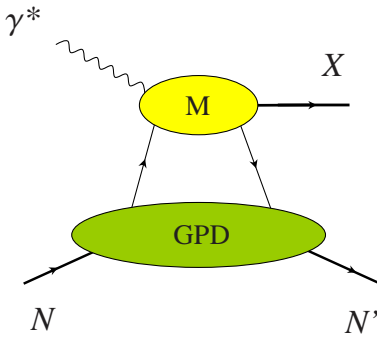


Figure 44: A generic exclusive diagram for virtual photoproduction of a gauge boson, hadronic system or jets, $X = \gamma, \gamma^*, Z, \rho, \pi, J/\psi, \text{jets}, \rho\rho, \dots$. The process-initiating particle can be a hadron instead of the photon.

6 Phenomenology of GPDs

In this section, we give a comprehensive discussion of a few major exclusive experiments where GPDs can be measured or accessed. All of the reactions involved can be divided into a few categories according to the underlying mechanism M of particle production, as demonstrated in Fig. 44. According to QCD factorization theorems, analogous to the one discussed in Section 5.1.1 for the VCS, the scattering amplitudes for the processes contain GPDs in convolution with a computable short-distance cross section. This is the latter which assorts processes to the corresponding group, which is either quark-photon Compton scattering, or hard re-scattering of quarks via the exchange of a far off-shell gluon, or production of quark (gluon) jets initiated by a photon or a meson from a quark/gluon in the target. Thus, we classify the processes as follow.

- Compton-induced processes, which include
 - leptonproduction of a real photon, $\ell N \rightarrow \ell' \gamma N'$: [2, 5, 342, 343, 344, 345, 321, 328, 346, 347, 348, 349, 350];
 - photoproduction of a lepton pair, $\gamma N \rightarrow (\ell^+ \ell^-) N'$: [351];
 - photoproduction of an electroweak boson, $\gamma N \rightarrow Z N'$: [352];
 - leptonproduction of a lepton pair, $\ell N \rightarrow \ell' (\ell^+ \ell^-) N'$: [353, 285, 354];
 - neutrino production of a real photon, $\nu_\ell N \rightarrow \ell N' \gamma$: [355, 356];
- Hard rescattering processes, which include
 - leptonproduction of a light meson, $\ell N \rightarrow \ell' M N'$: [357, 358, 142, 359, 360, 363, 361, 362, 364, 365, 366, 367];
 - leptonproduction of a heavy meson, $\ell N \rightarrow \ell' M_h N'$: [368, 369, 370, 371];
 - photoproduction of a heavy meson, $\gamma N \rightarrow M_h N'$: [372, 357, 371, 373];
 - mesoproduction of lepton pairs: $\pi N \rightarrow N' \ell \ell'$ [374];
 - hadron-antihadron annihilation into a lepton pair and a photon, $h\bar{h} \rightarrow \ell^+ \ell^- \gamma$ [375];
- Diffractive processes, which include
 - photoproduction of two jets, $\gamma N \rightarrow (2\text{jets}) N'$: [376, 377];

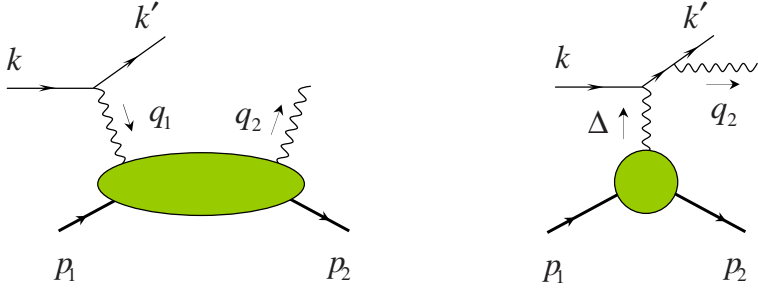


Figure 45: Subprocesses contributing to electroproduction of a real photon: deeply virtual Compton scattering (left) and Bethe-Heitler scattering (right).

- pion dissociation into two jets, $\pi N \rightarrow (2\text{jets})N'$: [378, 379, 380, 381, 382];
- neutrino production of heavy mesons, $\bar{\nu}_\mu N \rightarrow \mu D_s N'$ [383];
- lepton production of pion pairs, $\ell N \rightarrow \ell' \pi \pi N'$: [384];
- lepton production of two vector mesons with large rapidity gap, $\ell N \rightarrow \ell' \rho \rho N'$: [385];
- Higgs production, $pp \rightarrow pHp$: [386, 387].

In our subsequent presentation we will explore in detail three of the major processes: lepton production of γ , $\ell^+\ell^-$ pairs and light mesons. The reason for this choice is that these reactions can be used to measure GPDs to high accuracy. Moreover they have theoretically well-established and rigorous status over some of the other processes whose description in terms of GPDs is either not proven to all orders in strong coupling—like diffractive production in γN collisions or production of two vector mesons with a large rapidity gap—or is not even legitimate—for pion dissociation into jets and diffractive Higgs production,—since factorization theorems are broken for them. The light-cone dominance in virtual Compton scattering, on the other hand, is a consequence of the external kinematical conditions on the process in the same way as in deeply inelastic scattering. Therefore, one can expect the onset of the precocious scaling as early as at $Q^2 \sim 1 \text{ GeV}^2$. It is not the case for hard exclusive meson production, giving access to GPDs as well, where it is the dynamical behavior of the short-distance parton amplitude confined to a small transverse volume near the light cone that drives the applicability of the perturbative approach to the process. Here the reliability of perturbative QCD predictions is postponed to larger momentum transfer. However, the process of meson production is unique in its ability to potentially disentangle GPDs into separate flavor components. No other experimentally feasible⁴¹ reactions sharing this property are available.

6.1 Lepton production of a real photon

Exclusive lepton production of a photon off the nucleon serves as a clean electromagnetic probe of the nucleon’s internal structure and currently is the only measured reaction at present day experimental facilities in the required energy range [393, 394, 395, 396], which has a clear-cut legitimate description in terms of leading twist GPDs. Since GPDs carry information on both

⁴¹Though in principle, a deeply virtual Compton scattering with charged electroweak currents will serve the purpose of flavor separation, its actual experimental implementation faces gargantuan difficulties.

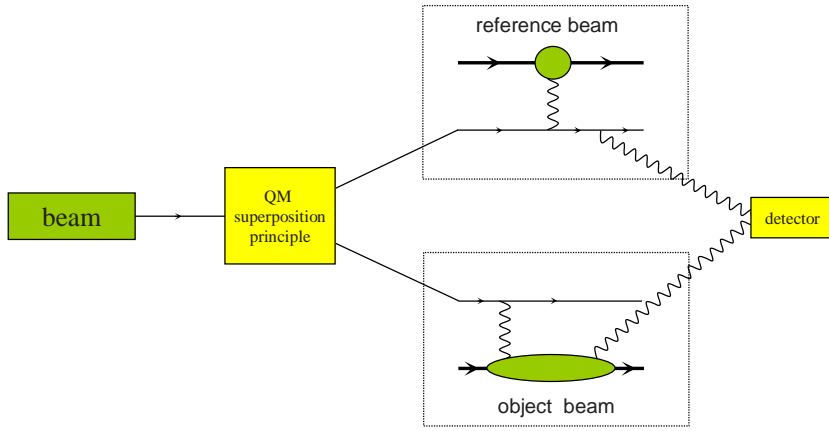


Figure 46: Proton “holography” with electroproduction of a real photon [118].

longitudinal and transverse degrees of freedom, their three-dimensional experimental exploration requires a complete determination of the DVCS amplitude, i.e., its magnitude and phase. For macroscopic objects viewed with visible light, a way to measure the phase is known as holography, which uses the interference of a source wave with the one diffracted off the test body: The laser beam is split into two rays. One of them serves as a reference source and the other reflects from the object’s surface. The reflected beam, which was in phase with the reference beam before hitting the “target”, interferes with the reference beam and forms fringes on the plate with varying intensity depending on the phase difference of both. For microscopic quantum-mechanical states, as we demonstrated in Section 2.1.4, one also resorts on analogous interferometric schemes (see Fig. 2). This technology allows for a complete measurement of the corresponding Wigner distribution. Unfortunately, the same method cannot be used for X-ray holography of crystals or γ -ray interferometry of hadrons via scattering experiments due to the absence of practical “splitters”. However, for lepton production of a photon from the nucleon there are actually two contributing amplitudes (see Fig. 45): the one due to deeply virtual Compton scattering off the nucleon $\mathcal{T}_{\text{DVCS}}$, we are interested in, and \mathcal{T}_{BH} from the “contaminating” Bethe-Heitler (BH) process, in which the real photon spills off the scattered lepton rather than the quark. The BH amplitude is completely known since the only long-distance input turns out to be nucleon form factors measured elsewhere. Thus the quantum-mechanical superposition principle lead to the presence of an interference term $\mathcal{T}_{\text{DVCS}}^* \mathcal{T}_{\text{BH}}$ between these amplitudes in addition to the intensities of each of the signals, $|\mathcal{T}_{\text{DVCS}}|^2$ and $|\mathcal{T}_{\text{BH}}|^2$, where the phase information is lost. Thus the BH process serves as a reference source for the measurement of the DVCS signal—its magnitude and phase (see Fig. 46). The most straightforward extraction of the interference term from the cross section measurement is achieved by making use of the opposite lepton charge conjugation properties of DVCS and BH amplitudes or their difference with respect to the lepton and nucleon spin dependence.

6.1.1 Kinematics of lepton production of the photon

We start our discussion of the process $e(k)N(p_1) \rightarrow e(k')N(p_2)\gamma(q_2)$ with discussion of its kinematics. The reality of the final state photon, immediately implies the equality of the skewness η and generalized Bjorken ξ variables, with the latter one expressed in terms of the standard x_B via

the equation

$$\eta = \xi \approx \frac{x_B}{2 - x_B}.$$

The most transparent consideration arises in the target rest frame in which the z -axis is directed opposite to the momentum of the spacelike virtual photon⁴², see Fig. 47. In this frame, we obviously have for the initial proton and virtual photon four-momenta

$$p_1^\mu = (M_N, 0, 0, 0), \quad q_1^\mu = (\omega_1, 0, 0, -q_1^z), \quad (6.1)$$

where the photon energy and the z -component of its three-momentum are expressed in terms of the variables (5.10) as

$$\omega_1 = \frac{Q}{\varepsilon}, \quad q_1^z = \frac{Q}{\varepsilon} \sqrt{1 + \varepsilon^2}. \quad (6.2)$$

Here and throughout our subsequent presentation we use the convention

$$\varepsilon \equiv 2x_B \frac{M_N}{Q}.$$

The outgoing nucleon four-momentum in the target rest frame has the components

$$p_2^\mu = (E_2, \mathbf{p}_2), \quad E_2 = M_N - \frac{\Delta^2}{2M_N}, \quad |\mathbf{p}_2| = \sqrt{-\Delta^2(1 - \Delta^2/(4M_N^2))}, \quad (6.3)$$

and the scattering angle of the recoiled nucleon is

$$\cos \theta_N = -\frac{\varepsilon^2(Q^2 - \Delta^2) - 2x_B \Delta^2}{4x_B M_N |\mathbf{p}_2| \sqrt{1 + \varepsilon^2}}. \quad (6.4)$$

The incoming electron four-momentum

$$k^\mu = (E, k^x, 0, k^z) = E(1, \sin \theta_e, 0, \cos \theta_e), \quad E = \frac{Q}{y\varepsilon}, \quad \cos \theta_e = -\frac{1 + y\varepsilon^2/2}{\sqrt{1 + \varepsilon^2}}, \quad (6.5)$$

depends on the variable proportional to the lepton energy loss

$$y = \frac{p_1 \cdot q_1}{p_1 \cdot k}, \quad q_1 = k - k'. \quad (6.6)$$

Notice that from the relation

$$\sin \theta_e = \frac{\varepsilon \sqrt{1 - y - y^2\varepsilon^2/4}}{\sqrt{1 + \varepsilon^2}},$$

it is clear that for large momentum transfer from the lepton to the target, the lepton beam experiences forward scattering with almost no deflection as $\theta_e \rightarrow 0$ for $Q^2 \gg M_N^2$. Finally, the four-vector of the real photon is given by

$$q_2^\mu = (\omega_2, \mathbf{v} \omega_2), \quad (6.7)$$

with momentum components and the scattering angle being

$$\omega_2 = \frac{Q}{\varepsilon} + \frac{\Delta^2}{2M_N}, \quad |\mathbf{v}| = 1, \quad \cos \theta_\gamma = -\frac{\varepsilon(Q^2 + \Delta^2) + 2Q\omega_2}{2Q\omega_2 \sqrt{1 + \varepsilon^2}}. \quad (6.8)$$

⁴²The transformation to the reference frame with the z -axis directed along the lepton beam is addressed in Ref. [398].

6.1.2 Cross section for lepton production of the photon

Now we are in a position to turn to physical observables, which give direct access to GPDs in the measurement of the five-fold cross section for the lepton production process

$$d\sigma = \frac{\alpha_{\text{em}}^3 x_B y}{16 \pi^2 Q^2 \sqrt{1 + \varepsilon^2}} \left| \frac{\mathcal{T}}{e^3} \right|^2 dx_B dy d(-\Delta^2) d\phi d\varphi. \quad (6.9)$$

Here the scattering amplitude \mathcal{T} is a sum of the DVCS $\mathcal{T}_{\text{DVCS}}$ and Bethe-Heitler (BH) \mathcal{T}_{BH} signals. The latter has no absorptive part at lowest order in the QED fine structure constant $\alpha_{\text{em}} = e^2/(4\pi)$, and is parametrized in terms of the electromagnetic form factors (2.16), which are assumed to be known from other measurements. For the electron beam, the separate contributions read

$$\mathcal{T}_{\text{DVCS}} = \frac{e^3}{q_1^2} \varepsilon_\mu^*(q_2) \bar{u}(k') \gamma_\nu u(k) T^{\mu\nu}, \quad (6.10)$$

$$\mathcal{T}_{\text{BH}} = \frac{e^3}{\Delta^2} \varepsilon_\mu^*(q_2) \bar{u}(k') \left(\gamma^\mu \frac{1}{k - \not{\Delta}} \gamma^\nu + \gamma^\nu \frac{1}{k' + \not{\Delta}} \gamma^\mu \right) u(k) J_\nu. \quad (6.11)$$

They correspond to diagrams (a) and (b) in Fig. 45, respectively, including the crossed contributions in the BH cases. Here the DVCS amplitude is expressed in terms of the tensor $T_{\mu\nu}$ from Eq. (5.51), while BH one via the nucleon electromagnetic current

$$J_\mu \equiv \langle p_2 | j_\mu(0) | p_1 \rangle, \quad (6.12)$$

expressed in terms of the Dirac and Pauli form factors in Eq. (2.16). It is very important to notice that the DVCS amplitude changes its sign when one goes from the electron to the positron beam,

$$\mathcal{T}_{\text{DVCS}}|_{e^+} = -\mathcal{T}_{\text{DVCS}}|_{e^-}, \quad (6.13)$$

while the BH process does not $\mathcal{T}_{\text{BH}}|_{e^+} = \mathcal{T}_{\text{BH}}|_{e^-}$.

The dependence of the cross section (6.9) on a number of kinematical variables allows for a thorough exploration of the DVCS amplitude. Apart from the Bjorken variable x_B , the t -channel momentum transfer Δ^2 and the lepton energy loss y , it depends on the azimuthal angle ϕ between the lepton and hadron scattering planes and the angle between the nucleon polarization vector and the scattered nucleon $\varphi = \Phi - \phi$, as shown in Fig. 47. We parametrize the polarization vector of the nucleon by polar and azimuthal angles Θ and Φ , respectively,

$$S^\mu = (0, \sin \Theta \cos \Phi, \sin \Theta \sin \Phi, \cos \Theta), \quad (6.14)$$

so that it has solely longitudinal polarization in the target rest frame when $\Theta = 0, \pi$, and the transverse one for $\Theta = \pi/2$.

At this point, it is instructive to point out the relation of our angular variables ϕ and Φ to ϕ_h and ϕ_s of the ‘‘Trento convention’’ [341]. They are simply related by

$$\phi + \phi_h = 2\pi, \quad \Phi + \phi_s = 2\pi. \quad (6.15)$$

As we emphasized in the previous section, the detailed experimental exploration of the DVCS amplitude is possible via the extraction of the interference term. One of the ways to achieve it is obvious from the charge-conjugation property of the DVCS amplitude (6.13). By performing

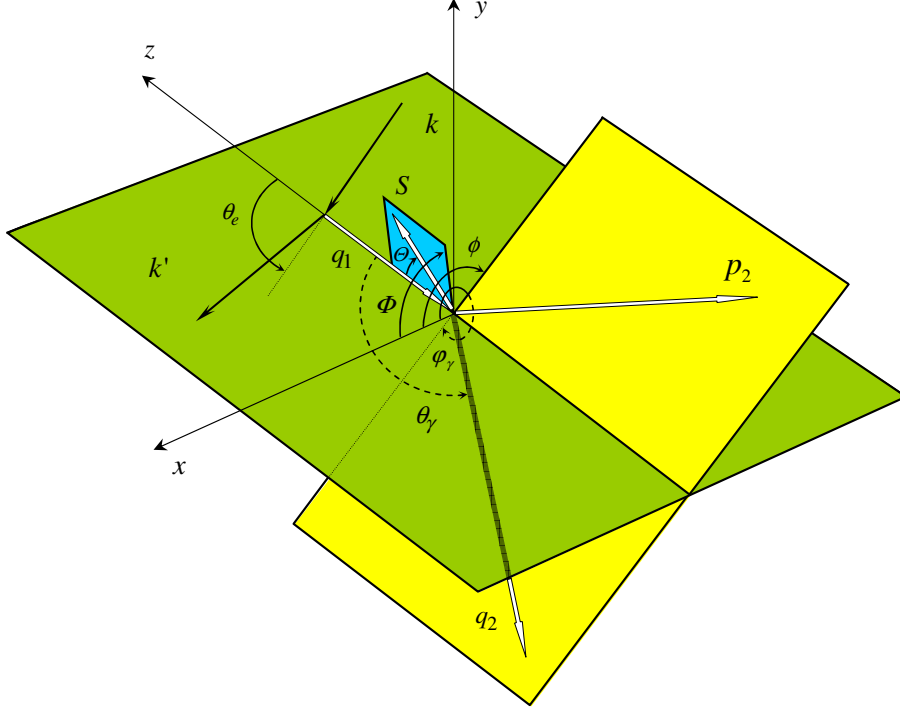


Figure 47: Kinematics of lepto-production in the target rest frame. The z -direction is chosen counter-along the three-momentum of the incoming virtual photon. The lepton three-momenta form the lepton scattering plane, while the recoiled proton and outgoing real photon define the hadron scattering plane. In this reference system the azimuthal angle between the lepton plane and the recoiled proton momentum is ϕ and is related in turn to the photon azimuthal angle $\varphi_\gamma = \phi + \pi$. The target polarization three-vector is described by two spherical angles in this frame (Θ, Φ) , so that the angle between the polarization vector and the scattered nucleon is $\varphi = \Phi - \phi$.

scattering experiments with electron and positron beams and taking their difference, one gets access to the interference

$$d\sigma_{e^-} - d\sigma_{e^+} \sim (\mathcal{T}_{\text{DVCS}}^* \mathcal{T}_{\text{BH}} + \mathcal{T}_{\text{DVCS}} \mathcal{T}_{\text{BH}}^*)_{e^-} \equiv \mathcal{I}_{e^-}$$

Although this set up is a perfect filter of \mathcal{I} , there is currently only one experimental facility possessing both types of the lepton beam, Deutsches Elektronen-Synchrotron. Therefore, in order to be able to study it with other machines, one has to resort to other techniques. As we will demonstrate below they are based on lepton and nucleon polarization observables and analysis of the azimuthal angle dependence of the outgoing nucleon or photon. The successful completion of this program calls for a detailed understanding of the spin and azimuthal angle dependence of the differential cross section (6.9). The azimuthal dependence of each of the three terms in

$$\mathcal{T}^2 = |\mathcal{T}_{\text{BH}}|^2 + |\mathcal{T}_{\text{DVCS}}|^2 + \mathcal{I} \quad (6.16)$$

arises from the Lorentz products of leptonic and hadronic four-momenta [342, 344, 328]. In our frame, these contractions yield finite sums of Fourier harmonics, whose maximal frequencies are defined by the rank m of the corresponding leptonic tensor⁴³ in the incoming lepton momentum

⁴³It is a product of two Dirac bilinear forms built from leptonic bispinors entering the two scattering amplitudes (6.10) and (6.11), i.e., $\bar{u}(k')\Gamma_1 u(k)\bar{u}(k)\Gamma_2 u(k')$.

k_μ . Note, however, that in the polarized part of the leptonic tensors, proportional to λ times the ε -tensor, one has one four-vector k_μ less than in the unpolarized part. Thus, the highest harmonic which is proportional to λ will be $\cos / \sin([m-1]\phi)$ instead of $\cos / \sin(m\phi)$. The parity and time reversal invariance provide further constraints on the Fourier coefficients.

There is an important difference between the interference term and the squared DVCS amplitude. The former has a contaminating ϕ -dependence due to the lepton BH propagators,

$$\mathcal{Q}^2 \mathcal{P}_1 \equiv (k - q_2)^2 = \mathcal{Q}^2 + 2k \cdot \Delta, \quad \mathcal{Q}^2 \mathcal{P}_2 \equiv (k - \Delta)^2 = -2k \cdot \Delta + \Delta^2, \quad (6.17)$$

where

$$k \cdot \Delta = -\frac{\mathcal{Q}^2}{2y(1+\varepsilon^2)} \left\{ 1 + 2K \cos \phi - \frac{\Delta^2}{\mathcal{Q}^2} \left(1 - x_B(2-y) + \frac{y\varepsilon^2}{2} \right) + \frac{y\varepsilon^2}{2} \right\}. \quad (6.18)$$

The $1/\mathcal{Q}$ -power suppressed kinematical factor K appearing here also shows up in the Fourier series

$$K \equiv \frac{1}{2\mathcal{Q}^2} \sqrt{-(1-y-y^2\varepsilon^2/4)(4x_B(1-x_B)+\varepsilon^2)(\Delta^2-\Delta_{\min}^2)(\Delta^2-\Delta_{\max}^2)}. \quad (6.19)$$

We expressed K in terms of the maximal and minimal momentum transfer in the t -channel,

$$\Delta_{\min,\max}^2 = -\frac{1}{4x_B(1-x_B)+\varepsilon^2} \left\{ 2(1-x_B)\mathcal{Q}^2 + \varepsilon^2\mathcal{Q}^2 \mp 2\sqrt{1+\varepsilon^2}(1-x_B)\mathcal{Q}^2 \right\}, \quad (6.20)$$

with $-$ ($+$) corresponding to Δ_{\min}^2 (Δ_{\max}^2). It vanishes at the kinematical boundary $\Delta^2 = \Delta_{\min}^2$, determined by the minimal value

$$-\Delta_{\min}^2 \approx \frac{M^2 x_B^2}{1 - x_B + x_B M^2 / \mathcal{Q}^2}, \quad (6.21)$$

as well as at

$$y \rightarrow y_{\max} \equiv 2 \frac{\sqrt{1+\varepsilon^2} - 1}{\varepsilon^2} \approx 1 - \frac{M_N^2 x_B^2}{\mathcal{Q}^2}.$$

As we see, the denominator of the u -channel lepton propagator \mathcal{P}_1 can be of order $1/\mathcal{Q}^2$ at large y . In the Bjorken limit it behaves like $(1-y)$. Moreover, if the outgoing photon is collinear to the incoming lepton, \mathcal{P}_1 vanishes. Of course, the photon then lies in the lepton scattering plane, i.e., $\varphi_\gamma = \phi + \pi = 0$, and both polar angles coincide with each other. This condition is fulfilled if

$$y \rightarrow y_{\text{col}} \equiv \frac{\mathcal{Q}^2 + \Delta^2}{\mathcal{Q}^2 + x_B \Delta^2} \approx 1 + (1-x_B) \frac{\Delta^2}{\mathcal{Q}^2}.$$

Therefore, for large y , the squared BH and interference terms are enhanced with respect to the squared DVCS one. Furthermore, the expansion of \mathcal{P}_1 in \mathcal{Q} is not justified, and, thus, the Fourier analysis of experimental data must be modified. For small y , it is legitimate to expand \mathcal{P}_1 and \mathcal{P}_2 in power series with respect to $1/\mathcal{Q}$. This generates higher harmonics suppressed by powers of K .

6.1.3 Angular dependence

Each of the terms in the squared amplitude (6.16) can be written as a finite Fourier sum of a few harmonic in the azimuthal angle ϕ ,

$$|\mathcal{T}_{\text{BH}}|^2 = \frac{e^6}{x_{\text{B}}^2 y^2 (1 + \varepsilon^2)^2 \Delta^2 \mathcal{P}_1(\phi) \mathcal{P}_2(\phi)} \left\{ c_0^{\text{BH}} + \sum_{n=1}^2 c_n^{\text{BH}} \cos(n\phi) + s_1^{\text{BH}} \sin(n\phi) \right\}, \quad (6.22)$$

$$|\mathcal{T}_{\text{DVCS}}|^2 = \frac{e^6}{y^2 Q^2} \left\{ c_0^{\text{DVCS}} + \sum_{n=1}^2 [c_n^{\text{DVCS}} \cos(n\phi) + s_n^{\text{DVCS}} \sin(n\phi)] \right\}, \quad (6.23)$$

$$\mathcal{I} = \frac{\pm e^6}{x_{\text{B}} y^3 \Delta^2 \mathcal{P}_1(\phi) \mathcal{P}_2(\phi)} \left\{ c_0^{\text{INT}} + \sum_{n=1}^3 [c_n^{\text{INT}} \cos(n\phi) + s_n^{\text{INT}} \sin(n\phi)] \right\}. \quad (6.24)$$

Here, the $+$ ($-$) sign in the interference stands for the negatively (positively) charged lepton beam. The results for the Fourier coefficients, presented below, show that the generation of new harmonics in the azimuthal angular dependence is terminated at the twist-three level. The coefficients c_1^{INT} , s_1^{INT} as well as c_0^{DVCS} arise at the twist-two level, and their dependence on GPDs has been investigated in Refs. [342, 344]. The remaining coefficients provide an additional angular dependence, with c_1^{DVCS} , s_1^{DVCS} , c_2^{INT} , and s_2^{INT} involving twist-three GPDs [345, 321, 328]. On the other hand, the harmonics proportional to $\cos(3\phi)$ ($\cos(2\phi)$) or $\sin(3\phi)$ ($\sin(2\phi)$) in the interference (squared DVCS) term originate from the twist-two double helicity-flip gluonic GPDs alone. They are not contaminated by the twist-two quark amplitudes, however, they are affected by twist-four power corrections [388]. In what follows, we neglect the effects of dynamical higher-twist (larger than three) contributions since we expect Bjorken scaling to be effective in the Compton amplitude starting with rather lower photon virtualities Q^2 .

To have a compact notation, we write the cross section for a polarized target as

$$d\sigma = d\sigma_{\text{unp}} + \cos \Theta d\sigma_{\text{LP}}(\Lambda) + \sin \Theta d\sigma_{\text{TP}}(\varphi), \quad (6.25)$$

where the polar angle Θ appears in the decomposition of the nucleon spin vector (6.14), $S^\mu = \cos \Theta S_{\text{LP}}^\mu(\Lambda) + \sin \Theta S_\perp^\mu(\Phi)$ with the longitudinal polarization $S_{\text{LP}}^\mu = (0, 0, 0, \Lambda)$ expressed in terms of the nucleon helicity. We will use the conventional definition of the lepton helicity, i.e., $\lambda = 1$ if the spin is aligned with the direction of the lepton three-momentum and $\lambda = -1$, when they are opposite.

6.1.4 Bethe-Heitler amplitude squared

This part of the lepto-production cross section is expressed solely in terms of $F_1(\Delta^2)$ and $F_2(\Delta^2)$, the known Dirac and Pauli form factors of the nucleon. There are several possibilities for the target polarization, and the relevant Fourier coefficients are:

- Unpolarized target:

$$\begin{aligned} c_{0,\text{unp}}^{\text{BH}} &= 8K^2 \left\{ (2 + 3\varepsilon^2) \frac{Q^2}{\Delta^2} \left(F_1^2 - \frac{\Delta^2}{4M^2} F_2^2 \right) + 2x_{\text{B}}^2 (F_1 + F_2)^2 \right\} \\ &+ (2 - y)^2 \left\{ (2 + \varepsilon^2) \left[\frac{4x_{\text{B}}^2 M^2}{\Delta^2} \left(1 + \frac{\Delta^2}{Q^2} \right)^2 + 4(1 - x_{\text{B}}) \left(1 + x_{\text{B}} \frac{\Delta^2}{Q^2} \right) \right] \left(F_1^2 - \frac{\Delta^2}{4M^2} F_2^2 \right) \right\} \end{aligned} \quad (6.26)$$

$$\begin{aligned}
& + 4x_B^2 \left[x_B + \left(1 - x_B + \frac{\varepsilon^2}{2} \right) \left(1 - \frac{\Delta^2}{Q^2} \right)^2 - x_B(1 - 2x_B) \frac{\Delta^4}{Q^4} \right] (F_1 + F_2)^2 \Big\} \\
& + 8(1 + \varepsilon^2) \left(1 - y - \frac{\varepsilon^2 y^2}{4} \right) \left\{ 2\varepsilon^2 \left(1 - \frac{\Delta^2}{4M^2} \right) \left(F_1^2 - \frac{\Delta^2}{4M^2} F_2^2 \right) \right. \\
& \quad \left. - x_B^2 \left(1 - \frac{\Delta^2}{Q^2} \right)^2 (F_1 + F_2)^2 \right\}, \\
c_{1,\text{unp}}^{\text{BH}} & = 8K(2 - y) \left\{ \left(\frac{4x_B^2 M^2}{\Delta^2} - 2x_B - \varepsilon^2 \right) \left(F_1^2 - \frac{\Delta^2}{4M^2} F_2^2 \right) \right. \\
& \quad \left. + 2x_B^2 \left(1 - (1 - 2x_B) \frac{\Delta^2}{Q^2} \right) (F_1 + F_2)^2 \right\}, \tag{6.27}
\end{aligned}$$

$$c_{2,\text{unp}}^{\text{BH}} = 8x_B^2 K^2 \left\{ \frac{4M^2}{\Delta^2} \left(F_1^2 - \frac{\Delta^2}{4M^2} F_2^2 \right) + 2(F_1 + F_2)^2 \right\}. \tag{6.28}$$

- Longitudinally polarized target:

$$\begin{aligned}
c_{0,\text{LP}}^{\text{BH}} & = 8\lambda\Lambda x_B(2 - y) y \frac{\sqrt{1 + \varepsilon^2}}{1 - \frac{\Delta^2}{4M^2}} (F_1 + F_2) \left\{ \frac{1}{2} \left[\frac{x_B}{2} \left(1 - \frac{\Delta^2}{Q^2} \right) - \frac{\Delta^2}{4M^2} \right] \left[2 - x_B \right. \right. \\
& \quad \left. - 2(1 - x_B)^2 \frac{\Delta^2}{Q^2} + \varepsilon^2 \left(1 - \frac{\Delta^2}{Q^2} \right) - x_B(1 - 2x_B) \frac{\Delta^4}{Q^4} \right] (F_1 + F_2) \\
& \quad \left. + \left(1 - (1 - x_B) \frac{\Delta^2}{Q^2} \right) \left[\frac{x_B^2 M^2}{\Delta^2} \left(1 + \frac{\Delta^2}{Q^2} \right)^2 + (1 - x_B) \left(1 + x_B \frac{\Delta^2}{Q^2} \right) \right] \left(F_1 + \frac{\Delta^2}{4M^2} F_2 \right) \right\}, \tag{6.29}
\end{aligned}$$

$$\begin{aligned}
c_{1,\text{LP}}^{\text{BH}} & = -8\lambda\Lambda x_B y K \frac{\sqrt{1 + \varepsilon^2}}{1 - \frac{\Delta^2}{4M^2}} (F_1 + F_2) \left\{ \left[\frac{\Delta^2}{2M^2} - x_B \left(1 - \frac{\Delta^2}{Q^2} \right) \right] \left(1 - x_B + x_B \frac{\Delta^2}{Q^2} \right) (F_1 + F_2) \right. \\
& \quad \left. + \left[1 + x_B - (3 - 2x_B) \left(1 + x_B \frac{\Delta^2}{Q^2} \right) - \frac{4x_B^2 M^2}{\Delta^2} \left(1 + \frac{\Delta^4}{Q^4} \right) \right] \left(F_1 + \frac{\Delta^2}{4M^2} F_2 \right) \right\}. \tag{6.30}
\end{aligned}$$

- Transversely polarized target:

$$\begin{aligned}
c_{0,\text{TP}}^{\text{BH}} & = -8\lambda \cos(\varphi)(2 - y) y \frac{Q}{M} \frac{\sqrt{1 + \varepsilon^2} K}{\sqrt{1 - y - \frac{\varepsilon^2 y^2}{4}}} (F_1 + F_2) \left\{ \frac{x_B^3 M^2}{Q^2} \left(1 - \frac{\Delta^2}{Q^2} \right) (F_1 + F_2) \right. \\
& \quad \left. + \left(1 - (1 - x_B) \frac{\Delta^2}{Q^2} \right) \left[\frac{x_B^2 M^2}{\Delta^2} \left(1 - \frac{\Delta^2}{Q^2} \right) F_1 + \frac{x_B}{2} F_2 \right] \right\}, \tag{6.31}
\end{aligned}$$

$$\begin{aligned}
c_{1,\text{TP}}^{\text{BH}} & = -16\lambda \cos(\varphi) x_B y \sqrt{1 - y - \frac{\varepsilon^2 y^2}{4}} \frac{M}{Q} \sqrt{1 + \varepsilon^2} (F_1 + F_2) \left\{ \frac{2K^2 Q^2}{\Delta^2 \left(1 - y - \frac{\varepsilon^2 y^2}{4} \right)} \left[\frac{\Delta^2}{4M^2} F_2 \right. \right. \\
& \quad \left. + x_B \left(1 - \frac{\Delta^2}{Q^2} \right) F_1 \right] + (1 + \varepsilon^2) x_B \left(1 - \frac{\Delta^2}{Q^2} \right) \left(F_1 + \frac{\Delta^2}{4M^2} F_2 \right) \Big\}, \tag{6.32}
\end{aligned}$$

$$s_{1,\text{TP}}^{\text{BH}} = 16\lambda \sin(\varphi) y x_B^2 \sqrt{1 - y - \frac{\varepsilon^2 y^2}{4}} \frac{M}{Q} \sqrt{(1 + \varepsilon^2)^3} \left(1 - \frac{\Delta^2}{Q^2} \right) (F_1 + F_2) \left(F_1 + \frac{\Delta^2}{4M^2} F_2 \right). \tag{6.33}$$

6.1.5 DVCS amplitude squared

$|\mathcal{T}_{\text{DVCS}}|^2$ is bilinear in the CFFs, and its coefficients are given in terms of $\mathcal{C}^{\text{DVCS}}$ functions, which are specified in Section 6.1.7:

- Unpolarized target:

$$c_{0,\text{unp}}^{\text{DVCS}} = 2(2 - 2y + y^2)\mathcal{C}_{\text{unp}}^{\text{DVCS}}(\mathcal{F}, \mathcal{F}^*), \quad (6.34)$$

$$\begin{Bmatrix} c_{1,\text{unp}}^{\text{DVCS}} \\ s_{1,\text{unp}}^{\text{DVCS}} \end{Bmatrix} = \frac{8K}{2 - x_B} \begin{Bmatrix} 2 - y \\ -\lambda y \end{Bmatrix} \begin{Bmatrix} \Re \\ \Im \end{Bmatrix} \mathcal{C}_{\text{unp}}^{\text{DVCS}}(\mathcal{F}^{\text{eff}}, \mathcal{F}^*), \quad (6.35)$$

$$c_{2,\text{unp}}^{\text{DVCS}} = -\frac{4Q^2 K^2}{M^2(2 - x_B)} \Re \mathcal{C}_{T,\text{unp}}^{\text{DVCS}}(\mathcal{F}_T, \mathcal{F}^*). \quad (6.36)$$

- Longitudinally polarized target:

$$c_{0,\text{LP}}^{\text{DVCS}} = 2\lambda\Lambda y(2 - y)\mathcal{C}_{\text{LP}}^{\text{DVCS}}(\mathcal{F}, \mathcal{F}^*), \quad (6.37)$$

$$\begin{Bmatrix} c_{1,\text{LP}}^{\text{DVCS}} \\ s_{1,\text{LP}}^{\text{DVCS}} \end{Bmatrix} = -\frac{8\Lambda K}{2 - x_B} \begin{Bmatrix} -\lambda y \\ 2 - y \end{Bmatrix} \begin{Bmatrix} \Re \\ \Im \end{Bmatrix} \mathcal{C}_{\text{LP}}^{\text{DVCS}}(\mathcal{F}^{\text{eff}}, \mathcal{F}^*), \quad (6.38)$$

$$s_{2,\text{LP}}^{\text{DVCS}} = -\frac{4\Lambda Q^2 K^2}{M^2(2 - x_B)} \Im \mathcal{C}_{T,\text{LP}}^{\text{DVCS}}(\mathcal{F}_T, \mathcal{F}^*). \quad (6.39)$$

- Transversely polarized target:

$$c_{0,\text{TP}}^{\text{DVCS}} = -\frac{QK}{M\sqrt{1-y}} \left[-\lambda y(2 - y) \cos(\varphi) \mathcal{C}_{\text{TP+}}^{\text{DVCS}} + (2 - 2y + y^2) \sin(\varphi) \Im \mathcal{C}_{\text{TP-}}^{\text{DVCS}} \right] (\mathcal{F}, \mathcal{F}^*), \quad (6.40)$$

$$\begin{Bmatrix} c_{1,\text{TP}}^{\text{DVCS}} \\ s_{1,\text{TP}}^{\text{DVCS}} \end{Bmatrix} = -\frac{4QK^2}{M(2 - x_B)\sqrt{1-y}} \times \left[\cos(\varphi) \begin{Bmatrix} -\lambda y \\ 2 - y \end{Bmatrix} \begin{Bmatrix} \Re \\ \Im \end{Bmatrix} \mathcal{C}_{\text{TP+}}^{\text{DVCS}} + \sin(\varphi) \begin{Bmatrix} 2 - y \\ \lambda y \end{Bmatrix} \begin{Bmatrix} \Im \\ \Re \end{Bmatrix} \mathcal{C}_{\text{TP-}}^{\text{DVCS}} \right] (\mathcal{F}^{\text{eff}}, \mathcal{F}^*), \quad (6.41)$$

$$\begin{Bmatrix} c_{2,\text{TP}}^{\text{DVCS}} \\ s_{2,\text{TP}}^{\text{DVCS}} \end{Bmatrix} = -\frac{4Q\sqrt{1-y}K}{M(2 - x_B)} \Im \left\{ \begin{Bmatrix} \sin(\varphi) \mathcal{C}_{T,\text{TP-}}^{\text{DVCS}} \\ \cos(\varphi) \mathcal{C}_{T,\text{TP+}}^{\text{DVCS}} \end{Bmatrix} \right\} (\mathcal{F}_T, \mathcal{F}^*). \quad (6.42)$$

The coefficient c_0^{DVCS} is expressed in terms of the twist-two CFFs $\mathcal{F} = \{\mathcal{H}, \mathcal{E}, \tilde{\mathcal{H}}, \tilde{\mathcal{E}}\}$, defined in Eq. (5.109), while the twist-three coefficients c_1^{DVCS} and s_1^{DVCS} arise from the interference of twist-two CFFs with the “effective” twist-three CFFs introduced in Eq. (5.112). These Fourier harmonics have the same functional dependence on CFFs as the leading twist-two ones [344]. However, this is not the case for the Fourier coefficients c_2^{DVCS} and s_2^{DVCS} , induced by the gluon transversity (5.57).

6.1.6 Interference of Bethe-Heitler and DVCS amplitudes

For the phenomenology of GPDs, the interference term \mathcal{I} is the most interesting quantity since it is linear in CFFs and thus simplifies their extraction from experimental measurements. The Fourier harmonics in this case have the following form:

- Unpolarized target:

$$c_{0,\text{unp}}^{\text{INT}} = -8(2-y)\Re e \left\{ \frac{(2-y)^2}{1-y} K^2 \mathcal{C}_{\text{unp}}^{\text{INT}}(\mathcal{F}) + \frac{\Delta^2}{Q^2} (1-y)(2-x_B) (\mathcal{C}_{\text{unp}}^{\text{INT}} + \Delta \mathcal{C}_{\text{unp}}^{\text{INT}})(\mathcal{F}) \right\}, \quad (6.43)$$

$$\begin{Bmatrix} c_{1,\text{unp}}^{\text{INT}} \\ s_{1,\text{unp}}^{\text{INT}} \end{Bmatrix} = 8K \begin{Bmatrix} -(2-2y+y^2) \\ \lambda y(2-y) \end{Bmatrix} \begin{Bmatrix} \Re e \\ \Im m \end{Bmatrix} \mathcal{C}_{\text{unp}}^{\text{INT}}(\mathcal{F}), \quad (6.44)$$

$$\begin{Bmatrix} c_{2,\text{unp}}^{\text{INT}} \\ s_{2,\text{unp}}^{\text{INT}} \end{Bmatrix} = \frac{16K^2}{2-x_B} \begin{Bmatrix} -(2-y) \\ \lambda y \end{Bmatrix} \begin{Bmatrix} \Re e \\ \Im m \end{Bmatrix} \mathcal{C}_{\text{unp}}^{\text{INT}}(\mathcal{F}^{\text{eff}}), \quad (6.45)$$

$$c_{3,\text{unp}}^{\text{INT}} = -\frac{8Q^2K^3}{M^2(2-x_B)^2} \Re e \mathcal{C}_{T,\text{unp}}^{\text{INT}}(\mathcal{F}_T). \quad (6.46)$$

- Longitudinally polarized target:

$$c_{0,\text{LP}}^{\text{INT}} = -8\Lambda\Lambda y \Re e \left\{ \left(\frac{(2-y)^2}{1-y} + 2 \right) K^2 \mathcal{C}_{\text{LP}}^{\text{INT}}(\mathcal{F}) + \frac{\Delta^2}{Q^2} (1-y)(2-x_B) (\mathcal{C}_{\text{LP}}^{\text{INT}} + \Delta \mathcal{C}_{\text{LP}}^{\text{INT}})(\mathcal{F}) \right\}, \quad (6.47)$$

$$\begin{Bmatrix} c_{1,\text{LP}}^{\text{INT}} \\ s_{1,\text{LP}}^{\text{INT}} \end{Bmatrix} = 8\Lambda K \begin{Bmatrix} -\lambda y(2-y) \\ 2-2y+y^2 \end{Bmatrix} \begin{Bmatrix} \Re e \\ \Im m \end{Bmatrix} \mathcal{C}_{\text{LP}}^{\text{INT}}(\mathcal{F}), \quad (6.48)$$

$$\begin{Bmatrix} c_{2,\text{LP}}^{\text{INT}} \\ s_{2,\text{LP}}^{\text{INT}} \end{Bmatrix} = \frac{16\Lambda K^2}{2-x_B} \begin{Bmatrix} -\lambda y \\ 2-y \end{Bmatrix} \begin{Bmatrix} \Re e \\ \Im m \end{Bmatrix} \mathcal{C}_{\text{LP}}^{\text{INT}}(\mathcal{F}^{\text{eff}}), \quad (6.49)$$

$$s_{3,\text{LP}}^{\text{INT}} = \frac{8\Lambda Q^2 K^3}{M^2(2-x_B)^2} \Im m \mathcal{C}_{T,\text{LP}}^{\text{INT}}(\mathcal{F}_T). \quad (6.50)$$

- Transversely polarized target:

$$c_{0,\text{TP}}^{\text{INT}} = \frac{8M\sqrt{1-y}K}{Q} \left[-\lambda y \cos(\varphi) \Re e \left\{ \left(\frac{(2-y)^2}{1-y} + 2 \right) \mathcal{C}_{\text{TP+}}^{\text{INT}}(\mathcal{F}) + \Delta \mathcal{C}_{\text{TP+}}^{\text{INT}}(\mathcal{F}) \right\} + (2-y) \sin(\varphi) \Im m \left\{ \frac{(2-y)^2}{1-y} \mathcal{C}_{\text{TP-}}^{\text{INT}}(\mathcal{F}) + \Delta \mathcal{C}_{\text{TP-}}^{\text{INT}}(\mathcal{F}) \right\} \right], \quad (6.51)$$

$$\begin{Bmatrix} c_{1,\text{TP}}^{\text{INT}} \\ s_{1,\text{TP}}^{\text{INT}} \end{Bmatrix} = \frac{8M\sqrt{1-y}}{Q} \quad (6.52)$$

$$\times \left[\cos(\varphi) \begin{Bmatrix} -\lambda y(2-y) \\ 2-2y+y^2 \end{Bmatrix} \begin{Bmatrix} \Re e \\ \Im m \end{Bmatrix} \mathcal{C}_{\text{TP+}}^{\text{INT}} + \sin(\varphi) \begin{Bmatrix} 2-2y+y^2 \\ \lambda y(2-y) \end{Bmatrix} \begin{Bmatrix} \Im m \\ \Re e \end{Bmatrix} \mathcal{C}_{\text{TP-}}^{\text{INT}} \right] (\mathcal{F}),$$

$$\begin{Bmatrix} c_{2,\text{TP}}^{\text{INT}} \\ s_{2,\text{TP}}^{\text{INT}} \end{Bmatrix} = \frac{16M\sqrt{1-y}K}{Q(2-x_B)} \quad (6.53)$$

$$\begin{aligned} & \times \left[\cos(\varphi) \begin{Bmatrix} -\lambda y \\ 2-y \end{Bmatrix} \begin{Bmatrix} \Re e \\ \Im m \end{Bmatrix} \mathcal{C}_{\text{TP+}}^{\text{INT}} + \sin(\varphi) \begin{Bmatrix} 2-y \\ \lambda y \end{Bmatrix} \begin{Bmatrix} \Im m \\ \Re e \end{Bmatrix} \mathcal{C}_{\text{TP-}}^{\text{INT}} \right] (\mathcal{F}^{\text{eff}}) , \\ s_{3,\text{TP}}^{\text{INT}} &= \frac{8Q\sqrt{1-y}K^2}{M(2-x_B)^2} \cos(\varphi) \Im m \mathcal{C}_{T,\text{TP+}}^{\text{INT}} (\mathcal{F}_T) , \end{aligned} \quad (6.54)$$

$$c_{3,\text{TP}}^{\text{INT}} = \frac{8Q\sqrt{1-y}K^2}{M(2-x_B)^2} \sin(\varphi) \Im m \mathcal{C}_{T,\text{TP-}}^{\text{INT}} (\mathcal{F}_T) . \quad (6.55)$$

The twist-three coefficients, i.e., c_2^{INT} and s_2^{INT} have again the same functional dependence as the twist-two ones. However, this is not the case for c_0^{INT} , which depends only on the twist-two CFFs \mathcal{F} , and for c_3^{INT} and s_3^{INT} , induced by \mathcal{F}_T .

6.1.7 Angular harmonics in terms of GPDs

The Fourier coefficients displayed above are expressed in terms of the coefficients \mathcal{C} . They depend on Compton form factors (5.109) summed over quark flavors weighted with their charges squared,

$$\mathcal{F} = \sum_q Q_q^2 \mathcal{F}^q ,$$

with $\mathcal{F}^q = \{\mathcal{H}^q, \mathcal{E}^q, \tilde{\mathcal{H}}^q, \tilde{\mathcal{E}}^q, \mathcal{H}_{\text{eff}}^q, \mathcal{E}_{\text{eff}}^q, \tilde{\mathcal{H}}_{\text{eff}}^q, \tilde{\mathcal{E}}_{\text{eff}}^q\}$.

- Squared DVCS amplitude:

$$\begin{aligned} \mathcal{C}_{\text{unp}}^{\text{DVCS}} (\mathcal{F}, \mathcal{F}^*) &= \frac{1}{(2-x_B)^2} \left\{ 4(1-x_B) \left(\mathcal{H}\mathcal{H}^* + \tilde{\mathcal{H}}\tilde{\mathcal{H}}^* \right) - x_B^2 \left(\mathcal{H}\mathcal{E}^* + \mathcal{E}\mathcal{H}^* + \tilde{\mathcal{H}}\tilde{\mathcal{E}}^* + \tilde{\mathcal{E}}\tilde{\mathcal{H}}^* \right) \right. \\ &\quad \left. - \left(x_B^2 + (2-x_B)^2 \frac{\Delta^2}{4M^2} \right) \mathcal{E}\mathcal{E}^* - x_B^2 \frac{\Delta^2}{4M^2} \tilde{\mathcal{E}}\tilde{\mathcal{E}}^* \right\} , \end{aligned} \quad (6.56)$$

$$\begin{aligned} \mathcal{C}_{\text{LP}}^{\text{DVCS}} (\mathcal{F}, \mathcal{F}^*) &= \frac{1}{(2-x_B)^2} \left\{ 4(1-x_B) \left(\mathcal{H}\tilde{\mathcal{H}}^* + \tilde{\mathcal{H}}\mathcal{H}^* \right) - x_B^2 \left(\mathcal{H}\tilde{\mathcal{E}}^* + \tilde{\mathcal{E}}\mathcal{H}^* + \tilde{\mathcal{H}}\mathcal{E}^* + \mathcal{E}\tilde{\mathcal{H}}^* \right) \right. \\ &\quad \left. - x_B \left(\frac{x_B^2}{2} + (2-x_B) \frac{\Delta^2}{4M^2} \right) \left(\mathcal{E}\tilde{\mathcal{E}}^* + \tilde{\mathcal{E}}\mathcal{E}^* \right) \right\} , \end{aligned} \quad (6.57)$$

$$\begin{aligned} \mathcal{C}_{\text{TP+}}^{\text{DVCS}} (\mathcal{F}, \mathcal{F}^*) &= \frac{1}{(2-x_B)^2} \left\{ 2x_B (\mathcal{H}\tilde{\mathcal{E}}^* + \tilde{\mathcal{E}}\mathcal{H}^*) - 2(2-x_B)(\tilde{\mathcal{H}}\mathcal{E}^* + \tilde{\mathcal{H}}^*\mathcal{E}) + x_B^2 (\mathcal{E}\tilde{\mathcal{E}}^* + \tilde{\mathcal{E}}\mathcal{E}^*) \right\} , \\ \mathcal{C}_{\text{TP-}}^{\text{DVCS}} (\mathcal{F}, \mathcal{F}^*) &= \frac{2}{(2-x_B)^2} \left\{ (2-x_B)(\mathcal{H}\mathcal{E}^* - \mathcal{E}\mathcal{H}^*) - x_B(\tilde{\mathcal{H}}\tilde{\mathcal{E}}^* - \tilde{\mathcal{E}}\tilde{\mathcal{H}}^*) \right\} . \end{aligned} \quad (6.58)$$

- Interference of Bethe-Heitler and DVCS amplitudes:

In this case, a part of the twist-two level result is expressed in terms of the functions, which appear in the lowest twist approximation, and they have the following form [344]

$$\mathcal{C}_{\text{unp}}^{\text{INT}} = F_1 \mathcal{H} + \frac{x_B}{2-x_B} (F_1 + F_2) \tilde{\mathcal{H}} - \frac{\Delta^2}{4M^2} F_2 \mathcal{E} , \quad (6.59)$$

$$\mathcal{C}_{\text{LP}}^{\text{INT}} = \frac{x_B}{2-x_B} (F_1 + F_2) \left(\mathcal{H} + \frac{x_B}{2} \mathcal{E} \right) + F_1 \tilde{\mathcal{H}} - \frac{x_B}{2-x_B} \left(\frac{x_B}{2} F_1 + \frac{\Delta^2}{4M^2} F_2 \right) \tilde{\mathcal{E}}, \quad (6.60)$$

$$\begin{aligned} \mathcal{C}_{\text{TP+}}^{\text{INT}} &= (F_1 + F_2) \left\{ \frac{x_B^2}{2-x_B} \left(\mathcal{H} + \frac{x_B}{2} \mathcal{E} \right) + \frac{x_B \Delta^2}{4M^2} \mathcal{E} \right\} - \frac{x_B^2}{2-x_B} F_1 \left(\tilde{\mathcal{H}} + \frac{x_B}{2} \tilde{\mathcal{E}} \right) \\ &\quad + \frac{\Delta^2}{4M^2} \left\{ 4 \frac{1-x_B}{2-x_B} F_2 \tilde{\mathcal{H}} - \left(x_B F_1 + \frac{x_B^2}{2-x_B} F_2 \right) \tilde{\mathcal{E}} \right\}, \\ \mathcal{C}_{\text{TP-}}^{\text{INT}} &= \frac{1}{2-x_B} \left(x_B^2 F_1 - (1-x_B) \frac{\Delta^2}{M^2} F_2 \right) \mathcal{H} + \left\{ \frac{\Delta^2}{4M^2} \left((2-x_B) F_1 + \frac{x_B^2}{2-x_B} F_2 \right) \right. \\ &\quad \left. + \frac{x_B^2}{2-x_B} F_1 \right\} \mathcal{E} - \frac{x_B^2}{2-x_B} (F_1 + F_2) \left(\tilde{\mathcal{H}} + \frac{\Delta^2}{4M^2} \tilde{\mathcal{E}} \right). \end{aligned} \quad (6.61)$$

The additional terms that appear in the power-suppressed contributions are defined as

$$\Delta \mathcal{C}_{\text{unp}}^{\text{INT}} = -\frac{x_B}{2-x_B} (F_1 + F_2) \left\{ \frac{x_B}{2-x_B} (\mathcal{H} + \mathcal{E}) + \tilde{\mathcal{H}} \right\}, \quad (6.62)$$

$$\Delta \mathcal{C}_{\text{LP}}^{\text{INT}} = -\frac{x_B}{2-x_B} (F_1 + F_2) \left\{ \mathcal{H} + \frac{x_B}{2} \mathcal{E} + \frac{x_B}{2-x_B} \left(\tilde{\mathcal{H}} + \frac{x_B}{2} \tilde{\mathcal{E}} \right) \right\}, \quad (6.63)$$

$$\Delta \mathcal{C}_{\text{TP+}}^{\text{INT}} = -\frac{\Delta^2}{M^2} \left\{ F_2 \tilde{\mathcal{H}} - \frac{x_B}{2-x_B} \left(F_1 + \frac{x_B}{2} F_2 \right) \tilde{\mathcal{E}} \right\}, \quad (6.64)$$

$$\Delta \mathcal{C}_{\text{TP-}}^{\text{INT}} = \frac{\Delta^2}{M^2} (F_2 \mathcal{H} - F_1 \mathcal{E}). \quad (6.65)$$

Let us now list the coefficients involving the gluon transversity:

- Squared DVCS amplitude:

$$\begin{aligned} \mathcal{C}_{T,\text{unp}}^{\text{DVCS}} &= \frac{1}{(2-x_B)^2} \left\{ \mathcal{H}_T \left[(2-x_B) \mathcal{E}^* - x_B \tilde{\mathcal{E}}^* \right] - 2(2-x_B) \tilde{\mathcal{H}}_T \left[\mathcal{H}^* + \frac{\Delta^2}{4M^2} \mathcal{E}^* \right] \right. \\ &\quad \left. - \mathcal{E}_T \left[(2-x_B) \mathcal{H}^* - x_B \tilde{\mathcal{H}}^* \right] + \tilde{\mathcal{E}}_T \left[x_B (\mathcal{H}^* + \mathcal{E}^*) - (2-x_B) \tilde{\mathcal{H}}^* \right] \right\}, \end{aligned} \quad (6.66)$$

$$\begin{aligned} \mathcal{C}_{T,\text{LP}}^{\text{DVCS}} &= \frac{1}{(2-x_B)^2} \left\{ \mathcal{H}_T \left[(2-x_B) \mathcal{E}^* - x_B \tilde{\mathcal{E}}^* \right] + \tilde{\mathcal{H}}_T \left[2(2-x_B) \tilde{\mathcal{H}}^* - x_B \left(x_B - \frac{\Delta^2}{2M^2} \right) \tilde{\mathcal{E}}^* \right] \right. \\ &\quad \left. - \mathcal{E}_T \left[x_B \mathcal{H}^* - (2-x_B) \tilde{\mathcal{H}}^* + \frac{x_B^2}{2} (\mathcal{E}^* + \tilde{\mathcal{E}}^*) \right] \right. \\ &\quad \left. + \tilde{\mathcal{E}}_T \left[(2-x_B) \left(\mathcal{H}^* + \frac{x_B}{2} \mathcal{E}^* \right) - x_B \left(\tilde{\mathcal{H}}^* + \frac{x_B}{2} \tilde{\mathcal{E}}^* \right) \right] \right\}, \end{aligned} \quad (6.67)$$

$$\begin{aligned} \mathcal{C}_{T,\text{TP+}}^{\text{DVCS}} &= \frac{1}{(2-x_B)^2} \left\{ \left[4(1-x_B) \mathcal{H}_T - x_B^2 \mathcal{E}_T + x_B (2-x_B) \tilde{\mathcal{E}}_T \right] (\mathcal{H}^* + \tilde{\mathcal{H}}^*) \right. \\ &\quad - \tilde{\mathcal{H}}_T \left(x_B^2 + (1-x_B) \frac{\Delta^2}{M^2} \right) (2 \tilde{\mathcal{H}}^* + x_B \tilde{\mathcal{E}}^*) \\ &\quad - x_B \left[x_B \mathcal{H}_T + \left(\frac{x_B^2}{2} + (2-x_B) \frac{\Delta^2}{4M^2} \right) \mathcal{E}_T \right] (\mathcal{E}^* + \tilde{\mathcal{E}}^*) \\ &\quad \left. + \tilde{\mathcal{E}}_T \left[(2-x_B) \left(\frac{x_B^2}{2} + (2-x_B) \frac{\Delta^2}{4M^2} \right) \mathcal{E}^* - x_B^2 \left(\frac{x_B}{2} - \frac{\Delta^2}{4M^2} \right) \tilde{\mathcal{E}}^* \right] \right\}, \end{aligned} \quad (6.68)$$

$$\begin{aligned} \mathcal{C}_{T,\text{TP}-}^{\text{DVCS}} = & \frac{1}{(2-x_B)^2} \left\{ \left[4(1-x_B)\mathcal{H}_T - x_B^2\mathcal{E}_T + x_B(2-x_B)\tilde{\mathcal{E}}_T \right] (\mathcal{H}^* + \tilde{\mathcal{H}}^*) \right. \\ & - 2\tilde{\mathcal{H}}_T \left(x_B^2 + (1-x_B)\frac{\Delta^2}{M^2} \right) (\mathcal{H}^* + \mathcal{E}^*) \\ & - x_B \left(x_B\mathcal{H}_T - (2-x_B)\frac{\Delta^2}{4M^2}\tilde{\mathcal{E}}_T \right) (\mathcal{E}^* + \tilde{\mathcal{E}}^*) \\ & \left. - \mathcal{E}_T \left[\left(x_B^2 + (2-x_B)^2\frac{\Delta^2}{4M^2} \right) \mathcal{E}^* + x_B^2\frac{\Delta^2}{4M^2}\tilde{\mathcal{E}}^* \right] \right\}. \end{aligned} \quad (6.69)$$

- Interference of Bethe-Heitler and DVCS amplitudes:

$$\mathcal{C}_{T,\text{unp}}^{\text{INT}} = -F_2\mathcal{H}_T + 2 \left(F_1 + \frac{\Delta^2}{4M^2}F_2 \right) \tilde{\mathcal{H}}_T + F_1\mathcal{E}_T, \quad (6.70)$$

$$\mathcal{C}_{T,\text{LP}}^{\text{INT}} = F_2 \left\{ \mathcal{H}_T + \frac{x_B}{2}(2\tilde{\mathcal{H}}_T + \mathcal{E}_T + \tilde{\mathcal{E}}_T) \right\} + F_1(x_B\tilde{\mathcal{H}}_T + \tilde{\mathcal{E}}_T), \quad (6.71)$$

$$\begin{aligned} \mathcal{C}_{T,\text{TP}+}^{\text{INT}} = & (2F_1 + x_B F_2)\mathcal{H}_T + x_B \left(\frac{x}{2} - \frac{\Delta^2}{4M^2} \right) \left[2(F_1 + F_2)\tilde{\mathcal{H}}_T + F_2\mathcal{E}_T \right] \\ & + \left\{ x_B F_1 + \left(\frac{x_B^2}{2} + (2-x_B)\frac{\Delta^2}{4M^2} \right) F_2 \right\} \tilde{\mathcal{E}}_T, \end{aligned} \quad (6.72)$$

$$\begin{aligned} \mathcal{C}_{T,\text{TP}-}^{\text{INT}} = & (2F_1 + x_B F_2)\mathcal{H}_T - (2-x_B)\frac{\Delta^2}{4M^2} \left[2(F_1 + F_2)\tilde{\mathcal{H}}_T + F_2\mathcal{E}_T \right] + x_B \left(F_1 + F_2\frac{\Delta^2}{4M^2} \right) \tilde{\mathcal{E}}_T. \end{aligned} \quad (6.73)$$

This set of formulas is the complete result for the real-photon lepto-production cross section in the twist-three approximation. Below, presenting quantitative estimates, we will not discuss the case of transversely polarized target, therefore, the integration on the right-hand side of Eq. (6.9) with respect to φ gives 2π .

6.1.8 Determination of Compton form factors from interference

Restricting the consideration to four leading twist CFFs $\mathcal{F} = \{\mathcal{H}, \mathcal{E}, \tilde{\mathcal{H}}, \tilde{\mathcal{E}}\}$, we have eight observables given by the first harmonics $\cos(\phi)$ and $\sin(\phi)$ of the interference term, which are accessible away from the kinematical boundaries in polarized beam and target experiments. Thus, experiments with both longitudinally and transversely polarized target can measure all eight Fourier coefficients $c_{1,\Lambda}^{\text{INT}}$ and $s_{1,\Lambda}^{\text{INT}}$ and, thus, also $\Re/\Im \mathcal{C}_\Lambda^{\text{INT}}$ with $\Lambda = \{\text{unp}, \text{LP}, \text{TP}_x, \text{TP}_y\}$. Knowing these \mathcal{C} functions, we can invert them to obtain the CFFs:

$$\begin{aligned} \mathcal{H} = & \frac{2-x_B}{(1-x_B)D} \left\{ \left[\left(2-x_B + \frac{4x_B^2 M^2}{(2-x_B)\Delta^2} \right) F_1 + \frac{x_B^2}{2-x_B} F_2 \right] \mathcal{C}_{\text{unp}}^{\text{INT}} \right. \\ & \left. - (F_1 + F_2) \left[x_B \mathcal{C}_{\text{LP}}^{\text{INT}} + \frac{2x_B^2 M^2}{(2-x_B)\Delta^2} (x_B \mathcal{C}_{\text{LP}}^{\text{INT}} - \mathcal{C}_{\text{TP}+}^{\text{INT}}) \right] + F_2 \mathcal{C}_{\text{TP}-}^{\text{INT}} \right\}, \end{aligned} \quad (6.74)$$

$$\begin{aligned} \mathcal{E} = & \frac{2-x_B}{(1-x_B)D} \left\{ \left[4 \frac{1-x_B}{2-x_B} F_2 - \frac{4M^2 x_B^2}{(2-x_B)\Delta^2} F_1 \right] \mathcal{C}_{\text{unp}}^{\text{INT}} \right. \\ & \left. + \frac{4x_B M^2}{(2-x_B)\Delta^2} (F_1 + F_2) (x_B \mathcal{C}_{\text{LP}}^{\text{INT}} - \mathcal{C}_{\text{TP}+}^{\text{INT}}) + \frac{4M^2}{\Delta^2} F_1 \mathcal{C}_{\text{TP}-}^{\text{INT}} \right\}, \end{aligned} \quad (6.75)$$

twist	sector \mathcal{C} 's	harmonics in \mathcal{I}				p of \mathcal{Q}^{-p}	Δ_\perp^l behavior	
		unp	LP	TP_x	TP_y		unp, LP	TP
two	$\Re \mathcal{C}(\mathcal{F}), \Delta \mathcal{C}(\mathcal{F})$	c_1, c_0	c_1, c_0	c_1, c_0	$s_1, -$	1,2	1,0	0,1
	$\Im \mathcal{C}(\mathcal{F}), \Delta \mathcal{C}(\mathcal{F})$	$s_1, -$	$s_1, -$	$s_1, -$	c_1, c_0	1,2	1,0	0,1
three	$\Re \mathcal{C}(\mathcal{F}^{\text{eff}})$	c_2	c_2	c_2	s_2	2	2	1
	$\Im \mathcal{C}(\mathcal{F}^{\text{eff}})$	s_2	s_2	s_2	c_2	2	2	1
two	$\Re \mathcal{C}_T(\mathcal{F}_T)$	c_3	-	-	-	1	3	2
	$\Im \mathcal{C}_T(\mathcal{F}_T)$	-	s_3	s_3	c_3	1	3	2

Table 6: Fourier coefficients c_i^{INT} and s_i^{INT} of the interference term defined in Section 6.1.6, while the corresponding \mathcal{C} coefficients are given in Section 6.1.7.

$$\begin{aligned} \tilde{\mathcal{H}} = & \frac{2 - x_B}{(1 - x_B)D} \left\{ (2 - x_B)F_1 \mathcal{C}_{\text{LP}}^{\text{INT}} \right. \\ & \left. - x_B(F_1 + F_2)\mathcal{C}_{\text{unp}}^{\text{INT}} + \left[\frac{2x_B M^2}{\Delta^2} F_1 + F_2 \right] (x_B \mathcal{C}_{\text{LP}}^{\text{INT}} - \mathcal{C}_{\text{TP+}}^{\text{INT}}) \right\}, \end{aligned} \quad (6.76)$$

$$\begin{aligned} \tilde{\mathcal{E}} = & \frac{2 - x_B}{(1 - x_B)D} \left\{ \frac{4M^2}{\Delta^2} (F_1 + F_2) (x_B \mathcal{C}_{\text{unp}}^{\text{INT}} + \mathcal{C}_{\text{TP-}}^{\text{INT}}) \right. \\ & \left. + \left[4 \frac{1 - x_B}{x_B} F_2 - \frac{4x_B M^2}{\Delta^2} F_1 \right] \mathcal{C}_{\text{LP}}^{\text{INT}} - \frac{4(2 - x_B)M^2}{x_B \Delta^2} F_1 \mathcal{C}_{\text{TP+}}^{\text{INT}} \right\}, \end{aligned} \quad (6.77)$$

where

$$D = 4 \left(F_1^2 - \frac{\Delta^2}{4M^2} F_2^2 \right) \left(1 - \frac{\Delta_{\min}^2}{\Delta^2} \right).$$

Consequently, the measurement of all four Fourier coefficients $c_{0,A}^{\text{INT}}$, as well as the four twist-two DVCS coefficients $c_{0,A}^{\text{DVCS}}$ can serve as experimental consistency checks. Alternatively, they can be used to extract CFFs. Thus, experiments with longitudinally polarized target have the potential to extract the real part of all four CFFs as well as two linear combinations of their imaginary parts from the interference term alone. The missing two imaginary parts could then, in principle, be obtained from the DVCS cross section, i.e., by measuring $c_{0,\text{unp}}^{\text{DVCS}}$ and $c_{0,\text{LP}}^{\text{DVCS}}$.

6.1.9 Physical observables and access to GPDs

As we have seen, the cross section for lepton production of the real photon possesses very rich angular structure. The goal of experimental measurements is to pin down the GPDs, and this requires a clean disentanglement of different components of the cross section (6.9). To go along this line, we introduce appropriate asymmetries in Section 6.1.10 and demonstrate how a Fourier transform can distinguish between the interference and squared DVCS contributions.

So far we have introduced eight CFFs at the twist-two level, with four of them from the gluonic transversity contribution. Four new CFFs appear at the twist-three level. These sectors can be separated due to their characteristic azimuthal dependence as summarized in Table 6 for the interference and in Table 7 for the squared DVCS amplitude, respectively.

Let us first examine the issue of the dominance of each of the three terms (6.22) – (6.24) in the lepton production cross section (6.9) in different kinematical regions. To do this, we need

interference of twist	\mathcal{C} 's	harmonics in $ \mathcal{T}_{\text{DVCS}} ^2$				p of \mathcal{Q}^{-p}	Δ_\perp^l behavior	
		unp	LP	TP_x	TP_y		unp, LP	TP
two & two	$\Re \mathcal{C}(\mathcal{F}, \mathcal{F}^*)$	c_0	c_0	c_0	-	2	0	1
	$\Im \mathcal{C}(\mathcal{F}, \mathcal{F}^*)$	-	-	-	c_0	2	-	1
two & three	$\Re \mathcal{C}(\mathcal{F}^{\text{eff}}, \mathcal{F}^*)$	c_1	c_1	c_1	s_1	3	1	0
	$\Im \mathcal{C}(\mathcal{F}^{\text{eff}}, \mathcal{F}^*)$	s_1	s_1	s_1	c_1	3	1	0
two & two	$\Re \mathcal{C}_T(\mathcal{F}_T, \mathcal{F}^*)$	c_2	-	-	-	2	2	-
	$\Im \mathcal{C}_T(\mathcal{F}_T, \mathcal{F}^*)$	-	s_2	s_2	c_2	2	2	1

Table 7: Fourier coefficients c_i^{DVCS} and s_i^{DVCS} of the squared DVCS amplitude $|\mathcal{T}_{\text{DVCS}}|^2$ defined in Section 6.1.5, while the corresponding \mathcal{C} coefficients are given in Section 6.1.7.

to know the functional dependence of the Fourier coefficients (6.22) – (6.24) on scaling variables and transferred momenta. Apart from the explicit x_B -dependence of the multiplicative prefactors there is also x_B -dependence hidden in CFFs. For instance, the unpolarized form factors \mathcal{H} and \mathcal{E} behave approximately like x_B^{-1} in the small- x_B region. Thus, for general kinematical settings, we expect from Eqs. (6.26), (6.34), and (6.44) that $c_0^{\text{BH}} \sim x_B^2 c_0^{\text{DVCS}} \sim x_B c_1^{\text{INT}}/K$ for the scattering on the unpolarized target. Taking now into account the kinematical prefactors in Eqs. (6.22) – (6.24) and the behavior of the BH-propagators (6.17), we realize that the ratio of the DVCS to BH amplitude behaves like $\sqrt{-(1-y)\Delta^2/y^2\mathcal{Q}^2}$. Obviously, for small (large) y the DVCS (BH) term dominates. As compared to the squared amplitudes, the interference term, after subtraction of c_0^{INT} , has an additional factor $\sqrt{\Delta_\perp^2/\Delta^2}$. Note, that the beam spin-flip contributions provide always an additional damping by a power of the factor y . For the unpolarized or longitudinally polarized target, higher harmonics in any of the three terms are suppressed by powers of K . However, in case of gluonic transversity, this goes in parallel with the enhancement by \mathcal{Q}^2/M_N^2 . It is important that the lower harmonics in the interference term, i.e., c_0^{INT} , appear at power suppressed level but expressed in terms of twist-two Compton form factors. Since, unlike c_1 , they are not proportional to the factor K , they can be rather important and sizable in the regions close to the kinematical boundaries. In case of the transversely polarized target, we observe that both higher and lower twist-three harmonics are suppressed by one power of K in the interference term.

The analytical structure and simple counting rules given above, provide a guideline on how to separate the three different parts in the lepto-production cross section. In single spin-flip experiments, which give access to the imaginary part of CFFs, the BH cross section drops out, while in unpolarized or double spin-flip experiments it does not and one needs to subtract it. This can certainly be done for not very small values of y . The interference and squared DVCS terms have different azimuthal angular dependence due to the presence of the BH-propagators in the interference term. In principle, this fact can be used to separate them by a Fourier analysis. However, this method requires very high-statistics data, from the experimental side, and a better understanding of twist-four contributions, from the theoretical side.

Due to different charge conjugation properties of individual components, it is possible to use the charge asymmetry to separate the interference and squared DVCS terms. The interference term is charge-odd and can be extracted in facilities that possess both positively and negatively

charged lepton beams [389, 390], i.e.,

$$d\sigma^+ - d\sigma^- \sim \frac{1}{x_B y^3 \mathcal{P}_1(\phi) \mathcal{P}_2(\phi) \Delta^2} \left\{ c_0^{\text{INT}} + \sum_{n=1}^3 [c_n^{\text{INT}} \cos(n\phi) + s_n^{\text{INT}} \sin(n\phi)] \right\}, \quad (6.78)$$

where we used the convention $d^\pm \sigma = d\sigma_{e^\pm}$. The measurement of the charge asymmetry and consequent extraction of separate harmonics provides the real (unpolarized or double spin-flip experiments) and imaginary (single spin-flip experiments) parts of linear combinations of twist-two and twist-three CFFs. The explicit projection procedure of these harmonics will be discussed below in Section 6.1.11. Moreover, the charge-even part is given by the sum of the BH and DVCS cross section. The subtraction of the BH part gives then the Fourier coefficients of the DVCS cross section:

$$d^+ \sigma + d^- \sigma - 2d^{\text{BH}} \sigma \sim \frac{1}{y^2 \mathcal{Q}^2} \left\{ c_0^{\text{DVCS}} + \sum_{n=1}^2 [c_n^{\text{DVCS}} \cos(n\phi) + s_n^{\text{DVCS}} \sin(n\phi)] \right\}. \quad (6.79)$$

For a polarized beam and target with all polarization options, the real and imaginary parts of all four CFFs in the twist-three sector can be extracted from the interference term alone by projecting onto the $\cos(2\phi)$ and $\sin(2\phi)$ harmonics and using Eqs. (6.74) – (6.77). Alternatively, knowing the twist-two sector and having only a longitudinally polarized target, one can employ, in addition, the squared DVCS term, i.e., its $\cos(\phi)$ and $\sin(\phi)$ harmonics, to access the full twist-three sector.

For gluonic transversity, the $\cos(3\phi)$ and $\sin(3\phi)$ harmonics in the interference term can only provide one imaginary and three real parts of certain linear combinations of \mathcal{F}_T . Missing information, in principle, can be obtained from the $\cos(2\phi)$ and $\sin(2\phi)$ harmonics of the squared DVCS term. Note here that again a polarized beam and target with all polarizations is necessary. Moreover, the gluonic transversity is suppressed by α_s/π , so one expects a stronger contamination by twist-four effects [388].

As we discussed, a combination of the charge asymmetry with different nucleon-lepton polarizations and projection of the corresponding harmonics provides, at least in principle, a way to explore the real and imaginary part of all CFFs. This gives maximal access to all GPDs, which enter in a convolution with the real or imaginary part of the coefficient functions. Since these formulas cannot be deconvoluted in practice [391], one has to rely on models with a set of free parameters, as discussed in Section 3.13, which has to be adjusted to experimental data on CFFs.

6.1.10 Asymmetries

The measurements of the cross section (6.9) in different setups, as discussed in the preceding section, would directly lead to determination of the CFFs. However, from the experimental point of view, it is simpler to measure asymmetries, thus avoiding the issue of the absolute normalization. Let us now discuss the separation of twist-two and twist-three sectors in terms of asymmetries.

The charge asymmetry

$$A_C = \left(\int_{-\pi/2}^{\pi/2} d\phi \frac{d^+ \sigma^{\text{unp}} - d^- \sigma^{\text{unp}}}{d\phi} - \int_{\pi/2}^{3\pi/2} d\phi \frac{d^+ \sigma^{\text{unp}} - d^- \sigma^{\text{unp}}}{d\phi} \right) \Bigg/ \int_0^{2\pi} d\phi \frac{d^- \sigma^{\text{unp}} + d^+ \sigma^{\text{unp}}}{d\phi}, \quad (6.80)$$

for unpolarized settings contains the contribution of all harmonics due to the presence of the non-negligible ϕ -dependence of BH propagators:

$$A_C \sim \sum_{n=0}^3 I_{1,n}^c c_n^{\text{INT}}, \quad (6.81)$$

with

$$I_{1,n}^c \sim \left(\int_{-\pi/2}^{\pi/2} d\phi \frac{\cos(n\phi)}{\mathcal{P}_1(\phi)\mathcal{P}_2(\phi)} - \int_{\pi/2}^{3\pi/2} d\phi \frac{\cos(n\phi)}{\mathcal{P}_1(\phi)\mathcal{P}_2(\phi)} \right), \quad (6.82)$$

while the normalization is not affected by twist-three corrections. If the final photon is collinear to the incoming (massless) lepton, $\mathcal{P}_1(\phi)$ is peaked around $\phi = \pi$. Thus, the ratio $I_{1,n}^c/I_{1,1}^c$ approaches plus or minus one, and all harmonics contribute on equal footing. However, since K is then of order Δ^2/\mathcal{Q}^2 , only c_0^{INT} and c_1^{INT} give essential contributions at the same order in Δ^2/\mathcal{Q}^2 . Thus, for this asymmetry, c_0^{INT} can give an essential effect for large y , since the twist-two part becomes small. For $y \ll y_{\text{col}}$, all twist-three harmonics are suppressed in addition by the K -factor. From the expansion of $I_{1,n}^c$ in powers of K we get

$$A_C \sim c_{1,\text{unp}}^{\text{INT}} - \frac{1}{3}c_{3,\text{unp}}^{\text{INT}} - \frac{2(3-2y)}{2-y} \frac{K}{1-y} \left(c_{0,\text{unp}}^{\text{INT}} - \frac{1}{3}c_{2,\text{unp}}^{\text{INT}} \right) + \dots \quad (6.83)$$

So, one would expect the contamination of the leading twist-two prediction by a $\sqrt{-\Delta^2/\mathcal{Q}^2}$ -suppressed term, which, however, contains only twist-two CFFs. Even if this $1/\mathcal{Q}$ -contamination is small, A_C still fails to extract solely the $c_{1,\text{unp}}^{\text{INT}}$ coefficient of the interference term since it gets an additive correction from $c_{3,\text{unp}}^{\text{INT}}$, induced by the gluon transversity and higher twist effects. Note, however, that the gluon contribution is suppressed by a power of the strong coupling α_s , so it probably does not strongly affect the twist-two coefficient $c_{1,\text{unp}}^{\text{INT}}$. Therefore, as a first order approximation, the definition (6.80) can be used for an order of magnitude estimate of the effect.

The (definite charge) beam-spin asymmetry on the unpolarized target,

$$A_{\text{SL}} = \left(\int_0^\pi d\phi \frac{d\sigma^\uparrow - d\sigma^\downarrow}{d\phi} - \int_\pi^{2\pi} d\phi \frac{d\sigma^\uparrow - d\sigma^\downarrow}{d\phi} \right) \Big/ \int_0^{2\pi} d\phi \frac{d\sigma^\uparrow + d\sigma^\downarrow}{d\phi}, \quad (6.84)$$

does not separate the interference term alone. It does contain contributions from the squared DVCS amplitude:

$$A_{\text{SL}} \sim \pm \sum_{n=1}^2 I_{1,n}^s s_{n,\text{unp}}^{\text{INT}} - \frac{\Delta^2}{y\mathcal{Q}^2} x_B s_{1,\text{unp}}^{\text{DVCS}}, \quad (6.85)$$

with

$$I_{1,n}^s = -\frac{1}{y^2} \left(\int_0^\pi d\phi \frac{\sin(n\phi)}{\mathcal{P}_1(\phi)\mathcal{P}_2(\phi)} - \int_\pi^{2\pi} d\phi \frac{\sin(n\phi)}{\mathcal{P}_1(\phi)\mathcal{P}_2(\phi)} \right). \quad (6.86)$$

In the collinear limit, the asymmetry vanishes. On the other hand, for $y \rightarrow 0$, it is determined by the twist-three coefficient $s_{1,\text{unp}}^{\text{DVCS}}$. The expansion with respect to K reads:

$$A_{\text{SL}} \sim s_{1,\text{unp}}^{\text{INT}} - \frac{2(3-2y)}{3(2-y)} \frac{K}{1-y} s_{2,\text{unp}}^{\text{INT}} - \frac{(1-y)(2-y)\Delta^2}{y\mathcal{Q}^2} x_B s_{1,\text{unp}}^{\text{DVCS}} + \dots \quad (6.87)$$

The $1/Q$ -suppressed effect generated by the BH propagators induces contamination due to the second harmonic suppressed by $K/(1-y)$. Depending on the kinematics and the size of multi-particle contributions, this contamination together with $s_{1,\text{unp}}^{\text{DVCS}}$ may prevent clean access to the twist-two GPDs even from high-precision measurements of this asymmetry. Note, that for general reasons, $s_{3,\text{unp}}^{\text{INT}}$ ($s_{2,\text{unp}}^{\text{DVCS}}$) is absent in the unpolarized interference (squared DVCS) term. However, the normalization of A_{SL} is affected by $1/Q$ -effects in the interference term, mainly due to the coefficient $c_{0,\text{unp}}^{\text{INT}}$.

6.1.11 Electron and positron beam options

When lepton beams of both charges are available, this provides clean separation of twist-two and twist-three GPDs. In these settings, one can discuss charge-odd and charge-even parts of the cross section (6.9), which extract the interference, and squared DVCS and BH amplitudes, respectively. The integrated charge-even part of the cross section does not contain any twist-three contributions—the interference term cancels there. On the other hand, after azimuthal averaging, the c_0 coefficient of the squared DVCS and all harmonics of squared BH amplitudes survive. So, it is convenient to use c_0 as a unique normalization of the asymmetries discussed below. Namely, independently from the target polarization we introduce

$$\mathcal{N}_{+-}^{-1} \equiv \int_0^{2\pi} d\phi \frac{d^+ \sigma^{\text{unp}} + d^- \sigma^{\text{unp}}}{d\phi} = 2 \int_0^{2\pi} d\phi \frac{d^{\text{BH}} \sigma^{\text{unp}} + d^{\text{DVCS}} \sigma^{\text{unp}}}{d\phi}. \quad (6.88)$$

- Charge-odd part:

In this case, one ends up with the interference term alone. However, because of the ϕ -dependence of the BH propagators we have to include an additional weight factor and use the measure

$$dw = 2\pi \frac{\mathcal{P}_1(\phi)\mathcal{P}_2(\phi)d\phi}{\int_0^{2\pi} \mathcal{P}_1(\phi')\mathcal{P}_2(\phi')d\phi'}, \quad (6.89)$$

for the azimuthal integration in order to compensate for the strong ϕ -dependence of the product of lepton propagators. The measure dw has the properties

$$\int_0^{2\pi} dw = 2\pi, \quad dw(\phi) = dw(-\phi) = dw(\phi + 2\pi).$$

Now we can exactly separate the Fourier coefficients in Eq. (6.24). Note that dw has its minimum at $\phi = \pi$, when the outgoing photon lies in the lepton scattering plane. In case when its momentum is collinear to the lepton beam, this minimum approaches zero in the massless limit.

To project out different harmonics, one can either (i) do the azimuthal averaging with appropriate weights, namely,

$$\cos(n\phi)dw, \quad \sin(n\phi)dw, \quad (6.90)$$

where $n = 0, \dots, 3$, or, (ii) use the fact that the Fourier sum for the cross section has only a finite number of terms, and integrate over different partitions of the azimuthal sphere. It is important to realize that the statistical error acquired via the extraction of the Fourier harmonics with the first weighting procedure is smaller compared to the latter, where the coefficients are found by

forming asymmetries⁴⁴. Let us present the charge odd asymmetries (CoA), which distinguish the cosine, $\cos(n\phi)$, and sine, $\sin(n\phi)$, harmonics.

The cos-harmonics, i.e., c_n^{INT} coefficients, are projected out by means of the integrals

$$\text{CoA}_{c(0)}^A = \mathcal{N}_{+-} \int_0^{2\pi} dw \frac{d^+ \sigma^A - d^- \sigma^A}{d\phi}, \quad (6.91)$$

$$\text{CoA}_{c(1)}^A = \mathcal{N}_{+-} \left(\int_{-\pi/2}^{\pi/2} dw \frac{d^+ \sigma^A - d^- \sigma^A}{d\phi} - \int_{\pi/2}^{3\pi/2} dw \frac{d^+ \sigma^A - d^- \sigma^A}{d\phi} \right) + \frac{1}{3} \text{CoA}_{c(3)}^A, \quad (6.92)$$

$$\text{CoA}_{c(n)}^A = \mathcal{N}_{+-} \sum_{k=1}^{2n} (-1)^{k+1} \int_{(2k-3)\pi/(2n)}^{(2k-1)\pi/(2n)} dw \frac{d^+ \sigma^A - d^- \sigma^A}{d\phi}, \quad (6.93)$$

with n running over $n = 2, 3$ in the last equation, and A stands for $A = \{\text{unp}, \text{LP}, \text{TP}\}$. The projection can be achieved by an appropriate flip of the target polarization vector. For the transversely polarized target, asymmetries are given in terms of two different combinations of CFFs. They are separable by the projection of the first odd and even harmonics in φ , while the average $\int_0^{2\pi} d\varphi \text{CoA}^{\text{TP}} = 0$ vanishes.

Next, the sin-harmonics, s_n^{INT} , can analogously be separated with the help of the formulas

$$\text{CoA}_{s(1)}^A = \mathcal{N}_{+-} \left(\int_0^\pi dw \frac{d^+ \sigma^A - d^- \sigma^A}{d\phi} - \int_\pi^{2\pi} dw \frac{d^+ \sigma^A - d^- \sigma^A}{d\phi} \right) - \frac{1}{3} \text{CoA}_{s(3)}^A, \quad (6.94)$$

$$\text{CoA}_{s(n)}^A = \mathcal{N}_{+-} \sum_{k=1}^{2n} (-1)^{k+1} \int_{(k-1)\pi/n}^{k\pi/n} dw \frac{d^+ \sigma^A - d^- \sigma^A}{d\phi}, \quad (6.95)$$

where $n = 2, 3$.

- Charge-even part:

Let us now define the azimuthal asymmetries of the charge-even part. To do this in the cleanest way, we subtract first the BH term. This might be possible in practice in the analysis of experimental data, since the BH cross section is known exactly (up to electromagnetic radiative corrections), see Section 6.1.4. Of course, it is assumed that the nucleon form factors are known from other measurements. This gives the squared DVCS amplitude

$$2d^{\text{DVCS}}\sigma = d^+ \sigma + d^- \sigma - 2d^{\text{BH}}\sigma.$$

Then an appropriate azimuthal averaging, now with the conventional measure $d\phi$, separates the cos-harmonics, c_n^{DVCS} , via

$$\text{CeA}_{c(0)}^A = 2\mathcal{N}_{+-} \int_0^{2\pi} d\phi \frac{d^{\text{DVCS}}\sigma^A}{d\phi}, \quad (6.96)$$

$$\text{CeA}_{c(n)}^A = 2\mathcal{N}_{+-} \sum_{k=1}^{2n} (-1)^{k+1} \int_{(2k-3)\pi/(2n)}^{(2k-1)\pi/(2n)} d\phi \frac{d^{\text{DVCS}}\sigma^A}{d\phi}, \quad (6.97)$$

⁴⁴This generic statement can be definitely made for a cross section of the form $d\sigma/d\phi = \alpha_0 + \alpha_1 \cos \phi$. The weights matching the above two methods are then $w_1 = \cos \phi$, and $w_2 = \text{sgn}(\cos \phi)$ corresponding to the left-right asymmetry. The former generates a smaller statistical error in the course of the extraction of α_1 compared to the latter.

with $n = 1, 2$, and sin-dependent coefficients by means of

$$\text{CeA}_{s(n)}^A = 2\mathcal{N}_{+-} \sum_{k=1}^{2n} (-1)^{k+1} \int_{(k-1)\pi/n}^{k\pi/n} d\phi \frac{d^{\text{DVCS}}\sigma^A}{d\phi}, \quad (6.98)$$

with $n = 1, 2$.

To conclude, an experimental facility having electron and positron beams is an ideal place to study GPDs.

6.1.12 Electron or positron beam option

Another situation is when only one kind of the lepton beam is available. Then, the study of single (lepton or nucleon) spin asymmetries allows one to remove the background BH cross section. Note, however, that when both the beam and target are polarized, and one studies double-spin asymmetries, one gets the contamination from the BH harmonics too. In the single (lepton or hadron) spin experiments, still the twist-two coefficient s_1^{INT} is contaminated by power-suppressed effects, since both the interference and squared DVCS terms contribute. The best one can do in these circumstances is to cancel completely the twist-three part of the interference term in the numerator. However, one will have still the power-suppressed DVCS cross section. For instance, for the single lepton-spin experiment one is able to probe $s_{1,\text{unp}}^{\text{INT}}$ plus $(1-y)\Delta^2/yQ^2$ corrections from $|\mathcal{T}_{\text{DVCS}}|^2$. This can be done using the formula

$$\text{SSA}_1 = \left(\int_0^\pi dw \frac{d\sigma^\uparrow - d\sigma^\downarrow}{d\phi} - \int_\pi^{2\pi} dw \frac{d\sigma^\uparrow - d\sigma^\downarrow}{d\phi} - \frac{1}{3} \sum_{k=1}^6 (-1)^{k+1} \int_{(k-1)\pi/6}^{k\pi/6} dw \frac{d\sigma^\uparrow - d\sigma^\downarrow}{d\phi} \right) \Bigg/ \int_0^{2\pi} d\phi \frac{d\sigma^\uparrow + d\sigma^\downarrow}{d\phi}. \quad (6.99)$$

Analogous extraction of the twist-two coefficient $s_{1,\text{LP}}^{\text{INT}}$ is available for the nucleon-spin asymmetry (with the unpolarized lepton beam). The projection of the same components can be achieved by weighting the integral with $\sin(\phi)dw$.

For smaller value of y , the contamination from the squared DVCS term may be large. Let us demonstrate that a separation of the interference and squared DVCS terms can be achieved by a Fourier transform. The multiplication of the cross section with $dw/d\phi$ induces new harmonics in the squared DVCS term. Projection of all three harmonics, i.e., measuring the asymmetries

$$\text{SSA}_n = \left(\sum_{k=1}^{2n} (-1)^{k+1} \int_{(k-1)\pi/n}^{k\pi/n} dw \frac{d\sigma^\uparrow - d\sigma^\downarrow}{d\phi} \right) \Bigg/ \int_0^{2\pi} d\phi \frac{d\sigma^\uparrow + d\sigma^\downarrow}{d\phi}, \quad (6.100)$$

(where $n = 2, 3$) provides the desired Fourier coefficients:

$$s_{1,\text{unp}}^{\text{INT}} \sim \left(\text{SSA}_1 - \frac{w_{s,11}}{w_{s,13}} \text{SSA}_3 \right), \quad s_{2,\text{unp}}^{\text{INT}} \sim \left(\text{SSA}_2 - \frac{w_{s,12}}{w_{s,13}} \text{SSA}_3 \right), \quad s_{1,\text{unp}}^{\text{DVCS}} \sim \text{SSA}_3, \quad (6.101)$$

with $w_{s,km} = \int_0^{2\pi} dw \sin(k\phi) \sin(m\phi)$. Thus, the extraction of twist-three harmonics is, in principle, possible, however, it requires high precision data. Such a modified Fourier analysis can be used to separate the coefficients of the interference and squared DVCS term also in the unpolarized and double spin-flip experiments. But one should realize that the weighted cross section contains now four odd and five even harmonics, and that the BH cross section must be removed.

6.1.13 Remarks on state-of-the-art of DVCS

To date, theoretical analyses of the deeply virtual Compton scattering were performed to next-to-leading order accuracy for a number of twist-two observables [399, 279, 280] and in Born approximation for certain twist-three asymmetries [400, 328]. These calculations agree rather well with the available experimental data [393, 394, 395, 396] (see Ref. [397] for a recent comprehensive summary) even with current crude knowledge of parameter dependence of GPDs, as we outlined in Section 3.13. Models for power suppressed effects in DVCS amplitudes were suggested based on renormalon analysis [402, 403] and an approach with introduction of the intrinsic transverse momentum dependence in GPDs [364] with the framework developed in Ref. [404] for light-cone distribution amplitudes.

The current experimental facilities do not possess complete exclusivity with respect to the final state particles. The usual situation is that the recoiled nucleon remains undetected and reconstructed using the missing mass technique. This represents an uncertainty in interpretation of the experimental data. Namely, the currently used technique cannot unambiguously establish whether it was a single nucleon or a nucleon accompanied by soft pion(s) that struck the detector. This calls for consideration of the associate soft-pion production along with DVCS. This problem has been addressed in several papers [405, 406, 407, 408] to which we refer for further reading (see also Ref. [409]).

6.2 Leptoproduction of lepton pairs

In the present section, we will discuss a process which allows to lift the kinematical restriction $\eta = \xi$ of the deeply virtual Compton scattering. As we have thoroughly discussed in the preceding sections, this restriction limited the measurement of GPDs via the imaginary part of the deeply virtual Compton scattering amplitudes in Born approximation solely to the line $\eta = \xi$ in the longitudinal momentum fraction space, $F^q(\xi, \xi, \Delta^2)$ (see Fig. 22). The way to eliminate this constraint is to have both the incoming and outgoing photons to be off-shell and carry unequal virtualities. This calls for consideration of the lepton pair production in the lepton scattering off the nucleon $e(k)N(p_1) \rightarrow e(k')N(p_2)\ell(\ell_-)\bar{\ell}(\ell_+)$.

6.2.1 Mapping the surface of GPDs

The advantage of having varying masses of the incoming and outgoing photons is that this allows to probe GPDs away from the diagonal $|\xi| = \eta$, the only kinematics which is accessible in DVCS. The skewness variable η is proportional to the sum $Q^2 + M_{\ell\bar{\ell}}^2$ (with $Q^2 = -q_1^2$ and $M_{\ell\bar{\ell}}^2 = q_2^2$) while ξ is essentially the difference $Q^2 - M_{\ell\bar{\ell}}^2$ (cf. Eq. (5.12)). The boundaries of the (ξ, η) region probed in the process are set by the following kinematical constraints:

- The skewness parameter lies in the region $\eta_{\min} < \eta < 0$, where the lower bound comes from the kinematical condition $|\Delta^2| \geq |\Delta_{\min}^2|$:

$$\eta_{\min} \leq \sqrt{-\Delta^2/(4M_N^2 - \Delta^2)}. \quad (6.102)$$

- The upper and lower value of ξ is a consequence of the quasi-real limit of the space- or timelike photon

$$-\eta < \xi < \eta. \quad (6.103)$$

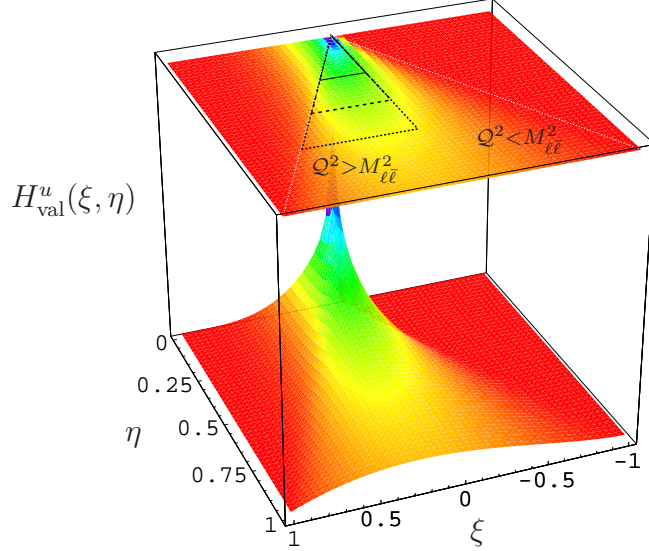


Figure 48: The coverage of a sample GPD surface—the valence component of the u -quark distribution—with electron beams of different energies [285, 354]. The three contours displayed on the figure embrace the areas to be probed for different values of the electron beam energy E , the lepton energy loss y , and the t -channel momentum transfer Δ^2 : (i) solid contour corresponds to $E = 11 \text{ GeV}$, $y = 0.5$, and $\Delta^2 = -0.3 \text{ GeV}^2$ ($M_N^2 \leq Q^2 \leq 10 \text{ GeV}^2$), (ii) dashed contour corresponds to $E = 25 \text{ GeV}$, $y = 0.75$, and $\Delta^2 = -1 \text{ GeV}^2$ ($-4\Delta^2 \leq Q^2 \leq 20 \text{ GeV}^2$), (iii) dotted contour corresponds to $E = 40 \text{ GeV}$, $y = 0.9$, and $\Delta^2 = -3 \text{ GeV}^2$ ($-4\Delta^2 \leq Q^2 \leq 35 \text{ GeV}^2$). We discarded in this plot the change of the GPD with Δ^2 for different kinematical settings.

It can be seen from Fig. 48 that the area of the surface probed in the production of the lepton pair with electron beam of increasing energy E is quite extensive: (solid contour) $E = 11 \text{ GeV}$, (dashed contour) $E = 25 \text{ GeV}$, (dotted contour) $E = 40 \text{ GeV}$. It is obvious that the higher the energy of the lepton beam, the higher Δ^2 are allowed with observed applicability of the perturbative analysis of the Compton amplitude, and thus the higher values of η are achieved.

Above, only the case $Q^2 > M_{\ell\bar{\ell}}^2$ was implied, which probes $\xi > 0$ component of GPDs. For the reversed inequality sign, one gets information on the region $\xi < 0$ and probes patches of the two-dimensional surface analogous to the previous case. The positive mass of the final-state photon allows to directly access only the “exclusive” component of GPDs, with $\eta > |\xi|$, where GPDs look like distribution amplitudes. To access the “inclusive” component characterized by $\eta < |\xi|$, with GPDs following the behavior of parton distributions, requires spacelike virtuality for the outgoing photon. Such a configuration is possible in two-photon exchange events in elastic electron-nucleon scattering. However, since the hadronic tensor (5.2) enters now via a loop integral, the single spin asymmetry measurements cannot be used for a direct extraction of GPDs.

6.2.2 Cross section for lepton pair electroproduction

The reaction we are going to discuss consists of three interfering processes, depicted in Fig. 49 (the crossed contributions are implied). However, only one of them is sensitive to the one-particle correlations in the nucleon when at least one of the photon virtualities is large compared to a

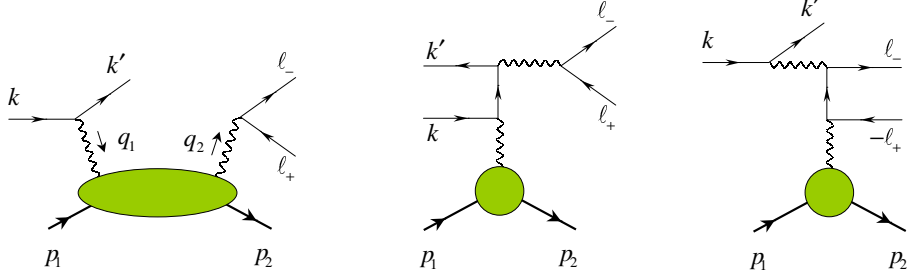


Figure 49: Subprocesses contributing to electroproduction of muon pairs.

typical hadronic scale. It arises from the virtual Compton scattering amplitude, shown on the left hand side in Fig. 49. The other two amplitudes represent the Bethe-Heitler background. We will discuss the simpler case of the production of the lepton pair of a different flavor compared to that of the beam, i.e., the muon pair production. The consideration of the electroproduction of electron pairs requires to add exchange contributions due to the identical nature of the electrons in the final state, i.e., $k' \rightarrow \ell_-$.

The generic form of the cross section of the exclusive electroproduction of lepton pairs off the nucleon, $e(k)N(p_1) \rightarrow e(k')N(p_2)\ell(\ell_-)\bar{\ell}(\ell_+)$, is

$$d\sigma = \frac{1}{4p_1 \cdot k} |\mathcal{T}|^2 d\text{LIPS}_4, \quad (6.104)$$

where \mathcal{T} is the sum of the amplitude of the virtual Compton scattering and two Bethe-Heitler processes, $\mathcal{T} = \mathcal{T}_{\text{VCS}} + \mathcal{T}_{\text{BH}_1} + \mathcal{T}_{\text{BH}_2}$, shown in Fig. 49. The four-particle Lorentz invariant phase space

$$d\text{LIPS}_4 = dM_{\ell\bar{\ell}}^2 d\text{LIPS}_3 d\Phi_{\ell\bar{\ell}}, \quad (6.105)$$

is factorized, by introducing integration over the invariant mass of the lepton pair $M_{\ell\bar{\ell}}^2$, into Lorentz invariant phase-space factors for the production of a heavy timelike photon off a nucleon

$$d\text{LIPS}_3 = (2\pi)^4 \delta^{(4)}(k + p_1 - k' - p_2 - q_2) \frac{d^4 p_2}{(2\pi)^3} \delta_+(p_2^2 - M_N^2) \frac{d^4 k'}{(2\pi)^3} \delta_+(k'^2) \frac{d^4 q_2}{(2\pi)^3} \delta_+(q_2^2 - M_{\ell\bar{\ell}}^2), \quad (6.106)$$

and its subsequent decay into a lepton pair

$$d\Phi_{\ell\bar{\ell}} = \frac{d^4 \ell_-}{(2\pi)^3} \delta_+(\ell_-^2 - m_\ell^2) \delta_+((q_2 - \ell_-)^2 - m_\ell^2). \quad (6.107)$$

A simple calculation gives for them

$$d\text{LIPS}_3 = \frac{dx_B dy d(-\Delta^2) d\phi}{16(2\pi)^4 \sqrt{1 + \varepsilon^2}}, \quad d\Phi_{\ell\bar{\ell}} = \frac{\beta d\Omega_\ell}{8(2\pi)^3}, \quad (6.108)$$

respectively. The graphical definition of the angles involved is demonstrated in Figs. 50 and 51. Here the solid angle and the velocity of the the final state lepton in the $\ell\bar{\ell}$ center-of-mass frame are

$$d\Omega_\ell = \sin \theta_\ell d\theta_\ell d\varphi_\ell, \quad \beta = \sqrt{1 - 4m_\ell^2/M_{\ell\bar{\ell}}^2}, \quad (6.109)$$

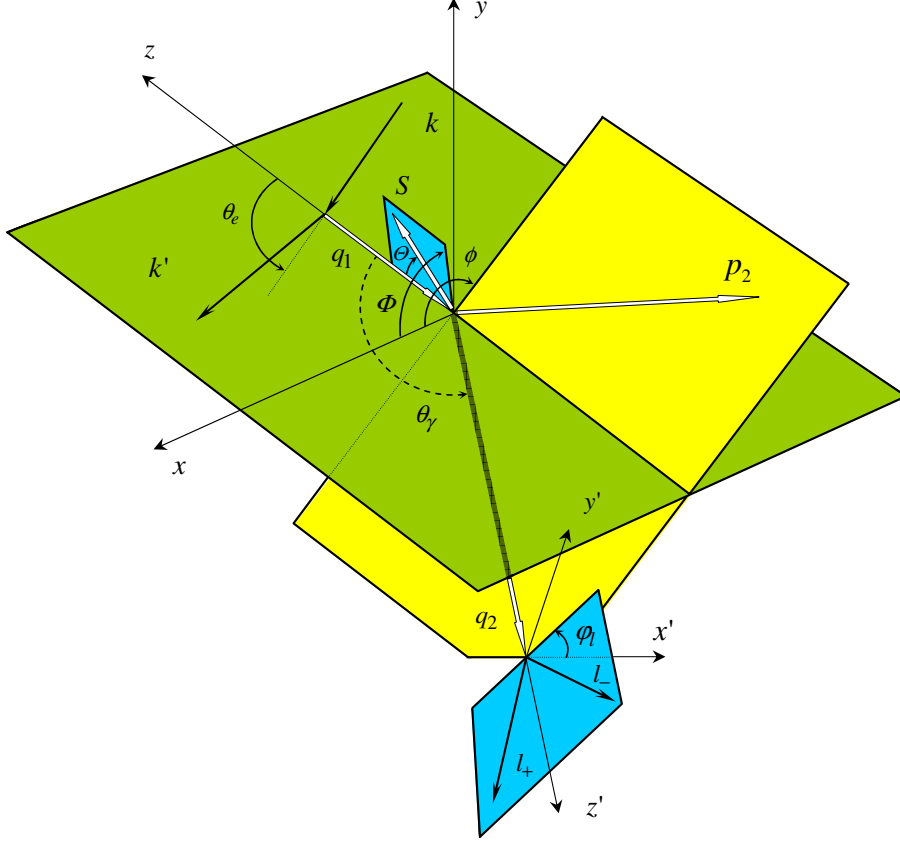


Figure 50: The kinematics of the lepton pair production in elastic electron-nucleon scattering. The coordinate system used in defining the kinematical variables is determined by the z -axis counter-aligned to the spacelike virtual photon. Another complimentary frame suited for evaluation of scalar products is the one with z' along the three-momentum of the timelike photon.

respectively. Introduction of the transverse polarization for the nucleon spin-vector Eq. (6.14) results in an extra integration variable in the phase space given by Eqs. (6.105) and (6.108),

$$d\text{LIPS}_4 \rightarrow \frac{d\Phi}{2\pi} \times d\text{LIPS}_4. \quad (6.110)$$

Extracting the lepton charge from the amplitudes, one gets for the cross section, expressed in terms of experimentally measurable variables,

$$d\sigma = \frac{\alpha_{\text{em}}^4}{16(2\pi)^3} \frac{x_B y \beta}{Q^2 \sqrt{1 + \varepsilon^2}} \left| \frac{T}{e^4} \right|^2 dx_B dy d(-\Delta^2) d\phi dM_{\ell\ell}^2 d\Omega_\ell. \quad (6.111)$$

6.2.3 Kinematics of the lepton pair electroproduction

There is a complementary rest frame to the conventional one discussed in Section 6.1.1 with the z -axis directed opposite to the three-momentum of the incoming virtual photon. It is very suitable for evaluation of scalar products of four-momenta at intermediate stages. The new frame is defined by rotating the z -axis in the hadronic plane such that it aligns with the three-momentum \mathbf{q}_2 of

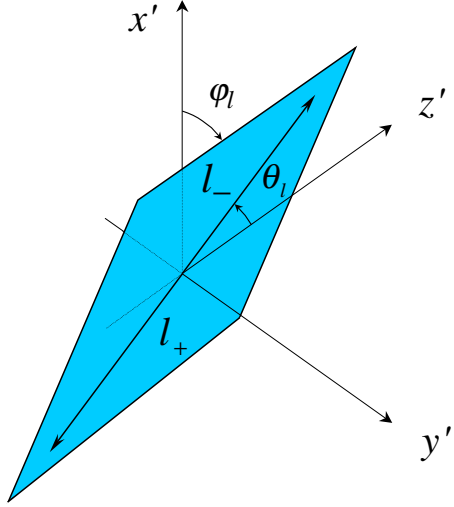


Figure 51: Azimuthal and polar angles of the lepton pair in the rest frame of the timelike photon.

the timelike virtual photon

$$q_2 = (\omega_2, \mathbf{v} \omega_2), \quad \omega_2 = \frac{\mathcal{Q}}{\varepsilon} + \frac{\Delta^2}{2M_N}, \quad v \equiv |\mathbf{v}| = \sqrt{1 - M_{\ell\ell}^2/\omega_2^2}. \quad (6.112)$$

Operationally, it is achieved by rotating the frame from Section 6.1.1 in the hadron scattering plane by the scattering angle θ_γ of the outgoing photon,

$$\cos \theta_\gamma = -\frac{\varepsilon (\mathcal{Q}^2 - M_{\ell\ell}^2 + \Delta^2) + 2\mathcal{Q}\omega_2}{2\mathcal{Q}\omega_2 v \sqrt{1 + \varepsilon^2}}, \quad (6.113)$$

as shown in Fig. 50. In the new frame with z' axis directed along \vec{q}_2 , the particle four-momenta read

$$q_2^\mu = (\omega_2, 0, 0, \omega_2 v), \quad q_1^\mu = (\omega_1, q_1^z \sin \theta_\gamma, 0, -q_1^z \cos \theta_\gamma), \quad p_1^\mu = (M_N, 0, 0, 0), \\ k^\mu = E (1, \sin \theta_e \cos \theta_\gamma \cos \varphi_\gamma - \cos \theta_e \sin \theta_\gamma, -\sin \theta_e \sin \varphi_\gamma, \sin \theta_e \sin \theta_\gamma \cos \varphi_\gamma + \cos \theta_e \cos \theta_\gamma),$$

with the azimuthal angle of the timelike photon $\varphi_\gamma = \pi + \phi$. The outgoing proton and scattered lepton momentum can be found from these equation using the momentum conservation laws. In these formulas, the sine of θ_γ can be expressed by means of invariants of scattering

$$\sin \theta_\gamma = \frac{\sqrt{4x_B(1-x_B) + \varepsilon^2}}{2\mathcal{Q}\omega_2 v \sqrt{1 + \varepsilon^2}} \sqrt{-(\Delta^2 - \Delta_{\min}^2)(\Delta^2 - \Delta_{\max}^2)}. \quad (6.114)$$

Here the maximal and minimal momentum transfer in the t -channel is

$$\Delta_{\min,\max}^2 = -\frac{1}{4x_B(1-x_B) + \varepsilon^2} \left\{ 2 \left((1-x_B)\mathcal{Q}^2 - x_B M_{\ell\ell}^2 \right) + \varepsilon^2 (\mathcal{Q}^2 - M_{\ell\ell}^2) \right. \\ \left. \mp 2\sqrt{1+\varepsilon^2} \sqrt{\left((1-x_B)\mathcal{Q}^2 - x_B M_{\ell\ell}^2 \right)^2 - \varepsilon^2 \mathcal{Q}^2 M_{\ell\ell}^2} \right\}, \quad (6.115)$$

with $-$ ($+$) corresponding to Δ_{\min}^2 (Δ_{\max}^2). Their approximate form, i.e., neglecting corrections of order $(p \cdot q)^{-1}$, in symmetrical variables (5.9) is

$$\Delta_{\max}^2 \simeq -Q^2 \frac{1-\eta^2}{\xi(1-\xi)}$$

and analogous result for Δ_{\min}^2 given before in Eq. (3.202). A boost from the timelike photon rest frame to the z' rest frame along the direction of motion of the photon with velocity \mathbf{v} (6.112) yields

$$\ell_- = \left(\frac{1}{2}\omega_2(1+v\beta \cos \theta_\ell), \frac{1}{2}M_{\ell\bar{\ell}}\beta \sin \theta_\ell \cos \varphi_\ell, \frac{1}{2}M_{\ell\bar{\ell}}\beta \sin \theta_\ell \sin \varphi_\ell, \frac{1}{2}\omega_2(v+\beta \cos \theta_\ell) \right), \quad (6.116)$$

where θ_ℓ and φ_ℓ are the solid angles of ℓ_- in the $\ell\bar{\ell}$ center-of-mass frame. The vector ℓ_+ is obtained by the reflection, $\varphi_\ell \rightarrow \varphi_\ell + \pi$ and $\theta_\ell \rightarrow \pi - \theta_\ell$, from ℓ_- , or equivalently by the substitution $\beta \rightarrow -\beta$.

For the bulk of our discussion it is enough to evaluate approximate forms of scalar products which enter the cross section. Namely, keeping only the leading and sub-leading terms in the $1/(p \cdot q)$ -expansion, one arrives at the following expressions

$$k \cdot \Delta \approx -\frac{Q^2}{y} \frac{\eta}{\xi} (1 - 2K \cos \varphi_\gamma), \quad (6.117)$$

$$\ell_- \cdot \Delta \approx -\frac{Q^2}{\tilde{y}} \frac{\eta}{\xi} (1 + 2\tilde{K} \cos \varphi_\ell), \quad (6.118)$$

$$\begin{aligned} \ell_- \cdot k &\approx \frac{Q^2}{y\tilde{y}} \frac{1}{\xi} \left\{ \frac{1}{2}(\xi - \eta)(1 - \tilde{y}) + \frac{1}{2}(\xi + \eta)(1 - y) \right. \\ &\quad \left. + \sigma \sqrt{(1-y)(1-\tilde{y})(\xi^2 - \eta^2)} \cos(\varphi_\gamma - \varphi_\ell) - 2\eta K \cos \varphi_\gamma - 2\eta \tilde{K} \cos \varphi_\ell \right\}. \end{aligned} \quad (6.119)$$

with

$$\left\{ \begin{array}{c} K \\ \tilde{K} \end{array} \right\} \approx \frac{1}{2\eta} \sqrt{-\xi \frac{\Delta^2}{Q^2}} \sqrt{1 - \frac{\Delta_{\min}^2}{\Delta^2}} \sqrt{\frac{1-\eta}{1+\eta}} \times \left\{ \begin{array}{c} \sqrt{(1-y)(\xi+\eta)} \\ \sqrt{(1-\tilde{y})(\xi-\eta)} \end{array} \right\}. \quad (6.120)$$

Note, that the original square root

$$\sqrt{(1-y)(1-\tilde{y})(1-\eta^2/\xi^2)Q^4}$$

in front of $\cos(\varphi_\gamma - \varphi_\ell)$ in Eq. (6.119) was replaced by

$$\sigma Q^2 / \xi \sqrt{(1-y)(1-\tilde{y})(\xi^2 - \eta^2)},$$

with

$$\sigma \equiv \text{sgn}(Q^2/\xi).$$

Since Q^2/ξ is positive for the kinematics we are considering, σ can be set to be equal to $+1$. However, discussing below relations between scattering amplitudes, we will make use of symmetries that induce the interchange $\xi \rightarrow -\xi$ and $Q^2 \rightarrow Q^2$ in the underlying expressions. Under these substitutions, σ changes the sign and takes the negative value -1 . Equation (6.117) reduces to

the known result [328] in the limit of the real final-state photon $M_{\ell\bar{\ell}} = 0$, discussed in the previous section. To make the results look symmetric, we introduce the variable \tilde{y}

$$\frac{1}{\tilde{y}} \equiv \frac{p_1 \cdot \ell_-}{p_1 \cdot q_2} = \frac{1 + v\beta \cos \theta_\ell}{2} \simeq \frac{1 + \cos \theta_\ell}{2}, \quad (6.121)$$

which varies in the interval $1 \leq \tilde{y} \leq \infty$ and enters in a fashion analogous to the fraction of the lepton energy loss y .

6.2.4 Generating function for angular dependence

In this section, we will discuss the electroproduction cross section involving the leading-twist Compton scattering amplitude. First, we present a generic form of the squared amplitude, where the hadronic part left intact, while the leptonic part is fully worked out. The square of the total amplitude, $\mathcal{T} = \mathcal{T}_{\text{VCS}} + \mathcal{T}_{\text{BH}_1} + \mathcal{T}_{\text{BH}_2}$, involves three essentially different contributions

$$\mathcal{T}^2 = |\mathcal{T}_{\text{VCS}}|^2 + \mathcal{I} + |\mathcal{T}_{\text{BH}_1} + \mathcal{T}_{\text{BH}_2}|^2, \quad (6.122)$$

the square of the virtual Compton scattering amplitude, — bilinear in Compton form factors, — the square of the Bethe-Heitler processes, — independent on GPDs and expressed solely in terms of elastic form factors, and the interference term

$$\mathcal{I} = \mathcal{T}_{\text{VCS}} \mathcal{T}_{\text{BH}_1}^\dagger + \mathcal{T}_{\text{VCS}} \mathcal{T}_{\text{BH}_2}^\dagger + \mathcal{T}_{\text{VCS}}^\dagger \mathcal{T}_{\text{BH}_1} + \mathcal{T}_{\text{VCS}}^\dagger \mathcal{T}_{\text{BH}_2}, \quad (6.123)$$

which is linear in Compton form factors. For the electron beam, the separate contributions to the total amplitude are given by

$$\mathcal{T}_{\text{VCS}} = \frac{e^4}{q_1^2 q_2^2} \bar{u}(\ell_-) \gamma_\mu u(-\ell_+) \bar{u}(k') \gamma_\nu u(k) T_{\mu\nu}, \quad (6.124)$$

$$\mathcal{T}_{\text{BH}_1} = \frac{e^4}{q_2^2 \Delta^2} \bar{u}(\ell_-) \gamma_\mu u(-\ell_+) \bar{u}(k') \left(\gamma_\mu \frac{1}{k - \not{\Delta}} \gamma_\nu + \gamma_\nu \frac{1}{k' + \not{\Delta}} \gamma_\mu \right) u(k) J_\nu, \quad (6.125)$$

$$\mathcal{T}_{\text{BH}_2} = \frac{e^4}{q_1^2 \Delta^2} \bar{u}(k') \gamma_\mu u(k) \bar{u}(\ell_-) \left(\gamma_\mu \frac{1}{-\ell_+ - \not{\Delta}} \gamma_\nu + \gamma_\nu \frac{1}{\ell_- + \not{\Delta}} \gamma_\mu \right) u(-\ell_+) J_\nu. \quad (6.126)$$

They correspond to the diagrams (a), (b), and (c) in Fig. 49, respectively, including the crossed contributions in the latter two cases. The VCS tensor $T_{\mu\nu}$ and the electromagnetic current J_μ were introduced previously in Eqs. (5.51) and (6.12), respectively. The two amplitudes \mathcal{T}_{VCS} and $\mathcal{T}_{\text{BH}_2}$ change the overall sign when one switches from the electron to the positron beam, and so do the interference terms involving them, while the term $\mathcal{T}_{\text{BH}_1}$ does not change sign. Obviously, both BH amplitudes are related by the interchange of the momenta $k' \leftrightarrow \ell_-$ and $k \leftrightarrow -\ell_+$. Moreover, the VCS and the first BH amplitude are even under the interchange of the produced leptons in the pair, while the second BH amplitude is odd. This symmetry property in the timelike DVCS plays an analogous role as the charge asymmetry in the spacelike case [351].

The evaluation of separate terms gives expressions which are represented as a Fourier sum of a few harmonics in the difference of the azimuthal angles $\varphi_l - \varphi_\gamma = \varphi_l - \phi - \pi$. Below, we list particular contributions to the total amplitude squared.

- The square of the VCS amplitude

$$|\mathcal{T}_{\text{VCS}}|^2 = \frac{2\xi^2 e^8}{Q^4 y^2 \tilde{y}^2 (\eta^2 - \xi^2)} \sum_{n=0}^2 (a_n^{\text{VCS}} + \lambda b_n^{\text{VCS}}) \cos(n(\varphi_l - \phi)), \quad (6.127)$$

has the following expansion coefficients

$$a_0^{\text{VCS}} = \frac{1}{2}(2 - 2y + y^2)(2 - 2\tilde{y} + \tilde{y}^2) \left(\mathcal{F}_1 \mathcal{F}_1^\dagger + \tilde{\mathcal{F}}_1 \tilde{\mathcal{F}}_1^\dagger \right) + 4(1 - y)(1 - \tilde{y}) \frac{\xi^2 - \eta^2}{\xi^2} \mathcal{F}_L \mathcal{F}_L^\dagger, \quad (6.128)$$

$$a_1^{\text{VCS}} = -\frac{\sigma}{\xi} \sqrt{(1 - y)(1 - \tilde{y})(\xi^2 - \eta^2)} (2 - y)(2 - \tilde{y}) \left(\mathcal{F}_1 \mathcal{F}_L^\dagger + \mathcal{F}_L \mathcal{F}_1^\dagger \right), \quad (6.129)$$

$$a_2^{\text{VCS}} = 2(1 - y)(1 - \tilde{y}) \left(\mathcal{F}_1 \mathcal{F}_1^\dagger - \tilde{\mathcal{F}}_1 \tilde{\mathcal{F}}_1^\dagger \right), \quad (6.130)$$

$$b_0^{\text{VCS}} = \frac{1}{2}y(2 - y)(2 - 2\tilde{y} + \tilde{y}^2) \left(\mathcal{F}_1 \tilde{\mathcal{F}}_1^\dagger + \tilde{\mathcal{F}}_1 \mathcal{F}_1^\dagger \right), \quad (6.131)$$

$$b_1^{\text{VCS}} = -\frac{\sigma}{\xi} \sqrt{(1 - y)(1 - \tilde{y})(\xi^2 - \eta^2)} y(2 - \tilde{y}) \left(\mathcal{F}_L \tilde{\mathcal{F}}_1^\dagger + \tilde{\mathcal{F}}_1 \mathcal{F}_L^\dagger \right), \quad (6.132)$$

$$b_2^{\text{VCS}} = 0. \quad (6.133)$$

Due to the virtuality of both the incoming and outgoing photons, the Lorentz structure accompanying \mathcal{F}_L , in contrast to the DVCS case, does contribute to the cross section and generates, e.g., the coefficient a_1^{VCS} .

The interference of the VCS and BH amplitude will involve lepton propagators from the latter which will bring conveniently rescaled factors in the denominator

$$(k' + \Delta)^2 \equiv 2\eta p \cdot q \mathcal{P}_1(k), \quad (k - \Delta)^2 \equiv 2\eta p \cdot q \mathcal{P}_2(k), \quad (6.134)$$

$$(\ell_+ + \Delta)^2 \equiv -2\eta p \cdot q \mathcal{P}_3(\ell_-), \quad (\ell_- + \Delta)^2 \equiv -2\eta p \cdot q \mathcal{P}_4(\ell_-). \quad (6.135)$$

The expressions are rather lengthy and are obtained by substituting Eqs. (6.117) and (6.120) into the left-hand side of the above definitions. We also introduce the following shorthand notations for the structures involving the nucleon matrix element of the quark electromagnetic current to make the formulas look as concise as possible,

$$\mathcal{S}_1 \equiv -\eta \left(k - \frac{1}{y} q_1 \right) \cdot J^\dagger - \frac{1}{p \cdot q} \left(k - \frac{1}{y} q_1 \right) \cdot \Delta q_1 \cdot J^\dagger, \quad (6.136)$$

$$\mathcal{S}_2 \equiv -\eta \left(\ell_- - \frac{1}{\tilde{y}} q_2 \right) \cdot J^\dagger - \frac{1}{p \cdot q} \left(\ell_- - \frac{1}{\tilde{y}} q_2 \right) \cdot \Delta q_2 \cdot J^\dagger, \quad (6.137)$$

$$\tilde{\mathcal{S}}_1 \equiv \frac{i}{p \cdot q} \varepsilon_{\mu\nu\rho\sigma} q_\mu k_\nu \Delta_\rho J_\sigma^\dagger, \quad \tilde{\mathcal{S}}_2 \equiv \frac{i}{p \cdot q} \varepsilon_{\mu\nu\rho\sigma} q_\mu \ell_{-\nu} \Delta_\rho J_\sigma^\dagger. \quad (6.138)$$

These functions depend on the azimuthal angles ϕ and φ_l . Combining these results, one finds, in full analogy with the previous analysis of $|\mathcal{T}_{\text{VCS}}|^2$, the interference contributions from the VCS and BH amplitudes.

- The interference $\mathcal{T}_{\text{VCS}} \mathcal{T}_{\text{BH}_1}^\dagger$

$$\mathcal{T}_{\text{VCS}} \mathcal{T}_{\text{BH}_1}^\dagger = \frac{2\xi^2 e^8}{y^2 \tilde{y}^2 \eta^2 (\eta^2 - \xi^2) Q^4 \Delta^2 \mathcal{P}_1(k) \mathcal{P}_2(k)} \sum_{n=0}^2 (a_n^1 + \lambda b_n^1) \cos(n(\varphi_l - \phi)), \quad (6.139)$$

is determined by

$$\begin{aligned} a_0^1 = & -4(1 - y)(1 - \tilde{y}) \left(\eta \mathcal{S}_1 \mathcal{F}_1 + \xi \tilde{\mathcal{S}}_1 \tilde{\mathcal{F}}_1 - 2 \frac{\xi^2 - \eta^2}{\xi} \mathcal{S}_1 \mathcal{F}_L \right) \\ & -(2 - 2y + y^2)(2 - 2\tilde{y} + \tilde{y}^2) \left(\xi \mathcal{S}_1 \mathcal{F}_1 - \eta \tilde{\mathcal{S}}_1 \tilde{\mathcal{F}}_1 \right) \end{aligned} \quad (6.140)$$

$$\begin{aligned}
& -2\frac{\tilde{y}}{y}(1-y)(2-y)(2-\tilde{y})(\xi+\eta)\left(\tilde{\mathcal{S}}_2\tilde{\mathcal{F}}_1-\frac{\eta}{\xi}\mathcal{S}_2\mathcal{F}_L\right), \\
a_1^1 &= 2\sigma\sqrt{(1-y)(1-\tilde{y})(\xi^2-\eta^2)} \\
&\times \left\{ (2-y)(2-\tilde{y})\left(\mathcal{S}_1\mathcal{F}_1+\tilde{\mathcal{S}}_1\tilde{\mathcal{F}}_1-\frac{\xi+\eta}{\xi}\mathcal{S}_1\mathcal{F}_L\right) + 4\frac{\tilde{y}}{y}\frac{1-y}{\xi-\eta}(\eta\mathcal{S}_2\mathcal{F}_1+\xi\tilde{\mathcal{S}}_2\tilde{\mathcal{F}}_1) \right\}, \tag{6.141}
\end{aligned}$$

$$a_2^1 = -4(\xi+\eta)(1-y)(1-\tilde{y})\left(\mathcal{S}_1\mathcal{F}_1+\tilde{\mathcal{S}}_1\tilde{\mathcal{F}}_1\right), \tag{6.142}$$

$$b_0^1 = -y(2-y)(2-2\tilde{y}+\tilde{y}^2)\left(\xi\mathcal{S}_1\tilde{\mathcal{F}}_1-\eta\tilde{\mathcal{S}}_1\mathcal{F}_1\right) - 2(\xi+\eta)(1-y)\tilde{y}(2-\tilde{y})\tilde{\mathcal{S}}_2(\mathcal{F}_1+\mathcal{F}_L), \tag{6.143}$$

$$b_1^1 = 2\sigma\sqrt{(1-y)(1-\tilde{y})(\xi^2-\eta^2)}y(2-\tilde{y})\left(\mathcal{S}_1\tilde{\mathcal{F}}_1+\tilde{\mathcal{S}}_1\mathcal{F}_1+\frac{\xi+\eta}{\xi}\tilde{\mathcal{S}}_1\mathcal{F}_L\right), \tag{6.144}$$

$$b_2^1 = 0. \tag{6.145}$$

- The interference $\mathcal{T}_{\text{VCS}}\mathcal{T}_{\text{BH}_2}^\dagger$

$$\mathcal{T}_{\text{VCS}}\mathcal{T}_{\text{BH}_2}^\dagger = \frac{2\xi^2 e^8}{y^2 \tilde{y}^2 \eta^2 (\eta^2 - \xi^2) Q^4 \Delta^2 \mathcal{P}_3(\ell_-) \mathcal{P}_4(\ell_-)} \sum_{n=0}^2 (a_n^2 + \lambda b_n^2) \cos(n(\varphi_l - \phi)), \tag{6.146}$$

is encoded into the following Fourier coefficients

$$\begin{aligned}
a_0^2 &= -4(1-y)(1-\tilde{y})\left(\eta\mathcal{S}_2\mathcal{F}_1+\xi\tilde{\mathcal{S}}_2\tilde{\mathcal{F}}_1+2\frac{\xi^2-\eta^2}{\xi}\mathcal{S}_2\mathcal{F}_L\right) \\
&+(2-2y+y^2)(2-2\tilde{y}+\tilde{y}^2)\left(\xi\mathcal{S}_2\mathcal{F}_1-\eta\tilde{\mathcal{S}}_2\tilde{\mathcal{F}}_1\right) \\
&-2\frac{y}{\tilde{y}}(1-\tilde{y})(2-y)(2-\tilde{y})(\xi-\eta)\left(\tilde{\mathcal{S}}_1\tilde{\mathcal{F}}_1-\frac{\eta}{\xi}\mathcal{S}_1\mathcal{F}_L\right), \tag{6.147}
\end{aligned}$$

$$\begin{aligned}
a_1^2 &= -2\sigma\sqrt{(1-y)(1-\tilde{y})(\xi^2-\eta^2)} \\
&\times \left\{ (2-y)(2-\tilde{y})\left(\mathcal{S}_2\mathcal{F}_1-\tilde{\mathcal{S}}_2\tilde{\mathcal{F}}_1-\frac{\xi-\eta}{\xi}\mathcal{S}_2\mathcal{F}_L\right) - 4\frac{y}{\tilde{y}}\frac{1-\tilde{y}}{\xi+\eta}(\eta\mathcal{S}_1\mathcal{F}_1+\xi\tilde{\mathcal{S}}_1\tilde{\mathcal{F}}_1) \right\}, \tag{6.148}
\end{aligned}$$

$$a_2^2 = 4(\xi-\eta)(1-y)(1-\tilde{y})\left(\mathcal{S}_2\mathcal{F}_1-\tilde{\mathcal{S}}_2\tilde{\mathcal{F}}_1\right), \tag{6.149}$$

$$b_0^2 = y(2-y)(2-2\tilde{y}+\tilde{y}^2)\left(\xi\mathcal{S}_2\tilde{\mathcal{F}}_1-\eta\tilde{\mathcal{S}}_2\mathcal{F}_1\right) - 2(\xi-\eta)\frac{y^2}{\tilde{y}}(2-\tilde{y})(1-\tilde{y})\tilde{\mathcal{S}}_1(\mathcal{F}_1+\mathcal{F}_L) \tag{6.150}$$

$$b_1^2 = -2\sigma\sqrt{(1-y)(1-\tilde{y})(\xi^2-\eta^2)}y(2-\tilde{y})\left(\mathcal{S}_2\tilde{\mathcal{F}}_1-\tilde{\mathcal{S}}_2\mathcal{F}_1-\frac{\xi-\eta}{\xi}\tilde{\mathcal{S}}_2\mathcal{F}_L\right), \tag{6.151}$$

$$b_2^2 = 0. \tag{6.152}$$

The unpolarized parts of the two interference terms must obey a symmetry relation, since the BH amplitudes (6.125) and (6.126) are related to each other by the substitutions of the lepton's momenta $k \leftrightarrow -\ell_+$ and $k' \leftrightarrow \ell_-$. Obviously, $q_1 \leftrightarrow -q_2$ under it. The Bose symmetry ensures on the other hand the invariance of the Compton amplitude (6.124) with respect to this interchange. As we mentioned above, all of the amplitudes possess definite symmetry properties under the permutation of leptons in the pair $\ell_- \leftrightarrow \ell_+$ and, thus, one can take the advantages of combining both transformations together, i.e., $k \leftrightarrow -\ell_-$ and $k' \leftrightarrow \ell_+$. From the definitions of the four-vectors (6.116) one can derive, after some algebra, a complete set of substitution rules reflecting them

$$Q^2 \rightarrow Q^2, \quad \xi \rightarrow -\xi, \quad \sigma \rightarrow -\sigma, \quad \Delta \rightarrow \Delta, \quad \eta \rightarrow \eta, \quad y \leftrightarrow \tilde{y}, \quad \varphi_\ell \leftrightarrow \phi. \tag{6.153}$$

The prefactors in the interference terms (6.139) and (6.146) are even under the transformation (6.153). Moreover, from the definitions (6.136), (6.137), and (6.138), one can conclude also that $\mathcal{S}_1 \leftrightarrow -\mathcal{S}_2; \tilde{\mathcal{S}}_1 \leftrightarrow -\tilde{\mathcal{S}}_2$ with (6.153). Taking all the results together, one obtains that the Fourier coefficients satisfy the equalities

$$a_n^2 = -a_n^1 \Big|_{y \leftrightarrow \tilde{y}; \xi \leftrightarrow -\xi}^{\mathcal{S}_1 \leftrightarrow -\mathcal{S}_2; \tilde{\mathcal{S}}_1 \leftrightarrow -\tilde{\mathcal{S}}_2}, \quad (6.154)$$

where \mathcal{F}_1 and $\tilde{\mathcal{F}}_1$ are even and odd functions in ξ , respectively. Finally, one observes that the product of the BH propagators (6.134) and (6.135) obeys the symmetry relation

$$\mathcal{P}_3 \mathcal{P}_4(Q^2, \Delta^2, \xi, \eta, y, \tilde{y}, \varphi_\ell) = \mathcal{P}_1 \mathcal{P}_2(Q^2, \Delta^2, -\xi, \eta, \tilde{y}, y, \phi = \varphi_\ell). \quad (6.155)$$

6.2.5 Angular dependence of the cross section

Having the generic expression for the total amplitude squared, one can proceed with the hadronic part and present the result as a Fourier expansion in terms of the azimuthal angle, ϕ of the recoiled nucleon and φ_ℓ of a lepton in the lepton pair. The starting point is to write down the general angular decomposition of the squared amplitudes, which results from the Lorentz structure of the contracted leptonic and hadronic tensors. The harmonics appearing here, can be classified with respect to the underlying twist expansion of the hadronic tensor (5.2), and the Fourier coefficients are in one-to-one correspondence with helicity amplitudes defined in the target rest frame. Extracting certain kinematical factors in order to match the normalization adopted for the lepton production cross section of the real photon in Ref. [328], the square of the VCS amplitude and its interference with the BH amplitudes as well as the squared BH amplitudes has the following expansion in these azimuthal angles

$$|\mathcal{T}_{\text{VCS}}|^2 = \frac{2\xi^2 e^8}{Q^4 y^2 \tilde{y}^2 (\eta^2 - \xi^2)} \sum_{n=0}^2 \{ c_n^{\text{VCS}}(\varphi_\ell) \cos(n\phi) + s_n^{\text{VCS}}(\varphi_\ell) \sin(n\phi) \}, \quad (6.156)$$

$$\begin{aligned} \mathcal{I} = & \frac{2\xi(1+\eta)e^8}{y^3 \tilde{y}^3 (\eta^2 - \xi^2) Q^2 \Delta^2} \sum_{n=0}^3 \left\{ \pm \frac{\tilde{y}}{\mathcal{P}_1 \mathcal{P}_2(\phi)} (c_n^1(\varphi_\ell) \cos(n\phi) + s_n^1(\varphi_\ell) \sin(n\phi)) \right. \\ & \left. + \frac{y}{\mathcal{P}_3 \mathcal{P}_4(\varphi_\ell)} (c_n^2(\phi) \cos(n\varphi_\ell) + s_n^2(\phi) \sin(n\varphi_\ell)) \right\}, \end{aligned} \quad (6.157)$$

$$\begin{aligned} |\mathcal{T}_{\text{BH}}|^2 = & \frac{\xi(1+\eta)^2}{y^4 \tilde{y}^4 \Delta^2 Q^2 \eta (\eta^2 - \xi^2)} \left\{ \sum_{n=0}^4 \left\{ \frac{\tilde{y}^2}{\mathcal{P}_1^2 \mathcal{P}_2^2(\phi)} (c_n^{11}(\varphi_\ell) \cos(n\phi) + s_n^{11}(\varphi_\ell) \sin(n\phi)) \right. \right. \\ & + \frac{y^2}{\mathcal{P}_3^2 \mathcal{P}_4^2(\varphi_\ell)} (c_n^{22}(\phi) \cos(n\varphi_\ell) + s_n^{22}(\phi) \sin(n\varphi_\ell)) \Big\} \\ & \left. \pm \sum_{n=0}^3 \frac{y \tilde{y}}{\mathcal{P}_1 \mathcal{P}_2 \mathcal{P}_3 \mathcal{P}_4} (c_n^{12}(\varphi_\ell) \cos(n\phi) + s_n^{12}(\varphi_\ell) \sin(n\phi)) \right\}. \end{aligned} \quad (6.158)$$

Here the $+$ ($-$) sign stands for the electron (positron) beam, and the relation between the azimuthal angles $\varphi_\gamma = \pi + \phi$ has been used in the expansion. The Fourier coefficients for the squared VCS term ($i = \text{vcs}$), the interference term with the first BH amplitude (6.125) ($i = 1$), and the squared BH amplitude (6.125) ($i = 11$) are expanded up to the second order harmonics in the

azimuthal angle φ_ℓ of the lepton pair and read

$$\begin{aligned} c_n^i(\varphi_\ell) &= \sum_{m=0}^2 \left\{ cc_{nm}^i \cos(m\varphi_\ell) + cs_{nm}^i \sin(m\varphi_\ell) \right\}, \\ s_n^i(\varphi_\ell) &= \sum_{m=0}^2 \left\{ sc_{nm}^i \cos(m\varphi_\ell) + ss_{nm}^i \sin(m\varphi_\ell) \right\}. \end{aligned} \quad (6.159)$$

The Fourier coefficients $ab_{nm}^i = (cc_{nm}^i, cs_{nm}^i, sc_{nm}^i, ss_{nm}^i)$ depend on the nucleon polarization vector (6.14) and can be decomposed further as

$$ab_{nm}^i = ab_{nm,\text{unp}}^i + \cos \Theta ab_{nm,\text{LP}}^i + \sin \Theta ab_{nm,\text{TP}}^i(\Phi). \quad (6.160)$$

A similar expansion in terms of the azimuthal angle ϕ is performed for the interference of the second BH amplitude (6.126) with the VCS amplitude ($i = 2$) and for the square of the second BH amplitude ($i = 22$). The interference of both BH amplitudes ($i = 12$) is analogous to Eq. (6.159), however, it contains now third order harmonics in the azimuthal angle φ_ℓ . The Fourier coefficients linearly depend on the polarization vector of the nucleon, see Eq. (6.160). At the edge of the phase space, the overall coefficient in the BH amplitude gets corrected according to

$$\frac{(1+\eta)^2}{\eta^2 - \xi^2} \rightarrow \frac{\left(1 + \eta + \frac{\xi \Delta^2}{2Q^2}\right)^2}{\eta^2 - \left(1 - \frac{\Delta^2}{4Q^2}\right)^2 \xi^2}. \quad (6.161)$$

We emphasize that $1/(\eta^2 - \xi^2)$ expressions in the squared VCS (6.156) and the interference (6.157) terms are corrected in an analogous manner to ensure their correct behavior in the limits $Q^2 \rightarrow 0$ and $M_{\ell\ell}^2 \rightarrow 0$.

Finally, we remark that all BH propagators, defined in Eqs. (6.134) and (6.135), are even functions of the azimuthal angle φ :

$$\mathcal{P}_i(\varphi) = \mathcal{P}_i(2\pi - \varphi) \quad \text{for } i = \{1, \dots, 4\}. \quad (6.162)$$

Thus, even and odd harmonics can be clearly separated from each other. It is also worth mentioning that the product $\mathcal{P}_3 \mathcal{P}_4$ as a function of the lepton-pair solid angles φ_ℓ and θ_ℓ satisfies the symmetry relation

$$\mathcal{P}_3 \mathcal{P}_4(\theta_\ell, \varphi_\ell) = \mathcal{P}_3 \mathcal{P}_4(\pi - \theta_\ell, \varphi_\ell + \pi). \quad (6.163)$$

As a consequence of this symmetry, any (anti)symmetric moment in θ_ℓ , after integration over $d\theta_\ell$ in a symmetric interval around the point $\theta_\ell = \pi/2$, has the following characteristic cos-Fourier expansion (for any integer r)

$$\int_{\pi/2-\vartheta}^{\pi/2+\vartheta} d \cos \theta_\ell \frac{\tau(\theta_\ell)}{[\mathcal{P}_3 \mathcal{P}_4]^r} = \sum_{n=0,1,2,\dots} \tau_n(\vartheta) \begin{Bmatrix} \cos([2n+1]\varphi_\ell) \\ \cos(2n\varphi_\ell) \end{Bmatrix} \quad \text{for } \begin{Bmatrix} \tau(\theta_\ell) = -\tau(\pi - \theta_\ell) \\ \tau(\theta_\ell) = \tau(\pi - \theta_\ell) \end{Bmatrix} \quad (6.164)$$

where $\vartheta \leq \frac{\pi}{2}$.

6.2.6 Squared virtual Compton amplitude

At leading twist, it turns out that $|\mathcal{I}_{\text{VCS}}|^2$ depends only on the harmonics $\cos[n(\varphi_\ell - \phi)]$ with $n = 0, 1, 2$. As a result, we find that in this approximation, there exist the following relations between the Fourier coefficients:

$$\begin{aligned} \text{ss}_{nn}^{\text{VCS}} &\simeq \text{cc}_{nn}^{\text{VCS}}, \\ \text{sc}_{nm}^{\text{VCS}} &\simeq \text{cs}_{nm}^{\text{VCS}} \simeq 0, \\ \text{ss}_{nm}^{\text{VCS}} &\simeq \text{cc}_{nm}^{\text{VCS}} \simeq 0, \quad n \neq m. \end{aligned} \quad (6.165)$$

The nonvanishing Fourier coefficients $\text{cc}_{nn}^{\text{VCS}}$ can be easily evaluated from Eqs. (6.128)-(6.133) and products of Compton form factors. The general structure of products of Compton form factors is given by

$$\frac{1}{4}\mathcal{F}_1\mathcal{F}_1^\dagger \equiv \mathcal{C}_{\mathcal{V}\mathcal{V},\text{unp}}^{\text{VCS}} + \mathcal{C}_{\mathcal{V}\mathcal{V},\text{LP}}^{\text{VCS}} \cos\Theta + i\sqrt{-\frac{\Delta^2}{4M_N^2}}\sqrt{1-\frac{\Delta_{\min}^2}{\Delta^2}}\sqrt{\frac{1-\eta}{1+\eta}}\mathcal{C}_{\mathcal{V}\mathcal{V},\text{TP}}^{\text{VCS}} \sin(\Phi-\phi)\sin\Theta, \quad (6.166)$$

$$\frac{1}{4}\mathcal{F}_1\tilde{\mathcal{F}}_1^\dagger \equiv \mathcal{C}_{\mathcal{V}\mathcal{A},\text{unp}}^{\text{VCS}} + \mathcal{C}_{\mathcal{V}\mathcal{A},\text{LP}}^{\text{VCS}} \cos\Theta + \sqrt{-\frac{\Delta^2}{4M_N^2}}\sqrt{1-\frac{\Delta_{\min}^2}{\Delta^2}}\sqrt{\frac{1-\eta}{1+\eta}}\mathcal{C}_{\mathcal{V}\mathcal{A},\text{TP}}^{\text{VCS}} \cos(\Phi-\phi)\sin\Theta, \quad (6.167)$$

with $\tilde{\mathcal{F}}_1\tilde{\mathcal{F}}_1^\dagger$ product having the decomposition similar to Eq. (6.166). The polar Θ and azimuthal Φ angles parametrize the nucleon polarization vector S according to Eq. (6.14). The functions $\mathcal{C}(\mathcal{F}, \mathcal{F}^*)$ depend on Compton form factors \mathcal{F} . For the case at hand, we find at leading order in $(p \cdot q)^{-1}$

$$\mathcal{C}_{\mathcal{V}\mathcal{V},\text{unp}}^{\text{VCS}}(\mathcal{F}, \mathcal{F}^*) = (1-\eta^2)\mathcal{H}\mathcal{H}^* - \eta^2(\mathcal{H}\mathcal{E}^* + \mathcal{E}\mathcal{H}^*) - \left(\frac{\Delta^2}{4M_N^2} + \eta^2\right)\mathcal{E}\mathcal{E}^*, \quad (6.168)$$

$$\mathcal{C}_{\mathcal{A}\mathcal{A},\text{unp}}^{\text{VCS}}(\mathcal{F}, \mathcal{F}^*) = (1-\eta^2)\tilde{\mathcal{H}}\tilde{\mathcal{H}}^* - \eta^2(\tilde{\mathcal{H}}\tilde{\mathcal{E}}^* + \tilde{\mathcal{E}}\tilde{\mathcal{H}}^*) - \eta^2\frac{\Delta^2}{4M_N^2}\tilde{\mathcal{E}}\tilde{\mathcal{E}}^*, \quad (6.169)$$

$$\mathcal{C}_{\mathcal{V}\mathcal{A},\text{unp}}^{\text{VCS}}(\mathcal{F}, \mathcal{F}^*) = 0. \quad (6.170)$$

The results for spin-dependent cases, including both longitudinally and transversely polarized target options, are presented below. The nonvanishing \mathcal{C} -coefficients in the squared VCS amplitude, defined in Eq. (6.166) – (6.167), for the polarized nucleon target are given by

$$\mathcal{C}_{\mathcal{V}\mathcal{A},\text{LP}}^{\text{VCS}}(\mathcal{F}, \mathcal{F}^*) = (1-\eta^2)\mathcal{H}\tilde{\mathcal{H}}^* - \eta^2(\mathcal{H}\tilde{\mathcal{E}}^* + \mathcal{E}\tilde{\mathcal{H}}^*) - \eta\left(\frac{\Delta^2}{4M_N^2} + \frac{\eta^2}{1+\eta}\right)\mathcal{E}\tilde{\mathcal{E}}^*, \quad (6.171)$$

$$\mathcal{C}_{\mathcal{V}\mathcal{V},\text{TP}}^{\text{VCS}}(\mathcal{F}, \mathcal{F}^*) = (1+\eta)(\mathcal{H}\mathcal{E}^* - \mathcal{E}\mathcal{H}^*), \quad (6.172)$$

$$\mathcal{C}_{\mathcal{A}\mathcal{A},\text{TP}}^{\text{VCS}}(\mathcal{F}, \mathcal{F}^*) = -(1+\eta)\eta\left(\tilde{\mathcal{H}}\tilde{\mathcal{E}}^* - \tilde{\mathcal{E}}\tilde{\mathcal{H}}^*\right), \quad (6.173)$$

$$\mathcal{C}_{\mathcal{V}\mathcal{A},\text{TP}}^{\text{VCS}}(\mathcal{F}, \mathcal{F}^*) = (1+\eta)\left(\eta\mathcal{H}\tilde{\mathcal{E}}^* - \mathcal{E}\tilde{\mathcal{H}}^*\right) + \eta^2\mathcal{E}\tilde{\mathcal{E}}^*. \quad (6.174)$$

Note, that in the (spacelike) DVCS limit, i.e., when one sets $\eta = \xi$, we retrieve our previous result from Ref. [328]

$$\mathcal{C}_{\text{unp}}^{\text{DVCS}} \stackrel{\text{DVCS}}{=} \mathcal{C}_{\mathcal{V}\mathcal{V},\text{unp}}^{\text{VCS}} + \mathcal{C}_{\mathcal{A}\mathcal{A},\text{unp}}^{\text{VCS}},$$

and analogous relations for the polarized case in the DVCS limit $\eta = \xi$,

$$\begin{aligned}\mathcal{C}_{\text{LP}}^{\text{DVCS}}(\mathcal{F}, \mathcal{F}^*) &\stackrel{\text{DVCS}}{=} \mathcal{C}_{\mathcal{V}\mathcal{A}, \text{LP}}^{\text{VCS}}(\mathcal{F}, \mathcal{F}^*) + \mathcal{C}_{\mathcal{V}\mathcal{A}, \text{LP}}^{\text{VCS}}(\mathcal{F}^*, \mathcal{F}), \\ \mathcal{C}_{\text{TP+}}^{\text{DVCS}}(\mathcal{F}, \mathcal{F}^*) &\stackrel{\text{DVCS}}{=} \mathcal{C}_{\mathcal{V}\mathcal{A}, \text{TP}}^{\text{VCS}}(\mathcal{F}, \mathcal{F}^*) + \mathcal{C}_{\mathcal{V}\mathcal{A}, \text{TP}}^{\text{VCS}}(\mathcal{F}^*, \mathcal{F}), \\ \mathcal{C}_{\text{TP-}}^{\text{DVCS}}(\mathcal{F}, \mathcal{F}^*) &\stackrel{\text{DVCS}}{=} \mathcal{C}_{\mathcal{V}\mathcal{V}, \text{TP}}^{\text{VCS}}(\mathcal{F}, \mathcal{F}^*) + \mathcal{C}_{\mathcal{A}\mathcal{A}, \text{TP}}^{\text{VCS}}(\mathcal{F}, \mathcal{F}^*).\end{aligned}\quad (6.175)$$

In this way, we find for the unpolarized target the following nonvanishing Fourier coefficients in the twist-two sector

$$\begin{aligned}\text{cc}_{00, \text{unp}}^{\text{VCS}} &= 2(2 - 2y + y^2)(2 - 2\tilde{y} + \tilde{y}^2) \{ \mathcal{C}_{\mathcal{V}\mathcal{V}, \text{unp}}^{\text{VCS}}(\mathcal{F}, \mathcal{F}^*) + \mathcal{C}_{\mathcal{A}\mathcal{A}, \text{unp}}^{\text{VCS}}(\mathcal{F}, \mathcal{F}^*) \} \\ &\quad + \frac{16}{\xi^2}(1 - y)(1 - \tilde{y})(\xi^2 - \eta^2)\mathcal{C}_{\mathcal{V}\mathcal{V}, \text{unp}}^{\text{VCS}}(\mathcal{F}_L, \mathcal{F}_L^*),\end{aligned}\quad (6.176)$$

$$\text{cc}_{11, \text{unp}}^{\text{VCS}} = \frac{4\sigma}{\xi}\sqrt{(1 - y)(1 - \tilde{y})(\xi^2 - \eta^2)}(2 - y)(2 - \tilde{y})\{\mathcal{C}_{\mathcal{V}\mathcal{V}, \text{unp}}^{\text{VCS}}(\mathcal{F}, \mathcal{F}_L^*) + \mathcal{C}_{\mathcal{V}\mathcal{V}, \text{unp}}^{\text{VCS}}(\mathcal{F}_L, \mathcal{F}^*)\}, \quad (6.177)$$

$$\text{cc}_{22, \text{unp}}^{\text{VCS}} = 8(1 - y)(1 - \tilde{y})\{\mathcal{C}_{\mathcal{V}\mathcal{V}, \text{unp}}^{\text{VCS}}(\mathcal{F}, \mathcal{F}^*) - \mathcal{C}_{\mathcal{A}\mathcal{A}, \text{unp}}^{\text{VCS}}(\mathcal{F}, \mathcal{F}^*)\}. \quad (6.178)$$

The remaining Fourier coefficients for longitudinally polarized target are given by

$$\begin{aligned}\text{cc}_{00, \text{LP}}^{\text{VCS}} &= 2\lambda(2 - y)y(2 - 2\tilde{y} + \tilde{y}^2)\{\mathcal{C}_{\mathcal{V}\mathcal{A}, \text{LP}}^{\text{VCS}}(\mathcal{F}, \mathcal{F}^*) + \mathcal{C}_{\mathcal{V}\mathcal{A}, \text{LP}}^{\text{VCS}}(\mathcal{F}^*, \mathcal{F})\}, \\ \text{cc}_{11, \text{LP}}^{\text{VCS}} &= \lambda\frac{4\sigma}{\xi}y(2 - \tilde{y})\sqrt{(1 - y)(1 - \tilde{y})(\xi^2 - \eta^2)}\{\mathcal{C}_{\mathcal{V}\mathcal{A}, \text{LP}}^{\text{VCS}}(\mathcal{F}_L, \mathcal{F}^*) + \mathcal{C}_{\mathcal{V}\mathcal{A}, \text{LP}}^{\text{VCS}}(\mathcal{F}_L^*, \mathcal{F})\},\end{aligned}\quad (6.179)$$

and, for transversely polarized target, they read

$$\begin{aligned}\text{cc}_{00, \text{TP}}^{\text{VCS}} &= \sqrt{-\frac{\Delta^2}{M_N^2}}\sqrt{1 - \frac{\Delta_{\min}^2}{\Delta^2}}\sqrt{\frac{1 - \eta}{1 + \eta}} \\ &\times \left\{ \lambda \cos(\Phi - \phi)(2 - y)y(2 - 2\tilde{y} + \tilde{y}^2)\{\mathcal{C}_{\mathcal{V}\mathcal{A}, \text{TP}}^{\text{VCS}}(\mathcal{F}, \mathcal{F}^*) + \mathcal{C}_{\mathcal{V}\mathcal{A}, \text{TP}}^{\text{VCS}}(\mathcal{F}^*, \mathcal{F})\} \right. \\ &\quad + i \sin(\Phi - \phi)(2 - 2y + y^2)(2 - 2\tilde{y} + \tilde{y}^2)\{\mathcal{C}_{\mathcal{V}\mathcal{V}, \text{TP}}^{\text{VCS}}(\mathcal{F}, \mathcal{F}^*) + \mathcal{C}_{\mathcal{A}\mathcal{A}, \text{TP}}^{\text{VCS}}(\mathcal{F}, \mathcal{F}^*)\} \\ &\quad \left. + 8i \sin(\Phi - \phi)(1 - y)(1 - \tilde{y})\frac{\xi^2 - \eta^2}{\xi^2}\mathcal{C}_{\mathcal{V}\mathcal{V}, \text{TP}}^{\text{VCS}}(\mathcal{F}_L, \mathcal{F}_L^*) \right\},\end{aligned}\quad (6.180)$$

$$\begin{aligned}\text{cc}_{11, \text{TP}}^{\text{VCS}} &= \sqrt{-\frac{\Delta^2}{M_N^2}}\sqrt{1 - \frac{\Delta_{\min}^2}{\Delta^2}}\sqrt{\frac{1 - \eta}{1 + \eta}}\frac{2\sigma}{\xi}\sqrt{(1 - y)(1 - \tilde{y})(\xi^2 - \eta^2)} \\ &\times \left\{ \lambda \cos(\Phi - \phi)y(2 - \tilde{y})\{\mathcal{C}_{\mathcal{V}\mathcal{A}, \text{TP}}^{\text{VCS}}(\mathcal{F}_L, \mathcal{F}^*) + \mathcal{C}_{\mathcal{V}\mathcal{A}, \text{TP}}^{\text{VCS}}(\mathcal{F}_L^*, \mathcal{F})\} \right. \\ &\quad \left. + i \sin(\Phi - \phi)(2 - y)(2 - \tilde{y})\{\mathcal{C}_{\mathcal{V}\mathcal{V}, \text{TP}}^{\text{VCS}}(\mathcal{F}_L, \mathcal{F}^*) + \mathcal{C}_{\mathcal{V}\mathcal{V}, \text{TP}}^{\text{VCS}}(\mathcal{F}_L^*, \mathcal{F})\} \right\},\end{aligned}\quad (6.181)$$

$$\begin{aligned}\text{cc}_{22, \text{TP}}^{\text{VCS}} &= \sqrt{-\frac{\Delta^2}{M_N^2}}\sqrt{1 - \frac{\Delta_{\min}^2}{\Delta^2}}\sqrt{\frac{1 - \eta}{1 + \eta}} \\ &\times 4i \sin(\Phi - \phi)(1 - y)(1 - \tilde{y})\{\mathcal{C}_{\mathcal{V}\mathcal{V}, \text{TP}}^{\text{VCS}}(\mathcal{F}, \mathcal{F}^*) - \mathcal{C}_{\mathcal{A}\mathcal{A}, \text{TP}}^{\text{VCS}}(\mathcal{F}, \mathcal{F}^*)\}.\end{aligned}\quad (6.182)$$

Here, according to the general twist-two relation (6.165),

$$\text{ss}_{11, \text{TP}}^{\text{VCS}} \simeq \text{cc}_{11, \text{TP}}^{\text{VCS}}, \quad \text{ss}_{22, \text{TP}}^{\text{VCS}} \simeq \text{cc}_{22, \text{TP}}^{\text{VCS}}. \quad (6.183)$$

All other coefficients are expressed using Eq. (6.165). Note, however, that the tensor-gluon contribution induces further second order harmonics, which are not displayed here since they are suppressed by a power of the coupling constant α_s .

6.2.7 Interference of virtual Compton and Bethe-Heitler amplitudes

In the leading-twist approximation, the following general relations can be established between the Fourier coefficients of the interference term

$$\begin{aligned} \text{ss}_{nm}^{\text{INT}} &\simeq \text{cc}_{nm}^{\text{INT}} \quad \text{and} \quad \text{cs}_{nm}^{\text{INT}} \simeq -\text{sc}_{nm}^{\text{INT}} \quad \text{for} \quad \{nm\} = \{12, 21, 32\}, \\ \text{ss}_{nm}^{\text{INT}} &\simeq \text{cc}_{nm}^{\text{INT}} \simeq \text{cs}_{nm}^{\text{INT}} \simeq \text{sc}_{nm}^{\text{INT}} \simeq 0 \quad \text{for} \quad n \neq m \pm 1, \end{aligned} \quad (6.184)$$

where $n, m + 1 \leq 3$ for $\text{INT} = \{1, 2\}$. For the unpolarized target, there are five nontrivial entries which arise for the unpolarized lepton beam, namely, $\text{cc}_{01,\text{unp}}^{\text{INT}}$, $\text{cc}_{10,\text{unp}}^{\text{INT}}$, $\text{cc}_{12,\text{unp}}^{\text{INT}}$, $\text{cc}_{21,\text{unp}}^{\text{INT}}$, and $\text{cc}_{32,\text{unp}}^{\text{INT}}$. They are supplemented by three additional Fourier coefficients for the polarized-beam option: $\text{cs}_{01,\text{unp}}^{\text{INT}}$, $\text{sc}_{10,\text{unp}}^{\text{INT}}$, and $\text{sc}_{21,\text{unp}}^{\text{INT}}$, while $\text{sc}_{12,\text{unp}}^{\text{INT}} \simeq \text{sc}_{32,\text{unp}}^{\text{INT}} \simeq 0$. To find the explicit form of these Fourier coefficients, one should evaluate the products of Dirac bilinears in Eqs. (6.139) – (6.146). This yields

$$\begin{aligned} \left\{ \begin{array}{l} \mathcal{S}_1 \\ \mathcal{S}_2 \end{array} \right\} \mathcal{F}_1 &\equiv 4Q^2 \frac{(1+\eta)\eta}{y\tilde{y}\xi} \left(\left\{ \begin{array}{l} \tilde{y}K \\ y\tilde{K} \end{array} \right\} \left[\mathcal{C}_{\mathcal{V},\text{unp}}(\mathcal{F}) \begin{Bmatrix} \cos \phi \\ \cos \varphi_\ell \end{Bmatrix} + \cos \Theta i\mathcal{C}_{\mathcal{V},\text{LP}}(\mathcal{F}) \begin{Bmatrix} \sin \phi \\ \sin \varphi_\ell \end{Bmatrix} \right] \right. \\ &\quad \left. + \sin \Theta \left\{ \begin{array}{l} \tilde{y}L \\ y\tilde{L} \end{array} \right\} \left[i\mathcal{C}_{\mathcal{V},\text{TP+}}(\mathcal{F}) \begin{Bmatrix} \sin \phi \\ \sin \varphi_\ell \end{Bmatrix} \cos(\Phi - \phi) + i\mathcal{C}_{\mathcal{V},\text{TP-}}(\mathcal{F}) \begin{Bmatrix} \cos \phi \\ \cos \varphi_\ell \end{Bmatrix} \sin(\Phi - \phi) \right] \right), \end{aligned} \quad (6.185)$$

$$\begin{aligned} \left\{ \begin{array}{l} \tilde{\mathcal{S}}_1 \\ \tilde{\mathcal{S}}_2 \end{array} \right\} \mathcal{F}_1 &\equiv 4Q^2 \frac{(1+\eta)\eta}{y\tilde{y}\xi} \left(\left\{ \begin{array}{l} \tilde{y}K \\ y\tilde{K} \end{array} \right\} \left[-i\mathcal{C}_{\mathcal{V},\text{unp}}(\mathcal{F}) \begin{Bmatrix} \sin \phi \\ \sin \varphi_\ell \end{Bmatrix} - \cos \Theta \mathcal{C}_{\mathcal{V},\text{LP}}(\mathcal{F}) \begin{Bmatrix} \cos \phi \\ \cos \varphi_\ell \end{Bmatrix} \right] \right. \\ &\quad \left. - \sin \Theta \left\{ \begin{array}{l} \tilde{y}L \\ y\tilde{L} \end{array} \right\} \left[\mathcal{C}_{\mathcal{V},\text{TP+}}(\mathcal{F}) \begin{Bmatrix} \cos \phi \\ \cos \varphi_\ell \end{Bmatrix} \cos(\Phi - \phi) - \mathcal{C}_{\mathcal{V},\text{TP-}}(\mathcal{F}) \begin{Bmatrix} \sin \phi \\ \sin \varphi_\ell \end{Bmatrix} \sin(\Phi - \phi) \right] \right), \end{aligned} \quad (6.186)$$

$$\begin{aligned} \left\{ \begin{array}{l} \mathcal{S}_1 \\ \mathcal{S}_2 \end{array} \right\} \tilde{\mathcal{F}}_1 &\equiv 4Q^2 \frac{(1+\eta)\eta}{y\tilde{y}\xi} \left(\left\{ \begin{array}{l} \tilde{y}K \\ y\tilde{K} \end{array} \right\} \left[i\mathcal{C}_{\mathcal{A},\text{unp}}(\mathcal{F}) \begin{Bmatrix} \sin \phi \\ \sin \varphi_\ell \end{Bmatrix} + \cos \Theta \mathcal{C}_{\mathcal{A},\text{LP}}(\mathcal{F}) \begin{Bmatrix} \cos \phi \\ \cos \varphi_\ell \end{Bmatrix} \right] \right. \\ &\quad \left. + \sin \Theta \left\{ \begin{array}{l} \tilde{y}L \\ y\tilde{L} \end{array} \right\} \left[\mathcal{C}_{\mathcal{A},\text{TP+}}(\mathcal{F}) \begin{Bmatrix} \cos \phi \\ \cos \varphi_\ell \end{Bmatrix} \cos(\Phi - \phi) - \mathcal{C}_{\mathcal{A},\text{TP-}}(\mathcal{F}) \begin{Bmatrix} \sin \phi \\ \sin \varphi_\ell \end{Bmatrix} \sin(\Phi - \phi) \right] \right), \end{aligned} \quad (6.187)$$

$$\begin{aligned} \left\{ \begin{array}{l} \tilde{\mathcal{S}}_1 \\ \tilde{\mathcal{S}}_2 \end{array} \right\} \tilde{\mathcal{F}}_1 &\equiv 4Q^2 \frac{(1+\eta)\eta}{y\tilde{y}\xi} \left(\left\{ \begin{array}{l} \tilde{y}K \\ y\tilde{K} \end{array} \right\} \left[-\mathcal{C}_{\mathcal{A},\text{unp}}(\mathcal{F}) \begin{Bmatrix} \cos \phi \\ \cos \varphi_\ell \end{Bmatrix} - \cos \Theta i\mathcal{C}_{\mathcal{A},\text{LP}}(\mathcal{F}) \begin{Bmatrix} \sin \phi \\ \sin \varphi_\ell \end{Bmatrix} \right] \right. \\ &\quad \left. - \sin \Theta \left\{ \begin{array}{l} \tilde{y}L \\ y\tilde{L} \end{array} \right\} \left[i\mathcal{C}_{\mathcal{A},\text{TP+}}(\mathcal{F}) \begin{Bmatrix} \sin \phi \\ \sin \varphi_\ell \end{Bmatrix} \cos(\Phi - \phi) + i\mathcal{C}_{\mathcal{A},\text{TP-}}(\mathcal{F}) \begin{Bmatrix} \cos \phi \\ \cos \varphi_\ell \end{Bmatrix} \sin(\Phi - \phi) \right] \right), \end{aligned} \quad (6.188)$$

where the angles Θ and Φ exhibit the dependence on the polarization of the target. We used, in analogy to the definitions (6.120), the shorthand notation for

$$\left\{ \begin{array}{l} L \\ \tilde{L} \end{array} \right\} \approx \frac{1}{2\eta} \sqrt{\frac{\xi M_N^2}{Q^2}} \left\{ \begin{array}{l} \sqrt{(1-y)(\xi+\eta)} \\ \sqrt{(1-\tilde{y})(\xi-\eta)} \end{array} \right\} \quad (6.189)$$

We also introduced universal electric- and magnetic-like combinations of electromagnetic form factors intertwined with CFFs

$$\mathcal{C}_{V,\text{unp}} = F_1 \mathcal{H} - \frac{\Delta^2}{4M_N^2} F_2 \mathcal{E}, \quad \mathcal{C}_{A,\text{unp}} = \eta(F_1 + F_2) \tilde{\mathcal{H}}. \quad (6.190)$$

For the longitudinally polarized nucleon, we get the following combinations of the electromagnetic and Compton form factors:

$$\mathcal{C}_{V,\text{LP}} = \eta(F_1 + F_2) \left(\mathcal{H} + \frac{\eta}{1+\eta} \mathcal{E} \right), \quad \mathcal{C}_{A,\text{LP}} = F_1 \tilde{\mathcal{H}} - \eta \left(\frac{\eta}{1+\eta} F_1 + \frac{\Delta^2}{4M_N^2} F_2 \right) \tilde{\mathcal{E}}, \quad (6.191)$$

while for the transversely polarized case we have four more combinations

$$\mathcal{C}_{V,\text{TP+}} = \frac{2\eta}{1-\eta} (F_1 + F_2) \left\{ \eta \left(\mathcal{H} - \frac{\eta}{1+\eta} \mathcal{E} \right) + \frac{\Delta^2}{4M_N^2} \mathcal{E} \right\}, \quad (6.192)$$

$$\mathcal{C}_{A,\text{TP+}} = -\frac{2}{1+\eta} \left\{ \eta^2 F_1 \left(\tilde{\mathcal{H}} + \frac{\eta}{1+\eta} \tilde{\mathcal{E}} \right) - \frac{\Delta^2}{4M_N^2} ((1-\eta^2) F_2 \tilde{\mathcal{H}} - \eta(F_1 + \eta F_2) \tilde{\mathcal{E}}) \right\}, \quad (6.193)$$

$$\mathcal{C}_{V,\text{TP-}} = \frac{2}{1+\eta} \left\{ \eta^2 F_1 (\mathcal{H} + \mathcal{E}) - \frac{\Delta^2}{4M_N^2} ((1-\eta^2) F_2 \mathcal{H} - (F_1 + \eta^2 F_2) \mathcal{E}) \right\}, \quad (6.194)$$

$$\mathcal{C}_{A,\text{TP-}} = -\frac{2\eta^2}{1+\eta} (F_1 + F_2) \left\{ \tilde{\mathcal{H}} + \frac{\Delta^2}{4M_N^2} \tilde{\mathcal{E}} \right\}. \quad (6.195)$$

Now, using Eqs. (6.139) – (6.145) and (6.157) it is straightforward to derive the following nonzero Fourier coefficients for the first interference term:

$$\text{cc}_{01,\text{unp}}^1 = 8\tilde{K}(1-y)(2-y)(2-\tilde{y}) \frac{\xi+\eta}{\eta} \Re \left\{ \mathcal{C}_{V,\text{unp}}(\mathcal{F}) + \mathcal{C}_{A,\text{unp}}(\mathcal{F}) - \frac{\xi-\eta}{\xi} \mathcal{C}_{V,\text{unp}}(\mathcal{F}_L) \right\}, \quad (6.196)$$

$$\text{cs}_{01,\text{unp}}^1 = 8\lambda\tilde{K}y(1-y)(2-\tilde{y}) \frac{\xi+\eta}{\eta} \Im \left\{ \mathcal{C}_{V,\text{unp}}(\mathcal{F}) + \mathcal{C}_{A,\text{unp}}(\mathcal{F}) + \frac{\xi-\eta}{\xi} \mathcal{C}_{V,\text{unp}}(\mathcal{F}_L) \right\}, \quad (6.197)$$

$$\begin{aligned} \text{cc}_{10,\text{unp}}^1 &= 8K \Re \left\{ -(2-2y+y^2)(2-2\tilde{y}+\tilde{y}^2) \left(\frac{\xi}{\eta} \mathcal{C}_{V,\text{unp}}(\mathcal{F}) + \mathcal{C}_{A,\text{unp}}(\mathcal{F}) \right) \right. \\ &\quad \left. + 8(1-y)(1-\tilde{y}) \frac{\xi^2-\eta^2}{\eta\xi} \mathcal{C}_{V,\text{unp}}(\mathcal{F}_L) \right\}, \end{aligned} \quad (6.198)$$

$$\text{cc}_{12,\text{unp}}^1 = 16K(1-y)(1-\tilde{y}) \frac{\xi-\eta}{\xi} \Re \left\{ \mathcal{C}_{V,\text{unp}}(\mathcal{F}) + \mathcal{C}_{A,\text{unp}}(\mathcal{F}) \right\}, \quad (6.199)$$

$$\text{sc}_{10,\text{unp}}^1 = -8\lambda Ky(2-y)(2-2\tilde{y}+\tilde{y}^2) \Im \left\{ \mathcal{C}_{V,\text{unp}}(\mathcal{F}) + \frac{\xi}{\eta} \mathcal{C}_{A,\text{unp}}(\mathcal{F}) \right\}, \quad (6.200)$$

$$\text{cc}_{21,\text{unp}}^1 = 8\tilde{K}(1-y)(2-y)(2-\tilde{y}) \frac{\xi+\eta}{\eta} \Re \left\{ \mathcal{C}_{V,\text{unp}}(\mathcal{F}) - \mathcal{C}_{A,\text{unp}}(\mathcal{F}) - \frac{\xi+\eta}{\xi} \mathcal{C}_{V,\text{unp}}(\mathcal{F}_L) \right\}, \quad (6.201)$$

$$\text{sc}_{21,\text{unp}}^1 = -8\lambda\tilde{K}y(1-y)(2-\tilde{y}) \frac{\xi+\eta}{\eta} \Im \left\{ \mathcal{C}_{V,\text{unp}}(\mathcal{F}) - \mathcal{C}_{A,\text{unp}}(\mathcal{F}) + \frac{\xi+\eta}{\xi} \mathcal{C}_{V,\text{unp}}(\mathcal{F}_L) \right\}, \quad (6.202)$$

$$\text{cc}_{32,\text{unp}}^1 = -16K(1-y)(1-\tilde{y}) \frac{\xi+\eta}{\eta} \Re \left\{ \mathcal{C}_{V,\text{unp}}(\mathcal{F}) - \mathcal{C}_{A,\text{unp}}(\mathcal{F}) \right\}. \quad (6.203)$$

One should also add to this list $\text{ss}_{12,\text{unp}}^1$, $\text{ss}_{21,\text{unp}}^1$, $\text{cs}_{21,\text{unp}}^1$, and $\text{ss}_{32,\text{unp}}^1$, which follow from Eq. (6.184).

Next, we display the explicit form of the Fourier coefficients in the interference term with the second BH process for an unpolarized nucleon target, which can be obtained through symmetry considerations as will be explained below. These coefficients are

$$cc_{01,\text{unp}}^2 = -8K(2-y)(1-\tilde{y})(2-\tilde{y})\frac{\xi-\eta}{\eta}\Re\left\{\mathcal{C}_{\mathcal{V},\text{unp}}(\mathcal{F}) - \mathcal{C}_{\mathcal{A},\text{unp}}(\mathcal{F}) - \frac{\xi+\eta}{\xi}\mathcal{C}_{\mathcal{V},\text{unp}}(\mathcal{F}_L)\right\}, \quad (6.204)$$

$$cs_{01,\text{unp}}^2 = 8\lambda Ky(1-\tilde{y})(2-\tilde{y})\frac{\xi-\eta}{\eta}\Im\left\{\mathcal{C}_{\mathcal{V},\text{unp}}(\mathcal{F}) - \mathcal{C}_{\mathcal{A},\text{unp}}(\mathcal{F}) + \frac{\xi+\eta}{\xi}\mathcal{C}_{\mathcal{V},\text{unp}}(\mathcal{F}_L)\right\}, \quad (6.205)$$

$$\begin{aligned} cc_{10,\text{unp}}^2 &= 8\tilde{K}\Re\left\{(2-2y+y^2)(2-2\tilde{y}+\tilde{y}^2)\left(\frac{\xi}{\eta}\mathcal{C}_{\mathcal{V},\text{unp}}(\mathcal{F}) + \mathcal{C}_{\mathcal{A},\text{unp}}(\mathcal{F})\right)\right. \\ &\quad \left.-8(1-y)(1-\tilde{y})\frac{\xi^2-\eta^2}{\eta\xi}\mathcal{C}_{\mathcal{V},\text{unp}}(\mathcal{F}_L)\right\}, \end{aligned} \quad (6.206)$$

$$cc_{12,\text{unp}}^2 = 16\tilde{K}(1-y)(1-\tilde{y})\frac{\xi+\eta}{\eta}\Re\left\{\mathcal{C}_{\mathcal{V},\text{unp}}(\mathcal{F}) - \mathcal{C}_{\mathcal{A},\text{unp}}(\mathcal{F})\right\}, \quad (6.207)$$

$$sc_{10,\text{unp}}^2 = 8\lambda\tilde{K}y(2-y)(2-2\tilde{y}+\tilde{y}^2)\Im\left\{\mathcal{C}_{\mathcal{V},\text{unp}}(\mathcal{F}) + \frac{\xi}{\eta}\mathcal{C}_{\mathcal{A},\text{unp}}(\mathcal{F})\right\}, \quad (6.208)$$

$$cc_{21,\text{unp}}^2 = -8K(2-y)(1-\tilde{y})(2-\tilde{y})\frac{\xi-\eta}{\eta}\Re\left\{\mathcal{C}_{\mathcal{V},\text{unp}}(\mathcal{F}) + \mathcal{C}_{\mathcal{A},\text{unp}}(\mathcal{F}) - \frac{\xi-\eta}{\xi}\mathcal{C}_{\mathcal{V},\text{unp}}(\mathcal{F}_L)\right\}, \quad (6.209)$$

$$sc_{21,\text{unp}}^2 = 8\lambda Ky(1-\tilde{y})(2-\tilde{y})\frac{\xi-\eta}{\eta}\Im\left\{\mathcal{C}_{\mathcal{V},\text{unp}}(\mathcal{F}) + \mathcal{C}_{\mathcal{A},\text{unp}}(\mathcal{F}) + \frac{\xi-\eta}{\xi}\mathcal{C}_{\mathcal{V},\text{unp}}(\mathcal{F}_L)\right\}, \quad (6.210)$$

$$cc_{32,\text{unp}}^2 = 16\tilde{K}(1-y)(1-\tilde{y})\frac{\xi-\eta}{\eta}\Re\left\{\mathcal{C}_{\mathcal{V},\text{unp}}(\mathcal{F}) + \mathcal{C}_{\mathcal{A},\text{unp}}(\mathcal{F})\right\}. \quad (6.211)$$

These expressions follow from Eqs. (6.146) – (6.152) and (6.157). For the unpolarized lepton beam, they appear from the application of the symmetry under the exchange $k \leftrightarrow -\ell_-$ and $k' \leftrightarrow \ell_+$, as discussed above in Section 6.2.4,

$$\{cc_{01}^2, cc_{10}^2, cc_{12}^2, cc_{21}^2, cc_{32}^2\}_{\text{unp}} = \{cc_{01}^1, cc_{10}^1, cc_{12}^1, cc_{21}^1, cc_{32}^1\}_{\text{unp}} \Big|_{\xi \rightarrow -\xi}^{y \leftrightarrow \tilde{y}}. \quad (6.212)$$

One should keep in mind that $\mathcal{C}_{\mathcal{V}}$ and $\mathcal{C}_{\mathcal{A}}$ are even and odd functions in $\xi - i0$, respectively, and $\tilde{K}(\xi, \tilde{y}) = K(-\xi, y = \tilde{y})$. It turns out that the remaining coefficients for the polarized lepton beam satisfy the following symmetry relations

$$\{cs_{01}^2, sc_{21}^2\}_{\text{unp}} = \sqrt{\frac{\tilde{y}-1}{1-y}}\{cs_{01}^1, sc_{21}^1\}_{\text{unp}} \Big|_{\xi \rightarrow -\xi}, \quad sc_{10,\text{unp}}^2 = -\sqrt{\frac{\tilde{y}-1}{1-y}}sc_{10,\text{unp}}^1 \Big|_{\xi \rightarrow -\xi}. \quad (6.213)$$

Next let us comment on the Fourier coefficients for the polarized target. From the results (6.185)-(6.188), we immediately deduce several relations which allow one to obtain the Fourier coefficients from Eqs. (6.196) – (6.203) and (6.204) – (6.211) for the unpolarized case by using simple substitution rules:

$$\{cc_{01}, cc_{10}, cc_{21}\}_{\text{LP}}^{\text{INT}} = \{cs_{01}, sc_{10}, sc_{21}\}_{\text{unp}}^{\text{INT}} \Big|_{\Im\mathcal{C}_{\text{unp}} \rightarrow \Re\mathcal{C}_{\text{LP}}}, \quad (6.214)$$

$$\{cs_{01}, sc_{10}, cs_{12}, sc_{21}, sc_{32}\}_{\text{LP}}^{\text{INT}} = \{cc_{01}, cc_{10}, cc_{12}, cc_{21}, cc_{32}\}_{\text{unp}}^{\text{INT}} \Big|_{\Re\mathcal{C}_{\text{unp}} \rightarrow \Im\mathcal{C}_{\text{LP}}}.$$

In case of the transversely polarized target, as before, one has an additional decomposition in $\cos(\Phi - \phi)$ and $\sin(\Phi - \phi)$ and has to replace K (\tilde{K}) by L (\tilde{L})

$$\begin{aligned} \{\text{cc}_{01}, \text{cc}_{10}, \text{cc}_{21}\}_{\text{TP+}}^{\text{INT}} &= \cos(\Phi - \phi) \{\text{cs}_{01}, \text{sc}_{10}, \text{sc}_{21}\}_{\text{unp}}^{\text{INT}} \Big|_{\substack{\Im m \mathcal{C}_{\text{unp}} \rightarrow \Re e \mathcal{C}_{\text{TP+}} \\ K \rightarrow L, \tilde{K} \rightarrow \tilde{L}}} , \\ \{\text{cs}_{01}, \text{sc}_{10}, \text{sc}_{21}\}_{\text{TP-}}^{\text{INT}} &= \sin(\Phi - \phi) \{\text{cs}_{01}, \text{sc}_{10}, \text{sc}_{21}\}_{\text{unp}}^{\text{INT}} \Big|_{\substack{\Im m \mathcal{C}_{\text{unp}} \rightarrow -\Re e \mathcal{C}_{\text{TP-}} \\ K \rightarrow L, \tilde{K} \rightarrow \tilde{L}}} , \\ \{\text{cs}_{01}, \text{sc}_{10}, \text{cs}_{12}, \text{sc}_{21}, \text{sc}_{32}\}_{\text{TP+}}^{\text{INT}} &= \cos(\Phi - \phi) \{\text{cc}_{01}, \text{cc}_{10}, \text{cc}_{12}, \text{cc}_{21}, \text{cc}_{32}\}_{\text{unp}}^{\text{INT}} \Big|_{\substack{\Re e \mathcal{C}_{\text{unp}} \rightarrow \Im m \mathcal{C}_{\text{TP+}} \\ K \rightarrow L, \tilde{K} \rightarrow \tilde{L}}} , \\ \{\text{cc}_{01}, \text{cc}_{10}, \text{cc}_{12}, \text{cc}_{23}, \text{cc}_{32}\}_{\text{TP-}}^{\text{INT}} &= \sin(\Phi - \phi) \{\text{cc}_{01}, \text{cc}_{10}, \text{cc}_{12}, \text{cc}_{23}, \text{cc}_{32}\}_{\text{unp}}^{\text{INT}} \Big|_{\substack{\Re e \mathcal{C}_{\text{unp}} \rightarrow \Im m \mathcal{C}_{\text{TP-}} \\ K \rightarrow L, \tilde{K} \rightarrow \tilde{L}}} . \end{aligned} \quad (6.215)$$

Applying the relation (6.184), the remaining nonvanishing Fourier coefficients, i.e., $\text{ss}_{21}^{\text{INT}}$, $\text{sc}_{12}^{\text{INT}}$, $\text{cs}_{21}^{\text{INT}}$, $\text{cs}_{23}^{\text{INT}}$ for LP and TP+ as well as $\text{ss}_{12}^{\text{INT}}$, $\text{ss}_{21}^{\text{INT}}$, $\text{ss}_{23}^{\text{INT}}$ and $\text{cs}_{21}^{\text{INT}}$ for TP- are easily found. Note also that

$$\tilde{K}(\xi, \tilde{y}) \approx \sqrt{(\tilde{y} - 1)/(1 - y)} K(-\xi, y) .$$

6.2.8 Squared Bethe-Heitler amplitude

The exact expressions for the Fourier coefficients of the pure BH term (6.158) are extremely lengthy and, therefore, will not be displayed here in analytic form. In the following, we limit ourselves instead to leading terms in the asymptotic expansion as $Q^2/\xi \rightarrow \infty$. Namely,

$$\begin{aligned} \text{cc}_{00,\text{unp}}^{11} &\approx -2 \frac{1-\eta}{1+\eta} \left(1 + \frac{\xi}{\eta}\right) (1-y) \left\{ (2-2y+y^2)(2-2\tilde{y}+\tilde{y}^2) \left(1 + \frac{\xi^2}{\eta^2}\right) \right. \\ &\quad \left. - 8(1-y)(1-\tilde{y}) \left(1 - \frac{\xi^2}{\eta^2}\right) \right\} \left\{ \left(1 - \frac{\Delta_{\min}^2}{\Delta^2}\right) \left(F_1^2 - \frac{\Delta^2}{4M^2} F_2^2\right) + \frac{2\eta^2}{1-\eta^2} (F_1 + F_2)^2 \right\} , \end{aligned} \quad (6.216)$$

$$\begin{aligned} \text{cc}_{02,\text{unp}}^{11} &\approx 2 \frac{1-\eta}{1+\eta} \left(1 + \frac{\xi}{\eta}\right) \left(1 - \frac{\xi^2}{\eta^2}\right) \left(1 - \frac{\Delta_{\min}^2}{\Delta^2}\right) (1-y) \left\{ (2-2y+y^2)(2-2\tilde{y}+\tilde{y}^2) \right. \\ &\quad \left. + 8(1-y)(1-\tilde{y}) \right\} \left(F_1^2 - \frac{\Delta^2}{4M^2} F_2^2\right) , \end{aligned} \quad (6.217)$$

$$\begin{aligned} \text{cc}_{11,\text{unp}}^{11} &\approx -4 \frac{1-\eta}{1+\eta} \left(1 + \frac{\xi}{\eta}\right) \frac{\sigma}{\eta} \sqrt{(1-y)(1-\tilde{y})(\xi^2 - \eta^2)} \\ &\quad \times (1-y)(2-y)(2-\tilde{y}) \left\{ \left(1 - 3\frac{\xi}{\eta}\right) \left(1 - \frac{\Delta_{\min}^2}{\Delta^2}\right) \left(F_1^2 - \frac{\Delta^2}{4M^2} F_2^2\right) - \frac{4\xi\eta}{1-\eta^2} (F_1 + F_2)^2 \right\} , \end{aligned} \quad (6.218)$$

$$\begin{aligned} \text{cc}_{13,\text{unp}}^{11} &\approx 4 \frac{1-\eta}{1+\eta} \left(1 + \frac{\xi}{\eta}\right)^2 \left(1 - \frac{\Delta_{\min}^2}{\Delta^2}\right) \frac{\sigma}{\eta} \sqrt{(1-y)(1-\tilde{y})(\xi^2 - \eta^2)} , \\ &\quad \times (1-y)(2-y)(2-\tilde{y}) \left(F_1^2 - \frac{\Delta^2}{4M^2} F_2^2\right) , \end{aligned} \quad (6.219)$$

$$\text{cc}_{20,\text{unp}}^{11} \approx -4 \frac{1-\eta}{1+\eta} \left(1 - \frac{\xi}{\eta}\right) \left(1 - \frac{\xi^2}{\eta^2}\right) \left(1 - \frac{\Delta_{\min}^2}{\Delta^2}\right) (1-y)^2 (1-\tilde{y}) \left(F_1^2 - \frac{\Delta^2}{4M^2} F_2^2\right) , \quad (6.220)$$

$$\begin{aligned} \text{cc}_{22,\text{unp}}^{11} &\approx 8 \frac{1-\eta}{1+\eta} \left(1 + \frac{\xi}{\eta}\right) \left(1 - \frac{\xi^2}{\eta^2}\right) (1-y)^2 (1-\tilde{y}) \\ &\quad \times \left\{ \left(1 - \frac{\Delta_{\min}^2}{\Delta^2}\right) \left(F_1^2 - \frac{\Delta^2}{4M^2} F_2^2\right) + \frac{2\eta^2}{1-\eta^2} (F_1 + F_2)^2 \right\} . \end{aligned} \quad (6.221)$$

The remaining coefficients are expressed via the already known ones

$$\begin{aligned} \text{cc}_{24,\text{unp}}^{11} &\approx \frac{(\eta + \xi)^2}{(\eta - \xi)^2} \text{cc}_{20,\text{unp}}^{11}, & \text{ss}_{11,\text{unp}}^{11} &\approx \text{cc}_{11,\text{unp}}^{11} + 2 \frac{\eta - \xi}{\eta + \xi} \text{cc}_{13,\text{unp}}^{11}, \\ \text{ss}_{13,\text{unp}}^{11} &\approx \text{cc}_{13,\text{unp}}^{11}, & \text{ss}_{22,\text{unp}}^{11} &\approx \text{cc}_{22,\text{unp}}^{11}, & \text{ss}_{24,\text{unp}}^{11} &\approx \text{cc}_{24,\text{unp}}^{11}. \end{aligned} \quad (6.222)$$

One should realize that this expansion is only valid if one stays away from kinematical boundaries, e.g., $y \ll 1$ is required. The reason for this is that the leading terms vanish with $(1 - y)$, and subleading corrections become important as $y \rightarrow 1$. In contrast to the DVCS case, no cancellations occur between the numerator and the denominator of the BH amplitude squared, so that, in general, the Fourier decomposition goes as high as up to the forth-order harmonics.

We also note that the Fourier coefficients for the second BH-amplitude squared simply follow from the symmetry under the exchange $k \leftrightarrow -\ell_-$ and $k' \leftrightarrow \ell_+$. Since we extracted a power of ξ in front of the squared BH amplitude (6.158), we obtain the substitution rule

$$\text{cc}_{nm}^{22} = -\text{cc}_{nm}^{11} \Big|_{\xi \rightarrow -\xi}^{\eta \leftrightarrow \tilde{\eta}} \quad \text{and} \quad \text{ss}_{nm}^{22} = -\text{ss}_{nm}^{11} \Big|_{\xi \rightarrow -\xi}^{\eta \leftrightarrow \tilde{\eta}}, \quad (6.223)$$

while the remaining variables $\{\eta, \Delta^2, Q^2\}$ are kept unchanged. For the interference term of the first and second BH amplitudes, the Fourier coefficients are

$$\begin{aligned} \text{cc}_{00,\text{unp}}^{12} &\approx 8 \frac{1 - \eta \xi}{1 + \eta \eta} \left(1 - \frac{\xi^2}{\eta^2} \right) (1 - y)(2 - y)(1 - \tilde{y})(2 - \tilde{y}) \\ &\times \left\{ \left(1 - \frac{\Delta_{\min}^2}{\Delta^2} \right) \left(F_1^2 - \frac{\Delta^2}{4M^2} F_2^2 \right) + \frac{2\eta^2}{1 - \eta^2} (F_1 + F_2)^2 \right\}, \end{aligned} \quad (6.224)$$

$$\begin{aligned} \text{cc}_{02,\text{unp}}^{12} &\approx 8 \frac{1 - \eta}{1 + \eta} \left(1 + \frac{\xi}{\eta} \right) \left(1 - \frac{\xi^2}{\eta^2} \right) (1 - y)(2 - y)(1 - \tilde{y})(2 - \tilde{y}) \left(1 - \frac{\Delta_{\min}^2}{\Delta^2} \right) \left(F_1^2 - \frac{\Delta^2}{4M^2} F_2^2 \right), \end{aligned} \quad (6.225)$$

$$\begin{aligned} \text{cc}_{11,\text{unp}}^{12} &\approx 8 \frac{1 - \eta \sigma}{1 + \eta \eta} \sqrt{(1 - y)(1 - \tilde{y})(\xi^2 - \eta^2)} \\ &\times \left\{ (2 - 2y + y^2)(2 - 2\tilde{y} + \tilde{y}^2) \left[\frac{\xi^2}{\eta^2} \left(1 - \frac{\Delta_{\min}^2}{\Delta^2} \right) \left(F_1^2 - \frac{\Delta^2}{4M^2} F_2^2 \right) + \frac{\xi^2 + \eta^2}{1 - \eta^2} (F_1 + F_2)^2 \right] \right. \\ &\left. - (1 - y)(1 - \tilde{y}) \left(1 - \frac{\xi^2}{\eta^2} \right) \left[9 \left(1 - \frac{\Delta_{\min}^2}{\Delta^2} \right) \left(F_1^2 - \frac{\Delta^2}{4M^2} F_2^2 \right) + 10 \frac{\eta^2}{1 - \eta^2} (F_1 + F_2)^2 \right] \right\}, \end{aligned} \quad (6.226)$$

$$\begin{aligned} \text{cc}_{20,\text{unp}}^{12} &\approx -8 \frac{1 - \eta}{1 + \eta} \left(1 - \frac{\xi}{\eta} \right) \\ &\times \left(1 - \frac{\xi^2}{\eta^2} \right) \left(1 - \frac{\Delta_{\min}^2}{\Delta^2} \right) (1 - y)(2 - y)(1 - \tilde{y})(2 - \tilde{y}) \left(F_1^2 - \frac{\Delta^2}{4M^2} F_2^2 \right), \end{aligned} \quad (6.227)$$

$$\begin{aligned} \text{cc}_{22,\text{unp}}^{12} &\approx 8 \frac{1 - \eta \xi}{1 + \eta \eta} \left(1 - \frac{\xi^2}{\eta^2} \right) \\ &\times (1 - y)(2 - y)(1 - \tilde{y})(2 - \tilde{y}) \left\{ \left(1 - \frac{\Delta_{\min}^2}{\Delta^2} \right) \left(F_1^2 - \frac{\Delta^2}{4M^2} F_2^2 \right) + \frac{2\eta^2}{1 - \eta^2} (F_1 + F_2)^2 \right\}, \end{aligned} \quad (6.228)$$

$$\begin{aligned} \text{ss}_{11,\text{unp}}^{12} &\approx \text{cc}_{11,\text{unp}}^{12} + 8 \frac{1 - \eta \sigma}{1 + \eta \eta} \sqrt{(1 - y)(1 - \tilde{y})(\xi^2 - \eta^2)} \left(1 - \frac{\xi^2}{\eta^2} \right) \\ &\times \left\{ (2 - 2y + y^2)(2 - 2\tilde{y} + \tilde{y}^2) + 8(1 - y)(1 - \tilde{y}) \right\} \left(1 - \frac{\Delta_{\min}^2}{\Delta^2} \right) \left(F_1^2 - \frac{\Delta^2}{4M^2} F_2^2 \right), \end{aligned} \quad (6.229)$$

$$\text{ss}_{22,\text{unp}}^{12} \approx \text{cc}_{22,\text{unp}}^{12}. \quad (6.230)$$

Again, under the interchanges $k \leftrightarrow -\ell_-$ and $k' \leftrightarrow \ell_+$, both amplitudes are odd, i.e., $\mathcal{T}_{\text{BH}_1} \leftrightarrow -\mathcal{T}_{\text{BH}_2}$, and, hence, their interference term is invariant. Thus, the Fourier coefficients must satisfy the relation

$$\text{cc}_{nm}^{12} = -\text{cc}_{mn}^{12} \Big|_{\xi \rightarrow -\xi}^{\eta \leftrightarrow \tilde{\eta}} \quad \text{and} \quad \text{ss}_{nm}^{12} = -\text{ss}_{mn}^{12} \Big|_{\xi \rightarrow -\xi}^{\eta \leftrightarrow \tilde{\eta}}, \quad (6.231)$$

which is indeed the case.

6.2.9 Single-spin asymmetries

Having introduced a complete angular dependence of the cross section, we will now have a closer look on the single-spin asymmetries, in particular, the beam-spin asymmetry for the proton

$$d\sigma^\uparrow - d\sigma^\downarrow \sim (\pm \mathcal{T}_{\text{BH}_1}^* + \mathcal{T}_{\text{BH}_2}^*) \Im \text{m} \mathcal{T}_{\text{VCS}} + \dots \quad (6.232)$$

Potentially, the interference term could be contaminated by the imaginary part $\Im \text{m} \mathcal{T}_{\text{VCS}} \mathcal{T}_{\text{VCS}}^\dagger$ arising from the interference of twist-two and twist-three Compton form factors. Just like in the DVCS case [328], we expect, that this contribution can be safely neglected, assuming the smallness of three-particle correlations. As we mentioned above, in the leading order of QCD perturbation theory, the single spin asymmetries are directly proportional to the linear combination of GPDs

$$\Im \text{m} \mathcal{F} = \pi \sum_q Q_q^2 \{ F^q(\xi, \eta, \Delta^2) \mp F^q(-\xi, \eta, \Delta^2) \} + \mathcal{O}(\alpha_s). \quad (6.233)$$

where (+) – applies for the (axial-) vector-type GPDs. For instance, eight leading-twist observables are measurable in the beam-spin asymmetry, which come in pairs from the interference of the VCS with the first and second BH amplitudes⁴⁵: $\text{cs}_{01}^1, \text{sc}_{10}^1, \text{sc}_{21}^1, \text{cs}_{12}^1$ as well as $\text{cs}_{01}^2, \text{sc}_{10}^2, \text{sc}_{21}^2, \text{cs}_{12}^2$, see Eq. (6.213). However, they depend only on two different linear combinations (6.190) of GPDs:

$$F_1(\mathcal{H} + \mathcal{H}_L) - \frac{\Delta^2}{4M_N^2} F_2(\mathcal{E} + \mathcal{E}_L), \quad \eta(F_1 + F_2)\tilde{\mathcal{H}} - \frac{\eta}{\xi} \left(F_1\mathcal{H}_L - \frac{\Delta^2}{4M_N^2} F_2\mathcal{E}_L \right). \quad (6.234)$$

Consequently, there exist six constraints among the whole set of coefficients, which can be expressed as

$$\begin{aligned} \text{sc}_{10}^1 &\simeq -\frac{(2-y)(2-2\tilde{y}+\tilde{y}^2)}{2(1-y)(2-\tilde{y})} \frac{\sqrt{(1-y)(\xi+\eta)}}{\sqrt{(1-\tilde{y})(\xi-\eta)}} \left\{ \text{cs}_{01}^1 + \frac{\xi-\eta}{\xi+\eta} \text{sc}_{21}^1 \right\}, \\ \frac{\text{cs}_{01}^2}{\text{sc}_{21}^1} &\simeq \frac{\text{sc}_{10}^2}{\text{sc}_{10}^1} \simeq \frac{\text{sc}_{21}^2}{\text{cs}_{01}^1} \simeq -\frac{\sqrt{(1-\tilde{y})(\xi-\eta)}}{\sqrt{(1-y)(\xi+\eta)}}, \end{aligned} \quad (6.235)$$

supplemented by the relation (6.184), i.e., $\text{cs}_{21}^1 \simeq -\text{sc}_{21}^1$ and $\text{cs}_{21}^2 \simeq -\text{sc}_{21}^2$. Another consequence of Eq. (6.234) is that the beam-spin asymmetry gives no handle on the Callan-Gross relation, i.e., the longitudinal Compton form factors cannot be separated from the leading ones. The Fourier

⁴⁵For brevity, throughout this section, we omit in the Fourier coefficients the subscript “unp”, which refers to the unpolarized target.

coefficients are projected out by taking the following moments when integrated over the scattering and azimuthal angles:

$$\begin{aligned} \sin \phi &\rightarrow \text{sc}_{10}^1, \quad \cos \theta_\ell \sin \varphi_\ell \rightarrow \text{cs}_{01}^1, \quad \cos \theta_\ell \cos \varphi_\ell \sin(2\phi) \rightarrow \text{sc}_{21}^1, \quad \cos \theta_\ell \sin \varphi_\ell \cos(2\phi) \rightarrow \text{cs}_{21}^1, \\ \sin \phi_\ell &\rightarrow \text{sc}_{10}^2, \quad \cos \theta_\ell \sin \phi \rightarrow \text{cs}_{01}^2, \quad \cos \theta_\ell \sin(2\varphi_\ell) \cos \phi \rightarrow \text{sc}_{21}^2, \quad \cos \theta_\ell \cos(2\varphi_\ell) \sin \phi \rightarrow \text{cs}_{21}^2, \end{aligned}$$

where the weight in the first (second) row is even (odd) under the reflection $\theta_\ell \rightarrow \pi - \theta_\ell$ and $\varphi_\ell \rightarrow \pi + \varphi_\ell$. In the same line of thinking, one can study the Fourier coefficients for the single target-spin asymmetries. Because of the substitution rules (6.214) and (6.215), the number of the Compton form factors will be the same as for the case of charge and angular asymmetries discussed below. Of course, single target-spin asymmetries are given by the imaginary part of new linear combinations of GPDs with a characteristic angular dependence.

From Eq. (6.235), one can conclude that the same information about GPDs is obtained by taking the appropriate moments in ϕ or φ_ℓ . However, the size of the complementary beam-spin asymmetries can vary. Moreover, if one takes the asymmetry from the interference with the second BH amplitude, the weight must be odd and, thus, we have no contamination from the squared VCS amplitude. To suppress the squared BH amplitude, one can integrate over the region $\pi/4 \leq \theta_\ell \leq 3\pi/4$ and form alternatively the $\sin \phi$ or $\sin \varphi_\ell$ moments. This procedure extracts the coefficients sc_{10}^1 and sc_{10}^2 , respectively, cf. Eqs. (6.157), (6.159), and (6.184). Thus, the beam-spin asymmetry

$$\begin{aligned} \left\{ \begin{array}{l} A_{\text{LU}}^{\sin \phi} \\ A_{\text{LU}}^{\sin \varphi_\ell} \end{array} \right\} &= \frac{1}{\mathcal{N}} \int_{\pi/4}^{3\pi/4} d\theta_\ell \int_0^{2\pi} d\varphi_\ell \int_0^{2\pi} d\phi \left\{ \begin{array}{l} 2 \sin \phi \\ 2 \sin \varphi_\ell \end{array} \right\} \frac{d\sigma^\uparrow - d\sigma^\downarrow}{d\Omega_\ell d\phi} \\ &\sim \Im \left\{ F_1 \mathcal{H} - \frac{\Delta^2}{4M_N^2} F_2 \mathcal{E} + \xi(F_1 + F_2) \tilde{\mathcal{H}} \right\}, \end{aligned} \quad (6.236)$$

with the normalization factor given by

$$\mathcal{N} = \int_{\pi/4}^{3\pi/4} d\theta_\ell \int_0^{2\pi} d\varphi_\ell \int_0^{2\pi} d\phi \frac{d\sigma^\uparrow + d\sigma^\downarrow}{d\Omega_\ell d\phi},$$

is analogous to that defined in the case of space- and timelike DVCS. For the proton target, it is mainly sensitive to the contribution $F_1 \Im \mathcal{H}$ and, therefore, it may not be useful for the estimate of the other two Compton form factors. The magnitude of the asymmetry can be as large as 20% depending on assumed models of GPDs.

6.2.10 Charge and angular asymmetries

Let us now comment on charge and angular asymmetries, in which the Fourier coefficients cc_{01}^1 , cc_{10}^1 , $\text{cc}_{12}^1 \simeq \text{ss}_{12}^1$, $\text{cc}_{21}^1 \simeq \text{ss}_{21}^1$, and $\text{cc}_{32}^1 \simeq \text{ss}_{32}^1$ as well as the complementary set due to the second interference term are accessible. The Fourier coefficients of both interference terms are related by

$$\frac{\text{cc}_{01}^2}{\text{cc}_{21}^1} \simeq \frac{\text{cc}_{10}^2}{\text{cc}_{10}^1} \simeq \frac{\text{cc}_{12}^2}{\text{cc}_{32}^1} \simeq \frac{\text{cc}_{21}^2}{\text{cc}_{01}^1} \simeq \frac{\text{cc}_{32}^2}{\text{cc}_{12}^1} \simeq -\frac{\sqrt{(1-\tilde{y})(\xi-\eta)}}{\sqrt{(1-y)(\xi+\eta)}}. \quad (6.237)$$

There are now three independent Compton form factors $\mathcal{C}_{V,\text{unp}}(\mathcal{F})$, $\mathcal{C}_{V,\text{unp}}(\mathcal{F}_L)$, and $\mathcal{C}_{A,\text{unp}}(\mathcal{F})$, introduced in Eq. (6.190). Consequently, there exist two constraints among five nontrivial Fourier

coefficients. If the Callan-Gross relation is assumed to be fulfilled, this number increases to three:

$$\begin{aligned} \text{cc}_{10}^1 &\simeq -\frac{(2-2y+y^2)(2-2\tilde{y}+\tilde{y}^2)}{2(2-y)(1-\tilde{y})(2-\tilde{y})} \frac{\sqrt{(1-\tilde{y})(\xi-\eta)}}{\sqrt{(1-y)(\xi+\eta)}} \left\{ \frac{\xi+\eta}{\xi-\eta} \text{cc}_{01}^1 + \text{cc}_{21}^1 \right\}, \\ \text{cc}_{12}^1 &\simeq \frac{-2(1-y)}{(2-y)(2-\tilde{y})} \frac{\sqrt{(1-\tilde{y})(\xi-\eta)}}{\sqrt{(1-y)(\xi+\eta)}} \text{cc}_{01}^1, \\ \text{cc}_{32}^1 &\simeq \frac{-2(1-\tilde{y})}{(2-y)(2-\tilde{y})} \frac{\sqrt{(1-y)(\xi+\eta)}}{\sqrt{(1-\tilde{y})(\xi-\eta)}} \text{cc}_{21}^1. \end{aligned} \quad (6.238)$$

The measurements of charge and angular asymmetries can be combined with double spin-flip experiments, which offer information on a new superposition of GPDs. As in the case of the beam-spin asymmetry, the number of independent Compton form factors is, however, reduced to two as a consequence of Eqs. (6.214) and (6.215).

The charge odd part is given by the interference of the first BH amplitude with the VCS amplitude as well as with the second BH amplitude. For unpolarized settings, the charge asymmetry yields

$$d\sigma^+ - d\sigma^- \sim \Re(\mathcal{T}_{\text{BH}_1}^* \mathcal{T}_{\text{BH}_2} + \mathcal{T}_{\text{BH}_1}^* \mathcal{T}_{\text{VCS}}). \quad (6.239)$$

Taking now the moments with respect to the solid angle of the final state lepton pair that are even under the reflection, e.g., by means of the weight function

$$w^{\text{even}}(\phi_\ell, \theta_\ell) = \{1, \cos \phi_\ell \cos \theta_\ell, \cos(2\phi_\ell), \sin \phi_\ell \cos \theta_\ell, \sin(2\phi_\ell), \dots\}, \quad (6.240)$$

the contaminating BH interference drops out and we find

$$\int d\Omega_\ell w^{\text{even}}(\phi_\ell, \theta_\ell) \frac{d\sigma^+ - d\sigma^-}{d\Omega_\ell} \sim \int d\Omega_\ell w^{\text{even}}(\phi_\ell, \theta_\ell) \Re(\mathcal{T}_{\text{BH}_1}^* \mathcal{T}_{\text{VCS}}). \quad (6.241)$$

Depending on the choice of the weight function, this average will provide Fourier series in ϕ , where the zeroth, first, second and third harmonics provide access to all leading-twist coefficients of the first interference term. In case when only the lepton beam of a specific charge—positive or negative—is available, one can form asymmetries with an odd weight

$$\begin{aligned} w^{\text{odd}}(\phi_\ell, \theta_\ell) \\ = \{\cos \theta_\ell, \cos \varphi_\ell, \cos(2\varphi_\ell) \cos \theta_\ell, \cos(3\varphi_\ell), \sin \varphi_\ell, \sin(2\varphi_\ell) \cos \theta_\ell, \sin(3\varphi_\ell), \dots\}, \end{aligned} \quad (6.242)$$

so that the squared amplitudes exactly drop out

$$\int d\Omega_\ell w^{\text{odd}}(\phi_\ell, \theta_\ell) \frac{d\sigma}{d\Omega_\ell} \sim \int d\Omega_\ell w^{\text{odd}}(\phi_\ell, \theta_\ell) \{\pm \mathcal{T}_{\text{BH}_1}^* \mathcal{T}_{\text{BH}_2} + \Re(\mathcal{T}_{\text{BH}_2}^* \mathcal{T}_{\text{VCS}})\}. \quad (6.243)$$

After the subtraction of the remaining BH interference is done, it allows to measure the leading twist-two Fourier coefficients. The procedure we just outlined may give a handle on the real part of the Compton form factors. If both types of the lepton-beam charge are available, the BH contribution disappears in the charge even combination and yields

$$\int d\Omega_\ell w^{\text{odd}}(\phi_\ell, \theta_\ell) \frac{d\sigma^+ + d\sigma^-}{d\Omega_\ell} \sim \int d\Omega_\ell w^{\text{odd}}(\phi_\ell, \theta_\ell) \Re(\mathcal{T}_{\text{BH}_2}^* \mathcal{T}_{\text{VCS}}). \quad (6.244)$$

To illustrate the feasibility of the subtraction procedure, consider the following charge and angular asymmetries

$$\left\{ \begin{array}{l} A_{\text{CA}}^{\cos \varphi_\ell} \\ A^{\cos \varphi_\ell} \end{array} \right\} = \frac{1}{\mathcal{N}} \int_{\pi/4}^{3\pi/4} d\theta_\ell \int_0^{2\pi} d\phi \int_0^{2\pi} d\varphi_\ell 2 \cos \varphi_\ell \left\{ \begin{array}{l} (d\sigma^+ + d\sigma^-)/2d\Omega_\ell d\phi \\ d\sigma^-/d\Omega_\ell d\phi \end{array} \right\}, \quad (6.245)$$

integrated with the weight $2 \cos \varphi_\ell$. In both cases, the normalization factor is given by

$$\mathcal{N} = \int_{\pi/4}^{3\pi/4} d\theta_\ell \int_0^{2\pi} d\phi \int_0^{2\pi} d\varphi_\ell \frac{d\sigma^-}{d\Omega_\ell d\phi}.$$

These asymmetries project the Fourier coefficient cc_{10}^2 of the second BH-VCS interference term, which, in the absence of \mathcal{F}_L , is proportional to

$$\text{cc}_{10}^2 \sim \Re \left\{ -\frac{\xi}{\eta} F_1 \mathcal{H} + \frac{\xi}{\eta} \frac{\Delta^2}{4M_N^2} F_2 \mathcal{E} - \eta (F_1 + F_2) \tilde{\mathcal{H}} \right\}, \quad (6.246)$$

making use of Eq. (6.206). One realizes that \mathcal{H} is now suppressed by a factor ξ/η and, thus, with decreasing $|\xi|$ the contribution of $\tilde{\mathcal{H}}$ starts to be important. We remark that as in case of DVCS, the charge and angular asymmetries might be contaminated stronger by twist-three effects than the beam-spin asymmetries. These coefficients are mainly of kinematical origin, i.e., they are expressed by twist-two GPDs and generate Fourier coefficients $\text{cc}_{00}^{\text{INT}}$, $\text{ss}_{11}^{\text{INT}} \simeq \text{cc}_{11}^{\text{INT}}$, and $\text{ss}_{22}^{\text{INT}} \simeq \text{cc}_{22}^{\text{INT}}$ that do not necessarily vanish at the kinematical boundaries.

6.2.11 Advantages of lepton pair electroproduction

In the preceding few sections, we have studied the process $eN \rightarrow e'N'\ell\bar{\ell}$. The structure of the cross section was obtained to the leading power in the hard momentum. We did not discuss here the power suppressed twist-three contributions, which generate further harmonics in the cross section. For instance, they induce off-diagonal elements in the coefficient matrix of the squared VCS amplitude, e.g., cc_{nm} with $n \neq m$ etc. However, they will not contaminate already existing Fourier harmonics, e.g., cc_{nn} etc. The process of the lepton pair production is the most favorable for experimental exploration of GPDs for a number of reasons:

- It is a clean electromagnetic process which does not involve other unknown non-perturbative function and, thus, has no contamination from other uncontrollable sources.
- The virtuality of the final state photon allows to disentangle the dependence of GPDs on both scaling variables and thus constrain the angular momentum sum rule.
- Studies of the angular distribution of the recoiled nucleon and of the lepton pair are complementary and lead to a rich angular structure of the cross section that can be used for separation of various combinations of GPDs.
- The variation of the relative magnitude of space- and timelike photon virtualities allows to access distributions of partons and anti-partons in the “exclusive” domain $\xi > |\eta|$.
- The higher one goes in skewness η , whose maximal value is limited by the magnitude of the momentum transfer to be within the region of applicability of QCD factorization $|\Delta^2| \ll p \cdot q$,

the larger surface in the exclusive domain ($\eta > |\xi|$) one measures in experiment. This diminishes the uncertainty coming from the inaccessible inclusive sector ($\eta < |\xi|$). The exclusive domain might saturate the spin sum rule (3.149) even for moderate η since the second moment of GPDs defining it is not extremely sensitive to the large- ξ behavior of GPDs where they are expected to behave just like conventional parton distributions.

- Another interesting feature of this process is that zero value of the generalized Bjorken variable can be exactly reached when the incoming and outgoing photons have about the same absolute values of virtualities $\mathcal{Q}^2 \simeq M_{\ell\bar{\ell}}^2$.
- The major complication in the experimental measurement of the process is a rather small magnitude of its cross section which is suppressed by two powers of the fine structure constant α_{em} compared to a typical deeply inelastic event. The other obstacle is the contamination of the heavy-photon events by the background of meson production. The latter can be circumvented in a relatively straightforward manner by avoiding the regions of $M_{\ell\bar{\ell}}^2$ close to meson-resonance thresholds. However, this also restricts the phase space in the measurements of GPDs. We also note that a numerical estimate of this contamination can be done by means of Eqs. (5.26) – (5.27). In fact, according to a perturbative QCD estimate [353], the ρ meson contribution to the beam spin asymmetry turns out to be small.
- A clear study of GPDs can be performed in experiments in which the tagged flavor of the lepton pair differs from that of the beam. When they are the same, one should add contributions in which the final electrons are interchanged, i.e., $k' \leftrightarrow \ell_-$. These will coherently interfere with each other. None of these results are available yet. They obviously will yield an essentially different dependence of the VCS amplitude on the external variables. To use the process with identical leptons for the extraction of information on GPDs, one needs to ensure that the momentum flow in the quark propagator of the handbag diagram remains large. Indeed, the scalar product

$$p \cdot q' = -p \cdot q \frac{2 - y - y \cos \theta_\ell}{2y} \left\{ 1 + \mathcal{O} \left(\frac{\Delta_\perp}{\sqrt{p \cdot q}} \right) \right\}, \quad (6.247)$$

that sets the scale in the exchanged VCS amplitude remains large. Note that here and in the following we denote the kinematical variables that enter the exchanged amplitudes with a prime. The power-suppressed contributions depend on all kinematical variables, in particular, on y , \tilde{y} and both azimuthal angles ϕ and φ_ℓ . Besides the condition $(2 - y)/y > \cos \theta_\ell$, which is fulfilled by the usual kinematical restriction $y < 1$, no other *kinematical cuts* are required to ensure the applicability of perturbative QCD. Moreover, η' is given by η in leading order

$$\eta' = \eta + \mathcal{O} \left(\frac{\Delta_\perp}{\sqrt{p \cdot q}} \right), \quad (6.248)$$

while ξ' receives strong dependence on the leptonic variables:

$$\xi' = \xi \frac{2 \cos \theta_\ell - y(1 + \cos \theta_\ell)}{2 - y(1 + \cos \theta_\ell)} - \frac{2\sqrt{1-y}\sqrt{\eta^2 - \xi^2} \sin \theta_\ell}{2 - y(1 + \cos \theta_\ell)} \cos(\phi - \varphi_\ell) + \mathcal{O} \left(\frac{\Delta_\perp}{\sqrt{p \cdot q}} \right). \quad (6.249)$$

It should be pointed out that if θ_ℓ approaches the edge of the phase space, i.e., $\theta_\ell \rightarrow \{0, \pi\}$, the absolute values of the scaling variables in Eq. (6.249) become identical $|\xi'| \simeq |\xi|$. The

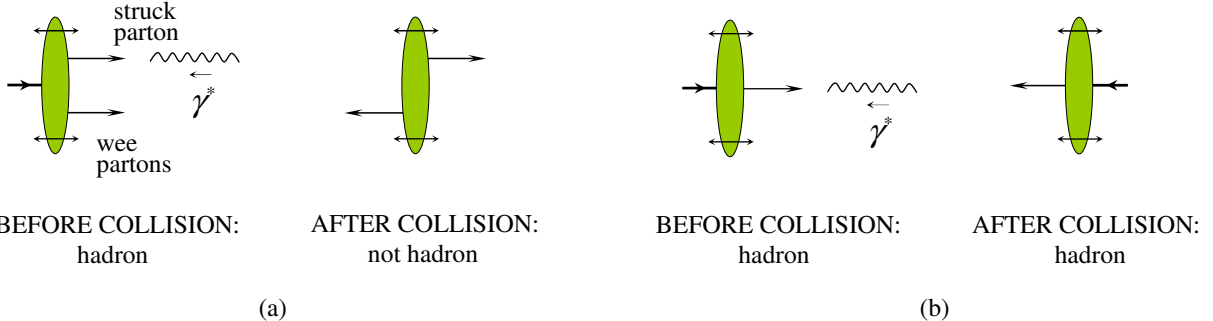


Figure 52: Feynman (or soft) mechanism for electromagnetic form factors. If more than one parton carries a large share of the parent’s hadron momentum (left diagram), after the absorption of the virtual photon the hadron disintegrates since the active partons move back to back in the opposite directions. However, provided a single parton carries the whole hadron’s momentum (right diagram), after the hard scattering the hadron as a whole merely changes its direction of motion.

conclusions we draw from our kinematical considerations are as follows. There are no crucial difficulties in the application of perturbative QCD as long as $p \cdot q$ is large. However, the analytic evaluation of observables and further studies are required to find an “optimal” method to extract the (ξ, η) shape of GPDs from the measurements of the reaction $e^\mp p \rightarrow e^\mp p e^+ e^-$.

We have discussed the most favorable observables, namely, various lepton-spin and azimuthal asymmetries that are sensitive to the imaginary part of the Compton form factors and, thus, directly to GPDs. We have not discussed in full, however, phenomenological consequences of using polarized targets, though we have presented the complete set of formulas with explicit angular dependence which can be used to extract complementary combinations of Compton form factors from experimental data. Longitudinal and transverse nucleon-spin asymmetries combined with the Fourier analysis will serve this purpose just like the lepton-spin asymmetries. In the case of DVCS (i.e., electroproduction of the real photon), the complete analysis along this line was given in Ref. [328]. The process $eN \rightarrow e'N'\ell\bar{\ell}$ with both photons being virtual provides a unique possibility to make the skewness parameter η independent from the generalized Bjorken variable ξ . Unfortunately, this process has a very low cross sections, the drawback which, hopefully, will be circumvented with future high-luminosity machines. The analysis of available events from the CLAS detector at Jefferson Laboratory is under way [410].

A closely related process to the one we addressed above is the photoproduction of lepton pairs [351]. It resembles the inverted deeply virtual Compton scattering. Namely, the virtual photon with negative helicity in timelike Compton scattering corresponds to a light quantum with positive helicity in DVCS. As compared to DVCS, the skewness is equal to the generalized Bjorken variable with the opposite sign, i.e., $\xi \simeq \eta$. The unpolarized and polarized photon beams allow to access the real and imaginary parts of a combination of Compton form factors $\mathcal{C}_T^{\text{unp}}$ identical to DVCS.

6.3 Hard exclusive production of mesons

To conclude the discussion of experimental probes of GPDs, we are going to briefly address the exclusive electroproduction of light mesons $\ell(k)N(p_1) \rightarrow \ell'(k')\gamma^*(q_1)N(p_1) \rightarrow \ell'(k')M(q_2)N(p_2)$. In the large- Q^2 limit, the amplitude of this process is dominated by the one-gluon-exchange

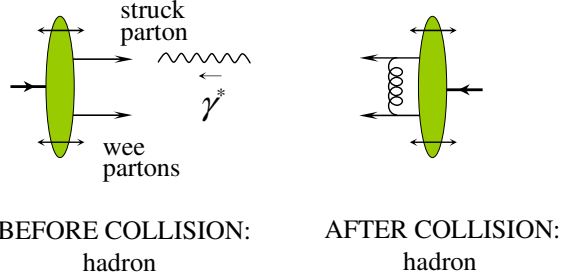


Figure 53: Hard mechanism for electromagnetic form factors.

mechanism, and can be calculated within perturbative QCD in terms of GPDs and distribution amplitudes of produced mesons. The meson electroproduction processes have one indisputable advantage over the Compton-initiated processes: by changing the type of produced mesons one can access different flavor combination of GPDs. This helps to perform the flavor decomposition of GPDs. It should be emphasized, however, that the pQCD diagrams for the hard exclusive meson electroproduction are similar to the one-gluon-exchange graphs determining the asymptotic behavior of hadronic form factors, and they share the same problem about the range of applicability of hard pQCD approach. The essence of the problem is that these are the virtualities of the internal lines of the hard subprocess (in particular, the virtuality of the exchanged gluon) which are much smaller than the virtuality Q^2 of the external probe, that determine whether the use of pQCD is justified or not.

6.3.1 Feynman versus hard mechanism in elastic form factors

Let us briefly recall the microscopic description of hadronic electromagnetic form factors. There are two basic mechanisms for their large- Δ^2 behavior. In general terms, the problem can be described in the following way. After the large momentum is transferred from the probing lepton to the hadron through the virtual photon interaction with a single quark, the latter radically changes the direction of its motion. However, in an exclusive reaction, it should eventually recombine together with the hadron's spectators to form the final state hadron. Imagine a hadron possesses at least two partons that almost equally share the bulk of its momentum, as shown in Fig. 52 (a). If only one of them absorbs the heavy photon, the active parton reverts its direction of motion, while the other fast parton continues to move forward in the original direction of the parent hadron. The probability for such momentum configuration to form an outgoing hadron is vanishing and thus should be discarded. In the mechanism proposed by Feynman [16], only one quark has a large momentum fraction $x \sim 1$ of the original hadron's momentum, and after the collision it carries the bulk part of the final hadron momentum. The “wee” spectators carry a very small $\sim 1/|\Delta|$ fraction of the hadron momentum, and can be associated either with initial or final hadron as in Fig. 52 (b). The more spectators one has, the smaller is the phase space for keeping the spectators within the $x_{\text{spect}} \sim 1/|\Delta|$ range. If the probability to have the momentum fraction of the active quark close to one is proportional to $q(x) \sim (1-x)^\nu$ where ν is proportional to the number of spectators, then the form factor drops like $\sim |\Delta|^{-\nu-1}$. Thus, Feynman mechanism suggests spectator counting rule: the larger is the number of quarks in a hadron, the faster its form factor drops with increasing $|\Delta|$.

In the hard perturbative QCD picture, all the valence quarks carry finite fractions of the initial

and final hadron momenta. The redistribution of the momentum transfer among the quarks goes through exchange of hard gluons (see Fig. 53). The minimal number of exchanges is $N - 1$ for a hadron composed of N valence quarks. The perturbative QCD prediction $F(-\Delta^2) \sim (\Delta^2)^{-N+1}$ for the spin-averaged form factors just counts the $1/\Delta^2$ powers due to the hard gluon propagators. The quark counting rules are the famous prediction of perturbative QCD for exclusive processes.

6.3.2 Quark counting rules

The derivation of the aforementioned counting rules is most transparent in the Breit frame, where the three-momenta of the incoming and outgoing hadrons are given in terms of the momentum transfer $\mathbf{p}_1 = -\mathbf{p}_2 = \Delta/2$. The partons momenta collinear to those of the incoming and outgoing hadrons are then given by

$$\mathbf{k}_i = \frac{x_i}{2}\Delta, \quad \mathbf{k}'_i = -\frac{y_i}{2}\Delta,$$

respectively. The momentum fractions obey the obvious energy-momentum conservation conditions

$$\sum_{i=1}^n x_i = \sum_{i=1}^n y_i = 1.$$

The main observation is that there are no other scales except for the hard scale Δ . Then the hard gluon exchange contribution to the form factor for a hadron made of n -quarks (see Fig. 54 for a typical diagram) can be written as

$$\begin{aligned} \langle p_2 | j_q^\mu(0) | p_1 \rangle &= L^\mu F(\Delta^2) \\ &\sim \Psi_{q \dots q}^* \{\bar{u}(k_n) \dots \bar{u}(k_1)\} \otimes \gamma^\mu D^{n-1} S^{n-1} \otimes \{u(k'_1) \dots u(k'_n)\} \Psi_{q \dots q}, \end{aligned} \quad (6.250)$$

where D stands for the exchanged gluons propagators, S for the quark propagators and $L^\mu = \bar{u}\gamma^\mu u$ is the quark current. Note, that all of the momenta associated with the internal lines of the hard subprocess are superpositions $[a(\{x_j\})p_1 - b(\{y_k\})p_2]$ of the initial and final hadron momenta, with the coefficients a and b given by sums of particular sets of fractions $\{x_j\}$ and $\{y_k\}$. Since $0 \leq a, b \leq 1$, the virtualities $(-ab\Delta^2)$ of the internal lines of the subprocess are spacelike and of the order of Δ^2 . In a situation when there are no other scales, the combinations $u(k_l)\bar{u}(k'_l)$ of Dirac spinors can only produce $\sim \Delta$ factors. Thus, we get the counting rules for building blocks of the amplitude

$$u, \bar{u} \sim |\Delta|^{1/2}, \quad D \sim |\Delta|^{-2}, \quad S \sim |\Delta|^{-1}. \quad (6.251)$$

Evidently, they could be guessed on dimensional grounds alone. For the form factor, we obtain

$$L^\mu F(\Delta^2) \sim \frac{|\Delta|}{(\Delta^2)^{n-1}}. \quad (6.252)$$

From the dimensional analysis, it also follows that the Lorentz structure L^μ has the dimension of mass, which gives the estimate $L \sim |\Delta|$. As a result, we find the scaling rule for the helicity non-flip form factor

$$F(\Delta^2) \sim \frac{1}{(\Delta^2)^{n-1}} = \frac{1}{(-\Delta^2)^{n-1}}. \quad (6.253)$$

The counting rules can be generalized for the contributions involving Fock components with different numbers n_i, n_f of quarks in the initial and final state. In this case, one should change

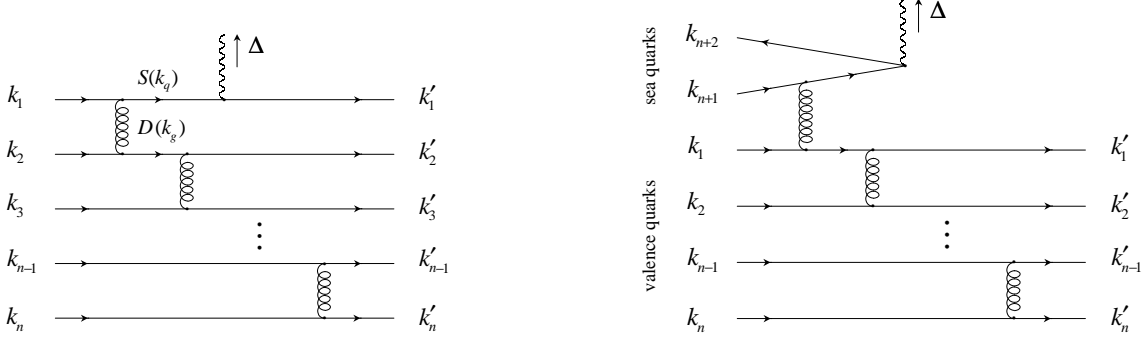


Figure 54: Origin of the quark counting rules from the hard exchange mechanism for $n \rightarrow n$ and $n_i \rightarrow n_f$ components of form factors.

$n \rightarrow (n_i + n_f)/2$. In particular, the annihilation-type $n + 2 \rightarrow n$ diagram shown in Fig. 54 has an extra factor

$$\bar{u}(k_{n+2}) S D u(k_{n+1}) \sim \frac{1}{\Delta^2}$$

resulting in an additional power of $1/\Delta^2$ in the form factor compared to (6.253).

It is rather popular to correlate the power behavior of form factors with the behavior of inclusive structure functions $F_1(x_B)$ of deeply inelastic scattering at large Bjorken variable x_B , when one approaches the exclusive single-hadron pole. The invariant mass $W^2 = (p_1 + q_1)^2$ of the produced hadronic system is related to x_B by

$$1 - x_B = x_B \frac{W^2 - M_h^2}{Q^2}, \quad (6.254)$$

where we shifted to the $Q^2 = \Delta^2$ notation. The single-hadron contribution to cross section is given by the form factor squared multiplied by $\delta(W^2 - m_h^2)$. According to Bloom and Gilman [411], the W^2 -integral of the hadron contribution is equal to the x -integral of the structure function $F_1(x)$ over a duality region with fixed boundaries in the variable W^2 . This gives a relation between the power ν specifying the $(1 - x)^\nu$ behavior of the structure function $F_1(x)$ in the $x \rightarrow 1$ region and the power-law behavior of the square elastic form factor: $F^2(Q^2) \sim (1/Q^2)^{\nu+1}$, or $\nu = 2n - 3$, if we use the counting of Eq. (6.250). In the proton case, with $n = 3$, one obtains $\nu = 3$, or a dipole behavior for the Dirac $F_1(Q^2)$ form factor.

It is worth emphasizing that one should not confuse the Bloom-Gilman duality with the Drell-Yan relation [206], which relates the integral of a nonforward parton density $f^q(x, Q^2)$, given in terms of the skewless GPD via

$$f^q(x, Q^2) \equiv F^q(x, \eta = 0, Q^2),$$

over the interval $x > 1 - \lambda/Q$ with the *first* power of the form factor. Also, the dominance of the region $x > 1 - \lambda/Q$ is a consequence of a specific structure of the density $f^q(x, Q^2)$. As we have seen before, the Drell-Yan relation does not work for the Gaussian model, but holds for the improved Regge-like model (3.333).

One should also realize that both relations were formulated in nonperturbative context. The shape of the structure function $F_1(x)$ or nonforward parton density $f^q(x, Q^2)$ is not necessarily

generated by pQCD dynamics. Knowing these functions, or building some models for them, one can use Bloom-Gilman or Drell-Yan relations to get predictions for form factors. Both relations have a common feature: change of the power ν in the $(1-x)^\nu$ behavior of the structure function results in a change of the $1/\mathcal{Q}^{\nu+1}$ power behavior of the form factor. Both relations give the same correlation between the two powers, and that is why they are sometimes confused.

Perturbative QCD predictions for asymptotic power behavior of form factors with definite powers, e.g., $(\alpha_s/\mathcal{Q}^2)^{n-1}$ for a spin-averaged form factor of n -quark hadron. It also predicts fixed powers $\alpha_s^{2n-2}(1-x)^{2n-3}$ for the $x \rightarrow 1$ behavior of the structure functions (see [240]). Formally, the powers of $(1-x)$, $1/\mathcal{Q}^2$ and α_s are correlated in pQCD as in Bloom-Gilman relation. However, a direct calculation of pQCD diagrams for $F_1(x)$ gives expressions which have more complicated structure than the squares of form factors (see, e.g., [156], where the $x \rightarrow 1$ behavior of GPDs is also discussed).

The Drell-Yan relation is invalid in pQCD, as emphasized in the pioneering paper [240]. In particular, the leading $(1-x)^3$ term in $F_1(x)$ is given in pQCD by diagrams involving four hard gluon exchanges and is accompanied by the α_s^4 factor. Integrating it over the region $x > 1 - \lambda/\mathcal{Q}$ one would get a contribution $\sim \alpha_s^4/\mathcal{Q}^4$ that has the same $1/\mathcal{Q}^4$ power as the pQCD prediction for the nucleon form factor, but is suppressed by two powers of α_s .

6.3.3 GPDs and form factors

The formalism of generalized parton distributions allows to combine the two mechanisms—the soft and hard—in a single description. Form factors result from integration of GPDs over the momentum fraction x as was demonstrated in Eq. (3.88),

$$\int_0^1 dx H^q(x, \eta, \Delta^2) = F^q(\Delta^2).$$

The result does not depend on the skewness η , so it is convenient to use here skewless generalized parton distributions, related via the Fourier transform to the impact parameter parton densities as discussed in Section 3.10.2. The simplest case of the meson electromagnetic form factor is also the most close diagram-wise to the meson electroproduction process. The soft contribution to $f^q(x, \Delta^2)$ in this case can be represented by the Drell-Yan formula

$$F_M(-\Delta_\perp^2) = \int_0^1 dx \int \frac{d^2 \mathbf{k}_\perp}{(2\pi)^3} \psi_{qq}^*(x, \mathbf{k}_\perp - (1-x)\Delta_\perp) \psi_{qq}(x, \mathbf{k}_\perp), \quad (6.255)$$

corresponding to overlap of two light cone wave functions. Taking the Gaussian ansatz

$$\psi_{qq}(x, \mathbf{k}_\perp) \sim \exp\left(-\frac{\mathbf{k}_\perp^2}{2x(1-x)\lambda^2}\right) \quad (6.256)$$

one can easily perform the \mathbf{k}_\perp integration and obtain

$$F_M^{\text{Gauss}}(-\Delta_\perp^2) = \int_0^1 dx q(x) \exp\left(-\frac{\Delta_\perp^2}{\lambda^2} \frac{1-x}{4x}\right), \quad (6.257)$$

where the integrand is a Gaussian model for the nonforward parton density. Its specific feature is the structure of the exponential factor that has a nontrivial non-factorized interplay between Δ_\perp^2 and x dependence. The pre-exponential factor may be interpreted as a forward quark density

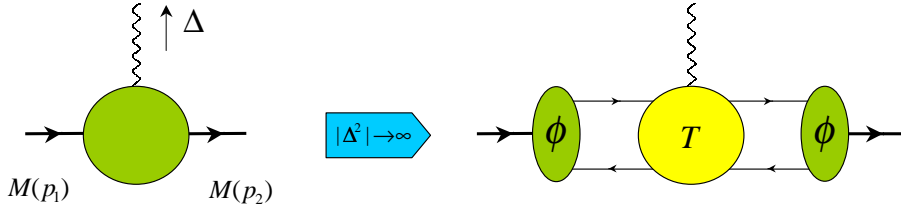


Figure 55: Factorized expression for the meson form factor at asymptotically large momentum transfer.

$q(x)$. Similar expressions were obtained more than twenty years ago in QCD sum rules for the soft contribution to hadronic form factors. In that approach, one considers a three-point correlator of the electromagnetic current with two local currents generating initial and final hadrons. It is convenient to work with the so-called Borel transforms of the correlation functions (for details, see [412, 421]), and in the pion form factor case, the double Borel transform of the basic triangle diagram has just a Gaussian form [421, 413])

$$\Phi[\Delta^2, \tau_1, \tau_2] = \frac{3}{2\pi^2(\tau_1 + \tau_2)} \int_0^1 dx x \bar{x} \exp\left(-\frac{\bar{x}}{x} \frac{\tau_1 \tau_2}{\tau_1 + \tau_2} \Delta^2\right), \quad (6.258)$$

where as usual $\bar{x} = 1 - x$. It should be noted that the application of the Borel transformation is equivalent to taking a Gaussian wave function with $\lambda_i^2 \sim 1/\tau_i$ for the vertices generating pions.

Turning back to the Gaussian ansatz (6.257), it is evident that the large- Δ^2 behavior of this expression is dominated by integration over the region where $(1-x)\Delta^2/\lambda^2 \sim 1$ or $1-x \sim \lambda^2/\Delta^2$. Hence, the result of integration is completely determined by the behavior of the pre-exponential factors (i.e., the model forward densities) at x close to 1. The ‘‘Borel’’ model (6.258) implies $\sim x(1-x)$ shape for $q_\pi(x)$, corresponding to the $1/\Delta^4$ asymptotic behavior. In a more general Gaussian model, if $q(x) \sim (1-x)^\nu$ for $x \rightarrow 1$, then the form factor asymptotically drops like $(\Delta^2)^{-\nu-1}$ at large Δ^2 .

In the nucleon case, the analogue of Eq. (6.258) for the F_1 form factor is [414, 413]

$$\Phi_1[\Delta^2, \tau_1, \tau_2] = \frac{1}{(2\pi)^4(\tau_1 + \tau_2)^3} \int_0^1 dx [3Q_u \bar{x}^2 - (2Q_u - Q_d) \bar{x}^3] \exp\left(-\frac{\bar{x}}{x} \frac{\tau_1 \tau_2}{\tau_1 + \tau_2} \Delta^2\right), \quad (6.259)$$

while in case of the magnetic form factor G_M it is given by

$$\Phi_M[\Delta^2, \tau_1, \tau_2] = \frac{3Q_u}{(2\pi)^4(\tau_1 + \tau_2)^3} \int_0^1 dx \bar{x}^2 \exp\left(-\frac{\bar{x}}{x} \frac{\tau_1 \tau_2}{\tau_1 + \tau_2} \Delta^2\right). \quad (6.260)$$

Since $G_M = F_1 + F_2$, one can derive the expression

$$\Phi_2[\Delta^2, \tau_1, \tau_2] = \frac{2Q_u - Q_d}{(2\pi)^4(\tau_1 + \tau_2)^3} \int_0^1 dx \bar{x}^3 \exp\left(-\frac{\bar{x}}{x} \frac{\tau_1 \tau_2}{\tau_1 + \tau_2} \Delta^2\right), \quad (6.261)$$

for the function related to the F_2 form factor. Looking at the $x \rightarrow 1$ behavior of the pre-exponential factors, we conclude that the Borel model, inspired by QCD sum rules, gives $1/\Delta^6$ for the large- Δ^2 behavior of the nucleon form factors $F_1(\Delta^2)$ and $G_M(\Delta^2)$, and $1/\Delta^8$ for $F_2(\Delta^2)$.

In a general Gaussian model, taking a more realistic $\sim (1-x)^3$ shape for the nucleon parton densities one would obtain $1/\Delta^8$ as the asymptotic behavior of $F_1(\Delta^2)$. Though this result seems to be in contradiction with the experimentally established dipole behavior of this form factor, the Gaussian model for the proton form factor $F_1^p(\Delta^2)$ [416, 204] successfully describes the data up to $\Delta^2 \sim 10 \text{ GeV}^2$. The explanation of this apparent ‘‘paradox’’ is very simple: the model Δ^2 -dependence for this and other form factors is given by more complicated functions than just pure powers of $1/\Delta^2$. Their nominal large- Δ^2 asymptotics is achieved only at very large values of Δ^2 , well beyond the accessible region. Thus, conclusions made on the basis of asymptotic relations might be of little importance in practice: a prediction with ‘‘wrong’’ large- Δ^2 behaviour might be quite successful phenomenologically in a rather wide range of Δ^2 . In fact, the improved model

$$f_{\text{Regge}}^q(x, \Delta^2) = q(x)x^{-\alpha'(1-x)\Delta^2}, \quad (6.262)$$

which imposes the correct Regge behavior $x^{-\alpha(\Delta^2)}$ for small momentum fractions x by a minimal modification $(2x\lambda^2)^{-1} \rightarrow -\alpha' \ln x$ of the Gaussian ansatz, allows to obtain a rather good description [205, 415] of all four nucleon form factors in the whole experimentally accessible region of spacelike momentum transfers. Note, that the exponential factor of the improved model behaves like $\exp[-\alpha'(1-x)^2\Delta^2]$ for x close to one. As a result, if the parton density behaves like $(1-x)^\nu$, then the relevant form factor decreases as $(\Delta^2)^{-(\nu+1)/2}$ for large Δ^2 , which exactly corresponds to the Drell-Yan relation [206]. We already pointed this property out in Section 3.13.2.

The asymptotic behavior of the form factor has a factorized form within perturbative QCD, see Fig. 55,

$$F_M^{\text{pQCD}}(\Delta^2) = f_M^2 \int_0^1 dx dy \phi_M(x) T(x, y; \Delta^2) \phi_M(y), \quad (6.263)$$

where $\phi_M(x)$ is the meson distribution amplitude and $T(x, y; \Delta^2)$ is the amplitude of the hard gluon exchange subprocess shown in Fig. 56. For the pion form factor, $M = \pi$,

$$T(x, y; \Delta^2) = \frac{8\pi\alpha_s}{9(1-x)(1-y)\Delta^2}.$$

Taking the asymptotic shape $\phi_\pi(x) = 6x(1-x)$, which apparently is a good approximation even at low normalization points [417], yields

$$F_\pi^{\text{pQCD}}(-\Delta^2) = \frac{8\pi\alpha_s f_\pi^2}{\Delta^2} = \frac{2\alpha_s}{\pi} \left(\frac{s_0}{\Delta^2} \right), \quad (6.264)$$

where $s_0 = 4\pi^2 f_\pi^2 \approx 0.7 \text{ GeV}^2$ is a typical hadronic scale for the pion. Since $s_0 \approx m_\rho^2$, the hard contribution has an obvious $2\alpha_s/\pi$ suppression compared to the vector meson dominance expectation $F^{\text{VMD}}(\Delta^2) \sim m_\rho^2/\Delta^2$. It is well known that the α_s/π is the standard price for each extra loop in a diagram.

It is also possible to include the perturbative QCD contribution as an addition to the nonforward parton density [418, 419, 420]

$$f_{\text{pQCD}}^q(x, -\Delta^2) = \frac{\alpha_s}{\pi} \left(\frac{s_0}{\Delta^2} \right) 4x \left\{ 1 - 2 \left[1 + x \ln \left(\frac{1-x}{x} \right) \right] \right\}. \quad (6.265)$$

This functional form is computed from the sum of the covariant-gauge Feynman diagrams in Fig. 56, where the electromagnetic current is replaced by the non-local light-ray operator (3.10), and

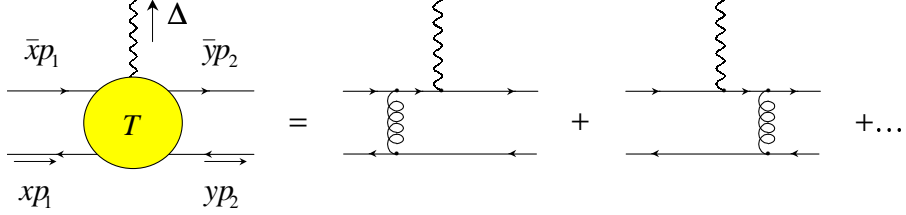


Figure 56: Hard rescattering in the meson form factor. The ellipses stand for the attachment of the photon to the lower quark line in the one-gluon exchange coefficient functions as well as for the higher order corrections.

Fig. 57 with the gluon line going out of the light-cone operator vertex. Note, that the term in the square brackets arises from such a graph. Therefore, it does not contribute to the form factor. The reason for vanishing of the discussed contribution becomes obvious when one realizes that it stems from the expansion of the Wilson line in the non-local light-cone operator determining the GPD. For the local current relevant for the form factor, the gauge link merely reduces to unity.

The comparison of the magnitude of the soft and hard contributions can be made in the local quark-hadron duality model [421, 422, 423], where both are present simultaneously. Just like the Borel model, this model is also inspired by QCD sum rules. However, instead of the Borel transform

$$\Phi[\Delta^2, \tau_1, \tau_2] = \frac{1}{\pi^2} \int_0^\infty ds_1 \int_0^\infty ds_2 \varrho^{\text{pert}}(s_1, s_2, \Delta) e^{-s_1 \tau_1 - s_2 \tau_2}, \quad (6.266)$$

in which the spectral density $\varrho^{\text{pert}}(s_1, s_2, \Delta^2)$ (calculated from diagrams of perturbation theory for the relevant correlator of three currents, e.g., electromagnetic and two axial ones, in case of the pion form factor) is integrated with the exponential weights $e^{-s_1 \tau_1}$, $e^{-s_2 \tau_2}$, one takes the function

$$T^{(3)}(\Delta^2, s_0) = \frac{1}{\pi^2} \int_0^{s_0} ds_1 \int_0^{s_0} ds_2 \varrho^{\text{pert}}(s_1, s_2, \Delta^2), \quad (6.267)$$

in which $\varrho^{\text{pert}}(s_1, s_2, \Delta^2)$ is integrated over the square $0 \leq s_1, s_2 \leq s_0$. Then one assumes that the pion contribution

$$\varrho_\pi(s_1, s_2, \Delta^2) = f_\pi^2 F_\pi(\Delta^2) \delta(s_1 - m_\pi^2) \delta(s_2 - m_\pi^2)$$

to the physical spectral density $\varrho^{\text{phys}}(s_1, s_2, \Delta^2)$ is dual to the “perturbative” spectral density $\varrho^{\text{pert}}(s_1, s_2, \Delta^2)$ in the appropriate “duality square” $[0 \leq s_1 \leq s_0] \otimes [0 \leq s_2 \leq s_0]$. The size of the duality interval s_0 is fixed from the local duality relation

$$f_\pi^2 = \frac{1}{\pi} \int_0^{s_0} ds \varrho^{\text{pert}}(s) \quad (6.268)$$

for the correlator of two axial currents. Since

$$\varrho^{\text{pert}}(s) = \frac{1}{4\pi} \left(1 + \frac{\alpha_s}{\pi} \right),$$

in the lowest order in α_s one obtains $s_0 = 4\pi^2 f_\pi^2 \approx 0.7 \text{ GeV}^2$, the scale we just discussed above. Thus, the local quark-hadron duality model corresponds to using the prescription $f_\pi^2 F_\pi(\Delta^2) = T^{(3)}(\Delta^2, s_0)$ and a similar relation Eq. (6.268) for f_π^2 . The spectral density $\varrho^{\text{pert}}(s_1, s_2, \Delta^2)$ is known

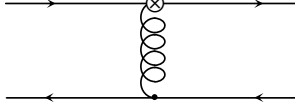


Figure 57: Additional hard rescattering diagram contributing to the leading order large- Δ^2 behavior of GPDs.

up to α_s level. The lowest order term found in Refs. [412, 421] can be easily integrated analytically over the duality square (see Ref. [421]. The $\mathcal{O}(\alpha_s)$ term [424] is much more complicated. However, its large- Δ^2 asymptotic behavior is fixed by the pQCD result (6.264), while the $\Delta^2 = 0$ value α_s/π is fixed by the Ward identity. Assuming the simplest interpolation [422] between these two values and combining the $\mathcal{O}(\alpha_s^0)$ and $\mathcal{O}(\alpha_s)$ contributions gives

$$\left(1 + \frac{\alpha_s}{\pi}\right) F_\pi^{\text{LD}}(-\Delta^2) = \left(1 - \frac{1 + 6s_0/\Delta^2}{(1 + 4s_0/\Delta^2)^{3/2}}\right) + \frac{\alpha_s/\pi}{1 + \Delta^2/2s_0}. \quad (6.269)$$

Just like the Borel model is equivalent to a Gaussian wave function, the local quark-hadron duality model corresponds to a step-like effective lightcone wave function $\psi_{qq}(x, \mathbf{k}) \sim \theta[x(1-x)s_0 - \mathbf{k}^2]$, and the first term in (6.269) which is due to the simplest triangle diagram, is given by an overlap of such soft wave functions. Hence, its large- Δ^2 behavior is governed by the Feynman mechanism.

On the other hand, the $\mathcal{O}(\alpha_s)$ term includes the one-gluon exchange contributions [237, 240] responsible for its leading asymptotic behavior at large Δ^2 . One should realize, however, that to get the “genuine hard” contribution, one should subtract from the $\mathcal{O}(\alpha_s)$ term of Eq. (6.269) the part produced by integration over a region where the virtuality of the exchanged gluon is small, say, smaller than s_0 . Such a subtraction, as argued in Refs. [414, 425] would reduce the hard part to a minuscule fraction of the $\mathcal{O}(\alpha_s)$ term. But, even without this subtraction, the purely soft term strongly exceeds the $\mathcal{O}(\alpha_s)$ term of Eq. (6.269) for all accessible momentum transfers. The two terms become equal to each other only for $\Delta^2 = 10 \text{ GeV}^2$. The bulk of the $\mathcal{O}(\alpha_s)$ term even at that point should be treated as a soft contribution. Within the local quark-hadron duality model, however, the question of dividing the $\mathcal{O}(\alpha_s)$ term into soft and hard parts does not have much of practical meaning. We only note, that with $\alpha_s/\pi = 0.1$ and $s_0 = 4\pi^2 f_\pi^2$, the local duality prediction is in perfect agreement with the latest Jefferson Lab measurements of the pion form factor [426] at the momentum transfer $0.6 \text{ GeV}^2 \leq \Delta^2 \leq 1.6 \text{ GeV}^2$.

For the nucleon form factors, the asymptotically leading two-gluon exchange term has an a priori $(\alpha_s/\pi)^2$ suppression resulting in a reduction by a factor of hundred. It is further complemented by a huge reduction due to the exclusion of the region of small gluon virtualities, so it is unlikely to be relevant at any imaginable momentum transfers. Thus, we do not expect that hard contributions will play a visible role in the nucleon case.

Comparing the Δ^2 -dependence of soft and hard parts of the nonforward parton density, we observe that the soft part decreases exponentially at large Δ^2 , i.e., faster than any power of $1/\Delta^2$. The power-law behavior for the form factor is produced only after integration over x . The resulting power depends on the $x \rightarrow 1$ behavior of $f^q(x, \Delta^2)$, in agreement with the Feynman/Drell-Yan picture. In contrast, the perturbative QCD term has a power-law behavior $(1/\Delta^2)^N$ before integration over x . As already mentioned, the power $N = n - 1$ is given by the number of gluon exchanges necessary to transfer the large momentum from the active quark to $n - 1$ spectators. Integration over x does not affect this power: there is no Drell-Yan/Feynman mechanism in perturbative

QCD. In this connection, it is worth recalling the pQCD prediction about the $x \rightarrow 1$ behavior of parton densities. As we discussed, in the nucleon case, the leading $(1 - x)^3$ term corresponds to four-gluon-exchange diagrams, with inevitable $(\alpha_s/\pi)^4 \sim 10^{-4}$ suppression. Furthermore, though the $(1 - x)^3$ behavior of this term and the $1/\Delta^4$ behavior of the asymptotic prediction for the nucleon Dirac form factor $F_1(\Delta^2)$ formally satisfy the Drell-Yan relation, they have nothing to do with it, because these results have different power in α_s . As noted in the pioneering paper [240], the Drell-Yan relation in pQCD is violated by two powers of α_s .

There is extensive and growing evidence that perturbative QCD contributions are just small $(\alpha_s/\pi)^n$ corrections incapable to explain the observed absolute magnitude of hadronic form factors. The only exception is the $\gamma^*\gamma \rightarrow \pi^0$ form factor for which the hard term has zero order in α_s . In this case, perturbative QCD should work, and it works starting with $Q^2 \sim 2 \text{ GeV}^2$. Correspondingly, as we discussed earlier, Compton scattering in which perturbative QCD also starts at α_s^0 is an analogue of the $\gamma^*\gamma \rightarrow \pi^0$ process—in a sense, $\gamma^*\gamma\pi^0$ is a part of the amplitude accounting for the most of the \bar{E} contribution—while the hard meson electroproduction, where the leading hard term is $\mathcal{O}(\alpha_s)$, is completely analogous to the pion form factor. In fact, the pion form factor is extracted from the σ_L part of the hard meson electroproduction cross section. For this reason, one may expect that extraction of GPDs through perturbative QCD formulas is justified for Compton-dominated processes starting at $Q^2 \sim 2 \text{ GeV}^2$, while the meson electroproduction is expected to be strongly contaminated by the soft contribution at least up to $Q^2 \sim 10 \text{ GeV}^2$. Such momentum transfers can be reached at upgraded Jefferson Lab accelerator energies. Anticipating these future developments, we present below the framework for perturbative description of hard meson electroproduction processes.

6.3.4 Exclusive meson production and QCD factorization

At sufficiently large Q^2 , the hard exclusive lepto-production of a meson M from a nucleon target N ,

$$\ell(k)N(p_1) \rightarrow \ell'(k')N'(p_2)M(q_2) \quad (6.270)$$

is a promising process to test our understanding of perturbative QCD description of exclusive reactions. It is also a unique tool to study the properties of nondiagonal transitions, $N \rightarrow N'$, with N' being a baryon from an $SU(3)$ multiplet, either octet or decuplet. The hadronic part of the $\gamma_L N \rightarrow MN'$ process can be written as the Fourier transform of the matrix element of the electromagnetic current Eq. (2.15)

$$\int d^4z e^{-iq_1 \cdot z} \langle M(q_2)N'(p_2) | j^\mu(z) | N(p_1) \rangle = i(2\pi)^4 \delta^{(4)}(q_1 + p_1 - q_2 - p_2) \mathcal{A}_M^\mu, \quad (6.271)$$

with $q_1 = k - k'$ being the momentum of the virtual photon, defined as the difference of incoming and outgoing lepton momenta.

If the intermediate photon is longitudinally polarized and has a large virtuality $Q^2 = -q_1^2$, the photoproduction amplitude $\gamma_L N \rightarrow N'M$ can be rigorously treated within pQCD [358]. A straightforward leading twist calculation gives the following expression for the amplitude

$$\mathcal{A}_M^\mu = \frac{1}{Q^2} \left(q_1^\mu + 2x_B p_1^\mu \right) \frac{4\pi f_M}{N_c} \mathcal{F}_{NN'}^M(\eta, \Delta^2) + \mathcal{O}(1/Q^3), \quad (6.272)$$

where f_M stands for the meson decay constant, defined in Section 3.7. The amplitude is explicitly gauge invariant,

$$q_1^\mu \mathcal{A}_\mu^M = 0.$$

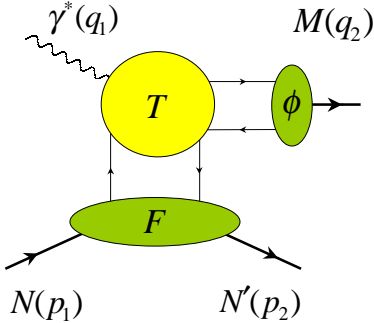


Figure 58: Factorization of the meson lepto-production at $-q_1^2 \rightarrow \infty$ into hard rescattering amplitude T and non-perturbative functions A , the generalized flavour changing parton distribution, and ϕ , the distribution amplitude of the outgoing meson.

Actually, it was reconstructed from the structure $2q^\mu + 3\eta p^\mu$, arising from the explicit calculation, by adding the transverse components of the momentum transfer. The generalized structure function \mathcal{F} depends on the skewness η , the t -channel momentum transfer Δ^2 and the resolution scale Q^2 . Neglecting the meson mass effects, the skewness is equal to the generalized Bjorken variable $\eta \approx \xi$. In the leading-twist approximation, \mathcal{F} is expressed through a convolution of a meson distribution amplitude $\phi_M(u)$, a quark or gluon GPD F^a and, correspondingly, the quark or gluon coefficient function T via [358]

$$\begin{aligned} & \mathcal{F}_{NN'}^M(\xi, \Delta^2) \\ & \equiv \int_0^1 du \int_{-1}^1 dx \phi_M(u) \{ T_M(u, x, \xi) F_{NN'}^M(x, \xi, \Delta^2) + T^g(u, x, \xi) F^g(x, \xi, \Delta^2) \}, \end{aligned} \quad (6.273)$$

(see Fig. 58). Here, the quark $F_{NN'}^M$ and gluon F^g GPDs provide a target-independent parametrization of the matrix elements of light-ray operators between hadronic states, see Eqs. (3.44) and (3.45). Choosing specific hadrons, one has to further decompose them into Dirac/Lorentz structures, as was done in Section 3. In case of the flavor exchange in the t -channel, the contribution of gluons is obviously absent, $T^g = 0$. It is also important to realize that only chiral even GPDs enter the production amplitudes. As was checked in [428] by an explicit next-to-leading order calculation following up an earlier all-order proof of Ref. [429], the chiral odd quark GPDs do not contribute to Eq. (6.273).

In the lowest order approximation, the function T_M is given by the one-gluon exchange mechanism shown in Fig. 56. It encodes the short distance dynamics of parton rescattering, and can be calculated in QCD perturbation theory as a series in the strong coupling constant α_s . The other two blocks, ϕ and F , are universal, i.e., process independent, and accumulate information about the long-distance physics. The Bjorken limit implies large invariant mass W of the hadronic final state, so that the produced baryon and meson are well separated in the phase space.

The amplitude for the meson electroproduction process is very similar to the pion form factor. Contributing diagrams can be decomposed into two sets. In the first set, the photon is attached to the quark line. In the second set, it is attached to the antiquark line. The momentum of the initial and final (anti-) quark is given in the collinear approximation by $k_1 = \frac{x+\xi}{2\xi} \Delta$ ($k_2 = \frac{x-\xi}{2\xi} \Delta$) and $k'_1 = u q_2$ ($k'_2 = (1-u) q_2$), respectively. In the leading twist approximation, both of these sets

separately respect current conservation. Obviously, if we formally replace $\frac{x+\xi}{2\xi} \rightarrow v$ and $\frac{x-\xi}{2\xi} \rightarrow 1-v$ with $0 < v < 1$, the kinematics reduces to that of the pion form factor. The essential difference is that we have to keep track of the emerging imaginary part, which is absent in the pion form factor case. The discontinuity develops in the region $|x| \geq \xi$ and can easily be restored.

In case of flavor-exchange GPDs, one can use the $SU(3)$ symmetry to relate them to the quark GPDs in the proton, as was discussed at length in Section 3.16.

6.3.5 Electroproduction of pseudoscalar mesons

The production of pseudoscalar mesons is sensitive to the polarized GPDs \tilde{H} , \tilde{E} . Therefore, in the present section, sometimes we will use the symbol F denoting either of them

$$F_{NN'}^M = \tilde{H}_{NN'}^M, \quad \tilde{E}_{NN'}^M.$$

We recall that, in general, GPDs here may induce flavor-changing transitions. For the function $\tilde{H}_{NN'}^M$, one can use the consequence of the $SU(3)$ symmetry in the form of relations (3.356). On the other hand, for the helicity-flip functions $\tilde{E}_{NN'}^M$, the effects of the symmetry breaking are rather large and one cannot use the symmetry arguments.

Let us present a compendium of leading order hard-scattering coefficient function which enter the amplitude (6.273).

- Charged pion production, $\gamma^* p \rightarrow n\pi^+$:

$$T_{\pi^+}(u, x, \xi) = C_F \alpha_s \left\{ \frac{Q_u}{(1-u)(\xi-x-i0)} - \frac{Q_d}{u(\xi+x-i0)} \right\} + \mathcal{O}(\alpha_s^2). \quad (6.274)$$

The function $\tilde{H}_{pn}^{\pi^+}$ that accompanies this coefficient function is the isovector combination of the proton ones

$$\tilde{H}_{pn}^{\pi^+} = \tilde{H}_{pn} = \tilde{H}^u - \tilde{H}^d,$$

see Eq. (3.356).

- Neutral pion production, $\gamma^* p \rightarrow p\pi^0$:

$$T_{\pi^0}(u, x, \xi) = C_F \alpha_s \left\{ \frac{1}{(1-u)(\xi-x-i0)} - \frac{1}{u(\xi+x-i0)} \right\} + \mathcal{O}(\alpha_s^2). \quad (6.275)$$

The functions $F_{pp}^{\pi^0}$, both $\tilde{H}_{pp}^{\pi^0}$ and $\tilde{E}_{pp}^{\pi^0}$ correspond to the combination

$$F_{pp}^{\pi^0} = -\frac{1}{\sqrt{2}} (Q_u F^u - Q_d F^d).$$

- Charged kaon production, $\gamma^* p \rightarrow Y^0 K^+$, with the neutral hyperon $Y^0 = \Lambda, \Sigma^0$ in the final state:

$$T_{K^+}(u, x, \xi) = -C_F \alpha_s \left\{ \frac{Q_u}{(1-u)(\xi-x-i0)} - \frac{Q_s}{u(\xi+x-i0)} \right\} + \mathcal{O}(\alpha_s^2). \quad (6.276)$$

The transition GPDs $\tilde{H}_{pY^0}^{K^+}$ with $Y = \Lambda, \Sigma^0$ are given by Eq. (3.356),

$$\tilde{H}_{p\Lambda}^{K^+} = \tilde{H}_{p\Sigma^0} = -\frac{1}{\sqrt{6}} (2\tilde{H}^u - \tilde{H}^d - \tilde{H}^s), \quad \tilde{H}_{p\Sigma^0}^{K^+} = \tilde{H}_{p\Sigma^0} = -\frac{1}{\sqrt{2}} (\tilde{H}^d - \tilde{H}^s).$$

- Neutral kaon production, $\gamma^* p \rightarrow K^0 \Sigma^+$:

$$T_{K^0}(u, x, \xi) = C_F \alpha_s \left\{ \frac{Q_d}{(1-u)(\xi-x-i0)} - \frac{Q_s}{u(\xi+x-i0)} \right\} + \mathcal{O}(\alpha_s^2). \quad (6.277)$$

The associated function $\tilde{H}_{p\Sigma^+}$ reads

$$\tilde{H}_{p\Sigma^+}^{K^0} = \tilde{H}_{p\Sigma^+} = -\tilde{H}^d + \tilde{H}^s.$$

As we know, the GPD \tilde{E} possesses a pseudoscalar meson pole (3.315). Since the mass difference between the pion and the kaon are rather large, these functions are more sensitive to the $SU(3)$ flavor symmetry breaking. Thus, it will be more accurate to refrain from incorporating the symmetry relations, and use instead the phenomenological values of low-energy parameters. As we discussed in Section 3.12, in first approximation one can just take the meson pole contribution only and use the following form for the helicity-flip functions

$$\tilde{E}_{pY}(x, \eta, \Delta^2) \simeq \frac{\theta(\eta - |x|)}{\eta} \phi_K \left(\frac{x+\eta}{2\eta} \right) \frac{g_{KpY} M_N}{m_K^2 - \Delta^2}, \quad (6.278)$$

with the couplings [9]

$$g_{Kp\Lambda} \approx -3.75\sqrt{4\pi}, \quad g_{Kp\Sigma} \approx 1.09\sqrt{4\pi}.$$

6.3.6 Electroproduction of vector mesons

The vector meson production process is sensitive to the unpolarized GPDs

$$F = H, E,$$

which enter in the spin sum rule (3.158). In case of flavor-changing transitions we will again use the $SU(3)$ relations since the symmetry breaking effects in these quantities are very small compared to the meson-pole-dominated function \tilde{E} . We have the following set of results for perturbative amplitudes and GPDs which contribute to cross sections.

- Neutral vector meson production, $\gamma^* p \rightarrow V_L^0 p$:

$$T_{V^0}(u, x, \xi) = C_F \alpha_s \left\{ \frac{1}{(1-u)(\xi-x-i0)} - \frac{1}{u(\xi+x-i0)} \right\} + \mathcal{O}(\alpha_s^2), \quad (6.279)$$

$$T_g(u, x, \xi) = 4T_F \alpha_s \frac{\sum_q Q_q}{u(1-u)(\xi-x-i0)(\xi+x-i0)} + \mathcal{O}(\alpha_s^2), \quad (6.280)$$

with $V^0 = \rho^0, \omega$. The flavor combinations of non-polarized GPDs are

$$F_{pp}^{\rho^0} = Q_u F^u - Q_d F^d, \quad F_{pp}^{\omega} = Q_u F^u + Q_d F^d. \quad (6.281)$$

The gluon GPD F^g is given by the standard formula (3.41).

- Charged vector meson production, $\gamma^* p \rightarrow \rho_L^+ n$:

$$T_{\rho^+}(u, x, \xi) = C_F \alpha_s \left\{ \frac{Q_u}{(1-u)(\xi-x-i0)} - \frac{Q_d}{u(\xi+x-i0)} \right\} + \mathcal{O}(\alpha_s^2). \quad (6.282)$$

The flavor combination of non-polarized GPDs is

$$F_{pn}^{\rho^+} = F^u - F^d. \quad (6.283)$$

6.3.7 Electroproduction of delta isobar

Just like in the production of pseudoscalar mesons with transitions within the baryon octet, the pion production involving transitions from octet to decuplet baryons is sensitive to the polarized GPDs, thus we identify $F_{NN'}^M$ in Eq. (6.273) with

$$F_{NN'}^M = \tilde{G}_{i,NN'}^M, \quad i = 1, \dots, 4.$$

The leading order perturbative amplitudes accompanying the corresponding nucleon-to-delta transition GPDs read as follows.

- π^+ production, $\gamma^* p \rightarrow \Delta^0 \pi^+$:

$$T_{\pi^+}(u, x, \xi) = C_F \alpha_s \left\{ \frac{Q_u}{(1-u)(\xi-x-i0)} - \frac{Q_d}{u(\xi+x-i0)} \right\} + \mathcal{O}(\alpha_s^2). \quad (6.284)$$

The function $\tilde{F}_{p\Delta^0}^{\pi^+}$ which comes with this coefficient function is the isovector combination of the proton GPDs

$$\tilde{G}_{p\Delta^0}^{\pi^+} = \tilde{G}_{p\Delta^0} = -\frac{1}{\sqrt{3}} \tilde{G}_{p\Delta^{++}},$$

see Eqs. (3.358) and (3.367).

- π^- production, $\gamma^* p \rightarrow \Delta^{++} \pi^-$:

$$T_{\pi^-}(u, x, \xi) = C_F \alpha_s \left\{ \frac{Q_d}{(1-u)(\xi-x-i0)} - \frac{Q_u}{u(\xi+x-i0)} \right\} + \mathcal{O}(\alpha_s^2). \quad (6.285)$$

The function $\tilde{F}_{p\Delta^{++}}^{\pi^+}$ accompanying T_{π^-} is again the isovector combination of the proton ones

$$\tilde{G}_{p\Delta^{++}}^{\pi^-} = \tilde{G}_{p\Delta^{++}},$$

see Eq. (3.358).

- π^0 production, $\gamma^* p \rightarrow \Delta^+ \pi^0$:

$$T_{\pi^0}(u, x, \xi) = C_F \alpha_s \frac{Q_u + Q_d}{2} \left\{ \frac{1}{(1-u)(\xi-x-i0)} - \frac{1}{u(\xi+x-i0)} \right\} + \mathcal{O}(\alpha_s^2), \quad (6.286)$$

and $\tilde{F}_{p\Delta^+}^{\pi^0}$ is given by

$$\tilde{G}_{p\Delta^+}^{\pi^0} = \tilde{G}_{p\Delta^+} = -\frac{2}{\sqrt{3}} \tilde{G}_{p\Delta^{++}},$$

see Eqs. (3.358) and (3.367).

6.3.8 Cross sections for electroproduction of mesons

Having found the amplitudes, one is ready to discuss the event rates. The cross section for exclusive electroproduction of mesons from the nucleon target is given by

$$d\sigma^M = \frac{1}{4k \cdot p_1} |4\pi \alpha_{\text{em}} L_\mu \mathcal{A}_M^\mu|^2 d\text{LISP}_3, \quad (6.287)$$

where the hadronic amplitude (6.272) is contracted with the leptonic current (which includes the photon propagator)

$$L^\mu = \frac{i}{Q^2} \bar{u}(k') \gamma^\mu u(k), \quad (6.288)$$

and the three-particle phase space volume has the standard form

$$d\text{LISP}_3 = (2\pi)^4 \delta^{(4)}(k + P_1 - k' - P_2 - q_2) \frac{d^3 k'}{2E'(2\pi)^3} \frac{d^3 P_2}{2E_2(2\pi)^3} \frac{d^3 q_2}{2\varepsilon_2(2\pi)^3}. \quad (6.289)$$

In the rest-frame of the target with the z -axis chosen counter-along the momentum of the virtual photon, as shown in Fig. 47, one obtains the following four-fold cross section

$$\frac{d\sigma^M}{dQ^2 dx_B d|\Delta^2| d\varphi_M} = \frac{\alpha_{\text{em}}^2}{2(4\pi)^2} \frac{x_B y^2}{Q^4} \left(1 + 4 \frac{M_N^2 x_B^2}{Q^2}\right)^{-1/2} |L_\mu \mathcal{A}_M^\mu|^2. \quad (6.290)$$

Here we use the standard variables as in VCS (5.10) and the azimuthal angle of the outgoing meson with respect to the lepton scattering plane is $\varphi_M = \varphi_\gamma$ with φ_γ defined in Fig. 47.

The conversion from lepto-production to photoproduction, $d\sigma_L^M$, with longitudinally polarized photons ε_L^μ is done by multiplying the result (6.292) with a kinematical factor, namely,

$$d\sigma_L^M = d\sigma^M \left(\frac{|\varepsilon_L \cdot p_1|^2}{q_1 \cdot p_1} \right) \left(\frac{|L \cdot p_1|^2}{k \cdot p_1} \frac{d^3 k'}{2E'(2\pi)^3} \right)^{-1} = d\sigma^M \frac{1}{\alpha_{\text{em}}} \frac{\pi}{1-y} \frac{x_B}{dx_B} \frac{Q^2}{dQ^2}. \quad (6.291)$$

To get the last equality, we used

$$|\varepsilon_L \cdot p_1|^2 = 4Q^2,$$

where the polarization vector of the longitudinal photon was defined in Eq. (5.101), and

$$|L \cdot p_1|^2 = 16 \frac{1-y}{y^2}, \quad \frac{d^3 k'}{2E'} = \frac{\pi y}{2} \frac{dx_B}{x_B} dQ^2.$$

Thus, the cross section for scattering on a transversely polarized nucleon target is given by

$$\frac{d\sigma_L^M}{d|\Delta^2| d\varphi_M} = \frac{\alpha_{\text{em}} \pi}{Q^6} \frac{f_M^2}{N_c^2} \frac{x_B^2}{(2-x_B)^2} \{ \sigma_M + \sigma_M^\perp \sin \Theta \sin(\Phi - \varphi_M) \}. \quad (6.292)$$

This generic form of the cross section should be supplemented by the explicit dependence of the unpolarized and transversely polarized components σ_M and σ_M^\perp on the corresponding GPDs. The calculations have been performed in Refs. [361, 362, 430, 9] for several types of outgoing baryons and mesons.

- Pion production:

$$\sigma_\pi = 8(1-x_B) |\tilde{\mathcal{H}}_{pN}^\pi|^2 - x_B^2 \frac{\Delta^2}{2M_N^2} |\tilde{\mathcal{E}}_{pN}^\pi|^2 - 4x_B^2 \Re \left(\tilde{\mathcal{H}}_{pN}^{\pi*} \tilde{\mathcal{E}}_{pN}^\pi \right), \quad (6.293)$$

$$\sigma_\pi^\perp = -4x_B \sqrt{1-x_B} \sqrt{-\frac{\Delta^2}{M_N^2}} \sqrt{1 - \frac{\Delta_{\min}^2}{\Delta^2}} \Im \left(\tilde{\mathcal{H}}_{pN}^{\pi*} \tilde{\mathcal{E}}_{pN}^\pi \right), \quad (6.294)$$

where the final state baryon $N = n, p$ corresponds to the produced $\pi = \pi^+, \pi^0$ meson, respectively. In this formula, we used the isospin symmetry between the proton and the neutron and thus neglected the mass difference between them, $M_p = M_n = M_N$.

- Kaon production:

$$\begin{aligned}\sigma_K &= 8(1 - x_B)|\tilde{\mathcal{H}}_{pY}^K|^2 - x_B^2 \left\{ \frac{\Delta^2}{2M_N^2} - \frac{1}{2} \left(1 - \frac{M_Y}{M_N} \right)^2 \right\} |\tilde{\mathcal{E}}_{pY}^K|^2 \\ &\quad - 2x_B \left\{ x_B \left(1 + \frac{M_Y}{M_N} \right) - (2 - x_B) \left(1 - \frac{M_Y}{M_N} \right) \right\} \Re \left(\tilde{\mathcal{H}}_{pY}^{K*} \tilde{\mathcal{E}}_{pY}^K \right),\end{aligned}\quad (6.295)$$

$$\sigma_K^\perp = -4x_B \sqrt{1 - x_B} \sqrt{-\frac{\Delta^2}{M_N^2}} \sqrt{1 - \frac{\Delta_{\min}^2}{\Delta^2}} \Im \left(\tilde{\mathcal{H}}_{pY}^{K*} \tilde{\mathcal{E}}_{pY}^K \right), \quad (6.296)$$

with the charged K^+ meson is produced with $Y = \Lambda, \Sigma^0$ and K^0 along with Σ^+ . Here, M_Y is the mass of the hyperon containing the strange quark.

- Vector mesons:

$$\sigma_V = 8(1 - x_B)|\mathcal{H}_{pN}^V|^2 - x_B^2 \left(2 + (2 - x_B)^2 \frac{\Delta^2}{2M_N^2} \right) |\mathcal{E}_{pN}^V|^2 - 4x_B^2 \Re \left(\mathcal{H}_{pN}^{V*} \mathcal{E}_{pN}^V \right), \quad (6.297)$$

$$\sigma_V^\perp = 4(2 - x_B) \sqrt{1 - x_B} \sqrt{-\frac{\Delta^2}{M_N^2}} \sqrt{1 - \frac{\Delta_{\min}^2}{\Delta^2}} \Im \left(\mathcal{H}_{pN}^{V*} \mathcal{E}_{pN}^V \right), \quad (6.298)$$

with the outgoing nucleon being the proton $N = p$ for $V = \rho, \omega$ and the neutron $N = n$ for $V = \rho^+$.

- Delta-isobar production:

$$\begin{aligned}\sigma_\Delta &= 4(1 - x_B)^2 |\tilde{\mathcal{G}}_{3,p\Delta}^\pi|^2 + x_B^2 \left\{ \frac{\Delta^4}{M_N^4} - 2 \frac{\Delta^2}{M_N^2} \left(1 + \frac{M_\Delta^2}{M_N^2} \right) + \left(1 - \frac{M_\Delta^2}{M_N^2} \right)^2 \right\} |\tilde{\mathcal{G}}_{4,p\Delta}^\pi|^2 \\ &\quad + 4x_B \left\{ 1 - \frac{M_\Delta^2 + \Delta^2}{M_N^2} - x_B \left(1 + \frac{M_\Delta^2 - \Delta^2}{M_N^2} \right) \right\} \Re \left(\tilde{\mathcal{G}}_{3,p\Delta}^{\pi*} \tilde{\mathcal{G}}_{4,p\Delta}^\pi \right),\end{aligned}\quad (6.299)$$

$$\sigma_\Delta^\perp = 4\sqrt{1 - x_B} \sqrt{-\frac{\Delta^2}{M_N^2}} \sqrt{1 - \frac{\Delta_{\min}^2}{\Delta^2}} \frac{M_\Delta}{M_N} \Im \left(\tilde{\mathcal{G}}_{3,p\Delta}^{\pi*} \tilde{\mathcal{G}}_{4,p\Delta}^\pi \right), \quad (6.300)$$

with the assignment of the reaction products specified in Section 6.3.7.

As a concluding remark, let us point out that the electroproduction of exotics has been discussed in Refs. [433, 434].

6.3.9 Perturbative corrections to meson production

Let us shortly discuss the role of radiative corrections to the leading order amplitudes taking the charged pion production as a case of study. At next-to-leading order, a question arises about the value of the momentum scale in the argument of the strong coupling constant. In estimates we will use two scale setting procedures: the naive $\mu_R = Q$ in the running $\alpha_s(Q^2)$ as at leading order with $\Lambda_{\text{QCD}}^{\text{LO}} = 220$ MeV and $N_f = 3$, in the first and the Brodsky-Lepage-Mackenzie scale setting [435, 430, 431, 432] with a fixed coupling at an ad hoc value $\alpha_s/\pi = 0.1$ below 1 GeV^2 in the second case. The leading order predictions [360, 361, 364] demonstrated in Fig. 59 (left) are plagued by

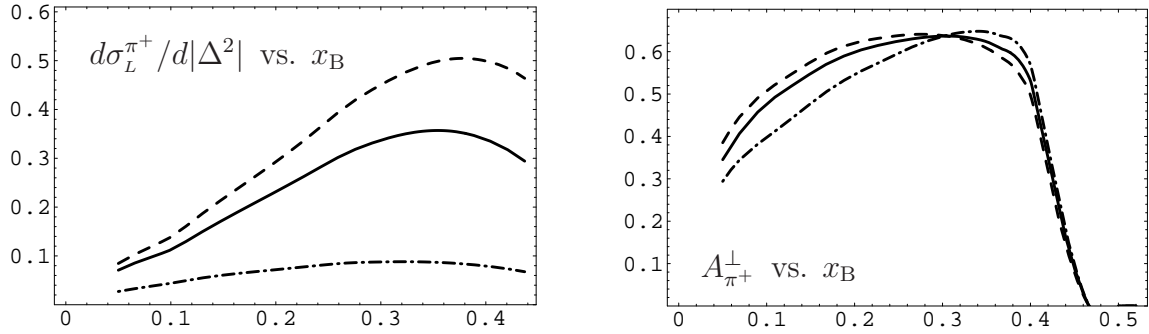


Figure 59: The leading twist predictions for the unpolarized photoproduction cross section in units of nbarns $d\sigma_L^{\pi^+}/d|\Delta^2|$ are shown for $\Delta^2 = -0.3 \text{ GeV}^2$ in the left panel. In the right panel, we display the transverse proton spin asymmetry \mathcal{A}_M^\perp for the same momentum transfer. The solid, dashed and dash-dotted curves represent the leading and next-to-leading order with naive and Brodsky-Lepage-Mackenzie scale setting, [430].

large uncertainties from the higher order corrections in absolute cross sections, however, they largely cancel in cross section ratios. For instance, the transverse target spin asymmetry defined by [361, 430]

$$\left(\int_0^\pi d\varphi_M \frac{d\sigma_L^M}{d|\Delta^2|d\varphi_M} - \int_\pi^{2\pi} d\varphi_M \frac{d\sigma_L^M}{d|\Delta^2|d\varphi_M} \right) \left(\int_0^{2\pi} d\varphi_M \frac{d\sigma_L^M}{d|\Delta^2|d\varphi_M} \right)^{-1} = -\frac{2}{\pi} \frac{\sigma_M^\perp}{\sigma_M} \sin \Theta \cos \Phi \\ \equiv -\mathcal{A}_M^\perp \sin \Theta \cos \Phi . \quad (6.301)$$

is shown in Fig. 59 (right) for $\Delta^2 = -(0.1, 0.3) \text{ GeV}^2$ and exhibits very little sensitivity to next-to-leading order corrections [430].

The next-to-leading order corrections are also available for heavy meson [436] and light neutral vector meson [431] production.

6.3.10 Nonperturbative corrections

The studies of higher-order perturbative corrections to the hard coefficient function in many physical observables have demonstrated that ambiguities generated by the perturbative resummation of fermion vacuum polarization insertions were of the same order of magnitude as available non-perturbative estimates of matrix elements of higher-twist operators [437]. The development and sophistication of these ideas provided some evidence that infrared renormalons may explain the magnitude of higher-twist contributions and even their functional dependence on scaling variables, and can thus be used to get rough estimates of power-suppressed effects [437]. On the practical side, to compute them one replaces the tree gluon propagator in loop diagrams by the one with resummed fermion bubbles and restores full β -function from the quark term—a procedure dubbed naive nonabelianization. In this so-called single-chain approximation, the propagator reads in the Landau gauge,

$$\mathcal{D}_{\mu\nu}(k) = -\frac{4\pi}{\alpha_s \beta_0} \int_0^\infty d\tau e^{4\pi/(\alpha_s \beta_0)\tau} \left(\frac{\mu^2 e^C}{-k^2} \right)^\tau \frac{1}{k^2} \left(g_{\mu\nu} - \frac{k_\mu k_\nu}{k^2} \right) ,$$

where $C_{\overline{\text{MS}}} = \frac{5}{3}$ in the $\overline{\text{MS}}$ and $C_{\text{MS}} = \frac{5}{3} - \gamma_E + \ln 4\pi$ in the MS scheme. As usual, β_0 is the (negative) one-loop beta function (G.29) and $\alpha_s = \alpha_s(\mu)$ is the running coupling constant (4.262). The quark coefficient function with resummed renormalon chains for the π^+ production has the form [58]

$$T_{\pi^+}(u, x, \eta; Q^2) = -\frac{4\pi C_F}{\beta_0} \int_0^\infty \frac{d\tau}{\eta} e^{4\pi/(\alpha_s \beta_0)\tau} \left(\frac{2\mu^2 e^C}{Q^2} \right)^\tau \times \left\{ \frac{Q_u}{[(1-u)(1-\frac{x}{\eta}-i0)]^{\tau+1}} - \frac{Q_d}{[u(1+\frac{x}{\eta}-i0)]^{\tau+1}} \right\}, \quad (6.302)$$

which is a straightforward modification of Eq. (6.274).

If we absorb the dependence on the momentum fraction into the argument of the coupling constant, $\alpha_s(\frac{1}{2}u(1 \pm \frac{x}{\eta})Q^2 e^{-C})$, it is easy to see that the end-point regions produce divergences. Infrared renormalons are caused by the end-point singularities [Feynman mechanism] in exclusive hard-gluon exchange amplitudes [438], see also [439, 440]. This can be viewed as an estimate of the ambiguity in the resummation of higher-order perturbative corrections or, taken to the extreme, as a model of higher-twist contributions [441]. Convolution of the coefficient function with the distribution amplitude generates renormalon poles. For the asymptotic distribution amplitude $\phi_{\text{asy}}(u) = 6u\bar{u}$, one gets two poles $\tau = 1$ and $\tau = 2$, corresponding to ambiguities on the level of Q^{-2} and Q^{-4} power corrections. Since the latter receives extra contributions from higher order diagrams as well, it makes sense to rely only on $\tau = 1$ pole for estimates of the form of higher-twist corrections. Taking the imaginary part (divided by π) arising from the contour deformation around the renormalon poles as a measure of their magnitude, we get

$$\tilde{\mathcal{H}}_{pn}(\eta, \Delta^2; Q^2) = \tilde{\mathcal{H}}_{pn}^{\text{PV}}(\eta, \Delta^2; Q^2) + \theta \frac{\Lambda_{\overline{\text{MS}}}^2 e^{5/3}}{Q^2} \int_{-1}^1 dx \Delta_{\tilde{H}}(x, \eta) \tilde{H}_{pn}(x, \eta, \Delta^2), \quad (6.303)$$

where $\theta = \pm 1$ reflects the ambiguity of the contour going around the renormalon pole in the Borel plane. Here, the one-loop expression for the QCD coupling constant was used and

$$\Delta_{\tilde{H}}(x, \eta) = -48 \frac{\pi C_F}{\beta_0 \eta} \left\{ \frac{Q_u}{(1-\frac{x}{\eta}-i0)^2} - \frac{Q_d}{(1+\frac{x}{\eta}-i0)^2} \right\}. \quad (6.304)$$

Within the DD-based models for GPDs discussed in Sections 3.13, the polarized GPDs and their first derivative are continuous functions at $x = \pm\eta$ [148], and therefore the integral over x is well-defined. If we allow for meson exchange-like contributions in GPDs, as we discussed in Section 3.9, this property would be lost. In the first term of (6.303) one should use the principal value prescription to go around the poles in the Borel plane. Assuming the pion-pole dominated form for \tilde{E} [9] one obtains

$$\tilde{\mathcal{E}}_{pn}(\eta, \Delta^2; Q^2) = \tilde{\mathcal{E}}_{pn}^{\text{PV}}(\eta, \Delta^2; Q^2) - \theta \frac{\Lambda_{\overline{\text{MS}}}^2 e^{5/3}}{Q^2} \Delta_{\tilde{E}}(\eta, \Delta^2; Q^2), \quad (6.305)$$

where only the single and double poles were kept at $\tau = 1$ in the second term, so that

$$\Delta_{\tilde{E}}(\eta, \Delta^2; Q^2) = -72 \frac{\pi C_F}{\beta_0 \eta} F_\pi(\Delta^2) \left(2 + \ln \frac{\Lambda_{\overline{\text{MS}}}^2 e^{5/3}}{Q^2} \right). \quad (6.306)$$

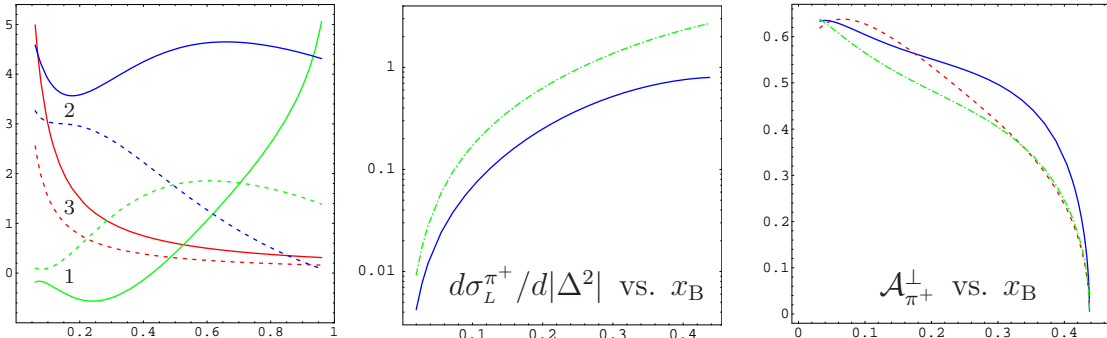


Figure 60: Generalized structure functions (left) in leading twist approximation (dashed) and including twist-four corrections (solid) as a function of x_B for $\Delta^2 = -0.3 \text{ GeV}^2$ and $Q^2 = 10 \text{ GeV}^2$: (1) $\Re e \tilde{\mathcal{H}}$, (2) $\Im m \tilde{\mathcal{H}}$, and (3) $10^{-2} \cdot \tilde{\mathcal{E}}$. The photoproduction cross section in units of nbarns (middle) without (solid) and with (dash-dotted) power suppressed contributions for the same values of the kinematical variables. The transverse spin asymmetry (right) at leading order (solid) and with twist-four power effects taken into account for $\Delta^2 = -0.3 \text{ GeV}^2$ and $Q^2 = 4 \text{ GeV}^2$ (dashed) and $Q^2 = 10 \text{ GeV}^2$ (dash-dotted). The maximal value of $x_{B,\max}$ is set by the kinematical constraint $|\Delta^2| > |\Delta_{\min}^2| = M_N^2 x_B^2 / (1 - x_B)$.

Notice that the consideration of \tilde{E} completely parallels the renormalon analysis of pion transition form factor [438, 439, 440]. In the vicinity of the pion pole one can approximate by $F_\pi(\Delta^2) = 4g_A M_N / (m_\pi^2 - \Delta^2)$ according to Eq. (3.315).

The estimates illustrated in Fig. 60 rely on GPDs discussed in Section 3.13.4. The values $\theta = 1$ and $A_{\overline{\text{MS}}} = 280 \text{ MeV}$ for $N_f = 4$ were used, and the tree level result for $\mathcal{F}^{\text{PV}} \rightarrow \mathcal{F}^{\text{LO}}$. Note, however, that to get the right magnitude of the higher-twist corrections suggested by experimental data in deeply inelastic scattering, one should take a larger value $|\theta| \approx 2 - 3$ [442]. The extremely large size of power corrections to the absolute cross section of the pion leptoproduction is in qualitative agreement with the earlier calculation of Ref. [403]. It is interesting to note that the renormalon model of higher-twist contributions only marginally affects the transverse target spin asymmetry and thus leads to the apparent conclusion of *the precocious scaling* in ratios of observables,—a fact pointed out previously in various circumstances [361, 430, 132].

7 Outlook

The last decade has witnessed substantial progress in unraveling the intriguing puzzle of hadron's structure through the newly developed concept of generalized parton distributions. Currently, theoretical understanding of various aspects of their physics and phenomenology have entered their early years of robust maturity. Different frontiers have been explored so far and have reached profound depth. As we discussed in this review, these developments include understanding of precise microscopic information accumulated by these functions about the inner content of hadrons and intuitive spatial picture encoded in GPDs; their symmetry and partonic properties; a new emphasis on the importance of the orbital angular momentum of hadron's constituents in building up helicity-flip transitions and the potential of GPDs to ultimately resolve the notorious proton spin crisis; the renormalization group evolution of GPDs with the change of the resolution scale up to the next-to-leading level of accuracy, just to name the most important ones.

The new functions, GPDs, are measurable in a number of exclusive reactions. The latter are promising tools to disentangle, in a quantitative manner, the intricate functional dependence of GPDs on intrinsic variables determining their shape. In certain cases, a precise theory has emerged from elaborate studies which includes understanding of higher order and higher twist corrections. Despite these impressive accomplishments, the subject is still in its early age of sophistication, and its theory is far from being complete. Thus, instead of repeating the success story, which we reviewed in the present work, let us give an outline of a few directions, where significant improvements can be made.

The theory of exclusive processes for GPDs needs to be developed in a number of directions, the major goal being increasing its predictive power. The leading approximation for the amplitudes of hard processes in QCD is affected by a number of multiplicative and additive corrections. To the first class we attribute radiative corrections in strong coupling, while the second set embraces higher-twist contributions, which decay according to a power law in the hard scale. When the given large scale Q (controlling the applicability of factorization to a reaction) becomes rather small, one must include power-suppressed effects since they can significantly modify the scaling behavior and the magnitude of the leading-twist predictions for corresponding cross sections. Power corrections are divided, as we explained above, into two classes according to their origin: dynamical and kinematical. The first consists of multiparton correlations inside hadrons and gives rise to new non-perturbative functions. The second arises from a separation of composite operators into components that have definite transformation properties with respect to the Lorentz group, i.e., these components possess a well-defined geometrical twist. This decomposition provides the so-called Wandzura-Wilczek type contributions appearing from separation into components with definite symmetry properties, as well as target mass corrections stemming from the subtraction of trace terms in the composite operators. All of these corrections should be under theoretical control to provide a reliable analysis of experimental data at current facilities, which allow to probe only moderately hard scales.

We have reviewed a formalism based on harmonic polynomials, which span a representation of the Lorentz group, to resum an infinite series of target mass corrections associated with twist-two operators. As we have seen, it was not possible to stay within the framework of single-variable functions (i.e., GPDs), so we needed to employ the framework of double distributions. The expansion in powers of M^2 can be cast in a conventional form of GPDs. Without performing this mass expansion, the inverse Radon transform, of course, directly converts the result into language of GPDs. However, a simpler representation should be available. Another reason for extending the analysis beyond the leading-twist level is the need to maintain electromagnetic gauge invariance. Thus, inclusion of target mass corrections to twist-three operators in off-forward Compton amplitudes and study of their implications for the validity of phenomenology of leading twist approximation at available momentum transfer is a natural next step. It would require a strong effort, since the twist-three sector is trickier because it requires a thorough disentangling of non-commuting procedures of twist separation and the use of Heisenberg equations of motions for elementary fields.

Experimental and theoretical studies of quark-gluon correlations represent a further extension of the analysis of one-particle distributions. Studies of the correlations between the “QCD partons” are interesting in two complimentary aspects. First, they provide important quantitative information towards understanding how the pointlike partons are bound together to produce hadrons. The goal is, therefore, to progress from the question “Of what are the hadrons built?” to “How they are built?” Second, quark-gluon correlations, as we already emphasized, are responsi-

ble for the higher-twist corrections to hard processes, the understanding of which is crucial in order to make QCD predictions truly quantitative. This task is attracting growing attention recently, as it has become clear that the discovery potential of the high-profile experimental programs searching for the physics beyond the standard model depends crucially on having effects of the strong interaction under control. A possible direction for development of the theory of twist-four corrections in the virtual Compton amplitude is a generalization of the Ellis-Furmanski-Petronzio formalism used earlier for deeply inelastic scattering. A very outstanding and elaborate problem is the construction of evolution equations for twist-four correlation functions.

We have outlined in this review the theory of the virtual Compton scattering within the context of GPDs for spin-zero and spin-one-half targets by including power-suppressed affects to twist-three accuracy. In order to explore the structure of the neutron, one must resort to using an $A > 1$ nuclear target, the lightest being the the spin-1 deuteron. In order to understand how precise one can determine neutron properties in hard reactions, one must understand completely the structure of contributions in measurements using deuteron targets. So far, the analysis has been performed only within the framework of the parton model [443, 76] (see also [444]). The consideration should be extended at least to the same level of precision as in the DVCS on the nucleon target, i.e., to twist-three accuracy.

A process unique in its ability to measure the surface of GPDs is the lepton-pair production off the proton, $ep \rightarrow e' p' \ell \bar{\ell}$. It has a doubly-virtual Compton scattering (DDVCS) amplitude as a subprocess, encoding information on GPDs. An immediate problem which has to be addressed is the calculation of the Bethe-Heitler amplitudes for the final state leptons identical to the one in the initial state $\ell = e$. This analysis requires the addition of exchange contributions and revisions of all cross sections where they coherently interfere with already available amplitudes, as discussed in Section 6.2. This will undoubtedly bring a vast variety of polarization and azimuthal observables which will further help to unveil the complicated structure of GPDs. Yet another development should include the study of twist-three effects in DDVCS in the same vein as it was done for DVCS.

Currently the bulk of predictions for exclusive processes are available only to zeroth order in strong coupling, excluding a few next-to-leading results for the leading-twist off-forward Compton amplitude [233, 316, 282] and certain final-state mesons in hard exclusive meson production [430, 436, 431]. An important problem is the calculation of one-loop corrections to twist-three Compton amplitudes with real and virtual final-state photons and numerical studies of their magnitude. The first results in the Wandzura-Wilczek approximation were reported in Ref. [302]. Continuous progress along these lines will allow one to extend the validity of factorization theorems beyond leading order in hard scales. A promising direction towards improvement of the leading-twist results is further development and use of the conformal scheme for exclusive processes. A particular goal is to predict two-loop corrections to the Compton scattering amplitude, starting from available next-to-next-to-leading order results for deeply inelastic scattering. Another project in higher order computation is to find one-loop corrections to the twist-two exclusive production of tensor mesons and to the contribution of the gluon transversity GPD in the double helicity flip production of vector mesons, which arises at subleading twist-three level [445].

The importance of Sudakov effects in exclusive processes calls for understanding an analogous mechanism in the leading-twist off-forward Compton scattering amplitudes and hard exclusive meson production. The Sudakov effects are known to reduce the sensitivity to edges of the phase space, which sometimes produce uncontrollable contributions that ruin clean theoretical predictions. However, in known circumstances this suppression happens away from the validity of

perturbative treatment, since the arguments of coupling run into the infrared region. This issue must be understood for the presently discussed processes.

The description of the hard exclusive meson production in the framework of QCD relies on essentially the same framework as developed to address exclusive form factors at large momentum transfer. Therefore, all subtle issues related to the description of helicity-flip form factors are immediately transferred to hard meson production with a transversely-polarized photon [446, 447]. In both cases, the endpoint contributions are uncontrollable in the naive form of factorization, appearing as a convolution of a hard part with two distribution amplitudes in case of form factors, or as a convolution of a hard part with a meson distribution amplitude and a GPD for meson production. And, in both cases, one faces singularities arising from the endpoint behavior of distribution amplitudes, which result in logarithmically divergent integrals. This clearly suggests that a part of the long-distance physics was erroneously included in the hard coefficient function and calls for a thorough re-factorization. A possible line of investigations is to start with the ρ -meson form factor, where these issues arise in the simplest circumstances, and analyze different regions of Feynman integrals. The effective field theory that emerges from this consideration is designed in terms of effective degrees of freedom parametrizing various regions in the momentum space, and allows for a systematic treatment of more involved cases like hard exclusive meson production or helicity-flip hadron form factors, including the nucleon Pauli form factor. The latter has received intensive scrutiny from the experimental side; it is one of the observables sensitive to the orbital motion of constituents inside the proton and is intrinsically related to the proton's spin content.

The study of hadron constituents that carry tiny momentum fractions allow to probe an essentially new state of partonic matter: the color glass condensate (for the most recent review see, e.g., [448]). This topic received a lot of attention recently from the point of view of inclusive deeply inelastic scattering. DVCS can contribute significantly toward advancement of the field. At small x , a dipole picture can be applied to its description, with emphasis on detailed understanding of the impact-parameter dependence of the two-dimensional hadron profile (another outstanding feature made available by the use of GPDs), which enters integrated in the analogous approach to deeply inelastic scattering. An immediate theoretical problem is to design non-linear QCD evolution equations to predict the small- x behavior of GPDs from first principles.

The most prominent problem of GPDs concerns, of course, their reliable modeling. Although we know their rough features in a limited range of parameter space, it still remains a rather weakly scrutinized area of the theory, and not because of a lack of efforts. A profound understanding can be achieved through elaborate simultaneous fits to both lattice simulations and experimental data.

Transition GPDs, as described in Section 3.16, stand for matrix elements of light-cone operators for which the hadron changes from the initial to the final state. Such contributions arise as a background to proton Compton scattering and must be clearly identified in order to be subtracted from observed rates. However, they are interesting on their own ground, as one can use them to unveil many deep facets of the structure of nucleon resonances, such as members of the baryon decuplet. Questions like the intrinsic deformation of hadrons can be studied in a new environment, distinct from the perspective of conventional form factor measurements. So far, a few relations have been established between diagonal octet-decuplet transitions and those of proton-proton GPDs by using large- N_c QCD and SU(3) flavor symmetry. These considerations, however, do not take into account any deformation effects. An interesting topic for further analysis is to study $1/N_c$ and SU(3) flavor violation corrections to these relations.

The small- Δ^2 dependence of GPDs can be revealed by making use of an effective theory description at scales of the order of chiral symmetry breaking as was demonstrated in Section 3.12. The conventional SU(2) chiral Lagrangian can be used to compute corrections to all twist-two generalized parton distributions to determine their dependence on momentum transfers up to $\mathcal{O}(m_\pi)$. This analysis should be performed for diagonal as well as transition GPDs. So far, an exploratory study has been done only for the parity-even GPDs as we reviewed above. Improvements which allow to go to higher momentum transfers can be done by systematically including the Δ -isobar as a dynamical degree of freedom in the microscopic Lagrangian.

Given the combined knowledge gained in recent years and anticipating the progress along the lines we outlined above, we hope that the theory of GPDs and related exclusive processes is capable to reach the level comparable to that achieved in the theory of inclusive deeply inelastic processes, and to provide access to new layers of information about hadronic structure.

Acknowledgements

This work was supported by the U.S. National Science Foundation under grant no. PHY-0456520 (A.B.) and by the U.S. Department of Energy contract DE-AC05-84ER40150 under which the Southeastern Universities Research Association (SURA) operates the Thomas Jefferson Accelerator Facility (A.R.). We are honored to dedicate this paper to Anatoly Vasilievich Efremov, our Teacher, who taught us his approach to physical phenomena and guided our first steps in physics. We were lucky to work in the inspiring atmosphere he created in his group, and enjoyed collaboration and discussions with A.V., and our friends, the members of his group, Alexander Bakulev, Eduard Kuraev, Gregory Korchemsky, Sergei Mikhailov, Rusko Ruskov, and Oleg Teryaev. Our work on generalized parton distributions was strongly influenced by our contacts and collaboration with I. Balitsky, V. Braun, K. Goeke, X. Ji, L. Mankiewicz, I. Musatov, D. Müller, M. Polyakov, A. Schäfer, and C. Weiss. One of us (A.B.) expresses his sincere gratitude to Dieter Müller for years of fruitful and inspiring collaboration. Over years, our GPD-effort was generously supported by the Alexander von Humboldt Foundation, and we express our deep gratitude to the Foundation and to our collaborators and colleagues with whom we worked and contacted in Germany: J. Blümlein, D. Diakonov, M. Diehl, Th. Feldmann, A. Freund, B. Geyer, V. Guzey, D. Ivanov, R. Jakob, A. Kirchner, N. Kivel, P. Kroll, M. Lazar, A. Mukherjee, N. Nikolaev, H.-C. Pauli, V. Petrov, G. Piller, P. Pobylitsa, M. Praszalowicz, D. Robaschik, J. Speth, L. Szymanowski, N. Stefanis, W. Schroers, M. Vanderhaeghen, and W. Weise. We thank S.J. Brodsky, M. Burkardt, J.-W. Chen, T. Cohen, J.C. Collins, L. Frankfurt, P. Hoodbhoy, G.P. Korchemsky, R. Lebed, A.D. Martin, G. Miller, B. Pire, M. Ryskin, M. Savage, M. Strikman, B. Tiburzi, and F. Yuan, for numerous stimulating discussions. Last but not least, we are indebted to Markus Diehl, who had generously agreed to be the first reader of this review, for his constructive criticism, numerous suggestions and corrections, which lead to a significant improvement of the manuscript.

A Conventions

We use the following convention for the metric tensor:

$$g_{\mu\nu} = g^{\mu\nu} = \text{diag}(1, -1, -1, -1). \quad (\text{A.1})$$

The contravariant and covariant vectors are defined as

$$v^\mu = (v_0, \mathbf{v}), \quad v_\mu = (v_0, -\mathbf{v}), \quad (\text{A.2})$$

respectively. For the totally antisymmetric Levi-Civita tensor $\varepsilon^{\mu\nu\rho\sigma}$, we adopt the normalization

$$\varepsilon^{0123} = 1, \quad \varepsilon_{0123} = -1. \quad (\text{A.3})$$

It obeys the Schouten identity

$$g^{\alpha\beta}\varepsilon^{\mu\nu\rho\sigma} - g^{\alpha\mu}\varepsilon^{\beta\nu\rho\sigma} + g^{\alpha\nu}\varepsilon^{\beta\mu\rho\sigma} - g^{\alpha\rho}\varepsilon^{\beta\mu\nu\sigma} + g^{\alpha\sigma}\varepsilon^{\beta\mu\nu\rho} = 0,$$

which stems from the absence of the totally antisymmetric rank-five tensor in four dimensions.

A.1 Representations of the Clifford algebra

The Dirac γ^μ matrices obey the four-dimensional Clifford algebra:

$$\{\gamma^\mu, \gamma^\nu\} = 2g^{\mu\nu} \cdot \mathbb{1}_{[4] \times [4]}, \quad (\text{A.4})$$

with $\mathbb{1}_{[4] \times [4]}$ being the $[4] \times [4]$ unit matrix. Let us introduce two representations for this algebra used in the main text.

• *Weyl representation*: In this representation, a bispinor is constructed from the left $\bar{\chi}_\downarrow$ and right λ_\uparrow Weyl spinors by merely putting them in the same multiplet

$$\psi = \begin{pmatrix} \lambda_\uparrow \\ \bar{\chi}_\downarrow \end{pmatrix}. \quad (\text{A.5})$$

This is the Dirac spinor. The main reason to arrange these two-component spinors in the same four-component vector is that the spatial parity is well defined for this object, i.e., the left and right spinors jump their places $\bar{\chi}_\downarrow \leftrightarrow \lambda_\uparrow$ under it. Recall that representations of the Lorentz group $L_+^\dagger = SO(3, 1) = SO(4, \mathbb{C})_{\perp R} \approx (SL(2, \mathbb{C}) \otimes SL(2, \mathbb{C}))_{\perp R}$ —a real form of the complexified group of four-dimensional rotations [449]—are labeled by a pair (j_1, j_2) of numbers, which are the eigenvalues $j_i(j_i + 1)$ of the $SL(2)$ Casimir operators \mathbf{J}_i^2 . The spinors $\bar{\chi}_\downarrow$ and λ_\uparrow transform according to the $(\frac{1}{2}, 0)$ and $(0, \frac{1}{2})$ representations, respectively. The complex conjugate of the $\bar{\chi}_\downarrow$ spinor transforms as λ_\uparrow , i.e.,

$$\bar{\chi}_\downarrow^* \sim i\sigma^y \lambda_\uparrow, \quad (\text{A.6})$$

where the second Pauli σ^y matrix serves as a charge conjugation matrix. The Dirac matrices have the following form in the Weyl representation

$$\gamma^\mu = \begin{pmatrix} 0 & \bar{\sigma}^\mu \\ \sigma^\mu & 0 \end{pmatrix}, \quad (\text{A.7})$$

where the two-by-two matrices are

$$\sigma^\mu = (1, \boldsymbol{\sigma}), \quad \bar{\sigma}^\mu = (1, -\boldsymbol{\sigma})$$

with $\boldsymbol{\sigma}$ being the vector of Pauli matrices $\boldsymbol{\sigma} = (\sigma^x, \sigma^y, \sigma^z)$. The chirality and charge conjugation matrices in this representation take the form

$$\gamma^5 = i\gamma^0\gamma^1\gamma^2\gamma^3 = \begin{pmatrix} 1 & 0 \\ 0 & -1 \end{pmatrix}, \quad C = i\gamma^2\gamma^0 = \begin{pmatrix} -i\sigma_2 & 0 \\ 0 & i\sigma_2 \end{pmatrix}. \quad (\text{A.8})$$

The latter obeys the following representation-independent relations

$$C^T = -C, \quad C^2 = -1, \quad C\gamma^\mu = -(\gamma^\mu)^T C. \quad (\text{A.9})$$

- *Dirac representation* is obtained from the Weyl representation by a unitary rotation

$$\gamma_D = \mathcal{U}^\dagger \gamma_W \mathcal{U}, \quad \mathcal{U} = \frac{1}{\sqrt{2}} \begin{pmatrix} 1 & 1 \\ 1 & -1 \end{pmatrix}. \quad (\text{A.10})$$

The Dirac matrices admit the form

$$\gamma^0 = \begin{pmatrix} 1 & 0 \\ 0 & -1 \end{pmatrix}, \quad \gamma = \begin{pmatrix} 0 & \boldsymbol{\sigma} \\ -\boldsymbol{\sigma} & 0 \end{pmatrix}, \quad \gamma^5 = \begin{pmatrix} 0 & 1 \\ 1 & 0 \end{pmatrix}, \quad C = \begin{pmatrix} 0 & -i\sigma_2 \\ -i\sigma_2 & 0 \end{pmatrix}. \quad (\text{A.11})$$

The transposed matrices can be brought to the usual form with the action of the charge conjugation matrices as follows

$$C\gamma_\mu^T C = \gamma_\mu, \quad C\gamma_5^T C = -\gamma_5, \quad C(\gamma_\mu \gamma_5)^T C = -\gamma_\mu \gamma_5, \quad C\sigma_{\mu\nu}^T C = \sigma_{\mu\nu}, \quad (\text{A.12})$$

where $\sigma_{\mu\nu} = \frac{i}{2} [\gamma_\mu, \gamma_\nu]$ is an antisymmetric matrix, which has the property $\gamma^5 \sigma^{\mu\nu} = \frac{i}{2} \varepsilon^{\mu\nu\rho\sigma} \sigma_{\rho\sigma}$. The product of three γ -matrices can be reduced to one by means of the identity

$$\gamma^\mu \gamma^\nu \gamma^\rho = g^{\mu\nu} \gamma^\rho + g^{\nu\rho} \gamma^\nu - g^{\mu\rho} \gamma^\nu + i\varepsilon^{\mu\nu\rho\sigma} \gamma_\sigma \gamma_5. \quad (\text{A.13})$$

A.2 Spin-1/2 spinors

The amplitude of the plane-wave solution to the Dirac equation satisfies the equation

$$(\not{p} - m) u(p) = 0. \quad (\text{A.14})$$

Using the Dirac representation of the γ -matrices, the Dirac bispinor can be written as

$$u_\lambda(p) = \begin{pmatrix} \sqrt{E_p + m} w_\lambda \\ \sqrt{E_p - m} (\mathbf{n} \cdot \boldsymbol{\sigma}) w_\lambda \end{pmatrix}. \quad (\text{A.15})$$

It defines a particle of the energy E_p and three-momentum \mathbf{p} , moving in the direction of the unit vector $\mathbf{n} \equiv \mathbf{p}/\sqrt{\mathbf{p}^2}$. The Weyl spinors w_λ are eigenfunctions of the helicity operator. Recall, that the Pauli-Lubanski vector

$$W^\mu = \frac{1}{2} \varepsilon^{\mu\nu\rho\sigma} P_\nu M_{\rho\sigma}$$

in the rest-frame of the particle gives the helicity operator

$$h = -\frac{i}{m} W^3 = i\Sigma^{12} = \frac{1}{2} \begin{pmatrix} \sigma^3 & 0 \\ 0 & \sigma^3 \end{pmatrix}, \quad (\text{A.16})$$

where the relation $\Sigma^{\mu\nu} = \frac{1}{4} [\gamma^\mu, \gamma^\nu]$ was used to write the representation for the spin matrix. Since

$$u_\lambda(0) = \sqrt{2m} \begin{pmatrix} w_\lambda \\ 0 \end{pmatrix}, \quad (\text{A.17})$$

in the particle's rest-frame, one finds two solutions of the eigenvalue equation $hu_\lambda(0) = \lambda u_\lambda(0)$ with helicity $+\frac{1}{2}$ and $-\frac{1}{2}$, respectively,

$$w_\uparrow(0) = \begin{pmatrix} 1 \\ 0 \end{pmatrix}, \quad w_\downarrow(0) = \begin{pmatrix} 0 \\ 1 \end{pmatrix}. \quad (\text{A.18})$$

If one chooses a different direction to define polarization states, the two-component spinor w obeys the equation $\frac{1}{2}(\mathbf{n} \cdot \boldsymbol{\sigma})w^\lambda = \lambda w^\lambda$. The solutions to it are

$$w_\uparrow = \begin{pmatrix} \cos \frac{\theta}{2} \\ \sin \frac{\theta}{2} e^{i\phi} \end{pmatrix} = \frac{1}{\sqrt{2|\mathbf{p}|(|\mathbf{p}| + p^3)}} \begin{pmatrix} |\mathbf{p}| + p^3 \\ p_\perp \end{pmatrix}, \quad (\text{A.19})$$

$$w_\downarrow = \begin{pmatrix} -\sin \frac{\theta}{2} e^{-i\phi} \\ \cos \frac{\theta}{2} \end{pmatrix} = \frac{1}{\sqrt{2|\mathbf{p}|(|\mathbf{p}| + p^3)}} \begin{pmatrix} -\bar{p}_\perp \\ |\mathbf{p}| + p^3 \end{pmatrix}. \quad (\text{A.20})$$

These Weyl spinors are normalized as $w_{\lambda'}^* w_\lambda = \delta_{\lambda'\lambda}$. Here, (θ, ϕ) are the polar and azimuthal angles specifying the direction of the vector \mathbf{n} . In the second set of equalities, we use the holomorphic and anti-holomorphic momenta, determined in terms of the components orthogonal to the z -axis,

$$p_\perp \equiv p^x + ip^y, \quad \bar{p}_\perp \equiv p^x - ip^y. \quad (\text{A.21})$$

The total Dirac bispinor is normalized as

$$\bar{u}_\lambda(p)u_{\lambda'}(p) = 2m \delta_{\lambda\lambda'}. \quad (\text{A.22})$$

The density matrix is constructed from them as a direct product

$$u(p) \otimes \bar{u}(p) = \frac{1}{2} (\not{p} + m) \left(1 + \gamma_5 \frac{\not{s}}{m} \right), \quad (\text{A.23})$$

with the four-dimensional spin-vector

$$s^\mu = 2m \left(\frac{(\mathbf{p} \cdot \mathbf{s})}{m}, \mathbf{s} + \frac{\mathbf{p}(\mathbf{p} \cdot \mathbf{s})}{m(E_p + m)} \right), \quad s^2 = -m^2.$$

The latter is obtained from the spin three-vector \mathbf{s} by a boost from the rest frame along \mathbf{p} . Both relations are valid for general spin states. Using the density matrix, we can find

$$\bar{u}(p)\gamma^\mu u(p) = 2p^\mu, \quad \bar{u}(p)\gamma^\mu\gamma^5 u(p) = 2s^\mu. \quad (\text{A.24})$$

The interpretation of the left and right spinors is transparent in Weyl representation. Namely, taking the ultrarelativistic limit of the Dirac equation, one can neglect the mass $m = 0$ and set $|\mathbf{p}| = E_p$, then Eq. (A.14) is reduced to two uncoupled equations

$$(1 + \mathbf{n} \cdot \boldsymbol{\sigma}) \bar{\chi}_\downarrow = 0, \quad (1 - \mathbf{n} \cdot \boldsymbol{\sigma}) \lambda_\uparrow = 0, \quad (\text{A.25})$$

for the left $\bar{\chi}_\downarrow$ and right λ_\uparrow components of the bispinor (A.5). Here, $\mathbf{n} = \mathbf{p}/E_p$ defines the direction of the particle's motion. Choosing it along the z -axis, $\mathbf{n} = (0, 0, 1)$, one obtains the solutions

$$\bar{\chi}_\downarrow \sim \begin{pmatrix} 0 \\ 1 \end{pmatrix}, \quad \lambda_\uparrow \sim \begin{pmatrix} 1 \\ 0 \end{pmatrix}. \quad (\text{A.26})$$

So that the left spinor $\bar{\chi}_\downarrow$ defines a particle with its helicity pointed in the opposite direction to its motion, while the right spinor λ_\uparrow corresponds to the aligned orientation of its spin and momentum.

Let us give expressions for certain Dirac bilinears $\bar{u}(p_2)\Gamma u(p_1)$ which arise in parametrizations of operator matrix elements in different Lorentz frames used throughout the paper.

- The Breit frame is defined by the condition $\mathbf{p}_1 + \mathbf{p}_2 = 0$ and the absence of the energy exchange $\Delta^0 = E_{\mathbf{p}1} - E_{\mathbf{p}2} = 0$, so that

$$E_{\mathbf{p}1} = E_{\mathbf{p}2} = m\sqrt{1 + \Delta^2/(4m^2)}, \quad \mathbf{p}_1 = -\mathbf{p}_2 = \Delta/2. \quad (\text{A.27})$$

Thus, the parity-even Dirac bilinears read in terms of the two-component Weyl spinors

$$\begin{aligned} \bar{u}(p_2)\gamma^0 u(p_1) &= 2mw_2^*w_1, & \bar{u}(p_2)\gamma^k u(p_1) &= iw_2^*[\Delta \times \boldsymbol{\sigma}]^k w_1, \\ \bar{u}(p_2)\frac{i\sigma^{\mu 0}\Delta_\mu}{2m}u(p_1) &= -\frac{\Delta^2}{2m}w_2^*w_1, & \bar{u}(p_2)\frac{i\sigma^{\mu k}\Delta_\mu}{2m}u(p_1) &= iw_2^*[\Delta \times \boldsymbol{\sigma}]^k w_1, \end{aligned} \quad (\text{A.28})$$

where $[\Delta \times \boldsymbol{\sigma}]^i \equiv \varepsilon^{ijk}\Delta^j\sigma^k$. As it can be seen, the helicity-flip and non-flip transitions in the Breit frame arise both from the γ^μ and $\sigma^{\mu\nu}$ vertices. Analogously, the parity-odd Dirac bilinears yield

$$\begin{aligned} \bar{u}(p_2)\gamma^0\gamma^5 u(p_1) &= 0, & \bar{u}(p_2)\gamma^k\gamma^5 u(p_1) &= 2m\sqrt{1 + \Delta^2/(4m^2)}w_2^*\sigma^k w_1 \\ \bar{u}(p_2)\gamma^5 u(p_1) &= w_2^*(\boldsymbol{\sigma} \cdot \Delta)w_1, & & -\frac{w_2^*\Delta^k(\boldsymbol{\sigma} \cdot \Delta)w_1}{2m(1 + \sqrt{1 + \Delta^2/(4m^2)})}. \end{aligned} \quad (\text{A.29})$$

- The Lorentz-covariant Breit frame is a form of the Breit frame used for applications involving heavy-baryon limit, see Section 3.12. In the large-mass approximation the temporal component of the incoming and outgoing nucleons' four-momenta dominates over the rest and they can be decomposed as

$$p_{1,2}^\mu = mv^\mu + k^\mu \pm \Delta^\mu/2, \quad (\text{A.30})$$

with the four-velocity $v^\mu = (1, \mathbf{0})$ and the residual momentum

$$k^\mu = \left(m(\sqrt{1 - \Delta^2/(4m^2)} - 1), \mathbf{0} \right).$$

The large components of the velocity-dependent heavy baryon spinor are found from the usual Eq. (A.15) with a projector

$$u_v(p_i) \equiv \frac{(1 + \not{v})u(p_i)}{\sqrt{2 + 2(v \cdot p_i)/m}}. \quad (\text{A.31})$$

They are normalized as $\bar{u}_v u_v = 2m$. With these results, the Dirac bilinears arising in Eq. (3.121) are reduced via equations

$$\begin{aligned} \bar{u}(p_2)\gamma_\mu u(p_1) &= v_\mu \bar{u}_v(p_2)u_v(p_1) + \frac{1}{m}\bar{u}_v(p_2)[S \cdot \Delta, S_\mu]u_v(p_1), \\ \bar{u}(p_2)\frac{i\sigma_{\mu\nu}\Delta^\nu}{2m}u(p_1) &= v_\mu \frac{\Delta^2}{4m^2}\bar{u}_v(p_2)u_v(p_1) + \frac{1}{m}\bar{u}_v(p_2)[S \cdot \Delta, S_\mu]u_v(p_1). \end{aligned}$$

Here $S^\mu \equiv \frac{i}{2}\sigma^{\mu\nu}\gamma^5 v_\nu$ is the Pauli-Lubanski spin vector. In the nucleon rest frame, it obviously coincides with the three-vector of spin $S^\mu = (0, \boldsymbol{\Sigma}/2)$, where $\boldsymbol{\Sigma} = \text{diag}(\boldsymbol{\sigma}, \boldsymbol{\sigma})$.

- The light-cone frame is another widely used frame, which has a unique quantization axis defined by the boosted hadron. Thus, the helicity of all states is defined with respect to this preferred direction. The spinors u^{LC} in the light-cone helicity basis are related to the conventional ones u , discussed above, via a unitary transformation [10]

$$\begin{pmatrix} u_\uparrow \\ u_\downarrow \end{pmatrix} = \frac{1}{\sqrt[4]{8\sqrt{p^+}|\mathbf{p}|(|\mathbf{p}| + p^3)(E_{\mathbf{p}} + |\mathbf{p}|)}} \times \begin{pmatrix} (|\mathbf{p}| + p^3)(E_{\mathbf{p}} + |\mathbf{p}|) & mp_\perp \\ -m\bar{p}_\perp & (|\mathbf{p}| + p^3)(E_{\mathbf{p}} + |\mathbf{p}|) \end{pmatrix} \begin{pmatrix} u_\uparrow^{\text{LC}} \\ u_\downarrow^{\text{LC}} \end{pmatrix}. \quad (\text{A.32})$$

The off-diagonal elements of this matrix vanish when the particle is moving fast and, therefore, the usual and light-cone helicities coincide. Below, we will drop the superscript LC , since we will talk only about the light-cone spinors for the rest of this subsection. Explicit form of bispinors with definite light-cone helicity can be found from the above equation. The result for the Dirac representation is [62]

$$u_\uparrow(p) = \frac{1}{\sqrt[4]{2\sqrt{p^+}}} \begin{pmatrix} p^+ + m/\sqrt{2} \\ p_\perp/\sqrt{2} \\ p^+ - m/\sqrt{2} \\ p_\perp/\sqrt{2} \end{pmatrix}, \quad u_\downarrow(p) = \frac{1}{\sqrt[4]{2\sqrt{p^+}}} \begin{pmatrix} -\bar{p}_\perp/\sqrt{2} \\ p^+ + m/\sqrt{2} \\ \bar{p}_\perp/\sqrt{2} \\ -p^+ + m/\sqrt{2} \end{pmatrix}. \quad (\text{A.33})$$

Note, that the negative-energy spinors $u_\lambda(-p) = C\bar{u}_\lambda^T(p)$, describing antiparticles, can be obtained from the positive-energy ones via the simple substitution $u_{\uparrow\downarrow}(-p) = -u_{\downarrow\uparrow}(p)|_{m \rightarrow -m}$. The bilinears which arise in the analysis of matrix elements can be computed utilizing the explicit form of the light-cone helicity spinors:

$$\begin{aligned} \bar{u}_\uparrow(p_2)\gamma^+u_\uparrow(p_1) &= 2\sqrt{p_1^+p_2^+}, & \bar{u}_\downarrow(p_2)\gamma^+u_\uparrow(p_1) &= 0, \\ \bar{u}_\uparrow(p_2)\sigma^{+k}_\perp u_\uparrow(p_1) &= 0, & \bar{u}_\downarrow(p_2)\sigma^{+k}_\perp u_\uparrow(p_1) &= 2i\sqrt{p_1^+p_2^+}\mathbf{e}_\perp^k, \\ \bar{u}_\uparrow(p_2)\sigma^{+-}u_\uparrow(p_1) &= im(p_2^+ - p_1^+)/\sqrt{p_1^+p_2^+}, & \bar{u}_\downarrow(p_2)\sigma^{+-}u_\uparrow(p_1) &= i(p_1^+p_{2\perp} + p_2^+p_{1\perp})/\sqrt{p_1^+p_2^+}, \\ \bar{u}_\uparrow(p_2)\gamma^+\gamma^5u_\uparrow(p_1) &= 2\sqrt{p_1^+p_2^+}, & \bar{u}_\downarrow(p_2)\gamma^+\gamma^5u_\uparrow(p_1) &= 0, \\ \bar{u}_\uparrow(p_2)\gamma^5u_\uparrow(p_1) &= m(p_1^+ - p_2^+)/\sqrt{p_1^+p_2^+}, & \bar{u}_\downarrow(p_2)\gamma^5u_\uparrow(p_1) &= (p_2^+p_{1\perp} - p_1^+p_{2\perp})/\sqrt{p_1^+p_2^+}, \end{aligned} \quad (\text{A.34})$$

where the two-dimensional vector is $\mathbf{e}^k = (1, i)$. Compared to the Breit-frame bilinears in terms of conventional spinors, the helicity-flip transitions in the present light-cone case arise from the chiral-odd Dirac matrix $\sigma^{\mu\nu}$ and the chiral γ^5 . Notice that, in general case, the bilinears depend on each of the momenta $\mathbf{p}_{i\perp}$ separately. Only when the plus-momenta are equal $p_1^+ = p_2^+$, do the bilinears depend solely on the combination $\Delta_\perp = \mathbf{p}_{1\perp} - \mathbf{p}_{2\perp}$ corresponding to the transverse momentum transfer. In the “transverse” Breit frame $\mathbf{p}_{1\perp} = -\mathbf{p}_{2\perp} = \Delta_\perp/2$ this also occurs even if $p_1^+ \neq p_2^+$.

A.3 Spin-1 vector field

To describe a spin-one field, let us introduce a definite-helicity polarization vectors $\boldsymbol{\varepsilon}$ in the particle’s rest frame. The spin operator acts on spin-one polarization vector as follows

$$\Sigma^{\mu\nu}\varepsilon^\rho(0) = g^{\mu\rho}\varepsilon^\nu(0) - g^{\nu\rho}\varepsilon^\mu(0). \quad (\text{A.35})$$

Therefore, the eigenvalue equation for the helicity operator acting on the three-vector $\boldsymbol{\varepsilon}$ of $\varepsilon^\mu = (0, \boldsymbol{\varepsilon})$ can be cast into the matrix form

$$h\boldsymbol{\varepsilon} = \begin{pmatrix} 0 & -i & 0 \\ i & 0 & 0 \\ 0 & 0 & 0 \end{pmatrix} \begin{pmatrix} \varepsilon^x \\ \varepsilon^y \\ \varepsilon^z \end{pmatrix} = \lambda \boldsymbol{\varepsilon}. \quad (\text{A.36})$$

One easily finds the eigenvectors of this equation corresponding to helicity +1 (right circular polarization), -1 (left circular polarization) and 0 (longitudinal polarization),

$$\boldsymbol{\varepsilon}_\uparrow = -\frac{1}{\sqrt{2}} \begin{pmatrix} 1 \\ i \\ 0 \end{pmatrix}, \quad \boldsymbol{\varepsilon}_\downarrow = -\frac{1}{\sqrt{2}} \begin{pmatrix} -1 \\ i \\ 0 \end{pmatrix}, \quad \boldsymbol{\varepsilon}_0 = \begin{pmatrix} 0 \\ 0 \\ 1 \end{pmatrix}, \quad (\text{A.37})$$

respectively. By boosting these rest-frame polarization vectors into the system moving with three-momentum \mathbf{p} , one gets the four-polarization vector in an arbitrary frame

$$\varepsilon_s^\mu(p) = \left(\frac{(\mathbf{p} \cdot \boldsymbol{\varepsilon}_s)}{m}, \boldsymbol{\varepsilon}_s + \frac{\mathbf{p}(\mathbf{p} \cdot \boldsymbol{\varepsilon}_s)}{m(E_\mathbf{p} + m)} \right) = L^\mu{}_\nu(p) \varepsilon_s^\nu(0). \quad (\text{A.38})$$

To get the last equation, we used the representation in terms of the Lorentz boost from the rest frame vector $\varepsilon_s^\mu(p) = (0, \boldsymbol{\varepsilon}_s)$, with

$$L^\mu{}_\nu(p) = \frac{1}{m} \begin{pmatrix} E_\mathbf{p} & p^j \\ p^i & m\delta^{ij} + \frac{p^i p^j}{E_\mathbf{p} + m} \end{pmatrix}. \quad (\text{A.39})$$

The polarization four-vector is normalized as

$$\varepsilon_{s_1}^* \cdot \varepsilon_{s_2} = -\delta_{s_1 s_2}. \quad (\text{A.40})$$

A.4 Spin-3/2 Rarita-Schwinger spin-vector

The Rarita-Schwinger spin-vector $u^\mu(p)$ describes the wave function of a spin-three-half particle [450], see Ref. [451] for a comprehensive summary. It satisfies the Dirac equation

$$(\not{p} - m)u^\mu(p) = 0,$$

and two subsidiary conditions

$$p_\mu u^\mu(p) = 0, \quad \gamma_\mu u^\mu(p) = 0.$$

The second condition projects out the spin-one-half component contaminating the spin-vector u^μ . The spin-vector is constructed as a superposition of the Dirac bispinor $u_\lambda(p)$ (A.15) and the covariant spin-one polarization vector (A.38)

$$u_S^\mu(p) = \sum_{s_1, s_2} \delta_{S, s_1 + s_2} \langle \frac{1}{2}, s_1, 1, s_2 | \frac{3}{2}, S \rangle u_{s_1}(p) \varepsilon_{s_2}^\mu(p), \quad (\text{A.41})$$

with the Clebsch-Gordan coefficients

$$\langle j_1, m_1, j_2, m_2 | j, m \rangle = (-1)^{j_1 - j_2 + m} \sqrt{2j_1 + 1} \begin{pmatrix} j_1 & j_2 & j \\ m_1 & m_2 & -m \end{pmatrix}.$$

Explicit form of different spin components of the Rarita-Schwinger spin-vector (A.41) is given by

$$u_{3/2}^\mu(p) = u_\uparrow(p)\varepsilon_\uparrow^\mu(p), \quad u_{1/2}^\mu(p) = \sqrt{\frac{1}{3}}u_\downarrow(p)\varepsilon_\uparrow^\mu(p) + \sqrt{\frac{2}{3}}u_\uparrow(p)\varepsilon_0^\mu(p), \quad (\text{A.42})$$

$$u_{-3/2}^\mu(p) = u_\downarrow(p)\varepsilon_\downarrow^\mu(p), \quad u_{-1/2}^\mu(p) = \sqrt{\frac{1}{3}}u_\uparrow(p)\varepsilon_\downarrow^\mu(p) + \sqrt{\frac{2}{3}}u_\downarrow(p)\varepsilon_0^\mu(p). \quad (\text{A.43})$$

Another widely used representation u^μ can be obtained from the above expressions by introducing a (transposed) four-component spinor for spin-three-half states,

$$\chi_S^T = (\delta_{S,3/2}, \delta_{S,1/2}, \delta_{S,-1/2}, \delta_{S,-3/2})$$

and explicit summation over s_1 and s_2 in Eq. (A.41). This yields

$$u_S^\mu(p) = L^\mu_\nu \begin{pmatrix} \sqrt{E_p + m} \mathbb{R}^\nu \chi_S \\ \sqrt{E_p - m} (\mathbf{n} \cdot \boldsymbol{\sigma}) \mathbb{R}^\nu \chi_S \end{pmatrix}, \quad (\text{A.44})$$

where $\mathbb{R}^0 = 0$, while the remaining $[2] \times [4]$ matrices are given by

$$\mathbb{R}^1 = \begin{pmatrix} -\frac{1}{\sqrt{2}} & 0 & \frac{1}{\sqrt{6}} & 0 \\ 0 & -\frac{1}{\sqrt{6}} & 0 & \frac{1}{\sqrt{2}} \end{pmatrix}, \quad \mathbb{R}^2 = \begin{pmatrix} -\frac{i}{\sqrt{2}} & 0 & -\frac{i}{\sqrt{6}} & 0 \\ 0 & -\frac{i}{\sqrt{6}} & 0 & -\frac{i}{\sqrt{2}} \end{pmatrix}, \quad \mathbb{R}^3 = \begin{pmatrix} 0 & \sqrt{\frac{2}{3}} & 0 & 0 \\ 0 & 0 & \sqrt{\frac{2}{3}} & 0 \end{pmatrix}. \quad (\text{A.45})$$

A.5 Particle states

Throughout this paper, the vector of state is normalized in the following way. For a one-particle state with three-momentum \mathbf{p} and energy $E_p = \sqrt{m^2 + \mathbf{p}^2}$, and other quantum numbers $\{\alpha\}$, like spin, flavor etc.,

$$|h(\mathbf{p}, E_p, \{\alpha\})\rangle \equiv |p\rangle, \quad (\text{A.46})$$

we have

$$\langle p'|p\rangle = 2E_p(2\pi)^3 \delta^{(3)}(\mathbf{p}' - \mathbf{p}) \delta_{\{\alpha'\}\{\alpha\}}, \quad (\text{A.47})$$

where $\delta_{\{\alpha'\}\{\alpha\}}$ is the Kronecker delta. For an n -particle state, we have an obvious generalization,

$$\langle p_1, \dots, p_N | p'_1, \dots, p'_N \rangle = \prod_{k=1}^N 2E_{\mathbf{p}_k}(2\pi)^3 \delta^{(3)}(\mathbf{p}'_k - \mathbf{p}_k) \delta_{\{\alpha'_k\}\{\alpha_k\}}, \quad (\text{A.48})$$

where we assume that there are no identical particles. If they are present, one simply needs to introduce symmetry factors. The completeness condition written symbolically as

$$\sum_n |n\rangle \langle n| = 1, \quad (\text{A.49})$$

is a shorthand notation for

$$\sum_N \sum_{\{\alpha_N\}} \int \prod_{k=1}^N \frac{d^3 \mathbf{p}_k}{2E_{\mathbf{p}_k}(2\pi)^3} |p_1, \dots, p_k\rangle \langle p_1, \dots, p_k| = 1, \quad (\text{A.50})$$

where the element of the phase space can be rewritten in a relativistically-invariant way:

$$\frac{d^3 \mathbf{p}_k}{2E_{\mathbf{p}_k}(2\pi)^3} = \frac{d^4 p_k}{(2\pi)^4} (2\pi) \delta_+(p_k^2 - m_k^2) \equiv \frac{d^4 p_k}{(2\pi)^4} (2\pi) \theta(p_k^0) \delta(p_k^2 - m_k^2), \quad (\text{A.51})$$

with the step function insuring the positivity of the energy flow.

A.6 Color algebra

The commutator algebra of the $SU(N_c)$ color group is

$$[T^a, T^b] = if^{abc}T^c. \quad (\text{A.52})$$

The generators in the fundamental $(T^a)_j^i \Phi^a = (t^a)_j^i \Phi^a$ and adjoint $(T^c)^{ab} \Phi^c = if^{acb} \Phi^c$ representations of the color group act on the quark and gluon fields, respectively. The generators in the fundamental representation t^a are normalized by the condition

$$\text{tr } t^a t^b = T_F \delta^{ab}. \quad (\text{A.53})$$

The color Casimir in the fundamental and adjoint representations are

$$(t^a)_j^i (t^a)_l^j = C_F \delta_l^i, \quad f^{abc} f^{abd} = C_A \delta^{cd}, \quad (\text{A.54})$$

respectively. The numerical values of the constants involved are

$$T_F = \frac{1}{2}, \quad C_F = \frac{N_c^2 - 1}{2N_c}, \quad C_A = N_c. \quad (\text{A.55})$$

B Light-cone vectors and tensors

In discussion of high-energy scattering, it is convenient to introduce a pair of light-cone vectors such that $n^2 = n^{*2} = 0$ and $n \cdot n^* \equiv n^\mu n_\mu^* = 1$. They can be chosen in the following way

$$n^\mu \equiv \frac{1}{\sqrt{2}}(1, 0, 0, -1), \quad n^{*\mu} \equiv \frac{1}{\sqrt{2}}(1, 0, 0, 1). \quad (\text{B.1})$$

Any four-vector z^μ can be decomposed into its light-cone components as

$$z^\mu = z^+ n^{*\mu} + z^- n^\mu + z_\perp^\mu, \quad (\text{B.2})$$

with

$$z^+ \equiv z \cdot n = \frac{1}{\sqrt{2}}(z^0 + z^z), \quad z^- \equiv z \cdot n^* = \frac{1}{\sqrt{2}}(z^0 - z^z). \quad (\text{B.3})$$

Scalar products are written as

$$z \cdot y \equiv z_\mu y^\mu = z^+ y^- + z^- y^+ - \mathbf{z}_\perp \cdot \mathbf{y}_\perp. \quad (\text{B.4})$$

The light-cone derivatives are conventionally defined as follows

$$\partial^+ = \frac{\partial}{\partial z^-}, \quad \partial^- = \frac{\partial}{\partial z^+}, \quad \partial_\perp^\mu = \frac{\partial}{\partial z_\mu^\perp} \quad (\text{B.5})$$

We use Euclidean notations for the transverse two-dimensional space with the metric

$$\delta_{\alpha\beta} = -g_{\alpha\beta}^\perp \equiv -(g_{\alpha\beta} - n_\alpha n_\beta^* - n_\alpha^* n_\beta) = \text{diag}(0, 1, 1, 0),$$

and the transverse projection of the totally antisymmetric tensor $\varepsilon_\perp^{\mu\nu} \equiv \varepsilon^{\mu\nu-+}$, which has the following nonzero components

$$\varepsilon_\perp^{12} = -\varepsilon_\perp^{21} = \varepsilon_{12}^\perp = -\varepsilon_{21}^\perp = 1.$$

Therefore, using the transverse Euclidean metric, we express $v_\perp \cdot u_\perp = -\mathbf{v}_\perp \cdot \mathbf{u}_\perp$ in terms of the two-dimensional vectors, $\mathbf{v} = (v^x, v^y)$. For contraction with transverse Dirac matrices, we use the convention

$$\mathbf{k}_\perp = \gamma_\perp \cdot \mathbf{k}_\perp = -\gamma_\perp \cdot k_\perp. \quad (\text{B.6})$$

Let us note that, due to the boost invariance along the z -axis, one can rescale the light-cone vectors,

$$n^{*\mu} \rightarrow \varrho n^{*\mu}, \quad n^\mu \rightarrow \varrho^{-1} n^\mu,$$

such that their product remains unchanged ($n \cdot n^* = 1$). One may choose the value of ϱ conveniently adjusting it to particular settings. Let us consider a few choices used in practical applications.

B.1 Compton frame

For most cases considered in this review, one can use the vectors defining the kinematics of physical processes to construct the pair of the light-cone vectors n^μ and $n^{*\mu}$. In particular, take the $2 \rightarrow 2$ particle kinematics, $p_1 + q_1 = p_2 + q_2$, of the Compton amplitude. We can choose a reference frame where the average momenta are collinear to the z -axis and are oppositely directed. Then we find

$$\begin{aligned} n_\mu &= \frac{2\xi}{Q^2 \sqrt{1+4(\xi\delta)^2}} q_\mu - \frac{1-\sqrt{1+4(\xi\delta)^2}}{2Q^2\delta^2 \sqrt{1+4(\xi\delta)^2}} p_\mu, \\ n_\mu^* &= -\frac{\xi\delta^2}{\sqrt{1+4(\xi\delta)^2}} q_\mu + \frac{1+\sqrt{1+4(\xi\delta)^2}}{4\sqrt{1+4(\xi\delta)^2}} p_\mu, \end{aligned} \quad (\text{B.7})$$

where we used the momenta

$$p = p_1 + p_2, \quad q = \frac{1}{2}(q_1 + q_2), \quad \Delta = p_1 - p_2 = q_2 - q_1, \quad (\text{B.8})$$

and the kinematical invariants

$$Q^2 = -q^2, \quad \xi = \frac{Q^2}{p \cdot q}, \quad \delta^2 \equiv \frac{M_N^2 - \frac{1}{4}\Delta^2}{Q^2}, \quad (\text{B.9})$$

introduced in Section 5.1.2. Using the reparametrization invariance, we attributed a mass dimension to the vector $n^{*\mu}$ and correspondingly the inverse mass dimension to n^μ .

The light-cone decomposition of momenta for a generic $2 \rightarrow 2$ scattering then can be found as an inverse transformation to Eq. (B.7),

$$\begin{aligned} p_\mu &= 2n_\mu^* + Q^2\delta^2 n_\mu, \\ q_\mu &= -\frac{2\xi}{1+\sqrt{1+4(\xi\delta)^2}} n_\mu^* - \frac{\xi Q^2\delta^2}{1-\sqrt{1+4(\xi\delta)^2}} n_\mu. \end{aligned} \quad (\text{B.10})$$

Expansion for the momentum difference may have slightly different coefficients depending on the way one introduces the skewness variable. It can be either defined as a Lorentz invariant of measurable (external) momenta,

$$\eta = \frac{\Delta \cdot q}{p \cdot q}, \quad (\text{B.11})$$

or through the light-cone coordinates,

$$\tilde{\eta} = \frac{\Delta^+}{p^+}. \quad (\text{B.12})$$

Looking at the explicit expressions of the kinematical variables in terms of light-cone vectors, one would expect a power-suppressed difference between these two definitions. Specifically,

$$\tilde{\eta} = \frac{\eta}{\sqrt{1 + 4(\xi\delta)^2}}. \quad (\text{B.13})$$

The momentum transfer in terms of these two definitions is given by

$$\Delta_\mu = \frac{2\eta}{\sqrt{1 + 4(\xi\delta)^2}} n_\mu^* - \frac{\eta Q^2 \delta^2}{\sqrt{1 + 4(\xi\delta)^2}} n_\mu + \Delta_\mu^\perp, \quad \Delta_\mu = 2\tilde{\eta} n_\mu^* - \tilde{\eta} Q^2 \delta^2 n_\mu + \Delta_\mu^\perp. \quad (\text{B.14})$$

This difference is irrelevant for our presentation since almost everywhere we are dealing with accuracy below the twist-four level, and we can take $\eta \approx \tilde{\eta}$. The magnitude of the transverse momentum component is expressed through the difference between the four-dimensional momentum squared and its minimal accessible value

$$\Delta_\perp^2 \equiv -\Delta_\perp^2 = (1 - \tilde{\eta}^2)(\Delta^2 - \Delta_{\min}^2), \quad \Delta_{\min}^2 = -\frac{4\tilde{\eta}^2 M_N^2}{1 - \tilde{\eta}^2}. \quad (\text{B.15})$$

In many cases, one can neglect the corrections $\mathcal{O}(\delta^2)$ and use approximate expressions for the momenta (B.8) in terms of the light-cone variables,

$$p_\mu \simeq 2n_\mu^*, \quad q_\mu \simeq \frac{Q^2}{2\xi} n_\mu - \xi n_\mu^*, \quad \Delta^\mu \simeq 2\eta n^{*\mu} + \Delta_\perp^\mu. \quad (\text{B.16})$$

There are similar forms for the incoming and outgoing momenta

$$q_{1\mu} \simeq \frac{Q^2}{2\xi} n_\mu - (\xi + \eta) n_\mu^* - \frac{1}{2} \Delta_\mu^\perp, \quad q_{2\mu} \simeq \frac{Q^2}{2\xi} n_\mu - (\xi - \eta) n_\mu^* + \frac{1}{2} \Delta_\mu^\perp, \quad (\text{B.17})$$

$$p_{1\mu} \simeq (1 + \eta) n_\mu^* + \frac{1}{2} \Delta_\mu^\perp, \quad p_{2\mu} \simeq (1 - \eta) n_\mu^* - \frac{1}{2} \Delta_\mu^\perp. \quad (\text{B.18})$$

As one can see, we have chosen the “transverse” Breit-frame assignment for transverse components of the proton momenta, i.e., $p_{1\perp}^\mu = -p_{2\perp}^\mu = \frac{1}{2} \Delta_\perp^\mu$. In certain cases, we will lift this condition, in particular, in Sections 3.10.3 and 5.3.6. Analogous relations apply to photons’ momenta. This approximation will be used throughout our analysis. Analogously, for the light-cone vectors one takes

$$n_\mu \simeq \frac{\xi}{Q^2} (2q_\mu + \xi p_\mu), \quad n_\mu^* \simeq \frac{1}{2} p_\mu. \quad (\text{B.19})$$

B.2 Breit frame

Let us introduce the “longitudinal” Breit frame for the $2 \rightarrow 2$ hard elastic scattering, which is useful in discussing the factorization theorems for exclusive meson production [358] addressed in Section 6.3.4. This is a frame where the incoming virtual photon has zero energy and moves along the z -axis. The initial-state proton moves head-on into this “brick-wall” photon, i.e., counter-along the z -axis, while the final-state hadron recoils backwards and goes in the same direction as the virtual photon. The current fragmentation system—the final state photon or meson—moves

in the same direction as the recoiled hadron. Neglecting the mass parameters and small transverse components, the relevant vectors can be written in terms of dimensionless light-like vectors (B.1)

$$q_1^\mu = \frac{\mathcal{Q}}{\sqrt{2}} n^{*\mu} - \frac{\mathcal{Q}}{\sqrt{2}} n^\mu, \quad (\text{B.20})$$

$$q_2^\mu = \frac{\mathcal{Q}}{\sqrt{2}} \frac{\xi - \eta}{\xi + \eta} n^{*\mu} - \frac{\mathcal{Q}}{\sqrt{2}} n^\mu, \quad (\text{B.21})$$

$$p_1^\mu = -\frac{\mathcal{Q}}{\sqrt{2}} \frac{1 + \eta}{\xi + \eta} n^{*\mu}, \quad (\text{B.22})$$

$$p_2^\mu = -\frac{\mathcal{Q}}{\sqrt{2}} \frac{1 - \eta}{\xi + \eta} n^{*\mu}, \quad (\text{B.23})$$

with $\mathcal{Q}^2 = -q_1^2$.

B.3 Drell-Yan frame

There is yet another useful frame for discussion of the deeply inelastic scattering of a virtual photon with momentum q on a on-shell quark l with production of a quark jet $p_J = q + l$ in the final state, see Fig. 7. It was used in Section 2.2.6. The frame is determined by transforming into the “center-of-mass” frame of the incoming quark l and the outgoing quark jet p_J and is dubbed the Drell-Yan frame [452, 453]. Namely, the four-momentum of the current jet p_J is light-like, $p_J^2 = 0$, and can be conveniently chosen as one of the light-like vectors, with the other one fixed by the hadron momentum $p_\mu = n_\mu^*$. Thus, we define a normalized null-vector \tilde{n}_μ tangent to n^μ ,

$$\tilde{n}_\mu \equiv \frac{p_{J\mu}}{p_J \cdot n^*}. \quad (\text{B.24})$$

Obviously, $\tilde{n}^2 = n^{*2} = 0$ and $n \cdot \tilde{n} = 1$. The Sudakov decomposition of all Lorentz vectors is straightforward

$$v_\mu = \tilde{n}_\mu v_- + n_\mu^* v_+ + v_\mu^\perp. \quad (\text{B.25})$$

We keep the same ‘+’-index notation for contractions with the vector \tilde{n} : $v^+ \equiv \tilde{n} \cdot v$. In the Bjorken limit, $q^- \rightarrow \infty$, the difference between p_J^- and q^- is negligible and, therefore, the Compton frame from Appendix B.1 and the present Drell-Yan frame [452, 453] coincide.

C Optical theorem

The optical theorem asserts that

$$\int d^4 z e^{iq \cdot z} \langle \Omega | [j_\mu^\dagger(z), j^\mu(0)]_- | \Omega \rangle = 2 \Im i \int d^4 x e^{iq \cdot z} \langle \Omega | T \{ j_\mu^\dagger(z) j^\mu(0) \} | \Omega \rangle, \quad (\text{C.1})$$

where $|\Omega\rangle$ stands for the vacuum state or any hadronic state. Let us derive the theorem for the polarization operator, i.e., when $|\Omega\rangle \rightarrow |0\rangle$ and the virtuality q^2 is timelike.

It is easy to derive that

$$\begin{aligned} \int d^4 z e^{iq \cdot z} \langle 0 | [j_\mu^\dagger(z), j^\mu(0)]_- | 0 \rangle &= \sum_n \langle 0 | j_\mu^\dagger(0) | n \rangle \langle n | j^\mu(0) | 0 \rangle (2\pi)^4 \delta^{(4)} \left(\sum_i^n p_i - q \right) \\ &\equiv -\varrho(q^2). \end{aligned} \quad (\text{C.2})$$

To this end, one should use the completeness property of the intermediate states (A.49), translation symmetry

$$j_\mu(z) = e^{iz \cdot \mathbb{P}} j_\mu(0) e^{-iz \cdot \mathbb{P}}, \quad (\text{C.3})$$

with

$$\exp(iz \cdot \mathbb{P}) |n\rangle = \exp\left(i \sum_i^n p_i \cdot z\right) |n\rangle, \quad (\text{C.4})$$

and the energy-momentum conservation $q = \sum_i^n p_i$. The latter is required, in particular, to show that the second term in the commutator does not contribute to the final result.

The function $\varrho(q^2)$ is a spectral density. Let us demonstrate this. Due to the current conservation, $\partial_\mu j^\mu = 0$, we have

$$\sum_i^n p_{i\mu} \langle n | j^\mu(0) | 0 \rangle = 0, \quad (\text{C.5})$$

with the timelike vector $(\sum_i^n p_i)^2 > 0$. Hence, to satisfy Eq. (C.5), the vector $\langle n | j_\mu(0) | 0 \rangle$ has to be space-like. Therefore, one gets

$$\langle n | j_\mu(0) | 0 \rangle^\dagger \langle n | j^\mu(0) | 0 \rangle < 0 \quad \implies \quad \varrho(q^2) > 0, \quad (\text{C.6})$$

which means that $\varrho(q^2)$ is positive definite.

Using Eq. (C.3), one can reduce the chronological product of currents in the integrand of the Fourier transform on the right-hand side of Eq. (C.1) to obtain

$$\begin{aligned} \langle 0 | T \{ j_\mu^\dagger(z) j^\mu(0) \} | 0 \rangle &= \sum_n \langle 0 | j_\mu^\dagger(0) | n \rangle \langle n | j^\mu(0) | 0 \rangle \\ &\times \left\{ \exp\left(-i \sum_i^n p_i \cdot z\right) \theta(z^0) + \exp\left(i \sum_i^n p_i \cdot z\right) \theta(-z^0) \right\}. \end{aligned} \quad (\text{C.7})$$

Inserting the unity

$$1 = \int d^4 q \delta^{(4)} \left(\sum_i^n p_i - q \right) \quad (\text{C.8})$$

into the sum, one can express this equation in terms of the spectral density $\varrho(q^2)$ of Eq. (C.2). Namely,

$$\begin{aligned} \langle 0 | T \{ j_\mu^\dagger(z) j^\mu(0) \} | 0 \rangle &= - \int \frac{d^4 q}{(2\pi)^4} \varrho(q^2) \{ e^{-iq \cdot z} \theta(z^0) + e^{iq \cdot z} \theta(-z^0) \} \\ &= - \frac{1}{2\pi} \int_0^\infty dE \int \frac{d^3 q}{(2\pi)^3} \varrho(q^2) e^{-i|z^0|E + i\mathbf{q} \cdot \mathbf{z}}. \end{aligned}$$

The final two steps involve the introduction of the spectral mass parameter M^2 via incorporating the unity

$$\int_0^\infty dM^2 \delta(M^2 - q^2) = 1 \quad (\text{C.9})$$

into the integrand of Eq. (C.9), and the use of the following contour integral representation

$$\frac{e^{-i|z^0|E}}{2E} = \frac{1}{2\pi} \int_{-\infty}^\infty \frac{dq_0}{(q^0)^2 - E^2 + i0} e^{-iz^0 q^0}. \quad (\text{C.10})$$

Integrating the result over E and combining q^0 and \mathbf{q} into one four-vector $q^\mu = (q^0, \mathbf{q})$, we get

$$i\langle 0 | T \{ j_\mu^\dagger(z) j^\mu(0) \} | 0 \rangle = \frac{1}{2\pi} \int \frac{d^4 q}{(2\pi)^4} e^{-iq \cdot z} \int_0^\infty dM^2 \frac{\varrho(M^2)}{q^2 - M^2 + i0}. \quad (\text{C.11})$$

After the inverse Fourier transformation, rewriting the spectral density according to its definition (C.2), and taking the imaginary part of both sides of Eq. (C.11), one obtains the optical theorem (C.1).

D Light-cone quantization of QCD

Consider the action of quantum chromodynamics,

$$S_{\text{QCD}} = \int d^4 z \mathcal{L}_{\text{QCD}}(z), \quad (\text{D.1})$$

with the Lagrangian (2.1). We will discuss it in the light-cone gauge; therefore, it is convenient to cast the Lagrangian in terms of the light-cone components of the elementary fields. Introducing the projectors for fermions $\Pi^\pm = \frac{1}{2}\gamma^\mp\gamma^\pm$, we can decompose the quark field into “good” and “bad” components via

$$\psi = \Pi^+ \psi + \Pi^- \psi \equiv \psi_+ + \psi_-.$$

The gauge potential can also be written in the light-cone coordinates as

$$A^\mu = (A^+, A^-, \mathbf{A}_\perp^i), \quad A^\pm \equiv \frac{1}{\sqrt{2}}(A^0 \pm A^3), \quad (\text{D.2})$$

where $\mathbf{A}_\perp^i = (A^x, A^y)$ is the transverse gauge field. The advantages of this parametrization becomes transparent and well suited for the light-cone gauge $A^+ = 0$. Note that the light-cone gauge can be implemented directly in the Lagrangian, without introducing a gauge-fixing term as one does for implementation of covariant gauges. Making use of the light-cone coordinates introduced in Appendix B, we immediately find that the QCD Lagrangian lacks terms with the light-cone time derivatives ∂^- acting on the bad field components ψ_- and A^- . This implies that the latter do not evolve with time and therefore they are not dynamical. Hence they can be integrated out in the functional integral without the loss of any dynamical information. This integration out can be implemented with a simple change of variables,

$$S_a = \partial^+ A_a^- - \frac{1}{\partial^+} \mathcal{D}_{\perp ab}^i \partial^+ \mathbf{A}_{\perp b}^i - g \frac{1}{\partial^+} \bar{\psi}_+ \gamma^+ t^a \psi_+, \quad \chi = \psi_- - \frac{1}{2\partial^+} \gamma^+ \boldsymbol{\gamma}_\perp^i \mathcal{D}_{\perp}^i \psi_+, \quad (\text{D.3})$$

where $\mathcal{D}_\perp^i = -\partial/\partial \mathbf{x}_\perp^i - ig \mathbf{A}_\perp^{ia} t^a$ and $\mathcal{D}_{\perp ab}^i = -\delta_{ab} \partial/\partial \mathbf{x}_\perp^i + g f_{acb} \mathbf{A}_\perp^{ic}$ are the fundamental and adjoint transverse covariant derivatives, respectively. This yields a two-component structure of the QCD Lagrangian

$$\mathcal{L}_{\text{QCD}} = \mathcal{L}_{\text{LC}} + \Delta \mathcal{L}, \quad (\text{D.4})$$

where

$$\begin{aligned} \mathcal{L}_{\text{LC}} = & i\bar{\psi}_+ \gamma^+ \partial^- \psi_+ - \frac{i}{2} \bar{\psi}_+ \boldsymbol{\gamma}_\perp^i \gamma^+ \boldsymbol{\gamma}_\perp^j \mathcal{D}_\perp^i \frac{1}{\partial^+} \mathcal{D}_\perp^j \psi_+ \\ & + (\partial^+ \mathbf{A}_{\perp a}^i) (\partial^- \mathbf{A}_{\perp a}^i) - \frac{1}{4} \mathbf{F}_{\perp ab}^i \mathbf{F}_{\perp ab}^i - \frac{1}{2} \left(\frac{1}{\partial^+} \mathcal{D}_{\perp ab}^i \partial^+ \mathbf{A}_{\perp b}^i + g \frac{1}{\partial^+} \bar{\psi}_+ \gamma^+ t^a \psi_+ \right)^2, \end{aligned} \quad (\text{D.5})$$

and

$$\Delta\mathcal{L} = \frac{1}{2}(S_a)^2 + i\bar{\chi}\gamma^-\partial^+\chi. \quad (\text{D.6})$$

The latter non-dynamical part of the Lagrangian, i.e., $\Delta\mathcal{L}$, does not depend on the light-cone time z^+ and can be completely absorbed into the normalization of the functional integral measure. Equivalently, this boils down to using the equations of motion for S_a and χ and thus setting both fields to zero,

$$S_a = 0, \quad \chi = 0. \quad (\text{D.7})$$

Thus, at the expense of the manifest Lorentz invariance, the QCD Lagrangian can be written in terms of the physical degrees of freedom only. At zero coupling, the “good” fields can be identified as QCD partons. As we discussed in Section 2.2.7, at zero light-cone time $z^+ = 0$ the quarks and gluons are free and one can decompose their fields in terms of creation and annihilation operators as [57]

$$\begin{aligned} \psi_+(z^-, \mathbf{z}_\perp, z^+ = 0) &= \sum_{\lambda=\uparrow\downarrow} \int \frac{dk^+ d^2\mathbf{k}_\perp}{2k^+(2\pi)^3} \\ &\times \left\{ b_\lambda(k^+, \mathbf{k}_\perp) u_{+\lambda}(k) e^{-i(k^+ z^- - \mathbf{k}_\perp \cdot \mathbf{z}_\perp)} + d_\lambda^\dagger(k^+, \mathbf{k}_\perp) u_{+\lambda}(-k) e^{i(k^+ z^- - \mathbf{k}_\perp \cdot \mathbf{z}_\perp)} \right\}, \end{aligned} \quad (\text{D.8})$$

$$\begin{aligned} \mathbf{A}_\perp(z^-, \mathbf{z}_\perp, z^+ = 0) &= \sum_{\lambda=\uparrow\downarrow} \int \frac{dk^+ d^2\mathbf{k}_\perp}{2k^+(2\pi)^3} \\ &\times \left\{ a_\lambda(k^+, \mathbf{k}_\perp) \boldsymbol{\varepsilon}_\perp^\lambda e^{-i(k^+ z^- - \mathbf{k}_\perp \cdot \mathbf{z}_\perp)} + a_\lambda^\dagger(k^+, \mathbf{k}_\perp) \boldsymbol{\varepsilon}_\perp^{\lambda*} e^{i(k^+ z^- - \mathbf{k}_\perp \cdot \mathbf{z}_\perp)} \right\}. \end{aligned} \quad (\text{D.9})$$

The bispinor u_+ is a “good” light-cone projection $u_+ = \Pi^+ u$ of the light-cone bispinor (A.33). It possesses a definite light-cone helicity [62], because it does not depend on the transverse momentum \mathbf{k}_\perp . While the two-dimensional gluon polarization vectors are

$$\boldsymbol{\varepsilon}_\perp^\uparrow = -\frac{1}{\sqrt{2}} \begin{pmatrix} 1 \\ i \end{pmatrix}, \quad \boldsymbol{\varepsilon}_\perp^\downarrow = -\frac{1}{\sqrt{2}} \begin{pmatrix} -1 \\ i \end{pmatrix}, \quad (\text{D.10})$$

for helicity up and down states, cf. Eq. (A.37). The (anti-) commutation relations between the creation and annihilation operators look as follows,

$$\{b_\lambda(k^+, \mathbf{k}_\perp), b_{\lambda'}^\dagger(k'^+, \mathbf{k}'_\perp)\} = 2k^+(2\pi)^3 \delta(k^+ - k'^+) \delta^{(2)}(\mathbf{k}_\perp - \mathbf{k}'_\perp) \delta_{\lambda\lambda'}, \quad (\text{D.11})$$

$$[a_\lambda(k^+, \mathbf{k}_\perp), a_{\lambda'}^\dagger(k'^+, \mathbf{k}'_\perp)] = 2k^+(2\pi)^3 \delta(k^+ - k'^+) \delta^{(2)}(\mathbf{k}_\perp - \mathbf{k}'_\perp) \delta_{\lambda\lambda'}. \quad (\text{D.12})$$

A drawback of the light-cone formalism is the loss of the Lorentz covariance, since the non-dynamical degrees of freedom are integrated out in the functional integral. If one keeps these degrees of freedom in the Lagrangian, then the Feynman rules for the gluon propagator change, while the rest remains the same as in covariant gauges. Notice that the light-cone gauge does not fix the gauge entirely, it allows for z^- -independent transformations $U(z^+, \mathbf{z})$, since $A^+(z) \rightarrow A^+(z) + U^\dagger(z^+, \mathbf{z}) \partial^+ U(z^+, \mathbf{z}) = 0$. The residual gauge freedom can be fixed by imposing a boundary condition on the gauge potential or other means, as described below.

Since only the physical degrees of freedom propagate in the light-cone gauge, the relation between the gauge potential and the field strength is linear,

$$\partial^+ A_\mu^\perp = F_\mu^{+\perp},$$

and can be easily inverted,

$$A_\mu^\perp(z^-, z^+, \mathbf{z}) = \int_{-\infty}^{\infty} dz'^- w(z'^- - z^-) F_{\mu}^{+\perp}(z'^-, z^+, \mathbf{z}). \quad (\text{D.13})$$

The weight w depends on the boundary condition imposed on the potential. It takes the following form

$$w(z^-) = \begin{cases} -\theta(z^-), & \mathbf{A}_\perp(z^- = \infty) = 0 \\ \theta(-z^-), & \mathbf{A}_\perp(z^- = -\infty) = 0 \\ -\frac{1}{2}\text{sgn}(z^-), & \mathbf{A}_\perp(z^- = \infty) + \mathbf{A}_\perp(z^- = -\infty) = 0 \end{cases}. \quad (\text{D.14})$$

Within perturbation theory, the incomplete gauge fixing elucidated above reveals itself in a spurious $1/k^+$ -singularity in the gluon Green function. The boundary conditions, in turn, translate into a regularization of this pole. This can be seen from the following representation of the gauge potential in terms of the field strength,

$$A_\mu^\perp(z^-, z^+, \mathbf{z}) = i \int_{-\infty}^{\infty} \frac{d\tau}{[\tau]_{\text{reg}}} e^{-i\tau z^-} \int_{-\infty}^{\infty} \frac{dz'^-}{2\pi} e^{i\tau z'^-} F_{\mu}^{+\perp}(z'^-, z^+, \mathbf{z}). \quad (\text{D.15})$$

The correspondence of the prescriptions with the boundary conditions is straightforward

$$\frac{1}{[\tau]_{\text{reg}}} = \begin{cases} \frac{1}{\tau - i0}, & \mathbf{A}_\perp(z^- = \infty) = 0 \\ \frac{1}{\tau + i0}, & \mathbf{A}_\perp(z^- = -\infty) = 0 \\ \frac{1}{2}\text{PV}\frac{1}{\tau}, & \mathbf{A}_\perp(z^- = \infty) + \mathbf{A}_\perp(z^- = -\infty) = 0 \end{cases}. \quad (\text{D.16})$$

This issue will be further discussed in Appendix G where we demonstrate some computational techniques which incorporate the light-cone gauge.

E Improved Belinfanté energy-momentum tensor

One can construct a symmetric energy-momentum tensor directly from the Lagrangian without going through the procedure of adding ad hoc extra terms to the original non-symmetric energy-momentum tensor [454]. To this end, let us promote the Minkowskian space QCD action to that in a curved background with the metric $g^{\mu\nu}(x)$,

$$S_{\text{QCD}} = \int d^4z \sqrt{-\det[g_{\mu\nu}(z)]} \mathcal{L}_{\text{QCD}}(z), \quad (\text{E.1})$$

where we introduced the inverse metric $g_{\mu\nu} = [g^{\mu\nu}]^{-1}$ satisfying $g^{\mu\rho}(z)g_{\rho\nu}(z) = \delta_\nu^\mu = \text{diag}(1, 1, 1, 1)$. The contraction of Lorentz indices in the QCD Lagrangian is accomplished with the help of the metric tensor, i.e.,

$$\mathcal{L}_{\text{QCD}}(z) = \frac{i}{2} \left[\bar{\psi}(z) \vec{\mathcal{D}}_{\{\mu} \gamma_{\nu\}} \psi(z) \right] g^{\mu\nu}(z) - \frac{1}{4} F_{\mu\nu}^a(z) F_{\rho\sigma}^a(z) g^{\mu\rho}(z) g^{\nu\sigma}(z), \quad (\text{E.2})$$

where the indices in the quark term are symmetrized $t_{\{\mu\nu\}} \equiv \frac{1}{2}(t_{\mu\nu} + t_{\nu\mu})$.

Under a general coordinate transformation $z^\mu \rightarrow z'^\mu$, the metric in two different coordinate systems transforms as a second-rank tensor

$$g'^{\mu\nu}(z') = g^{\rho\sigma}(z) \frac{\partial z'^\mu}{\partial z^\rho} \frac{\partial z'^\nu}{\partial z^\sigma}.$$

For an infinitesimal transformation $z' = z + \zeta(z)$, the change of the metric in different reference frames, but at the same space-time point z is

$$\delta g^{\mu\nu}(z) \equiv g'^{\mu\nu}(z) - g^{\mu\nu}(z) = g^{\mu\rho}(z)\partial_\rho\zeta^\nu(z) + g^{\nu\rho}(z)\partial_\rho\zeta^\mu(z) - \zeta^\rho(z)\partial_\rho g^{\mu\nu}(z). \quad (\text{E.3})$$

Neglecting the field variations $\delta\Phi$ due to the above general coordinate transformation, since they generate field equations of motion, we write the variation of the action as

$$\delta S_{\text{QCD}} = \frac{1}{2} \int d^4z \sqrt{-\det[g_{\rho\sigma}(z)]} \Theta_{\mu\nu}(z) \delta g^{\mu\nu}(z) + \sum_{\Phi} \Omega_{\Phi}, \quad (\text{E.4})$$

where we introduced the quantity

$$\frac{1}{2} \sqrt{-\det[g_{\rho\sigma}]} \Theta_{\mu\nu} = \frac{\partial}{\partial g^{\mu\nu}} \sqrt{-\det[g_{\rho\sigma}]} \mathcal{L}_{\text{QCD}} - \partial_\rho \frac{\partial}{\partial(\partial_\rho g^{\mu\nu})} \sqrt{-\det[g_{\rho\sigma}]} \mathcal{L}_{\text{QCD}}, \quad (\text{E.5})$$

after integrating by parts once in the second term and dropping the surface terms, $\delta g^{\mu\nu}(\text{surface}) = 0$.

The graviton is a spin-two particle, so it is a rank-two symmetric and traceless tensor $h^{\mu\nu}$, which arises as a first term in the expansion of the metric $g^{\mu\nu}$ around the flat Minkowskian space $\eta^{\mu\nu} = \text{diag}(1, -1, -1, -1)$, $g^{\mu\nu} = \eta^{\mu\nu} + h^{\mu\nu}$. Hence, the energy-momentum tensor $\Theta_{\mu\nu}$ coupled to it must be symmetric and traceless. It is called the Belinfanté energy momentum tensor. Note, that on the right-hand side of Eq. (E.5), one assumes that when differentiating with respect to a component of $g^{\mu\nu}$, one does not use the symmetry of the metric tensor in the differentiated function. For instance, while $g^{\mu\nu}$ is differentiated, the transposed tensor $g^{\nu\mu}$ is not. Using Eq. (E.3) in Eq. (E.4), it is easy to see that the energy-momentum tensor is covariantly conserved in the curved background, which translates into the usual conservation in the flat space, $\partial^\mu \Theta_{\mu\nu} = 0$.

To find the explicit form of the Belinfanté energy-momentum tensor for a given Lagrangian, one needs the variation of the determinant of the curved metric, which is easily to compute making use of its expansion in terms of minors M , and an analogous representation for the elements of the inverse metric, i.e.,

$$\det[g_{\mu\nu}] = \sum_{\nu=0}^{\mu} (-1)^{\mu+\nu} M_{\mu\nu} g_{\mu\nu}, \quad [g_{\mu\nu}]^{-1} = \frac{(-1)^{\mu+\nu} M_{\nu\mu}}{\det[g_{\mu\nu}]}.$$

Due to the fact that the metric is symmetric, one can interchange the indices of the minor in the last equality. Then

$$d \det[g_{\mu\nu}] = \sum_{\nu=0}^{\mu} (-1)^{\mu+\nu} M_{\mu\nu} dg_{\mu\nu} = \det[g_{\mu\nu}] g^{\mu\nu} dg_{\mu\nu} = -\det[g_{\mu\nu}] g_{\mu\nu} dg^{\mu\nu},$$

where, at the final step, we used the property $g_{\mu\nu} dg^{\mu\nu} = -g^{\mu\nu} dg_{\mu\nu}$ as a consequence of $g^{\mu\nu} g_{\mu\nu} = 4$. Since the QCD Lagrangian does not depend on the derivatives of the metric, only the first term

in Eq. (E.5) gives a non-vanishing contribution to the symmetric energy-momentum tensor. A calculation yields

$$\Theta^{\mu\nu} = -g^{\mu\nu}\mathcal{L}_{\text{QCD}} - F_a^{\mu\rho}F_{a\rho}^\nu + \frac{i}{4}\bar{\psi}\left\{\vec{\mathcal{D}}^\mu\gamma^\nu + \vec{\mathcal{D}}^\nu\gamma^\mu\right\}\psi, \quad (\text{E.6})$$

where we set the metric to the flat Minkowskian one.

Note, that although this technique produces a symmetric and also traceless (for spin one and spin one-half fields) tensor, in contrast to the Nöther procedure, it does not, however, generate automatically a traceless energy-momentum tensor if scalar fields are present in the Lagrangian, e.g.,

$$\mathcal{L}^{\text{sc}} = \frac{1}{2}(\partial^\mu\phi)(\partial_\mu\phi).$$

To cure the problem one should add a superpotential $X^{\mu\nu\rho\sigma}$, which results in the improved symmetric energy-momentum tensor for scalars [455, 456]

$$\Theta_{\text{sc}}^{\mu\nu} = \frac{1}{2}(\partial^\mu\phi)(\partial^\nu\phi) + \frac{1}{2}\partial_\rho\partial_\sigma X^{\mu\nu\rho\sigma} = \frac{1}{2}(\partial^\mu\phi)(\partial^\nu\phi) - \frac{1}{6}(\partial^\mu\partial^\nu - g^{\mu\nu}\square)\phi^2$$

with

$$X^{\mu\nu\rho\sigma} = g^{\mu\nu}X^{\rho\sigma} + g^{\rho\sigma}X^{\mu\nu} - g^{\mu\rho}X^{\nu\sigma} - g^{\nu\rho}X^{\mu\sigma} - \frac{1}{3}(g^{\mu\nu}g^{\rho\sigma} - g^{\mu\rho}g^{\nu\sigma})X^{\alpha\beta}g_{\alpha\beta},$$

expressed in terms of the symmetric tensor

$$X^{\mu\nu} = \frac{1}{2}g^{\mu\nu}\phi^2.$$

F Basics of the Skyrme model

In the multicolor limit, QCD becomes equivalent to a theory of mesons [457]. In the formal limit $N_c \rightarrow \infty$, this ‘‘artificial’’ world is populated with stable and noninteracting mesons. For large but finite values of the numbers of colors N_c , the mesons acquire nonvanishing width and two-particle cross sections of order N_c^{-1} and N_c^{-2} , respectively, they start to interact via the exchange of single mesons rather than quarks and gluons. The low-energy limit of the meson theory is given then by the chiral Lagrangian, which is a non-linear sigma model of the spontaneously broken chiral symmetry. Restricting to the two-flavor case, this effective theory is a theory of the pions as Goldstone bosons. The baryons appear in it as topologically stable solitons [458, 459], i.e., time-independent solutions to the classical equations of motion with conserved energy. They have masses that diverge as the inverse coupling constant $m \sim N_c = 1/(N_c^{-1})$. The solitons have the quantum numbers of the QCD baryons provided one takes into account the Wess-Zumino term [459].

The simplest chiral Lagrangian,

$$\mathcal{L} = \frac{f_\pi^2}{8}\text{tr}\left[(\partial_\mu\Sigma)(\partial^\mu\Sigma^\dagger)\right], \quad (\text{F.1})$$

which we discussed in Section 3.12, with the $SU(2)$ matrix Σ of mesons, leads to unstable solitons. This drawback can be cured by adding a four derivative ‘‘Skyrme’’ term

$$\Delta\mathcal{L} = \frac{\varepsilon_B^2}{32}\text{tr}[(\partial_\mu\Sigma)\Sigma^\dagger, (\partial_\nu\Sigma)\Sigma^\dagger][(\partial^\mu\Sigma)\Sigma^\dagger, (\partial^\nu\Sigma)\Sigma^\dagger],$$

where ε_B is a dimensionless parameter that characterizes the size of finite energy configurations. The choice of this addendum is unique since it provides a positive-definite Hamiltonian which is moreover second order in time derivatives. The resulting chiral Lagrangian $\mathcal{L} + \Delta\mathcal{L}$ admits a hedgehog soliton solution $\Sigma_0(\mathbf{r}) = \exp(iF(\mathbf{r})\tau_i\hat{r}_i)$, due to Skyrme, with topologically nontrivial boundary conditions $F(0) = -\pi$ and $F(\infty) = 0$ [460] (for a review, see Ref. [461]). Introducing the time-dependent matrix of collective coordinates

$$R(t) = a_0(t) + i\tau_i a_i(t) \quad \text{with} \quad \sum_{i=0}^3 a_i^2 = 1,$$

and substituting the ansatz $\Sigma(x) = R(t)\Sigma_0(\mathbf{r})R^\dagger(t)$ into the original Lagrangian yields a Lagrangian, which is of the second order in time derivatives of collective coordinates $\mathcal{L} \sim \sum_{i=0}^3 \dot{a}_i^2$. The canonical quantization procedure $\dot{a}_i \sim \pi_i = -i\partial/\partial a_i$ then leads to a Hamiltonian which is a Laplace operator $\nabla^2 = \sum_{i=0}^4 \partial^2/\partial a_i^2$ on a three-sphere. The eigenstates of this Laplacian are traceless symmetric polynomials, in complete analogy with conventional three-dimensional spherical harmonics. For instance, they satisfy $\nabla^2(a_0 + ia_1)^L = -L(L+2)(a_0 + ia_1)^L$, and possess equal eigenvalues $S = I = \frac{1}{2}L$ of the spin and isospin operators,

$$S_k = \frac{i}{2} \left(a_k \frac{\partial}{\partial a_0} - a_0 \frac{\partial}{\partial a_k} - \varepsilon_{klm} a_l \frac{\partial}{\partial a_m} \right), \quad (\text{F.2})$$

$$I_k = \frac{i}{2} \left(a_0 \frac{\partial}{\partial a_k} - a_k \frac{\partial}{\partial a_0} - \varepsilon_{klm} a_l \frac{\partial}{\partial a_m} \right), \quad (\text{F.3})$$

respectively.

Out of all hadronic states, we need for our purposes only the proton and delta isobar spin-up wave functions. Assuming the unit normalization for the Haar measure on the $SU(2)$ group, i.e.,

$$\int dR \equiv \frac{1}{\pi^2} \int d^4 a \delta \left(\sum_i^4 a_i^2 - 1 \right) = 1,$$

one can write the hadron states normalized to unity as⁴⁶ [460]

$$|p_\uparrow\rangle = \sqrt{2}(a_1 + ia_2), \quad |\Delta_\uparrow^+\rangle = 2(a_1 + ia_2)(1 - 3(a_0^2 + a_3^2)). \quad (\text{F.4})$$

They have spin and isospin $S_3 = I_3 = 1/2$. Since only the vector-isovector transitions survive in the large- N_c limit, and are of interest for the discussion in the main body of the paper, we write down the corresponding matrix elements

$$\langle p_\uparrow | \text{tr}(\tau^z R \tau^z R^\dagger) | p_\uparrow \rangle \equiv 2 \int dR (a_1^2 + a_2^2) \text{tr}(\tau^z R \tau^z R^\dagger) = -\frac{2}{3}, \quad (\text{F.5})$$

$$\langle \Delta_\uparrow^+ | \text{tr}(\tau^z R \tau^z R^\dagger) | p_\uparrow \rangle = -\frac{2\sqrt{2}}{3}. \quad (\text{F.6})$$

⁴⁶Notice that our normalization differs by a factor of $\sqrt{2}$ and a minus sign in the Δ^+ wave function compared to Ref. [460]. The first difference is a consequence of the normalization of the Haar measure and the requirement that $\langle H | H \rangle \equiv \int dR \langle H | H \rangle = 1$. Since we are interested in the relative magnitude of pp to $p\Delta^+$ transitions, this difference is totally irrelevant. The minus sign in the delta wave function is introduced so as to get the usual result for the magnetic moments (F.10).

From these relations, we find the result

$$\sqrt{2}\langle p_\uparrow | \text{tr}(\tau^z R \tau^z R^\dagger) | p_\uparrow \rangle = \langle \Delta_\uparrow^+ | \text{tr}(\tau^z R \tau^z R^\dagger) | p_\uparrow \rangle. \quad (\text{F.7})$$

we sought for. These matrix elements correspond to the following quark operator matrix elements

$$\langle B_2 | \text{tr}(\tau^a R \tau^j R^\dagger) | B_1 \rangle = g_0 \langle B_2 | \bar{\psi}_{q'} \tau_{q'q}^a \gamma^j \psi_q | B_1 \rangle,$$

up to an overall matching constant g_0 .

Decomposing the two light-flavor electromagnetic current into the isovector and isosinglet components $j_\mu = \frac{1}{2}(\bar{u}\gamma_\mu u - \bar{d}\gamma_\mu d) + \frac{1}{6}(\bar{u}\gamma_\mu u + \bar{d}\gamma_\mu d)$, one can neglect the singlet component in the matrix element between the proton and the delta-isobar and find

$$\langle \Delta^+ | j^\mu | p \rangle = \frac{1}{2} \langle \Delta^+ | \bar{u}\gamma^\mu u - \bar{d}\gamma^\mu d | p \rangle. \quad (\text{F.8})$$

This when combined with (F.7) gives a relation between the spatial components of the matrix elements of the quark electromagnetic current

$$\sqrt{2} \langle \Delta^+ | \mathbf{j}(0) | p \rangle = \langle p | \mathbf{j}(0) | p \rangle - \langle n | \mathbf{j}(0) | n \rangle. \quad (\text{F.9})$$

Here on the right-hand side, we have used the $SU(2)$ symmetry to relate the proton matrix element of the isovector quark current to the difference of matrix elements of the electromagnetic current between the proton and neutron states, i.e., $\langle p | \bar{u}\gamma_\mu u - \bar{d}\gamma_\mu d | p \rangle = \langle p | j^\mu | p \rangle - \langle n | j^\mu | n \rangle$. When Eq. (F.9) is re-expressed in terms of the magnetic moments (see Eq. (A.28)) we reproduce the well-known relation [460]

$$\mu_{p\Delta} = \frac{1}{\sqrt{2}}(\mu_p - \mu_n). \quad (\text{F.10})$$

G Computation techniques for evolution equations

In this Appendix we present a number of techniques for evaluation of one-loop evolution kernels in momentum and coordinate spaces.

G.1 Feynman rules

To start with, we give a comprehensive summary of Feynman rules for the QCD Lagrangian. The quark and gluon propagators are determined by the chronological product of two elementary fields,

$$\langle 0 | T \{ \psi(z_1) \bar{\psi}(z_2) \} | 0 \rangle = \int \frac{d^4 k}{(2\pi)^4} e^{-ik \cdot (z_1 - z_2)} i\mathcal{S}(k), \quad (\text{G.1})$$

$$\langle 0 | T \{ A_\mu^a(z_1) A_\nu^b(z_2) \} | 0 \rangle = \int \frac{d^4 k}{(2\pi)^4} e^{-ik \cdot (z_1 - z_2)} (-i) \delta^{ab} \mathcal{D}_{\mu\nu}(k), \quad (\text{G.2})$$

where the explicit gauge-dependent form of the momentum-space functions will be established below.

- For every internal quark line we write

$$\begin{array}{c} z_1 \xrightarrow{k} z_2 \\ \longleftarrow \longrightarrow \end{array} = i\mathcal{S}(k). \quad (\text{G.3})$$

- For every internal gluon line we write

$$\begin{array}{c} z_1 \xrightarrow[k]{\mu,a} z_2 \\ \curvearrowright \curvearrowleft \curvearrowright \curvearrowleft \curvearrowright \curvearrowleft \\ \nu,b \end{array} = -i\delta^{ab}\mathcal{D}^{\mu\nu}(k). \quad (\text{G.4})$$

- Quark-gluon vertex is

$$\begin{array}{c} \mu,a \\ \downarrow k_1 \\ \curvearrowright \curvearrowleft \curvearrowright \curvearrowleft \\ \nu,b \quad \rho,c \\ k_2 \quad k_3 \end{array} = \mathcal{V}_\mu^{qgq,a}(k_1, k_2, k_3) = igt^a\gamma_\mu(2\pi)^4\delta^{(4)}(k_1 + k_2 + k_3). \quad (\text{G.5})$$

- Three-gluon vertex is

$$\begin{array}{c} \mu,a \\ \downarrow k_1 \\ \curvearrowright \curvearrowleft \curvearrowright \curvearrowleft \\ \nu,b \quad \rho,c \\ k_2 \quad k_3 \end{array} = \mathcal{V}_{\mu\nu\rho}^{ggg,abc}(k_1, k_1, k_3) = g f^{abc} \{(k_1 - k_2)_\rho g_{\mu\nu} + (k_2 - k_3)_\mu g_{\nu\rho} + (k_3 - k_1)_\nu g_{\rho\mu}\} \times (2\pi)^4 \delta^{(4)}(k_1 + k_2 + k_3). \quad (\text{G.6})$$

- Four-gluon vertex reads

$$\begin{array}{c} \mu,a \quad \sigma,d \\ \curvearrowright \curvearrowleft \curvearrowright \curvearrowleft \\ \nu,b \quad \rho,c \\ k_1 \quad k_2 \quad k_3 \quad k_4 \end{array} = \mathcal{V}_{\mu\nu\rho\sigma}^{gggg,abcd}(k_1, k_1, k_3, k_4) = -ig^2 \{ f^{abe}f^{cde}(g_{\mu\rho}g_{\nu\sigma} - g_{\mu\sigma}g_{\nu\rho}) + f^{ace}f^{bde}(g_{\mu\nu}g_{\rho\sigma} - g_{\mu\sigma}g_{\nu\rho}) + f^{ade}f^{cbe}(g_{\mu\rho}g_{\nu\sigma} - g_{\mu\nu}g_{\rho\sigma}) \} (2\pi)^4 \delta^{(4)}(k_1 + k_2 + k_3 + k_4). \quad (\text{G.7})$$

- The resulting expression, constructed from propagators and vertices should be integrated with respect to the momentum of every internal line, i.e., multiplied by the factor

$$\int \prod_\ell \frac{d^d k_\ell}{(2\pi)^{\ell \cdot d}}. \quad (\text{G.8})$$

We have not specified so far the explicit form of the propagators. It is the following. The quark propagator we have

$$S(k) = \frac{k}{k^2 + i0}, \quad (\text{G.9})$$

The form of gluon propagator depends on the gauge assumed. In the covariant gauge $\partial \cdot A = 0$, it reads

$$\mathcal{D}^{\mu\nu}(k) = \frac{1}{k^2 + i0} \left(g^{\mu\nu} - (1 - \xi) \frac{k^\mu k^\nu}{k^2} \right), \quad (\text{G.10})$$

where ξ is the gauge fixing parameter. The gluon propagator in the light-cone gauge also depends on the fixing of residual gauge degrees of freedom. As we discussed earlier in Appendix D, the incomplete gauge fixing of the $A^+ = 0$ condition exhibits itself in a spurious $1/k^+$ -singularity in the gluon Green function, which has to be regularized as well

$$\mathcal{D}^{\mu\nu}(k) = \frac{d_{\text{reg}}^{\mu\nu}(k)}{k^+ + i0}, \quad d^{\mu\nu}(k) = g^{\mu\nu} - \frac{k^\mu n^\nu + k^\nu n^\mu}{[k^+]_{\text{reg}}}. \quad (\text{G.11})$$

There are several possibilities to fix the gauge completely. They are (we put the k^+ in square brackets to demonstrate that it is regularized via one of the prescriptions):

- Principal value prescription

$$\frac{1}{[k^+]_{\text{PV}}} = \frac{1}{2} \left(\frac{1}{k^+ + i0} + \frac{1}{k^+ - i0} \right). \quad (\text{G.12})$$

It corresponds to the anti-symmetric boundary conditions on the gauge potential $\mathbf{A}(\infty) = -\mathbf{A}(-\infty)$.

- Advanced prescription

$$d_{\text{Adv}}^{\mu\nu}(k) = g^{\mu\nu} - \frac{k^\mu n^\nu}{k^+ + i0} - \frac{k^\nu n^\mu}{k^+ - i0}, \quad (\text{G.13})$$

arises from imposing the condition of vanishing of the gauge potential at the light-cone future $\mathbf{A}(\infty) = 0$.

- Retarded prescription

$$d_{\text{Ret}}^{\mu\nu}(k) = g^{\mu\nu} - \frac{k^\mu n^\nu}{k^+ - i0} - \frac{k^\nu n^\mu}{k^+ + i0}, \quad (\text{G.14})$$

stems from the vanishing of the gauge potential in the past $\mathbf{A}(-\infty) = 0$. The direction of momentum flow k is very essential for the advanced and the retarded prescriptions. We assume in Eq. (G.11) the flow to be from the point z_1 to z_2 .

- Mandelstam-Leibbrandt prescription [463, 464]

$$\frac{1}{[k^+]_{\text{ML}}} = \frac{1}{k^+ + i0 \cdot k^-} = \frac{k^-}{k^+ k^- + i0}. \quad (\text{G.15})$$

This is prescription is not an obvious consequence of any boundary condition on the gauge potential, see though [465]. It is however a consequence of the equal-time (as opposed to the equal light-cone time) quantization [466].

G.2 Momentum integrals

The basic integrals which appear in the course of calculations are listed below.

- Minkowskian momentum integrals used in loop calculations ($d = 4 - 2\varepsilon$)

$$\int \frac{d^d k}{(2\pi)^d} e^{Ak^2 - iz \cdot k} = \frac{i}{(4\pi)^{d/2}} \frac{1}{A^{d/2}} e^{z^2/4A}, \quad (\text{G.16})$$

$$\int \frac{d^d k}{(2\pi)^d} e^{-ik \cdot z} \frac{1}{[-k^2]^m} = \frac{i}{2^{2m} \pi^{d/2}} \frac{\Gamma(d/2 - m)}{\Gamma(m)} \frac{1}{[-z^2]^{d/2-m}}. \quad (\text{G.17})$$

- Light-cone longitudinal integrals

$$\int_{-\infty}^{\infty} dk^+ dk^- e^{i(Ak^+ k^- + p^+ k^- + p^- k^+ + i0)} = \frac{2\pi}{A} e^{-ip^+ p^- / A}. \quad (\text{G.18})$$

- Euclidean transverse momentum integrals ($d = 2 - 2\varepsilon$)

$$\int \frac{d^d \mathbf{p}_\perp}{(2\pi)^d} e^{-i\alpha \mathbf{p}_\perp^2} = \frac{1}{(4\pi)^{d/2}} \frac{1}{(i\alpha)^{d/2}}. \quad (\text{G.19})$$

$$\int \frac{d^d \mathbf{p}_\perp}{(2\pi)^d} \frac{e^{i\mathbf{p}_\perp \cdot \mathbf{z}_\perp}}{\mathbf{p}_\perp^{2m}} = \frac{1}{2^{2m}\pi^{d/2}} \frac{\Gamma(d/2-m)}{\Gamma(m)} \frac{1}{\mathbf{z}_\perp^{d-2m}}. \quad (\text{G.20})$$

- Minkowskian space-time integrals

$$\int d^d z e^{ip \cdot z} \frac{1}{[-z^2]^k} = -i\pi^{d/2} 2^{d-2k} \frac{\Gamma(d/2-k)}{\Gamma(k)} \frac{1}{[-p^2]^{d/2-k}}, \quad (\text{G.21})$$

$$\int d^d z e^{Az^2 + ip \cdot z} = -i\pi^{d/2} \frac{1}{A^{d/2}} e^{p^2/4A}. \quad (\text{G.22})$$

G.3 Renormalization in covariant gauges

First, let us recall some of the basic equations of QCD. The dimensionally regularized and renormalized QCD Lagrangian in the covariant gauge is given by

$$\begin{aligned} \mathcal{L}_{\text{QCD}} &= \mathcal{Z}_2 \bar{\psi} i \not{\partial} \psi + \tilde{\mathcal{Z}}_1 \mu^\varepsilon g \bar{\psi} \not{A}^a t^a \psi \\ &- \frac{\mathcal{Z}_3}{4} (G_{\mu\nu}^a)^2 - \frac{1}{2} \mu^\varepsilon g \mathcal{Z}_1 f^{abc} G^{a,\mu\nu} A_\mu^b A_\nu^c - \frac{\mathcal{Z}_4}{4} \mu^{2\varepsilon} g^2 (f^{abc} A_\mu^b A_\nu^c)^2 - \frac{1}{2\xi} (\partial^\mu A_\mu^a)^2 \\ &+ \tilde{\mathcal{Z}}_3 \partial^\mu \bar{\omega}^a \partial_\mu \omega^a + \mu^\varepsilon g \tilde{\mathcal{Z}}_1 f^{abc} \partial^\mu \bar{\omega}^a A_\mu^b \omega^c, \end{aligned} \quad (\text{G.23})$$

where $d = 4 - 2\varepsilon$ is the space-time dimension and μ is a mass parameter, introduced in order to keep the coupling constant dimensionless. Here, the renormalized quark, gluon and (anti-)ghost fields $\Phi = \{\psi, A^\mu, \bar{\omega}, \omega\}$, respectively, and the renormalized coupling are expressed in terms of bare ones $\Phi_{(0)}$ and $g^{(0)}$ via

$$\Phi_{(0)} = \sqrt{\mathcal{Z}_\Phi} \Phi, \quad g^{(0)} = \mu^\varepsilon \mathcal{Z}_c g, \quad (\text{G.24})$$

with corresponding renormalization constants $\mathcal{Z}_\Phi = \{\mathcal{Z}_2, \mathcal{Z}_3, \tilde{\mathcal{Z}}_3\}$, for the quark, gluon and ghosts, respectively. The symbol $G_{\mu\nu}^a$ as a shorthand notation for the Abelian part of the full QCD field strength tensor $F_{\mu\nu}^a = G_{\mu\nu}^a + \mu^\varepsilon g \mathcal{X} f^{abc} A_\mu^b A_\nu^c$. The canonical dimensions of elementary fields are $d_q^{\text{can}} = 3/2 - \varepsilon$ for fermions, $d_g^{\text{can}} = 1 - \varepsilon$ for gluons, $d_{\bar{\omega}}^{\text{can}} = d - 2$ and $d_\omega^{\text{can}} = 0$ for the anti-ghost and ghost fields, respectively. The Lagrangian (G.23) is invariant under the following renormalized BRST-transformations:

$$\begin{aligned} \delta^{\text{BRST}} \psi &= -i\mu^\varepsilon g \tilde{\mathcal{Z}}_1 \omega^a t^a \psi \delta\lambda, \quad \delta^{\text{BRST}} A_\mu^a = \tilde{\mathcal{Z}}_3 \mathcal{D}_\mu \omega^a \delta\lambda, \\ \delta^{\text{BRST}} \omega^a &= \frac{1}{2} \mu^\varepsilon g \tilde{\mathcal{Z}}_1 f^{abc} \omega^b \omega^c \delta\lambda, \quad \delta^{\text{BRST}} \bar{\omega}^a = \frac{1}{\xi} \partial_\mu A_\mu^a \delta\lambda, \end{aligned} \quad (\text{G.25})$$

where $\delta\lambda$ is a renormalized Grassman variable. The covariant derivative is defined by $\mathcal{D}_\mu = \partial_\mu - i\mu^\varepsilon g \mathcal{X} T^a A_\mu^a$, where T^a is the generator in the fundamental ($T^a \phi_i = t_{ij}^a \phi_j$) or adjoint ($T^b \phi^a = i f^{abc} \phi^c$) representations depending on the object it is acting on. The Ward-Takahashi identities imply the following relations between the renormalization constants $\mathcal{Z}_1 \mathcal{Z}_3^{-3/2} = \mathcal{Z}_4^{1/2} \mathcal{Z}_3^{-1} = \tilde{\mathcal{Z}}_1 \tilde{\mathcal{Z}}_3^{-1} \mathcal{Z}_3^{-1/2} = \bar{\mathcal{Z}}_1 \mathcal{Z}_2^{-1} \mathcal{Z}_3^{-1/2}$. The charge renormalization constant is expressed in terms of the vertex and wave function renormalization constants via $\mathcal{Z}_c = \mathcal{X} \mathcal{Z}_3^{-1/2}$. In the minimal subtraction (MS) scheme, the \mathcal{Z} -factors are defined as Laurent series in ε :

$$\mathcal{Z}[g, \varepsilon] = 1 + \sum_{n=1}^{\infty} \frac{\mathcal{Z}^{[n]}[g]}{\varepsilon^n}.$$

For our consequent discussion, we take the renormalization constants \mathcal{Z}_2 , \mathcal{Z}_3 , $\tilde{\mathcal{Z}}_3$ and $\mathcal{X} \equiv \mathcal{Z}_1 \mathcal{Z}_3^{-1} = \tilde{\mathcal{Z}}_1 \tilde{\mathcal{Z}}_3^{-1} = \bar{\mathcal{Z}}_1 \mathcal{Z}_2^{-1}$ as independent ones.

The QCD Gell-Mann–Low function in d -dimensions is defined by

$$\beta_\varepsilon(g) = \frac{\partial g}{\partial \ln \mu} = -\varepsilon g + \beta(g), \quad (\text{G.26})$$

with $\beta(g)$ being the four-dimensional beta function. The anomalous dimensions of the physical fields and the gauge fixing parameter are

$$\gamma_q(g) = \frac{1}{2} \frac{d}{d \ln \mu} \ln \mathcal{Z}_2, \quad \gamma_g(g) = \frac{1}{2} \frac{d}{d \ln \mu} \ln \mathcal{Z}_3, \quad \sigma = \frac{d}{d \ln \mu} \ln \xi = -2\gamma_g, \quad (\text{G.27})$$

respectively. Their perturbative expansions are determined by the series

$$\frac{\beta(g)}{g} = \sum_{n=0}^{\infty} \left(\frac{\alpha_s}{4\pi} \right)^{n+1} \beta_n, \quad \gamma_a(g) = \sum_{n=0}^{\infty} \left(\frac{\alpha_s}{2\pi} \right)^{n+1} \gamma_{a(n)}. \quad (\text{G.28})$$

The first two terms of the β -function, used in the present review, are

$$\beta_0 = \frac{4}{3} T_F N_f - \frac{11}{3} C_A, \quad (\text{G.29})$$

$$\beta_1 = \frac{10}{3} C_A N_f + 2C_F N_f - \frac{34}{3} C_A^2. \quad (\text{G.30})$$

While the expressions for the one-loop anomalous dimensions of the elementary fields read

$$\gamma_{q(0)} = \frac{\xi}{2} C_F, \quad \gamma_{g(0)} = \frac{2}{3} T_F N_f + \frac{C_A}{4} \left(\xi - \frac{13}{3} \right). \quad (\text{G.31})$$

A full set of renormalization constants and anomalous dimensions in QCD up to four-loop order can be found in Ref. [467].

G.4 Renormalization of composite operators

The subtracted operator⁴⁷ $\mathcal{O}^R[\Phi]$, constructed from the renormalized elementary fields $\Phi = \{\psi, \bar{\psi}, A^\mu\}$, are expressed in terms of the bare ones $\mathcal{O}[\Phi_{(0)}]$ —built from the unrenormalized fields $\Phi_{(0)} = \{\psi_{(0)}, \bar{\psi}_{(0)}, A_{(0)}^\mu\}$ —through the multiplication with a renormalization factor

$$\mathcal{O}^R[\Phi] = \mathcal{Z} \mathcal{O}[\sqrt{\mathcal{Z}_\Phi} \Phi], \quad (\text{G.32})$$

⁴⁷A vector of dimension N , composed from different operators with the same quantum numbers, which mix under renormalization group flow. For instance, in the flavor singlet case it is a two-dimensional object (4.146).

which admits Laurent expansion in the parameter ε of dimensional regularization,

$$\mathcal{Z}[g, \varepsilon] = 1 + \sum_{n=1}^{\infty} \frac{\mathcal{Z}^{[n]}[g]}{\varepsilon^n}. \quad (\text{G.33})$$

In turn, each term of this series $\mathcal{Z}^{[n]}[g]$ has an infinite series expansion in the strong coupling. The operators $\mathcal{O}^R[\Phi]$ generate finite contributions when inserted into Green functions with elementary field operators:

$$\langle \mathcal{O}^R[\Phi] \Phi(z_1) \Phi(z_2) \dots \Phi(z_N) \rangle = \text{finite}. \quad (\text{G.34})$$

The renormalization factors determine the anomalous dimensions of the corresponding operators,

$$\begin{aligned} \gamma &= -\left(\frac{d}{d \ln \mu} \mathcal{Z}\right) \mathcal{Z}^{-1} + \frac{d}{d \ln \mu} \ln \mathcal{Z}_\Phi = g \frac{d}{dg} \left(\mathcal{Z}^{[1]} - \mathcal{Z}_\Phi^{[1]} \right) \\ &= g \frac{d}{dg} \mathcal{Z}^{[1]} + 2\gamma_\Phi, \end{aligned} \quad (\text{G.35})$$

where at the second step we used the fact that only the single pole of the Laurent series determine anomalous dimensions since

$$\frac{d}{d \ln \mu} = -\varepsilon \frac{d}{d \ln g} + \dots$$

All higher order terms in the Laurent expansion are expressed through it. Here, the matrix \mathcal{Z}_Φ is diagonal and its entries are determined by the renormalization constants of elementary fields forming a given bilocal composite operator

$$\mathcal{Z}_\Phi = \begin{pmatrix} \mathcal{Z}_\Phi & 0 & 0 & \dots \\ 0 & \mathcal{Z}_{\Phi'} & 0 & \dots \\ 0 & 0 & \mathcal{Z}_{\Phi''} & \dots \\ \vdots & \vdots & \vdots & \ddots \end{pmatrix} \quad (\text{G.36})$$

In order to calculate the renormalization factor, one computes the amputated⁴⁸ Green function with insertion of the bare composite operator, and uses the renormalized perturbation theory to find the residue of the pole

$$\langle \mathcal{O}[\Phi] \Phi(z_1) \Phi(z_2) \rangle_{\text{amp}} = -\frac{1}{\varepsilon} \mathcal{R} \langle \mathcal{O}[\Phi] \Phi(z_1) \Phi(z_2) \rangle_{\text{amp}}^{\text{tree}} + \dots \quad (\text{G.37})$$

Since the renormalized operator generates divergence-free Green functions (G.34), one immediately finds

$$\mathcal{R} = \mathcal{Z}^{[1]}. \quad (\text{G.38})$$

G.5 Construction of evolution equations in coordinate space

In this appendix, we intend to review different approaches to the construction of the renormalization group equations for non-local light-cone operators. We will discuss two of them: one based on the use of covariant gauges, Ref. [228, 229], and the other one relying on the light-cone gauge

⁴⁸The amputated Green function is defined as a Green function with removed propagators corresponding to the external lines $\langle \mathcal{O}[\Phi'] \Phi(z_1) \dots \Phi(z_L) \rangle_{\text{amp}} = \langle \mathcal{O}[\Phi'] \Phi(z_1) \dots \Phi(z_L) \rangle / \prod_{k=1}^L \langle \Phi' \Phi(z_k) \rangle$.

with different prescriptions on the spurious pole in the gluon density matrix. The machinery will be demonstrated on a simple example of the unrenormalized quark string operator

$$\mathcal{O}^{qq}(z_1^-, z_2^-) = \bar{\psi}_{(0)}(z_1^-)[z_1^-, z_2^-]\gamma^+\psi_{(0)}(z_2^-), \quad (\text{G.39})$$

expressed in terms of the bare fields $\psi_{(0)}$. In the covariant gauge, one needs the following Feynman rules for \mathcal{O}^{qq} to one-loop accuracy,

$$\begin{array}{ccc} \psi & & \psi \\ \otimes \uparrow k_1 & & k_2 \uparrow \otimes \downarrow \\ \end{array} = [\mathcal{O}_2^{qq}(k_1, k_2)] = \gamma^+ e^{-iz_1^- k_1^+ - iz_2^- k_2^+}, \quad (\text{G.40})$$

$$\begin{array}{ccc} \psi & A^+ & \psi \\ \otimes \uparrow k_1 & k_3 \uparrow \otimes \downarrow & k_2 \uparrow \otimes \downarrow \\ \mu, a & & \end{array} = [\mathcal{O}_3^{qq}(k_1, k_2, k_3)]_\mu^a = g t^a n_\mu \gamma^+ e^{-iz_1^- k_1^+ - iz_2^- k_2^+} \frac{e^{-iz_3^- k_3^+} - e^{-iz_2^- k_3^+}}{k_3^+}. \quad (\text{G.41})$$

Here the second contribution (G.41) obviously arises from the expansion of the path-ordered exponential in Eq. (G.39) to the first non-trivial order in the coupling. In the light-cone gauge $A^+ = 0$, only the first one, i.e., Eq. (G.40), contributes. Let us discuss both frameworks in turn.

G.5.1 Covariant gauge formalism

In covariant gauges, we need to evaluate Feynman diagrams shown in Fig. 61. The diagrams (a) and (b) contribute to the renormalization constant \mathcal{R} in Eq. (G.37), while the diagram (c) corresponds to the field renormalization which produces the addendum due to the field anomalous dimension γ_φ defined by Eq. (G.35).

The most efficient method for computation of momentum integrals containing Fourier exponents is to use the so-called α -representation for Feynman propagators,

$$\frac{1}{(k^2 + i0)^n} = \frac{(-i)^n}{\Gamma(n)} \int_0^\infty d\alpha \alpha^{n-1} e^{i\alpha(k^2 + i0)}, \quad (\text{G.42})$$

taken here with an arbitrary power n for generality. Exponentiating all propagators, it is instructive to rescale the integration variables,

$$\alpha_j \equiv x_j \varrho, \quad (\text{G.43})$$

and switch to the integration over ϱ and the Feynman parameters x_j

$$\int_0^\infty \prod_j^N d\alpha_j = \int_0^\infty d\varrho \varrho^{N-1} \int_0^1 \prod_j^N dx_j \delta \left(\sum_{k=1}^N x_k - 1 \right). \quad (\text{G.44})$$

After integration over the loop momentum k , the subsequent integral over the overall scale ϱ results in poles in the parameter ε of dimensional regularization. A typical integral reads

$$\begin{aligned} & \int \frac{d^d k}{(2\pi)^d} \frac{e^{-iz^- k^+}}{k^2 \prod_{i=1}^n (k - q_i)^2} \\ &= \frac{i(-1)^{n+1}}{(4\pi)^{d/2}} \Gamma \left(n + 1 - \frac{d}{2} \right) \int_0^1 \prod_{i=1}^{n+1} dx_i \delta \left(\sum_{i=1}^{n+1} x_i - 1 \right) \frac{e^{-iz^- \sum_{i=1}^n x_i q_i^+}}{\left[-\sum_{i=1}^n x_i q_i^2 + (\sum_{i=1}^n x_i q_i)^2 \right]^{n+1-d/2}}. \end{aligned} \quad (\text{G.45})$$

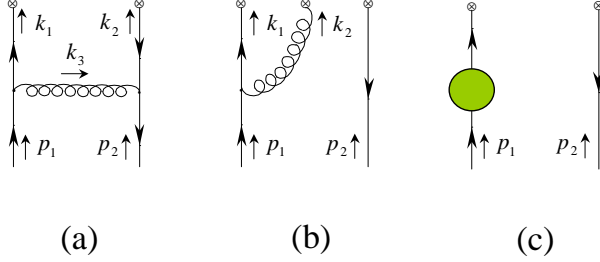


Figure 61: Feynman diagrams contributing to the one-loop quark-quark mixing kernel.

After these general preliminary remarks, we are now in a position to present a step-by-step procedure of calculating the evolution kernel for the above light-ray vector operator (G.39) in the covariant Feynman gauge $\xi = 1$.

- Use Feynman rules from Section G.1 and Eqs. (G.40) and (G.40) to assign momentum intergals for the amputated Green function

$$\mathcal{M} = \langle \mathcal{O}^{qq}(z_1^-, z_2^-) \psi_{(0)}(k_1) \bar{\psi}_{(0)}(k_2) \rangle_{\text{amp}} \equiv \langle \mathcal{O}^{qq}(z_1^-, z_2^-) \psi_{(0)}(k_1) \bar{\psi}_{(0)}(k_2) \rangle / \prod_{j=1}^2 i\mathcal{S}(k_j),$$

coming from each diagram in Fig. 61

- Project out the color and Dirac (or Lorentz) structures of the corresponding vertex

$$\mathcal{M} = \frac{1}{4N_c} \gamma^+ \text{tr}_c \text{tr} \{ \gamma^- \mathcal{M} \}. \quad (\text{G.46})$$

The contributions of the diagrams Fig. 61 (a) and (b) are then given by

$$\begin{aligned} \mathcal{M}_{\text{cov}}^{(a)} &= \frac{1}{4N_c} \gamma^+ \int \prod_{j=1}^3 \frac{d^d k_j}{(2\pi)^4} (-i) \mathcal{D}^{\mu\nu}(k_3) \\ &\quad \times \text{tr}_c \text{tr} \{ \gamma^- \mathcal{V}_\mu^a(k_3, -k_2, p_2) i\mathcal{S}(-k_2) [\mathcal{O}_2^{qq}(k_1, k_2)] i\mathcal{S}(k_1) \mathcal{V}_\nu^a(-k_3, p_1, -k_1) \}, \\ \mathcal{M}_{\text{cov}}^{(b)} &= \frac{1}{4N_c} \gamma^+ \int \prod_{j=1}^2 \frac{d^d k_j}{(2\pi)^4} (-i) \mathcal{D}^{\mu\nu}(k_2) \text{tr}_c \text{tr} \{ \gamma^- [\mathcal{O}_3^{qq}(k_1, k_2, p_2)]_\mu^a i\mathcal{S}(k_1) \mathcal{V}_\nu^a(-k_2, p_1, -k_1) \}. \end{aligned} \quad (\text{G.47})$$

Perform integration over the redundant momenta using the energy-momentum delta functions leaving k_3 and k_2 as the loop momenta in diagrams (a) and (b), respectively.

- Compute traces. Use the fact that one can treat external momenta as light-like $p_i^\mu = p_i^+ n^{*\mu}$. We end up with momentum integrals

$$\begin{aligned} \mathcal{M}_{\text{cov}}^{(a)} &= 2ig^2 C_F \gamma^+ \int \frac{d^d k}{(2\pi)^d} \frac{\mathbf{k}_\perp^2}{k^2(p_1 - k)^2(p_2 + k)^2} e^{-iz_1^-(p_1 - k)^+ - iz_2^-(p_2 + k)^+}, \\ \mathcal{M}_{\text{cov}}^{(b)} &= 2ig^2 C_F \gamma^+ \int \frac{d^d k}{(2\pi)^d} \frac{1}{k^2(p_1 - k)^2} \frac{(p_1 - k)^+}{k^+} \left(e^{-iz_1^- p_1^+ - iz_2^- p_2^+} - e^{-iz_1^-(p_1 - k)^+ - iz_2^-(p_2 + k)^+} \right). \end{aligned} \quad (\text{G.48})$$

- Compute the momentum integrals.

In the $\mathcal{M}^{(a)}$ amplitude, the lack of the d -dimensional covariance of the integrand, due to the presence of the $d - 2$ dimensional transverse momentum \mathbf{k}_\perp , results in a slight complication in the use of the generic integral (G.45). However, with the help of Eqs. (G.18) and (G.19), the integration is easily performed in the light-cone (or Sudakov) coordinates

$$k^\mu = k^+ n^{*\mu} + k^- n^\mu + k_\perp^\mu, \quad (\text{G.49})$$

with the volume element being

$$d^d k = dk^+ dk^- d^{d-2} \mathbf{k}_\perp. \quad (\text{G.50})$$

For the pole part⁴⁹ (PP) of the dimensionally regularized integral, we thus find

$$\text{PP} \mathcal{M}_{\text{cov}}^{(a)} = \frac{1}{\varepsilon} \frac{\alpha_s}{2\pi} C_F \int_0^1 dx_1 dx_2 \theta(1 - x_1 - x_2) e^{-ip_1^+(\bar{x}_1 z_1^- + x_1 z_2^-) - ip_2^+(\bar{x}_2 z_1^- + x_2 z_2^-)}. \quad (\text{G.51})$$

Since we have set the external momenta to be light-like, we have no scale in the integral. However, if introduced, it would simply add an exponential for the integral with respect to the overall scale ϱ , and we can use the substitution

$$\int_0^\infty d\varrho \varrho^{1-d/2} \rightarrow \int_0^\infty d\varrho \varrho^{1-d/2} e^{-im^2 \varrho} = \frac{\Gamma(\varepsilon)}{(im^2)^\varepsilon} \simeq \frac{1}{\varepsilon} + \dots$$

In the $\mathcal{M}^{(b)}$ amplitude, the integral with $1/k^+$ pole can be computed making the trick

$$\frac{1}{k^+} (1 - e^{-iz^- k^+}) = iz^- \int_0^1 d\tau e^{-i\tau z^- k^+}. \quad (\text{G.52})$$

Then, using the generic momentum integral (G.45), and after that integrating over τ , we get

$$\text{PP} \mathcal{M}_{\text{cov}}^{(b)} = \frac{1}{\varepsilon} \frac{\alpha_s}{2\pi} C_F \int_0^1 dx_1 \left[\frac{\bar{x}_1}{x_1} \right]_+ e^{-ip_1^+(\bar{x}_1 z_1^- + x_1 z_2^-) - ip_2^+ z_2^-}, \quad (\text{G.53})$$

with the plus-prescription defined in Eq. (4.29).

- Add the mirror symmetric contribution for the diagram (b) $\mathcal{M}^{(\tilde{b})}$, which is obtained by the interchange $p_1 \leftrightarrow p_2$ in the Eq. (G.53), and notice that, according to Eq. (G.37), the $\mathcal{Z}^{[1]}$ constant is determined to be

$$\text{PP} \left(\mathcal{M}^{(a)} + \mathcal{M}^{(b)} + \mathcal{M}^{(\tilde{b})} \right)_{\text{cov}} = -\frac{1}{\varepsilon} \mathcal{Z}^{[1]} \cdot [\mathcal{O}_2^{qq}(p_1, p_2)], \quad (\text{G.54})$$

with

$$\begin{aligned} \mathcal{Z}_{qq}^{[1]} \cdot [\mathcal{O}_2^{qq}(p_1, p_2)] &\equiv -\frac{\alpha_s}{2\pi} C_F \int_0^1 dx_1 dx_2 \theta(1 - x_1 - x_2) \gamma^+ e^{-ip_1^+(\bar{x}_1 z_1^- + x_1 z_2^-) - ip_2^+(\bar{x}_2 z_1^- + x_2 z_2^-)} \\ &\quad \times \left\{ 1 + \left[\frac{\bar{x}_1}{x_1} \right]_+ \delta(x_2) + \left[\frac{\bar{x}_2}{x_2} \right]_+ \delta(x_1) \right\}. \end{aligned} \quad (\text{G.55})$$

⁴⁹The PP is defined as $\text{PP} \{A\Gamma(\varepsilon)\} = \frac{1}{\varepsilon} A$.

By comparing Eqs. (4.140) and (4.12), we find that the evolution kernel is

$$\mathcal{K} = -\alpha_s \frac{d}{d\alpha_s} \mathcal{Z}^{[1]} - \gamma_\Phi, \quad (\text{G.56})$$

where $\gamma_\Phi = \gamma_q = \frac{\alpha_s C_F}{2\pi} + \dots$ in the Feynman gauge $\xi = 1$ (see Eq. (G.31)). Changing $x_1 = u$ and $x_2 = v$ we get the $\mathcal{K}_{(0)}^{qq,V}$ kernel in Eq. (4.19).

In order to study the singlet evolution involving mixing with gluonic operators, we should consider definite C -parity combinations of quark operators. The summary of the corresponding Feynman rules, with the same conventions as used here, can be found in Appendices A.1 and A.2 of Ref. [253]. The calculation of these evolution kernels goes through without any changes.

Yet another technique to evaluate the momentum integrals was developed in Refs. [228, 229]. According to it, the propagators are combined using the standard Feynman parametrization, and the resulting momentum integrals take the form

$$\int \frac{d^d k}{(2\pi)^d} e^{-ik^+(z_2^- - z_1^-)} \frac{P(p_i, x_i | k)}{[k^2 - L]^n}, \quad (\text{G.57})$$

where $P(p_i, x_i | k)$ is a polynomial function in k , p_i and the Feynman parameters x_i . The divergences can be evaluated by Taylor expanding the exponential factor in the integrand: $e^{-ik^+(z_2^- - z_1^-)} = 1 - ik^+(z_2^- - z_1^-) + \dots$. Since the denominator depends on k^2 only, we can average with respect to possible orientations of k . Due to the light-like character of the vector n , just the first few terms survive after integration (we maximally need to expand up to $(k^+)^3$). To present the result in the conventional form, we have to remove terms proportional to $(z_2^- - z_1^-)^m$. This is achieved through the integration by parts with respect to the Feynman parameters which play now the rôle of positions on the light-cone. A typical integration for a test function $\tau(y, z)$ looks like

$$i(z_2^- - z_1^-) p_1^+ \mathbb{J} \cdot \tau(y, z) = \mathbb{J} \cdot \left\{ \delta(y)\tau(0, z) + \frac{\partial \tau(y, z)}{\partial y} - \delta(1-y-z)\tau(y, \bar{y}) \right\},$$

where we have introduced the following shorthand notation for the integral

$$\mathbb{J} \cdot \tau(u, v) \equiv \int_0^1 dv \int_0^{\bar{v}} du e^{-ip_1^+(\bar{u}z_1^- + uz_2^-) - ip_2^+(\bar{v}z_2^- + vz_1^-)} \tau(u, v). \quad (\text{G.58})$$

Similar equations hold for the p_2^+ contributions. When double and triple integration by parts is required, it turns out that, after the first integration, the dangerous terms proportional to $\delta(1-u-v)$ that might cause a problem vanish identically in all cases.

For diagrams which originate from the expansion of the phase factor (G.41), there appear terms in the integrand which possess the structure

$$E(k, p_1, u) \equiv \frac{1}{(k^+ + up_1^+)} \left[1 - e^{-i(z_2^- - z_1^-)(up_1^+ + k^+)} \right], \quad (\text{G.59})$$

with k being the momentum of integration and u one of the Feynman parameters. The best way to treat them is to factorize the k -dependence using the following identity utilizing the translation invariance

$$E(k, p_1, u) = \frac{1}{u} \exp \left(\frac{k^+}{u} \frac{\partial}{\partial p_1^+} \right) \frac{1 - e^{-iu(z_2^- - z_1^-)p_1^+}}{p_1^+}. \quad (\text{G.60})$$

As previously, expanding the exponential which depends on the differential operator in power series of $(k^+)^n$, one can easily perform the final momentum integration, since only a limited number of the lowest order terms contribute as a consequence of the light-like character of the vector n .

However, this is not the end of the story in case of gluonic operators. There, some contributions possess apart from the factor desired factor $p_1^+ p_2^+$ accompanying the gluon operator vertex, also the factors with $(p_i^+)^2$ dependence, which does not have the momentum structure of the product of two field strength tensors. For completeness, let us outline a few steps allowing to convert these structures into the required one, i.e., $(p_i^+)^2 \rightarrow p_1^+ p_2^+$. At first notice, that in the sum of all diagrams, the coefficient in front of, e.g., $(p_1^+)^2$ has the following general structure

$$\tau_1(u) + \tau_2(u)\delta(v) + \tau_3(u)\delta(1-u-v). \quad (\text{G.61})$$

The integration by parts reduces this expression to the desired form up to contributions proportional to $\delta(1-u-v)$. Namely,

$$\begin{aligned} (p_1^+)^2 \mathbb{J} \cdot \tau_1(u) &= (p_1^+)^2 \mathbb{J} \cdot \{ [\tau_1(u)v + \tau_2(u)] \delta(1-u-v) - \tau_2(u)\delta(v) \} \\ &\quad + p_1^+ p_2^+ \mathbb{J} \cdot \{ [\tau_1(u)v + \tau_2(u)] \delta(1-u-v) \\ &\quad - [\tau_1(0)v + \tau_2(0)] \delta(u) - [\tau'_1(u)v + \tau'_2(u)] \}. \end{aligned} \quad (\text{G.62})$$

Note also, that the resulting function

$$(p_1^+)^2 [\tau_1(u)v + \tau_2(u) + \tau_3(u)] \delta(1-u-v) \quad (\text{G.63})$$

can, in all known cases, be safely discarded on the grounds of the Bose symmetry properties of the string operators it is convoluted with. Similar equations hold for structures accompanying $(p_2^+)^2$. In particular, for the parity-even gluon operator $\mathcal{O}^{gg}(z_1^-, z_2^-)$, the test functions involved above take the following explicit form $\tau_1(u) = 2u(1-u) - 1$ and $\tau_2(u) = \frac{1}{2}(1-u)(2-u)$, and similarly, for the $u \rightarrow v$ contribution.

G.5.2 Light-cone gauge formalism with ML prescription

Turning to the calculation in the light-cone gauge, we will use the causal prescription on the spurious light-cone pole in the gluon propagator, i.e., the Mandelstam-Leibbrandt (ML) prescription [466, 464]. The most important feature of this prescription is the presence of an additional absorptive part of the vector boson Green function, namely

$$\text{Disc} \left\{ \frac{d_{\text{ML}}^{\mu\nu}(k)}{k^2 + i0} \right\} = -2\pi i\theta(k_+) \left\{ d_{\text{PV}}^{\mu\nu}(k)\delta(k^2) - \frac{k^-}{k^2} (k^\mu n^\nu + k^\nu n^\mu) \delta(k^+ k^-) \right\}. \quad (\text{G.64})$$

The second contribution is of the “ghost” type, since it has the opposite sign compared to the conventional one. As was proved in Ref. [466], the ML prescription is not an optional choice, rather, it is an unavoidable consequence of the equal-time canonical quantization. The outcome of having this additional term can be easily seen in the calculation of the one-loop evolution kernels. Basically, it leads to the absence of spurious singularities in separate diagrams, and to finiteness of individual contributions, in contrast to the regularization by means of the principal value, which we will review next.

The momentum integrals with the Mandelstam-Leibbrandt prescription are most easily computed with the help of the light-cone decomposition of momenta, Eq. (G.49). The longitudinal

integrals are evaluated using the Cauchy theorem, which yields

$$\int_{-\infty}^{\infty} \frac{dk^+ dk^-}{[k^+]_{\text{ML}}^j} e^{i(Ak^+ k^- + k^+ p^- + k^- p^+)} = -\frac{2\pi}{p^+} \left(-\frac{A}{p^+} \right)^{j-1} \left(e^{-ip^+ p^- / A} - \sum_{k=0}^{j-1} \left(-i \frac{p^+ p^-}{A} \right)^k \right). \quad (\text{G.65})$$

For $j = 0$, it agrees with Eq. (G.18). The remaining Euclidean integrals are evaluated via Eq. (G.19). Combining two integrations, one gets the following result for a generic one-loop integral with a $1/k^+$ -pole regularized via the Mandelstam-Leibbrandt prescription

$$\begin{aligned} & \int \frac{d^d k}{(2\pi)^d} \frac{e^{-iz^- k^+}}{[k^+]_{\text{ML}}} \frac{1}{k^2 \prod_{i=1}^n (k - q_i)^2} \\ &= \frac{i(-1)^{n+1}}{(4\pi)^{d/2}} \Gamma(n+1 - \frac{d}{2}) \int_0^1 \prod_{i=1}^{n+1} dx_i \delta \left(\sum_{i=1}^{n+1} x_i - 1 \right) \frac{1}{\sum_{i=1}^n x_i q_i^+} \\ & \times \left\{ \frac{e^{-iz^- \sum_{i=1}^n x_i q_i^+}}{\left[-\sum_{i=1}^n x_i q_i^2 + (\sum_{i=1}^n x_i q_i)^2 \right]^{n+1-d/2}} - \frac{1}{\left[-\sum_{i=1}^n x_i q_i^2 - (\sum_{i=1}^n x_i \mathbf{q}_{i\perp})^2 \right]^{n+1-d/2}} \right\}, \end{aligned} \quad (\text{G.66})$$

which agrees for $z^- = 0$ with results of Refs. [468, 469, 470].

The anomalous dimensions of quarks and gluons are, of course, gauge dependent and their one-loop values for the present choice are given by

$$\gamma_{(0)q} = \frac{3}{2} C_F, \quad \gamma_{(0)g} = \frac{\beta_0}{2}. \quad (\text{G.67})$$

More generally, the anomalous dimension of the gluon field in the light-cone gauge is equal to the renormalization group function of the running coupling,

$$\gamma_g = \frac{\beta(g)}{g},$$

to all orders in the coupling constant.

In the light-cone gauge, only the diagrams (a) and (c) contribute. The Feynman integral for the contribution (a) remains the same as in Eq. (G.47), where we have to use now the gauge propagator (G.11) with (G.15). Using the projection (G.46) to evaluate the trace, we find

$$\begin{aligned} \mathcal{M}_{\text{lc}}^{(a)} &= 2ig^2 C_F \gamma^+ \int \frac{d^d k}{(2\pi)^d} \frac{e^{-iz_1^-(p_1-k)^+ - iz_2^-(p_2+k)^+}}{k^2(p_1-k)^2(p_2+k)^2} \\ & \times \left\{ \mathbf{k}_\perp^2 + \frac{(p_1-k)^+}{[k^+]_{\text{ML}}} (p_2+k)^2 + \frac{(p_2+k)^+}{[k^+]_{\text{ML}}} (p_1-k)^2 \right\}. \end{aligned} \quad (\text{G.68})$$

The first term in the curly brackets produces the amplitude $\mathcal{M}_{\text{cov}}^{(a)}$, while the integrals with the regularized pole are given by Eq. (G.66) adjusted for the present needs

$$\text{PP} \int \frac{d^d k}{(2\pi)^d} \frac{e^{-ik^+ z^-}}{[k^+]_{\text{ML}}^n k^2(p-k)^2} = \frac{i}{(4\pi)^2 \varepsilon} \int_0^1 \frac{dx}{x^n} \left(e^{-ixp^+ z^-} - \sum_{l=0}^{n-1} (-ixp^+ z^-)^l \right). \quad (\text{G.69})$$

Since $k^+/[k^+]_{\text{ML}} = 1$, one can use Eq. (G.45) for other terms. Finally, adding the light cone gauge quark anomalous dimensions to Eq. (G.56), one recovers the same result as obtained with the covariant gauge fixing before, see Eq. (4.19).

G.6 Construction of evolution equations in momentum space

Now we outline the momentum-space formalism for the calculation of evolution kernels developed in Ref. [234]. It relies heavily on the use of the light-cone gauge with the principal value prescription. To begin with, we outline the basics of the one-loop renormalization of the QCD Lagrangian in this gauge.

G.6.1 Renormalization in light-cone gauge with PV prescription

The principal value prescription on the unphysical pole at $k^+ = 0$ (G.12) can be operationally formulated as a regularization

$$\frac{1}{[k_+]_{\text{PV}}} = \lim_{\delta \rightarrow 0} \frac{k_+}{k_+^2 + \delta^2}, \quad (\text{G.70})$$

with a parameter δ . The introduction of this extra parameter allows one to disentangle the spurious light-cone divergences from the conventional ultraviolet and infrared poles in ε . They would be unseparable otherwise if δ was set to zero from the onset.

As a first step, let us compute the one-loop quark self-energy due to the gluon which is given by the momentum integral

$$\Sigma(q) = \mu^{2\varepsilon} \int \frac{d^d k}{(2\pi)^d} \gamma^\mu \frac{\not{q} - \not{k}}{(q - k)^2} \gamma^\nu \frac{d_{\mu\nu}(k)}{k^2}. \quad (\text{G.71})$$

Reorganizing the numerator, we can cast it in the form

$$\Sigma(q) = -2(1 - \varepsilon)\gamma_\mu J_2^\mu(q) - (\not{q}\gamma_\mu\gamma_+ + \gamma_+\gamma_\mu\not{q}) J_{2+}^\mu(q), \quad (\text{G.72})$$

where we set the dimensionally regularized tadpole $\int d^d k / k_+ k^2$ to zero. The contributing integrals are

$$J_2^\mu(q) = \mu^{2\varepsilon} \int \frac{d^d k}{(2\pi)^d} \frac{(q - k)^\mu}{k^2(q - k)^2} = \frac{i\Gamma(\varepsilon)}{(4\pi)^2} \left(-\frac{4\pi\mu^2}{q^2}\right)^\varepsilon \frac{q^\mu}{2} \int_0^1 \frac{du}{(u\bar{u})^\varepsilon}, \quad (\text{G.73})$$

$$\begin{aligned} J_{2+}^\mu(q) &= \mu^{2\varepsilon} \int \frac{d^d k}{(2\pi)^d} \frac{(q - k)^\mu}{k^2(q - k)^2 [k_+]_{\text{PV}}} \\ &= \frac{i\Gamma(\varepsilon)}{(4\pi)^2} \left(-\frac{4\pi\mu^2}{q^2}\right)^\varepsilon \int_0^1 \frac{du}{(u\bar{u})^\varepsilon [uq_+]_{\text{PV}}} \left\{ \bar{\alpha} q^\mu - (1 - 2u) \frac{q^2}{2q_+} n^\mu \right\}. \end{aligned} \quad (\text{G.74})$$

Let us add a comment on the calculation procedure involving the integrals with $1/k_+$ pole in the integrand [469]. Since its regularization via the principal value prescription does not depend on k_- , after exponentiation of propagators (G.42), one easily performs the dk_- integral resulting in a delta-functions with the argument being an equality between the plus-components of the loop and external momenta. Thus, the k_+ integration is trivial making use of this delta-function. The transverse integral is performed using the Gaussian integration (G.19). Also, notice that if we would not use the regularization with the parameter δ in Eq. (G.70) this would lead to an extra pole in the dimensionally regularized Feynman-parameter integral and yield a double-pole in a one-loop diagram. Having distinct regularization parameters, we disentangle the ultraviolet poles from the spurious poles due to the light-cone singularity in the gauge propagator. Assembling everything together, we get

$$\Sigma(q) = \not{q}\Sigma_1(q) + \frac{q^2}{2q_+}\gamma_+\Sigma_2(q) \quad (\text{G.75})$$

where the functions in front of independent Dirac structures are

$$\Sigma_1(q) = -(1 - \varepsilon) \frac{i\Gamma(\varepsilon)}{(4\pi)^2} \left(-\frac{4\pi\mu^2}{q^2} \right)^\varepsilon \int_0^1 \frac{du}{(u\bar{u})^\varepsilon}, \quad \Sigma_2(q) = -\frac{i\Gamma(\varepsilon)}{(4\pi)^2} \left(-\frac{4\pi\mu^2}{q^2} \right)^\varepsilon \int_0^1 \frac{du}{(u\bar{u})^\varepsilon} \frac{4\bar{u}q_+}{[uq_+]_{\text{PV}}}. \quad (\text{G.76})$$

The Feynman-parameter integral involving the principal-value regularized denominator is computed as an expansion in the parameter of dimensional regularization,

$$\int_0^1 \frac{d\alpha}{(\alpha\bar{\alpha})^\varepsilon} \frac{\bar{\alpha}q_+}{[\alpha q_+]_{\text{PV}}} = -1 - \ln \frac{\delta}{q_+} - \varepsilon \left(2 - \frac{1}{2} \ln^2 \frac{\delta}{q_+} - \frac{5}{4} \zeta(2) \right) + \mathcal{O}(\varepsilon^2). \quad (\text{G.77})$$

The arising dependence on the plus-momentum is a well-known property of light cone gauge regularized with principal value prescription, which propagates into the anomalous dimensions of elementary field operators. Of course, the dependence on δ (and q^+) cancels out in all gauge invariant quantities.

Keeping only the pole contributions in one-loop self-energies, the one-loop gluon and quark propagators can be represented as a unitary rotations of the tree propagators

$$\mathcal{D}^{\mu\nu} \rightarrow \mathcal{D}_{[1]}^{\mu\nu}, \quad \mathcal{S} \rightarrow \mathcal{S}_{[1]}. \quad (\text{G.78})$$

The renormalization constants are no longer numbers, but rather they are matrices acting on the spinor (Lorentz) indices of the fermion (gluon) field operators. Moreover as we emphasized above, the renormalization constants depend on the plus components of the particles' momenta k_i^+ . The origin of this can be traced back to the lack of the rescaling invariance,

$$d_{\text{PV}}^{\mu\nu}(\varrho k) \neq d_{\text{PV}}^{\mu\nu}(k), \quad (\text{G.79})$$

which is otherwise obeyed by the unregularized propagator and the propagator with Mandelstam-Leibbrandt prescription. We can represent the one-loop propagators as follows.

- Quark propagator is

$$\mathcal{S}_{[1]}(k) = \bar{U}(k) \not{k} U(k) \frac{\mathcal{Z}_q(k)}{k^2 + i0}, \quad (\text{G.80})$$

where

$$U(k) = 1 - \frac{\tilde{\mathcal{Z}}_q(k)}{2k^+} \not{k} \gamma^+, \quad \bar{U}(k) \equiv \gamma^0 U^\dagger(k) \gamma^0 = 1 - \frac{\tilde{\mathcal{Z}}_q(k)}{2k^+} \gamma^+ \not{k}. \quad (\text{G.81})$$

The renormalization constants are

$$\mathcal{Z}_q(k) = 1 + \frac{\alpha_s}{\pi} C_F \frac{1}{\varepsilon} \left\{ \int dq^+ \frac{k^+}{q^+ - k^+} \vartheta_{11}^0(q^+, q^+ - k^+) + \frac{3}{4} \right\}, \quad (\text{G.82})$$

$$\tilde{\mathcal{Z}}_q(k) = \frac{\alpha_s}{2\pi} C_F \frac{1}{\varepsilon} \left\{ 1 + \int dq^+ \frac{k^+}{q^+ - k^+} \vartheta_{11}^0(q^+, q^+ - k^+) \right\}, \quad (\text{G.83})$$

- Gluon propagator reads

$$\mathcal{D}_{[1]}^{\mu\nu}(k) = U^{\mu\rho}(k) d_{\rho\sigma}(k) U^{\sigma\nu}(k) \frac{\mathcal{Z}(k)}{k^2 + i0}. \quad (\text{G.84})$$

The presence of the divergent tensor $U^{\mu\nu}$,

$$U^{\mu\nu}(k) = g^{\mu\nu} - \tilde{\mathcal{Z}}_g(k) \frac{k^\mu n^\nu + k^\nu n^\mu}{k^+}, \quad (\text{G.85})$$

is an artifact of the Lorentz symmetry breaking effects by the gauge fixing vector n^μ and of using the principal value prescription which leads to different renormalization constants for “good” and “bad” components of tensor fields. Namely,

$$\mathcal{Z}_g(k) = 1 + \frac{\alpha_s}{\pi} C_A \frac{1}{\varepsilon} \left\{ \int dq^+ \frac{k^+}{q^+ - k^+} \vartheta_{11}^0(q^+, q^+ - k^+) - \frac{1}{4} \frac{\beta_0}{C_A} \right\}, \quad (\text{G.86})$$

$$\tilde{\mathcal{Z}}_g(k) = \frac{\alpha_s}{2\pi} C_A \frac{1}{\varepsilon} \left\{ 1 + \int dq^+ \frac{k^+}{q^+ - k^+} \vartheta_{11}^0(q^+, q^+ - k^+) \right\}. \quad (\text{G.87})$$

Note that the “good” components of the fields are renormalized by \mathcal{Z} and are not affected by $\tilde{\mathcal{Z}}$.

The appearing \mathcal{Z} -factors depend on the integral involving the light-cone singularity

$$\int dq^+ \frac{k^+}{[q^+ - k^+]_{\text{PV}}} \vartheta_{11}^0(q^+, q^+ - k^+) = \ln \frac{\delta}{k^+}. \quad (\text{G.88})$$

However, for the consequent use we will not use the explicit form of this integral.

Finally, notice that if one relies on the cut-off regularization with an ultraviolet scale μ^2 rather than dimensional regularization, then one would be able to obtain one from the other by making the substitution

$$\frac{1}{\varepsilon} \rightarrow \frac{\mu^{2\varepsilon}}{\varepsilon} \rightarrow \ln \mu^2, \quad (\text{G.89})$$

where μ^2 is the standard mass parameter of dimensional regularization.

G.6.2 Evolution kernels in momentum space

Computing the evolution kernels we have to isolate ultraviolet divergences occurring in transverse-momentum integrals of partons interacting with a bare quark operator (G.39). To extract this dependence properly, it is sufficient to separate the perturbative loop from the correlation function in question. To this end, the latter can be represented in the form of the momentum integral in which the integration over the fractional energies of the particles attached to the vertex is removed

$$\mathcal{O}^{qq}(x_1, x_2) = \int \frac{d^4 k_1}{(2\pi)^4} \frac{d^4 k_2}{(2\pi)^4} \delta(k_1^+ - x_1) \delta(k_2^+ - x_2) \mathcal{O}^{qq}(k_1, k_2), \quad (\text{G.90})$$

where the momentum-space operator is given here by

$$\mathcal{O}^{qq}(k_1, k_2) = \int d^4 z_1 d^4 z_2 e^{ik_1 \cdot z_1 + ik_2 \cdot z_2} \bar{\psi}(z_1) \gamma^+ \psi(z_2) \equiv \bar{\psi}(k_1) \gamma^+ \psi(k_2). \quad (\text{G.91})$$

Here in the last step we introduced the momentum-space quark fields.

The calculation of one-loop diagrams is extremely simple within the framework of momentum-fraction space with the light-cone gauge [234, 63, 471, 472, 473]. Let us describe again a step-by-step procedure for computing the kernel.

- Use Feynman rules from Section G.1 to write the one-loop expression for the correlation function (G.90).
- Project the color and Dirac structure on the operator vertex as in Eq. (G.46). These two steps result in

$$\begin{aligned}\mathcal{O}_{\text{1-loop}(a)}^{qq}(x_1, x_2) &= \frac{1}{4N_c} \int \frac{d^4 p_1}{(2\pi)^4} \frac{d^4 p_2}{(2\pi)^4} \mathcal{O}^{qq}(p_1, p_2) \int \prod_{i=1}^3 \frac{d^4 k_i}{(2\pi)^4} \delta(k_1^+ - x_1) \delta(k_2^+ - x_2) \quad (\text{G.92}) \\ &\times \text{tr}_c \text{tr} \left\{ \gamma^- \mathcal{V}_\mu^a(-k_3, p_1, -k_1) i\mathcal{S}(-k_2) \gamma^+ i\mathcal{S}(k_1) \mathcal{V}_\nu^a(k_3, -k_2, p_2) \right\} (-i) \mathcal{D}^{\mu\nu}(k_3).\end{aligned}$$

- Eliminate the momentum conservation delta-functions keeping k_3^μ as the loop momentum k^μ .
- Use the Sudakov decomposition for four-momenta in Eq. (G.49). Compute the trace extracting only the piece which results in the logarithmically divergent transverse-momentum integral. Namely, since the loop-momentum volume element produces the factor $\mathbf{k}_\perp^2 d\mathbf{k}_\perp^2$, and the denominators of the three propagators give the factor $(\mathbf{k}_\perp^2)^{-3}$, one needs to extract the term proportional to \mathbf{k}_\perp^2 from the trace, i.e.,

$$\begin{aligned}\frac{1}{4} \text{tr} \left\{ \gamma^- \gamma_\mu (\not{k}_1 - \not{p}_1 - \not{p}_2) \gamma^+ \not{k}_1 \gamma_\nu \right\} d^{\mu\nu}(k_1 - p_1) \\ \simeq -2\mathbf{k}_{1\perp}^2 \left\{ 1 + \frac{x_1 - p_1^+ - p_2^+}{x_1 - p_1^+} [x_1 \beta_1 - 1] + \frac{x_1}{x_1 - p_1^+} [(x_1 - p_1^+ - p_2^+) \beta_1 - 1] \right\}.\end{aligned}\quad (\text{G.93})$$

- Use the strong-ordering approximation (4.3), $|\mathbf{k}_{1\perp}| \gg |\mathbf{p}_{1\perp}|$ and $k_1^- \gg p_1^-$. For a typical propagator denominator this gives

$$(k_1 - p_1)^2 + i0 \simeq \mathbf{k}_{1\perp}^2 [(x_1 - p_1^+) \beta_1 - 1 + i0], \quad (\text{G.94})$$

where one conveniently introduces a rescaled k^- component

$$\beta \equiv \frac{2k^-}{\mathbf{k}_\perp^2}. \quad (\text{G.95})$$

The last three steps yield

$$\begin{aligned}\mathcal{O}_{\text{1-loop}(a)}^{qq}(x_1, x_2) &= -\frac{\alpha_s}{2\pi^2} C_F \int \frac{d^4 p_1}{(2\pi)^4} \frac{d^4 p_2}{(2\pi)^4} \mathcal{O}^{qq}(p_1, p_2) \delta(x_1 + x_2 - p_1^+ - p_2^+) \int \frac{d^2 \mathbf{k}_{1\perp}}{\mathbf{k}_{1\perp}^2} \quad (\text{G.96}) \\ &\times \frac{1}{x_1 - p_1^+} \int \frac{d\beta_1}{2\pi i} \frac{(x_1 - p_1^+) + (x_1 - p_1^+ - p_2^+) [x_1 \beta_1 - 1] + x_1 [(x_1 - p_1^+ - p_2^+) \beta_1 - 1]}{[x_1 \beta_1 - 1 + i0][(x_1 - p_1^+ - p_2^+) \beta_1 - 1 + i0][(x_1 - p_1^+) \beta_1 - 1 + i0]},\end{aligned}$$

- Compute the transverse-momentum integral with a cut-off

$$\int^{\mu^2} \frac{d^2 \mathbf{k}_{1\perp}}{\mathbf{k}_{1\perp}^2} = \pi \ln \mu^2. \quad (\text{G.97})$$

- Use the generalized step functions from Appendix G.7.

As can be seen, Eq. (G.96) diverges at $x_1 = p_1^+$. The divergencies disappear after one adds the virtual radiative corrections (renormalization of the field operators) discussed in the previous subsection.

- Virtual corrections are computed using the one-loop propagator given in Eq. (G.80), namely, one gets

$$\mathcal{O}_{\text{1-loop}(b)}^{qq}(x_1, x_2) = \int \frac{d^4 p_1}{(2\pi)^4} \frac{d^4 p_2}{(2\pi)^4} \sqrt{\mathcal{Z}_q(p_1) \mathcal{Z}_q(p_2)} \bar{\psi}(p_1) U(p_1) \gamma^+ \bar{U}(p_2) \psi(p_2), \quad (\text{G.98})$$

where the quark-field operators are renormalized as

$$\psi(k) = \sqrt{\mathcal{Z}_q(k)} U(k) \psi_{(0)}(k). \quad (\text{G.99})$$

Using the obvious fact that

$$U(p) \gamma^+ = \gamma^+ \bar{U}(p) = 1$$

and explicit form of the one-loop renormalization constant (G.82), one finally gets the contribution due to the virtual corrections

$$\begin{aligned} \mathcal{O}_{\text{1-loop}(b)}^{qq}(x_1, x_2) &= \frac{\alpha_s}{2\pi} C_F \ln \mu^2 \int dx'_1 dx'_2 \delta(x_1 + x_2 - x'_1 - x'_2) \\ &\times \left\{ \frac{3}{2} \delta(x_1 - x'_1) + \delta(x_1 - x'_1) \int dx''_1 \frac{x'_1}{x''_1 - x'_1} \vartheta_{11}^0(x''_1, x''_1 - x'_1) \right. \\ &\quad \left. + \delta(x_2 - x'_2) \int dx''_2 \frac{x'_2}{x''_2 - x'_2} \vartheta_{11}^0(x''_2, x''_2 - x'_2) \right\} \mathcal{O}^{qq}(x'_1, x'_2), \end{aligned} \quad (\text{G.100})$$

where $p_i^+ \equiv x'_i$.

- Adding Eqs. (G.96) and (G.98) yields

$$\mathcal{O}_{\text{1-loop}}^{qq}(x_1, x_2) = -\frac{\alpha_s}{2\pi} C_F \ln \mu^2 \int dx'_1 dx'_2 \delta(x_1 + x_2 - x'_1 - x'_2) K_{(0)}^{qq,V}(x_1, x_2 | x'_1, x'_2) \mathcal{O}^{qq}(x'_1, x'_2), \quad (\text{G.101})$$

with the kernel given in Eq. (4.42), where the regularization of the end-point behavior $y_i \rightarrow x_i$ results in the plus-prescription,

$$\left[\frac{y_1}{x_1 - y_1} \vartheta_{11}^0(x_1, x_1 - y_1) \right]_+ \equiv \frac{y_1}{x_1 - y_1} \vartheta_{11}^0(x_1, x_1 - y_1) - \delta(x_1 - y_1) \int dy'_1 \frac{y_1}{y'_1 - y_1} \vartheta_{11}^0(y'_1, y'_1 - y_1). \quad (\text{G.102})$$

G.7 Generalized step functions

The momentum space evolution kernels presented in Section 4.4.1 are expressed in terms of the generalized step-functions

$$\vartheta_{\alpha_1 \dots \alpha_j}^k(x_1, \dots, x_j) \equiv \int \frac{d\beta}{2\pi i} \beta^k \prod_{\ell=1}^j (x_\ell \beta - 1 + i0)^{-\alpha_\ell}. \quad (\text{G.103})$$

In general case, the reduction of the higher-rank functions is performed making multiple use of the following identities

$$\begin{aligned}\vartheta_{ijk\dots}^n(x_1, x_2, x_3, \dots) &= \frac{1}{x_1 - x_2} \left\{ \vartheta_{i-1jk\dots}^{n-1}(x_1, x_2, x_3, \dots) - \vartheta_{ij-1k\dots}^{n-1}(x_1, x_2, x_3, \dots) \right\} \quad (\text{G.104}) \\ &= \frac{1}{x_1 - x_2} \left\{ x_2 \vartheta_{i-1jk\dots}^n(x_1, x_2, x_3, \dots) - x_1 \vartheta_{ij-1k\dots}^n(x_1, x_2, x_3, \dots) \right\}.\end{aligned}$$

In case of two coinciding arguments, the function collapses to a lower rank,

$$\vartheta_{ijk\dots}^n(x_1, x_1, x_3, \dots) = \vartheta_{i+j,k\dots}^n(x_1, x_3, \dots).$$

Along this line of reasoning, all the functions can be reduced to the lowest one ϑ_{11}^0 , which is given by

$$\vartheta_{11}^0(x_1, x_2) = \frac{\theta(x_1)\theta(-x_2) - \theta(-x_1)\theta(x_2)}{x_1 - x_2} = \frac{\theta(x_1) - \theta(x_2)}{x_1 - x_2}. \quad (\text{G.105})$$

It is defined in terms of the conventional step function $\theta(x) = \{1, x \geq 0 ; 0, x < 0\}$.

As a demonstration of how Eq. (G.104) works, we give a list of formulas for the generalized step functions that appear in the lowest order calculations,

$$\vartheta_1^0(x) = 0, \quad (\text{G.106})$$

$$\vartheta_{21}^0(x_1, x_2) = \frac{x_2}{x_1 - x_2} \vartheta_{11}^0(x_1, x_2), \quad (\text{G.107})$$

$$\vartheta_{22}^0(x_1, x_2) = -\frac{2x_1 x_2}{(x_1 - x_2)^2} \vartheta_{11}^0(x_1, x_2), \quad (\text{G.108})$$

$$\vartheta_{22}^1(x_1, x_2) = -\frac{x_1 + x_2}{(x_1 - x_2)^2} \vartheta_{11}^0(x_1, x_2), \quad (\text{G.109})$$

$$\vartheta_{21}^1(x_1, x_2) = \frac{1}{x_1 - x_2} \vartheta_{11}^0(x_1, x_2) - \frac{1}{x_1 - x_2} \vartheta_{11}^0(x_1), \quad (\text{G.110})$$

$$\vartheta_{111}^0(x_1, x_2, x_3) = \frac{x_2}{x_1 - x_2} \vartheta_{11}^0(x_2, x_3) - \frac{x_1}{x_1 - x_2} \vartheta_{11}^0(x_1, x_3), \quad (\text{G.111})$$

$$\vartheta_{111}^1(x_1, x_2, x_3) = \frac{1}{x_1 - x_2} \vartheta_{11}^0(x_2, x_3) - \frac{1}{x_1 - x_2} \vartheta_{11}^0(x_1, x_3), \quad (\text{G.112})$$

$$\vartheta_{112}^1(x_1, x_2, x_3) = \frac{x_2}{(x_1 - x_2)(x_3 - x_2)} \vartheta_{11}^0(x_2, x_3) + \frac{x_1}{(x_1 - x_2)(x_1 - x_3)} \vartheta_{11}^0(x_1, x_3). \quad (\text{G.113})$$

H Evolution of nonsymmetric double distributions

Let us discuss the evolution of double distribution in nonsymmetric longitudinal variables⁵⁰ s and r originally used in Refs. [3, 4, 6] rather than symmetric α and β introduced in Section 3.8. These conventions will simplify somewhat the explicit form of evolution kernels. The variables of the corresponding the nonsymmetric double distribution $Q(s, r, \Delta^2)$ parametrize the four-momentum of the initial parton

$$k_1^\mu = s p_1^\mu + r \Delta^\mu$$

⁵⁰These variables were denoted in the original work [3, 4, 6] by x and y , respectively. We have changed the notation to s and r to avoid confusion with already used conventions in Section 4.4.4 and later.

in terms of the s -channels momentum of the incoming hadron p_1 and the t -channel momentum transfer Δ . The four-momentum of the final parton is then $k_2^\mu = sp_1^\mu - (1-r)\Delta^\mu$, i.e., the momentum transfer Δ is shared by the partons in fractions r and $1-r \equiv \bar{r}$. The relation between the parameters s, r and the symmetric variables β, α from Eq. (3.205) is evidently given by

$$s = \beta, \quad r = \frac{1}{2}(1 + \alpha - \beta). \quad (\text{H.1})$$

Notice that by redefining the negative- β part of as an antiquark distribution (or using the β -symmetry property of the gluon distribution), the variable s can always be taken positive, with the support region being $0 \leq s, r, s+r \leq 1$. In particular, for quarks in the nucleon, the nonsymmetric DDs for the vector operator are defined by the following representation [3]:

$$\langle p_2 | \mathcal{O}^{qq}(0, z^-) | p_1 \rangle = \int_0^1 ds \int_0^{\bar{s}} dr \left\{ e^{-isz^- p_1^+ - irz^- \Delta^+} \left[h^+ Q^q(s, r) + \frac{b}{M_N} (sp_1^+ + r\Delta^+) P^q(s, r) \right] - e^{isz^- p_1^+ - i\bar{r}z^- \Delta^+} \left[h^+ Q^{\bar{q}}(s, r) + \frac{b}{M_N} (sp_1^+ + r\Delta^+) P^{\bar{q}}(s, r) \right] \right\}, \quad (\text{H.2})$$

where we did not display the dependence of DDs Q and P on Δ^2 , since it will be irrelevant throughout our discussion. At $\Delta^2 = 0$, the r -integral of the combination $Q^{q,\bar{q}}(s, r) + sP^{q,\bar{q}}(s, r)$ produces the usual quark and antiquark densities $q(s)$ and $\bar{q}(s)$ as can be seen by matching (H.2) into Eq. (3.66). In a similar way, one can introduce the nonsymmetric double distributions for gluons

$$\begin{aligned} \langle p_2 | \mathcal{O}^{gg}(0, z^-) | p_1 \rangle &= \frac{1}{2} \int_0^1 ds \int_0^{\bar{s}} dr \left\{ e^{-isz^- p_1^+ - irz^- \Delta^+} + e^{isz^- p_1^+ - i\bar{r}z^- \Delta^+} \right\} \\ &\quad \times \left[h^+ p_1^+ s Q^g(s, r) + \frac{b}{M_N} (sp_1^+ + r\Delta^+)^2 P^g(s, r) \right]. \end{aligned} \quad (\text{H.3})$$

Due to the factor s included in this definition, the combination of gluon DDs in the zero-recoil $\Delta^2 = 0$ limit $Q^g(s, r) + sP^g(s, r)$ reduces to the usual gluon density $g(s)$ (3.71) after integration over r . Analogous functions can be introduced in the odd parity sector, whose definitions can be read from Eqs. (H.2) and (H.4) by dressing the symbols on the right- and left-hand sides with tildes, i.e., $\mathcal{O}^{aa} \rightarrow \tilde{\mathcal{O}}^{aa}$ and $Q^a \rightarrow \tilde{Q}^a$, $P^a \rightarrow \tilde{P}^a$, as well as changing the relative sign between the momentum exponentials.

The use of $Q(s, r)$ DDs has some disadvantages when the symmetry properties are discussed. In particular, the symmetry of the $f(\beta, \alpha)$ DDs with respect to the change $\alpha \rightarrow -\alpha$ corresponds to the “München symmetry” of $Q(s, r)$ with respect to the interchange $r \leftrightarrow 1-s-r$ [142]. However, evolution kernels for $Q(s, r)$ look simpler than their symmetric analogues.

H.1 Evolution kernels for nonsymmetric double distributions

The μ -dependence of parton helicity-independent DDs $Q^a(s, r)$ is governed by the evolution equation

$$\frac{d}{d \ln \mu^2} Q^a(s_1, r_1; \mu^2) = \sum_b \int_0^1 ds_2 \int_0^1 dr_2 \theta(1 - s_2 - r_2) R^{ab;V}(s_1, r_1; s_2, r_2) Q^b(s_2, r_2; \mu^2), \quad (\text{H.4})$$

where $a, b = q, g$. A similar set of equations, with the kernels denoted by $R^{ab;A}(s_1, r_1; s_2, r_2)$ governs the evolution of the parton helicity sensitive double distributions $\tilde{Q}^a(s_1, r_1; \mu^2)$.

Integration over r_1 converts $Q^a(s_1, r_1; \mu^2)$ for $\Delta^2 = 0$ into the parton distribution functions, whose evolution is described by the DGLAP equations (4.9). The kernels $R^{ab}(s_1, r_1; s_2, r_2)$ must satisfy the reduction relation

$$\int_0^{1-s_1} dr_1 R^{ab}(s_1, r_1; s_2, r_2) = \frac{1}{s_2} P^{ab}(s_1/s_2). \quad (\text{H.5})$$

Alternatively, integration over s_1 converts $Q^a(s_1, r_1; \mu^2)$ at the point $\Delta^2 = 0$ into an object similar to a meson distribution amplitude, so one may expect that the result of integration of $R^{ab}(s_1, r_1; s_2, r_2)$ over s_1 should be related to the ER-BL kernels governing the evolution of distribution amplitudes [237, 240] e.g., in case of the qq kernel

$$\int_0^{1-r_1} ds_1 R^{qq}(s_1, r_1; s_2, r_2) = V^{qq}(r_1, r_2). \quad (\text{H.6})$$

These reduction properties of the $R^{qq,V}(s_1, r_1; s_2, r_2)$ kernel can be illustrated using its explicit one-loop form,

$$R^{ab}(s_1, r_1; s_2, r_2) = \frac{\alpha_s}{2\pi} R_{(0)}^{ab}(s_1, r_1; s_2, r_2) + \mathcal{O}(\alpha_s^2), \quad (\text{H.7})$$

with [3]

$$\begin{aligned} R_{(0)}^{qq;V}(s_1, r_1; s_2, r_2) &= \frac{C_F}{s_2} \left\{ \frac{\theta(0 \leq s_1/s_2 \leq 1) s_1/s_2}{(1 - s_1/s_2)} \left[\frac{1}{r_2} \delta\left(\frac{s_1}{s_2} - \frac{r_1}{r_2}\right) + \frac{1}{\bar{r}_2} \delta\left(\frac{s_1}{s_2} - \frac{\bar{r}_1}{\bar{r}_2}\right) \right] \right. \\ &\quad \left. + \theta\left(0 \leq \frac{s_1}{s_2} \leq \min\left\{\frac{r_1}{r_2}, \frac{\bar{r}_1}{\bar{r}_2}\right\}\right) - \delta\left(1 - \frac{s_1}{s_2}\right) \delta(r_1 - r_2) \left[\frac{1}{2} + 2 \int_0^1 dz \frac{z}{\bar{z}} \right] \right\}. \end{aligned} \quad (\text{H.8})$$

Here the last (formally divergent) term, as usual, provides the regularization for the $1/(s_1 - s_2)$ singularities present in the kernel. This singularity can be also written as $1/(r_2 - r_1)$ for the term containing $\delta(s_1/s_2 - r_1/r_2)$ and as $1/(r_1 - r_2)$ for the term accompanying $\delta(s_1/s_2 - \bar{r}_1/\bar{r}_2)$. In each particular case, incorporating the $1/(1 - z)$ term into a plus-type distribution, one should treat z as s_1/s_2 , r_1/r_2 or \bar{r}_1/\bar{r}_2 , respectively. One can check that integrating $R_{(0)}^{qq;V}(s_1, r_1; s_2, r_2)$ over r_1 or s_1 gives the DGLAP splitting function (4.55) or the ER-BL kernel (4.76) with (4.77).

A convenient way to get explicit expressions for $R^{ab}(s_1, r_1; s_2, r_2)$ is to extract them from the light-cone kernels $\mathcal{K}_{(0)}^{ab}(u, v)$ describing the evolution equations for the light-ray operators (4.12)). Parametrizing nonforward matrix elements in terms of DDs, we can express $R_{(0)}^{ab}(s_1, r_1; s_2, r_2)$ in terms of the universal $\mathcal{K}_{(0)}^{ab}(u, v)$ kernels. Since the definitions of the gluon distributions $Q^g(s, r)$, $\tilde{F}^g(s, r)$ contain an extra p_1^+ factor on the right-hand side, which results in the differentiation $\partial/\partial s$ of the relevant kernel, it is convenient to proceed in two steps. First, we introduce the auxiliary kernels $r_{(0)}^{ab}(s_1, r_1; s_2, r_2)$ directly related by to the light-ray evolution kernels $\mathcal{K}_{(0)}^{ab}(u, v)$,

$$\begin{aligned} r_{(0)}^{ab}(s_1, r_1; s_2, r_2) &= \int_0^1 du \int_0^{\bar{u}} dv \delta(s_1 - s_2(\bar{u} - v)) \delta(r_1 - u - r_2(\bar{u} - v)) \mathcal{K}_{(0)}^{ab}(u, v) \\ &= \frac{1}{s_2} \mathcal{K}_{(0)}^{ab} \left(r_1 - \frac{r_2 s_1}{s_2}, \bar{r}_1 - \frac{\bar{r}_2 s_1}{s_2} \right) \vartheta \left(\frac{r_2 s_1}{s_2} - r_1, 0 \right) \vartheta \left(\frac{s_1}{s_2} - 1, \frac{r_2 s_1}{s_2} - r_1 \right). \end{aligned} \quad (\text{H.9})$$

Here the spectral constraint arises as a result of the integration (4.52) and expressing the appearing generalized step-functions by means of Eq. (4.46) in terms of $\vartheta(x, y)$, Eq. (4.39).

The second step is to get the R -kernels using the relations

$$R_{(0)}^{qq}(s_1, r_1; s_2, r_2) = r_{(0)}^{qq}(s_1, r_1; s_2, r_2), \quad (\text{H.10})$$

$$R_{(0)}^{gg}(s_1, r_1; s_2, r_2) = \frac{s_2}{s_1} r_{(0)}^{gg}(s_1, r_1; s_2, r_2), \quad (\text{H.11})$$

$$\frac{\partial}{\partial s_1} \left[s_1 R_{(0)}^{gg}(s_1, r_1; s_2, r_2) \right] = -r_{(0)}^{gg}(s_1, r_1; s_2, r_2), \quad (\text{H.12})$$

$$R_{(0)}^{gg}(s_1, r_1; s_2, r_2) = -s_2 \frac{\partial}{\partial s_1} r_{(0)}^{gg}(s_1, r_1; s_2, r_2). \quad (\text{H.13})$$

Hence, to obtain $R_{(0)}^{gg}(s_1, r_1; s_2, r_2)$, we should integrate $r_{(0)}^{gg}(s_1, r_1; s_2, r_2)$ with respect to s_1 . We fix the integration ambiguity by the requirement that $R_{(0)}^{gg}(s_1, r_1; s_2, r_2)$ vanishes for $s_1 > 1$. Then

$$R_{(0)}^{gg}(s_1, r_1; s_2, r_2) = \frac{1}{s_1} \int_{s_1}^1 ds r_{(0)}^{gg}(s, r_1; s_2, r_2). \quad (\text{H.14})$$

This convention guarantees a simple relation (H.5) to the DGLAP kernels.

At one loop, $R_{(0)}^{gg;A}(s_1, r_1; s_2, r_2) = R_{(0)}^{gg;V}(s_1, r_1; s_2, r_2)$, and this kernel was already displayed in Eq. (H.8). Other kernels, including the $R_{(0)}^{gg;V}(s_1, r_1; s_2, r_2)$ kernel originally obtained in Ref. [4], are given by

$$R_{(0)}^{gg;A}(s_1, r_1; s_2, r_2) = 2T_F N_f \frac{s_1}{s_2^2} \left\{ \delta \left(\frac{s_1}{s_2} - \frac{r_1}{r_2} \right) \theta(r_2 - r_1) + \delta \left(\frac{s_1}{s_2} - \frac{\bar{r}_1}{\bar{r}_2} \right) \theta(r_1 - r_2) - \frac{s_2}{s_1} \theta \left(0 \leq \frac{s_1}{s_2} \leq \min \left\{ \frac{r_1}{r_2}, \frac{\bar{r}_1}{\bar{r}_2} \right\} \right) \right\}, \quad (\text{H.15})$$

$$R_{(0)}^{gg;A}(s_1, r_1; s_2, r_2) = 2C_F \frac{1}{s_1} \left\{ \left(\frac{s_1}{s_2} - \frac{r_1}{r_2} \right) \theta \left(\frac{s_1}{s_2} \leq \frac{r_1}{r_2} \leq 1 \right) + \left(\frac{s_1}{s_2} - \frac{\bar{r}_1}{\bar{r}_2} \right) \theta \left(\frac{s_1}{s_2} \leq \frac{\bar{r}_1}{\bar{r}_2} \leq 1 \right) + \frac{1}{2} \delta(r_2 - r_1) \theta(0 \leq s_1 \leq s_2) \right\}, \quad (\text{H.16})$$

$$R_{(0)}^{gg;A}(s_1, r_1; s_2, r_2) = \frac{C_A}{s_2} \left\{ \frac{\theta(0 \leq s_1/s_2 \leq 1) s_1/s_2}{(1 - s_1/s_2)} \left[\frac{1}{r_2} \delta \left(\frac{s_1}{s_2} - \frac{r_1}{r_2} \right) + \frac{1}{\bar{r}_2} \delta \left(\frac{s_1}{s_2} - \frac{\bar{r}_1}{\bar{r}_2} \right) \right] + 4\theta \left(0 \leq \frac{s_1}{s_2} \leq \min \left\{ \frac{r_1}{r_2}, \frac{\bar{r}_1}{\bar{r}_2} \right\} \right) - \delta \left(1 - \frac{s_1}{s_2} \right) \delta(r_1 - r_2) \left[\frac{\beta_0}{2C_A} + 2 \int_0^1 \frac{dz}{\bar{z}} \right] \right\}, \quad (\text{H.17})$$

in the odd parity sector, and

$$R_{(0)}^{gg;V}(s_1, r_1; s_2, r_2) = R_{(0)}^{gg;A}(s_1, r_1; s_2, r_2) + 8T_F N_f \frac{r_2 \bar{r}_2}{s_2} \left(\frac{r_1}{r_2} + \frac{\bar{r}_1}{\bar{r}_2} - 2 \frac{s_1}{s_2} \right) \theta \left(0 \leq \frac{s_1}{s_2} \leq \min \left\{ \frac{r_1}{r_2}, \frac{\bar{r}_1}{\bar{r}_2} \right\} \right), \quad (\text{H.18})$$

$$R_{(0)}^{gg;V}(s_1, r_1; s_2, r_2) = 2C_F \frac{1}{s_1} \left\{ \left(\frac{r_1}{r_2} - \frac{s_1}{s_2} \right) \theta \left(\frac{s_1}{s_2} \leq \frac{r_1}{r_2} \leq 1 \right) + \left(\frac{\bar{r}_1}{\bar{r}_2} - \frac{s_1}{s_2} \right) \theta \left(\frac{s_1}{s_2} \leq \frac{\bar{r}_1}{\bar{r}_2} \leq 1 \right) + \frac{1}{2} \delta(r_2 - r_1) \theta(0 \leq s_1 \leq s_2) \right\}, \quad (\text{H.19})$$

$$\begin{aligned} R_{(0)}^{gg;V}(s_1, r_1; s_2, r_2) &= R_{(0)}^{gg,A}(s_1, r_1; s_2, r_2) \\ &\quad + 12C_A \frac{1}{s_1} \left(r_1 - \frac{r_2 s_1}{s_2} \right) \left(\bar{r}_1 - \frac{\bar{r}_2 s_1}{s_2} \right) \theta \left(0 \leq \frac{s_1}{s_2} \leq \min \left\{ \frac{r_1}{r_2}, \frac{\bar{r}_1}{\bar{r}_2} \right\} \right), \end{aligned} \quad (\text{H.20})$$

for the even parity case. The equations (H.4) with above evolution kernels can be also solved analytically, with the result for the s_1 -moments of DDs given by an expansion in the Gegenbauer polynomials as we will explain in Section 4.11.8.

H.2 Solution of evolution equation for double distributions

Having discussed the evolution of GPDs, let us turn to the analogous analysis of scale dependence of DDs, limiting our consideration however to leading order in coupling constant. The analytic solution to the evolution equations for double distributions (H.4) introduced in Section H.1 was obtained in Refs. [3, 4] by combining standard methods of solving evolution equations for parton densities and distribution amplitudes. First, one should take moments with respect to s . Utilizing the rescaling property $R^{ab}(s_1, r_1; s_2, r_2) = R^{ab}(s_1/s_2, r_1; 1, r_2)/s_2$, one obtains

$$\frac{d}{d \ln \mu^2} Q_n^a(r_1; \mu^2) = \sum_b \int_0^1 dr_2 R_n^{ab;V}(r_1, r_2) Q_n^b(r_2; \mu^2), \quad (\text{H.21})$$

where $Q_n^a(r; \mu^2)$ is the n -th s -moment of $Q^a(s, r; \mu^2)$

$$Q_n^a(r; \mu^2) = \int_0^1 ds s^n Q^a(s, r; \mu^2). \quad (\text{H.22})$$

The one-loop kernels $R_{(0)n}^{ab;V}(r_1, r_2)$ and analogous kernels $R_{(0)n}^{ab;A}(r_1, r_2)$ governing the evolution of parton helicity dependent double distributions $\tilde{Q}_n^a(y; \mu^2)$ are given by [231, 140]

$$\begin{aligned} R_{(0)n}^{qq;A}(r_1, r_2) &= C_F \left\{ \left(\frac{r_1}{r_2} \right)^{n+1} \left[\frac{1}{n+1} + \frac{1}{r_2 - r_1} \right] \theta(r_2 - r_1) \right. \\ &\quad \left. + \left(\frac{\bar{r}_1}{\bar{r}_2} \right)^{n+1} \left[\frac{1}{n+1} + \frac{1}{r_1 - r_2} \right] \theta(r_1 - r_2) - \delta(r_1 - r_2) \left[\frac{1}{2} + 2 \int_0^1 dz \frac{z}{\bar{z}} \right] \right\}, \end{aligned} \quad (\text{H.23})$$

$$R_{(0)n}^{gg;A}(r_1, r_2) = 2T_F N_f \frac{n}{n+1} \left\{ \left(\frac{r_1}{r_2} \right)^{n+1} \theta(r_2 - r_1) + \left(\frac{\bar{r}_1}{\bar{r}_2} \right)^{n+1} \theta(r_1 - r_2) \right\}, \quad (\text{H.24})$$

$$R_{(0)n}^{gg;A}(r_1, r_2) = C_F \frac{1}{n} \left\{ \delta(r_1 - r_2) - \frac{2}{n+1} \left[\left(\frac{r_1}{r_2} \right)^{n+1} \theta(r_2 - r_1) + \left(\frac{\bar{r}_1}{\bar{r}_2} \right)^{n+1} \theta(r_1 - r_2) \right] \right\}, \quad (\text{H.25})$$

$$\begin{aligned} R_{(0)n}^{gg;A}(r_1, r_2) &= C_A \left\{ \left(\frac{r_1}{r_2} \right)^{n+1} \left[\frac{4}{n+1} + \frac{1}{r_2 - r_1} \right] \theta(r_2 - r_1) \right. \\ &\quad \left. + \left(\frac{\bar{r}_1}{\bar{r}_2} \right)^{n+1} \left[\frac{4}{n+1} + \frac{1}{r_1 - r_2} \right] \theta(r_1 - r_2) - \delta(r_1 - r_2) \left[\frac{\beta_0}{2C_A} + 2 \int_0^1 dz \frac{z}{\bar{z}} \right] \right\}, \end{aligned} \quad (\text{H.26})$$

for odd parity sector, and

$$R_{(0)n}^{qq;V}(r_1, r_2) = R_{(0)n}^{qq,A}(r_1, r_2), \quad (\text{H.27})$$

$$R_{(0)n}^{gg;V}(r_1, r_2) = R_{(0)n}^{gg;A}(r_1, r_2) + 8T_F N_f \frac{n}{n+1} \left\{ \left(\frac{r_1}{r_2} \right)^{n+1} \left[\frac{r_2 \bar{r}_1}{n} - \frac{r_1 \bar{r}_2}{n+2} \right] \theta(r_2 - r_1) + \left(\frac{\bar{r}_1}{\bar{r}_2} \right)^{n+1} \left[\frac{\bar{r}_2 r_1}{n} - \frac{\bar{r}_1 r_2}{n+2} \right] \theta(r_1 - r_2) \right\} \quad (\text{H.28})$$

$$R_{(0)n}^{gq;V}(r_1, r_2) = C_F \frac{1}{n} \left\{ \delta(r_1 - r_2) + \frac{2}{n+1} \left[\left(\frac{r_1}{r_2} \right)^{n+1} \theta(r_2 - r_1) + \left(\frac{\bar{r}_1}{\bar{r}_2} \right)^{n+1} \theta(r_1 - r_2) \right] \right\}, \quad (\text{H.29})$$

$$R_{(0)n}^{gg;V}(r_1, r_2) = R_{(0)n}^{gg;A}(r_1, r_2) + 12C_A \frac{1}{n+1} \left\{ \left(\frac{r_1}{r_2} \right)^{n+1} \left[\frac{r_2 \bar{r}_1}{n} - \frac{r_1 \bar{r}_2}{n+2} \right] \theta(r_2 - r_1) + \left(\frac{\bar{r}_1}{\bar{r}_2} \right)^{n+1} \left[\frac{\bar{r}_2 r_1}{n} - \frac{\bar{r}_1 r_2}{n+2} \right] \theta(r_1 - r_2) \right\}, \quad (\text{H.30})$$

for even parity double distributions.

From Eqs. (H.24), (H.25) and (H.28), (H.29) one can derive the following reduction formulas for the nondiagonal kernels:

$$\frac{\partial}{\partial r_1} R_{(0)1}^{gg}(r_1, r_2) = -V_{(0)}^{gg}(r_1, r_2), \quad (\text{H.31})$$

$$\lim_{n \rightarrow 0} n R_{(0)n}^{gq}(r_1, r_2) = -\frac{\partial}{\partial r_1} V_{(0)}^{gq}(r_1, r_2), \quad (\text{H.32})$$

which hold for both even and odd parity sectors. To understand the structure of these relations, one should realize that constructing nondiagonal qg and gq kernels, one faces mismatching p_1^+ factors which are converted in the ER-BL limit into derivatives with respect to r_1 .

It is straightforward to check that all the kernels $R_{(0)n}^{ab;V}(r_1, r_2)$ and $R_{(0)n}^{ab;A}(r_1, r_2)$ obey the property

$$w_n(r_2) R_{(0)n}^{ab}(r_1, r_2) = w_n(r_1) R_{(0)n}^{ab}(r_2, r_1),$$

where $w_n(r) = (r\bar{r})^{n+1}$. Hence, the eigenfunctions of the evolution equations are orthogonal with the weight $w_n(r) = (r\bar{r})^{n+1}$, i.e., they are proportional to the Gegenbauer polynomials $C_k^{n+3/2}(r - \bar{r})$, see Refs. [240, 278] and also the papers [241, 256, 242, 243], where the general algorithm was applied to the evolution of flavor-singlet distribution amplitudes. Expanding the moment functions $Q_n^a(r; \mu^2)$ over the Gegenbauer polynomials $C_k^{n+3/2}(r - \bar{r})$

$$Q_n^a(r; \mu^2) = (r\bar{r})^{n+1} \sum_{k=0}^{\infty} C_k^{n+3/2}(r - \bar{r}) Q_{nk}^a(\mu) \quad (\text{H.33})$$

we get the one-loop evolution equation for the expansion coefficients

$$\frac{d}{d \ln \mu^2} Q_{nk}^a(\mu^2) = \frac{\alpha_s}{2\pi} \sum_b \Gamma_{(0)nk}^{ab;V} Q_{nk}^b(\mu^2), \quad (\text{H.34})$$

where $\Gamma_{(0)nk}^{ab;V}$ are the eigenvalues of the kernels $R_{(0)}^{ab;V}(r_1, r_2)$ related to the elements $\gamma_{(0)j}^{ab;V}$ of the usual flavor-singlet anomalous dimension matrix given in Eq. (4.152)

$$\Gamma_{(0)nk}^{qq;V} = -\frac{1}{2} \gamma_{(0)n+k}^{qq,V}, \quad \Gamma_{(0)nk}^{gq;V} = -\frac{n}{2} \gamma_{(0)n+k}^{gq,V}, \quad \Gamma_{(0)nk}^{gg;V} = -\frac{1}{2n} \gamma_{(0)n+k}^{gg,V}, \quad \Gamma_{(0)nk}^{gg;V} = -\frac{1}{2} \gamma_{(0)n+k}^{gg,V}; \quad (\text{H.35})$$

and similarly for the helicity-sensitive quantities $\Gamma_{(0)nk}^{ab;A}$, which are expressed through $\gamma_{(0)n+k}^{ab;A}$ of Eqs. (4.156) – (4.159).

In the approach outlined above, the outcome that the index j of the anomalous dimensions $\gamma_{(0)j}^{ab}$ is given just by the sum $n+k$ looks like an unexpected miracle. But it can be easily explained within the framework of the lightcone operators [230], where the solution of the evolution equation is known in the operator form, with the μ -dependence of multiplicatively renormalizable operators \mathbb{O}_j governed by a single anomalous dimension γ_j . In subsection 4.11.8, we discuss how this evolution on the operator level translates into the evolution of double distributions.

H.3 Asymptotic shape of double distributions

It is instructive to consider first two simplified situations for evolution of double distributions. In the quark nonsinglet case, the evolution is governed by γ_{n+k}^{qq} alone and the solution to Eq. (H.34) can be written in the form (H.33) as

$$Q_n^{q,\text{NS}}(r; \mu^2) = (r\bar{r})^{n+1} \sum_{k=0}^{\infty} C_k^{n+3/2}(r - \bar{r}) Q_{nk}^{q,\text{NS}}(\mu_0^2) \left(\frac{\alpha_s(\mu_0^2)}{\alpha_s(\mu^2)} \right)^{\gamma_{(0)n+k}^{qq;V}/\beta_0}, \quad (\text{H.36})$$

Since $\gamma_{(0)0}^{qq;V} = 0$ while all the anomalous dimensions $\gamma_{(0)j}^{qq;V}$ with $j \geq 1$ are positive, only $Q_0^{\text{NS}}(r; \mu^2)$ survives in the asymptotic limit $\mu^2 \rightarrow \infty$ while all the moments $Q_n^{q,\text{NS}}(r; \mu^2)$ with $n \geq 1$ evolve to zero values. Hence, in the formal $\mu^2 \rightarrow \infty$ limit, we have

$$Q^{q,\text{NS}}(s, r; \mu^2 \rightarrow \infty) \sim \delta(s) r\bar{r}, \quad (\text{H.37})$$

i.e., in each of its variables, the limiting function $Q^{\text{NS}}(s, r; \mu^2 \rightarrow \infty)$ acquires the characteristic asymptotic form dictated by the nature of the variable: $\delta(s)$ is the limiting form of parton densities [19, 27], while the $r\bar{r}$ -form is the asymptotic shape for the lowest-twist two-body distribution amplitudes [237, 240].

Another example is the evolution of the gluon distribution in pure gluodynamics. It is governed by $\gamma_{(0)n+k}^{gg;V}$ with $\beta_0 = -11N_c/3$. Note that the lowest local operator in this case corresponds to $n = 1$. Furthermore, in pure gluodynamics, $\gamma_{(0)1}^{gg;V}$ vanishes while $\gamma_{(0)j}^{gg;V} > 0$ if $j \geq 2$. This means that in the $\mu^2 \rightarrow \infty$ limit we have

$$s Q^g(s, r; \mu^2 \rightarrow \infty) \sim \delta(s) (r\bar{r})^2. \quad (\text{H.38})$$

Finally, in QCD one should take into account the effects due to the quark-gluon mixing. Performing the analysis identical to the one in Section 4.11.6, we find

$$\sum_q Q_{10}^q(\mu^2 \rightarrow \infty) \rightarrow \frac{N_f}{4C_F + N_f}, \quad Q_{10}^g(\mu^2 \rightarrow \infty) \rightarrow \frac{4C_F}{4C_F + N_f}. \quad (\text{H.39})$$

Since all the combinations of moments Q_{nk}^a with $n+k \geq 2$ vanish in the $\mu^2 \rightarrow \infty$ limit, we obtain

$$s \sum_q Q^q(s, r; \mu^2 \rightarrow \infty) \rightarrow 30 \frac{N_f}{4C_F + N_f} \delta(s) (r\bar{r})^2, \quad (\text{H.40})$$

$$s Q^g(s, r; \mu^2 \rightarrow \infty) \rightarrow 30 \frac{4C_F}{4C_F + N_f} \delta(s) (r\bar{r})^2. \quad (\text{H.41})$$

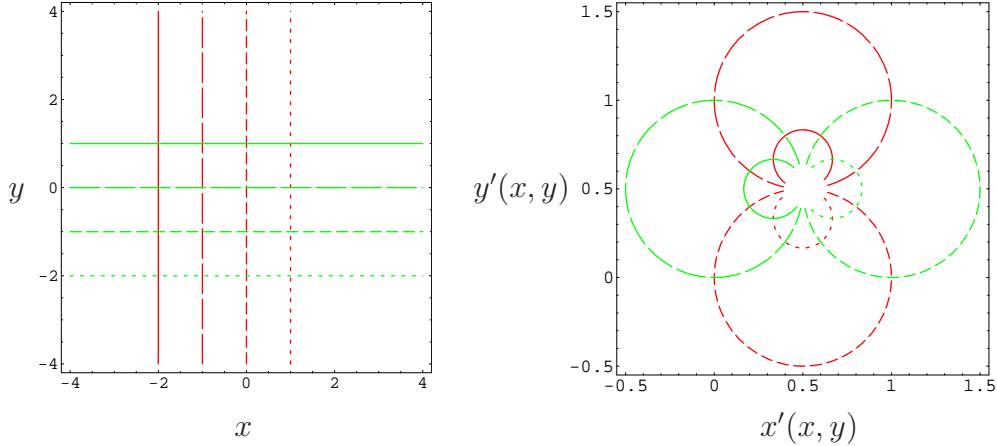


Figure 62: Visualization of the finite conformal boost (I.8) for $t = z = 0$ and transformation parameter $d^\mu = (0, -1, -1, 0)$. The angles are preserved under the transformation.

The former equation here can be rewritten in the form

$$\sum_q Q^q(s, r; \mu^2 \rightarrow \infty) \rightarrow -30 \frac{N_f}{4C_F + N_f} \delta'(s) (r\bar{r})^2. \quad (\text{H.42})$$

When reduced to GPDs, the asymptotic solutions found here reproduces the results established in Sections 4.11.2 and 4.11.6.

I Elements of the conformal group

The conformal group is the maximal extension of the Poincaré group that leaves the light cone invariant. It is the symmetry of the classical QCD Lagrangian and is thus of physical interest for light-cone-dominated as well as high-energy processes, where the asymptotic freedom of QCD implies that its approximation by a non-interacting theory is good starting point.

Conformal transformations are coordinate transformation of the metric of the d -dimensional space of the form

$$g'^{\mu\nu}(z') = \Omega(z) g^{\mu\nu}(z). \quad (\text{I.1})$$

Let us consider the infinitesimal transformation,

$$\Omega(z) \approx 1 + \omega(z), \quad (\text{I.2})$$

and count the number of independent parameters involved. The variation of the metric at different space-time points is (cf. Eq. (E.3))

$$\delta g^{\mu\nu}(z) = g'^{\mu\nu}(z') - g^{\mu\nu}(z) = \omega(z) g^{\mu\nu}(z) = \partial^\mu \epsilon^\nu(z) + \partial^\nu \epsilon^\mu(z), \quad (\text{I.3})$$

with $\delta z^\mu \equiv \epsilon^\mu(z)$. Contracting both sides with the inverse metric tensor $[g^{\mu\nu}]^{-1} = g_{\mu\nu}$, we get

$$\omega(z) = \frac{2}{d} \partial \cdot \epsilon(z). \quad (\text{I.4})$$

Substituting it back into (I.3) we obtain the Killing equation

$$\partial^\mu \epsilon^\nu(z) - \partial^\nu \epsilon^\mu(z) - \frac{2}{d} g^{\mu\nu}(z) \partial \cdot \epsilon(z) = 0. \quad (\text{I.5})$$

Differentiating this expression with respect to z^μ and z^ν , i.e., applying ∂^μ and ∂^ν , respectively, and summing up the results, we use the Killing equation (I.5) to find

$$\{(d-2)\partial^\mu \partial^\nu + g^{\mu\nu}(z)\partial^2\} \partial \cdot \epsilon(z) = 0. \quad (\text{I.6})$$

Here we have assumed that $\partial \cdot \epsilon(z)$ is nonsingular. We will not consider the case of $d = 2$ which leads to an infinite-dimensional algebra. For other $d \neq 2$, the solution for the Killing vector reads

$$\epsilon^\mu(z) = d^\mu z^2 + (c \delta^{\mu\nu} + b^{\mu\nu}) z_\nu + a^\mu. \quad (\text{I.7})$$

These infinitesimal transformations can be easily integrated to produce finite transformations. As a result, one finds from the form of the general solution (I.7) that the well-known Poincaré transformations, are augmented by dilatations

$$z^\mu \xrightarrow{D} z'^\mu = e^c z^\mu,$$

and special conformal boosts

$$z^\mu \xrightarrow{K} z'^\mu = \frac{z^\mu + d^\mu z^2}{1 + 2d \cdot z + d^2 z^2}. \quad (\text{I.8})$$

The latter are composed of the sequence of an inversion $z^\mu \rightarrow z^\mu/z^2$, a translation $z^\mu \rightarrow z^\mu + d^\mu$, and a further inversion. The finite conformal boost is visualized in Fig. 62. It clearly demonstrates the angle-preserving nature of the transformation: all angles remain rectangular before and after the transformation is applied.

The conformal factor $[1 + 2d \cdot z + d^2 z^2]^{-1}$ is singular on the light-cone cone $z^2 = 0$. As a result, the special conformal transformations are not well defined as global transformations in the Minkowski space-time. Moreover, it is possible to transform non-causally connected regions into one another, which violates fundamental principles of nature. To apply the conformal group to the quantum field theory in Minkowski space-time, it is sufficient in our studies to restrict to infinitesimal special conformal transformations: this eliminates both of the aforementioned problems.

I.1 Conformal algebra

The conformal transformations form a group. In four space-time dimensions it is a fifteen-parameter group $SO(4, 2)$. Below, we summarize specific types of transformations and display the change of the space-time coordinates which they induce:

- | | | |
|--------------------------|------------------------|--|
| • Lorentz transformation | $\mathbb{M}^{\mu\nu}:$ | $\delta^M z^\mu = \omega^{\mu\nu} z_\nu$ |
| • Translation | $\mathbb{P}^\mu:$ | $\delta^P z^\mu = a^\mu$ |
| • Dilatation | $\mathbb{D}:$ | $\delta^D z^\mu = \lambda z^\mu$ |
| • Conformal boost | $\mathbb{K}^\mu:$ | $\delta^K z^\mu = c_\nu (2z^\mu z^\nu - z^2 g^{\mu\nu})$ |

The corresponding generators act in the Hilbert space of field operators and obey the commutator algebra:

$$\begin{aligned}
i[\mathbb{M}^{\mu\nu}, \mathbb{M}^{\rho\sigma}] &= g^{\mu\rho}\mathbb{M}^{\nu\sigma} + g^{\nu\sigma}\mathbb{M}^{\mu\rho} - g^{\mu\sigma}\mathbb{M}^{\nu\rho} - g^{\nu\rho}\mathbb{M}^{\mu\sigma}, \\
i[\mathbb{M}^{\mu\nu}, \mathbb{P}^\rho] &= g^{\mu\rho}\mathbb{P}^\nu - g^{\nu\rho}\mathbb{P}^\mu, \\
i[\mathbb{M}^{\mu\nu}, \mathbb{K}^\rho] &= g^{\mu\rho}\mathbb{K}^\nu - g^{\nu\rho}\mathbb{K}^\mu, \\
i[\mathbb{P}^\mu, \mathbb{D}] &= -\mathbb{P}^\mu, \\
i[\mathbb{P}^\mu, \mathbb{K}^\nu] &= -2g^{\mu\nu}\mathbb{D} + 2\mathbb{M}^{\mu\nu}, \\
i[\mathbb{D}, \mathbb{K}^\mu] &= -\mathbb{K}^\mu.
\end{aligned} \tag{I.9}$$

The remaining commutators vanish.

I.2 Induced representations

The infinitesimal conformal variation of a quantum field $\Phi(x)$ is determined by its commutator

$$\delta^G \Phi(z) = i[\Phi(z), \mathbb{G}], \tag{I.10}$$

with one of the generators from the conformal algebra $\mathbb{G} = \mathbb{P}^\mu, \mathbb{M}^{\mu\nu}, \dots$. We are interested in the representation of these generators, acting on the Hilbert space, in terms of differential operators,

$$[\mathbb{G}, \Phi(z)] \equiv \hat{G}\Phi(z). \tag{I.11}$$

The differential representation of these generators can be easily derived with the help of the standard technique of induced representations [462] making use of the coset parametrization of the Minkowski space

$$\Phi(z) = e^{iz \cdot \mathbb{P}} \Phi(0) e^{-iz \cdot \mathbb{P}}. \tag{I.12}$$

Let us consider the stability subgroup of the conformal group, i.e., transformations which leave the plane $z^\mu = 0$ unaffected. This small group contains the generators $\{\mathbb{M}^{\mu\nu}, \mathbb{D}, \mathbb{K}^\mu\}$,

$$[\mathbb{M}^{\mu\nu}, \Phi(0)] = -i\Sigma^{\mu\nu}\Phi(0), \quad [\mathbb{D}, \Phi(0)] = -i\Delta\Phi(0), \quad [\mathbb{K}^\mu, \Phi(0)] = \kappa^\mu\Phi(0). \tag{I.13}$$

The representation matrices $\Sigma_{\mu\nu}$, Δ and κ_μ , obey the algebra

$$[\Delta, \kappa^\mu] = \kappa^\mu, \quad [\Sigma^{\mu\nu}, \Delta]_- = 0, \quad [\Delta, \Delta] = 0. \tag{I.14}$$

We take $\Sigma_{\mu\nu}$ that forms an irreducible representation of the homogeneous Lorentz group, acting on the fields as follows

$$\Sigma^{\mu\nu}\psi = \frac{1}{4}[\gamma^\mu, \gamma^\nu]\psi, \quad \Sigma^{\mu\nu}A^\rho = g^{\mu\rho}A^\nu - g^{\nu\rho}A^\sigma, \quad \Sigma^{\mu\nu}F^{\rho\sigma} = g^{\mu\rho}F^{\nu\sigma} - g^{\nu\rho}F^{\mu\sigma} - (\rho \leftrightarrow \sigma). \tag{I.15}$$

Since Δ commutes with the generators of the small group, by the Shur's lemma it must be multiple of unity,

$$\Delta = d \cdot \mathbb{1}_{[n] \times [n]}, \tag{I.16}$$

with $\mathbb{1}_{[n] \times [n]}$ being an $[n] \times [n]$ unity matrix acting on the n -dimensional vector Φ , which is a number for the scalar field, and a four-component column for the Dirac fermion. The value of d gives the mass dimensions of fields

$$d_g = 1, \quad d_q = \frac{3}{2}. \tag{I.17}$$

Then from (I.14) we have

$$\kappa^\mu = 0. \quad (\text{I.18})$$

Our goal now is to find the representation of the generators of scaling \mathbb{D} and special conformal \mathbb{K}^μ transformations in the basis of field operators depending on the space-time coordinate z^μ . Acting with $e^{iz \cdot \mathbb{P}}$ and $e^{-iz \cdot \mathbb{P}}$ from the left and from the right on (I.13), we get

$$[\Phi(z), e^{iz \cdot \mathbb{P}} \mathbb{D} e^{-iz \cdot \mathbb{P}}] = id\Phi(z). \quad (\text{I.19})$$

A little algebra leads to the result

$$\begin{aligned} e^{iz \cdot \mathbb{P}} \mathbb{D} e^{-iz \cdot \mathbb{P}} &= \sum_{n=0}^{\infty} \frac{i^n}{n!} z_{\mu_1} \dots z_{\mu_n} [\mathbb{P}^{\mu_1}, [\dots, [\mathbb{P}^{\mu_n}, \mathbb{D}]]] \\ &= \mathbb{D} + iz_\mu [\mathbb{P}^\mu, \mathbb{D}] = \mathbb{D} - z \cdot \mathbb{P}, \end{aligned} \quad (\text{I.20})$$

where only one commutator has survived in the sum, while all the other have vanished by the use of the conformal algebra. Substituting this back into Eq. (I.19), we get finally the representation of the dilatation in the basis of field operators

$$[\Phi(z), \mathbb{D}] = i(d + z \cdot \partial)\Phi(z). \quad (\text{I.21})$$

Obviously, d is the canonical dimension of the field.

In a similar way, we find the action of the special conformal boosts

$$[\Phi(z), e^{iz \cdot \mathbb{P}} \mathbb{K}^\mu e^{-iz \cdot \mathbb{P}}] = 0. \quad (\text{I.22})$$

With the first three terms surviving in the series, we can write

$$\begin{aligned} e^{iz \cdot \mathbb{P}} \mathbb{K}^\mu e^{-iz \cdot \mathbb{P}} &= \sum_{n=0}^{\infty} \frac{i^n}{n!} z_{\mu_1} \dots z_{\mu_n} [\mathbb{P}^{\mu_1}, [\dots, [\mathbb{P}^{\mu_n}, \mathbb{K}^\mu]]] \\ &= \mathbb{K}^\mu - 2z_\nu (g^{\mu\nu} \mathbb{D} + \mathbb{M}^{\mu\nu}) + (2z^\mu z^\nu - z^2 g^{\mu\nu}) \mathbb{P}_\nu. \end{aligned} \quad (\text{I.23})$$

Making use of the representation of \mathbb{P}^μ , $\mathbb{M}^{\mu\nu}$ and \mathbb{D} , we finally find

$$[\Phi(z), \mathbb{K}^\mu] = i \{(2z^\mu z^\nu - z^2 g^{\mu\nu}) \partial_\nu + 2dz^\mu + 2\Sigma^{\mu\nu} z_\nu\} \Phi(z). \quad (\text{I.24})$$

To summarize, the representation of all generators from the conformal algebra reads

$$\begin{aligned} i\widehat{P}^\mu &= \partial^\mu, \\ i\widehat{M}^{\mu\nu} &= z^\mu \partial^\nu - z^\nu \partial^\mu + \Sigma^{\mu\nu}, \\ i\widehat{D} &= d + z^\mu \partial_\mu, \\ i\widehat{K}^\mu &= 2dz^\mu - z^2 \partial^\mu + 2z^\mu z^\nu \partial_\nu + 2z_\nu \Sigma^{\mu\nu}. \end{aligned} \quad (\text{I.25})$$

J Scheme transformation matrix

Let us prove Eq. (4.224). Using Eq. (4.195), written in the form

$$a(j, k) \gamma_{jk}^{\text{ND}} = (\gamma_j - \gamma_k) \gamma_{jk}^c(l) + [\boldsymbol{\gamma}^{\text{ND}}, \boldsymbol{\gamma}^c(l)]_{jk}, \quad (\text{J.1})$$

we get

$$a(k', k'') b_{k' k''}(k) = -\gamma_{k' k''}^c(k) - \frac{1}{\gamma_{k'} - \gamma_k} [\boldsymbol{\gamma}^{\text{ND}}, \boldsymbol{\gamma}^c(l)]_{k' k''} + \frac{1}{\gamma_{k'} - \gamma_k} \gamma_{k' k''}^c(l) (\gamma_{k''} - \gamma_k). \quad (\text{J.2})$$

Note, that Eq. (4.198) ensures that the right-hand side of this equation does not depend on l , i.e.,

$$a(k', k'') b_{k' k''}(k)|_{l+n} = a(k', k'') b_{k' k''}(k)|_l, \quad (\text{J.3})$$

for any $n \in \mathbb{N}$. Using the property

$$a(k_0, k_N) = \sum_{i=0}^{N-1} a(k_i, k_{i+1}), \quad (\text{J.4})$$

one proves by induction that

$$\begin{aligned} a(k', k'') \{ \mathbf{b}^N(k) \}_{k' k''} &= -\gamma_{k' k''}^c(l) \{ \mathbf{b}^{N-1}(k) \}_{k''' k''} \\ &\quad + \sum_{n=0}^{N-2} \{ \mathbf{b}^n(k) \mathbf{M}(k) \mathbf{b}^{N-n-2}(k) \}_{k' k''} \\ &\quad - \sum_{n=0}^{N-1} \{ \mathbf{b}^n(k) \mathbf{M}(k) \mathbf{b}^{N-n-1}(k) \}_{k' k''} \\ &\quad + \{ \mathbf{b}^{N-1}(k) \}_{k' k''} \frac{1}{\gamma_{k''} - \gamma_k} \gamma_{k''}^c(l) (\gamma_{k''} - \gamma_k), \end{aligned} \quad (\text{J.5})$$

where the matrix $\mathbf{M}(k)$ has the following elements

$$M_{k' k''}(k) \equiv \frac{1}{\gamma_{k'} - \gamma_k} [\boldsymbol{\gamma}^{\text{ND}}, \boldsymbol{\gamma}^c(l)]_{k' k''}, \quad (\text{J.6})$$

with the l -dependence made implicit in the notation for \mathbf{M} .

For the value $k = k''$, which enters (4.195), the last term in Eq. (J.5) is proportional to $\{ \mathbf{b}(k'') \}_{k' k''} \gamma_{k''}^c(l)$. Therefore, using the l -independence of the right-hand side of (J.5), one can get rid of this term by setting $l = k''$. Thus,

$$\begin{aligned} a(k', k'') \mathcal{B}_{k' k''} &= -\gamma_{k' k''}^c(k'') \sum_{N=1}^{\infty} \{ \mathbf{b}^{N-1}(k) \}_{k''' k''} \\ &\quad + \sum_{N=1}^{\infty} \left\{ \sum_{n=0}^{N-2} \{ \mathbf{b}^n(k) \mathbf{M}(k) \mathbf{b}^{N-n-2}(k) \}_{k' k''} - \sum_{n=0}^{N-1} \{ \mathbf{b}^n(k) \mathbf{M}(k) \mathbf{b}^{N-n-1}(k) \}_{k' k''} \right\}, \end{aligned} \quad (\text{J.7})$$

so that the infinite sum of contributions in the curly brackets vanishes identically. Therefore, we find that the transformation matrix from the modified minimal subtraction scheme to the conformal scheme reads

$$\mathcal{B}_{jk} = \left\{ \frac{1}{1 + \mathbf{A}} \right\}_{jk}, \quad \text{with} \quad \mathbf{A}_{jk} = \frac{\gamma_{jk}^c(k)}{a(j, k)}. \quad (\text{J.8})$$

K Two-loop anomalous dimensions

In this appendix we give a concise summary of results about two-loop anomalous dimensions: their explicit form for all twist-two sectors as well as equalities among them arising in the minimal supersymmetric extension of QCD. Before we do this, a few comments are in order.

First of all, we have to keep in mind the difference between the diagonal anomalous dimensions of conformal operators, as defined in Eq. (4.141), and the forward anomalous dimensions of the conventional Wilson operators (4.67). They are related in the following way

$$\gamma_j^{qq} = \gamma_j^{qq;fw}, \quad \gamma_j^{gg} = \frac{6}{j} \gamma_j^{gg;fw}, \quad \gamma_j^{gq} = \frac{j}{6} \gamma_j^{gq;fw}, \quad \gamma_j^{gq} = \gamma_j^{gq;fw}. \quad (\text{K.1})$$

The pre-factors in the off-diagonal matrix elements of the two-by-two anomalous dimension matrix come from the standard definition of the Gegenbauer polynomials, as explained in Section 4.7.1.

The anomalous dimensions for even and odd moments of the forward parton densities are not analytic functions of the spin. They depend on the signature factor $\sigma = (-1)^{j+1}$.

As it is well known, provided one is not restricted to particular flavor combinations of quark operators, they start to mix with gluons, and the resulting renormalization group equation takes a matrix form.

Let us now set up the terminology, which was implicitly used in the main text. The combination of quark densities of the form

$$q_{\text{NS}}^{(+)} = (u + \bar{u}) - (d + \bar{d}), \quad (\text{K.2})$$

is called the nonsinglet combination with positive signature. It is distinct from yet another nonsinglet combination

$$q_{\text{NS}}^{(-)} = q - \bar{q} \equiv q_v, \quad (\text{K.3})$$

which is known as the valence quark distribution. It does not mix with gluons either. Finally, the singlet quark distribution

$$q_s = q + \bar{q}, \quad (\text{K.4})$$

has the positive $\sigma = 1$ parity.

Without further ado, let us give the two-loop anomalous dimensions in all twist-two sectors of QCD making use of the following harmonic sums

$$S_\ell(j) = \sum_{k=1}^j \frac{1}{k^\ell}, \quad S'_\ell(j) = 2^{\ell-1} \sum_{k=1}^j [1 + (-1)^k] \frac{1}{k^\ell}, \quad \tilde{S}(j) = \sum_{k=1}^j \frac{(-1)^k}{k^2} S_1(k).$$

K.1 Even-parity sector

The non-singlet anomalous dimension is [474]

$$\begin{aligned} \gamma_{(1)j}^{\text{NS},\text{fw}} &= \left(C_F^2 - \frac{1}{2} C_F C_A \right) \left\{ \frac{4(2j+3)}{(j+1)^2(j+2)^2} S(j+1) - 2 \frac{3j^3 + 10j^2 + 11j + 3}{(j+1)^3(j+2)^3} \right. \\ &\quad + 4 \left(2S_1(j+1) - \frac{1}{(j+1)(j+2)} \right) (S_2(j+1) - S'_2(j+1)) \\ &\quad \left. + 16\tilde{S}(j+1) + 6S_2(j+1) - \frac{3}{4} - 2S'_3(j+1) + 4(-1)^{j+1} \frac{2j^2 + 6j + 5}{(j+1)^3(j+2)^3} \right\} \end{aligned}$$

$$\begin{aligned}
& + C_F C_A \left\{ S_1(j+1) \left(\frac{134}{9} + \frac{2(2j+3)}{(j+1)^2(j+2)^2} \right) \right. \\
& - 4S_1(j+1)S_2(j+1) + S_2(j+1) \left(-\frac{13}{3} + \frac{2}{(j+1)(j+2)} \right) \\
& - \frac{43}{24} - \frac{1}{9} \frac{151j^4 + 867j^3 + 1792j^2 + 1590j + 523}{(j+1)^3(j+2)^3} \Big\} \\
& + C_F T_F N_f \left\{ -\frac{40}{9} S_1(j+1) + \frac{8}{3} S_2(j+1) + \frac{1}{3} + \frac{4}{9} \frac{11j^2 + 27j + 13}{(j+1)^2(j+2)^2} \right\}. \tag{K.5}
\end{aligned}$$

The singlet anomalous dimensions are [475]

$$\gamma_{(1)j}^{qg;\text{fw},V} = \gamma_{(1)j}^{\text{NS,fw}} - 4C_F T_F N_f \frac{5j^5 + 57j^4 + 227j^3 + 427j^2 + 404j + 160}{j(j+1)^3(j+2)^3(j+3)^2}, \tag{K.6}$$

$$\begin{aligned}
\gamma_{(1)j}^{qg;\text{fw},V} &= -2C_A T_F N_f \left\{ (-2S_1^2(j+1) + 2S_2(j+1) - 2S'_2(j+1)) \frac{j^2 + 3j + 4}{(j+1)(j+2)(j+3)} \right. \\
&+ \frac{960 + 2835j + 4057j^2 + 3983j^3 + 3046j^4 + 1777j^5 + 731j^6 + 195j^7 + 30j^8 + 2j^9}{j(j+1)^3(j+2)^3(j+3)^3} \\
&+ (-1)^{j+1} \frac{141 + 165j + 92j^2 + 27j^3 + 3j^4}{(j+1)(j+2)^3(j+3)^3} + 8 \frac{(2j+5)}{(j+2)^2(j+3)^2} S_1(j+1) \Big\} \\
&- 2C_F T_F N_f \left\{ (2S_1^2(j+1) - 2S_2(j+1) + 5) \frac{j^2 + 3j + 4}{(j+1)(j+2)(j+3)} \right. \\
&- 4 \frac{S_1(j+1)}{(j+1)^2} + \frac{11j^4 + 70j^3 + 159j^2 + 160j + 64}{(j+1)^3(j+2)^3(j+3)} \Big\}, \tag{K.7}
\end{aligned}$$

$$\begin{aligned}
\gamma_{(1)j}^{gg;\text{fw},V} &= -C_F^2 \left\{ (-2S_1^2(j+1) + 10S_1(j+1) - 2S_2(j+1)) \frac{j^2 + 3j + 4}{j(j+1)(j+2)} \right. \\
&- 4 \frac{S_1(j+1)}{(j+2)^2} - \frac{12j^6 + 102j^5 + 373j^4 + 740j^3 + 821j^2 + 464j + 96}{j(j+1)^3(j+2)^3} \Big\} \\
&- 2C_A C_F \left\{ (S_1^2(j+1) + S_2(j+1) - S'_2(j+1)) \frac{j^2 + 3j + 4}{j(j+1)(j+2)} \right. \\
&+ \frac{1296 + 10044j + 30945j^2 + 47954j^3 + 42491j^4 + 22902j^5 + 7515j^6 + 1384j^7 + 109j^8}{9j^2(j+1)^3(j+2)^2(j+3)^2} \\
&+ (-1)^{j+1} \frac{8 + 9j + 4j^2 + j^3}{(j+1)^3(j+2)^3} - \frac{17j^4 + 68j^3 + 143j^2 + 128j + 24}{3j^2(j+1)^2(j+2)} S_1(j+1) \Big\} \\
&- \frac{8}{3} C_F T_F N_f \left\{ \left(S_1(j+1) - \frac{8}{3} \right) \frac{j^2 + 3j + 4}{j(j+1)(j+2)} + \frac{1}{(j+2)^2} \right\}, \tag{K.8}
\end{aligned}$$

$$\begin{aligned}
\gamma_{(1)j}^{gg;\text{fw},V} &= C_A T_F N_f \left\{ -\frac{40}{9} S_1(j+1) + \frac{8}{3} + \frac{8}{9} \frac{19j^4 + 114j^3 + 275j^2 + 312j + 138}{j(j+1)^2(j+2)^2(j+3)} \right\} \\
&+ C_F T_F N_f \left\{ 2 + 4 \frac{2j^6 + 16j^5 + 51j^4 + 74j^3 + 41j^2 - 8j - 16}{j(j+1)^3(j+2)^3(j+3)} \right\} \\
&+ C_A^2 \left\{ \frac{134}{9} S_1(j+1) + 16S_1(j+1) \frac{2j^5 + 15j^4 + 48j^3 + 81j^2 + 66j + 18}{j^2(j+1)^2(j+2)^2(j+3)^2} \right\}
\end{aligned}$$

$$\begin{aligned}
& - \frac{16}{3} + 8S'_2(j+1) \frac{j^2 + 3j + 3}{j(j+1)(j+2)(j+3)} - 4S_1(j+1)S'_2(j+1) \\
& + 8\tilde{S}(j+1) - S'_3(j+1) - \frac{1}{9} \frac{1457j^9 + 6855j^8 + 44428j^7 + 163542j^6}{j^2(j+1)^3(j+2)^3(j+3)^3} \\
& - \frac{1}{9} \frac{1376129j^5 + 557883j^4 + 529962j^3 + 308808j^2 + 101088j + 15552}{j^2(j+1)^3(j+2)^3(j+3)^3} \Big\}. \tag{K.9}
\end{aligned}$$

K.2 Odd-parity sector

The forward anomalous dimensions in the odd parity sector are given by [476]:

$$\gamma_{(1)j}^{qg;\text{fw},A} = \gamma_{(1)j}^{\text{NS,fw}} + 4C_F T_F N_f \frac{(j+3)(4+5j+3j^2+j^3)}{(j+1)^3(j+2)^3}, \tag{K.10}$$

$$\begin{aligned}
\gamma_{(1)j}^{qg;\text{fw},A} &= 2C_F T_F N_f \left\{ -\frac{j(16+49j+60j^2+30j^3+5j^4)}{(j+1)^3(j+2)^3} + \frac{4j}{(j+1)^2(j+2)} S_1(j+1) \right. \\
&\quad \left. - \frac{2j}{(j+1)(j+2)} (S_1^2(j+1) - S_2(j+1)) \right\} + 4C_A T_F N_f \left\{ \frac{8+4j-7j^2-10j^3-6j^4-j^5}{(j+1)^3(j+2)^3} \right. \\
&\quad \left. - \frac{4S_1(j+1)}{(j+1)(j+2)^2} + \frac{j}{(j+1)(j+2)} (S_1^2(j+1) - S_2(j+1) + S'_2(j+1)) \right\}, \tag{K.11}
\end{aligned}$$

$$\begin{aligned}
\gamma_{(1)j}^{qg;\text{fw},A} &= 8C_F T_F N_f \left\{ \frac{(j+3)(5j+7)}{9(j+1)(j+2)^2} - \frac{(j+3)}{3(j+1)(j+2)} S_1(j+1) \right\} \\
&\quad + C_F^2 \left\{ \frac{(j+3)(3j+4)(3+14j+12j^2+3j^3)}{(j+1)^3(j+2)^3} - \frac{2(j+3)(3j+4)}{(j+1)(j+2)^2} S_1(j+1) \right. \\
&\quad \left. + \frac{2(j+3)}{(j+1)(j+2)} (S_1^2(j+1) + S_2(j+1)) \right\} \\
&\quad + 2C_A C_F \left\{ -\frac{750+2380j+3189j^2+2098j^3+651j^4+76j^5}{9(j+1)^3(j+2)^3} \right. \\
&\quad \left. + \frac{45+44j+11j^2}{3(j+1)^2(j+2)} S_1(j+1) + \frac{j+3}{(j+1)(j+2)} (-S_1^2(j+1) - S_2(j+1) + S'_2(j+1)) \right\}, \tag{K.12}
\end{aligned}$$

$$\begin{aligned}
\gamma_{(1)j}^{qg;\text{fw},A} &= 2C_F T_F N_f \frac{8+30j+70j^2+71j^3+35j^4+9j^5+j^6}{(j+1)^3(j+2)^3} \\
&\quad + 8C_A T_F N_f \left\{ \frac{35+75j+52j^2+18j^3+3j^4}{9(j+1)^2(j+2)^2} - \frac{5}{9} S_1(j+1) \right\} \\
&\quad + C_A^2 \left(-\frac{1768+5250j+7075j^2+4974j^3+1909j^4+432j^5+48j^6}{9(j+1)^3(j+2)^3} \right. \\
&\quad \left. + \frac{2}{9} \frac{484+948j+871j^2+402j^3+67j^4}{(j+1)^2(j+2)^2} S_1(j+1) \right. \\
&\quad \left. + \frac{8S'_2(j+1)}{(j+1)(j+2)} - 4S_1(j+1)S'_2(j+1) - S'_3(j+1) + 8\tilde{S}(j+1) \right\}. \tag{K.13}
\end{aligned}$$

K.3 Maximal-helicity sector

Since the quark and gluon operators of the maximal helicity have different quantum numbers with respect to the helicity operator (A.16), they do not mix with each other under renormalization and thus have an autonomous scale dependence. The anomalous dimension of the quark transversity sector is [477]

$$\begin{aligned} \gamma_{(1)j}^{qg;fw,T} = & C_F^2 \left\{ -\frac{1}{4} - 2S_1(j+1) + S_2(j+1) \right\} + \frac{8}{9} C_F T_F N_f \left\{ \frac{3}{8} - 5S_1(j+1) + 3S_2(j+1) \right\} \\ & + \frac{C_A C_F}{4} \left\{ -\frac{20}{3} + \frac{572}{9} S_1(j+1) - \frac{58}{3} S_2(j+1) - 16S_1(j+1)S_2(j+1) \right\} \\ & - 2C_F \left(C_F - \frac{C_A}{2} \right) \left\{ \frac{1}{4} + \frac{1 + (-1)^j}{(j+1)(j+2)} - \frac{5}{2} S_2(j+1) + S'_3(j+1) - 8\tilde{S}(j+1) \right. \\ & \left. - S_1(j+1) (1 + 4S_2(j+1) - 4S'_2(j+1)) \right\}, \end{aligned} \quad (\text{K.14})$$

while the gluon it reads [478]

$$\begin{aligned} \gamma_{(1)j}^{gg;fw,T} = & C_A^2 \left\{ S_1(j+1) \left(\frac{134}{9} - 4S'_2(j+1) \right) - S'_3(j+1) + 8\tilde{S}(j+1) - \frac{1}{j(j+3)} - \frac{16}{3} \right\} \\ & + C_A T_F N_f \left\{ \frac{8}{3} - \frac{40}{9} S_1(j+1) - \frac{2}{j(j+3)} \right\} + C_F T_F N_f \frac{2(j+1)(j+2)}{j(j+3)}. \end{aligned} \quad (\text{K.15})$$

K.4 Supersymmetric relations between anomalous dimensions

The twist-two anomalous dimensions quoted in the previous appendix for conventional Wilson operators and in Section 4.9.4 for conformal operators are defined by rather lengthy expressions and an independent check on their correctness is very instructive. In QCD per se, there are no relations between the elements of the quark-gluon mixing matrix. However, in its closest cousin—the $\mathcal{N} = 1$ super-Yang-Mills theory which operates in terms of a single Majorana quark (gaugino) coupled to gluodynamics—the presence of the space-time supersymmetry, which transforms a gaugino into a gluon and then back, allows one to establish a set of equations between the elements of the mixing matrix. In perturbation theory the adjustments which have to be made are minimal. Merely, one has to equate the color Casimir operators in all QCD expression to the rank of the color group N_c , accounting for the fact that contrary to QCD in $\mathcal{N} = 1$ super-Yang-Mills there is just a single flavor of quarks and that it belongs to the adjoint representation of the color group. Thus, the “supersymmetric limit” of ordinary QCD is achieved via the identification $C_A = C_F = 2T_F = N_c$ in all QCD anomalous dimensions. This is not the end of the story however, since the conventional procedure of dimensional regularization, used to operate with infinities in perturbation theory, explicitly breaks supersymmetry. A way out was proposed a long time ago in the form of a regularization procedure dubbed dimensional reduction [479, 480]. According to it, the dimension of space-time is reduced from four down to $d = 4 - 2\varepsilon$, while all fields have the same number of components as in four dimensions thus preserving the equality of bosonic and fermionic degrees of freedom. Instead of redoing all calculations anew with the modified regularization procedure, one can merely perform the scheme transformation via a finite rotation of the two-vector (4.146) of quark and gluon conformal operators (4.138) from the standard dimensional regularization

(DREG) to the dimensional reduction (DRED) schemes

$$\mathbf{O}_{\text{DRED}}^{\text{R}} = \mathbf{z} \cdot \mathbf{O}_{\text{DREG}}^{\text{R}}.$$

Thus, the quark-gluon anomalous dimension mixing matrix, γ , for the regularization with DRED is related to the one with DREG via

$$\gamma^{\text{DRED}} = \mathbf{z} \cdot \gamma^{\text{DREG}} \cdot \mathbf{z}^{-1} - \beta(g) \frac{\partial}{\partial g} \mathbf{z} \cdot \mathbf{z}^{-1}. \quad (\text{K.16})$$

The transformation matrix \mathbf{z} is deduced from the difference of counterterms determining the anomalous dimensions of the quark and gluon conformal operators in the above two schemes. It takes the following form to one-loop order in coupling constant [483]

$$\mathbf{z}_{jk} = \mathbb{1}_{[2] \times [2]} \delta_{jk} + \frac{\alpha_s}{2\pi} N_c \left\{ \mathbf{z}_j \delta_{jk} + \mathbf{z}_{jk}^{\text{ND}} \theta_{j-2,k} [1 + (-1)^{j-k}] \right\}, \quad (\text{K.17})$$

with the following matrices

$$\mathbf{z}_j^V = \begin{pmatrix} -\frac{j(j+3)}{2(j+1)(j+2)} & \frac{12}{j(j+2)(j+3)} \\ \frac{j}{6(j+2)} & -\frac{1}{6} \end{pmatrix}, \quad \mathbf{z}_j^A = \begin{pmatrix} -\frac{j(j+3)}{2(j+1)(j+2)} & \frac{12}{j(j+1)(j+2)} \\ -\frac{j}{3(j+1)(j+2)} & -\frac{1}{6} - \frac{4}{(j+1)(j+2)} \end{pmatrix}, \quad (\text{K.18})$$

for the vector [481, 482, 483] and axial [476, 482, 483] channels, respectively, and a universal non-diagonal (in the conformal spin) part [483]

$$\mathbf{z}_{jk}^{\text{ND}} = \begin{pmatrix} 0 & \frac{6(2k+3)}{k(k+1)(k+2)(k+3)} \\ -\frac{(2k+3)}{6(k+1)(k+2)} & -\frac{(2k+3)(j-k)(j+k+3)}{k(k+1)(k+2)(k+3)} \end{pmatrix}. \quad (\text{K.19})$$

On the other hand, no rotation matrices are needed at the two-loop order for the maximal-helicity operators, i.e., $z^T = 1$.

As a consequence of supersymmetric Ward identities and the commutator algebra of the $\mathcal{N} = 1$ superconformal group [484], the transformed anomalous dimensions in the DRED scheme obey a set of relations which hold to all orders in perturbation theory [483, 485]. They can be naturally classified as follows.

- Autonomous relations for the vector and axial channels [224] (as before, we set $\gamma_{jj} \equiv \gamma_j$ and we do not display the superscript ‘‘DRED’’ for brevity)

$$\gamma_j^{qq;a} + \frac{6}{j} \gamma_j^{gg;a} = \frac{j}{6} \gamma_j^{gg;a} + \gamma_j^{gg;a}, \quad a = V, A. \quad (\text{K.20})$$

- Relations between the axial and vector channels [63, 486, 483, 485]

$$\gamma_{j+1}^{qq;V} + \frac{6}{j+1} \gamma_{j+1}^{gg;V} = \gamma_j^{qq;A} - \frac{j}{6} \gamma_j^{gg;A}, \quad \gamma_{j+1}^{qq;A} + \frac{6}{j+1} \gamma_{j+1}^{gg;A} = \gamma_j^{qq;V} - \frac{j}{6} \gamma_j^{gg;V}. \quad (\text{K.21})$$

- Relations between the diagonal and non-diagonal elements of anomalous dimensions in the axial and vector channels [483, 485]

$$\frac{6}{j} \gamma_j^{gg;V} - \frac{j+3}{6} \gamma_j^{gg;V} = \frac{j+1}{2j+1} \Delta_{j+1,j-1}^{\text{ND},A}, \quad \frac{6}{j} \gamma_j^{gg;A} - \frac{j+3}{6} \gamma_j^{gg;A} = \frac{j+1}{2j+1} \Delta_{j+1,j-1}^{\text{ND},V}, \quad (\text{K.22})$$

where

$$\Delta_{j+1,j-1}^{\text{ND},a} \equiv \frac{j-1}{j+1} \gamma_{j+1,j-1}^{gg;\text{ND},a} + \frac{j-1}{6} \gamma_{j+1,j-1}^{gg;\text{ND},a} - \frac{6}{j+1} \gamma_{j+1,j-1}^{gg;\text{ND},a} - \gamma_{j+1,j-1}^{gg;\text{ND},a}. \quad (\text{K.23})$$

- Relation between the anomalous dimensions of the maximal-helicity operators [478, 483]

$$\gamma_j^{qg;T} = \gamma_j^{gg;T}. \quad (\text{K.24})$$

As we established in Section 4.6.3, conformal operators do not mix with each other at leading order in coupling constant. As a consequence, the right-hand side of equations (K.22) is zero, i.e., the expansion starts from $\mathcal{O}(\alpha_s^2)$. Beyond one loop, as we have seen in the main presentation, the Eqs. (K.20) – (K.24) provide a very non-trivial check of the existing results. As a final remark, let point out that the above relations are merely particular cases of more generic relations between the anomalous dimensions of conformal operators γ_{jk} for any $j \geq k$ [483, 485].

L Twist separation in light-ray operators

The non-local form of the twist-two operators was introduced in the main text in Eq. (3.112). An analogous representation for the twist-three operators arises from the difference of \mathcal{O}_ρ^{qq} and $\mathcal{R}_\rho^{2,qq}$. The result can be cast into the form [230]

$$\begin{aligned} \mathcal{R}_\rho^{3,qq}(-z, z) &= \mathcal{O}_\rho^{qq}(-z, z) - \mathcal{R}_\rho^{2,qq}(-z, z) \\ &= \int_0^1 du z^\mu \left(g_{\nu\rho} \frac{\partial}{\partial z^\mu} - g_{\nu\mu} \frac{\partial}{\partial z^\rho} \right) \mathcal{O}^{qq,\nu}(-uz, uz), \end{aligned} \quad (\text{L.1})$$

(up to terms of higher order in z^2) making use of an obvious identity

$$\int_0^1 du z^\mu \frac{\partial}{\partial z^\mu} \mathcal{O}_\rho^{qq}(-uz, uz) = \int_0^1 du u \frac{\partial}{\partial u} \mathcal{O}_\rho^{qq}(-uz, uz) = \mathcal{O}_\rho^{qq}(-z, z) - \int_0^1 du \mathcal{O}_\rho^{qq}(-uz, uz).$$

Next, we have to differentiate the light-ray operator on the right-hand side of Eq. (L.1). This action involves differentiation of the path ordered exponential

$$[z_2, z_1] = P \exp \left(ig \int_{z_1}^{z_2} dz^\mu A_\mu(z) \right).$$

For a Wilson line (which is neither restricted to the light-cone here nor its path is given by a straight line), a generic variation of the gauge link under an infinitesimal deformation of the path/contour can be written as [487],

$$\begin{aligned} \delta[z_2, z_1] &= ig A_\mu(z_2) \delta z_2^\mu [z_2, z_1] - ig [z_2, z_1] A_\mu(z_1) \delta z_1^\mu \\ &\quad + ig \int_{-1}^1 d\tau [z_2, z(\tau)] F_{\mu\nu}(z(\tau)) \delta z^\mu(\tau) \dot{z}^\nu(\tau) [z(\tau), z_1]. \end{aligned} \quad (\text{L.2})$$

Here the dot on top of the path $z^\mu(\tau)$ from the initial to final points stands for the differentiation with respect to the proper time τ on it, $\dot{z}^\nu(\tau) \equiv dz^\nu(\tau)/d\tau$. The field strength appears here because, in evaluating the infinitesimal displacement of the path, one forms a closed loop, and thus induces a curvature, in it. The straight-line parametrization of the path $z^\mu(\tau)$ from z_1 to z_2 is

$$z_1^\mu = a^\mu + z^\mu \rightarrow z_2^\mu = a^\mu - z^\mu : \quad z^\mu(\tau) = a^\mu - \tau z^\mu.$$

Therefore, depending on whether the variation in Eq. (L.2) will be performed with respect to the total translation a^μ of the path as a whole or, rather, with respect to the relative distance between the ends z^μ , one will not or will, respectively, acquire a factor of the proper time τ under the integral. Namely:

- Differentiation with respect to the relative distance

$$\delta z^\mu(\tau) = -\tau dz^\mu, \quad \dot{z}^\nu(\tau) = -z^\mu, \quad \delta z_1^\mu = dz^\mu, \quad \delta z_2^\mu = -dz^\mu,$$

results into the equation

$$\frac{\partial}{\partial z^\mu}[-z, z] = -igA_\mu(-z)[-z, z] - ig[-z, z]A_\mu(z) - ig \int_{-1}^1 d\tau \tau [-z, \tau z]F_{\mu\nu}(\tau z)z^\nu[\tau z, z]. \quad (\text{L.3})$$

- Differentiation with respect to the total translation

$$\delta z^\mu(\tau) = da^\mu, \quad \dot{z}^\nu(\tau) = -z^\mu, \quad \delta z_1^\mu = da^\mu, \quad \delta z_2^\mu = da^\mu,$$

gives instead

$$\begin{aligned} \frac{\partial}{\partial a^\mu}[-z + a, z + a] &= igA_\mu(-z + a)[-z + a, z + a] - ig[-z + a, z + a]A_\mu(z + a) \\ &\quad - ig \int_{-1}^1 d\tau [-z + a, \tau z + a]F_{\mu\nu}(\tau z + a)z^\nu[\tau z + a, z + a]. \end{aligned} \quad (\text{L.4})$$

Thus, the differentiation in Eq. (L.1) is performed using Eq. (L.3) and yields

$$\begin{aligned} \frac{\partial}{\partial z^\mu} \mathcal{O}_\nu^{qq}(-z, z) &= -\bar{\psi}(-z) \vec{\mathcal{D}}_\mu \gamma_\nu[-z, z]\psi(z) + \bar{\psi}(-z)[-z, z] \vec{\mathcal{D}}_\mu \gamma_\nu \psi(z) \\ &\quad - ig \int_{-1}^1 d\tau \tau \bar{\psi}(-z)\gamma_\nu[-z, \tau z]F_{\mu\rho}(\tau z)z^\rho[\tau z, z]\psi(z), \end{aligned} \quad (\text{L.5})$$

where the left derivative acts on the argument $-z^\mu$ of the field $\bar{\psi}$ with the sign, i.e., $\bar{\psi}(-z)\vec{\mathcal{D}}_\mu = \bar{\psi}(-z)[\partial/\partial(-z^\mu) + igA_\mu(-z)]$. We substitute this expression back into Eq. (L.1) and an analogous one with changed indices. For further reduction we have to use the Heisenberg equation of motion for the quark field $\vec{\mathcal{D}}\psi = 0$ in the two-particle operators containing total derivatives,

$$\left(\gamma_\mu \vec{\mathcal{D}}_\nu - \gamma_\nu \vec{\mathcal{D}}_\mu \right) \psi \stackrel{\text{EOM}}{=} \frac{i}{2} \vec{\mathcal{D}} \sigma_{\mu\nu} \psi, \quad \bar{\psi} \left(\gamma_\mu \vec{\mathcal{D}}_\nu - \gamma_\nu \vec{\mathcal{D}}_\mu \right) \stackrel{\text{EOM}}{=} \frac{i}{2} \bar{\psi} \sigma_{\mu\nu} \vec{\mathcal{D}}. \quad (\text{L.6})$$

Assembling everything together, we get for the twist-three operator

$$\begin{aligned} \mathcal{R}_\rho^{3,qq}(-z, z) &= iz^\nu \int_0^1 du \left\{ \frac{u}{2} \bar{\psi}(-uz) \left(\sigma_{\rho\nu} \vec{\mathcal{D}} [-uz, uz] + [-uz, uz] \vec{\mathcal{D}} \sigma_{\rho\nu} \right) \psi(uz) \right. \\ &\quad \left. + g \int_{-u}^u d\tau \tau \bar{\psi}(-uz) \gamma_\nu F_{\rho\mu}(\tau z) z^\mu \psi(uz) \right\}. \end{aligned}$$

Now, the two-particle operators in round brackets can be further reduced to operators with total derivatives and three-particle operators by means of Eq. (L.4) and the use of the quark equation of motion, namely,

$$\begin{aligned} \frac{\partial}{\partial a_\rho} \Big|_{a=0} \bar{\psi}(a-z) \left\{ \begin{array}{c} \sigma_{\mu\nu} \gamma_\rho \\ \gamma_\rho \sigma_{\mu\nu} \end{array} \right\} \psi(a+z) &= \bar{\psi}(-z) \left\{ \begin{array}{c} \sigma_{\mu\nu} \vec{\mathcal{D}} \\ \vec{\mathcal{D}} \sigma_{\mu\nu} \end{array} \right\} \psi(z) \\ &\quad - ig \int_{-1}^1 d\tau \bar{\psi}(-z) \left\{ \begin{array}{c} \sigma_{\mu\nu} \gamma_\rho \\ \gamma_\rho \sigma_{\mu\nu} \end{array} \right\} F^{\rho\sigma}(\tau z) z_\sigma \psi(z). \end{aligned} \quad (\text{L.7})$$

Summing these contributions and reducing the product of three Dirac matrices with Eq. (A.13) to one, we find

$$\bar{\psi}(-z) \left(\sigma^{\mu\nu} \vec{\mathcal{D}}[-z, z] + [-z, z] \vec{\mathcal{D}}\sigma^{\mu\nu} \right) \psi(z) = -2\varepsilon^{\mu\nu\rho\sigma} \partial_\rho \tilde{\mathcal{O}}_\sigma^{qq}(-z, z) - 2ig\varepsilon^{\mu\nu\rho\sigma} \int_{-1}^1 d\tau \bar{\psi}(-z) \gamma_\sigma \gamma^5 F_{\rho\lambda}(\tau z) z^\lambda \psi(z), \quad (\text{L.8})$$

with $\partial_\mu = \vec{\partial}_\mu + \vec{\partial}_\mu$ being the total derivative as defined in Eq. (5.39). Thus, we express the twist-three parity-even operator in terms of the total derivative of the parity-odd bilocal operator and three-particle operators. Substituting the result into (L.1), we derive the following equation [230]

$$\begin{aligned} \mathcal{O}_\rho^{qq}(-z^-, z^-) &= \mathcal{R}_\rho^{2,qq}(-z^-, z^-) + z^- \int_0^1 du \left\{ -iu \varepsilon_\rho^{+\mu\nu} \partial_\mu \tilde{\mathcal{O}}_\nu^{qq}(-uz^-, uz^-) \right. \\ &\quad \left. + \frac{z^-}{2} \int_{-u}^u d\tau \left[(u-\tau) \mathcal{S}_{[+]^\rho}^{ggq}(-uz^-, \tau z^-, uz^-) - (u+\tau) \mathcal{S}_{[-]^\rho}^{ggq}(-uz^-, \tau z^-, uz^-) \right] \right\}, \end{aligned} \quad (\text{L.9})$$

where we set $z^\mu = z^- n^\mu$ and use the three-particle operators introduced in Eq. (5.40). An analogous equation holds for the parity-odd twist-three operator with obvious dressing or removal of tildes from the functions involved,

$$\begin{aligned} \tilde{\mathcal{O}}_\rho^{qq}(-z^-, z^-) &= \tilde{\mathcal{R}}_\rho^{2,qq}(-z^-, z^-) + z^- \int_0^1 du \left\{ -iu \varepsilon_\rho^{+\mu\nu} \partial_\mu \mathcal{O}_\nu^{qq}(-uz^-, uz^-) \right. \\ &\quad \left. + \frac{z^-}{2} \int_{-u}^u d\tau \left[(u-\tau) \tilde{\mathcal{S}}_{[+]^\rho}^{ggq}(-uz^-, \tau z^-, uz^-) - (u+\tau) \tilde{\mathcal{S}}_{[-]^\rho}^{ggq}(-uz^-, \tau z^-, uz^-) \right] \right\}. \end{aligned} \quad (\text{L.10})$$

Notice that, on the right-hand side of this equation (L.9), one gets the operator $\tilde{\mathcal{O}}_\rho^{qq}$, which does not possess a definite twist. The same statement applies to (L.10). Therefore, Eq. (L.9) combined with (L.10) forms a coupled system of recursion relations, which should be solved in order to determine the twist-three operators in terms of twist-two and twist-three three-particle ones. These equations can be easily solved iteratively. Namely, one substitutes $\tilde{\mathcal{O}}_\rho^{qq}$ from (L.10) into (L.9) and so on. It is easier to perform this straightforward calculation rather than describe it. The final result is given in Eq. (5.66) for $z^2 = z_\mu z^\mu = 0$ [289].

For certain applications—the resummation of target mass corrections addressed in Section 5.6 at leading twist level and accounting for twist-four effects due to Δ^2/Q^2 effects in amplitudes, just to name a few—one needs to keep non-light-like inter-field separations, i.e., $z^2 \neq 0$. For the present discussion, the multiparticle operators will be irrelevant and thus will be neglected. We decompose a given non-local, say of even parity, operator $\mathcal{O}_\rho^{qq}(-z, z)$ into its symmetric and antisymmetric parts

$$\mathcal{O}_\rho^{qq}(-z, z) = \mathcal{O}_\rho^{qq,\text{sym}}(-z, z) + \mathcal{O}_\rho^{qq,\text{asym}}(-z, z). \quad (\text{L.11})$$

The symmetric operator is easily constructed from \mathcal{O}_ρ^{qq} as was previously done in Eq. (3.112),

$$\mathcal{O}_\rho^{qq,\text{sym}}(-z, z) = \int_0^1 du \frac{\partial}{\partial z^\rho} z^\sigma \mathcal{O}_\sigma^{qq}(-uz, uz). \quad (\text{L.12})$$

When expanded in Taylor series it generates a tower of Wilson operators symmetric in all Lorentz indices, however, since $z^2 \neq 0$ here, it is not automatically traceless.

The antisymmetric operator is given by the difference between the “full” operator and its symmetric component. After some algebra, which led to Eq. (L.9), one finds the antisymmetric even-parity operator in terms of the odd-parity one

$$\mathcal{O}_\rho^{qq,\text{asym}}(-z, z) = \mathcal{O}_\rho^{qq}(-z, z) - \mathcal{O}_\rho^{qq,\text{sym}}(-z, z) = -i\varepsilon_\rho^{\mu\nu\sigma} z_\mu \partial_\nu \int_0^1 du u \tilde{\mathcal{O}}_\sigma^{qq}(ux, -ux). \quad (\text{L.13})$$

Notice, that when we expand the second equality in Taylor series, we get Eq. (5.155). As we know, $\mathcal{O}_\rho^{qq,\text{asym}}(-z, z)$ can be expressed in terms of $\mathcal{O}_\rho^{qq,\text{sym}}(-z, z)$ and $\tilde{\mathcal{O}}_\rho^{qq,\text{sym}}(-z, z)$ and higher twist multi-particle operators, which we ignore. Thus, to find the antisymmetric operator $\mathcal{O}^{\text{asym}}$, we need to solve the system of equations given by (L.13) and a similar one for the axial vector operator. Excluding, for instance, the axial operator we get an equation

$$\begin{aligned} \mathcal{O}_\rho^{qq}(-z, z) &= \mathcal{O}_\rho^{qq,\text{sym}}(-z, z) - i\varepsilon_\rho^{\mu\nu\sigma} z_\mu \partial_\nu \int_0^1 du u \tilde{\mathcal{O}}_\sigma^{qq,\text{sym}}(-uz, uz) \\ &\quad + \left\{ [(z \cdot \partial)^2 - z^2 \partial^2] g_\rho^\sigma - [(z \cdot \partial) \partial_\rho - \partial^2 z_\rho] z^\sigma \right\} \int_0^1 du u \bar{u} \mathcal{O}_\sigma^{qq}(-uz, uz). \end{aligned} \quad (\text{L.14})$$

As before $\bar{u} \equiv 1 - u$. In the course of the calculation, the contraction of two ε -tensors have produced six terms, four of them are displayed above, and the other two are neglected since they are proportional to total derivatives $\partial^\sigma \mathcal{O}_\sigma(-z, z)$. This contribution, my means of the equations of motion, is expressed in terms of the twist-four antiquark-gluon-quark operator (cf. (L.5))

$$\partial^\sigma \mathcal{O}_\sigma^{qq}(-z, z) \stackrel{\text{EOM}}{=} -ig \int_{-1}^1 du \bar{\psi}_q(-z) \gamma_\mu z_\nu F^{\mu\nu}(uz) \psi_q(z). \quad (\text{L.15})$$

Solving iteratively the recurrence relations (L.14), we find to twist-four accuracy

$$\begin{aligned} \mathcal{O}_\rho^{qq,\text{asym}}(-z, z) &= -\frac{1}{2} \int_0^1 du u \left\{ i\varepsilon_\rho^{\mu\nu\sigma} z_\mu \partial_\nu \left[\tilde{\mathcal{O}}_\sigma^{qq,\text{sym}}((\bar{u} - u)z, z) + \tilde{\mathcal{O}}_\sigma^{qq,\text{sym}}(-z, (u - \bar{u})z) \right] \right. \\ &\quad \left. + (\partial_\rho z_\sigma - g_{\rho\sigma}(z \cdot \partial)) [\mathcal{O}_\sigma^{qq,\text{sym}}((\bar{u} - u)z, z) - \mathcal{O}_\sigma^{qq,\text{sym}}(-z, (u - \bar{u})z)] \right\} \\ &\quad + \frac{1}{4} z^2 \partial^2 \int_0^1 du u \bar{u} \int_0^1 dv \\ &\quad \times \left\{ i\bar{u} \varepsilon_\rho^{\mu\nu\sigma} z_\mu \partial_\nu \left[\tilde{\mathcal{O}}_\sigma^{qq,\text{sym}}((v\bar{u} - u)z, (v\bar{u} + u)z) + \tilde{\mathcal{O}}_\sigma^{qq,\text{sym}}(-(v\bar{u} + u)z, -(v\bar{u} - u)z) \right] \right. \\ &\quad + v\bar{u} (\partial_\rho z^\sigma - g_\rho^\sigma(z \cdot \partial)) [\mathcal{O}_\sigma^{qq,\text{sym}}((v\bar{u} - u)z, (v\bar{u} + u)z) - \mathcal{O}_\sigma^{qq,\text{sym}}(-(v\bar{u} + u)z, -(v\bar{u} - u)z)] \\ &\quad \left. + \frac{2}{z^2} (z_\rho z^\sigma - g_\rho^\sigma z^2) [\mathcal{O}_\sigma^{qq,\text{sym}}((v\bar{u} - u)z, (v\bar{u} + u)z) + \mathcal{O}_\sigma^{qq,\text{sym}}(-(v\bar{u} + u)z, -(v\bar{u} - u)z)] \right\}. \end{aligned} \quad (\text{L.16})$$

Here we dropped terms $\mathcal{O}(z^4)$. The corrections we accounted here generate Δ^2/Q^2 power suppressed effect in the Compton amplitude.

References

- [1] D. Müller, D. Robaschik, B. Geyer, F.M. Dittes, J. Horejsi, Fortsch. Phys. 42 (1994) 101.

- [2] X. Ji, Phys. Rev. Lett. 78 (1997) 610.
- [3] A.V. Radyushkin, Phys. Lett. B 380 (1996) 417.
- [4] A.V. Radyushkin, Phys. Lett. B 385 (1996) 333.
- [5] X. Ji, Phys. Rev. D 55 (1997) 7114.
- [6] A.V. Radyushkin, Phys. Rev. D 56 (1997) 5524.
- [7] X. Ji, J. Phys. G 24 (1998) 1181.
- [8] A.V. Radyushkin, *Generalized parton distributions*, in At the Frontier of Particle Physics. Handbook of QCD, Ed. M. Shifman, vol. 2 (World Scientific, 2001) p. 1037; hep-ph/0101225.
- [9] K. Goeke, M.V. Polyakov, M. Vanderhaeghen, Prog. Part. Nucl. Phys. 47 (2001) 401.
- [10] M. Diehl, Phys. Rept. 388 (2003) 41.
- [11] I. Estermann, O.C. Simpson, O. Stern, Phys. Rev. 52 (1937) 535.
- [12] R. Hofstadter, R.W. McAllister, Phys. Rev. 102 (1956) 851.
- [13] M. Breidenbach et al., Phys. Rev. Lett. 23 (1969) 935.
- [14] J. Bjorken, Phys. Rev. 179 (1969) 1547.
- [15] R.P. Feynman, Phys. Rev. Lett. 23 (1969) 1415.
- [16] R.P. Feynman, *Photon-Hadron Interactions*, Benjamin (New York, 1972).
- [17] C.G. Callan, D.J. Gross, Phys. Rev. Lett. 22 (1968) 156.
- [18] G. 't Hooft, Marseilles Meeting, 1973.
- [19] D.J. Gross, F. Wilczek, Phys. Rev. Lett. 30 (1973) 1343.
- [20] H.D. Politzer, Phys. Rev. Lett. 30 (1973) 1346.
- [21] L.D. Landau, I.Ya. Pomeranchuk, Dokl. Akad. Nauk Ser. Fiz. 102 (1955) 489.
- [22] I.Ya. Pomeranchuk, Dokl. Akad. Nauk Ser. Fiz. 103 (1955) 1005.
- [23] N.K. Nielsen, Am. J. Phys. 49 (1981) 1171.
- [24] R.J. Hughes, Nucl. Phys. B 186 (1981) 376.
- [25] H. Fritzsch, M. Gell-Mann, H. Leutwyler, Phys. Lett. B 47 (1973) 365.
- [26] D.J. Gross, F. Wilczek, Phys. Rev. D 8 (1973) 3633.
- [27] H. Georgi, H.D. Politzer, Phys. Rev. D 9 (1974) 416.
- [28] J.G.H. de Groot et al., Phys. Lett. B 82 (1979) 456.

- [29] R.K. Ellis, W.J. Stirling, B.R. Webber, *QCD and collider physics*, Cambridge Monographs in Particle Physics, Nuclear Physics and Cosmology, Cambridge Univ. Press, (Cambridge, 1996).
- [30] D.M. Ceperley, Rev. Mod. Phys. 67 (1995) 279.
- [31] E.P. Wigner, Phys. Rev. 40 (1932) 749.
- [32] N. Balasz, B. Jennings, Phys. Rept. 104 (1984) 347;
M. Hillery, R.F. O'Connell, M.O. Scully, E.P. Wigner, Phys. Rept. 106 (1984) 121;
H.-W. Lee, Phys. Rept. 259 (1995) 147.
- [33] H.J. Groenewold, Physica 12 (1946) 405.
- [34] A. Dragt, S. Habib, *How Wigner function transforms under symplectic maps*, in *Quantum Aspects of Beam Physics*, ed. P. Chen, Word Scientific (Singapore, 1998) p. 651, quant-ph/9806056.
- [35] K. Vogel, H. Risken, Phys. Rev. A 40 (1989) 2847.
- [36] D.T. Smithey, M. Beck, M.G. Raymer, A. Faridani, Phys. Rev. Lett. 70 (1993) 1244;
G. Breitenbach, S. Schiller, J. Mlynek, Nature 387 (1997) 471.
- [37] U. Leonhardt, *Measuring the quantum state of light*, Cambridge Studies in Modern Optics, Cambridge Univ. Press, (Cambridge, 1997).
- [38] K. Banaszek, C. Radzewicz, K. Wodkiewicz, J.S. Krasiński, Phys. Rev. A 60 (1999) 674.
- [39] D. Yennie, M. Ravenhall, M. Levy, Rev. Mod. Phys. 29 (1957) 144.
- [40] E.J. Ernst, R.G. Sachs, K.C. Wali, Phys. Rev. 119 (1960) 1105;
R.G. Sachs, Phys. Rev. 126 (1962) 2256.
- [41] A.V. Belitsky, X. Ji, F. Yuan, Phys. Rev. D 69 (2004) 074014.
- [42] A.L. Licht, A. Pagnamenta, Phys. Rev. D 2 (1970) 1150.
- [43] J. Kelly, Phys. Rev. C 66 (2002) 065203.
- [44] X. Ji, Phys. Lett. B 254 (1991) 456;
G. Holzwarth, Z. Phys. A 356 (1996) 339.
- [45] G. Sterman, Int. J. Mod. Phys. A 16 (2001) 3041.
- [46] S. Coleman, R.E. Norton, Nuovo Cim. 38 (1965) 438.
- [47] V.N. Gribov, B.L. Ioffe, I.Ya. Pomeranchuk, Sov. J. Nucl. Phys. 2 (1966) 549;
B.L. Ioffe, Phys. Lett. B 30 (1969) 123.
- [48] S.J. Brodsky, P. Hoyer, N. Marchal, S. Peigné, F. Sannino, Phys. Rev. D 65 (2002) 114025.
- [49] J.C. Collins, Phys. Lett. B 536 (2002) 43.

- [50] A.V. Belitsky, X. Ji, F. Yuan, Nucl. Phys. B 656 (2003) 165.
- [51] A.V. Efremov, A.V. Radyushkin, Theor. Math. Phys. 44 (1981) 774.
- [52] J.C. Collins, D.E. Soper, Nucl. Phys. B 194 (1982) 445.
- [53] J.M.F. Labastida, G. Sterman, Nucl. Phys. B 254 (1985) 425.
- [54] D. Boer, P.J. Mulders, F. Pijlman, Nucl. Phys. B 667 (2003) 201.
- [55] F.J. Gilman, Phys. Rev. 167 (1968) 1365.
- [56] L.N. Hand, Phys. Rev. 129 (1963) 1834.
- [57] S.J. Brodsky, H.C. Pauli, S.S. Pinsky, Phys. Rept. 301 (1998) 299.
- [58] A.V. Belitsky, AIP Conf. Proc. 698 (2004) 607.
- [59] X. Ji, Phys. Rev. Lett. 91 (2003) 062001.
- [60] A.D. Martin, M.G. Ryskin, Phys. Rev. D 64 (2001) 094017.
- [61] D.E. Soper, Phys. Rev. D 15 (1977) 1141.
- [62] J.B. Kogut, D.E. Soper, Phys. Rev. D 1 (1970) 2901.
- [63] A.P. Bukhvostov, G.V. Frolov, L.N. Lipatov, E.A. Kuraev, Nucl. Phys. B 258 (1985) 601.
- [64] P.V. Landshoff, J.C. Polkinghorne, R.D. Short, Nucl. Phys. B 28 (1971) 225.
- [65] R.L. Jaffe, Nucl. Phys. B 229 (1983) 205.
- [66] M. Diehl, T. Gousset, Phys. Lett. B 428 (1998) 359.
- [67] L. Frankfurt, A. Freund, V. Guzey, M. Strikman, Phys. Lett. B 418 (1998) 345; (Erratum) Phys. Lett. B 429 (1998) 414.
- [68] X. Ji, R.F. Lebed, Phys. Rev. D 63 (2001) 076005.
- [69] M. Diehl, Eur. Phys. J. C 19 (2001) 485.
- [70] Ph. Hägler, Phys. Lett. B 594 (2004) 164.
- [71] Z. Chen, X. Ji, Phys. Rev. D 71 (2005) 016003.
- [72] M.V. Polyakov, Nucl. Phys. B 555 (1999) 231.
- [73] P. Hoodbhoy, X. Ji, Phys. Rev. D 58 (1998) 054006.
- [74] A.V. Belitsky, D. Müller, Phys. Lett. B 486 (2000) 369.
- [75] E.R. Berger, F. Cano, M. Diehl, B. Pire, Phys. Rev. Lett. 87 (2001) 142302.
- [76] F. Cano, B. Pire, Eur. Phys. J. A 19 (2004) 423.

- [77] G. Sterman, *An introduction to quantum field theory*, Cambridge University Press, (Cambridge, 1993).
- [78] M. Glück, E. Reya, A. Vogt, Z. Phys. C 53 (1992) 651;
M. Glück, E. Reya, I. Schienbein, Eur. Phys. J. C 10 (1999) 313.
- [79] P.J. Sutton, A.D. Martin, R.G. Roberts, W.J. Stirling, Phys. Rev. D 45 (1992) 2349.
- [80] J. Pumplin, D.R. Stump, J. Huston, H.L. Lai, P. Nadolsky, W.K. Tung, J. High Ener. Phys. 0207 (2002) 012.
- [81] A.D. Martin, R.G. Roberts, W.J. Stirling, R.S. Thorne, Eur. Phys. J. C 23 (2002) 73; Eur. Phys. J. C 28 (2003) 455; Eur. Phys. J. C 35 (2004) 325.
- [82] M. Glück, E. Reya, A. Vogt, Eur. Phys. J. C 5 (1998) 461.
- [83] T. Gehrmann, W.J. Stirling, Phys. Rev. D 53 (1996) 6100.
- [84] M. Glück, E. Reya, M. Stratmann, W. Vogelsang, Phys. Rev. D 63 (2001) 094005.
- [85] J. Blümlein, H. Bottcher, Nucl. Phys. B 636 (2002) 225.
- [86] E. Leader, A.V. Sidorov, D.B. Stamenov, Eur. Phys. J. C 23 (2002) 479.
- [87] M. Hirai, S. Kumano, N. Saito, Phys. Rev. D 69 (2004) 054021.
- [88] P. Hoodbhoy, R.L. Jaffe, A. Manohar, Nucl. Phys. B 312 (1989) 571.
- [89] A.V. Efremov, O.V. Teryaev, Sov. J. Nucl. Phys. 36 (1982) 557; *On The Oscillations Of The Tensor Spin Structure Function*, hep-ph/9910555.
- [90] F.E. Close, S. Kumano, Phys. Rev. D 42 (1990) 2377.
- [91] A. Schäfer, L. Szymanowski, O.V. Teryaev, Phys. Lett. B 464 (1999) 94.
- [92] H. Gao, Int. J. Mod. Phys. E 12 (2003) 1; (Erratum) E 12 (2003) 567.
- [93] T. Frederico, E.M. Henley, S.J. Pollock, S. Ying, Phys. Rev. C 46 (1992) 347.
- [94] R.G. Arnold, C.E. Carlson, F. Gross, Phys. Rev. C 23 (1981) 363.
- [95] A.P. Kobushkin, A.I. Syamtomov, Phys. Atom. Nucl. 58 (1995) 1477.
- [96] S.J. Brodsky, J.R. Hiller, Phys. Rev. D 46 (1992) 2141.
- [97] D. Abbott et al., Eur. Phys. J. A 7 (2000) 421.
- [98] G. Altarelli, G.G. Ross, Phys. Lett. B 212 (1988) 391.
- [99] R.D. Carlitz, J.C. Collins, A. Mueller, Phys. Lett. B 214 (1988) 229.
- [100] A.V. Efremov, O.V. Teryaev, JINR Report E2-88-287 (1988).
- [101] R.L. Jaffe, A. Manohar, Nucl. Phys. B 337 (1990) 509.

- [102] M. Anselmino, A.V. Efremov, E. Leader, Phys. Rep. 261 (1995) 1; (Erratum) Phys. Rept. 281 (1997) 399.
- [103] B. Lampe, E. Reya, Phys. Rep. 332 (2000) 1.
- [104] B.W. Fillipone, X. Ji, Adv. Nucl. Phys. 26 (2001) 1.
- [105] S.D. Bass, *The spin structure of the proton*, hep-ph/0411005.
- [106] P.L. Anthony et al., Phys. Lett. B 493 (2000) 19.
- [107] B. Adeva et al., Phys. Rev. D 58 (1998) 112001.
- [108] B. Adeva et al., Phys. Rev. D 58 (1998) 112002.
- [109] J.J. de Swart, Rev. Mod. Phys. 35 (1963) 916.
- [110] K. Hagiwara et al., Phys. Rev. D 66 (2002) 010001.
- [111] S.A. Larin, T. van Ritbergen, J.A.M. Vermaseren, Phys. Lett. B 404 (1997) 153.
- [112] V.B. Berestetsky, E.M. Lifshitz, L.P. Pitaevsky, *Quantum Electrodynamics*, Pergamon Press (Oxford, 1982).
- [113] S.V. Bashinsky, R.L. Jaffe, Nucl. Phys. B 536 (1998) 303.
- [114] R.L. Jaffe, Phil. Tras. Roy. Soc. Lond. A 359 (2001) 391.
- [115] X. Ji, Phys. Rev. D 58 (1998) 056003.
- [116] H. Page, Phys. Rev. 144 (1966) 1250.
- [117] A.V. Belitsky, X. Ji, Phys. Lett. B 538 (2002) 289.
- [118] A.V. Belitsky, D. Müller, Nucl. Phys. A 711 (2002) 118.
- [119] M.V. Polyakov, Phys. Lett. B 555 (2003) 57.
- [120] M.V. Polyakov, A.G. Shuvaev, *On ‘dual’ parametrizations of generalized parton distributions*, hep-ph/0207153.
- [121] L. Okun, I.Yu. Kobzarev, J. Exp. Theor. Phys. 16 (1963) 1343.
- [122] I.Yu. Kobzarev, V.I. Zakharov, Annals Phys. 60 (1970) 448.
- [123] S.J. Brodsky, D.S. Hwang, B.Q. Ma, I. Schmidt, Nucl. Phys. B 593 (2001) 311.
- [124] O.V. Teryaev, *Spin structure of nucleon and equivalence principle*, hep-ph/9904376.
- [125] P. Ball, V.M. Braun, Phys. Rev. D 54 (1996) 2182.
- [126] A.V. Bakulev, S.V. Mikhailov, N.G. Stefanis, Phys. Lett. B 578 (2004) 91;
A.P. Bakulev, K. Passek-Kumericki, W. Schroers, N.G. Stefanis, Phys. Rev. D 70 (2004) 033014; (Erratum) Phys. Rev. D 70 (2004) 079906.

- [127] V.M. Braun, A. Lenz, Phys. Rev. D 70 (2004) 074020.
- [128] A. Khodjamirian, Th. Mannel, M. Melcher, Phys. Rev. D 70 (2004) 074002.
- [129] P. Ball, M. Boglione, Phys. Rev. D 68 (2003) 094006.
- [130] B. Clerbaux, M.V. Polyakov, Nucl. Phys. A 679 (2000) 185.
- [131] X. Ji, J.P. Ma, F. Yuan, Nucl. Phys. B 652 (2003) 383.
- [132] A.V. Belitsky, X. Ji, F. Yuan, Phys. Rev. Lett. 91 (2003) 092003.
- [133] M. Jacob, G.C. Wick, Ann. Phys. 7 (1959) 404.
- [134] S.J. Brodsky, S.D. Drell, Phys. Rev. D 22 (1980) 2236.
- [135] R. Buniy, J.P. Ralston, P. Jain, AIP Conf. Proc. 549 (2000) 302;
J.P. Ralston, P. Jain, Phys. Rev. D 68 (2004) 053008.
- [136] V.M. Braun, R.J. Fries, N. Mahnke, E. Stein, Nucl. Phys. B 589 (2000) 381; (Erratum)
Nucl. Phys. B 607 (2001) 433.
- [137] K.J. Golec-Biernat, A.D. Martin, Phys. Rev. D 59 (1999) 014029.
- [138] M. Diehl, T. Feldmann, R. Jakob, P. Kroll, Nucl. Phys. B 596 (2001) 33; (Erratum) Nucl.
Phys. B 605 (2001) 647.
- [139] S.J. Brodsky, M. Diehl, D.S. Hwang, Nucl. Phys. B 596 (2001) 99.
- [140] A.V. Radyushkin, Phys. Rev. D 59 (1999) 014030.
- [141] A.V. Radyushkin, Phys. Lett. B 131 (1983) 179.
- [142] L. Mankiewicz, G. Piller, T. Weigl, Eur. Phys. J. C 5 (1998) 119.
- [143] M.V. Polyakov, C. Weiss, Phys. Rev. D 60 (1999) 114017.
- [144] O.V. Teryaev, Phys. Lett. B 510 (2001) 125.
- [145] B.C. Tiburzi, Phys. Rev. D 70 (2004) 057504; *Light-front dynamics and generalized parton
distributions*, nucl-th/0407005.
- [146] A.V. Belitsky, D. Müller, A. Kirchner, A. Schäfer, Phys. Rev. D 64 (2001) 116002.
- [147] P.V. Pobylitsa, Phys. Rev. D 67 (2003) 034009.
- [148] A.V. Radyushkin, Phys. Lett. B 449 (1999) 81.
- [149] I.M. Gelfand, G.E. Shilov, *Generalized functions*, vol. 1, *Properties and operations*, Academic Press, (New York and London, 1964).
- [150] I.M. Gelfand, G.E. Shilov, N.Ya. Vilenkin, *Generalized functions*, vol. 5, *Integral geometry
and representation theory*, Academic Press, (New York and London, 1966).

- [151] M. Burkardt, Phys. Rev. D 62 (2000) 071503, (Erratum) Phys. Rev. D 66 (2002) 119903.
- [152] M. Burkardt, Int. J. Mod. Phys. A 18 (2003) 173.
- [153] M. Burkardt, Phys. Rev. D 66 (2002) 114005.
- [154] M. Diehl, Eur. Phys. J. C 25 (2002) 223; (Erratum) Eur. Phys. J. C 31 (2003) 277.
- [155] M. Burkardt, Phys. Lett. B 595 (2004) 245.
- [156] F. Yuan, Phys. Rev. D 69 (2004) 051501.
- [157] P. Hagler, J. Negele, D.B. Renner, W. Schroers, T. Lippert, K. Schilling, Phys. Rev. D 68 (2003) 034505; Phys. Rev. Lett. 93 (2004) 112001.
- [158] J.P. Ralston, B. Pire, Phys. Rev. D 66 (2002) 111501.
- [159] A. Freund, Eur. Phys. J. C 31 (2003) 203.
- [160] A.D. Martin, M.G. Ryskin, Phys. Rev. D 57 (1998) 6692.
- [161] B. Pire, J. Soffer, O.V. Teryaev, Eur. Phys. J. C 8 (1999) 103.
- [162] M. Diehl, T. Feldmann, R. Jakob, P. Kroll, Nucl. Phys. B 596 (2001) 33; (Erratum) Nucl. Phys. B 605 (2001) 647.
- [163] P.V. Pobylitsa, Phys. Rev. D 65 (2002) 114015.
- [164] P.V. Pobylitsa, Phys. Rev. D 65 (2002) 077504.
- [165] M. Burkardt, *Generalized parton distributions and distribution of partons in the transverse plane*, hep-ph/0105324.
- [166] M. Burkardt, Nucl. Phys. A 711 (2002) 127.
- [167] M. Burkardt, Phys. Lett. B 582 (2004) 151.
- [168] P.V. Pobylitsa, Phys. Rev. D 66 (2002) 094002.
- [169] P.V. Pobylitsa, Phys. Rev. D 67 (2003) 094012.
- [170] A. Mukherjee, I.V. Musatov, H.-C. Pauli, A.V. Radyushkin, Phys. Rev. D 67 (2003) 073014.
- [171] B.C. Tiburzi, G.A. Miller, Phys. Rev. D 67 (2003) 013010; Phys. Rev. D 67 (2003) 113004.
- [172] E. Jenkins, A.V. Manohar, Phys. Lett. B 255 (1991) 558.
- [173] D. Arndt, M.J. Savage, Nucl. Phys. A 697 (2002) 429; J.-W. Chen, X. Ji, Phys. Lett. B 523 (2001) 107.
- [174] J.-W. Chen, X. Ji, Phys. Rev. Lett. 88 (2002) 052003.
- [175] V. Bernard, N. Kaiser, U.-G. Meißner, Int. J. Mod. Phys. E 4 (1995) 193.

- [176] N.A. Kivel, M.V. Polyakov, *One loop chiral corrections to hard exclusive processes. I: Pion case*, hep-ph/0203264; Nucl. Phys. A 711 (2002) 211.
- [177] M. Diehl, A. Manashov, A. Schäfer, *Generalized parton distributions for the pion in chiral perturbation theory*, hep-ph/0505269.
- [178] J. Gasser, H. Leutwyler, Annals Phys. 158 (1984) 142.
- [179] J.F. Donoghue, H. Leutwyler, Z. Phys. C 52 (1991) 343;
B. Kubis, U.-G. Meißner, Nucl. Phys. A 671 (2000) 332; (Erratum) Nucl. Phys. A 692 (2001) 647.
- [180] V. Bernard, N. Kaiser, J. Kambor, U.-G. Meißner, Nucl. Phys. B 388 (1992) 315.
- [181] V. Bernard, H.W. Fearing, T.R. Hemmert, U.-G. Meißner, Nucl. Phys. A 635 (1998) 121;
(Erratum) Nucl. Phys. A 642 (1998) 563.
- [182] V.Yu. Petrov, P.V. Pobylitsa, M.V. Polyakov, I. Bornig, K. Goeke, C. Weiss, Phys. Rev. D 57 (1998) 4325.
- [183] M. Pentinen, M.V. Polyakov, K. Goeke, Phys. Rev. D 62 (2000) 014024.
- [184] P. Schweitzer, S. Boffi, M. Radici, Phys. Rev. D 66 (2002) 114004.
- [185] P. Schweitzer, M. Colli, S. Boffi, Phys. Rev. D 67 (2003) 114022.
- [186] J. Ossmann, M.V. Polyakov, P. Schweitzer, D. Urbano, K. Goeke, Phys. Rev. D 71 (2005) 034011.
- [187] M. Praszalowicz, A. Rostworowski, Acta Phys. Polon. B 34 (2003) 2699.
- [188] W. Broniowski, E. Ruiz Arriola, Phys. Lett. B 574 (2003) 57.
- [189] X.D. Ji, W. Melnitchouk, X. Song, Phys. Rev. D 56 (1997) 5511.
- [190] I.V. Anikin, D. Binosi, R. Medrano, S. Noguera, V. Vento, Eur. Phys. J. A 14 (2002) 95.
- [191] S. Boffi, B. Pasquini, M. Traini, Nucl. Phys. B 649 (2003) 243; Nucl. Phys. B 680 (2004) 147.
- [192] S. Scopetta, V. Vento, Eur. Phys. J. A 16 (2003) 527; Phys. Rev. D 69 (2004) 094004; Fizika B 13 (2004) 397; Phys. Rev. D 71 (2005) 014014;
S. Noguera, S. Scopetta, V. Vento, Phys. Rev. D 70 (2004) 094018.
- [193] I.V. Anikin, A.E. Dorokhov, A.E. Maksimov, L. Tomio, Phys. Atom. Nucl. 63 (2000) 489;
I.V. Anikin, A.E. Dorokhov, A.E. Maksimov, L. Tomio, V. Vento, Nucl. Phys. A 678 (2000) 175.
- [194] S. Simula, *Generalized parton distributions in the light-front constituent quark model*, hep-ph/0406074.

- [195] A. Mukherjee, M. Vanderhaeghen, Phys. Lett. B 542 (2002) 245; Phys. Rev. D 67 (2003) 085020;
 D. Chakrabarti, A. Mukherjee, Phys. Rev. D 71 (2005) 014038.
- [196] L. Theußl, S. Noguera, V. Vento, Eur. Phys. J. A 20 (2004) 483.
- [197] B.C. Tiburzi, G.A. Miller, Phys. Rev. C 64 (2001) 065204. Phys. Rev. D 65 (2002) 074009; *Light-front Bethe-Salpeter equation applied to form factors, GPDs and GDAs*, hep-ph/0205109; Phys. Rev. D 67 (2003) 054015;
- [198] H.M. Choi, C.R. Ji, L.S. Kisslinger, Phys. Rev. D 64 (2001) 093006. Phys. Rev. D 66 (2002) 053011.
- [199] B.C. Tiburzi, W. Detmold, G.A. Miller, Phys. Rev. D 68 (2003) 073002; Phys. Rev. D 70 (2004) 093008.
- [200] M. Gockeler, R. Horsley, D. Pleiter, P.E.L. Rakow, A. Schäfer, G. Schierholz, W. Schroers, Phys. Rev. Lett. 92 (2004) 042002. Nucl. Phys. Proc. Suppl. 128 (2004) 203; Nucl. Phys. Proc. Suppl. 135 (2004) 156; *Generalized parton distributions and structure functions from full lattice QCD*, hep-lat/0409162; *Generalized parton distributions in full lattice QCD*, hep-lat/0410023.
- [201] J.W. Negele, R.C. Brower, P. Dreher, R. Edwards, George T. Fleming, P. Hagler, T. Lippert, A.V. Pochinsky, D.B. Renner, D. Richards, K. Schilling, W. Schroers, Nucl. Phys. Proc. Suppl. 129 (2004) 910; Nucl. Phys. Proc. Suppl. 129 (2004) 907; Nucl. Phys. Proc. Suppl. 128 (2004) 170.
- [202] P. Hagler, J.W. Negele, D.B. Renner, W. Schroers, T. Lippert, K. Schilling, *Helicity dependent and independent generalized parton distributions of the nucleon in lattice QCD*, hep-ph/0410017.
- [203] J. Bratt, S. Dalley, B. van de Sande, E.M. Watson, Phys. Rev. D 70 (2004) 114502;
 S. Dalley, Phys. Lett. B 570 (2003) 191.
- [204] M. Diehl, T. Feldmann, R. Jakob, P. Kroll, Eur. Phys. J. C 8 (1999) 409.
- [205] M. Diehl, T. Feldmann, R. Jakob, P. Kroll, Eur. Phys. J. C 39 (2005) 1.
- [206] S.D. Drell, T.M. Yan, Phys. Rev. Lett. 24 (1970) 181.
- [207] V. Gadiyak, X. Ji, C. Jung, Phys. Rev. D 65 (2002) 094510.
- [208] M. Strikman, C. Weiss, Phys. Rev. D 69 (2004) 054012;
- [209] L. Frankfurt, M. Strikman, C. Weiss, Annalen Phys. 13 (2004) 665;
 L. Frankfurt, M. Strikman, C. Weiss, M. Zhalov, *Transverse structure of strong interactions at LHC: from diffraction to new particle production*, hep-ph/0412260.
- [210] S.L. Adler, Annals Phys. 50 (1968) 189; Phys. Rev. D 12 (1975) 2644.
- [211] H.F. Jones, M.D. Scadron, Annals Phys. 81 (1973) 1.

- [212] R.C.E. Devenish, T.S. Eisenschitz, J.G. Körner, Phys. Rev. D 14 (1976) 3063.
- [213] C.H. Llewellyn Smith, Phys. Rept. 3 (1972) 261.
- [214] L. Alvarez-Ruso, S.K. Singh, M.J. Vicente Vacas, Phys. Rev. C 57 (1998) 2693;
S.K. Singh, M.J. Vicente-Vacas, E. Oset, Phys. Lett. B 416 (1998) 23; (Erratum) Phys. Lett. B 423 (1998) 428.
- [215] S.K. Singh, Nucl. Phys. Proc. Suppl. 112 (2002) 77.
- [216] M.N. Butler, M.J. Savage, R.P. Springer, Nucl. Phys. B 399 (1993) 69.
- [217] R.F. Lebed, Nucl. Phys. B 430 (1994) 295.
- [218] R.F. Dashen, E. Jenkins, A.V. Manohar, Phys. Rev. D 51 (1995) 3697.
- [219] A.V. Manohar, *Large-N QCD*, In Proc. of Les Houches Summer School in Theoretical Physics, Session 68: Probing the Standard Model of Particle Interactions, hep-ph/9802419.
- [220] E. Jenkins, Ann. Rev. Nucl. Part. Sci. 48 (1998) 81.
- [221] R.K. Ellis, H. Georgi, M. Machacek, H.D. Politzer, G.G. Ross, Phys. Lett. B 78 (1978) 281;
Nucl. Phys. B 152 (1979) 285.
- [222] V.N. Gribov, L.N. Lipatov, Sov. J. Nucl. Phys. 15 (1972) 438;
A.P. Bukhvostov, L.N. Lipatov, N.P. Popov, Sov. J. Nucl. Phys. 20 (1974) 287;
L.N. Lipatov, Sov. J. Nucl. Phys. 20 (1975) 94.
- [223] G. Altarelli, G. Parisi, Nucl. Phys. B 126 (1977) 298.
- [224] Yu.L. Dokshitzer, Sov. Phys. JETP 46 (1977) 641.
- [225] S. Chekanov et al., Phys. Rev. D 67 (2003) 012007.
- [226] M. Bordag, D. Robaschik, Theor. Math. Phys. 49 (1982) 1063.
- [227] I.I. Balitsky, Phys. Lett. B 124 (1983) 230.
- [228] M. Bordag, L. Kaschluhn, G. Petrov, D. Robaschik, Sov. J. Nucl. Phys. 37 (1983) 112;
T. Braunschweig, J. Horejsi, D. Robaschik, Z. Phys. C 23 (1984) 19;
B. Geyer, D. Robaschik, M. Bordag, J. Horejsi, Z. Phys. C 26 (1985) 591;
T. Braunschweig, B. Geyer, J. Horejsi, D. Robaschik, Z. Phys. C 33 (1986) 275.
- [229] T. Braunschweig, B. Geyer, D. Robaschik, Annalen Phys. 44 (1987) 403.
- [230] I.I. Balitsky, V.M. Braun, Nucl. Phys. B 311 (1989) 541.
- [231] J. Blümlein, B. Geyer, D. Robaschik, Phys. Lett. B 406 (1997) 161. *Twist-2 light-ray operators: Anomalous dimensions and evolution equations*, hep-ph/9711405.
- [232] I.I. Balitsky, A.V. Radyushkin, Phys. Lett. B 413 (1997) 114.
- [233] A.V. Belitsky, D. Müller, Phys. Lett. B 417 (1998) 129.

- [234] A.P. Bukhvostov, E.A. Kuraev, L.N. Lipatov, Sov. J. Nucl. Phys. 38 (1983) 263; Sov. J. Nucl. Phys. 39 (1984) 121; Sov. Phys. JETP 60 (1984) 22.
- [235] A.V. Belitsky, D. Müller, Nucl. Phys. B 527 (1998) 207.
- [236] A.V. Belitsky, Nucl. Phys. B 574 (2000) 407 (2000).
- [237] A.V. Efremov, A.V. Radyushkin, Phys. Lett. B 94 (1980) 245; Theor. Math. Phys. 42 (1980) 97.
- [238] V.L. Chernyak, A.R. Zhitnitsky, V.G. Serbo, JETP Lett. 26 (1977) 594.
- [239] G.R. Farrar, D.R. Jackson, Phys. Rev. Lett. 43 (1979) 246.
- [240] S.J. Brodsky, G.P. Lepage, Phys. Lett. B 87 (1979) 359; Phys. Rev. D 22 (1980) 2157.
- [241] M.K. Chase, Nucl. Phys. B 174 (1980) 109.
- [242] Th. Ohrndorf, Nucl. Phys. B 186 (1981) 153.
- [243] V.N. Baier, A.G. Grozin, Nucl. Phys. B 192 (1981) 476.
- [244] V.K. Dobrev, V.B. Petkova, S.G. Petrova, I.T. Todorov, Phys. Rev. D 13 (1976) 887.
- [245] A.A. Migdal, Annals Phys. 109 (1977) 365.
- [246] Yu.M. Makeenko, Sov. J. Nucl. Phys. 33 (1981) 440.
- [247] S.J. Brodsky, Y. Frishman, G.P. Lepage, C. Sachradja, Phys. Lett. B 91 (1980) 239.
- [248] Th. Ohrndorf, Nucl. Phys. B 198 (1982) 26.
- [249] N.S. Craigie, V.K. Dobrev, I.T. Todorov, Ann. Phys. 159 (1985) 411.
- [250] D. Müller, Z. Phys. C 49 (1991) 293.
- [251] D. Müller, Phys. Rev. D 49 (1994) 2525.
- [252] D. Müller, Phys. Rev. D 58 (1998) 054005.
- [253] A.V. Belitsky, D. Müller, Nucl. Phys. B 537 (1999) 397.
- [254] S.É. Derkachov, S.K. Kehrein, A.N. Manashov, Nucl. Phys. B 493 (1997) 660.
- [255] A.V. Belitsky, S.É. Derkachov, G.P. Korchemsky, A.N. Manashov, *Superconformal operators in Yang-Mills theories on the light-cone*, hep-th/0503137.
- [256] M.A. Shifman, M.I. Vysotsky, Nucl. Phys. B 186 (1981) 475.
- [257] H. Bateman, A. Erdélyi, *Higher transcendental functions*, vol. 1, McGraw-Hill (New York, 1953).
- [258] R. Jackiw, Phys. Rev. Lett. 41 (1978) 1635; *Topological investigations of quantized gauge theories*, in Proc. of Les Houches Summer School on Theoretical Physics: *Relativity, Groups and Topology II*, eds. B.S. DeWitt and R. Stora, (North-Holland, 1984) p. 221.

- [259] S.D. Joglekar, B.W. Lee, Ann. Phys. 97 (1975) 160;
 S.D. Joglekar, Ann. Phys. 108 (1977) 233; Ann. Phys. 109 (1977) 210.
- [260] N.A. Kivel, L. Mankiewicz, Nucl. Phys. B 557 (1999) 271; Phys. Lett. B 458 (1999) 338;
 N.A. Kivel, Nucl. Phys. A 663 (2000) 1011.
- [261] J. Pestieau, P. Roy, H. Terazawa, Phys. Rev. Lett. 25 (1970) 402; (Erratum) Phys. Rev. Lett. 25 (1970) 704;
 V. Del Duca, S.J. Brodsky, P. Hoyer, Phys. Rev. D 46 (1992) 931;
 V.M. Braun, P. Gornicki, L. Mankiewicz, Phys. Rev. D 51 (1995) 6036;
 Yu.V. Kovchegov, M. Strikman, Phys. Lett. B 516 (2001) 314.
- [262] V.M. Braun, G.P. Korchemsky, D. Müller, Prog. Part. Nucl. Phys. 51 (2003) 311.
- [263] A.N. Manashov, M. Kirch, A. Schäfer, *Solving the leading order evolution equation for GPDs*, hep-ph/0503109.
- [264] M. Kantorovich, N. Lebedev, J. Exp. Theor. Phys. 8 (1938) 1192.
- [265] A.G. Shuvaev, Phys. Rev. D 60 (1999) 116005.
- [266] J.D. Noritzsch, Phys. Rev. D 62 (2000) 054015.
- [267] A.V. Belitsky, B. Geyer, D. Müller, A. Schäfer, Phys. Lett. B 421 (1998) 312.
- [268] M. Abramowitz, I.A. Stegun, *Handbook on mathematical functions*, Dover Publications, Inc., (New York, 1965).
- [269] A.V. Belitsky, D. Müller, L. Niedermeier, A. Schäfer, Phys. Lett. B 437 (1998) 160;
 A.V. Belitsky, D. Müller, Nucl. Phys. B (Proc. Suppl.) 79 (1999) 573.
- [270] A.V. Belitsky, D. Müller, L. Niedermeier, A. Schäfer, Nucl. Phys. B 546 (1999) 279.
- [271] W. Furmanski, R. Petronzio, Z. Phys. C 11 (1982) 293.
- [272] M. Glück, E. Reya, A. Vogt, Z. Phys. C 48 (1990) 471.
- [273] G. Shaw, Nucl. Phys. A 675 (2000) 84;
 G. Parisi, N. Sourlas, Nucl. Phys. B 151 (1979) 421;
 I.S. Barker, C.S. Langensiepen, G. Shaw, Nucl. Phys. B 186 (1981) 61;
 I.S. Barker, B.R. Martin, G. Shaw, Z. Phys. C 19 (1983) 147;
 V.G. Krivokhizhin, S.P. Kurlovich, V.V. Sanadze, I.A. Savin, A.V. Sidorov, N.B. Skachkov, Z. Phys. C 36 (1987) 51.
- [274] A. Freund, V. Guzey, *Numerical methods in the LO evolution of nondiagonal parton distributions: The DGLAP case*, hep-ph/9801388; Phys. Lett. B 462 (1999) 178;
- [275] A.V. Belitsky, D. Müller, A. Freund, Phys. Lett. B 461 (1999) 270; Nucl. Phys. B 574 (2000) 347; Phys. Lett. B 493 (2000) 341;
 A.V. Belitsky, D. Müller, Phys. Lett. B 464 (1999) 249.
- [276] M.H. Sarmadi, Phys. Lett. B 143 (1984) 471.

- [277] F.-M. Dittes, A.V. Radyushkin, Phys. Lett. B 134 (1984) 359.
- [278] S.V. Mikhailov, A.V. Radyushkin, Nucl. Phys. B 254 (1985) 89; Nucl. Phys. B 273 (1986) 161.
- [279] A. Freund, M.F. McDermott, Phys. Rev. D 65 (2002) 056012; (Erratum) Phys. Rev. D 66 (2002) 079903.
- [280] A. Freund, M.F. McDermott, Phys. Rev. D 65 (2002) 091901; Phys. Rev. D 65 (2002) 074008; Eur. Phys. J. C 23 (2002) 651;
- [281] A.V. Afanasev, S.J. Brodsky, C.E. Carlson, Y.C. Chen, M. Vanderhaeghen, Phys. Rev. Lett. 93 (2004) 122301; *The two-photon exchange contribution to elastic electron nucleon scattering at large momentum transfer*, hep-ph/0502013.
- [282] X. Ji, J. Osborne, Phys. Rev. D 58 (1998) 094018.
- [283] J.C. Collins, A. Freund, Phys. Rev. D 59 (1999) 074009.
- [284] C.W. Bauer, S. Fleming, D. Pirjol, I.Z. Rothstein, I.W. Stewart, Phys. Rev. D 66 (2002) 014017.
- [285] A.V. Belitsky, D. Müller, Phys. Rev. D 68 (2003) 116005.
- [286] M.A. Shifman, A.I. Vainshtein, V.I. Zakharov, Nucl. Phys. B 147 (1979) 347.
- [287] I.V. Anikin, B. Pire, O.V. Teryaev, Phys. Rev. D 62 (2000) 071501.
- [288] M. Pentinen, M.V. Polyakov, A.G. Shuvaev, M. Strikman, Phys. Lett. B 491 (2000) 96.
- [289] A.V. Belitsky, D. Müller, Nucl. Phys. B 589 (2000) 611.
- [290] N.A. Kivel, M.V. Polyakov, A. Schäfer, O.V. Teryaev, Phys. Lett. B 497 (2001) 73.
- [291] A.V. Radyushkin, C. Weiss, Phys. Lett. B 493 (2000) 332.
- [292] N.A. Kivel, M.V. Polyakov, Nucl. Phys. B 600 (2001) 334.
- [293] A.V. Radyushkin, C. Weiss, Phys. Rev. D 63 (2001) 114012.
- [294] A.V. Radyushkin, C. Weiss, Phys. Rev. D 64 (2001) 097504.
- [295] B.E. White, J. Phys. G 28 (2002) 203.
- [296] I.V. Anikin, O.V. Teryaev, Phys. Lett. B 509 (2001) 95.
- [297] P. Ball, M. Lazar, Phys. Lett. B 515 (2001) 131.
- [298] D.V. Kiptily, M.V. Polyakov, Eur. Phys. J. C 37 (2004) 105.
- [299] J. Blümlein, D. Robaschik, Nucl. Phys. B 581 (2000) 449.
- [300] J. Blümlein, B. Geyer, D. Robaschik, Nucl. Phys. B 560 (1999) 283.

- [301] P.A.M. Guichon, M. Vanderhaeghen, Prog. Part. Nucl. Phys. 41 (1998) 125.
- [302] N.A. Kivel, L. Mankiewicz, Nucl. Phys. B 672 (2003) 357.
- [303] P. Ball, V.M. Braun, Y. Koike, K. Tanaka, Nucl. Phys. B 529 (1998) 323.
- [304] B. Geyer, M. Lazar, D. Robaschik, Nucl. Phys. B 618 (2001) 99; (Erratum) B 652 (2003) 408;
- [305] J. Eilers, B. Geyer, M. Lazar, Phys. Rev. D 69 (2004) 034015.
- [306] B. Geyer, D. Robaschik, J. Eilers, Nucl. Phys. B 704 (2005) 279.
- [307] B. Geyer, D. Robaschik, Phys. Rev. D 71 (2005) 054018.
- [308] F. Bissey, J.R. Cudell, J. Cugnon, J.P. Lansberg, P. Stassart, Phys. Lett. B 587 (2004) 189; Nucl. Phys. Proc. Suppl. 133 (2004) 77;
F. Bissey, J.R. Cudell, J. Cugnon, M. Jaminon, J.P. Lansberg, P. Stassart, Phys. Lett. B 547 (2002) 210; AIP Conf. Proc. 660 (2003) 339.
- [309] V.M. Braun, S.E. Derkachov, A.N. Manashov, Phys. Rev. Lett. 81 (1998) 2020;
V.M. Braun, S.E. Derkachov, G.P. Korchemsky, A.N. Manashov, Nucl. Phys. B 553 (1999) 355.
- [310] A.V. Belitsky, Phys. Lett. B 453 (1999) 59; Nucl. Phys. B 558 (1999) 259; Nucl. Phys. B 574 (2000) 407.
- [311] S.E. Derkachov, G.P. Korchemsky, A.N. Manashov, Nucl. Phys. B 566 (2000) 203.
- [312] V.M. Braun, G.P. Korchemsky, A.N. Manashov, Phys. Lett. B 476 (2000) 455; Nucl. Phys. B 603 (2001) 69.
- [313] A.V. Belitsky, V.M. Braun, A.S. Gorsky, G.P. Korchemsky, Int. J. Mod. Phys. A 19 (2004) 4715.
- [314] S. Wandzura, F. Wilczek, Phys. Lett. B 72 (1977) 195.
- [315] X. Ji, J. Osborne, Phys. Rev. D 57 (1998) 1337.
- [316] L. Mankiewicz, G. Piller, E. Stein, M. Vänttinen, T. Weigl, Phys. Lett. B 425 (1998) 186.
- [317] H. Burkhardt, W.N. Cottingham, Annals Phys. 56 (1970) 453.
- [318] A.V. Efremov, O.V. Teryaev, E. Leader, Phys. Rev. D 55 (1997) 4307.
- [319] P.L. Anthony et al., Phys. Lett. B 553 (2003) 18;
G.S. Mitchell, *Spin structure functions g_1 and g_2 for the proton and deuteron*, hep-ex/9903055;
P. Bosted, Nucl. Phys. A 663 (2000) 297.
- [320] M. Gockeler et al., Phys. Rev. D 63 (2001) 074506.
- [321] A.V. Belitsky, A. Kirchner, D. Müller, A. Schäfer, Phys. Lett. B 510 (2001) 117.

- [322] B.I. Ermolaev, F.I. Olness, A.G. Shuvaev, Phys. Rev. D 60 (1999) 034013.
- [323] I.I. Balitsky, E. Kuchina, Phys. Rev. D 62 (2000) 074004.
- [324] L. Favart, M.V.T. Machado, Eur. Phys. J. C 34 (2004) 429; Eur. Phys. J. C 29 (2003) 365.
L. Favart, Eur. Phys. J. C 33 (2004) S509.
- [325] A.V. Vinnikov, *Regge and factorized GPD models in ρ^0 elastic electroproduction* hep-ph/0501061.
- [326] A.G. Shuvaev, K.J. Golec-Biernat, A.D. Martin, M.G. Ryskin, Phys. Rev. D 60 (1999) 014015.
- [327] A. Hebecker, T. Teubner, Phys. Lett. B 498 (2001) 16.
- [328] A.V. Belitsky, D. Müller, A. Kirchner, Nucl. Phys. B 629 (2002) 323.
- [329] V.N. Gribov, A.A. Migdal, Sov. J. Nucl. Phys. 8 (1969) 583.
- [330] J.B. Bronzan, G.L. Kane, U.P. Sukhatme, Phys. Lett. B 49 (1974) 272.
- [331] J. Noritzsch, Phys. Rev. D 69 (2003) 094016.
- [332] S. Ferrara, R. Gatto, A.F. Grillo, *Conformal algebra in space-time and operator product expansion*, Springer Tracts in Modern Physics 67 (1973) 1.
- [333] G.T. Bodwin, J. Qiu, Phys. Rev. D 41 (1990) 2755;
A.V. Manohar, Phys. Rev. Lett. 66 (1991) 289.
- [334] H.D. Politzer, Nucl. Phys. B 172 (1980) 349.
- [335] H. Georgi, H.D. Politzer, Phys. Rev. D 14 (1976) 1829.
- [336] O. Nachtmann, Nucl. Phys. B 63 (1973) 237.
- [337] P. Ball, V.M. Braun, Nucl. Phys. B 543 (1999) 201.
- [338] B. Geyer, M. Lazar, D. Robaschik, Nucl. Phys. B 559 (1999) 339; B. Geyer, M. Lazar, Nucl. Phys. B 581 (2000) 341.
- [339] A.V. Belitsky, D. Müller, Phys. Lett. B 507 (2001) 173.
- [340] N.Ya. Vilenkin, *Special Functions and the Theory of Group Representations*, American Mathematical Society (Providence, RI, 1968).
- [341] A. Bacchetta, U. D'Alesio, M. Diehl, C.A. Miller, Phys. Rev. D 70 (2005) 117504.
- [342] M. Diehl, T. Gousset, B. Pire, J.P. Ralston, Phys. Lett. B 411 (1997) 193.
- [343] A. Freund, M. Strikman, Phys. Rev. D 60 (1999) 071501;
L. Frankfurt, A. Freund, M. Strikman, Phys. Lett. B 460 (1999) 417.
- [344] A.V. Belitsky, D. Müller, L. Niedermeier, A. Schäfer, Nucl. Phys. B 593 (2001) 289.

- [345] A.V. Belitsky, D. Müller, A. Kirchner, A. Schäfer, Phys. Rev. D 64 (2001) 116002.
- [346] A. Donnachie, J. Gravelis, G. Shaw, Eur. Phys. J. C 18 (2001) 539;
M. McDermott, R. Sandapen, G. Shaw, Eur. Phys. J. C 22 (2002) 655.
- [347] A. Donnachie, H.G. Dosch, Phys. Lett. B 502 (2001) 74; Phys. Rev. D 65 (2002) 014019.
- [348] A. Freund, M. McDermott, M. Strikman, Phys. Rev. D 67 (2003) 036001.
- [349] A. Gardestig, A.P. Szczepaniak, J.T. Londergan, Phys. Rev. D 68 (2003) 034005.
- [350] A. Freund, Phys. Rev. D 68 (2003) 096006.
- [351] E.R. Berger, M. Diehl, B. Pire, Eur. Phys. J. C 23 (2002) 675.
- [352] J. Bartels, M. Loewe, Z. Phys. C 12 (1982) 263.
- [353] M. Guidal, M. Vanderhaeghen, Phys. Rev. Lett. 90 (2003) 012001.
- [354] A.V. Belitsky, D. Müller, Phys. Rev. Lett. 90 (2003) 022001.
- [355] P. Amore, C. Corianò, M. Guzzi, *Deeply virtual neutrino scattering*, hep-ph/0404121;
C. Corianò, M. Guzzi, Phys. Rev. D 71 (2005) 0503002.
- [356] A. Psaker, *Probing generalized parton distributions with neutrino beams*, hep-ph/0412321.
- [357] S.J. Brodsky, L. Frankfurt, J.F. Gunion, A.H. Mueller, M. Strikman, Phys. Rev. D 50 (1994) 3134.
- [358] J.C. Collins, L. Frankfurt, M. Strikman, Phys. Rev. D 56 (1997) 2982.
- [359] L. Mankiewicz, G. Piller, T. Weigl, Phys. Rev. D59, 017501 (1999).
- [360] L. Mankiewicz, G. Piller, A.V. Radyushkin, Eur. Phys. J. C 10 (1999) 307.
- [361] L. Frankfurt, P.V. Pobylitsa, M.V. Polyakov, M. Strikman, Phys. Rev. D 60 (1999) 014010;
- [362] L. Frankfurt, M.V. Polyakov, M. Strikman, M. Vanderhaeghen, Phys. Rev. Lett. 84 (2000) 2589.
- [363] M.I. Eides, L. Frankfurt, M.I. Strikman, Phys. Rev. D 59 (1999) 114025.
- [364] M. Vanderhaeghen, P.A.M. Guichon, M. Guidal, Phys. Rev. Lett. 80 (1998) 5064; Phys. Rev. D 60 (1999) 094017.
- [365] F. Cano, J.M. Laget, Phys. Lett. B 551 (2003) 317.
- [366] M. Diehl, A.V. Vinnikov, Phys. Lett. B 609 (2005) 286.
- [367] S.V. Goloskokov, P. Kroll, *Vector meson electroproduction at small Bjorken- x and generalized parton distributions*, hep-ph/0501242.
- [368] M.G. Ryskin, Phys. Lett. B 403 (1997) 335.

- [369] P. Hoodbhoy, Phys. Rev. D 56 (1997) 388.
- [370] M. Vänttinen, L. Mankiewicz, Phys. Lett. B 434 (1998) 141.
- [371] L. Frankfurt, W. Koepf, M. Strikman, Phys. Rev. D 57 (1998) 512.
- [372] M.G. Ryskin, Z. Phys. C 57 (1993) 89.
- [373] M. Vänttinen, L. Mankiewicz, Phys. Lett. B 440 (1998) 157.
- [374] E.R. Berger, M. Diehl, B. Pire, Phys. Lett. B 523 (2001) 265.
- [375] B. Pire, L. Szymanowski, *Hadron-hadron annihilation into two photons and backword VCS in the scaling regime of QCD*, hep-ph/0411387.
- [376] K. Golec-Biernat, J. Kwiecinski, A.D. Martin, Phys. Rev. D 58 (1998) 094001.
- [377] V.M. Braun, S. Gottwald, D.Yu. Ivanov, A. Schäfer, L. Szymanowski, Phys. Rev. Lett. 89 (2002) 172001.
- [378] G. Bertsch, S.J. Brodsky, A.S. Goldhaber, J.F. Gunion, Phys. Rev. Lett. 47 (1981) 297.
- [379] L. Frankfurt, G.A. Miller, M. Strikman, Phys. Lett. B 304 (1993) 1; Found. Phys. 30 (2000) 533; Phys. Rev. D 65 (2002) 094015.
- [380] N.N. Nikolaev, W. Schäfer, G. Schwiete, Phys. Rev. D 63 (2001) 014020.
- [381] V.M. Braun, D.Yu. Ivanov, A. Schäfer, L. Szymanowski, Phys. Lett. B 509 (2001) 43; Nucl. Phys. B 638 (2002) 111.
- [382] V.L. Chernyak, Phys. Lett. B 516 (2001) 116;
V.L. Chernyak, A.G. Grozin, Phys. Lett. B 517 (2001) 119.
- [383] B. Lehmann-Dronke, A. Schäfer, Phys. Lett. B 521 (2001) 55.
- [384] B. Lehmann-Dronke, M. Maul, S. Schäfer, E. Stein, A. Schäfer, Phys. Lett. B 457 (1999) 207;
B. Lehmann-Dronke, P.V. Pobylitsa, M.V. Polyakov, A. Schäfer, K. Goeke, Phys. Lett. B 475 (2000) 147;
B. Lehmann-Dronke, M.V. Polyakov, A. Schäfer, K. Goeke, Phys. Rev. D 63 (2001) 114001.
- [385] D.Yu. Ivanov, B. Pire, L. Szymanowski, O.V. Teryaev, Phys. Lett. B 550 (2002) 65.
- [386] V.A. Khoze, A.D. Martin, M.G. Ryskin, Eur. Phys. J. C 14 (2000) 525; Eur. Phys. J. C 19 (2001) 477; (Erratum) Eur. Phys. J. C 20 (2001) 599.
- [387] A. De Roeck, V.A. Khoze, A.D. Martin, R. Orava, M.G. Ryskin, Eur. Phys. J. C 25 (2002) 391.
- [388] N. Kivel, L. Mankiewicz, Eur. Phys. J. C 21 (2001) 621.
- [389] S.J. Brodsky, F.E. Close, J.F. Gunion, Phys. Rev. D 5 (1972) 1384; Phys. Rev. D 6 (1972) 177; Phys. Rev. D 8 (1973) 3678.

- [390] P. Kroll, M. Schürmann, P.A.M. Guichon, Nucl. Phys. A 598 (1996) 435.
- [391] A. Freund, Phys. Lett. B 472 (2000) 412.
- [392] J. Balla, M.V. Polyakov, C. Weiss, Nucl. Phys. B 510 (1998) 327.
- [393] M. Airapetian, et al., Phys. Rev. Lett. 87 (2001) 182001.
- [394] S. Chekanov et al., Phys. Lett. B 573 (2003) 46.
- [395] C. Adloff et al., Phys. Lett. B 517 (2001) 47.
- [396] S. Stepanyan et al., Phys. Rev. Lett. 87 (2001) 182002.
- [397] W.D. Nowak, *Deeply virtual Compton scattering: results and future*, hep-ex/0503010.
- [398] M. Diehl, S. Sapeta, *On the analysis of lepton scattering on longitudinally or transversely polarized protons*, hep-ph/0503023.
- [399] A.V. Belitsky, D. Müller, L. Niedermeier, A. Schäfer, Phys. Lett. B 474 (2000) 163; Chech. J. Phys. 50/S1 (2000) 123.
- [400] N. Kivel, M.V. Polyakov, M. Vanderhaeghen, Phys. Rev. D 63 (2001) 114014.
- [401] V.A. Korotkov, W.D. Nowak, Eur. Phys. J C 23 (2002) 455; Nucl. Phys. A 711 (2002) 175; W.D. Nowak, Nucl. Phys. (Proc. Suppl.) 105 (2002) 171.
- [402] A.V. Belitsky, A. Schäfer, Nucl. Phys. B 527 (1998) 235.
- [403] M. Vänttinen, L. Mankiewicz, E. Stein, *Higher-twist contributions in exclusive processes*, in *The Structure of baryons*, eds. D.W. Menze and B. Metsch, World Scientific (Singapore, 1998) p. 316; hep-ph/9810527.
- [404] R. Jakob, P. Kroll, M. Raufks, J. Phys. G 22 (1996) 45,
- [405] P.A.M. Guichon, L. Mosse, M. Vanderhaeghen, Phys. Rev. D 68 (2003) 034018.
- [406] J.-W. Chen, M.J. Savage, Nucl. Phys. A 735 (2004) 411.
- [407] N.A. Kivel, M.V. Polyakov, S. Stratmann, *Soft-pion emmission from the nucleon induced by twist-two light-cone operators*, nucl-th/0407052.
- [408] M.C. Birse, *Comment on soft-pion emission in DVCS*, hep-ph/0503076.
- [409] J. Blümlein, J. Eilers, B. Geyer, D. Robaschik, Phys. Rev. D 65 (2002) 054029.
- [410] M. Garçon, talk at *User group symposium and annual meeting: A celebration of JLab physics*, <http://www.jlab.org/intralab/calendar/archive03/ugm/talks/garcon.pdf>; *Generalized parton distributions and deep exclusive reactions: present program at JLab*, hep-ex/0501041.
- [411] E.D. Bloom, F.J. Gilman, Phys. Rev. Lett. 25 (1970) 1140; Phys. Rev. D 4 (1971) 2901.

- [412] B.L. Ioffe, A.V. Smilga, Nucl. Phys. B 216 (1983) 373.
- [413] A.V. Radyushkin, Annalen Phys. 13 (2004) 718.
- [414] V.A. Nesterenko, A.V. Radyushkin, Sov. J. Nucl. Phys. 39 (1984) 811; Phys. Lett. B 128 (1983) 439.
- [415] M. Guidal, M.V. Polyakov, A.V. Radyushkin, M. Vanderhaeghen, *Nucleon form factors from generalized parton distributions*, hep-ph/0410251.
- [416] A.V. Radyushkin, Phys. Rev. D 58 (1998) 114008.
- [417] A.P. Bakulev, S.V. Mikhailov, N.G. Stefanis, Phys. Part. Nucl. 354 (2004) 7.
- [418] M. Diehl, T. Feldmann, P. Kroll, C. Vogt, Phys. Rev. D 61 (2000) 074029.
- [419] C. Vogt, Phys. Rev. D 64 (2001) 057501; (Erratum) Phys. Rev. D 69 (2004) 079901.
- [420] P. Hoodbhoy, X. Ji, F. Yuan, Phys. Rev. Lett. 92 (2004) 012003.
- [421] V.A. Nesterenko, A.V. Radyushkin, Phys. Lett. B 115 (1982) 410.
- [422] A.V. Radyushkin, Nucl. Phys. A 532 (1991) 141.
- [423] A.V. Radyushkin, Acta Phys. Polon. B 26 (1995) 2067.
- [424] V.V. Braguta, A.I. Onishchenko, Phys. Lett. B 591 (2004) 267.
- [425] N. Isgur, C.H. Llewellyn Smith, Phys. Rev. Lett. 52 (1984) 1080.
- [426] J. Volmer et al., Phys. Rev. Lett. 86 (2001) 1713.
- [427] N.G. Stefanis, Eur. Phys. J. direct C 1 (1999) 7.
- [428] P. Hoodbhoy, Phys. Rev. D 65 (2002) 077501.
- [429] J.C. Collins, M. Diehl, Phys. Rev. D 61 (2000) 114015; M. Diehl, T. Gousset, B. Pire, Phys. Rev. D 59 (1999) 034023.
- [430] A.V. Belitsky, D. Müller, Phys. Lett. B 513 (2001) 349.
- [431] D.Yu. Ivanov, L. Szymanowski, G. Krasnikov, JETP Lett. 80 (2004) 226.
- [432] I.V. Anikin, B. Pire, L. Szymanowski, O.V. Teryaev, S. Wallon, *On BLM scale fixing in exclusive processes*, hep-ph/0411408.
- [433] M. Diehl, B. Pire, L. Szymanowski, Phys. Lett. B 584 (2004) 58.
- [434] I.V. Anikin, B. Pire, L. Szymanowski, O.V. Teryaev, S. Wallon, Phys. Rev. D 70 (2004) 011501; Phys. Rev. D 71 (2005) 034021.
- [435] S.J. Brodsky, G.P. Lepage, P.B. Mackenzie, Phys. Rev. D 28 (1984) 228.
- [436] D.Yu. Ivanov, A. Schäfer, L. Szymanowski, G. Krasnikov, Eur. Phys. J. C 34 (2004) 297.

- [437] M. Beneke, Phys. Rept. 317 (1999) 1.
- [438] S.S. Agaev, Phys. Lett. B 360 (1996) 117; Nucl. Phys. B Proc. Suppl. 74 (1999) 155.
- [439] P. Godzinski, N. Kivel, Nucl. Phys. B 521 (1998) 274.
- [440] A.I. Karanikas, N.G. Stefanis, Phys. Lett. B 504 (2001) 225.
- [441] M. Beneke, V.M. Braun, L. Magnea, Nucl. Phys. B 497 (1998) 297.
- [442] M. Maul, E. Stein, A. Schäfer, L. Mankiewicz, Phys. Lett. B 401 (1997) 100.
- [443] A. Kirchner, D. Müller, Eur. Phys. J. C 32 (2003) 347.
- [444] A. Freund, M. Strikman, Phys. Rev. C 69 (2004) 015203; Eur. Phys. J. C 33 (2004) 53.
- [445] N.A. Kivel, Phys. Rev. D 65 (2002) 0540101.
- [446] L. Mankiewicz, G. Piller, Phys. Rev. D 61 (2000) 074013.
- [447] I.V. Anikin, O.V. Teryaev, Phys. Lett. B 554 (2003) 51.
- [448] H. Weigert, *Evolution at small x : the color glass condensate*, hep-ph/0501087.
- [449] A.O. Barut, R. Raczka, *Theory of group representations and applications*, World Scientific (Singapore, 1986).
- [450] W. Rarita, J.S. Schwinger, Phys. Rev. 60 (1941) 61.
- [451] T.R. Hemmert, B.R. Holstein, J. Kambor, J. Phys. G 24 (1998) 1831.
- [452] R. Meng, F.I. Olness, D.E. Soper, Nucl. Phys. B 371 (1992) 79.
- [453] J.C. Collins, Nucl. Phys. B 396 (1993) 161.
- [454] L.D. Landau, E.M. Lifshitz, *The classical theory of fields*, vol. 2, Elsevier (North Holland, 2004).
- [455] C.G. Callan, S.R. Coleman, R. Jackiw, Annals Phys. 59 (1970) 42.
- [456] R. Jackiw, *Field theoretic investigations in current algebra*, in *Current algebra and anomalies*, S.B. Treiman, E. Witten, R. Jackiw, B. Zumino, World Scientific (Singapore, 1985) p. 81.
- [457] G. 't Hooft, Nucl. Phys. B 72 (1974) 461; Nucl. Phys. B 75 (1974) 461.
- [458] G.T.H. Skyrme, Proc. R. Soc. London A 260 (1961) 127.
- [459] E. Witten, Nucl. Phys. B 160 (1979) 57; Nucl. Phys. B 223 (1983) 422; Nucl. Phys. B 223 (1983) 433.
- [460] G.S. Adkins, C.R. Nappi, E. Witten, Nucl. Phys. B 228 (1983) 552.
- [461] I. Zahed, G.E. Brown, Phys. Rept. 142 (1986) 1.

- [462] G. Mack, A. Salam, Ann. Phys. 53 (1969) 174.
- [463] S. Mandelstam, Nucl. Phys. B 213 (1983) 149.
- [464] G. Leibbrandt, *Noncovariant gauges. Quantization of Yang-Mills and Chern-Simons theory in axial-type gauges*, World Scientific, (Singapore, 1994).
- [465] A.A. Slavnov, S.A. Frolov, Theor. Math. Phys. 73 (1987) 1158.
- [466] A. Bassutto, G. Nardelli, R. Soldati, *Yang-Mills theories in the algebraic non covariant gauges*, World Scientific, (Singapore, 1991).
- [467] K.G. Chetyrkin, *Four-loop renormalization of QCD: full set of renormalization constants and anomalous dimensions*, hep-ph/0405193.
- [468] M. Ögren, Class. Quant. Grav. 3 (1986) 581.
- [469] D.M. Capper, J.J. Dulwich, M.J. Litvak, Nucl. Phys. B 241 (1984) 463.
- [470] G. Heinrich, Z. Kunszt, Nucl. Phys. B 519 (1998) 405;
A. Bassutto, G. Heinrich, Z. Kunszt, W. Vogelsang, Phys. Rev. D 58 (1998) 094020.
- [471] A.V. Belitsky, E.A. Kuraev, Nucl. Phys. B 499 (1997) 301.
- [472] A.V. Belitsky, D. Müller, Nucl. Phys. B 503 (1997) 279.
- [473] A.V. Belitsky, *Leading-order analysis of the twist-3 space- and timelike cut vertices in QCD*, in Proc. of XXXI PNPI Winter School, ed. V.A. Gordeev (St. Petersburg, 1997) p. 369; hep-ph/9703432.
- [474] E.G. Floratos, D.A. Ross, C.T. Sachrajda, Nucl. Phys. B 129 (1977) 66; (Erratum) Nucl. Phys. B 139 (1978) 545;
A. Gonzales-Arroyo, C. Lopez, F.J. Yndurain, Nucl. Phys. B 153 (1979) 161;
G. Curci, W. Furmanski, R. Petronzio, Nucl. Phys. B 175 (1980) 27;
E.G. Floratos, R. Lacaze, C. Kounnas, Phys. Lett. B 98 (1981) 89.
- [475] E.G. Floratos, D.A. Ross, C.T. Sachrajda, Nucl. Phys. B 152 (1979) 493;
A. Gonzales-Arroyo, C. Lopez, Nucl. Phys. B 166 (1980) 429;
E.G. Floratos, C. Kounnas, R. Lacaze, Nucl. Phys. B 192 (1981) 417;
W. Furmanski, R. Petronzio, Phys. Lett. B 97 (1980) 437;
E.G. Floratos, R. Lacaze, C. Kounnas, Phys. Lett. B 98 (1981) 285;
R. Hamberg, W.L. van Neerven, Nucl. Phys. B 379 (1992) 143;
R.K. Ellis, W. Vogelsang, *The evolution of parton distributions beyond leading order: singlet case*, hep-ph/9602356.
- [476] R. Mertig, W.L. van Neerven, Z. Phys. C 70 (1996) 637;
W. Vogelsang, Phys. Re. D 54 (1996) 2023; Nucl. Phys. B 475 (1996) 47.
- [477] W. Vogelsang, Phys. Rev. D 57 (1998) 1886;
S. Kumano, M. Miyama, Phys. Rev. D 56 (1997) 2504;
A. Hayashigaki, Y. Kanazawa, Y. Koike, Phys. Rev. D 56 (1997) 7350.

- [478] W. Vogelsang, *Acta Phys. Polon. B* 29 (1998) 1189.
- [479] W. Siegel, *Phys. Lett. B* 84 (1979) 193.
- [480] D.M. Capper, D.R.T. Jones, P. van Nieuwenhuizen, *Nucl. Phys. B* 167 (1980) 479.
- [481] R.K. Ellis, D.A. Ross, A.E. Terrano, *Nucl. Phys. B* 178 (1981) 421;
 I. Antoniadis, E.G. Floratos, *Nucl. Phys. B* 191 (1981) 217;
 G.A. Schuler, S. Sakakibara, J.G. Körner, *Phys. Lett. B* 194 (1987) 125;
 J.G. Körner, M.M. Tung, *Z. Phys. C* 64 (1994) 255;
 Z. Kunszt, A. Singer, Z. Trócsányi, *Nucl. Phys. B* 411 (1994) 397.
- [482] J. Blümlein, V. Ravindran, W.L. van Neerven, *Acta Phys. Polon. B* 29 (1998) 2581.
- [483] A.V. Belitsky, D. Müller, A. Schäfer, *Phys. Lett. B* 450 (1999) 126;
 A.V. Belitsky, D. Müller, *Phys. Rev. D* 65 (2002) 054037.
- [484] M.F. Sohnius, *Phys. Rept.* 128 (1985) 39.
- [485] A.V. Belitsky, D. Müller, *Nucl. Phys. B (Proc. Suppl.)* 79 (1999) 576.
- [486] A.P. Bukhvostov, G.V. Frolov, L.N. Lipatov, E.A. Kuraev, *JETP Lett.* 41 (1985) 92.
- [487] J.L. Gervais, A. Neveu, *Phys. Lett. B* 80 (1979) 255;
 E. Corrigan, B. Hasslacher, *Phys. Lett. B* 81 (1979) 181;
 L. Durand, E. Mendel, *Phys. Lett. B* 85 (1979) 241.